

# THE SECRETION AND STRUCTURE OF THE SKELETON OF LIVING AND FOSSIL BRYOZOA

BY R. TAVENER-SMITH AND A. WILLIAMS, F.R.S.

*Department of Geology, The Queen's University, Belfast*

(Received 5 August 1971 – Revised 31 December 1971)

[Plates 6 to 30]

## CONTENTS

	PAGE		PAGE
INTRODUCTION	98	(2) Rectanguloid, cancelloid and cerioporoid zooecia	135
MATERIALS AND METHODS	100	(3) Hederelloid, dactylethroid and salpingoid zooecia	138
ORIGIN AND STRUCTURE OF PERIOSTRACUM	100	(c) Structure of trepostome zooecium	139
(a) Periostracum secretion in <i>Membranipora</i>	101	(1) <i>Leioclema</i> zooecium	140
(b) Periostracum secretion in other bryozoans	105	(2) <i>Peronopora</i> zooecium	142
(c) General structure of the periostracum	107	(3) <i>Constellaria</i> zooecium	143
ORIGIN AND STRUCTURE OF MINERAL EXOSKELETON	109	(4) Other trepostome zooecia	143
(a) Structure of cheilostome zooecium	110	(d) Structure of cystoporate zooecium	144
(1) Anascan zooecium	111	(e) Structure of cryptostome zooecium	148
(2) Cribrimorphan zooecium	117	(1) Ptilodictyoid zooecium	148
(3) Gymnocystidean and ascophoran zooecia	118	(2) Rhabdomesoid zooecium	150
(b) Structure of cyclostome zooecium	122	(3) Fenestelloid zooecium	150
(1) Articuloid and tubuloporoid zooecia	124	CONCLUSIONS	153
		REFERENCES	158
		LIST OF ABBREVIATIONS	<i>pull-out facing p. 159</i>

Eighty species of living and extinct bryozoans have been studied to ascertain the mode of secretion of the skeleton and its structural diversity throughout geological time.

In the growing tip of the cheilostomes *Membranipora* and *Electra* and the ctenostome *Bowerbankia*, periostracum secreted by a cap of palisade cells expands forwards by intussusception. Older periostracum, left behind by the advancing cell cap in cheilostomes and cyclostomes, becomes the seeding sheet of a calcitic layer (primary layer) of vertically disposed crystallites with minor banding, nodules and lenses, deposited by epithelium generated immediately proximal of the cell cap. The periostracum is composed of mucopolysaccharide and some chitin but its outer surface varies, being a fibrillar triple-unit membrane in cheilostomes and the cyclostomes *Berenicea* and *Lichenopora*, and a homogenous granular layer in *Bowerbankia* and the cyclostome *Crisidia*.

The mineral skeleton of most cheilostomes is secreted on periostracum by succeeding epithelium. But coelocystic structures, deposited within folds of epithelium, also occur and vary from frontal walls and cryptocysts to almost complete skeletons of *Cupuladria* and *Iodictyum*. In some living cheilostomes and in

Vol. 264. B. 859. (Price £3.65; U.S. \$10.20) 13

[Published 25 May 1972]

most fossil species examined, only a primary shell, more commonly calcitic than aragonitic, is found, but in the majority of living species there occurs an organic-carbonate secondary layer usually composed of discrete laminar or lenticular aggregates of vertically disposed crystallites enclosed in proteinous sheets. In *Celleporella*, however, the laminae are more strongly defined because they consist of spirally growing calcitic plates separated from one another by simultaneously secreted proteinous sheets. More rarely, a tertiary layer is found in some species. It is almost entirely calcitic or aragonitic and may be banded, granular or composed of acicular crystallites. Puncta and basal kenozooids, as in *Schizoporella* and *Cupuladria*, penetrate the shell of some species and accommodate papillae with storage cells.

The mineral skeleton of most cyclostomes, including the earliest known genera like the Ordovician *Corynotrypa*, has always been subperiostracal, and may also be pierced by puncta accommodating storage papillae and distally closed by periostracal plugs (e.g. *Crisidia*, *Berenicea*). The skeleton of *Heteropora*, *Hornera*, *Lichenopora* and related genera which first appeared in early Mesozoic times, is coelocystic. It may also be ornamented by inwardly pointing cones of secondary shell (pseudopuncta) with or without axial rods of granular calcite (e.g. *Hornera*), or include vesicular tissue between radiating rows of zooecia as in *Lichenopora*. All cyclostomes, however, have always had a double-layered calcitic skeleton consisting of a primary layer of vertically disposed acicular crystallites, granules or tablets altered to a granular texture in the fossil state, and a laminar secondary layer with spirally growing plates and/or overlapping fibres coated by protein sheets.

The mineral skeleton of the remaining stenolaemates represented by extinct trepostomes, cystoporates and cyclostomes, is exclusively double-layered and coelocystic. The primary layer is granular, the secondary composed of lenticular fibres. Pseudopuncta were almost invariably developed and interzooecial cavities (mesopores) commonly occurred and were filled with vesicular tissue as in *Lichenopora*.

Phylogenetic considerations suggest that the prototypic bryozoans possessed a pseudopunctate coelocystic skeleton, indented by mesopores and composed of a chitinous or proteinous periostracum, a primary layer of acicular crystallites and a secondary layer of lenticular fibres. This structure was inherited by trepostomes, cystoporates and cryptostomes. It reappeared in Mesozoic cyclostomes subsequent to their divergence from a cystoporate-like ancestor by the development of a variably punctate subperiostracal skeleton which, however, was composed of the same shell types. The sub-peripheral skeleton of early cheilostomes may have evolved by extension of the ctenostome secretory regime. In any event a new type of secondary shell, composed of acicular crystallites arranged in protein-bound laminae and lenticles, became characteristic mainly of Tertiary and Recent species. Nevertheless, a coelocystic skeleton and even a stenolaemate-like secondary shell have already appeared within the Order.

## INTRODUCTION

Since their first appearance during the Ordovician period, bryozoans (or ectoprocts) have become progressively important marine benthos, so that living species represent about one-third of all those described. They, therefore, command the attention of both the palaeontologist and the biologist, and literature about the phylum reflects this community of interest. Yet, except for the works of a few researchers like Borg (1965), little attempt has been made to study living and fossil groups simultaneously in order to understand the processes of skeletal growth in extinct forms. This procedure is not the same as correlating independently derived observations on related living and fossil species, because information required by the palaeontologist about skeletal accretion, is subtly different from that given by the biologist in his description of epithelial secretion. In some respects technical inadequacies have been responsible for this deficiency in the past. The bryozoan exoskeleton (zooecium) is typically a delicate framework with a structural variation that can never be fully appreciated under the light microscope. Indeed, some of the fundamental differences in the fabric of the bryozoan exoskeleton have only become apparent with recent electron microscopic studies (Boardman & Cheetham 1969; Söderqvist 1968; Schopf & Travis 1968; Tavener-Smith 1969a; Tavener-Smith & Williams 1970; Armstrong 1970). Consequently, it seemed opportune to undertake an ultrastructural survey of the skeleton of living and extinct bryozoans to find out if a consistent pattern of zooecial differentiation exists among the various Orders.

The procedure adopted for the investigation was dictated by the nature of fossil preservation.



The chief hazard in determining the skeletal succession of an extinct group is to misidentify the fabric of recrystallized specimens as an original structure. Fortunately two of the three living Orders studied, the Cheilostomata and Cyclostomata, embrace species as far back as the Cretaceous and Ordovician respectively. It has therefore been possible to check the amount of structural alteration certain fossil cheilostomes and cyclostomes have undergone as a result of fossilization, and then to use such specimens as standards in assessing the authenticity of skeletal fabrics of extinct species recovered from the same horizon and locality.

As a prelude to establishing reliable standards for the comparative study of zooecia throughout time, an account of the skeletal secretion and structure in certain living species is presented, beginning with *Membranipora membranacea* (Linn.). This species, which has a simple zooecium, is easily obtainable and cultivable, and its growth has been the subject of an outstanding investigation by Lutaud (1961). Moreover, no bryozoan has yet been found with a growing edge or tip differing structurally from that of *Membranipora*. Consequently, the growth of the tip of *Membranipora* may be regarded as typical of all bryozoans and has been confirmed at least for another cheilostome *Electra pilosa* (Linn.), the cyclostome *Crisidia cornuta* (Linn.) and the ctenostome *Bowerbankia imbricata* (Adams).

Study of the growth tip itself reveals only the steps leading to the exudation of the external organic layer of the zooecium. This constituent, however, is destroyed during fossilization so that the rest of the paper is concerned with the mineral part of the exoskeleton, and the organic cover has been considered mainly in its role as a seeding sheet for crystallite growth. Accordingly, no fossil Ctenostomata has been described. Even the few allegedly calcified ctenostomes available, like some Ordovician specimens of *Vinella*, were not only of questionable affinities but entirely recrystallized. Fossils belonging to all the remaining Orders, however, have been examined as far back in geologic time as collections at our disposal have allowed. In this way it has been possible to build up a reasonably complete picture of the main evolutionary changes affecting the calcareous exoskeleton of bryozoans during phyletic history.

Finally it seems appropriate to comment briefly on the terminology of this paper. In general, we have followed the lead of Ryland (1970) who has done much to clarify a confused vocabulary. We have, however, retained 'zooecium' in place of 'cystid' (Ryland 1970, p. 18) to mean the entire exoskeleton of an individual (zooid) on the grounds that the noun has won a permanent place in bryozoan terminology through usage alone. We have also revised the terms used in describing skeletal successions. The zooecium varies greatly in structure but characteristically consists of an external organic cover underlain by a calcareous frame. Both constituents may be regarded as independent parts of the skeletal succession, yet their terminological distinction has not been clearly drawn by modern writers. Bobin & Prenant (1968, p. 159), for example, used 'ectocyst' for the entire succession and 'pellicle' for the external organic layer which has been called 'ectocyst' by Lutaud (1961, p. 175) and 'cuticle' by Silén (1944, p. 434), Hyman (1959, p. 287), Söderqvist (1968, p. 115) and Boardman & Cheetham (1969, p. 209). Ryland (1970, p. 17) and Schneider (1963, p. 358), on the other hand, used 'cuticle' to mean the full skeletal succession, while Banta (1968, p. 504), having concluded that the calcite within the zooecium of *Watersipora* is 'intracuticular', maintained that the entire succession should be referred to as 'ectocyst'. These contradictions have prompted us to adopt other names already well established for the exoskeletal successions of other invertebrates, particularly the related lophophorate Brachiopoda. Terms of immediate relevance are: 'periostracum' for the *external* organic cover, 'primary shell (or layer)' for the first-formed mineral layer secreted on the

inner surface of the periostracum and 'secondary shell (or layer)' for a distinguishable succeeding layer normally composed of persistent bands or laminae of calcium carbonate separated from one another by interconnected organic membranes. Other terms, identifying canals or rods penetrating various parts of the successions, will be introduced in the course of the paper. The use of such terms in describing the structure of the bryozoan zooecium is defensible, not merely because they reduce ambiguity but because they can signify homologous structures in different phyla.

#### MATERIALS AND METHODS

Specimens used in this study were obtained in the living, dried or fossilized state, and a number of procedures have been adopted to exact information.

For general histochemical investigations under the light microscope, living specimens were fixed in 10 % neutral formalin. Required parts of specimens were then decalcified in Gooding and Stewart's fluid (Culling 1963) and the organic residues embedded in 56 °C paraffin wax. Prepared sections were subjected to Mazia protein stain, periodic acid-Schiff reaction (PAS), and alcian blue, Mayer's haemalum and eosin. Frozen sections of formalin-fixed specimens and residues prepared by a modified Van Wisselingh-Brunswik test (Campbell 1929) were used for the identification of lipids, and chitin respectively.

For transmission electron microscopic study of soft parts, living specimens were fixed in 4 % gluteraldehyde made up in 3 % sodium chloride, then decalcified in 10 % EDTA, washed in sucrose and treated for 1 h with 2 % osmic acid; all solutions were buffered to pH 7.2 with phosphate buffer. Following dehydration, specimens were embedded in an Epoxy resin and the sections stained with aqueous uranyl acetate and aqueous lead citrate.

All carbonate skeletons of living and fossil species were studied under a Stereoscan scanning electron microscope (purchased by NERC grant RB/ST/E5). For this purpose, the mineral skeleton of living bryozoans were freed of soft parts by immersion in sodium hypochlorite for some hours. Many fossils examined were embedded in rock matrix and are preferred to specimens free of matrix which have almost invariably suffered enough weathering to affect the fabric of the superficial parts. However, fossils in rock cannot be successfully prepared to show the true texture of natural and fracture surfaces, and details of their skeletal successions are best seen in cut sections. Consequently, Recent shells have also been sectioned in the same way to ensure that the constituents of fossil successions have been correctly identified. For this purpose, both fossils in matrix and free shells were embedded in a resin like Araldite and cut with a diamond-edged blade along any preferred direction to provide surfaces containing the required sections. These were then polished with tin oxide or alumina and etched in 2 % EDTA for between 15 and 30 min, dependent on the texture of the shell, to enhance topographic differences between various constituents. All natural surfaces, fracture surfaces and differentially etched sections were coated with gold/palladium for examination under the Stereoscan.

#### ORIGIN AND STRUCTURE OF PERIOSTRACUM

The outer organic cover of bryozoans, the periostracum, is secreted at the growing edges or tips of a colony. In a simple adnate colony, like that of *Membranipora*, a growing tip (figure 1) is the youngest of a linear series of zooids illustrating successive stages in the development of a single zooid. In more complex colonies, growing tips have the same basic arrangement even if

they are precursory to specialized zooids such as the stoloniferous kenozooids of *Bowerbankia*. As far as is known, the growth tips of all bryozoans are alike in being composed of epithelial cells grouped around a peritoneal core and bounded by a continuous layer of periostracum. The growth tip itself may be defined as extending proximally to the edge of the first calcium carbonate layer to be secreted beneath the periostracum. In *Bowerbankia* and other Ctenostomata lacking an organized mineral skeleton, the tip has been identified proximally as far as the first transverse partition. Such boundaries broadly indicate those zones where epithelium first becomes more or less permanently attached to the zoecium. It is, therefore, practicable to describe periostracal secretion and structure in relation to the growth tips of various species before giving a comparative account of the exoskeleton of mature zooids in living and extinct Orders.

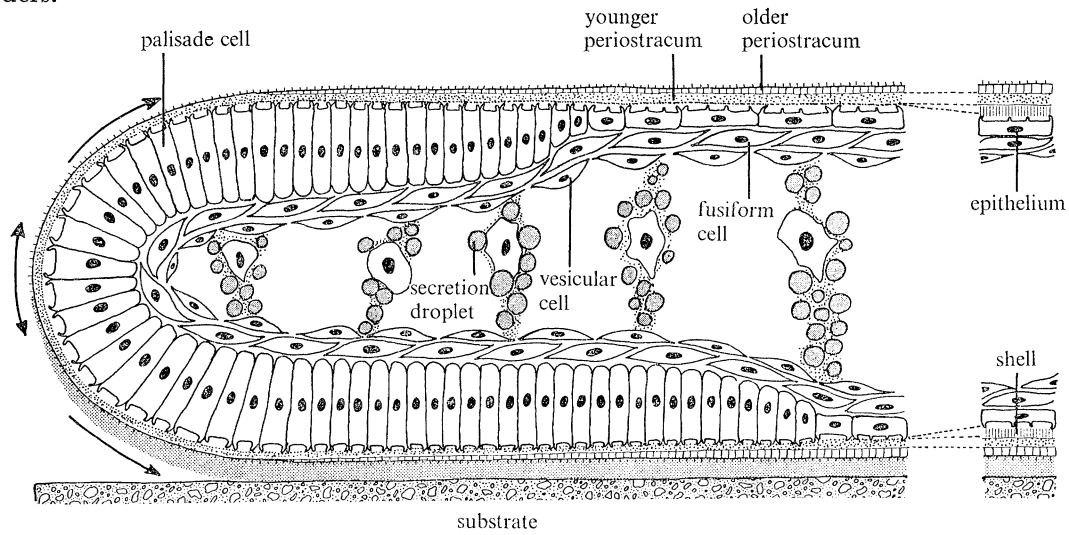


FIGURE 1. Diagrammatic sagittal section of a cheilostome growth tip showing the relationship between periostracum of the palisade cell cap and the skeletal cover of the mature zooid; the fine stippling between the tip and substrate represents mucin.

(a) *Periostracum secretion in Membranipora*

In the growth tip of *Membranipora membranacea*, the epithelial cells (or palisade cells of Lutaud 1961, p. 176) are closely packed into a single layer, shaped like an asymmetrical capsule, about 120  $\mu\text{m}$  in diameter, with the basal and frontal surfaces extending proximally for about 170 and 120  $\mu\text{m}$  respectively. This structure has been designated the 'apical cell plate' by Schneider (1963, p. 364) in another cheilostome *Bugula*; but, in this account, it will be referred to as the 'palisade cell cap' (or 'cap') which better describes its form even when it is undergoing a re-orientation during growth (figure 1). The palisade cells, of which there are about 70 in a sagittal section of the cap, are about 28  $\mu\text{m}$  long, 5  $\mu\text{m}$  wide and roughly prismatic in shape (figures 2; and 3 and 4, plate 6). All cells have the same internal organization indicative of youth and intense secretory activity. The proximal three-quarters of the cell includes a large nucleus with a prominent nucleolus and only small quantities of deeply staining heterochromatin, densely distributed granular endoplasmic reticulum, and scattered mitochondria. The distal quarter of the cell is dominated by a conspicuous Golgi apparatus and a large globular vesicle (figure 5, plate 6). The groundmass of this part of the cell consists of a smooth endoplasmic reticulum with well-dispersed mitochondria and many small secretion droplets. Here adjacent membranes are tightly folded parallel to the long axes of the cells and locked by terminal bars in the form of

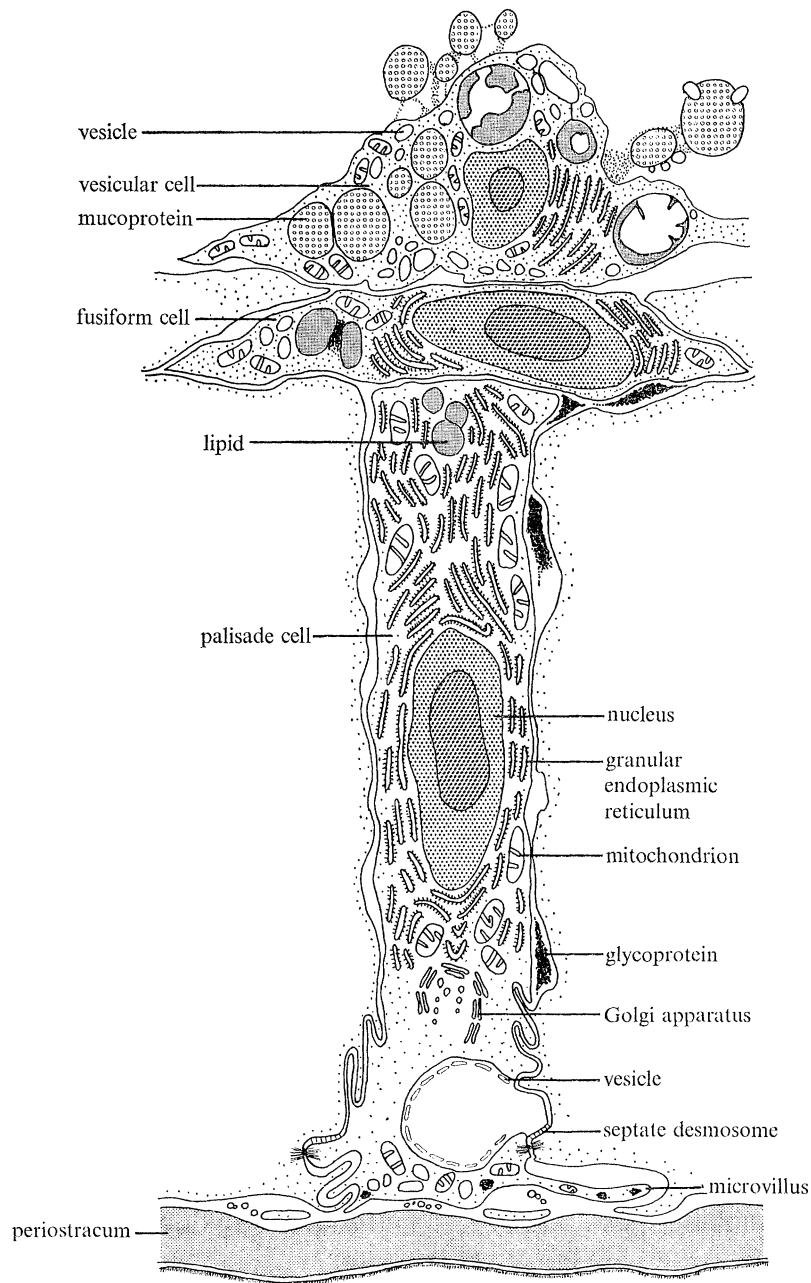


FIGURE 2. Diagrammatic sagittal section through part of the palisade cell cap showing its relation to the periostracum.

#### DESCRIPTION OF PLATE 6

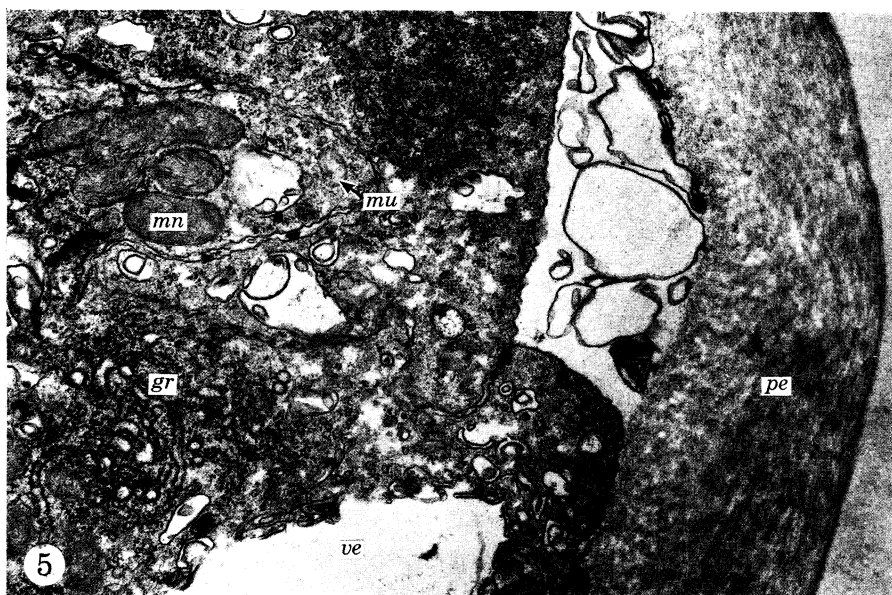
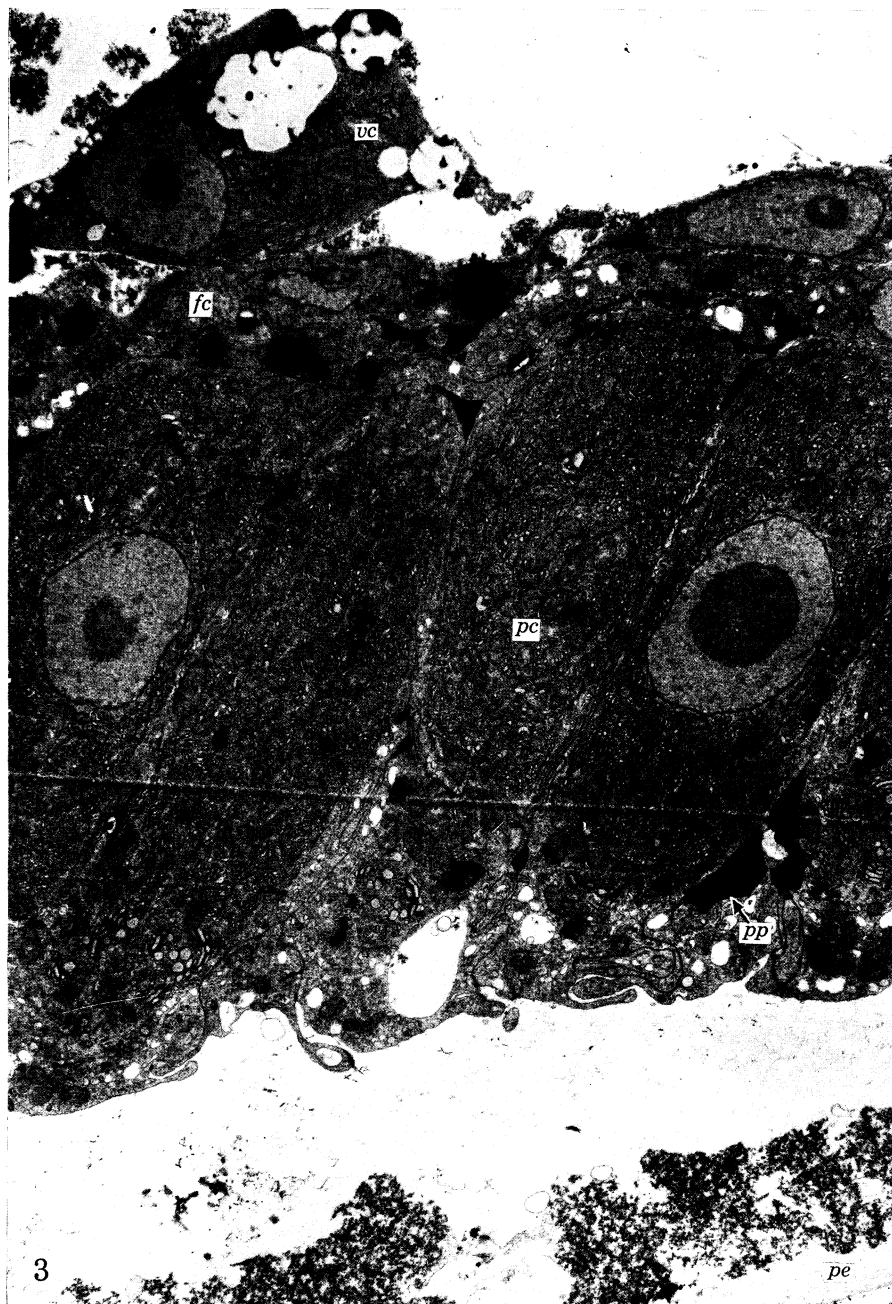
Electron micrographs of the growth tip of *Membranipora membranacea* (Linnaeus), Portaferry, Co. Down, N. Ireland:

FIGURE 3. Vesicular, fusiform and palisade cells in relation to the periostracum ( $\times 5500$ ).

FIGURE 4. Palisade cells with well-developed intercellular spaces and microvillous extensions of the external plasmalemma ( $\times 5500$ ).

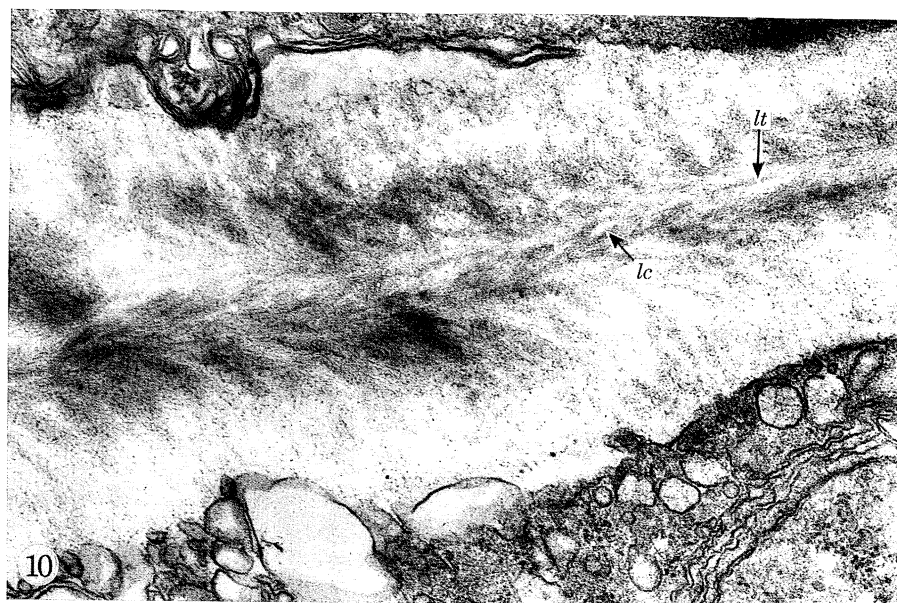
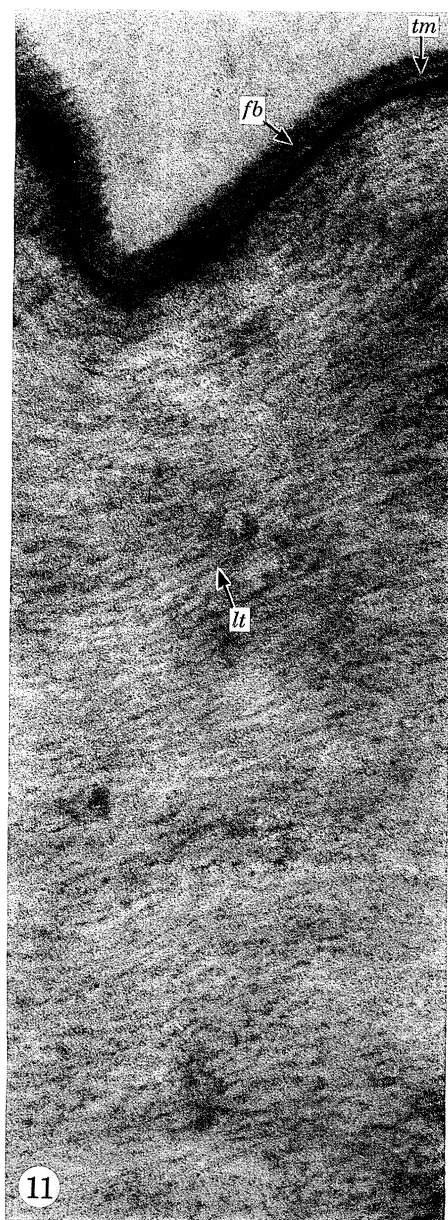
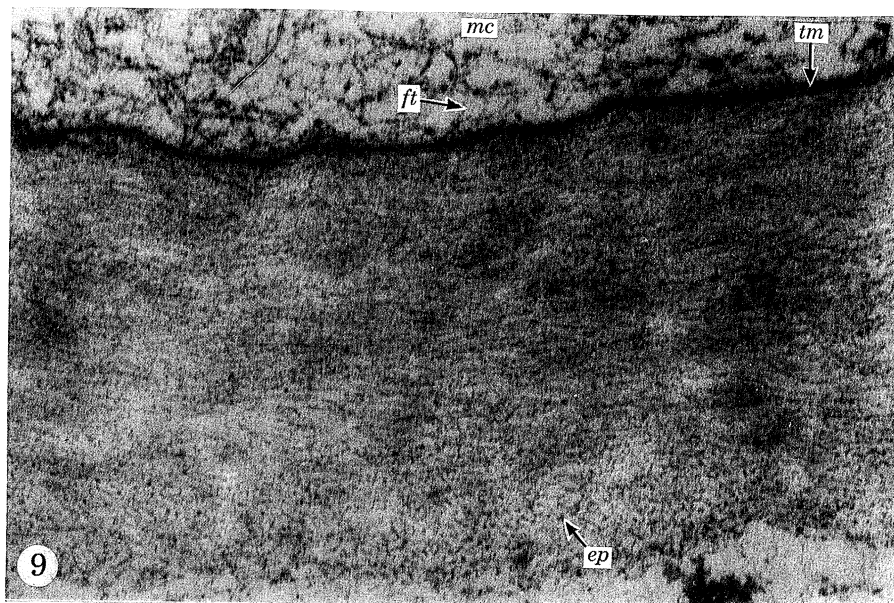
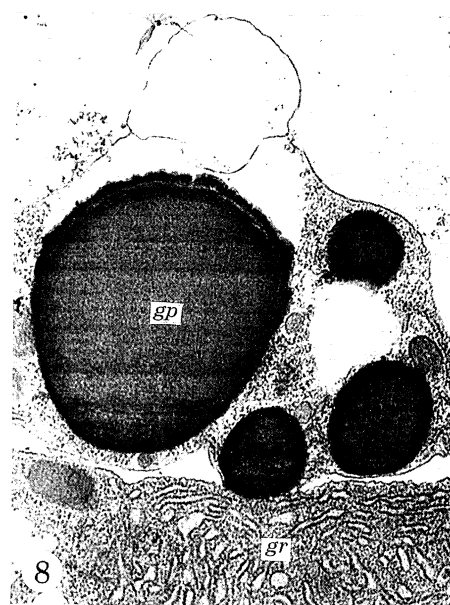
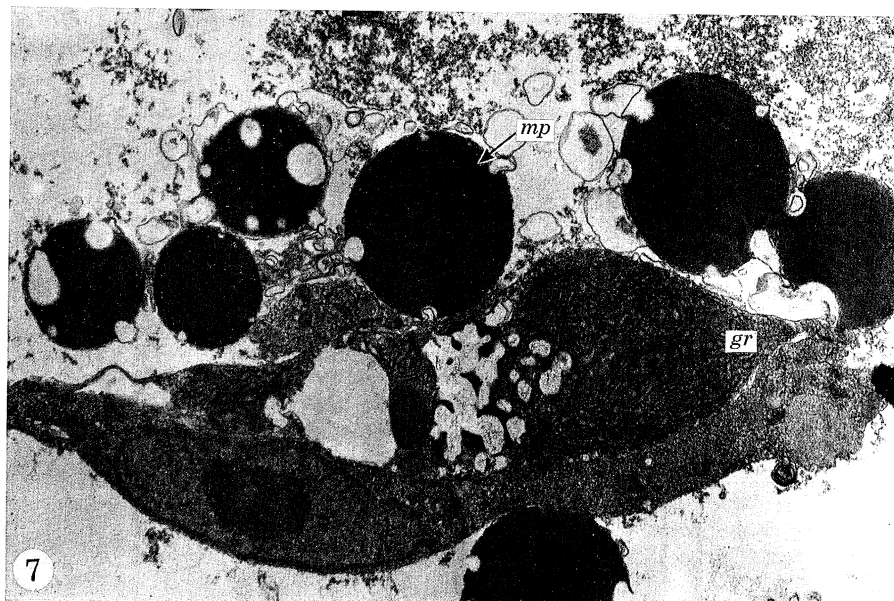
FIGURE 5. Distal part of palisade cells in association with the periostracum ( $\times 20000$ ).

FIGURE 6. Detail of distal part of palisade cells showing intercellular polysaccharide-protein secretion ( $\times 20600$ ).



FIGURES 3 TO 6. For legends see facing page.





FIGURES 7 TO 11. For legends see facing page.

undifferentiated or septate desmosomes (figure 6, plate 6). The external plasmalemma responsible for the secretion of the periostracum is thrown into recumbent microvilli up to 7  $\mu\text{m}$  long and 300 nm in diameter. The microvilli are generally concentrated into two or three rows along the cell edges and are so arranged in adjacent cells as to interdigitate across the external openings of intercellular spaces (figure 3, plate 6).

A variety of secretion droplets are found scattered throughout the palisade cells. A Sudan black B test on formalin-fixed frozen sections of *Membranipora* indicated the presence of some neutral lipid droplets in the internal pole of the cell. These droplets are identifiable as patchily electron-dense bodies up to 500 nm in diameter and lack limiting membranes. Other electron-dense secretions, also without bounding membranes but with a granular texture, occur as irregular bodies in intercellular spaces (figure 6, plate 6) where they may be more than 2  $\mu\text{m}$  long, and as subrounded droplets about 500 nm across within the cells near the external plasmalemma. These secretion bodies coincide with that part of the cell registering a positive PAS reaction which persisted in saliva-treated sections. These bodies are, therefore, likely to be polysaccharide-protein complexes which would account for their intimate association with glycogen rosettes seen under the electron microscope. Glycogen particles are also found elsewhere in the cells especially near the Golgi apparatus, while electron-light droplets within membrane-bound vesicles in the outer region of the cell have been identified as a mucopolysaccharide (figure 5, plate 6).

On the proximal side of the terminal cap, columnar palisade cells pass rapidly into cuboidal epithelium in which individual cells become progressively more flattened until they may be more than 20  $\mu\text{m}$  wide and only 5  $\mu\text{m}$  high. The internal organization of the cell also changes, with the Golgi apparatus and principal vesicle becoming smaller and the granular endoplasmic reticulum losing definition, so that ribosomes are more evenly distributed throughout the groundmass.

The peritoneum forming the core of the growing tip of *Membranipora* consists of two layers of cells and a more sporadically distributed medial group: the fusiform cells, the vesicular cells and the spheroidal leucocytes respectively of Lutaud (1961, p. 186) (figure 2). The spindle-shaped fusiform cells which are up to 20  $\mu\text{m}$  wide and about 4  $\mu\text{m}$  thick, lie adjacent to the inner plasmalemma of the palisade cells (figures 3 and 4, plate 6). They, too, have large nuclei, granular endoplasmic reticulum and mitochondria, and secretion droplets particularly lipids. The vesicular cells are similar in dimensions and disposition but are distinguished by an abundance of vesicles, membrane-bound droplets of an electron-dense material and inclusions of unsaturated lipids (figure 3, plate 6).

A number of vaguely defined cells, weakly attached to the inner plasmalemma of the vesicular cells, also occur within the medial zone of the growing tip and are charged with a variety

---

#### DESCRIPTION OF PLATE 7

Electron micrographs of the growth tip of *Membranipora membranacea*:

FIGURES 7, 8. Spheroidal leucocytes with secretion droplets of mucoprotein and glycoprotein ( $\times 8250$ ).

FIGURE 9. The apical periostracum with a poorly differentiated triple-unit membrane bearing filaments in the external mucin film ( $\times 82500$ ).

FIGURE 10. Lacunae developed in the periostracum of a transverse wall ( $\times 27500$ ).

FIGURE 11. Outer part of a fully developed periostracum showing the triple-unit membrane and its external filamentous brush ( $\times 165000$ ).



of secretion droplets (figures 7 and 8, plate 7). Some of these inclusions are lipids but the majority consist of either electron-dense spherical bodies, about 3  $\mu\text{m}$  across, lacking a bounding membrane and associated with glycogen particles, or electron-dense granular droplets, about 2.5  $\mu\text{m}$  in diameter, each enclosed in a membrane which may be distended here and there into small vesicles. In wax-embedded sections, the electron-dense secretion droplets in the spheroidal leucocytes and vesicular cells showed a strong positive PAS reaction which persisted after glycogen digestion. They also reacted positively to mercury bromphenol blue and are probably complexes of protein with mucin and glycogen.

Although all cell layers identified above probably contribute to its synthesis, the periostracum is secreted by the microvillous outer plasmalemma of the palisade cells (figures 9 to 11, plate 7). The periostracum appears to form a continuous cover for the growing tip, differing only in thickness. Reliable estimates of thickness are difficult to obtain because newly formed parts of the periostracum are usually less compact than more mature portions and may include closely distributed lacunae up to 100 nm across, which represent either a temporary vesicular condition immediately following exudation or tensional artefacts (figure 10). However, periostracum around the palisade cell cap, showing the same degree of compaction throughout, varies in thickness from 2.5 to 1.5  $\mu\text{m}$  adjacent to the proximal and apical parts of the cap respectively.

On the proximal side of the growth tip, the external cover of the periostracum is fully developed as a triple-unit membrane consisting of an outer and inner electron-dense layer, about 3.5 and 4.5 nm thick respectively, separated by an electron-light zone about 5.5 nm thick (figure 11.) The external surface of the outer layer bears an evenly topped, filamentous brush about 18 nm high with individual filaments occasionally distinguishable as bulbous-tipped rods up to 7 nm wide. The main periostracal layer is usually differentiated into two zones of about equal thickness. The electron-light groundmass of the outer zone is seamed with linear trails of electron-dense particles about 1.5 nm across. The trails are up to 200 nm long and mostly lie parallel with the external cover, but they are also sporadically disposed normal to that cover. Inwardly the electron-dense particles become more evenly distributed so that the inner zone has a finely stippled appearance. Various histochemical tests, including performic acid-Schiff, alcian blue, Mallory's triple strain and the Van Wisselingh-Brunswik test for chitin, confirm the findings of Schneider (1963, p. 358) that the periostracum is composed of mucopolysaccharides and proteins with some chitin. It is, therefore, possible that the electron-dense particles represent the chitinous constituent in a dominantly proteinous periostracum.

The apical segment of the periostracum is not only the thinnest part of that cover, but also the least well defined. Here, the triple-unit membrane is not uniformly developed while the filaments do not usually form an even brush and may extend outwards as much as 150 nm as an irregular web of threads, each about 3.5 nm thick (figure 9, plate 7). Also, on the basal side of

#### DESCRIPTION OF PLATE 8

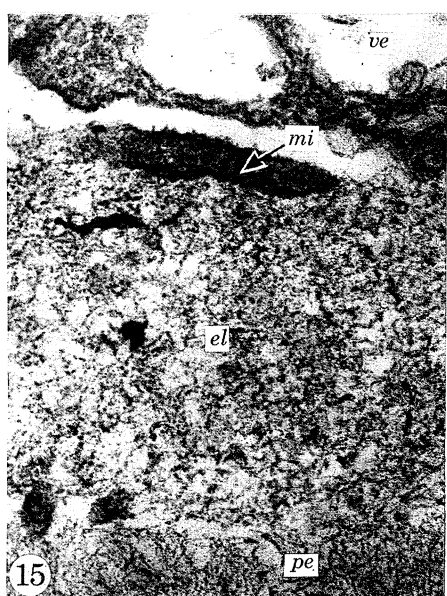
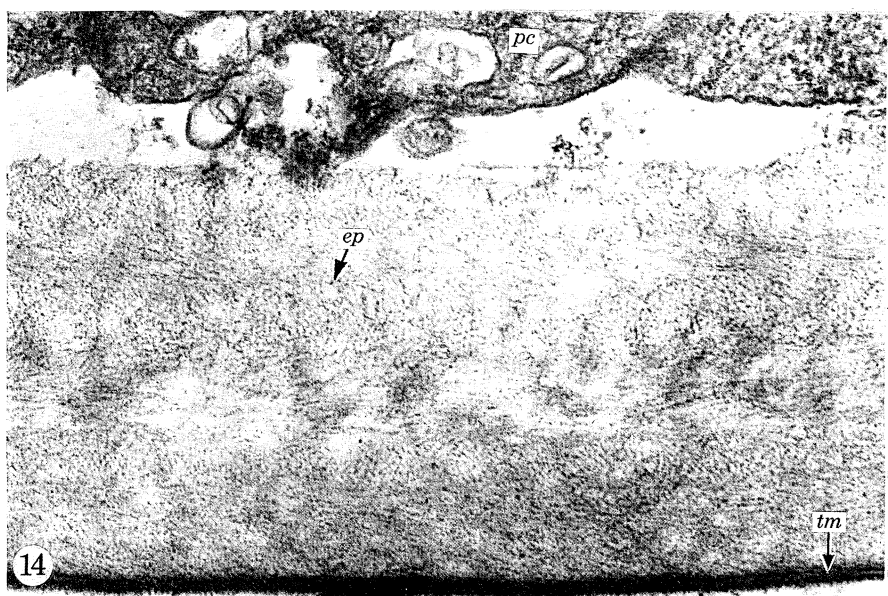
Electron micrographs of the growth tip of *Electra pilosa* (Linnaeus), Portaferry, Co. Down, N. Ireland:

FIGURE 12. Palisade cells in relation to the periostracum ( $\times 8250$ ).

FIGURE 13. Vesicular, fusiform and palisade cells showing secretion droplets ( $\times 5500$ ).

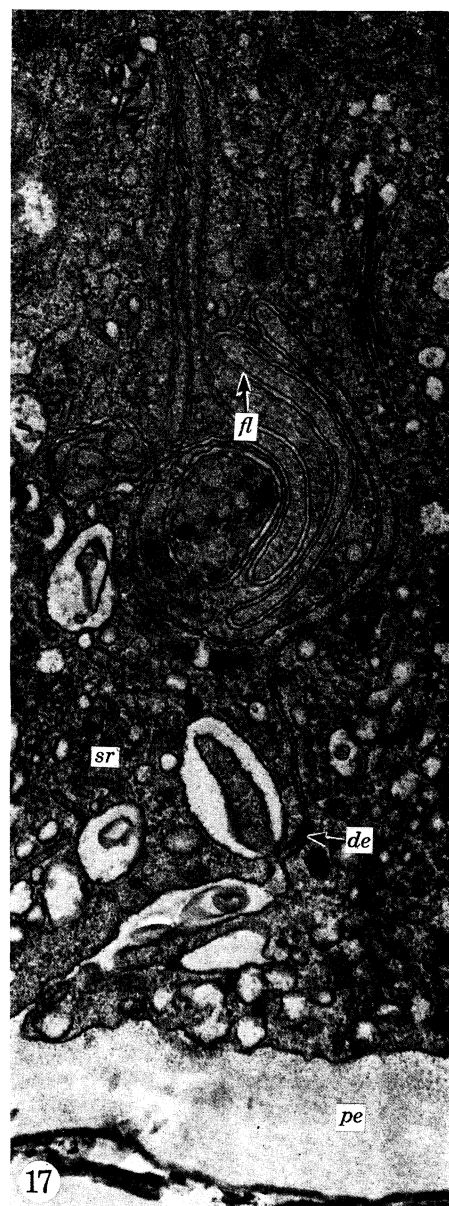
FIGURE 14. The periostracum with its external triple-unit membrane and electron-dense trails ( $\times 55000$ ).

FIGURE 15. The layer of extraneous material intervening between the periostracum and the outer plasmalemma of a palisade cell ( $\times 68700$ ).



FIGURES 12 TO 15. For legends see facing page.





FIGURES 16 TO 19. For legends see facing page.

the tip, a coating of mucin occurs external to the periostracum. The mucin is merely a film entangled with filaments at the central part of the apex, but it thickens proximally into a layer, up to 4  $\mu\text{m}$  thick, intervening between the tip and substrate where it acts as an adhesive for the attachment of the colony.

Variation in the thickness and texture of the apical periostracum is consistent with its growth by intussusception (Schneider 1963, p. 360). As periodic examination of a zooidal tip grown on a marked glass surface shows, the periostracum remains entire even during active enlargement. Moreover, at any moment during growth, the inner periostracal surface, being secreted simultaneously, is an isochronous boundary. Hence if the thickness of the periostracum around the palisade cell cap is a function of age, the filamentous triple-unit membrane bounding the periostracum is progressively older away from the central apical zone (figure 1). Presumably, during periods of colonial extension the forward movement of the palisade cell cap is always accompanied by a distension of the existing central apical zone of the periostracum which is gradually pushed aside as newly secreted material displaces it either physically or by continual impregnation of an adjustable protein-chitin fabric that has not yet polymerized. Polymerization as well as tanning effects more fully account for the better definition of the triple-unit membrane and its shortened, filamentous coat in older periostracum.

Concomitantly with distension of the apical periostracum, mucin must diffuse on to the external surface. It is possible that only a few apical palisade cells are involved in this secretory process, but that once the mucin reaches the exterior it gravitates towards the basal wall and accumulates between the substrate and the advancing tip.

In this way, the first-formed part of the periostracum is secreted and then left behind by the advancing palisade cell cap as a cover for the newly differentiating parts of the colony, and as a seeding sheet for mineral components of zooecia. The periostracum is secreted by both epithelial and palisade cells but growth relationships between these two cell types is complex. Although all palisade cells have the characteristics of young tissue, we agree with Lutaud (1961, p. 249) that only those along the basal wall are involved in high mitotic activity. It therefore seems likely that new palisade cells originate from the basal generative zone. On the frontal surface, the main proliferation of cells takes place proximally of the cap, and additional cell surface needed to maintain secretion of the periostracum on this side is provided by changes in cell shape as columnar palisade cells flatten proximally (figure 24, plate 10).

(b) *Periostracum secretion in other bryozoans*

Sections of other bryozoans suggest that the structure of the zooidal growing tip throughout the phylum is basically the same as that of *Membranipora*.

In the cheilostome *Electra pilosa* the palisade cell cap is about 100  $\mu\text{m}$  long and half as wide,

---

DESCRIPTION OF PLATE 9

Electron micrographs of the growth tip of *Bowerbankia imbricata* (Adams), Ardkeen, Co. Down, N. Ireland:

FIGURE 16. Palisade cells in relation to the periostracum ( $\times 20\,600$ ).

FIGURE 17. The outer parts of palisade cells with tightly folded lateral plasmalemmas in relation to the periostracum ( $\times 27\,500$ ).

FIGURE 18. The periostracum with its granular external coat ( $\times 55\,000$ ).

Electron micrograph of the growth tip of *Crisidia cornuta* (Linnaeus), Ardkeen, Co. Down, N. Ireland:

FIGURE 19. The periostracum with its granular external coat and internal sealing surface ( $\times 90\,000$ ).

and consists in sagittal section of about 45 cells each up to 11  $\mu\text{m}$  long and 3.5  $\mu\text{m}$  wide. The cells are differentiated into a larger inner zone with granular endoplasmic reticulum and an outer vesicular zone (figures 12 and 13, plate 8). When the cap is actively secreting periostracum, however, very large vesicles develop to serve groups of three or four cells. Consequently, the outer part of the cap forms a narrow, irregular, microvillous layer adjacent to the periostracum, which is separated from the rest of the cap by a more or less continuous zone of vesicles.

The periostracum of *Electra* is structurally and histochemically comparable with that of *Membranipora*. Its outer coat is a triple-unit membrane about 13.5 nm thick bearing a dense filamentous coat up to 9 nm high (figure 14, plate 8). Beneath this membrane, the main layer is usually about 1  $\mu\text{m}$  thick adjacent to the proximal part of the cap. In section it consists of electron-light material seamed with thread-like trails of electron-dense particles up to 100 nm long and about 3 nm thick, presumably representing a dominantly proteinous layer with chitinous filaments. Electron-dense trails next to the triple-unit membrane usually lie more or less parallel to the external surface, but zones of highly inclined and subparallel trails may alternate inwardly. The innermost zone may be separated from the palisade cells by a distinctive layer up to 500 nm thick (figure 15, plate 8). This layer contains filaments of variable length, vesicle membranes, and electron-dense clots in a groundmass of medium electron-density. Its presence does not represent an intermediate stage in periostracal deposition because, where the periostracum rests on the palisade cell cap, electron-dense particles already organized into trails are seen to arise directly from the secreting plasmalemma. The layer is, therefore, more likely to be a temporary accumulation of organic residue which is either reconstituted or removed prior to an episode of periostracal secretion.

The palisade cell cap of the ctenostome *Bowerbankia imbricata* is smaller than that of other living bryozoans studied, being only about 50  $\mu\text{m}$  deep and 85  $\mu\text{m}$  in diameter. In sagittal section, the cap consists of about 20 palisade cells. Each is conventionally differentiated into an inner zone of predominantly granular endoplasmic reticulum and an outer one containing abundant vesicles and secretion droplets (figure 16, plate 9). The lateral walls are usually thrown into tight folds lying parallel with the long axis of the cell (figure 17, plate 9). The exits of intercellular spaces are overlain by up to three pairs of interdigitating microvilli, some over 1  $\mu\text{m}$  long.

The periostracum is about 700 nm thick proximally (figure 18, plate 9) and consists of a medium electron-dense granular external coat about 40 nm thick underlain by a layer of electron-light material forming a groundmass for closely distributed electron-dense particles

---

#### DESCRIPTION OF PLATE 10

FIGURE 20. Electron micrograph of the periostracum at the growth tip of *Crisidia cornuta* (Linnaeus), Ardkeen, Co. Down, N. Ireland ( $\times 22500$ ).

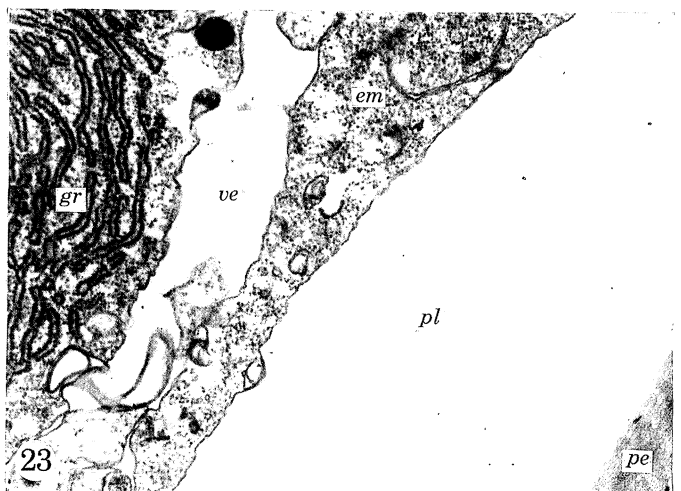
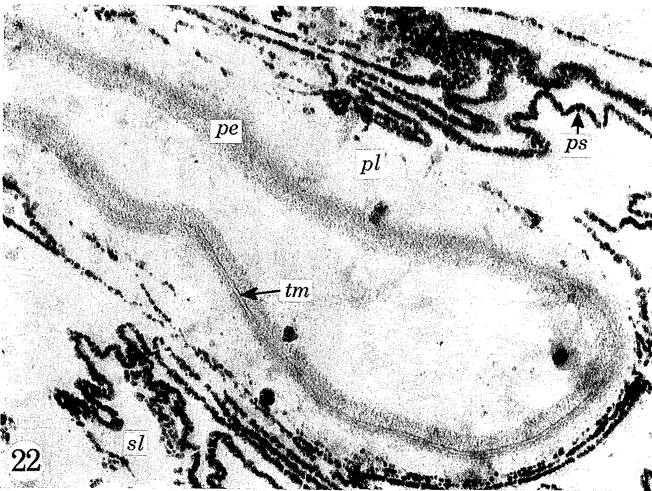
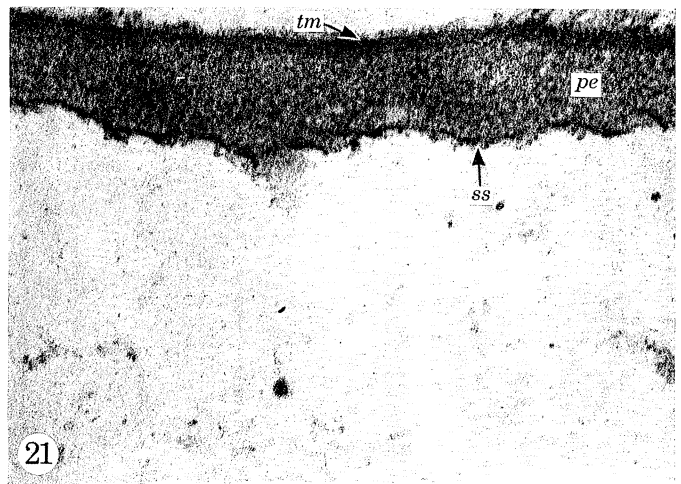
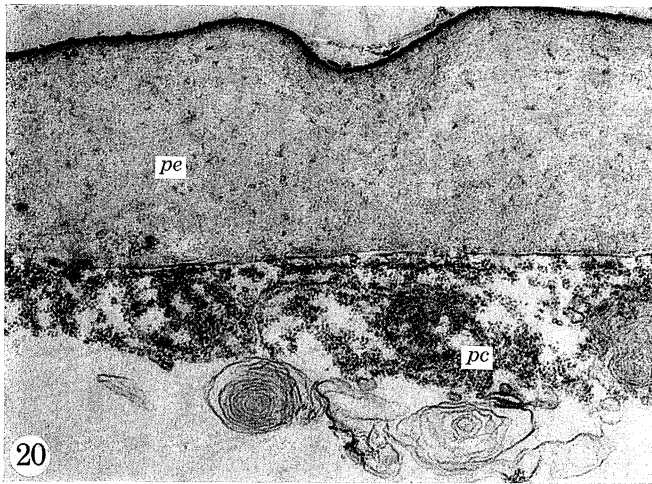
FIGURE 21. Electron micrograph of the periostracum of *Berenicea patina* (Lamarck), Killyleagh, Co. Down, N. Ireland ( $\times 82500$ ).

FIGURE 22. Electron micrograph of the periostracum and proteinous sheets within the secondary shell of *Lichenopora radiata* (Audouin), Plymouth, England ( $\times 34000$ ).

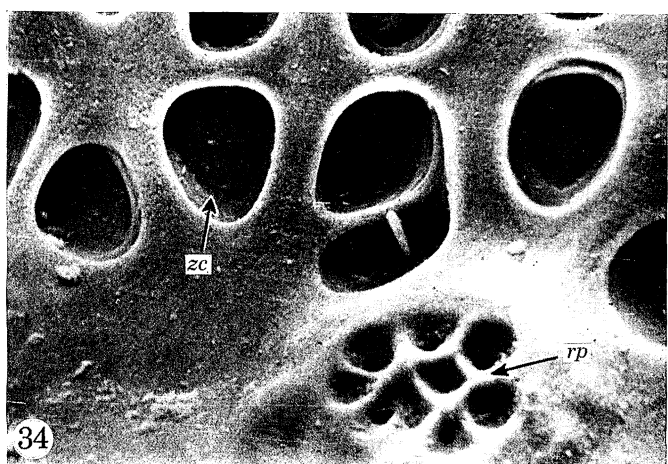
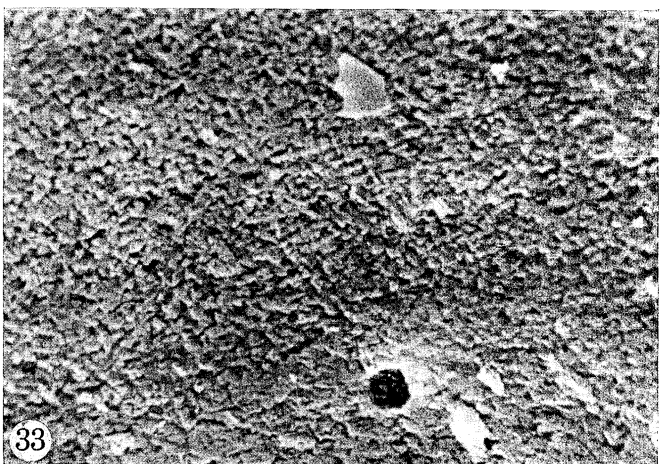
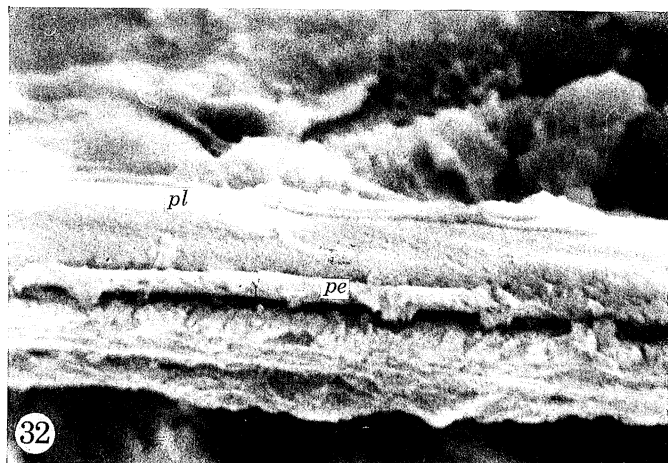
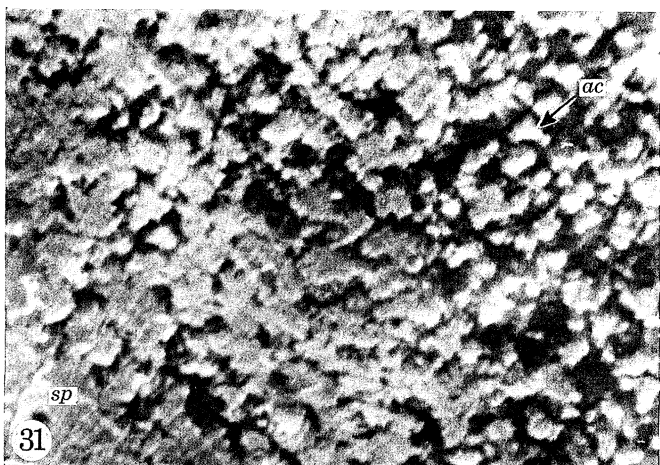
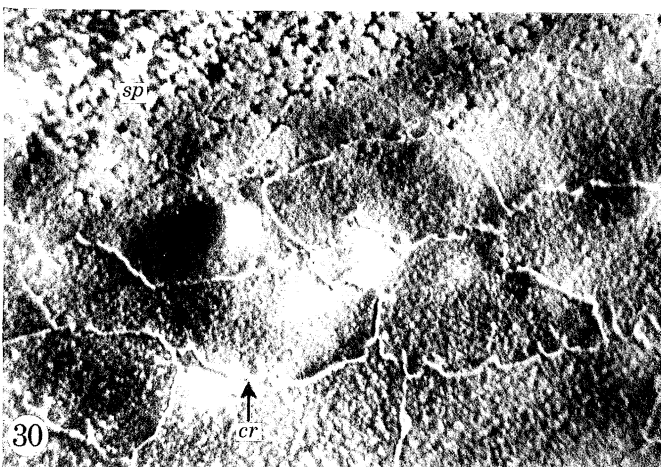
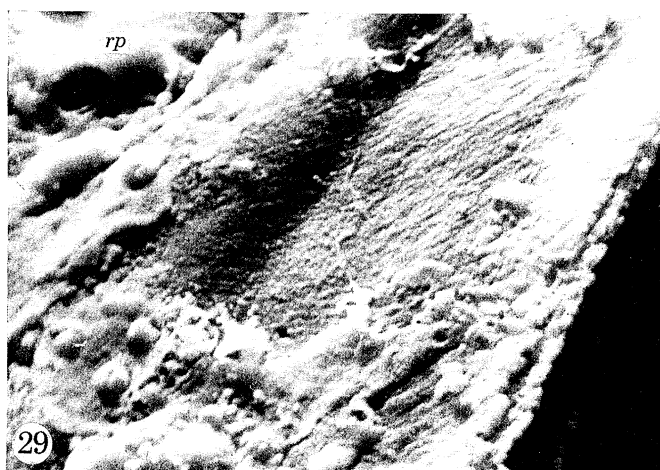
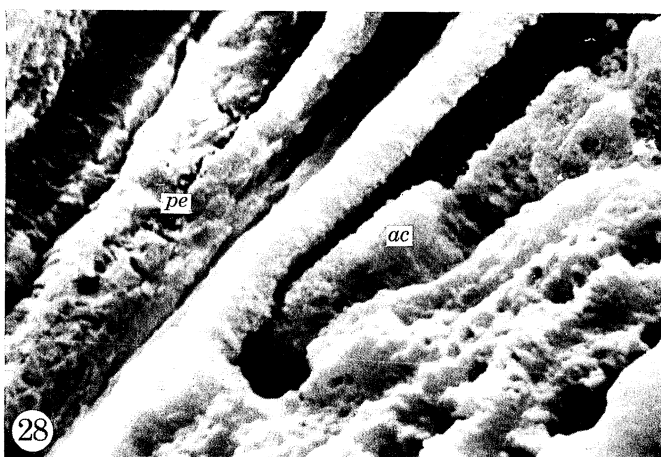
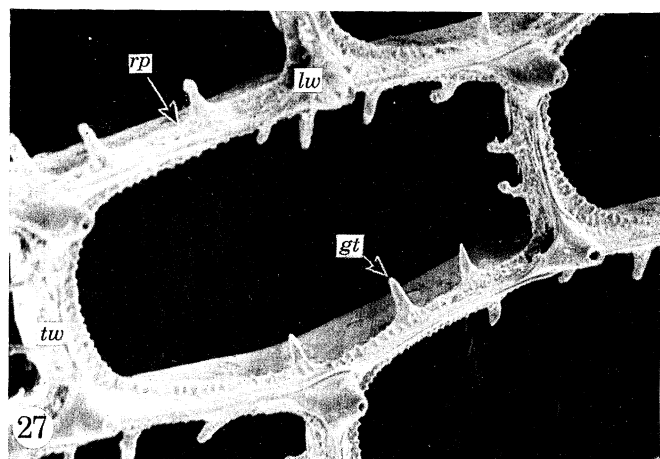
FIGURE 23. Electron micrograph of the epithelium adjacent to the transverse wall of *Membranipora membranacea* ( $\times 12000$ ).

FIGURE 24. Electron micrograph of the epithelium adjacent to the basal and transverse walls of *Celleporella hyalina* (Linnaeus), Plymouth, England ( $\times 11000$ ).





FIGURES 20 TO 24. For legends see facing page.



FIGURES 27 TO 34. For legends see facing page.



about 2.5 nm across. These generally impart a stippled appearance to the layer but may be alined in trails normal to, or parallel with, the external surface. The external coat is only sparsely filamentous on the outside being, more commonly, slightly fretted as if bands, a few nanometres thick, are flaking off the main part of the coat. A modified Van Wisselingh-Brunswick test shows abundant chitin in the periostracum, and the texture and electron-density of the external coat suggest that it may be chitinous. The electron-dense particles in the rest of the periostracum which is composed of mucopolysaccharides and proteins (Bobin 1958), may also be chitinous.

The palisade cell cap of *Crisidia cornuta* has not been observed in occupation of the distal end of a growth tip. However, microvilli, have been seen resting on an incomplete layer of newly formed periostracum about 650 nm thick. Thus skeletal secretion in the cyclostome *Crisidia* proceeds in the same way as in cheilostomes and ctenostomes.

The fully developed periostracum of *Crisidia* (figures 19 and 20, plates 9 and 10) averages 1.5  $\mu\text{m}$  in thickness exclusive of rounded folds, up to 250 nm in height crenulating the outer surface. The outer coat, essentially an electron-dense granular zone about 25 to 30 nm thick, may bear an impersistent mat of scattered, uneven fibrils up to 75 nm long or a dense nap about 13 nm high and sporadically distributed vesicles up to 25 nm across. More commonly, the outer surface of the coat appears slightly fretted like that of *Bowerbankia* (figure 19). This outer coat passes internally into a zone of closely spaced electron-dense trails, 20 nm or more in length, which are disposed normal to the external surface. Similar trails, about 2 nm thick and alined either parallel with, or normal to the exterior, may also occur within the underlying stippled main layer of the periostracum. An electron-dense membrane, up to 10 nm thick, seals the periostracum internally and serves as a seeding sheet for the crystallites of the succeeding primary layer.

(c) *General structure of the periostracum*

Despite variation in thickness, texture and structure, the only important difference among bryozoan periostraca so far examined is the presence or absence of a triple-unit membrane in the outer coat (figure 25). In *Membranipora* the electron-dense bounding layers of the membrane are distinguishable at the tip; and, as maturation proceeds, all components become better defined proximally of the advancing cap. In particular, the filamentous mat on the outer layer develops into a dense short nap, while the inner electron-dense layer becomes thicker. These

---

#### DESCRIPTION OF PLATE 11

Scanning electron micrographs of the zooecia of *Membranipora membranacea*:

FIGURE 27. Frontal view of zooecia showing gymnocystal spines ( $\times 120$ ).

FIGURE 28. Section of a lateral wall showing the periostracal layer and lenses of primary acicular crystallites ( $\times 2900$ ).

FIGURE 29. Internal surface of a lateral wall showing the lineated fabric of the primary layer ( $\times 2400$ ).

FIGURES 30, 31. Internal surface of a lateral wall showing scarp-like fronts of acicular crystallites and crenulated ridges of calcite ( $\times 2400$ ;  $\times 5700$ ).

Scanning electron micrographs of the zooecia of *Electra pilosa*:

FIGURE 32. Section of a lateral wall showing the periostracal layer between two primary layers of acicular crystallites ( $\times 2600$ ).

FIGURE 33. External surface of a lateral wall showing the granular texture ( $\times 2600$ ).

FIGURE 34. Internal surface of a lateral wall showing craters and a rosette plate ( $\times 670$ ).

variations tend to blur the nature of the membrane in other species although the invariable presence of the middle electron-light layer is a reliable indication of its existence.

The presence of filamentous triple-unit membranes in the periostraca of *Schizoporella* and *Umbonula* (Tavener-Smith & Williams 1970, pp. 239, 247), *Celleporella*, *Cupuladria* and *Electra* suggests that such coats have always been a feature of the cheilostome exoskeleton, varying only in the thickness of their bounding layers. Even the main periostracal layer of all these genera shows a similar differentiation into electron-dense trails permeating an electron-light ground-mass. Hence the periostracum of *Membranipora* may be regarded as typical of living and fossil species of the Cheilostomata.

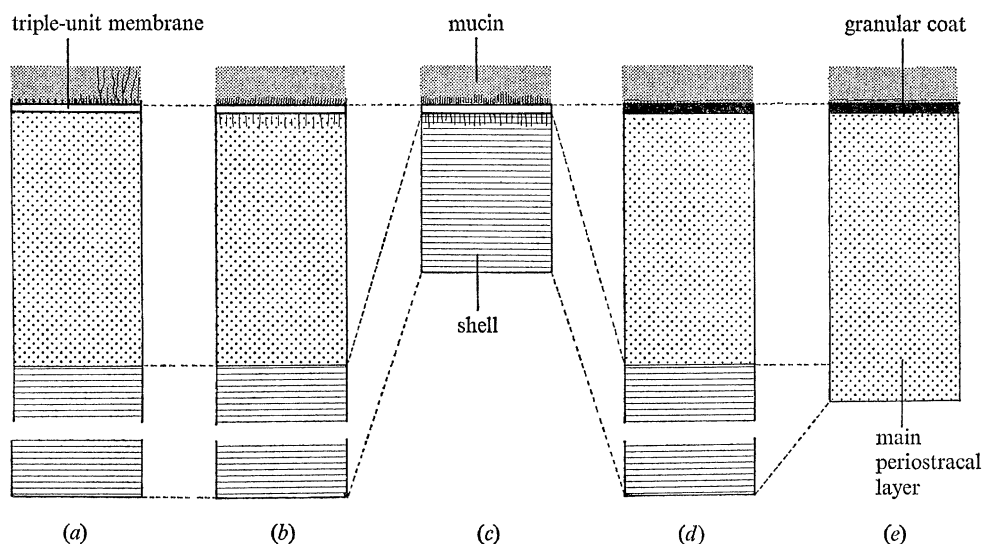


FIGURE 25. Diagram showing a correlation of periostracum and carbonate shell in *Membranipora* (a), *Berenicea* (b), *Lichenopora* (c), *Crisidia* (d) and *Bowerbankia* (e).

In contrast, the outer periostracal coat of *Bowerbankia* and *Crisidia*, which may be as thick as a fully developed cheilostome membrane, consists of a homogeneous medium electron-dense layer with a granular texture and a slightly fretted external surface; filaments are rare. Even the main periostracal layers of both species are alike in the small extent to which electron-dense particles are alined in trails within a mucoprotein groundmass.

There are, therefore, some ctenostomes and cyclostomes with a different periostracum from that characteristic of cheilostomes. There are, also, at least two cyclostomes with periostraca containing triple-unit membranes. In *Berenicea patina* (Lamarck) and *Lichenopora radiata* (Audouin), a triple-unit membrane, up to 10 nm thick, is consistently developed in two otherwise variable periostraca. In *Berenicea*, the external surface of the membrane usually bears filaments in dense coats about 12 nm thick (figure 21, plate 10), or in more dispersed arrays when they may be up to 45 nm long. The rest of the periostracum can also vary from a dense filamentous mat about 20 nm thick overlying papillose outgrowths of the mantle, to a layer up to ten times as thick. This contains electron-dense particles, either closely clustered to give a granular appearance or roughly alined parallel to the exterior, in an electron-light matrix. In *Lichenopora*, the succession is like that overlying the papillae of *Berenicea*, because both the internal and external surfaces of the triple-unit membrane support a simple coat of closely distributed filaments up to 50 nm long (figure 22, plate 10).

In terms of periostracal ultrastructure, then, the Cyclostomata appears to be a composite Order. The periostracal succession of *Crisidia* (and possibly related Articulata) is close to that of the Ctenostomata if *Bowerbankia* is typical of that Order. *Berenicea* and *Lichenopora* (and possibly other Tubuloporina and Rectangulata) possess periostraca similar to those of the Cheilostomata, if differences in the main periostracal layer are attributable solely to variation in the rate of its secretion. Which is the dominant type of periostracum within the Cyclostomata and whether the development of different types has any evolutionary significance, remain to be seen.

#### ORIGIN AND STRUCTURE OF MINERAL EXOSKELETON

The epithelium secreting the mineral constituents of the zooecium originates from a ring of generative cells immediately proximal of the palisade cell cap. The new cells do not differ much from palisade cells except for their cuboidal shape. As they arise they are accommodated within the surface layer by movement of the generative zone and the palisade cell cap in a distal direction. This distal movement is adjusted to the intussusceptive growth of the periostracum, the oldest part of which is constantly being left behind as a cover for the newly generated cells. Even in bryozoans with well-developed mineral skeletons, the new epithelium initially exudes periostracum, although this soon comes to an end with the secretion of an irregularly developed electron-dense sheet up to 10 nm thick (figures 19 and 21, plates 9 and 10). This is the seeding surface for the first crystallites of the mineral skeleton, which are usually deposited among sporadically distributed proteinous threads trailing up to 150 nm inwardly from the seeding surface.

By the time it is secreting carbonate, the epithelium differs from the columnar palisade cells in many ways. In *Celleporella hyalina* (Linn.), each epithelial cell is greatly stretched in a plane parallel to the inner shell surface so that it may be up to 25  $\mu\text{m}$  across and usually less than 1  $\mu\text{m}$  high except around the nucleus (figure 24, plate 10). The outer, secreting plasmalemma is free of microvilli, although it is usually thrown into folds with an amplitude of about 200 nm. Internally the chief difference is that the granular endoplasmic reticulum consists of widely scattered individual cisternae up to 2.5  $\mu\text{m}$  long within a groundmass containing densely distributed ribosomes. Lipids and lysosomes rarely occur, but small vesicles and membrane-bound secretion droplets of proteinous complexes about 150 nm in diameter, are frequently present just below the surface of the secreting plasmalemma.

The fabric of any bryozoan skeleton with a predominantly mineral composition may be greatly affected by changes in zooidal as well as colonial growth. The thickening shell may accommodate persistent papillae of outer epithelium in well-defined canals (puncta) or enclose cylinders of differently textured carbonate (pseudopuncta). The succession itself can vary from one species to another, reflecting differences in secretory regimes and changes in the growth habit of a colony. Thus in some species with identical modes of colonial growth, the carbonate phase of epithelial secretion can involve the deposition of up to three distinct mineral layers. Other variations are related to whether colonies are encrusting or erect when extra skeletal rigidity is acquired by the secretion of more carbonate, or whether the carbonate skeleton is secreted within folds of epithelium independently of the outer periostracum-epithelium cover. These complications prompt the use of a number of specific skeletal successions as standards for the correlation of the zoecial fabric of the currently recognized Orders, the Cheilostomata, Cyclostomata, Trepotomata, Cryptostomata and Cystoporata. In every Order, there

are species with specialized zooecia (heterozooecia). Such specialization, however, has not affected skeletal textures or successions which have always been found to be similar although not necessarily complete throughout the colony of every species examined. Consequently the successions given below may be regarded as typical of the colony even when they are described solely in terms of autozooecia.

(a) *Structure of cheilostome zooecium*

The completeness of the cheilostome zooecium and the full range of skeletal succession depend on the nature and origin of the mineral frontal wall. Five different kinds of walls are recognized, four being distinguishable by the arrangement of their carbonate successions in relation to those for the rest of the zooecia (figure 26).

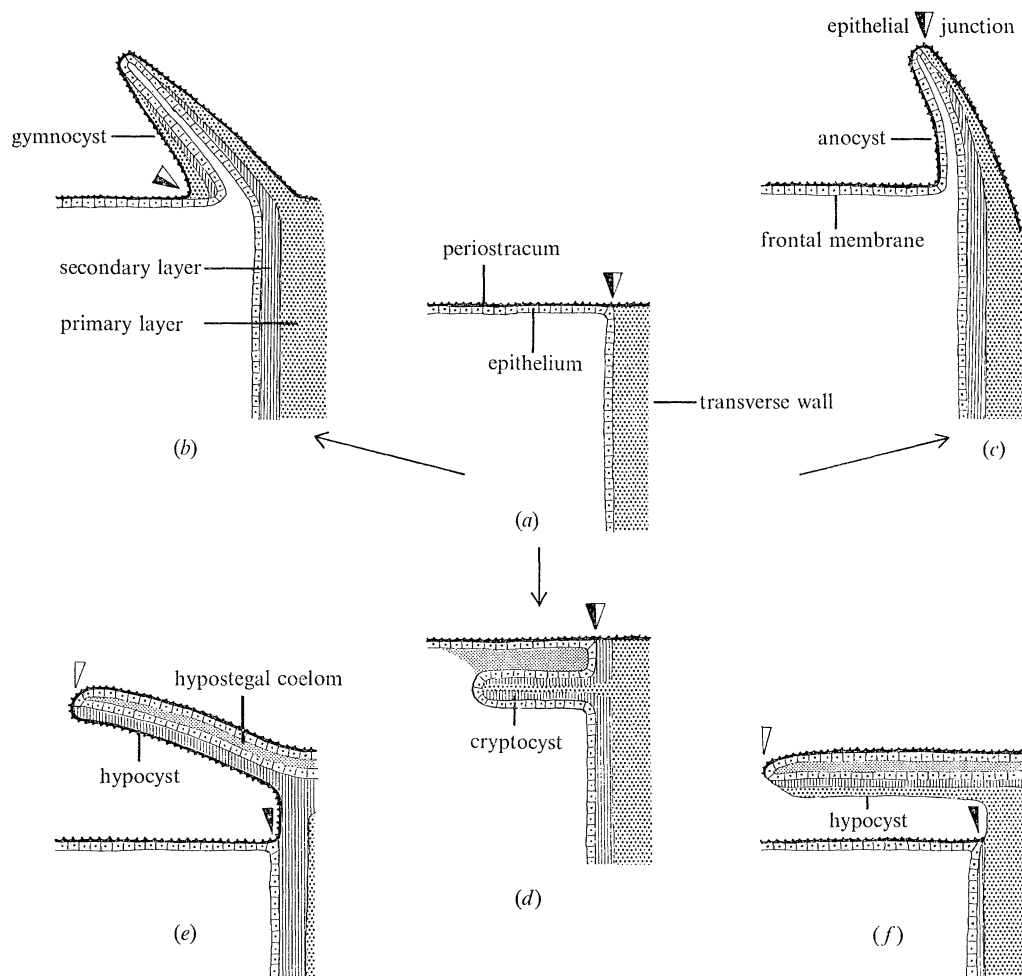


FIGURE 26. Diagram showing various types of frontal walls developed among *Membranipora* (a), *Membraniporella* (b), *Celleporella* (c), *Cellaria* (d), *Umbonula* (e) and *Schizoporella* (f).

In the anascan *Membranipora*, the frontal cover consists of periostracum and underlying epithelium (eustegal epithelium) only and can be contracted to cause protrusion of the lophophore. In most anascan and cribrimorph cheilostomes, however, this pliable frontal membrane is protected by extensions of the carbonate layers of the lateral and transverse walls. In some species, the mineral outgrowths are secreted on frontal periostracum with which they form

continuous skeletal successions. These outgrowths (gymnocysts) vary from discrete spines to solid plates lying external to the frontal membrane. In other species, carbonate ledges or platforms (cryptocysts) grow centripetally from the lateral and transverse walls internally to the frontal periostracum from which they are separated by a double layer of epithelium enclosing hypostegal coelom. Both structures are composed of one or more carbonate layers secreted symmetrically about the medial plane, but the external carbonate surface of the gymnocyst is the first-secreted mineral part of the structure, whereas that of the cryptocyst is the last-secreted part.

The Orders Gymnocystidea and Ascophora, which broadly correspond to the Ascophora imperfecta and Ascophora vera of Harmer (1957, p. 645), were erected on differences in the structure of the ascus and its skeletal cover (Ryland 1970, p. 40). The distinction depends on whether the frontal skeletal wall grows out over the periostracum forming the ascus, or whether the periostracum migrates proximally beneath a completed frontal wall to define an ascus (Tavener-Smith & Williams 1970, p. 253). Both structures are fundamentally alike because each is secreted by an epithelial sheet which lines only the frontal surface of the wall and is separated from an outer layer of eustegal epithelium by hypostegal coelom. Consequently, the carbonate successions are not symmetrically disposed about the medial planes of either frontal wall and, since the first-secreted mineral parts line the inner surface, the structure may be referred to as a hypocyst.

Both Harmer and Silén believed that the ascus is formed from a fold of eustegal epithelium which lies dorsal of another fold around an inner envelope of hypostegal epithelium enclosing the frontal wall. Silén (1944, pp. 41 *et seq.*) compared this feature with a gymnocyst but, in respect of its growth, it is a cryptocyst. In any event, neither structure has yet been identified with an ascus. The nearest approach to an ascophoran gymnocyst is the frontal wall of *Celleporella*, which is secreted by epithelium lining only its dorsal surface. Hence the carbonate succession is not symmetrically disposed about the medial plane of the frontal wall and, since the first-secreted crystallites constitute the frontal carbonate surface immediately underlying the periostracum, the structure may be described as an anocyst.

The phylogenetic implications of these differences in the growth of carbonate frontal walls are unknown but, in terms of zooecial secretion, the cheilostomes fall into two main groups; the Anasca and Cribrimorpha with the frontal wall secreted symmetrically about a medial plane either outside or inside a fold of epithelium; and the Gymnocystidea and Ascophora with the frontal wall secreted on the frontal or basal side only. Such a grouping is used in the following account.

(1) *Anascan zooecium*

The calcareous framework of the anascans, *Membranipora* and *Electra*, consists solely of transverse and lateral walls and a variably developed gymnocyst (figure 27, plate 11), and is an impunctate primary shell with a variable texture. In *Membranipora*, the periostracum forming the medial seeding sheet for adjacent lateral and transverse walls (figure 28, plate 11) is up to 10 µm thick and consists exclusively of the inner part of the main layer. Calcite crystallites seeded on the inner surface of the periostracum grow out at right angles to form closely packed arrays of acicular crystallites (figure 28), about 200 nm thick and up to 1 µm long, with rare traces of organic cement. These arrays usually form ill-defined successions passing into impersistent lenses, between 400 and 800 nm thick, with crystallites lying vertical to the long axes of the

lenses. Some idea of how these lenses accumulate is given by the microtopography of the inner surface of carbonate secretion at the moment of death. Here, superimposed on a finely granular or lineated texture (figure 29, plate 11) are impersistent overlapping scarp-like fronts of calcite (figure 30, plate 11). In front of each scarp and at the same level occur groups of crystallites up to 1  $\mu\text{m}$  across, which reduce outwards to isolated crystallites no more than 150 nm across (figure 31, plate 11). Such a scarp is the continuous edge of a spirally growing lens with the scattered crystallites in front representing newly secreted nuclei which, by peripheral accretion, gradually amalgamate with one another and the scarp thereby promoting lateral expansion of the lens. In this way, several lenses at different levels in a spiral arrangement may be secreted simultaneously by epithelium. Low ridges of calcite about 40 nm thick also occur as crenulated boundaries of enclosures up to 20  $\mu\text{m}$  across (figure 30). These might represent cell outlines recorded by excessive secretion along intercellular boundaries.

Although lenticular stacks of crystallites occur within the *Membranipora* skeleton, they are not separated from one another by protein sheets (figure 23, plate 10) and are too scattered to form a distinct layer. Consequently the entire calcareous zooecial succession, which may be up to 30  $\mu\text{m}$  thick may be designated primary shell.

The structure of the *Electra* wall does not differ significantly from that of *Membranipora* (figure 32, plate 11). Vertical crystallites, up to 500 nm thick and 4  $\mu\text{m}$  long, make up much of the fabric. They impart a granular texture to zooecial surfaces (figure 33, plate 11) including the floors of regularly spaced shallow craters indenting the lateral walls (figure 34, plate 11). On intercrater surfaces, the granules may be strongly lineated more or less parallel to the crater edges (figure 36, plate 12). Rhomb seeds, about 200 nm across, are occasionally identifiable on the surfaces as are traces of overlapping aggregates of crystallites representing spirally growing lenses. Even the external surfaces of both the gymnocyst and spines, which must be composed of the first crystallites seeded on the periostracum, may show spirally disposed crystallites. The structure of a hollow spine, with its entire periostracal coat lined by primary calcite indicates how similar its growth must be to that of the gymnocyst. Growth must first involve the formation of a tube by intussusceptive expansion of periostracum and proliferation of lining epithelium. Thereafter, secretion of primary shell takes place between the periostracum and the retreating epithelium which occupies an increasingly restricted core.

The pseudostegoidean anascan *Cellaria fistulosa* (Linn.) differs from *Membranipora* in habit and structure. The erect colony is composed of cylindrical branches, each articulated with its

#### DESCRIPTION OF PLATE 12

FIGURE 36. Scanning electron micrograph of the internal surface of a lateral wall of *Electra pilosa* ( $\times 2700$ ).

Scanning electron micrographs of the zooecia of *Cellaria fistulosa* (Linnaeus), Portaferry, Co. Down, N. Ireland:

FIGURE 37. Transverse section showing the structure of the cryptocyst and zooecial walls; frontal surface of zooecium to the right ( $\times 625$ ).

FIGURE 38. Transverse section showing detail of cryptocyst structure ( $\times 2500$ ).

FIGURE 39. View of fracture surfaces of the walls and the internal surface of a zooecial chamber ( $\times 2700$ ).

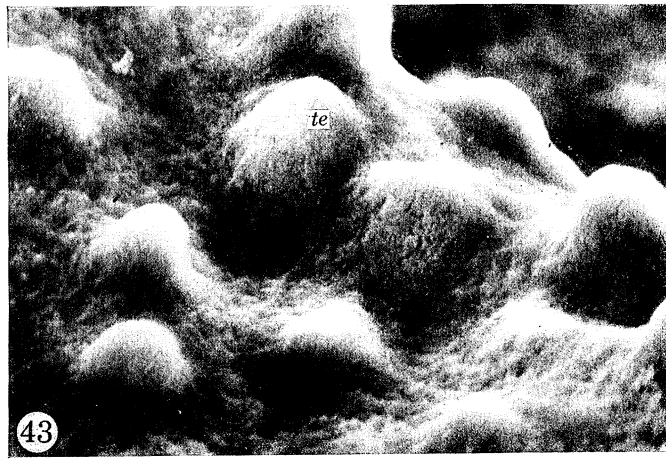
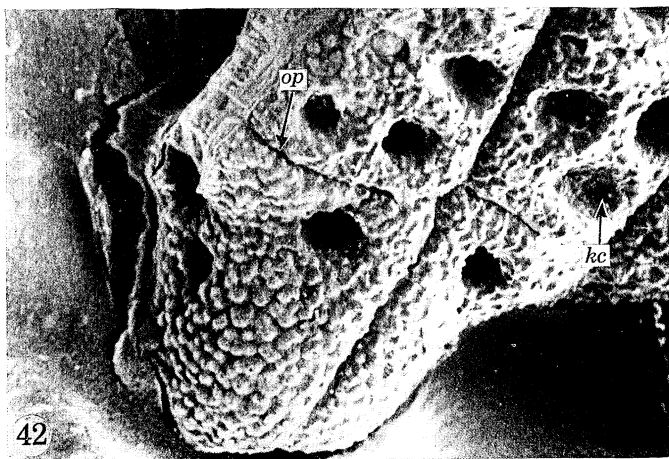
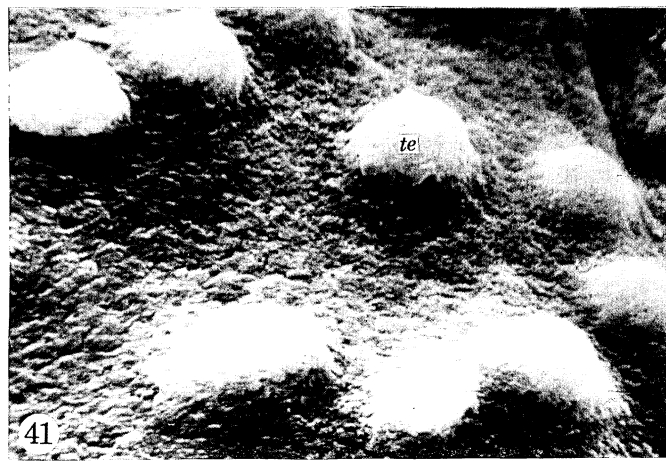
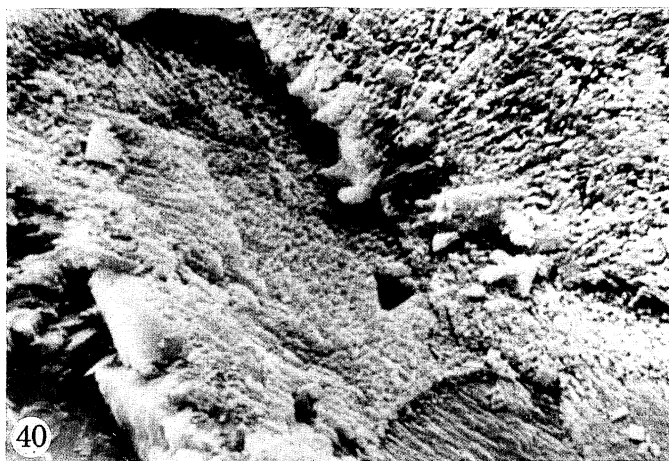
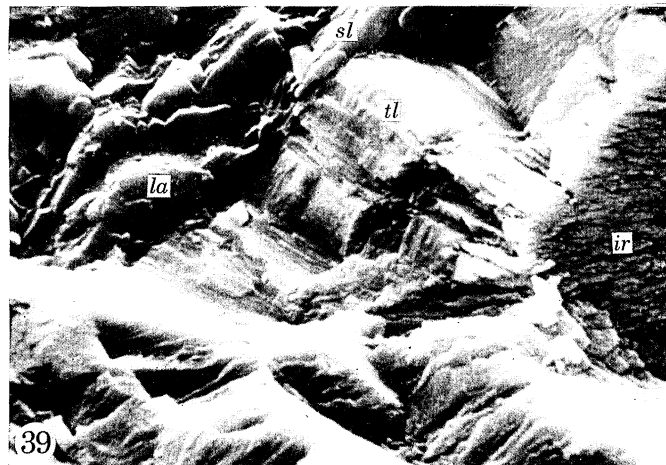
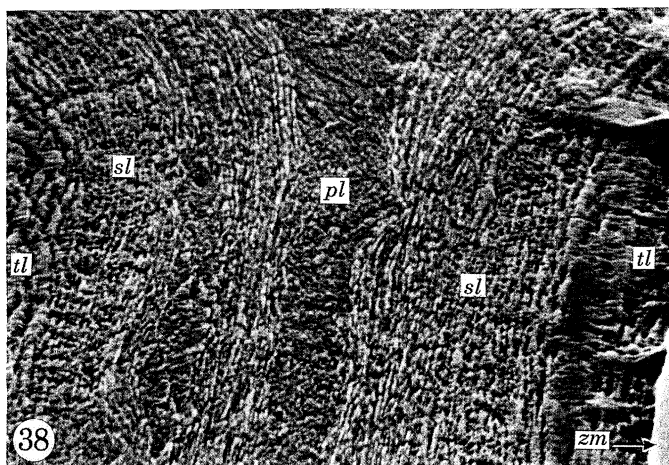
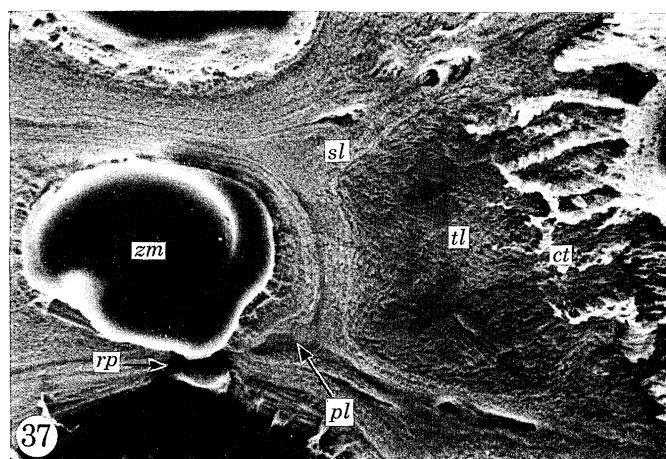
FIGURE 40. Internal surface of a zooecial chamber showing the stacking of acicular crystallites ( $\times 2700$ ).

FIGURE 41. External surface of cryptocyst with tubercles ( $\times 2800$ ).

Scanning electron micrographs of the zooecia of *Cupuladria biporosa* Cann and Bassler, Pointe-Noire, Ghana:

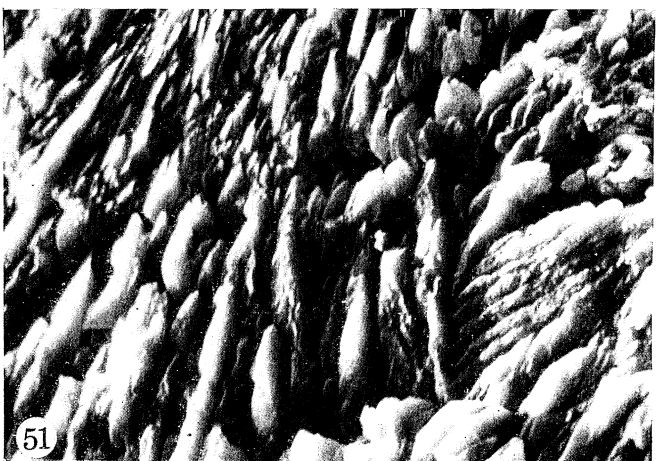
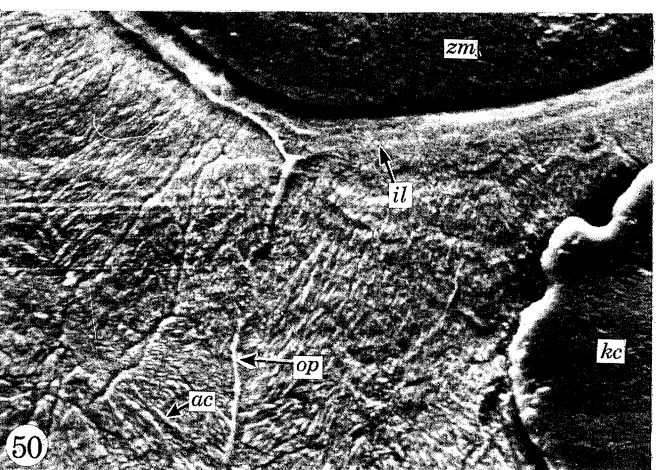
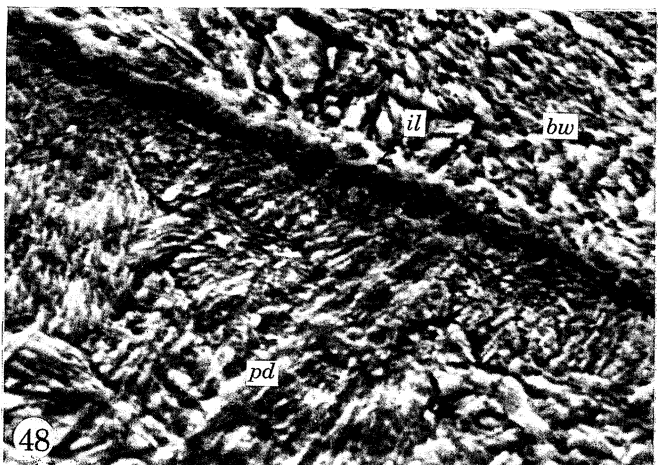
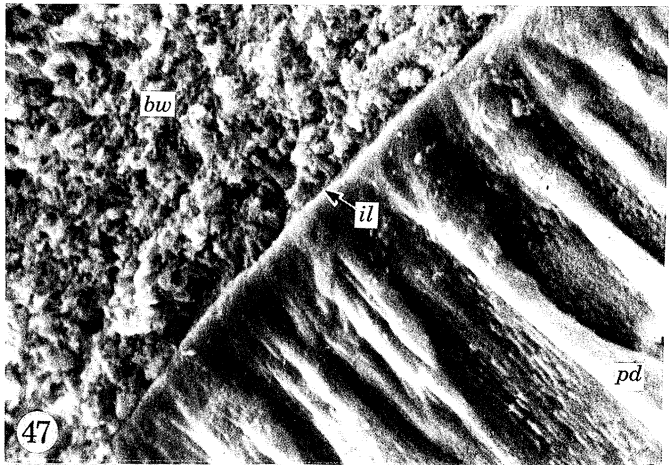
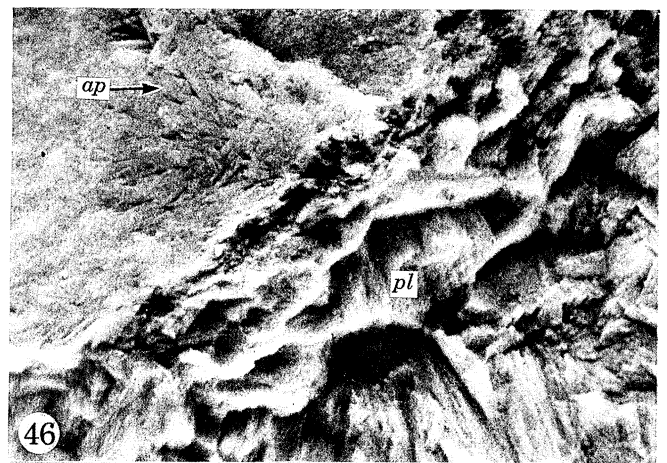
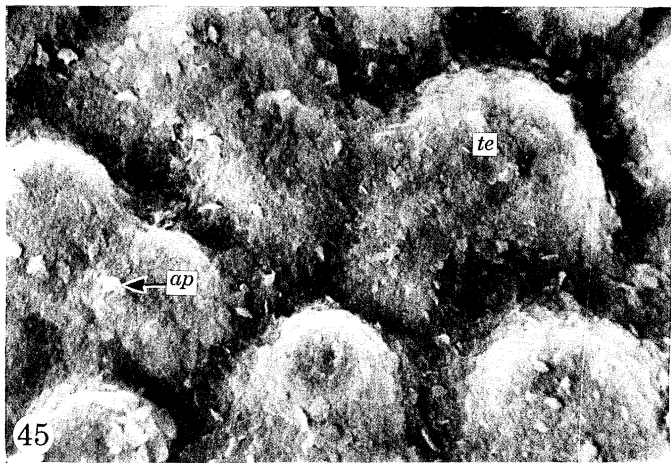
FIGURE 42. View of the basal surface showing organic partitions and kenozooid chambers ( $\times 135$ ).

FIGURE 43. Detail of basal surface showing the tubercles and granular surface ( $\times 2600$ ).



FIGURES 36 TO 43. For legends see facing page.





FIGURES 45 TO 52. For legends see facing page.

neighbour by a narrow constriction in which a flexible periostracum is the only part of the exoskeleton secreted. The zooecial fronts forming the surface of a branch are regularly arranged in alternating rows describing a low spiral about the long axis of a branch. Consequently, although five zooecia can be counted in one turn, a cross-section will show relatively large distal sections of five zooecia alternating with smaller proximal sections of the five zooecia making up the adjacent distal row, all facing outwards from a central axis of solid shell (figure 35).

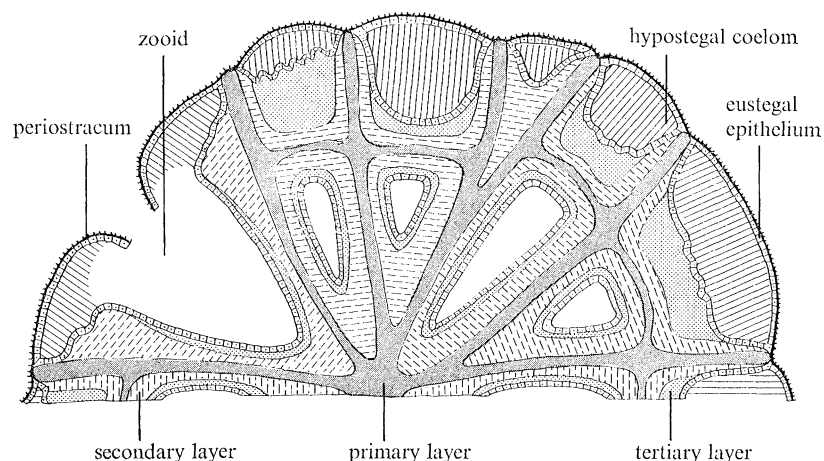


FIGURE 35. Diagram showing the arrangement of secretory epithelium in relation to the skeleton of *Cellaria* as seen in transverse section.

The arrangement of the skeletal succession in the zooecium of *Cellaria* is further complicated by the growth of a cryptocyst. A fully developed periostracum can only exist as an external cover for the colony as a whole, and is, therefore, restricted to the frontal surface of a zooecium. Elsewhere any organic sheet, separating the lateral walls of adjacent zooecia (the intercalary cuticle of Harmer) and acting as a seeding sheet at the core of a branch for a much reduced basal wall, must be a very thin extension of the inner surface of the periostracum because it is rarely identifiable. The primary layer (figures 37 and 38, plate 12) is also not always continuously developed although it is normally present as a string of irregular nodules, up to 3  $\mu\text{m}$  in thickness, consisting of acicular crystallites as small as 150 nm in diameter disposed vertically to the surface of secretion.

#### DESCRIPTION OF PLATE 13

Scanning electron micrographs of the zooecia of *Cupuladria biporosa*:

FIGURE 45. External surface of the frontal part of a zooecial wall showing tubercles and aragonite prisms ( $\times 1400$ ).

FIGURE 46. View of a fracture surface of the basal wall and the internal surface of a zooecial chamber ( $\times 1400$ ).

FIGURES 47, 48. Fracture surface and differentially etched section of the junction between the basal zooecial wall and the pad (47,  $\times 1300$ ; 48,  $\times 2500$ ).

FIGURE 49. Section of the basal part of the pad showing an organic partition extending through primary shell of acicular crystallites; basal surface to the left ( $\times 650$ ).

FIGURE 50. Section of the pad at its junction with the basal wall of a zooecium showing the connexion between an organic partition and the intrabasal sheet ( $\times 650$ ).

FIGURE 51. Scanning electron micrograph of the external basal surface of *Onychocella cyclostoma* Goldfuss from the Cretaceous (Upper Maastrichtian), Maastricht, The Netherlands ( $\times 2400$ ).

FIGURE 52. Scanning electron micrograph of the medial junction of the frontal spines of *Membraniporella nitida* (Johnston), Killyleagh, Co. Down, N. Ireland ( $\times 600$ ).

The succeeding secondary layer, which is usually about 15  $\mu\text{m}$  thick, is immediately recognizable as the finely banded member of the succession (figure 38). It consists of impermanent lenses and parallel-sided laminae, 200 nm thick on average and up to 13  $\mu\text{m}$  long, disposed parallel with the inner zooecial surfaces. Their truncated or tapering lateral ends, their clustering into small groups transgressing one another and their sharply defined boundaries, indicate that the laminae grow spirally and that they are probably separated from one another by interconnected protein sheets. Oblique fracture surfaces confirm that the laminae are composed of vertically stacked crystallites.

The zooecia of *Cellaria* are lined by a tertiary layer, up to 10  $\mu\text{m}$  thick, composed of faintly banded calcite with well-defined cleavages running continuously for more than 5  $\mu\text{m}$  throughout parts of the succession (figures 38 and 39, plate 12). The layer is built up of platelets and flat-lying acicular crystallites up to 1.5  $\mu\text{m}$  in length, which may appear on the inner surface as lineations disposed parallel to rhombic cleavages (figure 40, plate 12).

Complications in the bryozoan skeletal succession arising from the presence of a cryptocyst are illustrated by its growth in *Cellaria*. The inner periostracal extension and the primary and secondary layers of adjacent walls extend to the external cover of fully developed periostracum and eustegal epithelium. In early stages of zooecial growth, folds of epithelium must develop about 15  $\mu\text{m}$  below the frontal edges of the zooecial walls and, as they expand medially, secrete a shelf-like extension of the zooecial walls (compare figure 26). A section through this cryptocyst from basal to frontal surface (figures 35; and 37, plate 12) showed the following succession: a banded and cleaved layer (10  $\mu\text{m}$  thick), a laminar layer (5  $\mu\text{m}$ ), a coarsely granular layer (13  $\mu\text{m}$ ), a less well-defined laminar layer (3  $\mu\text{m}$ ) and another coarsely granular layer with sporadically strong cleavage (20  $\mu\text{m}$ ). Correlation suggests that the second, third and fourth layers represent primary granular shell flanked by secondary laminar shell which is consistent with secretion within a fold of epithelium. The fifth, outer granular layer, which has an external surface bearing tubercles about 4.5  $\mu\text{m}$  across (figure 41, plate 12), is deposited by the outer part of the epithelial fold which, in turn, is separated from periostracum and eustegal epithelium by hypostegal coelom. Evidently this granular layer is a correlative of the tertiary layer lining the lateral and basal zooecial walls.

*Cupuladria* is one of the most elaborate anascan cheilostomes, although the zooecial succession is comparatively simple. Living specimens of *C. biporosa* Canu and Bassler used in this study were dredged and fixed by Mr W. Pople and we are deeply appreciative of the trouble he took to provide suitable material. Unfortunately, the fixed specimens did not travel well, but they did show that the structure of the periostracum was like that of *Electra* and that the organic sheets dividing the colony radially, concentrically and equatorially were extensions of only the inner part of the periostracum.

The discoidal colonial skeleton of *Cupuladria* is composed of zooecia (with distal vibracula), arranged radially and alternately in linear and adjacent sets respectively, underlain by a calcareous pad (figures 42 and 43, plate 12). The pad is not a simple thickening of the zooecial basal wall (figure 44), from which it is separated by a proteinous sheet, the intrabasal sheet, up to 400 nm thick (figures 48 and 50, plate 13). The pad is divided into blocks about 200  $\mu\text{m}$  square by radially and transversely disposed organic partitions connecting with one another and with the intrabasal sheet (figures 49 and 50, plate 13). These organic partitions are also extensions of the inner part of the periostracum and are about as thick as the intrabasal sheet. Ellipsoidal kenozooid chambers occur within a block (figure 42, plate 12) each about 120  $\mu\text{m}$

wide and lined with a proteinous membrane about 35 nm thick. They contain traces of cells and membrane-bound, electron-dense proteinous droplets up to 4  $\mu\text{m}$  across. Three or four chambers in various stages of completion are normally seen on the basal surface of a block; and each is usually the basal member of a group of 3 or 4 closely stacked, earlier-defined ones forming a beaded column within the pad. Chambers within a column communicate with one another and through the basal wall of the overlying zooecium by a canal piercing the relatively thin, interchamber partitions. Each block underlies approximately one-quarter of each of two diagonally adjacent zooecia so that the radial partitions more or less coincide with the zooecial plane of bilateral symmetry.

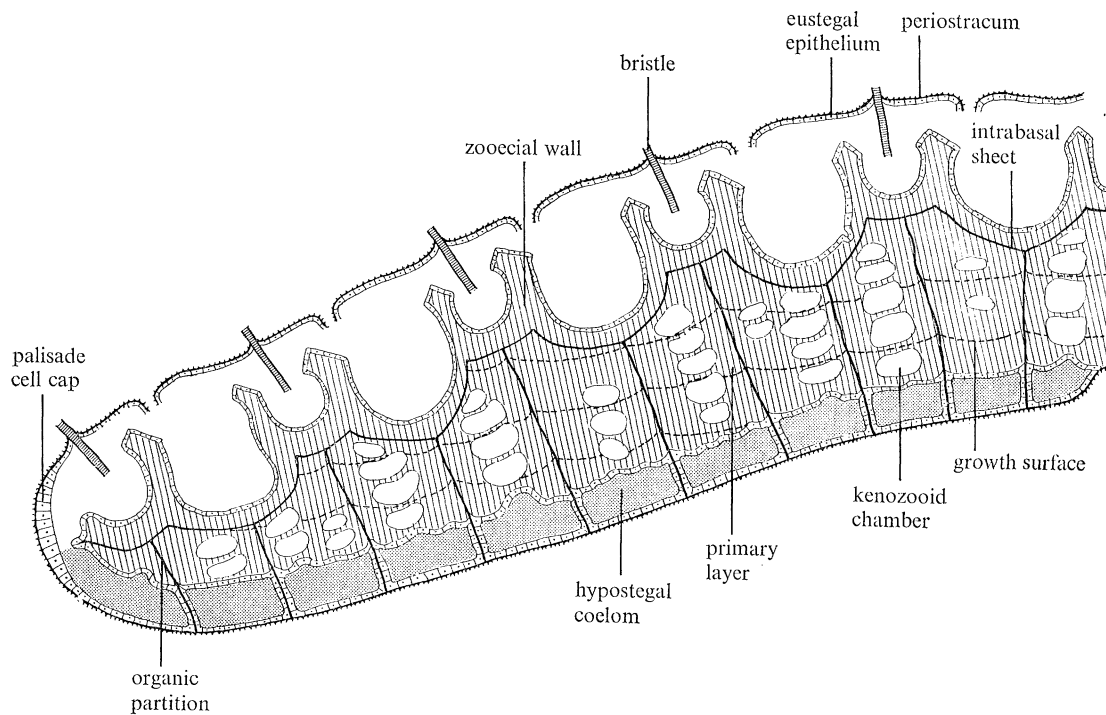


FIGURE 44. Diagram showing the arrangement of secretory epithelium in relation to the skeleton of *Cupuladria* as seen in sagittal section; organic contents of kenozooid chambers omitted for clarity.

Despite its division into discrete units by organic sheets, the carbonate skeleton is simple. It is composed exclusively of aragonite secreted mainly as acicular crystallites, between 200 and 300 nm thick and up to 15  $\mu\text{m}$  long, arranged in arrays parallel with the rhombic {110} and pinacoid {010} faces (figures 46 and 47, plate 13). The crystallites of the zooecial walls and pad are disposed steeply or vertically to all organic sheets and growth surfaces (figure 49, plate 13). Many of the latter are indicated within the skeleton by impersistent proteinous sheets, up to 50 nm thick, representing temporary changes from carbonate to organic secretion. Consequently they appear in sections as variably spaced isochronous lines, up to 20  $\mu\text{m}$  apart. More persistent anastomosing proteinous sheets usually appear within a micrometre or so of the skeletal surfaces bounding zooids and defining kenozooid chambers. Among these sheets, aragonite can occur as flat-lying orthorhombic prisms which are also well seen in the tubercular frontal parts of the zooecial walls (figure 45, plate 13) where they may even be arranged in spiral growth scarps. Such constituents may mark the beginnings of the secondary layer.

The structure and attitude of the organic partitions pervading *Cupuladria* are the best clues

to its skeletal growth. A complete periostracal succession is found only as an external wrapping to the entire colony where it is underlain by eustegal epithelium and everywhere separated from the inner carbonate-secreting hypostegal epithelium by hypostegal coelom. The periostracum is exuded around the periphery of the colony by palisade cell caps (the common buds of Cook 1965, p. 156), one located at each of the distal apices of a zooidal ray. The vertical partition, longitudinally bisecting the sector of the pad beneath a zooecial ray, originates periodically as an extension of the inner part of the periostracum within the palisade cell cap which subsequently divides into two. The partition then develops like a new lateral wall in *Membranipora* and is lined on each side with epithelial cells which secrete aragonitic extensions of the pad near the partition. The intrabasal partition, which is continuous with the vertical partition, is secreted within a pair of epithelial folds expanding distally and laterally in the equatorial plane from the frontal edge of the vertical partition. Proliferating epithelium on the frontal and basal surfaces of the intrabasal partition secrete zooecial walls and pad respectively. The basal kenozooid chambers are defined by differential secretion of hypostegal epithelium lining the pad in the same way as tremopores penetrating the frontal wall of ascophoran cheilostomes, and have the same storage function.

Finally, a transverse partition can only be continuous with the basal periostracum, lateral wall, and the intrabasal and vertical partitions if it is secreted later than those boundaries but in advance of the distal end of the pad. It is therefore formed by secretion within expanding folds of epithelium, which meet medially. Completion of a transverse partition does not seal off a block of the pad because communication is maintained through the kenozooid chambers and secretion of aragonite takes place on the proximal surface of the newly formed transverse partitions.

Only one fossil anascan cheilostome, *Onychocella*, represented by two species, *O. stigmatophora* Goldfuss and *O. cyclostoma* Goldfuss, from the Cretaceous (Maastrichtian) of the Netherlands, was available for study. The species were simple encrusting forms with a uniform succession of variously inclined acicular crystallites (figure 51, plate 13), up to 15  $\mu\text{m}$  long and 1.25  $\mu\text{m}$  wide, even in frontal walls as much as 200  $\mu\text{m}$  thick. Such a succession, which was secreted on a periostracum between 2 and 3  $\mu\text{m}$  thick, must have been primary layer exclusively.

#### DESCRIPTION OF PLATE 14

Scanning electron micrographs of the zooecia of *Membraniporella nitida*:

FIGURE 53. External frontal surface of a spine showing the alinement of acicular crystallites ( $\times 2300$ ).

FIGURE 54. Internal surface of an ovicell showing laminae composed of rhombic crystallites ( $\times 2300$ ).

FIGURE 55. Section of an ovicell showing the skeletal succession ( $\times 2500$ ).

Scanning electron micrographs of the zooecia of cribrimorph cheilostomes from the Cretaceous (Upper Maastrichtian), Maastricht, The Netherlands:

FIGURE 56. Section of *Ubaghsia reticulata* (Ubaghs) showing the granular structure of the primary layer ( $\times 2500$ ).

FIGURE 57. Section of *Batrachopora ornata* (Goldfuss) showing the granular primary layer and lenticles lining a zooecial chamber ( $\times 2400$ ).

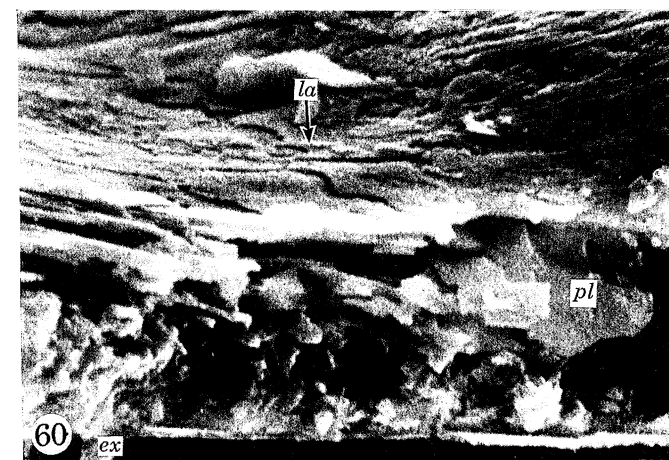
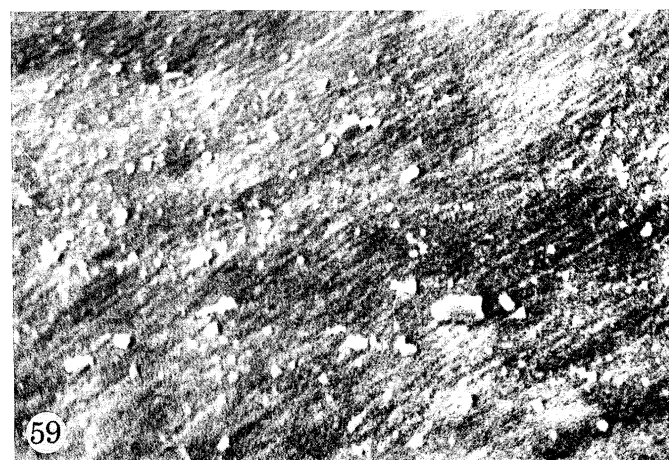
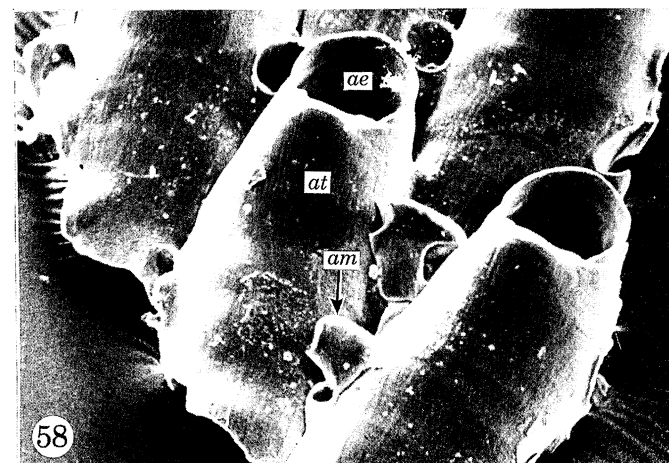
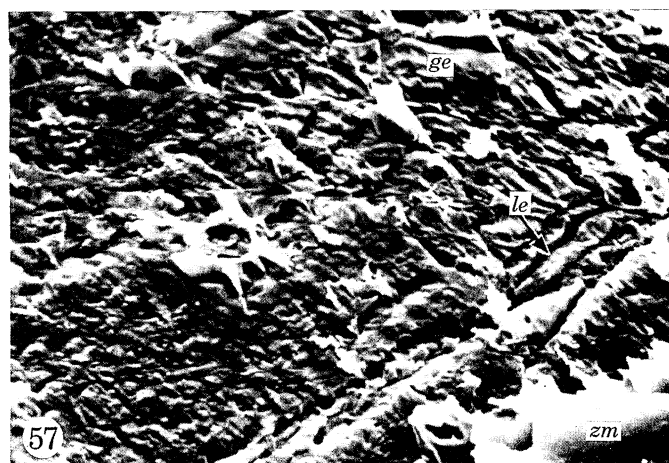
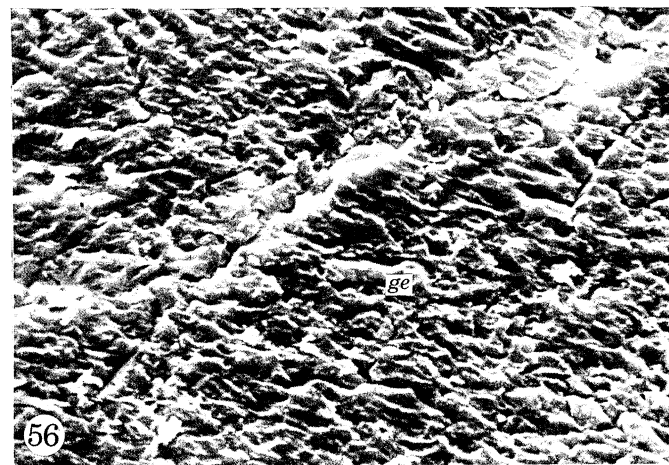
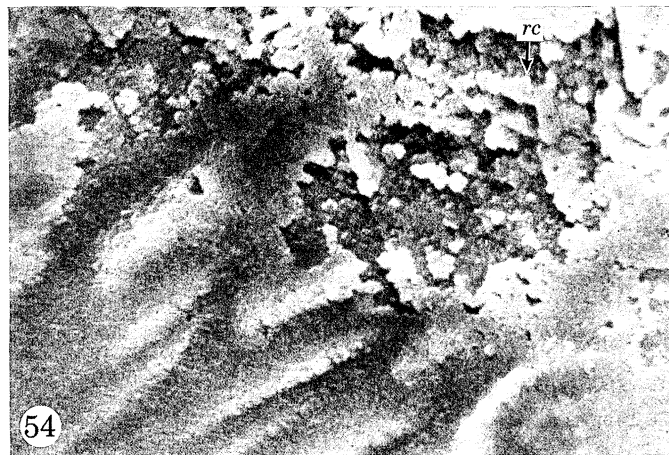
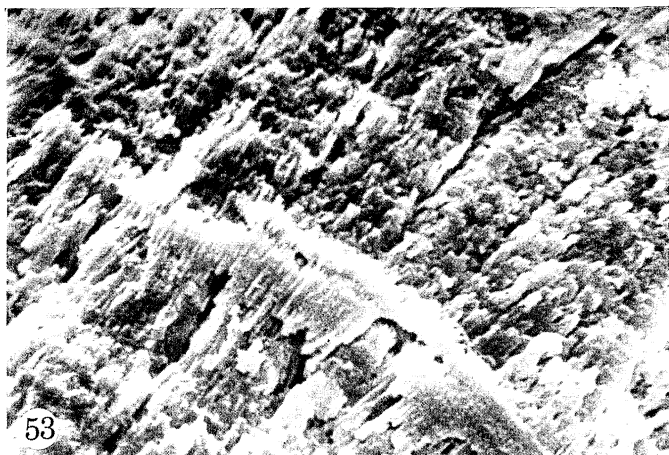
Scanning electron micrographs of the zooecia of *Celleporella hyalina*:

FIGURE 58. Frontal view of zooecia showing the position of the anocyst ( $\times 120$ ).

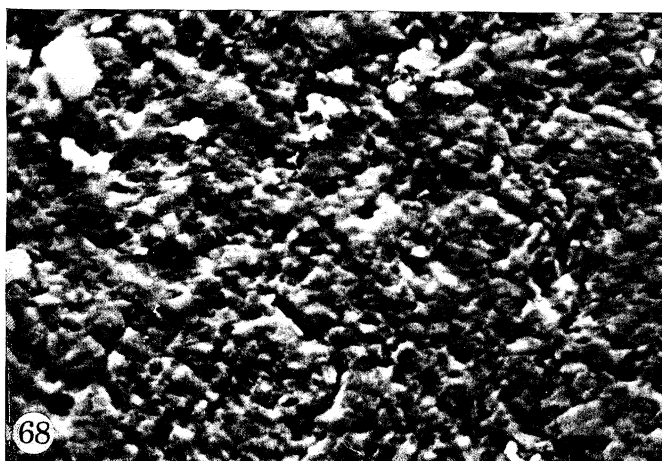
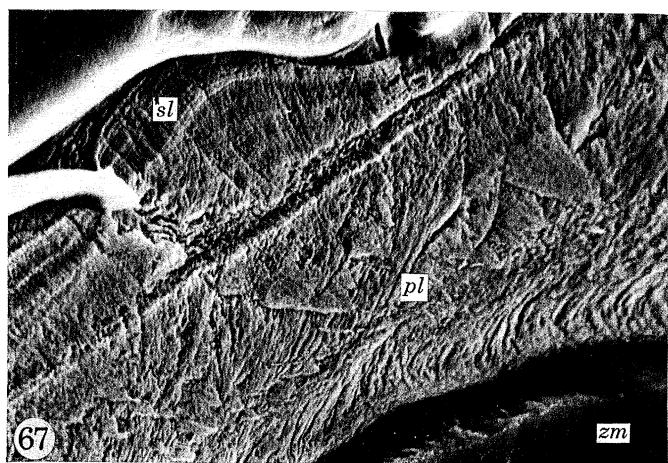
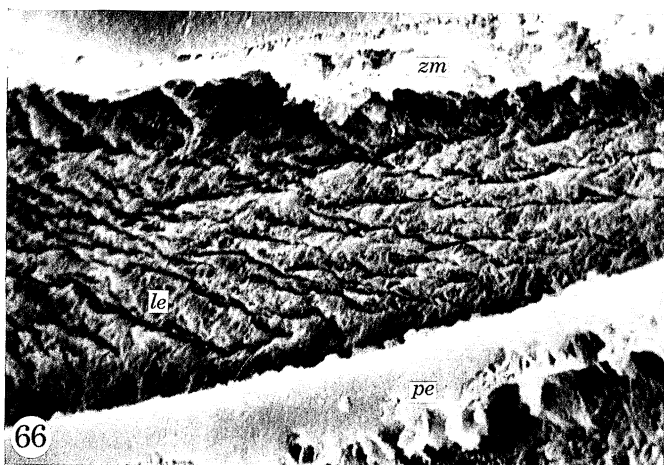
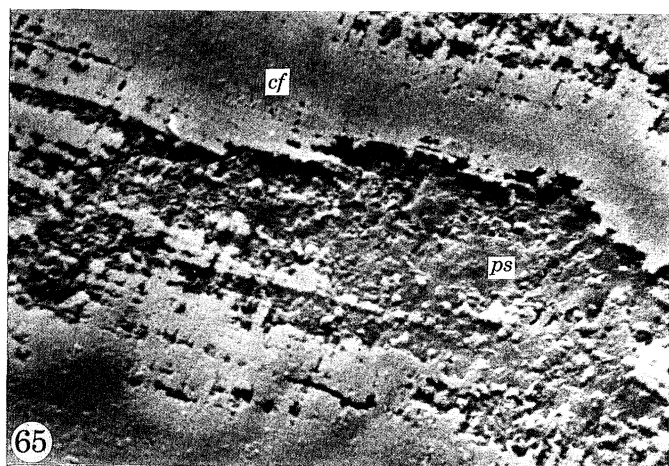
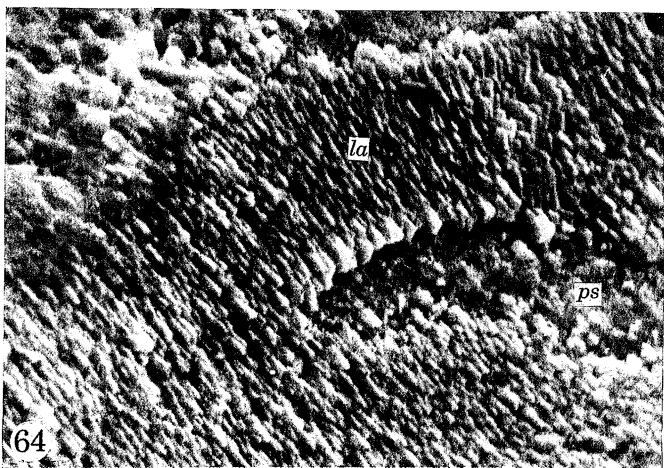
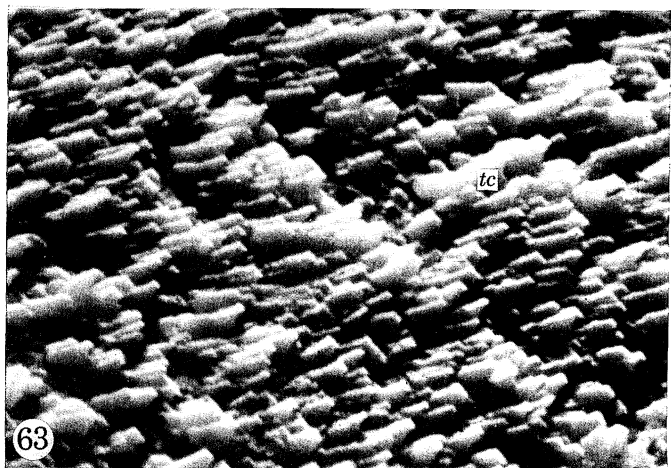
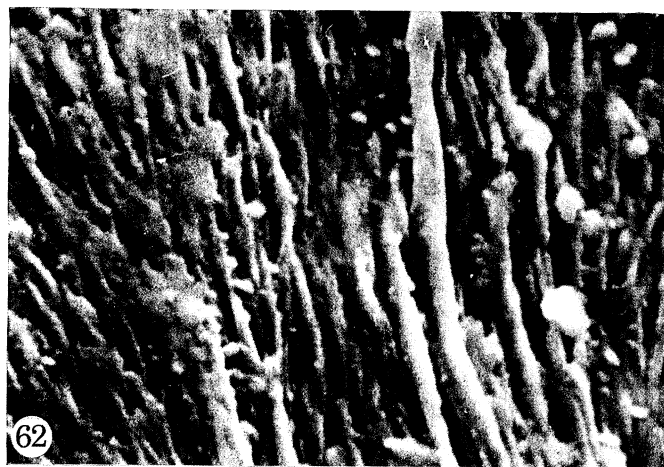
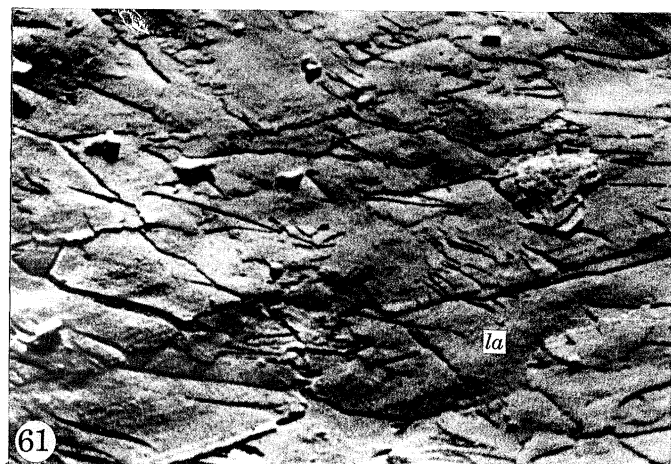
FIGURE 59. External surface of a zooecium showing lineations of the primary layer ( $\times 6000$ ).

FIGURE 60. View of the fracture surface of a wall and the internal surface of a zooecial chamber ( $\times 3200$ ).





FIGURES 53 TO 60. For legends see facing page.



FIGURES 61 TO 68. For legends see facing page.



(2) *Cribrimorphan zooecium*

There is some doubt about the systematic position of *Membraniporella* which is included among the Cribriliniidae (Bassler 1953, p. 186), but has recently been reassigned to the anascan Malacostegoidea by Ryland (1970, p. 159). However, the cage of medially fused spines (figure 52, plate 13) arching over the frontal periostracal membrane of *Membraniporella nitida* (Johnston) is homologous with the cribrimorph frontal shields and may be regarded as typical of living cribriliniids.

In dried specimens of *M. nitida*, the periostracum covers external surfaces, ensheathes spines and intervenes between their tips along their medial plane of contact. The outer, primary calcite layer is 7  $\mu\text{m}$  thick on average, and is mainly coarsely granular although crystallites, about 200 to 300 nm in size, frequently occur and may be epitaxially arranged to give a lineation on the external surfaces (figure 53, plate 14). The inner primary layer is about 5  $\mu\text{m}$  thick and consists of lenses with crenulated boundaries, up to 9  $\mu\text{m}$  long and 1.3  $\mu\text{m}$  wide (figure 55, plate 14). Although the lenses are crudely stratified parallel to the external surface they are sharply distinguishable from the regular laminae averaging 250 nm in thickness, which constitute the banded secondary layer (figure 55). The laminae are composed of rhombic crystallites (figure 54, plate 14) about 170 to 200 nm in size and grow spirally in the same way as those found in *Membranipora*. This succession is evident everywhere including the frontal spines where a granular primary layer surrounds a core of banded secondary shell. A cribrimorph (and anascan) spine is, therefore, strictly comparable in structure and growth with a gymnocyst.

The cribrimorphs are first recorded and most richly represented in the Cretaceous. Four Maastrichtian species have been examined and only *Decurtaria cornuta* Beissel was too badly recrystallized to provide evidence of shell fabric. In the other species, *Batrachopora ornata* (Goldfuss), *Leptocheilopora magna* Land and *Ubaghsia reticulata* (Ubaghs), haloes of recrystallization up to 10  $\mu\text{m}$  wide usually surround zooecial spaces, while the rest of the skeleton tends to be seamed with diagenetically induced pores and cracks which become enlarged and subsequently filled with resin during the preparation of sections. None the less, sufficient original fabric survives to indicate the nature of the skeletal succession. In *Leptocheilopora* and *Ubaghsia* (figure 56, plate 14), the texture is exclusively granular, commonly with irregular crystallites, about

## DESCRIPTION OF PLATE 15

Scanning electron micrographs of the zooecia of *Celleporella hyalina*:

FIGURE 61. Internal surface of the frontal wall showing overlapping laminae of the secondary shell ( $\times 2200$ ).

FIGURE 62. Part of a muscle scar on the internal surface of a lateral wall ( $\times 6200$ ).

Scanning electron micrographs of the zooecia of *Celleporella pumicosa* Hincks, Strangford, Co. Down, N. Ireland:

FIGURE 63. Undersurface of the base of a colony showing tabular crystallites ( $\times 6000$ ).

FIGURE 64. Internal surface of the basal wall of a zooecial chamber showing the crystallite structure of laminae ( $\times 2300$ ).

FIGURE 65. Internal surface of the basal wall of a zooecial chamber showing a protein sheet overlain by a film of calcite ( $\times 2600$ ).

FIGURE 66. Section of basal zooecial wall showing the disposition of primary lenticles ( $\times 2600$ ).

FIGURE 67. Section of the frontal wall showing the carbonate succession ( $\times 1300$ ).

FIGURE 68. Scanning electron micrograph of the frontal wall of *Acanthionella typica* Gabb and Horn from the Palaeocene (Vincentown Limesand), Vincentown, New Jersey ( $\times 2400$ ).

10  $\mu\text{m}$  long and 2  $\mu\text{m}$  wide, disposed normal to surfaces of deposition but also including more massive nodules. In *Batrachopora* (figure 57, plate 14), a similarly textured layer prevails but the zooecial spaces are lined with another layer up to 8  $\mu\text{m}$  thick, consisting of lenticles arranged parallel with the internal zooecial surfaces. This layer is at least transitional into a laminar secondary shell so that the granular skeletal succession in all fossil cribrimorphs studied may be described as wholly primary.

### (3) *Gymnocystidean and ascophoran zooecia*

A description has already been given of the skeletal successions of the two species, *Umbonula littoralis* Hastings and *Schizoporella unicornis* (Johnston), generally accepted as representative of the Gymnocystidea and Ascophora respectively (Tavener-Smith & Williams 1970) and characterized by the possession of a hypocyst. Both species have a threefold carbonate layering with similar primary and secondary successions, although a preliminary survey of living and fossil species suggests such variation in skeletal fabric to be atypical of the ascus-bearing Cheilostomata. The calcitic primary layer is granular and grades quickly into a well-banded secondary calcitic layer with laminae or coarser lenticles, up to 500 nm thick and 10  $\mu\text{m}$  in extent, separated from one another by anastomosing protein sheets about 5 nm thick. The bands are usually made up of acicular crystallites in epitaxial arrangement from one level to the next so that a strong cleavage lineation, more or less normal to the banding, is commonplace and may dominate massive calcitic lenticles up to 20  $\mu\text{m}$  thick that develop in the distal part of the *Umbonula* frontal wall. Surface views of the laminae show them in attitudes of spiral growth with overlapping scarps and, more rarely, with left- and right-handed screw dislocation edges. The tertiary layers are quite different from each other. In *Umbonula*, the tertiary layer consists of highly inclined acicular crystallites of calcite, about 250 nm thick, forming a thin continuous external layer of the frontal wall and impersistent patches elsewhere in the zooecium. In *Schizoporella*, it is limited to the frontal wall where it occurs as an external coat of acicular crystallites of aragonite, up to 2  $\mu\text{m}$  long and 500 nm thick, disposed epitaxially at variable angles to growth surfaces.

The frontal wall of *Schizoporella* is pierced by canals (tremopores) about 10  $\mu\text{m}$  in diameter. They are lined by a proteinous membrane which thickens into a wad about 250 nm thick plugging the dorsal entrance of the tremopore. The lining is secreted by papillose extensions of hypostegal epithelium covering the ventral surface of the frontal wall, which contain numerous secretion droplets. This kind of punctation, originating by differential secretion on the *outer* surface of the frontal wall, is fundamentally different from canals accommodating papillose extensions of the epithelium lining *inner* zooecial surfaces as in many cyclostomes. Identification of the different types in fossil species, however, is hazardous except when skeletal growth has been affected by changes in the rate of secretion. In section, such changes are usually expressed as growth 'lines', and these, because of lack of carbonate secretion within the canals, invariably form acute angles with the long axes of puncta pointing away from the bases of papillae.

Although *Celleporella hyalina* (Linn.) is equipped with an ascus, the frontal wall or anocyst is different from that of *Schizoporella* because it is secreted by a basal epithelial lining and is, consequently, an unmodified extension of the lateral and transverse walls (figures 26; and 58, plate 14). The primary layer which may be up to 6  $\mu\text{m}$  thick, consists of epitaxially arranged, highly inclined crystallites imparting a finely granular and linear aspect to the external surface (figure 59, plate 14) and a strong cleavage to fracture surfaces (figure 60, plate 14). Massive

lenticles, up to 8  $\mu\text{m}$  across, also occur sporadically. The secondary layer is banded with individual laminae, averaging 250 nm in thickness and enclosed in anastomosing sheets of protein about 5 nm thick. The laminae crop out on the internal surface of the frontal wall as a series of rhombic plates. They are commonly about 6  $\mu\text{m}$  across with concentric banding occasionally preserved on the faces at intervals of 300 nm, and overlap one another in attitudes of spiral growth (figure 61, plate 15). Decalcified sections of epithelium and protein sheets indicate that four or five plates, each with its protein cover, may be secreted simultaneously by a single cell (figure 24, plate 10). The interiors of *Celleporella* have also afforded rare examples of bryozoan muscle scar impressions (figure 62, plate 15). These are subparallel ridges, up to 1  $\mu\text{m}$  thick and 20  $\mu\text{m}$  long, superimposed on the secondary fabric which is not completely destroyed by the emplacement of muscle bases.

In contrast to the species described above, most ascophorans appear to have a restricted skeletal succession. In living *Cellepora pumicosa* Hincks zooecial walls may be as much as 35  $\mu\text{m}$  thick, yet only two fabrics are found. The basic units of the primary layer are tabular crystallites, up to 2  $\mu\text{m}$  across and between 170 and 200 nm thick, set epitaxially in highly inclined arrays on proteinous sheets (figures 63 and 64, plate 15). The free-growing ends of the tablets are closed by faces subtending rhombic or dihexagonal angles. Changes in stacking do occur in lenses up to 22  $\mu\text{m}$  across. These lenticular segregations can be delineated by proteinous sheets or thin deposits of calcite (figure 65, plate 15) and simulate banding in section (figure 66, plate 15). The banding, however, differs from that of the secondary shell of other ascophorans in its coarseness, irregularity and disposition being inclined at an angle to, and not parallel with, surfaces of deposition. These lenses of tabular crystallites, therefore, constitute a primary shell of different texture from those previously described. They are the chief constituent of the *Cellepora* zooecium, but a secondary shell up to 7  $\mu\text{m}$  thick and composed of laminae about 600 nm thick, is deposited as an external coat of the frontal wall by hypostegal epithelium (figure 67, plate 15).

The skeletal structure of fossil Celleporidae is not like that of living *Cellepora* Hincks. *Cellepora accumulata* (von Hagenow) from the Maastrichtian chalk drift near Hamburg showed no differentiation of fabric other than a coarsely granular aspect with crystallites normal to the surface of deposition. The entire carbonate succession is evidently primary, although whether the fabric is original remains to be seen. *Acanthionella typica* Gabb & Horn from the Palaeocene of New Jersey, has been assigned to the family (Bassler 1953, p. G 220) but without conclusive proof that the stock is a celleporid. It is noteworthy that although the frontal walls are granular (figure 68, plate 15), a distinct banding, about 600 nm thick has been identified in the carbonate layer on either side of a medial organic sheet about 2  $\mu\text{m}$  thick (figure 69, plate 16). The bands, however, are evenly developed parallel to the medial sheet and are much more likely secondary laminae than the primary lenticles of *C. pumicosa*. If this similarity is a key to correlation, the granular frontal wall represents a tertiary layer and the retention of *Acanthionella* within the Celleporidae becomes even more controversial.

The retoporids *Iodictyum* and *Sertella* are ascophorans with an erect fenestrate skeleton consisting of box-like zooecia in rows on one side only of a branch and a thick basal succession on the reverse side. The mineral skeleton of both genera is divided into compartments about 600 to 700  $\mu\text{m}$  across by interconnected extensions of the inner part of the periostracum up to 2  $\mu\text{m}$  thick (figure 77). A principal sheet intervenes between the basal zooecial walls and the basal layer of the colony. Extensions from it run medially through the lateral zooecial walls to the frontal surface and along extrapolated mid-lines of zooecia through the basal layer (figure

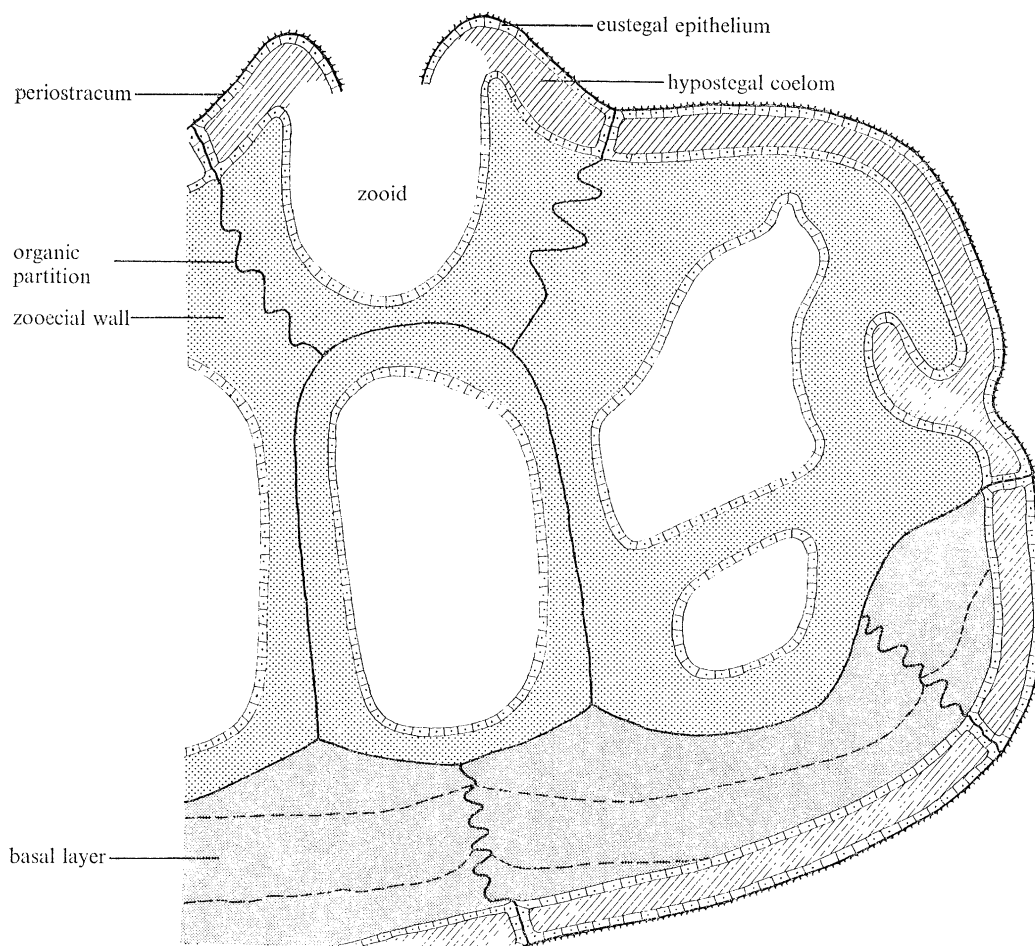


FIGURE 77. Diagram showing the arrangement of secretory epithelium in relation to the skeleton of *Iodictyum* as seen in transverse section.

#### DESCRIPTION OF PLATE 16

FIGURE 69. Scanning electron micrograph of a longitudinal section of the axial part of *Acanthionella typica* showing medial organic sheet separating banded carbonate successions ( $\times 2300$ ).

Scanning electron micrographs of the zooecia of *Iodictyum sanguineum* (Ortmann), Misaki, Japan:

FIGURE 70. View of the basal surface showing the occurrence of organic sheets ( $\times 125$ ).

FIGURE 71. Section of the basal layer showing the disposition of crystallites ( $\times 2200$ ).

FIGURE 72. Section of a basal zooecial wall separated from the basal layer by an organic partition ( $\times 1300$ ).

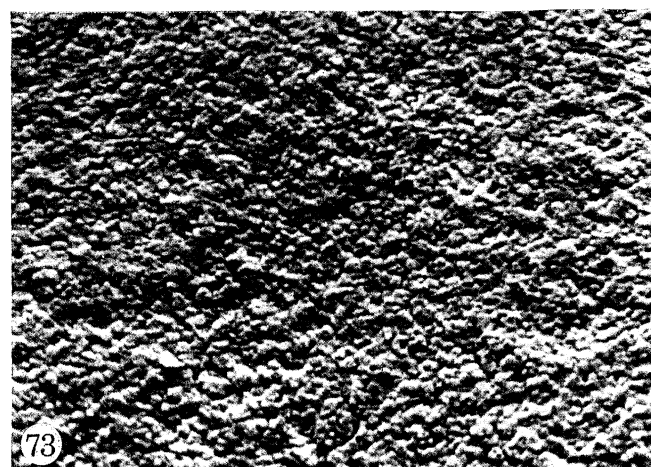
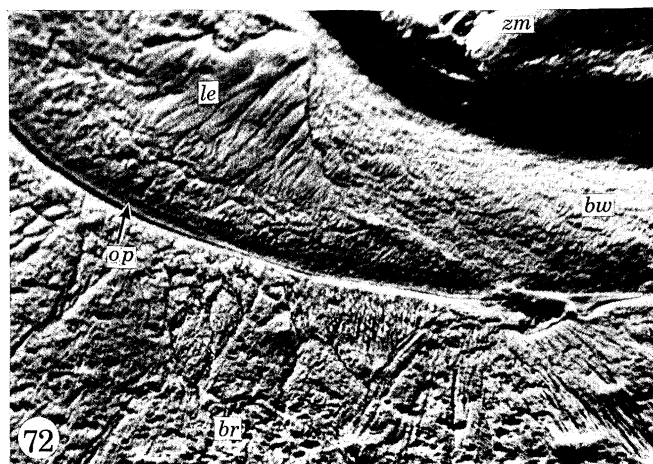
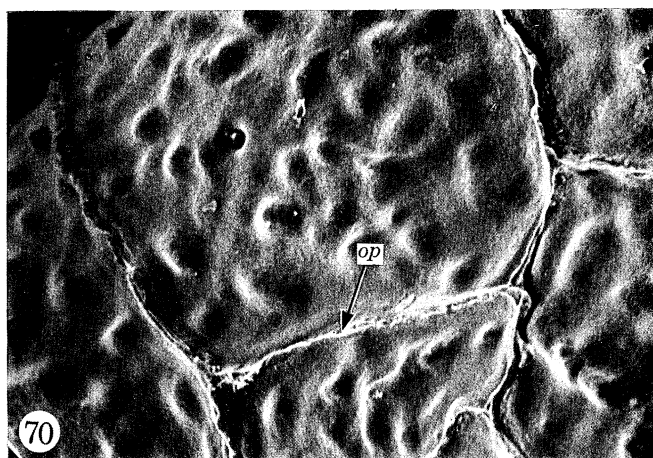
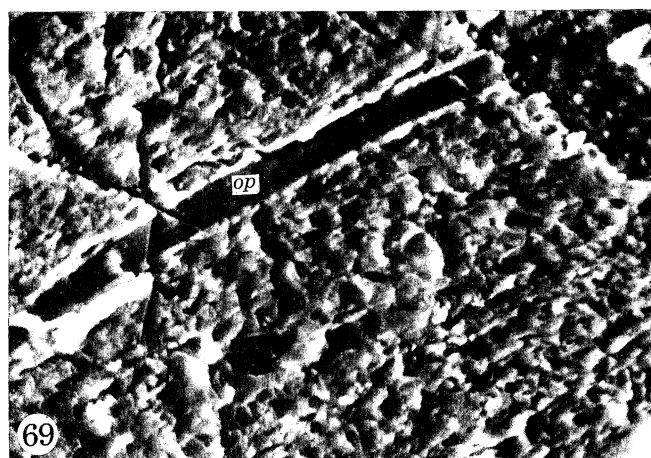
FIGURE 73. External surface of the frontal wall showing a finely granular texture ( $\times 2500$ ).

Scanning electron micrographs of the zooecia of *Sertella carinata* (MacGillivray), Murray Island, Australia:

FIGURE 74. External surface of the basal layer showing its tuberculate nature ( $\times 1300$ ).

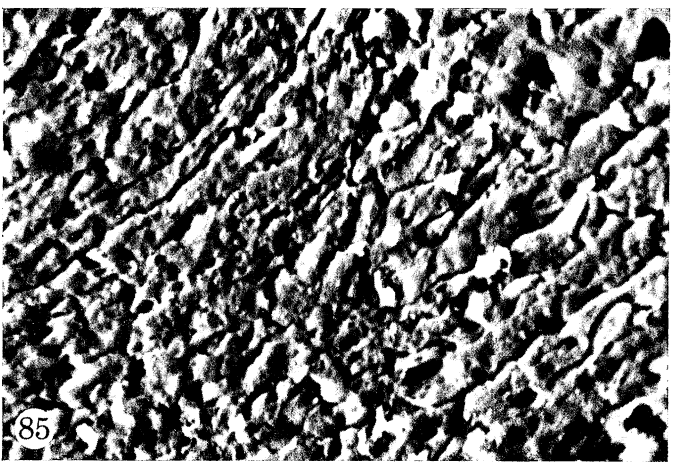
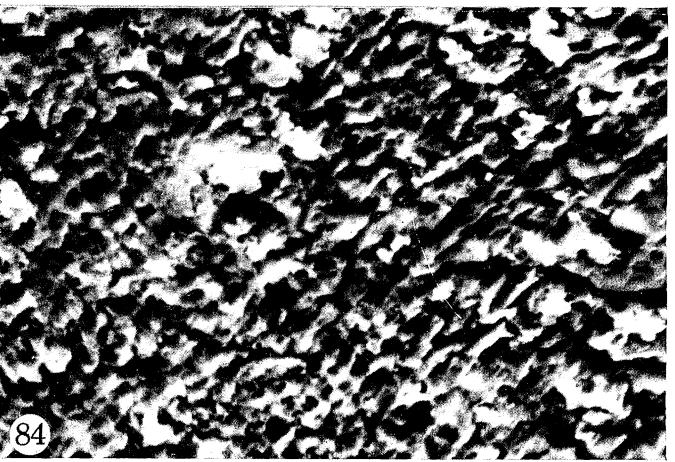
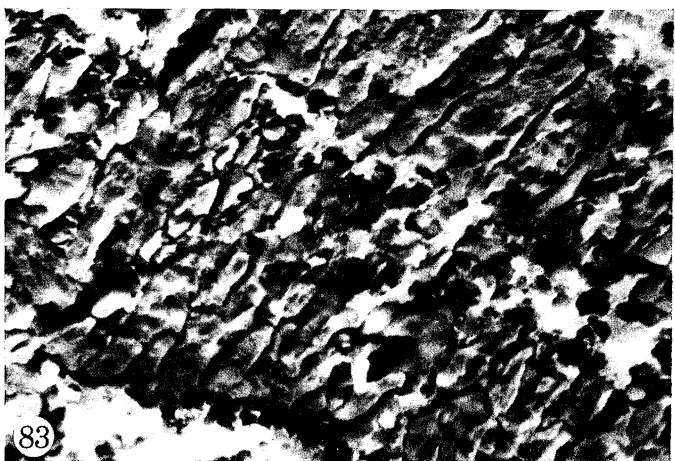
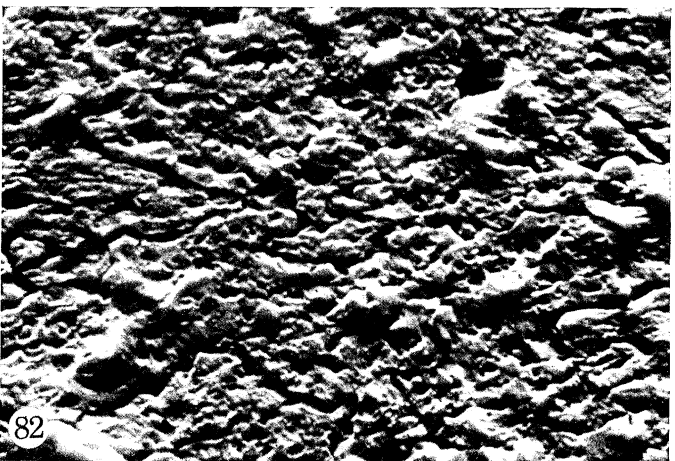
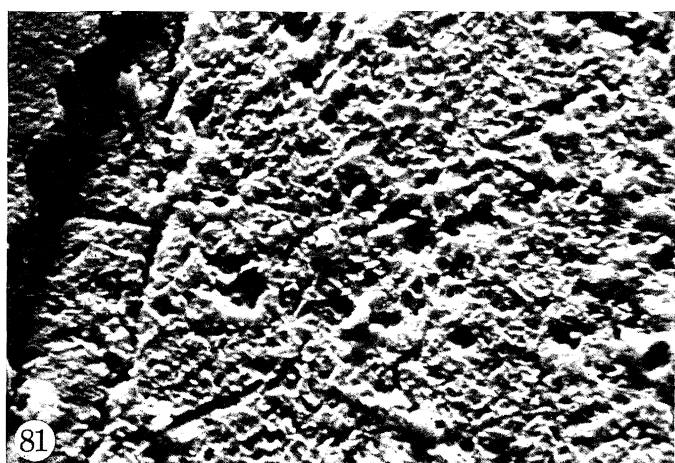
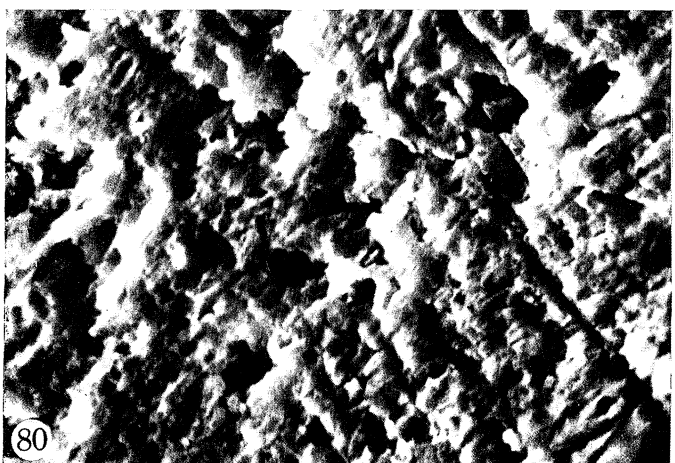
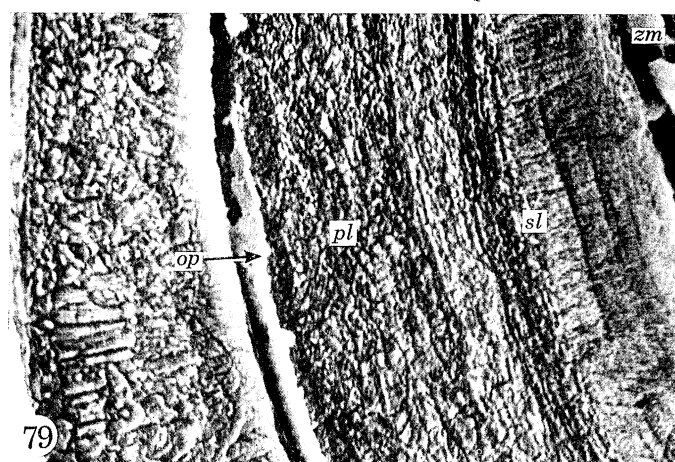
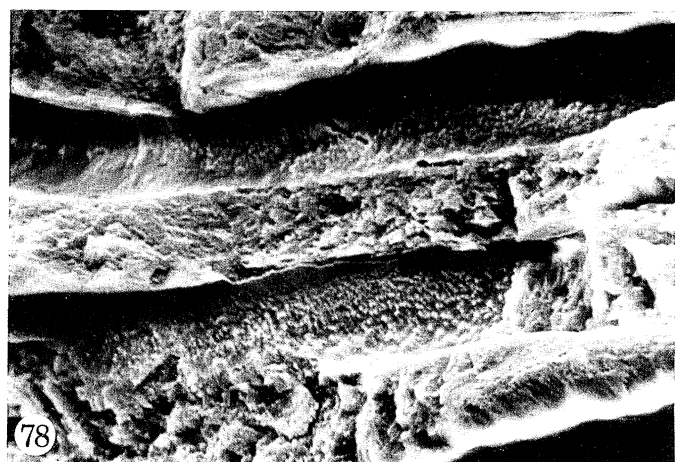
FIGURE 75. Section of the basal layer showing the disposition of acicular crystallites; zooecial chambers and frontal surface to the right ( $\times 2400$ ).

FIGURE 76. Section of the basal layer showing a tightly folded organic partition; zooecial chambers and frontal surface to the right ( $\times 1200$ ).



FIGURES 69 TO 76. For legends see facing page.





FIGURES 78 TO 85. For legends see facing page.

70, plate 16). The extensions within the basal and frontal layers are usually thrown into regular folds parallel with surfaces of deposition (figure 76, plate 16). These sheets provide seeding surfaces for calcite nuclei secreted by epithelium forming a frontal and basal envelope for the colony as well as the zooecial lining, and there are consistent differences between the skeletal fabric of the two genera.

In *Iodictyum sanguineum* (Ortmann), the basal layer is made up of epitaxial groups of acicular crystallites, up to 250 nm thick and 20  $\mu$ m long, secreted at high angles to the bounding periostracal sheets so that differences in crystallite disposition may occur from one group to the next (figure 71, plate 16). This fabric is the same throughout the basal layer, the external surface of which is also finely granular through the presence of rhombic heads of crystallites about 240 nm across. The entire succession may therefore be designated primary shell. The zooecial lining may be about 35  $\mu$ m thick and is somewhat different from the basal layer because it consists of short or obliquely inclined acicular crystallites about 300 nm thick commonly grouped into fairly regular lenses about 1.5  $\mu$ m thick and exceptionally up to 20  $\mu$ m long, and scattered calcitic nodules up to 35  $\mu$ m across (figure 72, plate 16). This fabric is also characteristic of the frontal wall where acicular crystallites commonly occur in irregular lenses and are responsible for the finely granular appearance of both the external surface of the frontal wall (figure 73, plate 16) and the internal zooecial surface. Thus the zooecia and the basal mineral layer of *Iodictyum* are exclusively primary shell, composed mainly of epitaxial acicular crystallites with differences only in their aggregation.

As in *Iodictyum*, *Sertella granulata* (MacGillivray) shows some difference between the fabric of the primary shell of zooecia and the basal layer with its finely tuberculate external surface (figure 74, plate 16). In the basal layer, acicular crystallites (figure 75, plate 16) are inclined at high angles to periostracal seeding surfaces (figure 76, plate 16) so that in fracture surfaces near folded sheets the calcite appears as alternating bands of cleaved plates and cross sections of crystallites (figure 78, plate 17). The zooecial primary layer, usually between 5 and 15  $\mu$ m thick, is also composed of groups of acicular crystallites arranged in irregular lenses. Unlike *Iodictyum*, however, all zooid chambers are lined with a secondary layer, up to 10  $\mu$ m thick,

---

#### DESCRIPTION OF PLATE 17

Scanning electron micrographs of the zooecia of *Sertella carinata*:

FIGURE 78. Fracture surface of the basal layer showing alternating bands of differently disposed calcite crystallites ( $\times 1200$ ).

FIGURE 79. Section showing the skeletal succession between adjacent zooecial chambers ( $\times 6000$ ).

Scanning electron micrographs of sections of the zooecial walls of fossil cheilostomes:

FIGURE 80. *Psilosecos muralis* (Gabb & Horn) from the Palaeocene (Vincentown Limesand), Vincentown, New Jersey ( $\times 2500$ ).

FIGURE 81. *Porina filigrana* (Goldfuss) from the Cretaceous (Upper Maastrichtian), Maastricht, The Netherlands ( $\times 2400$ ).

FIGURE 82. *Pachythecella variegata* (d'Orbigny) from the Cretaceous (Upper Maastrichtian), Hemmoor, W. Germany ( $\times 2300$ ).

FIGURE 83. *Cryptostomella gastroporum* (Marsson) from the Cretaceous (Upper Maastrichtian), Hemmoor, W. Germany ( $\times 2400$ ).

FIGURE 84. *Bathystomella cordiformis* (von Hagenow) from the Cretaceous (Campanian), Rügen, E. Germany ( $\times 2400$ ).

FIGURE 85. *Systemostoma asperulum* (Marsson) from the Cretaceous (Lower Maastrichtian), Rügen, E. Germany ( $\times 2400$ ).



distinguished by a fine banding about 350 nm thick and strong cleavage normal to the surface of deposition (figure 79, plate 17).

The fossil genus *Psilosecos* has been classified as a reteporid (Bassler 1953, p. 213) but, as Professor E. Voigt has pointed out (personal communication), it bears little resemblance to other members of the family and its taxonomic position is uncertain. The skeletal fabric of *Psilosecos muralis* (Gabb & Horn) from the Palaeocene of New Jersey (figure 80, plate 17), consists of crystallites up to 800 nm thick, disposed normal to surfaces of deposition including inner periostracal extensions, about 1.7  $\mu\text{m}$  thick, forming the framework of the colony. The skeleton therefore, is composed exclusively of primary shell as in *Iodictyum* and sporadic traces of lenses about 3  $\mu\text{m}$  thick emphasize the comparison.

A survey of some extinct ascophoran species suggests that their carbonate successions were generally simpler than those of living ascophorans. Among the Porinidae, the shell structure of the Upper Maastrichtian *Beisselina striata* (Goldfuss), *Pachythecella variegata* (d'Orbigny) and *Porina filograna* (Goldfuss) from the Netherlands and Germany is granular (figure 81, plate 17), or dominated by coarse crystallites up to 10  $\mu\text{m}$  long and 2  $\mu\text{m}$  thick having no preferred orientation in *Beisselina*, but arranged normal to secreting surfaces as in *Pachythecella* (figure 82, plate 17). Although zooecial walls may be 400  $\mu\text{m}$  thick, the fabric is the same throughout and is primary shell. A fabric of relatively coarse crystallites up to 12.5  $\mu\text{m}$  long and 3  $\mu\text{m}$  wide disposed normal to zooecial surfaces and representing only primary shell (figures 83, 84 and 85, plate 17) is also characteristic of other Maastrichtian species from Germany and the Netherlands including the cycloporid *Taeniporina arachnoidea* (Goldfuss), the mucronellid *Cryptostomella gastroporum* (Marsson), the parmulariid *Bathystomella cordiformis* (von Hagenow) and *Systenostoma asperulum* (Marsson) of uncertain familial status. Even the Maastrichtian *Platyglena ocellata* Marsson from Denmark which may be an excessively calcified cribrimorph (E. Voigt, personal communication) is characterized by an exclusively primary shell of long crystallites lying normal to zooecial surfaces; and although the granular skeleton of the contemporaneous *Dysnoetopora celleporoides* Canu and Bassler from Tennessee is affected by strong cleavage, it is still primary shell only.

#### (b) Structure of cyclostome zooecium

The cyclostomes are more diverse and have a longer geological history than the cheilostomes. Eight cyclostome superfamilies are currently recognized and, although some of these groups (Articuloidea, Tubuloporoidea, Hederelloidea) are first recorded from the Lower Palaeozoic and the remainder (Cancelloidea, Cerioporoidea, Rectanguloidea, Dactylethroidea, Salpingoidea) from Lower and Middle Mesozoic successions, only three (Hederelloidea, Dactylethroidea, Salpingoidea) are extinct. Despite this range the skeletal succession is less variable than that of cheilostomes. Two calcitic layers of primary crystallites and secondary laminae are typical of nearly all living and fossil species, while variation in this succession depends solely on the nature of zooidal replication from the common bud.

In most cyclostomes (Borg 1926, p. 255; Illies 1968, p. 227) developing zooids are partitioned off from the common bud (and from each other) by one septum, or more, originating within folds of the calcite-secreting epithelium lining the walls of the common bud (or parent zooecium). These folds grow centripetally (figure 86) and spread distally until they involve the subcircular junction (secretory epithelial junction) between the calcite-secreting epithelium and the periostracum-secreting epithelium of the terminal membrane which forms the frontal part of the zooecium. As growth proceeds, two oppositely situated folds of the secretory epithelial

junction must advance and meet medially to give rise to two separate disks of terminal membrane representing the frontal parts of the distally expanding parent and offspring zooids. In this way, interzooidal partitions composed exclusively of carbonate layer(s) can arise to connect walls with fully developed skeletal successions including the periostracum. The articuloid *Crisidia* and the tubuloporoid *Berenicea* are representative of cyclostomes with this kind of colonial growth.

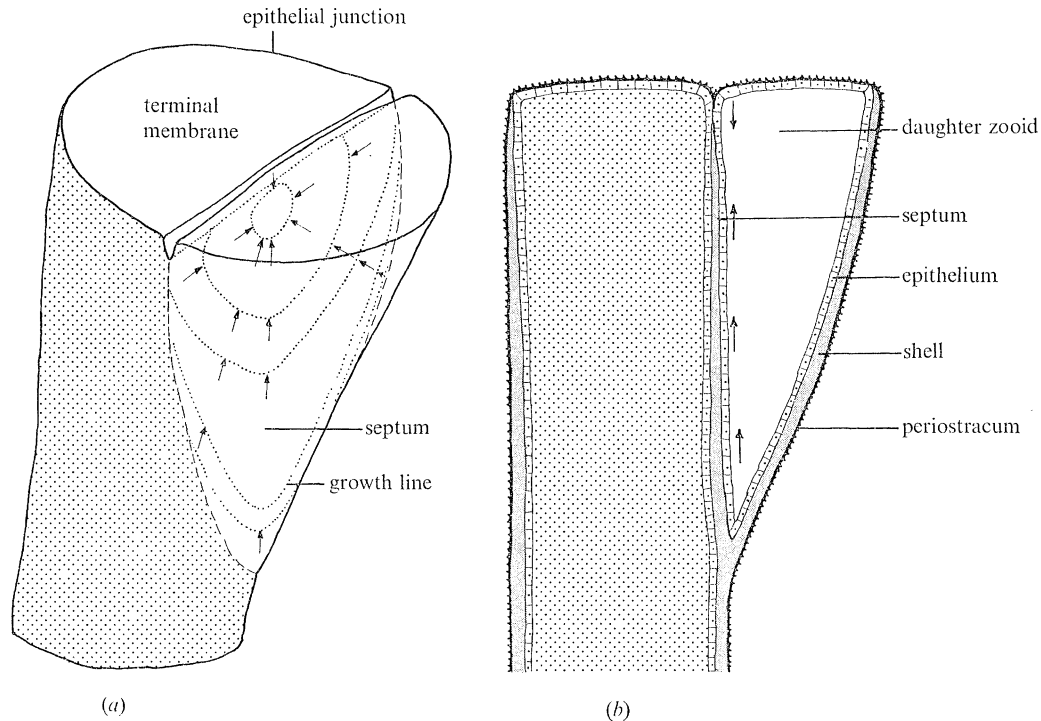


FIGURE 86. Diagram showing the skeletal growth relationship between a daughter and parent zooid of *Crisidia* seen in semiperspective (a) and sagittal section (b).

In contrast to the mode of growth described above, zooidal development from the common bud of a minority of species involves the secretion of all interzooidal walls independently of a colonial membrane composed of periostracum and the eustegal epithelium (Ryland 1970, p. 105) and homologous with the terminal membranes in other cyclostomate colonies. In *Lichenopora*, the common bud is funnel shaped. It overlaps the primary disk, from which it originates, onto the substrate and continues to act as the expanding boundary of the colony throughout life. Inside this growing edge which generates an ever-increasing colonial cover of periostracum and eustegal epithelium, carbonate zooecial walls are secreted within folds of basal epithelium (figure 132). These folds never connect with eustegal epithelium so that the calcified zooecial walls are always separated from the frontal periostracal cover of the colony by the hypostegal coelomic cavity (Borg 1926, p. 315). The astogeny of *Hornera* is less well known (Borg 1926, pp. 305–7), but it seems that the first group of up to six zooid offspring originates in the vicinity of the primary zooid, all growing upright from the primary disc (figure 136, plate 23); and that branching which is usually dichotomous, takes place almost immediately, and thereafter at regular intervals. Periostracum and eustegal epithelium must therefore extend as a colonial cover from the primary disk to the common buds at the apices of each

branch. The mineral skeleton of the cerioporoid *Heteropora* is also deposited within epithelial folds as were the zooecia of related fossil species examined by us.

(1) *Articuloid and tubuloporous zooecia*

The mineral skeletal succession of *Crisia eburnea* (Linn.) has been described by Söderqvist (1968). His findings have been confirmed by our studies of *Crisidia cornuta* (Linn.) and can now be considered in relation to associated organic constituents identifiable in sections of decalcified shell. The primary layer of *Crisidia* is secreted on an inner electron-dense sealing surface of the

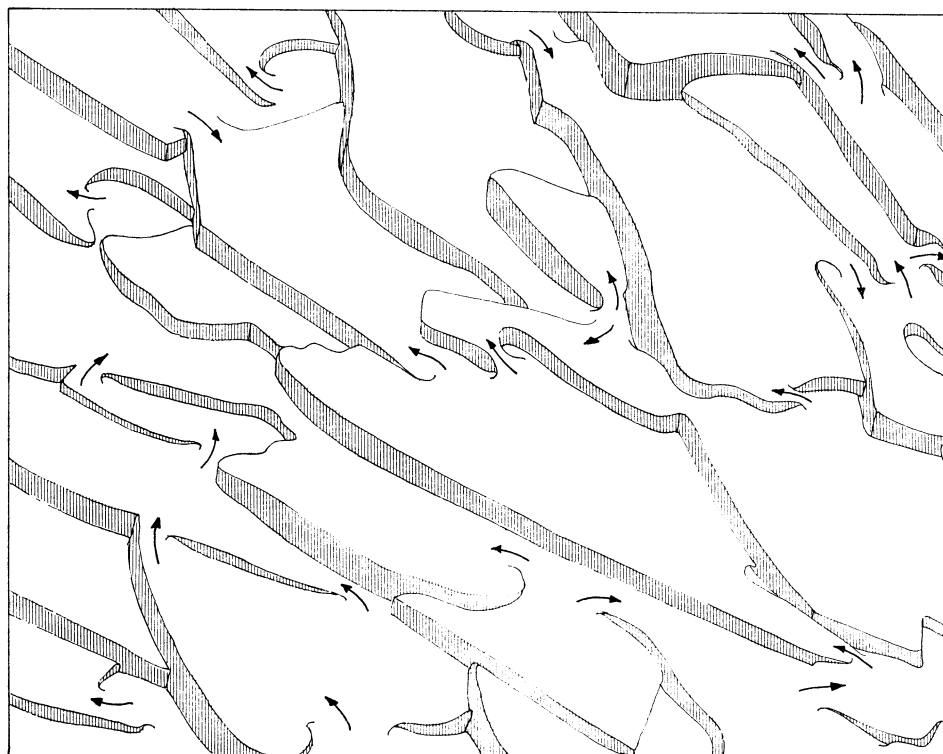


FIGURE 87. Diagram showing overlapping laminae of the secondary shell of *Crisidia* in attitudes of spiral growth; vertically lined strips represent laterally growing scarp faces of calcite, and the arrows indicate unbroken connexions in the interlaminar protein sheets from one level to the next.

#### DESCRIPTION OF PLATE 18

Electron micrographs of *Crisidia cornuta* (Linnaeus), Ardkeen, Co. Down, N. Ireland:

FIGURE 88. External surface of a zooecium showing the strips of primary acicular crystallites ( $\times 2500$ ).

FIGURE 89. Section of zooecial walls showing the skeletal succession ( $\times 7000$ ).

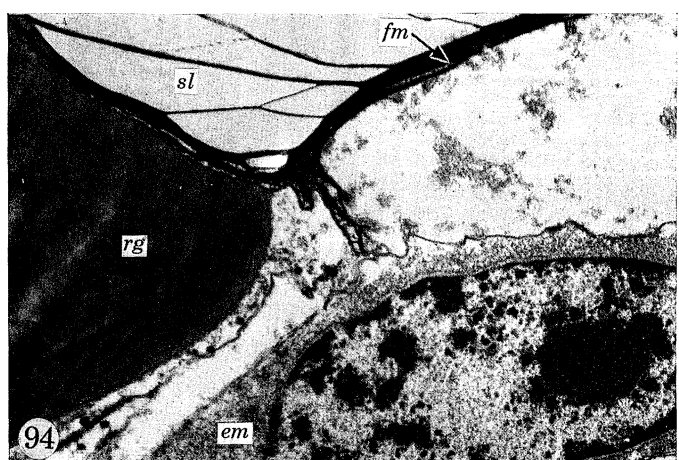
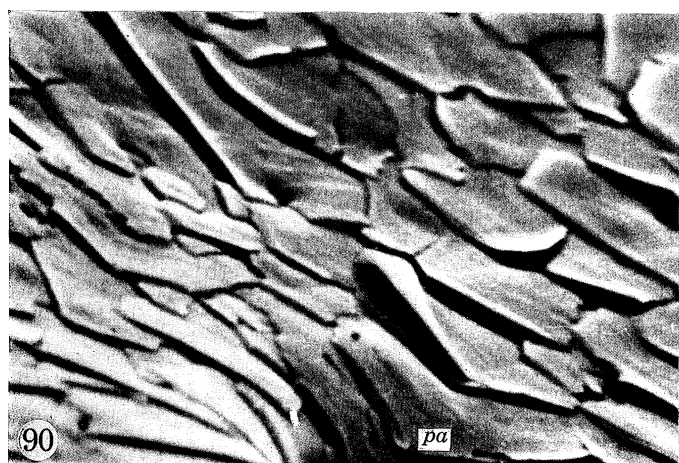
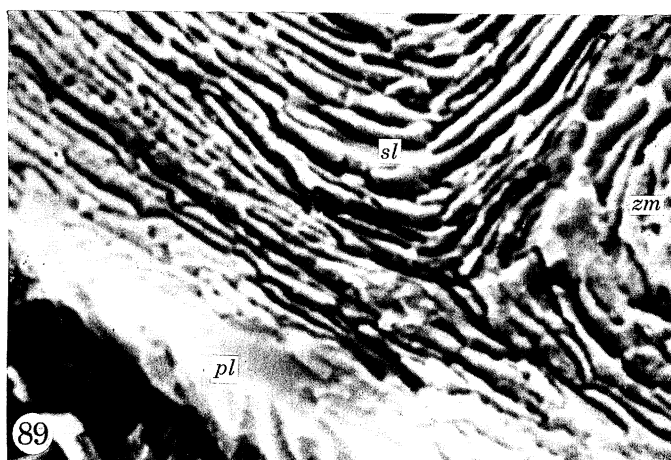
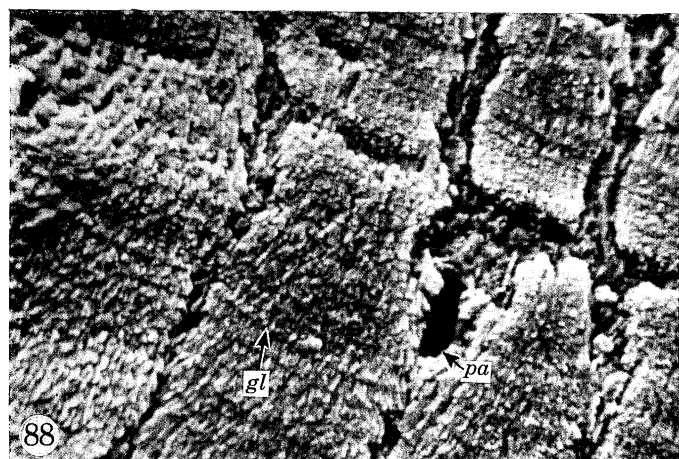
FIGURES 90, 91. Views of the internal surfaces of zooecia showing overlapping tablets and fibres of the secondary shell ( $\times 6500$ ).

FIGURE 92. Internal view of a punctum penetrating laminae of the secondary layer ( $\times 6500$ ).

FIGURE 93. View of the socket component of a nodal joint indenting the surface of a stoloniferous kenozoecium ( $\times 600$ ).

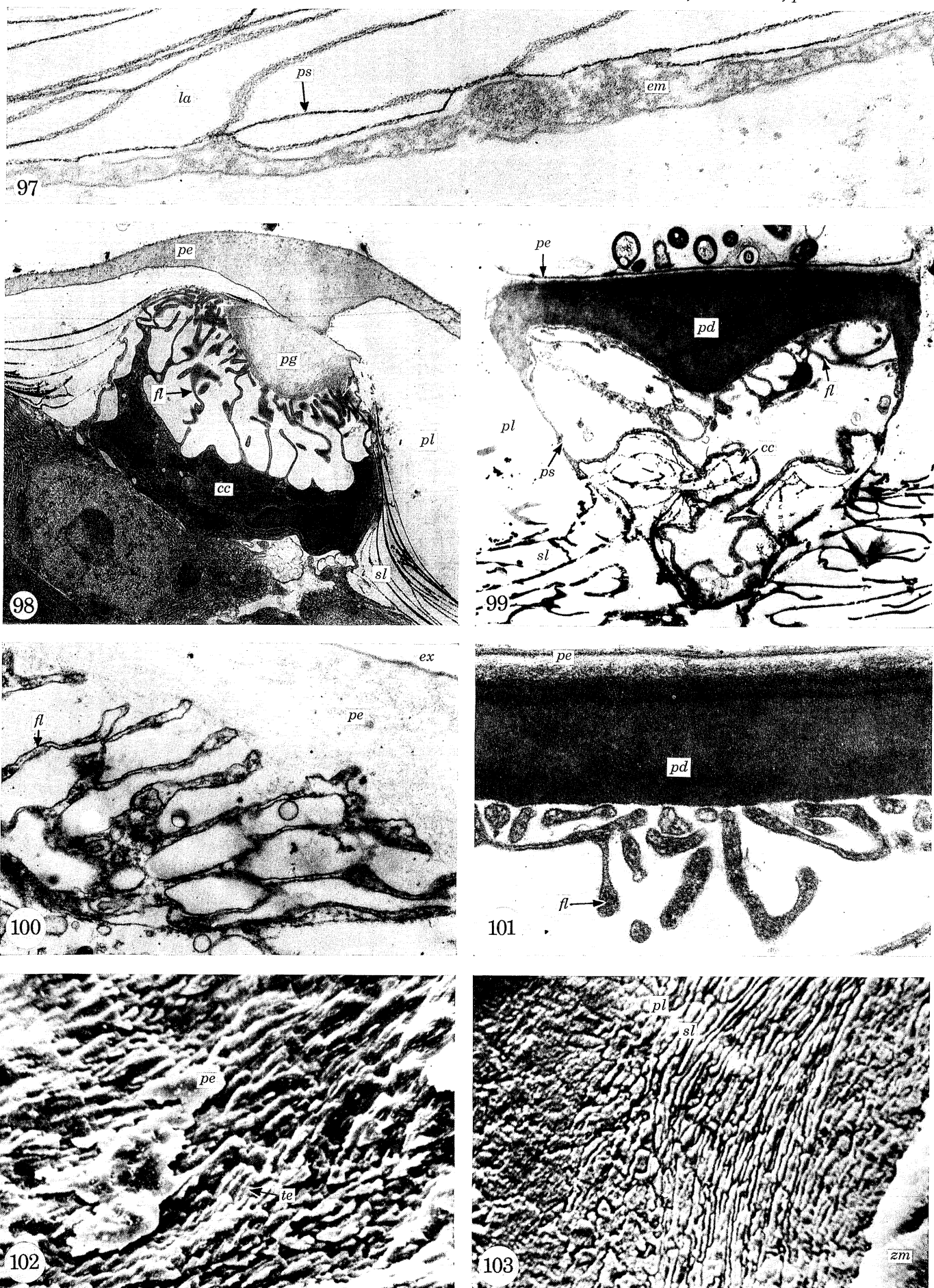
FIGURE 94. Section of the decalcified tissue at the node between two zooids showing the relative position of the protein ring ( $\times 22500$ ).

FIGURE 95. Section of a zooecial wall of *Crisia corbini* Canu from the Tertiary (Lower Lutetian), Chaumont en Vexin, France, showing the laminar secondary layer ( $\times 7000$ ).



FIGURES 88 TO 95. For legends see facing page.





FIGURES 97 TO 103. For legends see facing page.

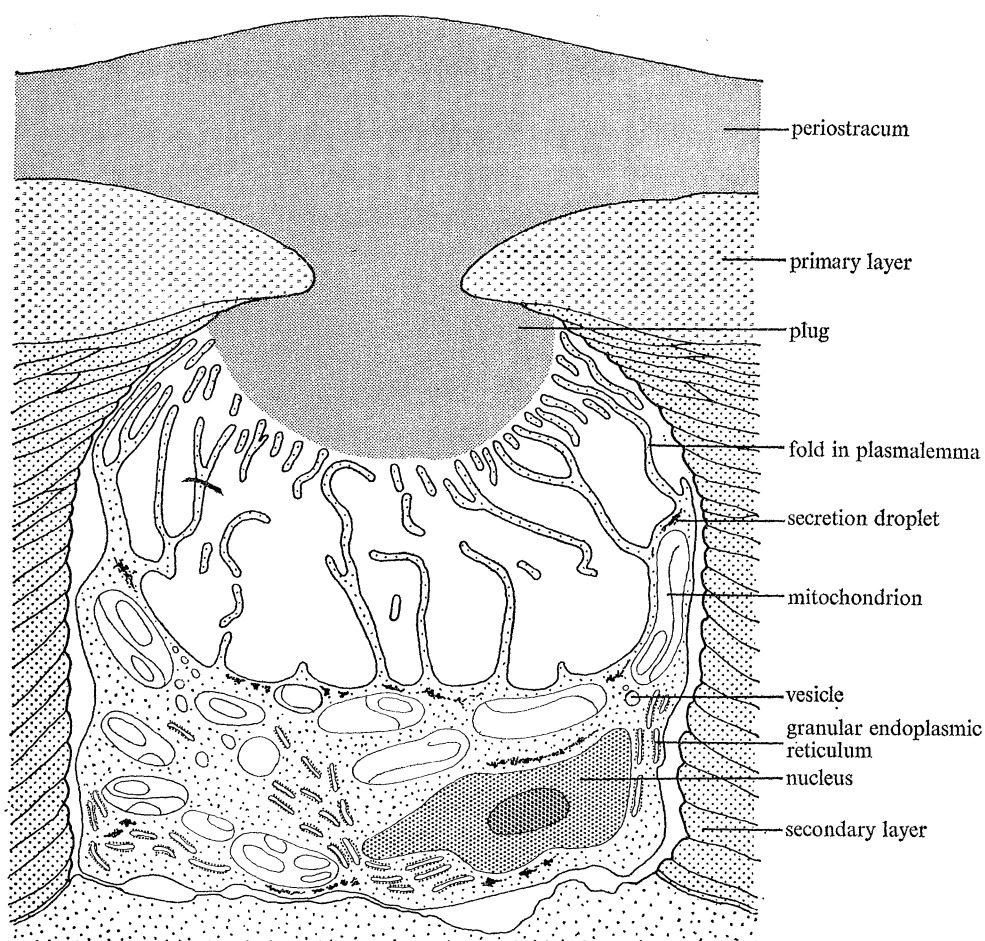


FIGURE 96. Diagram showing the structure of a papilla and punctum in the shell of *Crisidia*.

#### DESCRIPTION OF PLATE 19

Transmission electron micrographs of *Crisidia cornuta*:

FIGURE 97. Decalcified section showing secretory epithelium in association with protein sheets of the secondary shell ( $\times 55\,000$ ).

FIGURE 98. Decalcified section showing the structure of a papilla occupying a punctum in the shell ( $\times 10\,700$ ).

FIGURE 100. Decalcified section showing the folds in the plasmalemmas of core cells in relation to the periostracum near the growing tip ( $\times 41\,000$ ).

Electron micrographs of *Berenicea patina* (Lamarck), Killyleagh, Co. Down, N. Ireland:

FIGURE 99. Decalcified section showing the structure of a papilla occupying a punctum in the shell ( $\times 9\,200$ ).

FIGURE 101. Decalcified section showing the folds in the plasmalemmas of core cells in relation to the protein pad ( $\times 41\,000$ ).

FIGURE 102. External view of the basal wall with adherent periostracum showing the tuberculate surface of the primary layer ( $\times 650$ ).

FIGURE 103. Section of a zooecial wall showing the skeletal succession ( $\times 2\,800$ ).

periostracum about 6 nm thick (figure 19, plate 9), in long parallel strips about 10.5  $\mu\text{m}$  wide (figure 88, plate 18). The primary layer is up to 3.5  $\mu\text{m}$  thick (figure 89, plate 18) and is mineral in composition except for rare proteinous trails from the periostracum. Calcite is secreted on the periostracum as gently inclined acicular crystallites, about 300 nm thick and up to 1.2  $\mu\text{m}$  long, disposed more or less parallel with the long axis of the zooecium. Internally, however, the crystallites tend to have irregular, interlocking boundaries giving a granular effect, although the frequent prevalence of one cleavage direction on fracture surfaces suggests that there is general crystallographic alinement.

This granular primary layer is abruptly succeeded by a laminar secondary layer which may be up to 15  $\mu\text{m}$  thick (figure 89, plate 18). The laminae consist predominantly of tablets with rhombic or dihexagonal corner angles (figures 90 and 91, plate 18). The tablets are, on average, 240 nm thick and 4  $\mu\text{m}$  wide, although two or three in the same plane may unite laterally. Fibres of about the same width and average thickness but with a medial keel on the outer surface, also occur. On internal surfaces both constituents are disposed like overlapping tiles about 2.5  $\mu\text{m}$  apart, but the scarp-like exposed edges are impersistent laterally or interleaved with one another in attitudes of spiral growth (figure 87). The laminae are separated from one another by interconnected protein sheets about 6 nm thick which appear in sections of decalcified zooecium and associated epithelium as anastomosing threads (figure 97, plate 19). Some sheets are seen to arise at the secreting plasmalemma and to be separated from a complete outer sheet by a gap along the plasmalemma which must have been occupied by a laminar edge *in vivo*. Calcite and protein are therefore simultaneously secreted at different levels by an epithelial cell. Moreover, lateral expansion of any one lamina in spiral arrangement with its neighbours, increases the area of its inner surface available for settlement by protein molecules which simultaneously form the seeding sheet over which an inner lamina can encroach by lateral growth. The progress of the lateral growth of laminae is commonly indicated by faint concentric banding, with a periodicity of 150 nm, on their inner surfaces (figure 91, plate 18).

This process of skeletal growth by the simultaneous secretion of protein and carbonate is invariably characteristic of the secondary layer of all cyclostome species investigated irrespective of the shape of the calcitic constituents.

The mineral skeleton of *Crisidia* is pierced by unbranched canals (pseudopores of Levinson 1909, p.V.) arranged alternately in rows at intervals of about 16  $\mu\text{m}$ . A mature canal is elliptical in outline in the secondary layer, but it becomes constricted to a relatively narrow slit, less than 2  $\mu\text{m}$  across, in the primary layer and appears as a lenticular opening on the external surface (figure 92, plate 18). The canal is lined with a protein sheet about 10 nm thick and contains a papillose extension of epithelium consisting of a layer of peripheral cells surrounding a few core cells with numerous membrane-lined vesicles (figures 96; and 98, plate 19). Distally just below the constricted neck of the canal the plasmalemmas of core and peripheral cells are thrown into highly convoluted folds usually about 120 nm wide and up to 1.5  $\mu\text{m}$  long. The constricted slit is occupied by a plug of material of the same composition as the main part of the periostracum, with which it is continuous. The plug, consisting mainly of protein complexes, is secreted by the plasmalemma folds especially of the vesicular core cells which may actively exude material into the distal part of the canal throughout the life of the zooid. It is lacking distally of newly developed papillae near the growth tip where plasmalemma folds directly underlie the main periostracal layer (figure 100, plate 19).

The secretion of proteinous rings (Hyman 1959, p. 389) instead of shell at regularly spaced

nodes in the *Crisidia* colony provides branches with flexible joints. Each joint consists of a truncated cone up to 15  $\mu\text{m}$  high and wide accommodated by a socket (figure 93, plate 18). Although both cone and socket penetrate secondary shell, their surfaces are finely granular and are lined by electron-dense proteinous films about 250 nm thick (figure 94, plate 18) which also extend onto the internal surfaces of adjacent calcareous walls. Each ring which may be up to 5  $\mu\text{m}$  thick extends between these proteinous films. It must be formed after secretion of the proteinous films had broken the continuity of the mineral part of the skeleton and furnished a space beneath the periostracum for its deposition.

The only fossil Articuloidea studied was a specimen of *Crisia corbini* Canu, from the Lower Lutetian of Dîse, France, which showed a granular primary layer and a well-developed secondary layer of laminae with an average thickness of 300 nm (figure 95, plate 18). This may prove to be one of the earliest known Crisiidae because, although the family has been recorded in the Cretaceous, Professor E. Voigt (personal communication) has pointed out that it is doubtful whether the pre-Tertiary 'crisiids' are jointed and, accordingly whether they are Articuloidea.

In contrast to true Articuloidea, the Tubuloporoidea have a well-authenticated geological record. One of the key families, the Diastoporidae, includes the longest surviving bryozoan stocks for not only are constituent species recorded from Lower Palaeozoic rocks, but those assigned to one genus, *Berenicea*, range from the Ordovician to the present day. Accordingly, the encrusting discoidal colony of living *Berenicea patina* (Lamarck) is an appropriate example of tubuloporoid skeletal structure.

The skeletal succession of living *Berenicea* is like that of *Crisidia*. The primary layer is only about 6  $\mu\text{m}$  thick basally but may be twice as much in zooecial walls. The calcite seeds of the primary surface usually occur as gently to vertically disposed acicular crystallites up to 2.5  $\mu\text{m}$  wide and 10 or more  $\mu\text{m}$  long (figure 102, plate 19). The surface crystallites are normally succeeded by a more granular type of calcite which grades laterally and inwardly into coarse lenses over 500 nm thick and up to 15  $\mu\text{m}$  across arranged more or less parallel to the zooecial surfaces (figure 103, plate 19). The lenses may even develop keels on their outer surfaces like the fibres of *Entalophora*. They are sheathed in protein sheets and herald the regular banding, on average 250 nm thick, of the inner part of the secondary layer, which is seen on internal surfaces to be composed of tabular laminae, with rhombic or dihexagonal corner angles, in attitudes of spiral growth (figures 105 and 106, plate 20).

The canals and papillae of *Berenicea* differ from those of *Crisidia* in detail. They occur alternately in rows at intervals of about 13  $\mu\text{m}$ , and are unbranched and elliptical in cross-section. The distal opening of each canal is star-shaped because of the centripetal growth of seven or eight subtriangular projections of finely granular calcite from a depressed marginal border about 1.5  $\mu\text{m}$  wide (figure 107, plate 20). The papillae occupying the canals are bounded by a protein sheet about 30 nm thick (figure 99, plate 19, figure 104). Distally the dominant feature of a papilla is an electron-dense pad which is composed of fine granules, about 8 nm in diameter, aligned linearly at high angles to the flat outer surface but varying in spacing to define successive growth surfaces (figure 101, plate 19). The outer surface of the pad lies about 45 nm beneath the periostracum to which it is attached by fibrils. The pad varies in thickness because it extends up to 3  $\mu\text{m}$  proximally as a thick peripheral rim and a central cone. Immediately beneath the pad and, presumably, responsible for its secretion, occur many branched microvilli arising from the peripheral and core cells occupying the pseudopores. Immediately below the microvillous



zone the papilla is sharply constricted in conformity with the distal stellate aperture of the canal so that the pad fits over the front of the aperture with the peripheral rim resting on the depressed border.

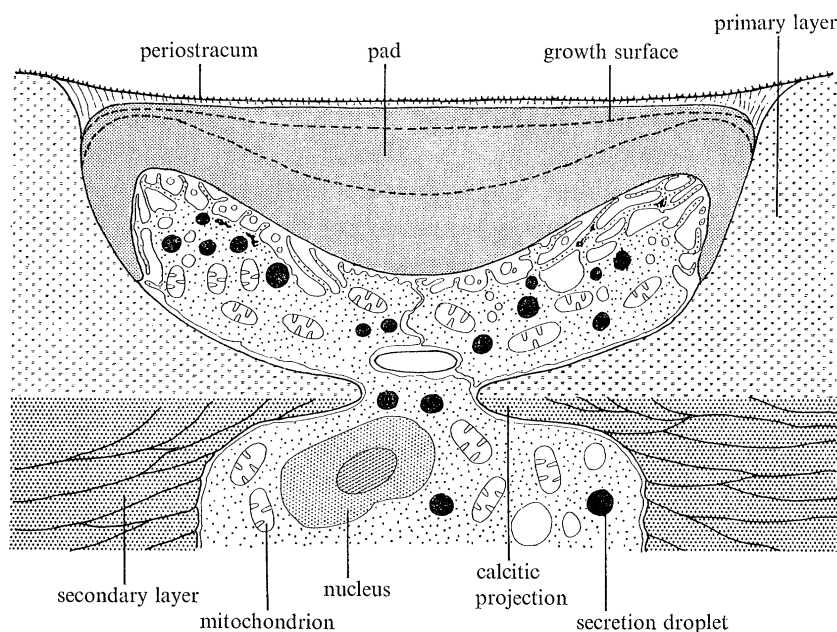


FIGURE 104. Diagram showing the structure of a papilla and punctum in the shell of *Berenicea*.

Three fossil genera studied showed how representative the *Berenicea* carbonate succession is of extinct diastoporids. The skeletal succession of *Discosparsa simplex* d'Orbigny from the Upper Cretaceous Chalk of Kent, was normally developed with a granular primary layer, up to 17  $\mu\text{m}$  thick and a secondary layer of relatively coarse lenses passing inwardly into regularly arranged laminae averaging 750 nm in thickness (figure 108, plate 20). *Sagenella consimilis* (Lonsdale) from the Middle Silurian Wenlock Limestone of England also possessed a thin secondary layer preserved as calcite lenses arranged parallel with the zooecial surface and normal to irregular columns of calcite up to 24  $\mu\text{m}$  long constituting the primary layer. The most

#### DESCRIPTION OF PLATE 20

Scanning electron micrographs of the zooecia of *Berenicea patina*:

FIGURES 105, 106. Internal surfaces of zooecia showing the tabular laminae of the secondary shell in attitudes of spiral growth ( $\times 6500$ ,  $\times 2600$ ).

FIGURE 107. External surface of zooecial wall showing the star-shaped distal opening of a punctum ( $\times 2600$ ).

FIGURE 108. Scanning electron micrograph of a section of a zooecial wall of *Discosparsa simplex* d'Orbigny from the Cretaceous (Upper Chalk), Chatham, England, showing the skeletal succession ( $\times 1200$ ).

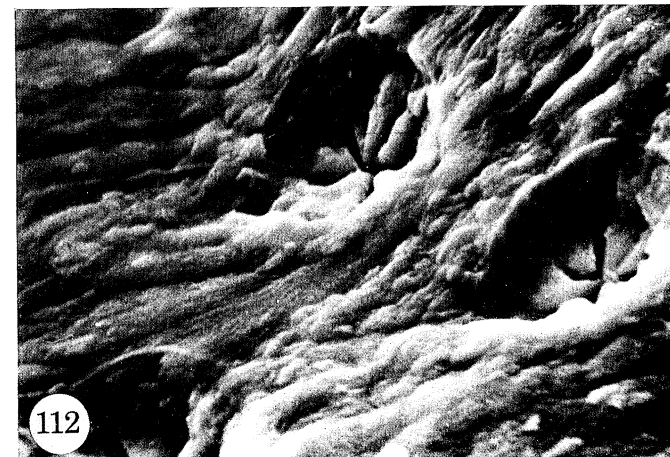
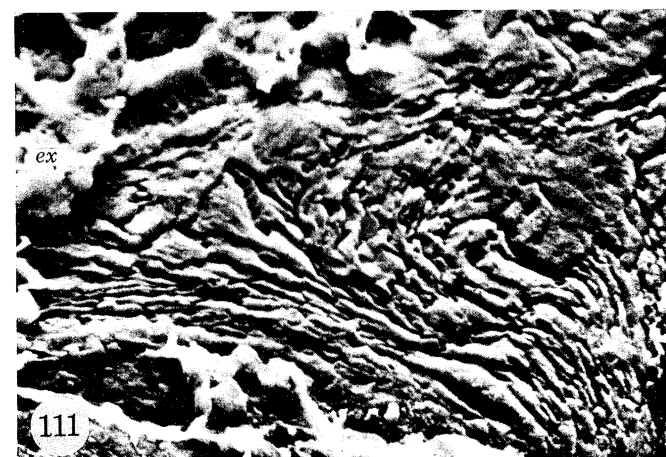
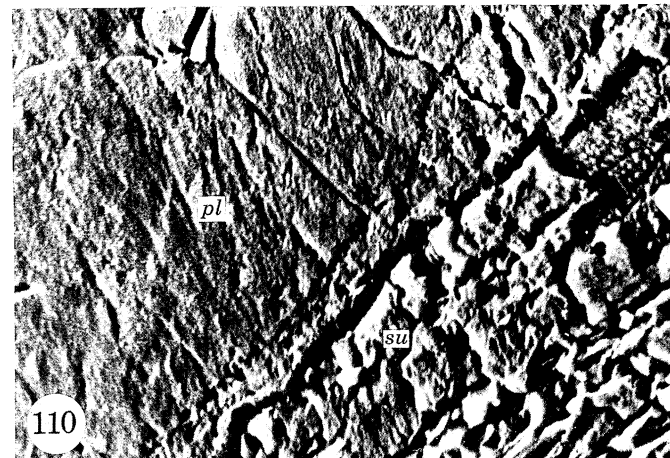
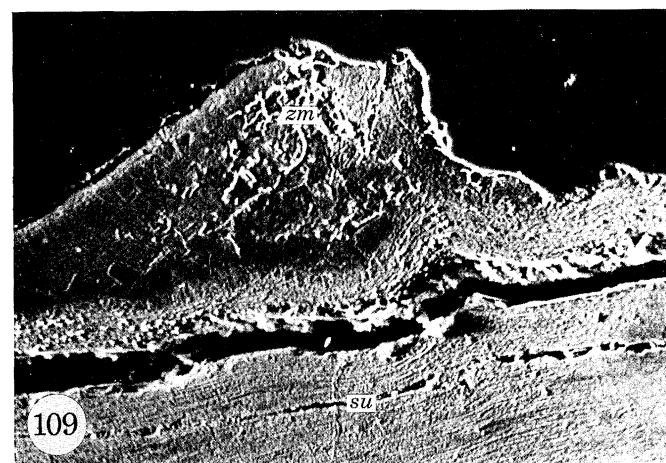
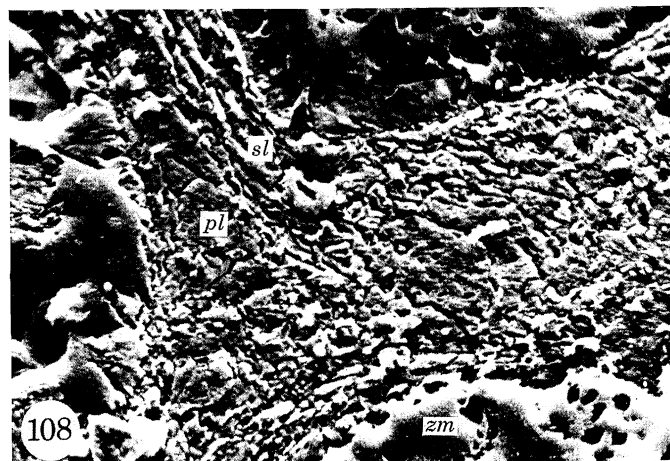
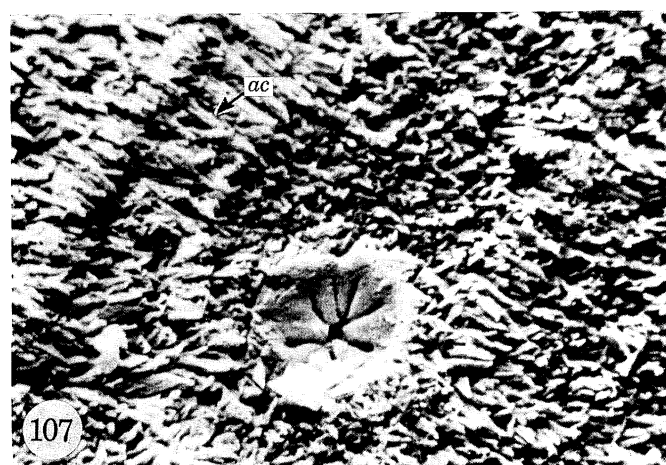
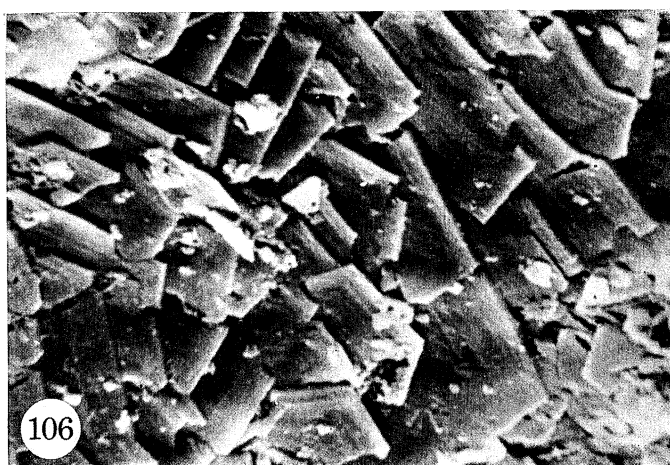
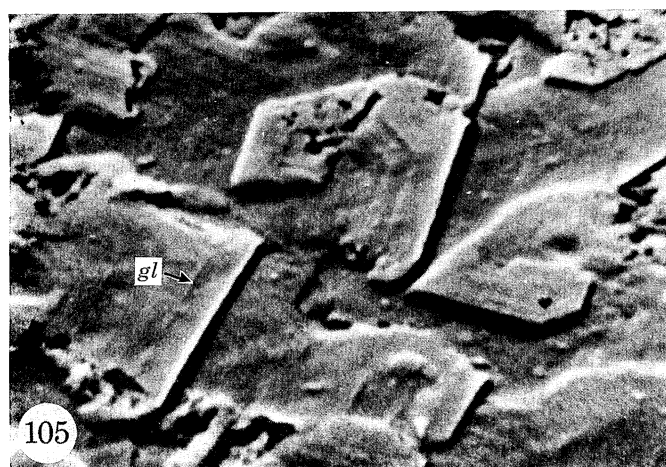
Scanning electron micrographs of a zooecium of *Corynotrypa* sp. from the Ordovician (Bromide Formation), Spring Creek, Oklahoma:

FIGURE 109. Sagittal section of a zooecium showing its relation to the substrate ( $\times 230$ ).

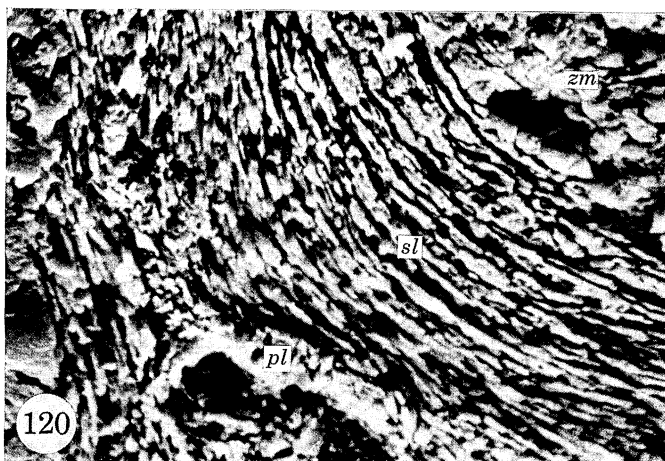
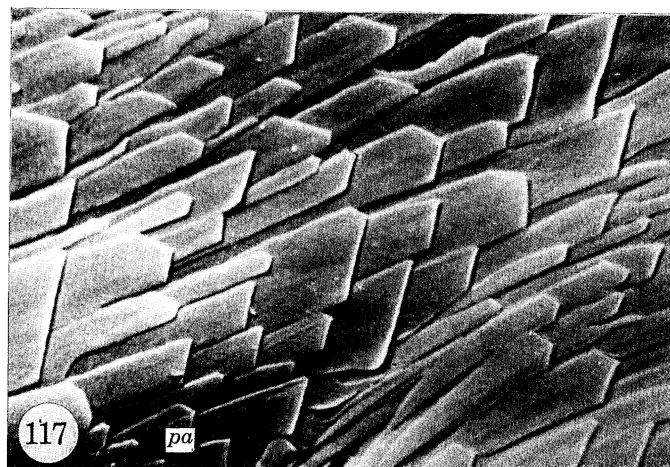
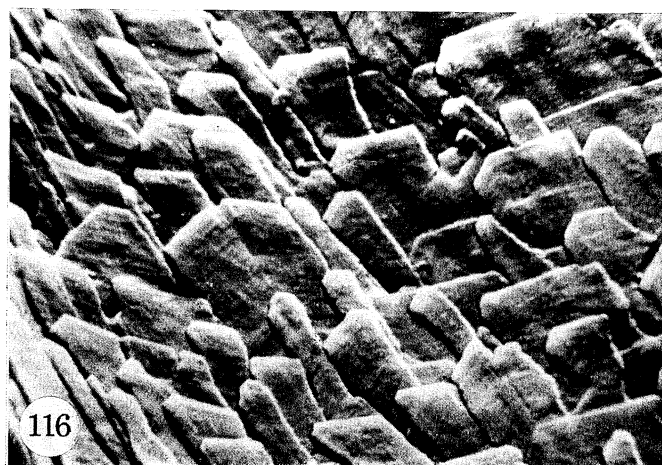
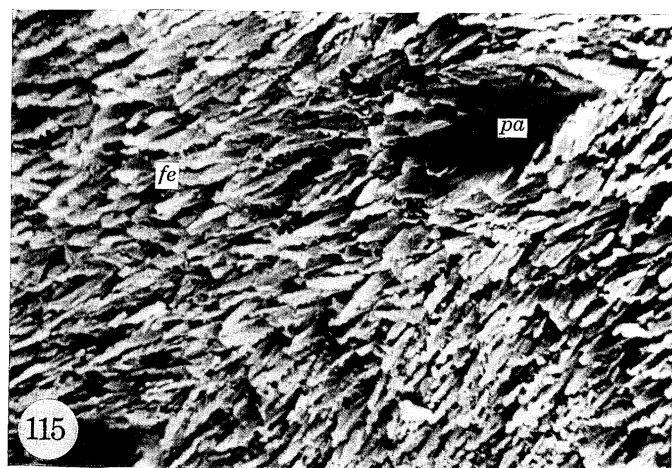
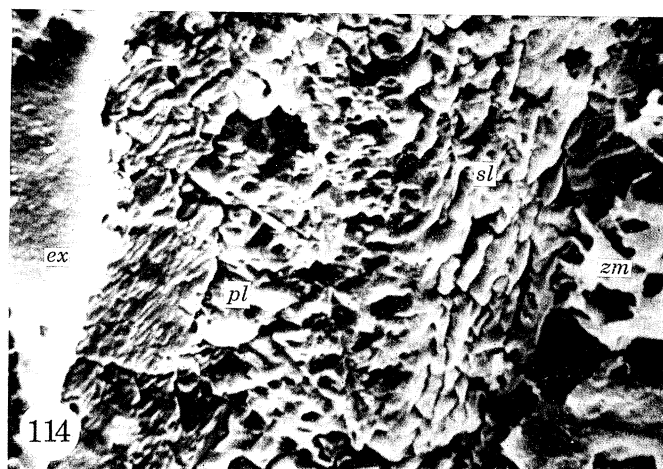
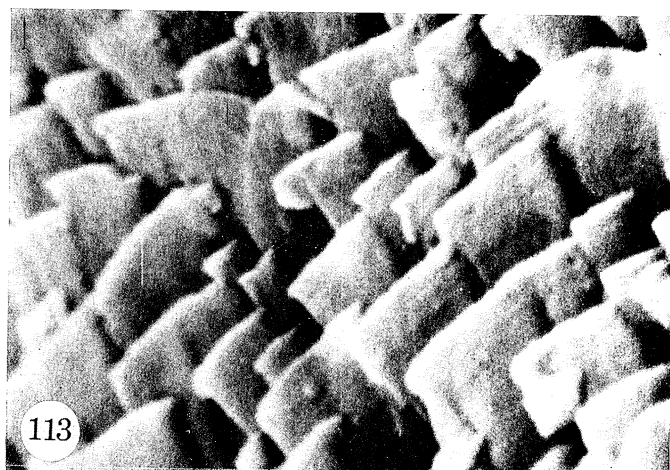
FIGURE 110. Section showing the primary shell of a zooecium ( $\times 2300$ ).

FIGURE 111. Section showing the secondary shell of a zooecium ( $\times 2300$ ).

FIGURE 112. Scanning electron micrographs of an external zooecial surface of *Tubulipora phalangea* Couch, Killyleagh, Co. Down, N. Ireland, showing the primary shell and distal openings of puncta ( $\times 2600$ ).



FIGURES 105 TO 112. For legends see facing page.



FIGURES 113 TO 120. For legends see facing page.



significant discovery, however, was that both shell layers were present in *Corynotrypa*, one of the earliest and most primitive cyclostomes. Specimens of an unnamed species (figure 109, plate 20) from the Upper Ordovician Bromide Formation of Oklahoma, consisted mainly of coarsely granular calcite representing primary shell (figure 110, plate 20). In addition, the zooidal chambers are lined by a secondary layer composed of laminae and lenses of calcite varying in thickness from 400 to 2000 nm (figure 111, plate 20).

The skeletal structure of living and fossil *Tubulipora*, the pre-eminent member of the Tubuliporidae, is almost indistinguishable from that of *Berenicea*. In living *T. phalangea* Couch, the primary layer is usually a few microns thick and consists of acicular crystallites or platelets less than 1  $\mu\text{m}$  across (figure 112, plate 20), while the secondary layer is composed of overlapping tablets or truncated fibres, up to 6  $\mu\text{m}$  wide, affected by left- and right-hand screw dislocations and bearing parallel growth steps at intervals of about 200 nm (figure 113, plate 21). The canals are like those of *Berenicea* in distribution, size and morphology (figure 112, plate 20). *T. chathamensis* Gregory from the Upper Cretaceous (Chalk) of Kent differs only in possessing a more massive skeleton with the granular primary layer up to 20  $\mu\text{m}$  thick and fibres of the secondary layer averaging 400 nm in thickness (figure 114, plate 21).

The skeletal succession of *Entalophora*, the oldest surviving representative of the tubuliporoid Entalophoridae, is affected by the ramose growth of the stock. In an undescribed living species from the Antarctic, the succession seen in zooecial walls between mature zooids is diverse (figure 121). A medial zone of coarsely granular calcite, about 7  $\mu\text{m}$  thick, represents the first-formed part of the primary layer (figure 118, plate 21) and is succeeded on either side by coarse lenses of calcite up to 8  $\mu\text{m}$  wide and 2  $\mu\text{m}$  thick. Some of the lenses may develop keels on their medial or outer surfaces, a prevalent condition in the fibres of the succeeding layer, which are arranged more regularly and alternately in rows (figure 119, plate 21). These fibres may be up to 1  $\mu\text{m}$  thick and 12  $\mu\text{m}$  wide, but inwardly they become thinner averaging 300 nm and are seen on internal surfaces as successions of laths or even tablets, with rhombic and dihexagonal corner angles, varying from 1 to 4.5  $\mu\text{m}$  in width and overlapping one another at intervals of 5  $\mu\text{m}$  (figures 116 and 117, plate 21). The keeled part of a fibre may develop as a narrow prong in advance of the broader base (figure 122). Parallel ridges with a periodicity of 180 nm occur on laths and prongs and show the progress of lateral accretion.

This succession is characteristic of axially placed zooecia, but peripherally in a transverse

---

#### DESCRIPTION OF PLATE 21

FIGURE 113. Scanning electron micrograph of the internal zooecial surface of *Tubulipora phalangea* showing the overlapping fibres of the secondary shell ( $\times 6800$ ).

FIGURE 114. Scanning electron micrograph of a section of external zooecial wall of *Tubulipora chathamensis* Gregory from the Cretaceous (Upper Chalk), Chatham, England, showing the skeletal succession ( $\times 2800$ ).

Scanning electron micrographs of the zooecia of *Entalophora* sp., The Antarctic:

FIGURE 115. View of the external zooecial surface showing the calcite blades of the inner primary layer and the distal opening of a punctum ( $\times 1300$ ).

FIGURES 116, 117. View of an internal zooecial surface showing the disposition of fibres of the secondary layer ( $\times 2800$ ).

FIGURE 118. Section of a zooecial wall showing the skeletal succession ( $\times 2500$ ).

FIGURE 119. Section of the secondary layer showing keeled fibres ( $\times 6800$ ).

FIGURE 120. Scanning electron micrograph of a section of a zooecial wall of *Lopholepsis radians* von Hagenow from the Cretaceous (Lower Greensand), Farrington, England, showing the skeletal succession ( $\times 2300$ ).



section the granular layer becomes thinner and less continuous, eventually forming a line of discrete lenses about  $4\text{ }\mu\text{m}$  wide, intersecting the external boundary in a distinct notch (figure 121). Similar notches occur between adjacent zooecia around the section boundary and correspond to narrow furrows on the external surface of a branch. These furrows are so arranged that a pair running longitudinally and parallel to each other define the proximal extent of a zooecium.

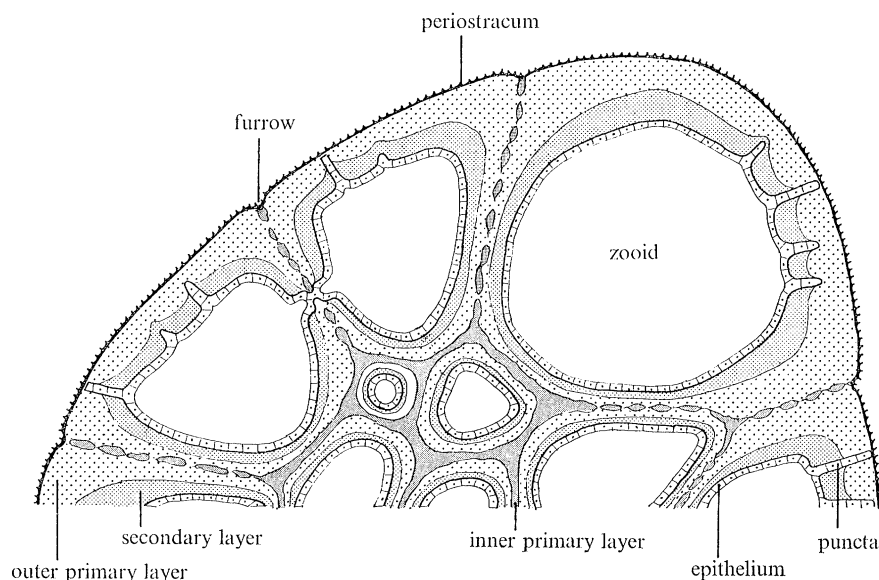


FIGURE 121. Diagrammatic transverse section showing the secretory epithelium in relation to skeletal structure in *Entalophora*.

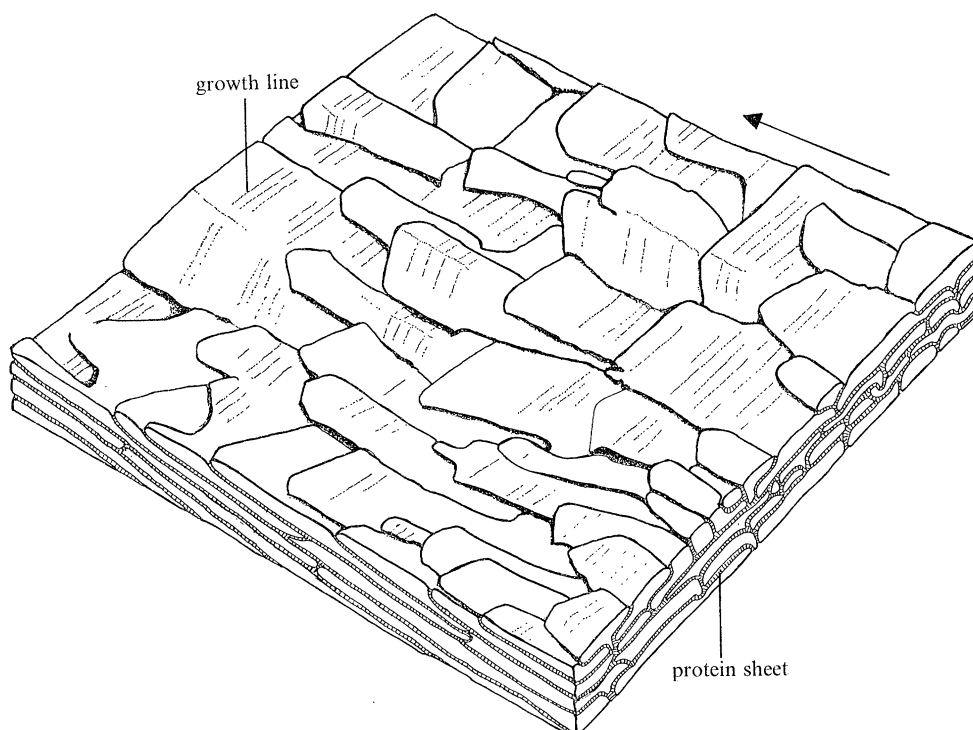


FIGURE 122. Diagram showing the relationship between fibres, some of them keeled, in the secondary shell of *Entalophora*.

They then converge to encircle the zooecial tube immediately distally of its separation from the main part of the branch. The two furrows defining the limits of the next distal zooecium in the same sector of the branch arise from either side of the convergent arc. Between the furrows, the branch surface is composed of overlapping, gently inclined calcitic blades about 2  $\mu\text{m}$  wide and up to 15  $\mu\text{m}$  long (figure 115, plate 21). The blades make acute angles with the furrows alternately pointing proximally and distally on both sides of adjacent furrows in a herring-bone pattern. These blades are unlike the acicular crystallites generally found in the primary layer. Their loose stacking suggests that they are sheathed in protein sheets, and the narrower ones appear to be keels of wider underlying blades. They are, therefore, identical with the coarse fibres which, in section, are seen to succeed the primary granular calcite in the interzooecial walls. Yet they could only have been secreted on periostracum if they occur on the external surface of branches and, in that respect, they are also primary.

The growth of such a distinctive fabric appears to proceed in the following way. When a zooid is first released from the common bud occupying the axis of a branch, it secretes a septum of granular calcite which may be envisaged as the primary layer of the common bud and immature zooecia. Its growth is controlled at its distal edge by the secretory epithelial junction where the periostracum, on which the granular layer is seeded, forms a narrow strip along the edge bordering the terminal membrane. As distal accretion continues, the zooecium expands gradually into a cone so that its outer wall of granular calcite overlain by a secretory epithelial junction ultimately becomes part of the colonial surface. At this stage, the edge of the granular calcite wall forms an ellipse sloping proximally from the central common bud (Borg 1926, fig. 48). Further distal growth initially involves more secretion of granular calcite along the inner and lateral boundaries of the zooecium. But on the outer surface and then elsewhere as the complete zooecium takes shape, the terminal membrane migrates away from the granular calcite wall in conjunction with the proliferation of cells at the secretory epithelial junction. The newly generated epithelium must first secrete an external layer of periostracum followed inwardly by flat-lying fibres. This order of succession is verified by the disposition of fibre keels and of the edges of fibres defining canals which are morphologically similar to those of *Crisidia*. Both keels and fibre edges point outwardly indicating deposition by epithelium lining the internal surface of the zooecium.

Notwithstanding the restricted nature of the granular calcite and the laminar aspect of the underlying layer of coarse fibres, it seems appropriate to classify them as outer and inner primary layers respectively. Attention can then be drawn to the fact that the latter is deposited directly on periostracum in some parts of the colony, but is structurally precursory to a secondary layer of regularly arranged fibrous laminae.

The remaining tubuloporoids investigated confirm the prevalence of the skeletal succession already described. In the theonoid *Lopholepsis radians* Hagenow from the Lower Cretaceous (Greensands) of Farringdon, England, a two-layered carbonate skeleton of primary acicular and granular crystallites and secondary fibrous laminae averaging about 300 nm, is developed (figure 120, plate 21). In the punctate frondiporid *Meandropora aurantium* (Milne-Edwards) from the Pliocene Crag of Cromer, England, the dominant fabric is a primary layer of acicular crystallites about 450 nm thick and granular calcite. A secondary layer of fibrous laminae up to 2  $\mu\text{m}$  across and averaging 350 nm in thickness, is usually restricted to the basal and adjoining parts of the lateral walls of zooecia (figure 123, plate 22). In two oncousoeciid species, *Proboscina wetherelli* Morris from the Upper Cretaceous (Chalk) of Chatham, England, and *Proboscina*

*frondosa* (Nicholson) from the Upper Ordovician (Richmond) of Richmond, Ohio, a granular primary layer is succeeded by secondary laminae consisting of regular tabular units averaging 400 nm in thickness in the younger species, but of much coarser fibres up to 1.3  $\mu\text{m}$  thick in the older (figure 124, plate 22).

Finally, the colonial growth of the plagioeciid *Terebellaria ramosissima* Lamaroux, from the Middle Jurassic (Inferior Oolite) of France, deserves special consideration. The colony forms an erect screw-like body with a central core of erect zooecia which included the common bud and gave rise to a spirally disposed ledge of autozooecia (figure 125, plate 22). The latter became detached from the core by bending over to grow proximally so that three or four rows of alternating zooecia may be counted on the face of a spiral immediately distal of the ledge border (figure 131). Distally of these open zooecia the spiral surface slopes inwardly to the next ledge. This surface is covered by a thin carbonate film beneath which can be seen the outlines of five or six rows of buried zooecia. These were once functional, but during the proximally directed growth of each spiral ledge which must have involved proliferation of extra rows of zooecia, older more distal zooecia became buried under a carbonate film which, as shown by growth lines, advanced proximally from each ledge. Despite these complexities, the carbonate succession is normal (figure 126, plate 22) consisting of a granular primary layer, about 2  $\mu\text{m}$  thick and a secondary layer of fibrous laminae with an average thickness of 650 nm. Canals penetrate at least the secondary layer (figure 126, plate 22) at intervals of about 6  $\mu\text{m}$  and are distinct from mural pores (figure 127, plate 22).

The distribution of primary layer is the key to the restoration of the soft parts of *Terebellaria* (figure 131). At the border of each ledge there occurs a thin layer of primary shell flanked by secondary laminae (figure 126, plate 22). This must represent the floor of zooecia at the ledge while the underlying secondary laminae belong to zooecia forming the adjacent proximal edge. The carbonate film covering the distal part of each spiral face is also primary shell. It must have been secreted on periostracum intervening between it and the older zooecia. This could only be so if there had been a secretory epithelial junction at the proximal edge of the primary film of calcite, and a complementary external cover of periostracum with its epithelial lining.

#### DESCRIPTION OF PLATE 22

FIGURE 123. Scanning electron micrograph of a section of the lateral wall of *Meandropora aurantium* (Milne-Edwards) from the Tertiary (Pliocene Crag), Cromer, England ( $\times 2300$ ).

FIGURE 124. Scanning electron micrograph of a section of the lateral wall of *Proboscina frondosa* (Nicholson) from the Upper Ordovician (Richmond Group), Cincinnati, Ohio ( $\times 2400$ ).

Scanning electron micrographs of the zooecia of *Terebellaria ramosissima* Lamaroux from the Middle Jurassic (Inferior Oolite), Calvados, France:

FIGURE 125. Transverse section of part of a colony showing a primary carbonate film between two zooecial rows ( $\times 120$ ).

FIGURE 126. Transverse section showing the relationship between the primary carbonate film and adjacent zooecial walls ( $\times 2400$ ).

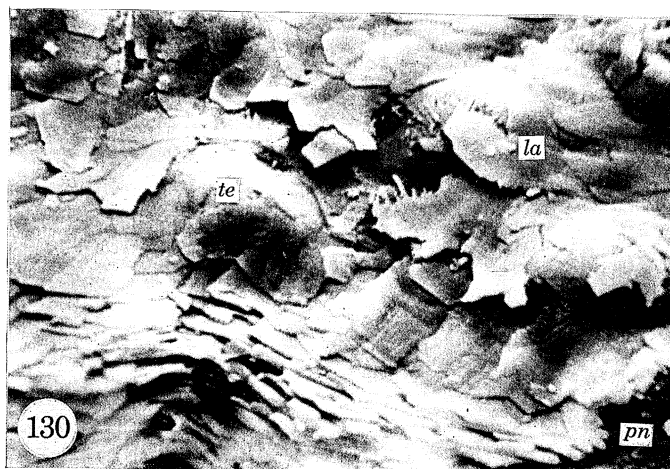
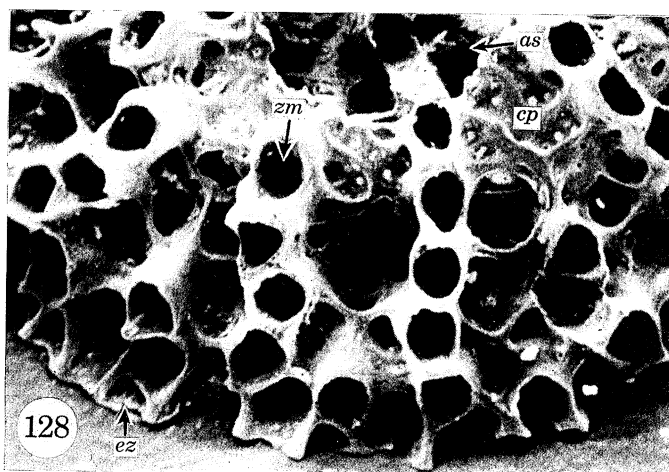
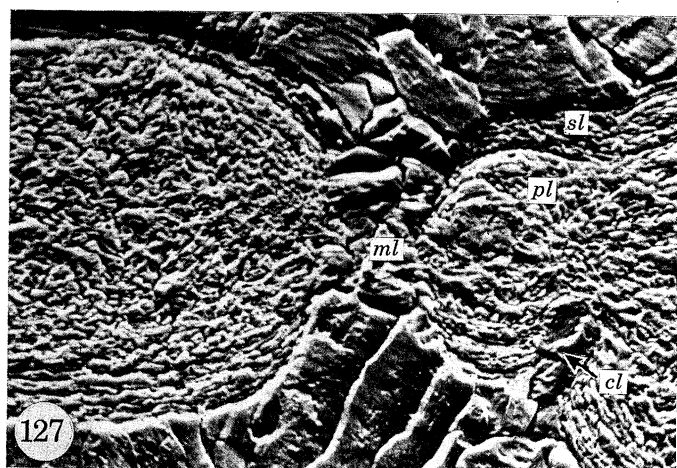
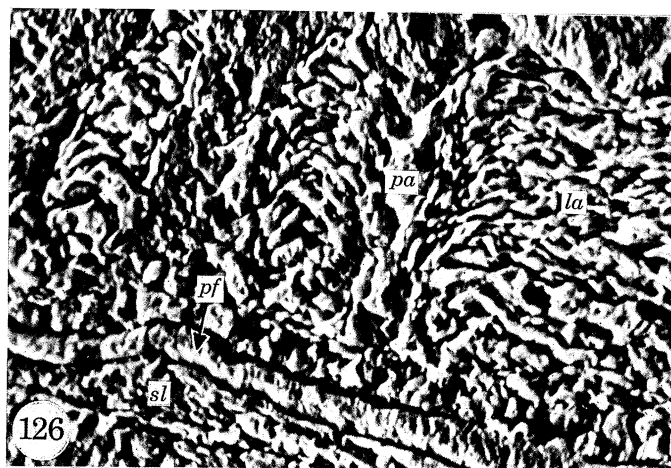
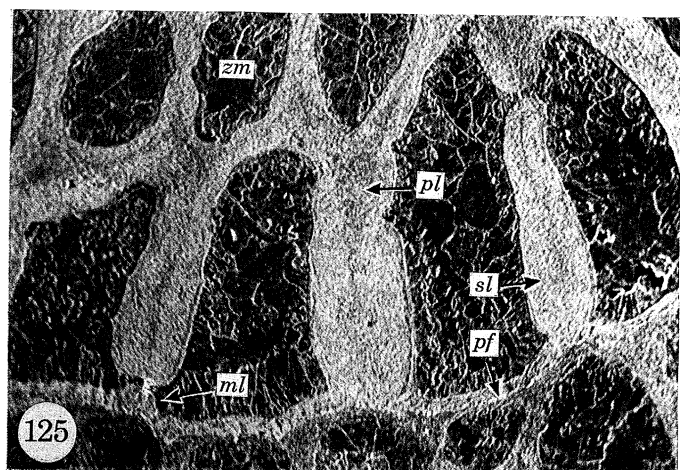
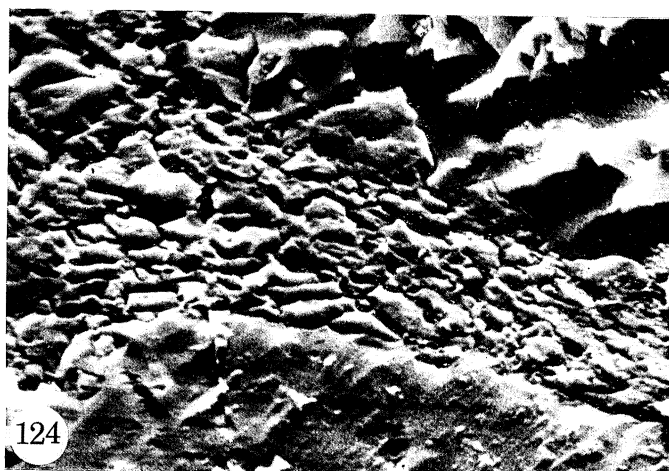
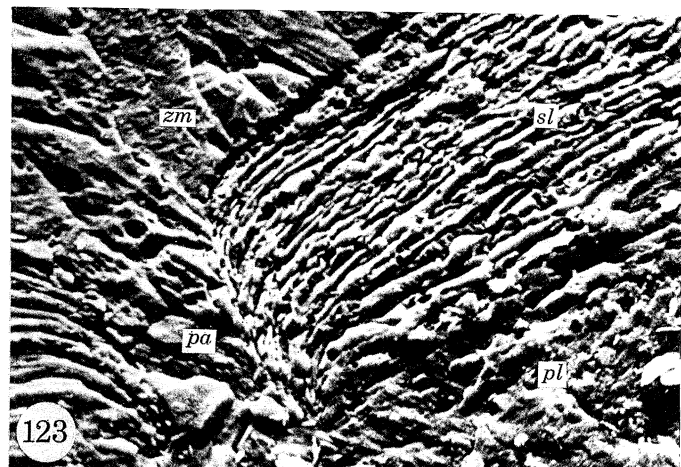
FIGURE 127. Transverse section of zooecial wall showing a mural pore and a canal penetrating the secondary layer ( $\times 1200$ ).

Scanning electron micrographs of the zooecia of *Lichenopora radiata* (Audouin), Plymouth, England:

FIGURE 128. View of part of a colony showing the relationship between zooecia and alveoli ( $\times 100$ ).

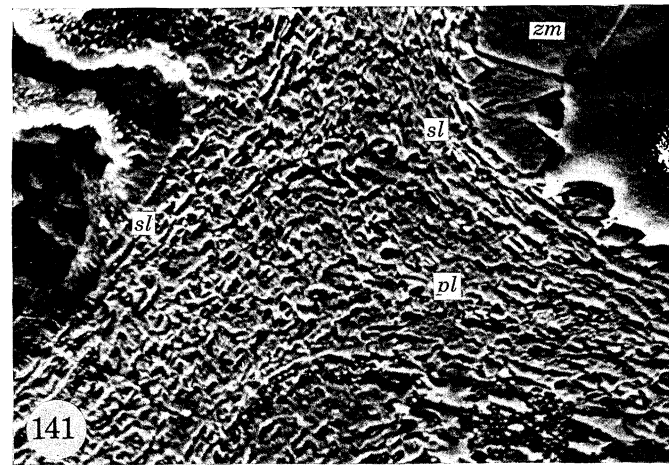
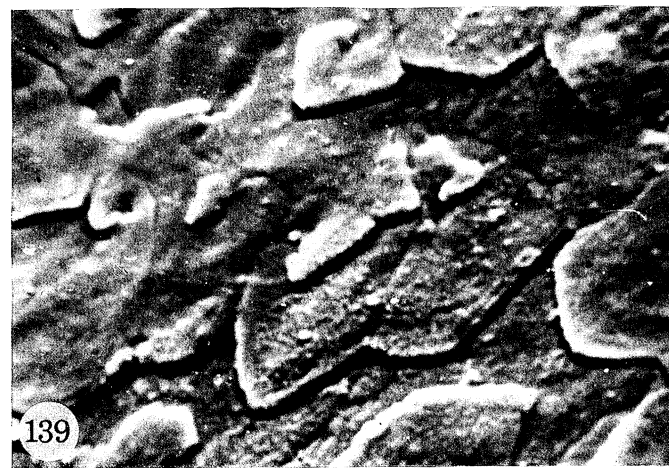
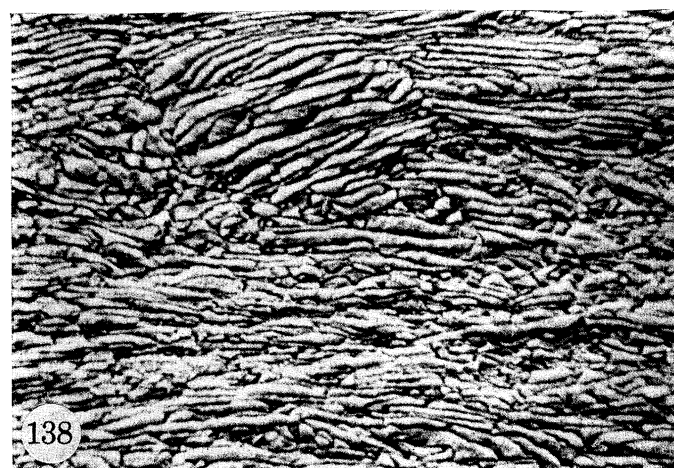
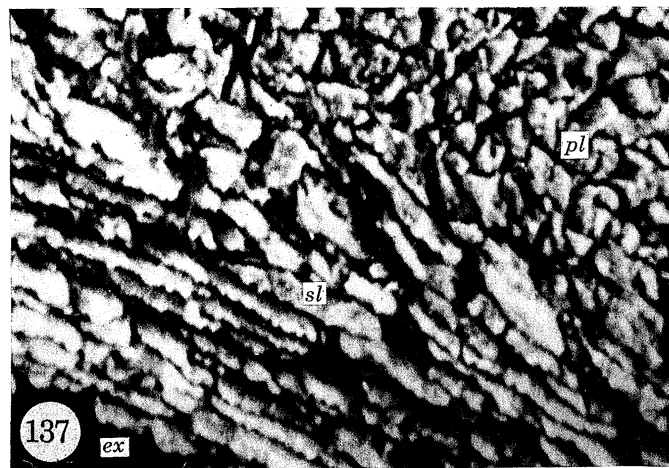
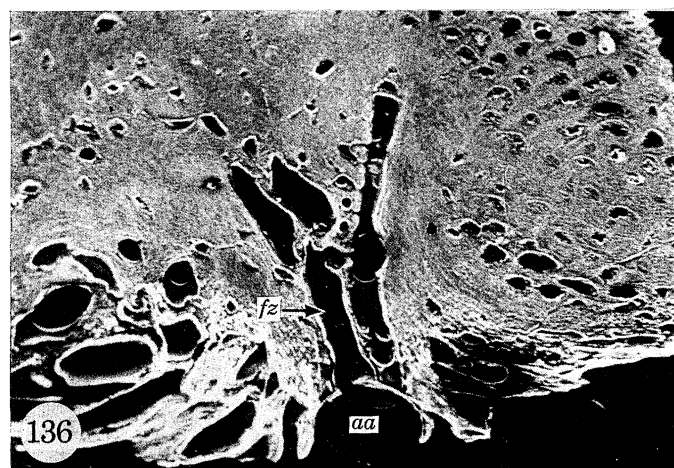
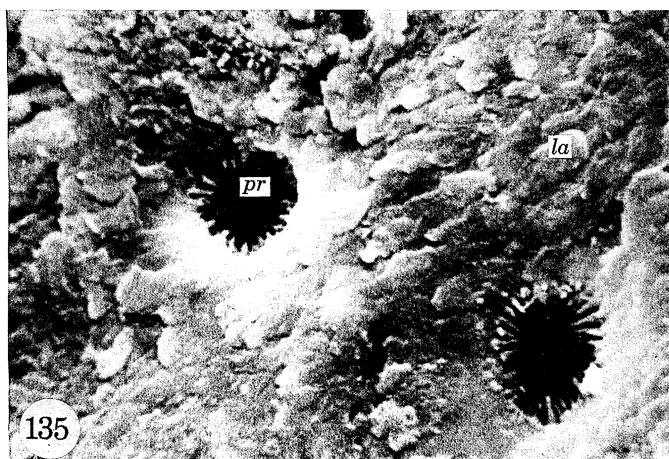
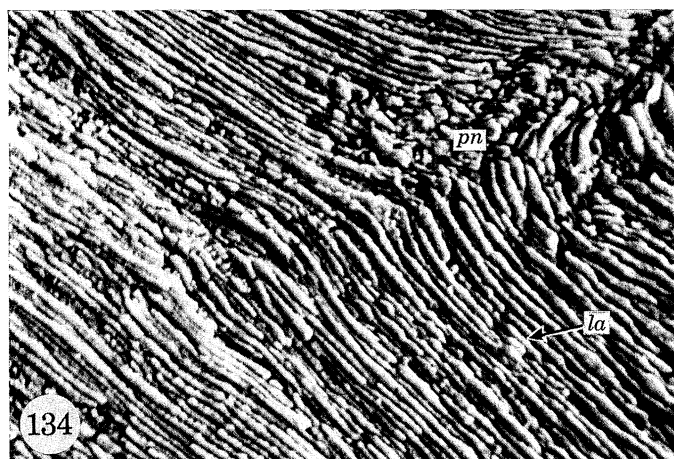
FIGURE 129. Section of the base of a colony showing the carbonate succession ( $\times 2700$ ).

FIGURE 130. View of the internal surface of zooecium showing the tubercles associated with pseudopuncta ( $\times 2700$ ).



FIGURES 123 TO 130. For legends see facing page.





FIGURES 134 TO 141. For legends see facing page.

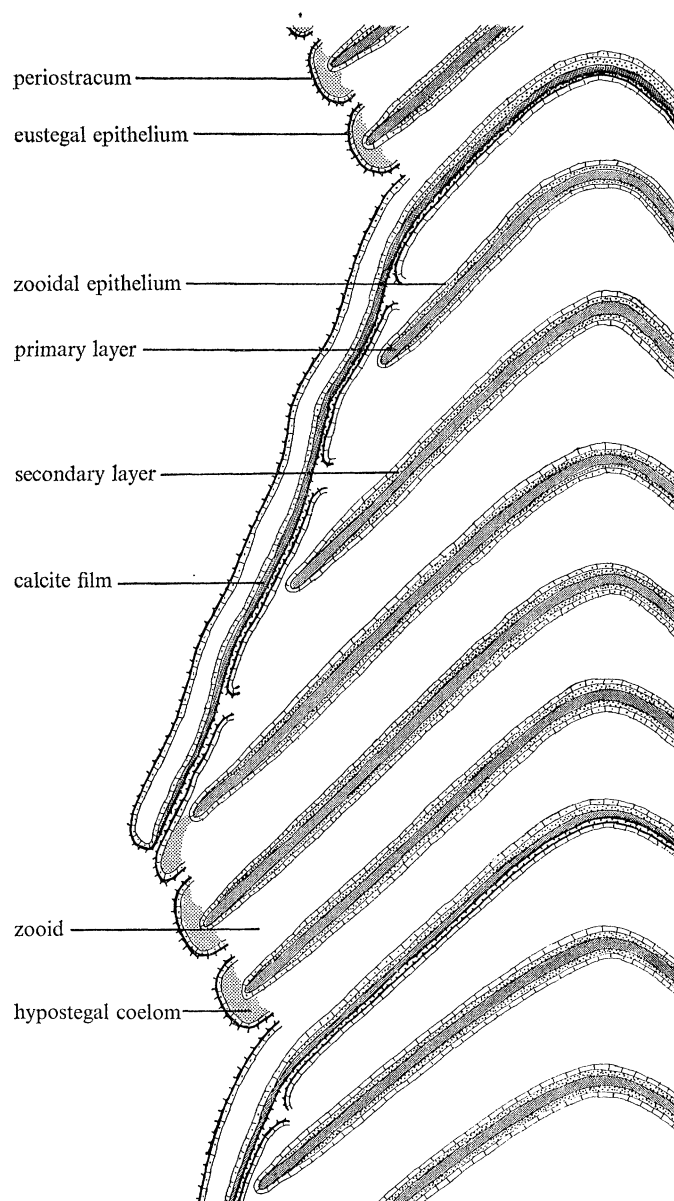


FIGURE 131. Diagram showing the arrangement of secretory epithelium in relation to the skeleton of *Terebellaria* as seen in sagittal section.

#### DESCRIPTION OF PLATE 23

Scanning electron micrographs of *Lichenopora radiata*:

FIGURE 134. Section of the secondary layer of the basal wall showing the structure of a pseudopunctum ( $\times 2700$ ).

FIGURE 135. External surface of an alveolar partition showing pores ( $\times 2700$ ).

Scanning electron micrographs of *Hornera frondiculata* (Lamouroux), off Malta:

FIGURE 136. Medial section of the base of a colony showing the arrangement of the first formed zooecia ( $\times 65$ ).

FIGURE 137. Section of a branch showing the skeletal succession ( $\times 6800$ ).

FIGURE 138. Section of a branch showing the development of laminae in the secondary shell ( $\times 2700$ ).

FIGURE 139. Internal surface of a zooecium showing the presence of tabular laminae in attitudes of spiral growth ( $\times 6800$ ).

FIGURE 140. External surface of a branch showing overlapping fibres of the secondary shell ( $\times 2600$ ).

FIGURE 141. Scanning electron micrograph of a section of *Bicavea urnula* (d'Orbigny) from the Cretaceous (Upper Chalk), Chatham, England ( $\times 1200$ ).

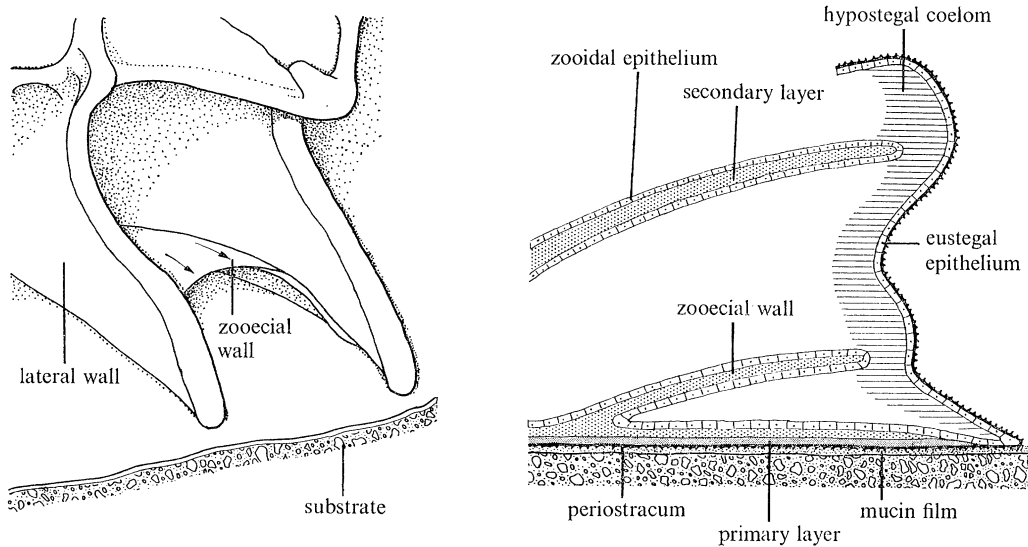


FIGURE 132. Diagram showing the skeletal differentiation of a newly formed zooid at the growing edge of *Lichenopora*.

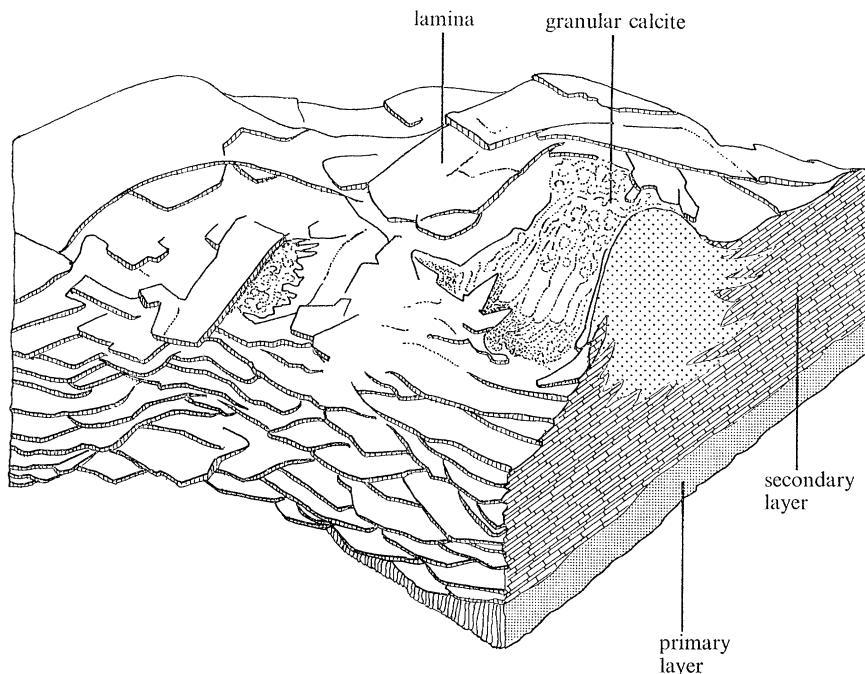


FIGURE 133. Diagram showing the structure of a pseudopunctum in the secondary shell of *Lichenopora*.

The structure of the zooecia between successive primary carbonate films indicates that they behaved as members of a single fascicle bounded distally by periostracum with eustegal epithelium (figure 131). Each zooecial wall within a fascicle consists of a medial layer of primary granular calcite flanked by fibrous secondary shell. Such walls must have been secreted within folds of hypostegal epithelium originating as invaginations from the colonial base. The carbonate film was, therefore, the visible part of the floor of the colony which extended from the base

as a continuous helicoidal strip and supported rows of zooids all growing towards the outer side of the spiral. *Terebellaria* is, therefore, much more like rectanguloids than tubuloporoids, and its systematic position should be reconsidered.

(2) *Rectanguloid, cancelloid and cerioporoid zooecia*

Secretion of an entire calcareous colony apart from its foundation within folds of basal epithelium has already been alluded to as characteristic of *Lichenopora*, *Hornera* and *Heteropora*. These genera are representatives of the Rectanguloidea, Cancellioidea and Cerioporoida respectively and this mode of secretion has been confirmed in related fossil and living species.

In *Lichenopora radiata* (Audoin) from Plymouth (figure 128, plate 22), the primary shell is restricted to a narrow zone succeeding the basal periostracum, presumably with binding mucopolysaccharide attaching the colony to the substrate. Here it is a sharply delineated layer, averaging 1.6  $\mu\text{m}$  in thickness and composed of vertically stacked calcitic granules usually about 200 nm wide and up to 1  $\mu\text{m}$  long (figure 129, plate 22).

The remaining carbonate part of the colony, including radiating rows of zooecia and convex partitions defining coelomic spaces (alveoli) in the intervening sectors (figure 128, plate 22), consists exclusively of a variable secondary shell (figure 132). The first few micrometres is usually composed of blades averaging 500 nm and 6  $\mu\text{m}$  in thickness and width respectively. In section, the blades are normally horizontally arranged and like all laminae segregated from one another by protein sheets about 10 nm thick; in surface view they are either parallel to one another or, more rarely, randomly disposed. The rest of the secondary layer is dominated by more regular laminae averaging 380 nm in thickness and consisting of blades about 5  $\mu\text{m}$  wide and overlapping at intervals of between 6 and 12  $\mu\text{m}$  (figures 130 and 135, plates 22 and 23). Concentric ridges with a periodicity of 300 nm and rarer screw dislocation figures, confirm their spiral growth. The laminar successions may pass laterally and vertically into granular calcite, occurring as nodules or, more commonly, as fine crystallites in various stages of accretion.

Internal surfaces of zooecia are studded with subconical tubercles about 5  $\mu\text{m}$  in height and basal diameter (figure 130, plate 22). The tubercles have a core of granular calcite passing peripherally into laminae (figure 133; figure 134, plate 23). This relationship and the inwardly convex disposition of surrounding laminae recall the calcitic rods (taleolae) associated with the pseudopuncta found in articulate Brachiopoda (Williams 1968, p. 39).

The frontal and lateral surfaces of the colonies are also pierced by subcircular pores at intervals of about 15  $\mu\text{m}$  (figure 135, plate 23). The pores have a mean diameter of 7  $\mu\text{m}$  and are constricted by centripitally arranged spines. They afford connexion between the hypostegal coelom and the alveoli and zooidal interiors. In that respect the pores are different from the canals characteristic of other cyclostomes.

No rectanguloid fossil species have been examined, but since *Lichenopora* is the longest ranging member of the superfamily no radical changes in skeletal structure are likely ever to have occurred.

Living and fossil species belonging to the Horneridae and Cytididae respectively, the two most important families of the Cancellioidea, have been investigated and indicate a survival of a similar skeletal fabric from Jurassic to Recent times.

*Hornera frondiculata* (Lamouroux) off Malta grows as branched colonies with each branch comprising erect autozooids connected to one another by a network of transverse and longitudinal walls defining chambers which communicate externally by narrow slits (figure 142).



Primary shell forms the base of the colony (figure 136, plate 23) and occurs as a medial layer, commonly about 3  $\mu\text{m}$  thick, throughout the entire skeleton (figure 137, plate 23). The texture is variably granular with calcitic grains about 350 nm across or, more commonly, coarse crystallites up to 2  $\mu\text{m}$  long which may be aligned normal to the shell boundaries. Except at zooecial edges, the primary layer permeating the branches is invariably sandwiched between two secondary layers (figure 138, plate 23) averaging 350 and 370 nm thick respectively, and seen on both surfaces as spirally arranged tablets with rhombic and dihexagonal corner angles (figure 139, plate 23) and concentric growth ridges with a mean periodicity of 160 nm. The internal primary–secondary boundary is much sharper than the external where a few rows of relatively coarse laminae are normally developed (figures 137 and 140, plate 23). Tubercles, varying from 20 to 120  $\mu\text{m}$  in diameter, are surface expressions of laminae outwardly arched in localized patches around granular cores. Contrary to Brood (1970, p. 192) these structures are typical pseudopuncta.

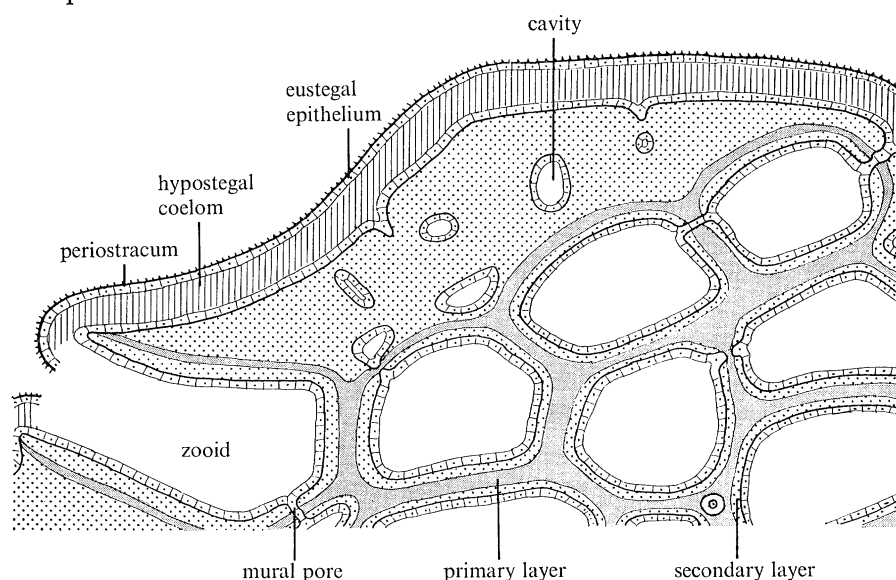


FIGURE 142. Diagram showing the arrangement of secretory epithelium in relation to the skeleton of *Hornera* as seen in transverse section: cavities within the skeleton represent extensions of the hypostegal coelom delineated by skeletal thickening.

#### DESCRIPTION OF PLATE 24

FIGURE 143. Scanning electron micrograph of a transverse section of *Homoeosolen ramulosus* (Lonsdale) from the Cretaceous (Upper Chalk), Chatham, England showing the skeletal succession ( $\times 1300$ ).

Scanning electron micrographs of the zooecia of *Heteropora* sp., The Antarctic:

FIGURE 144. Section of a zooecial wall showing the skeletal succession ( $\times 2800$ ).

FIGURE 145. View of the side of an aperture showing overlapping laminae of the secondary layer ( $\times 1400$ ).

FIGURE 146. Section of a zooecial wall showing keeled fibres of the secondary layer ( $\times 6800$ ).

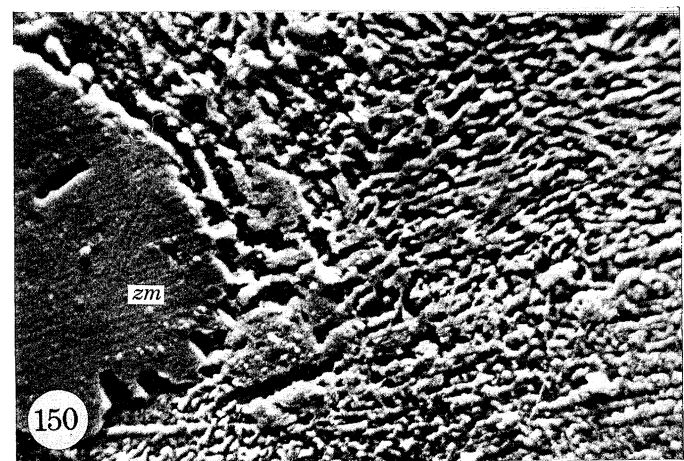
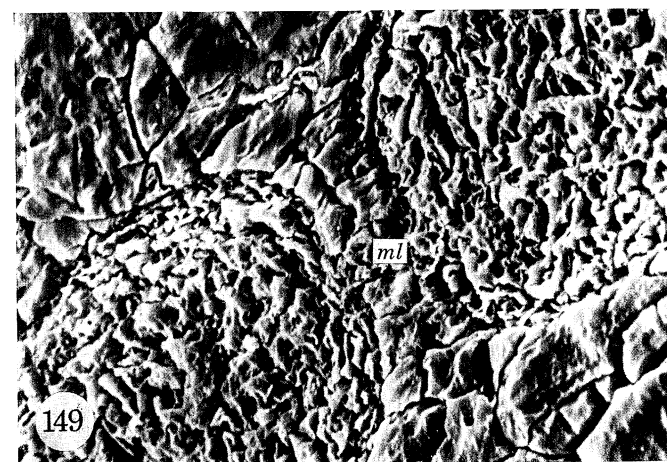
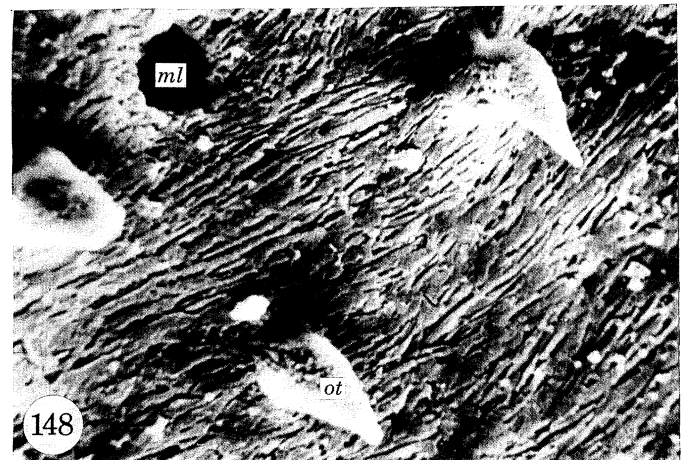
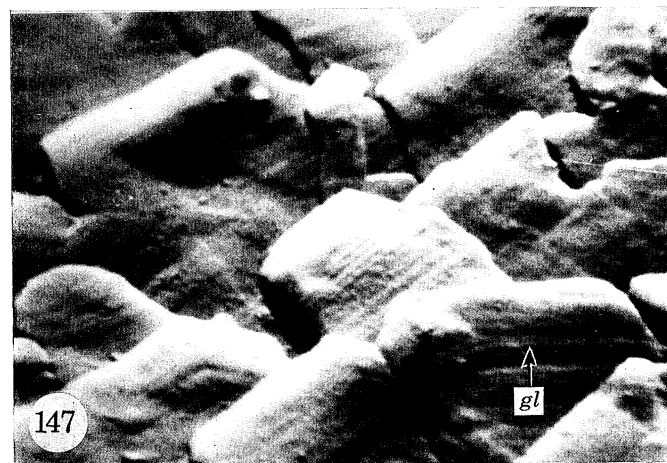
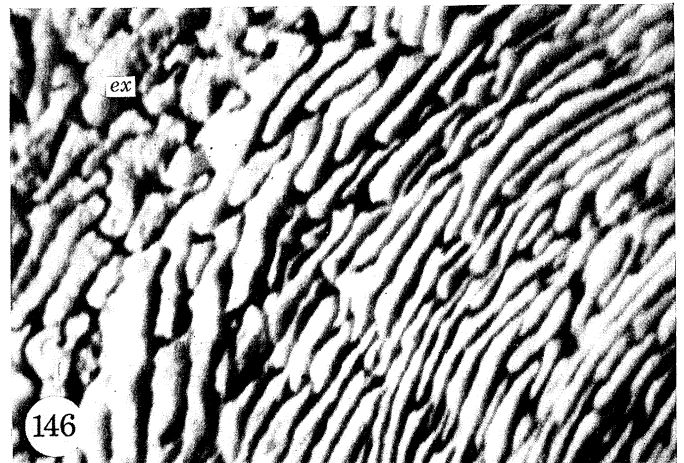
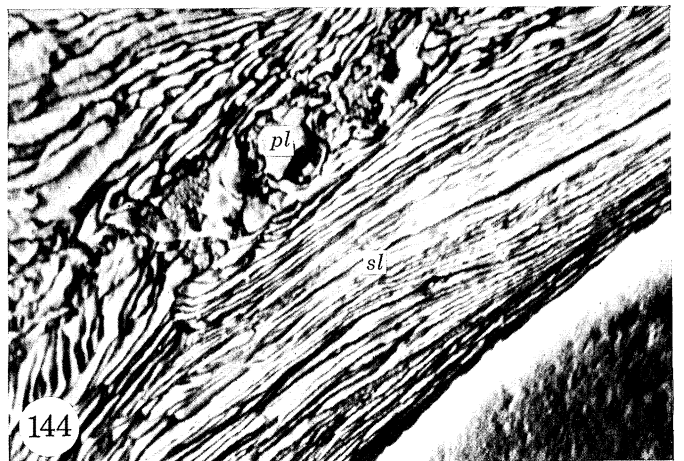
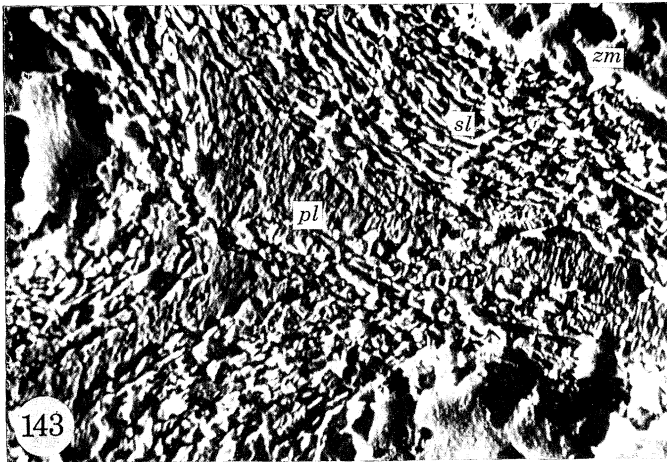
FIGURE 147. Internal surface of a zooecium showing overlapping fibres with growth lines ( $\times 6800$ ).

FIGURE 148. Internal surface of a zooecium showing a mural pore and hook-like outgrowths ( $\times 1500$ ).

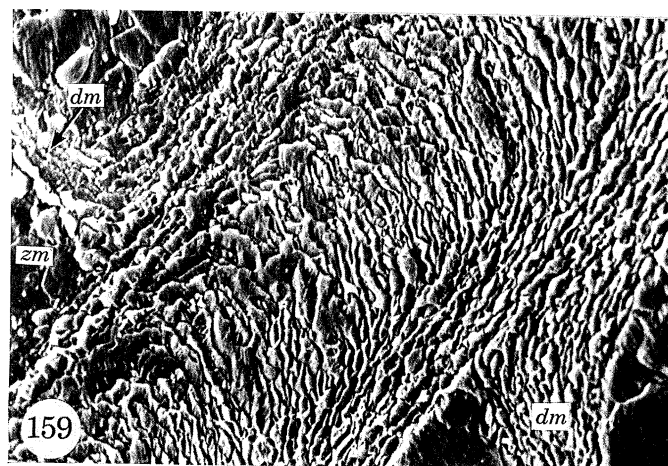
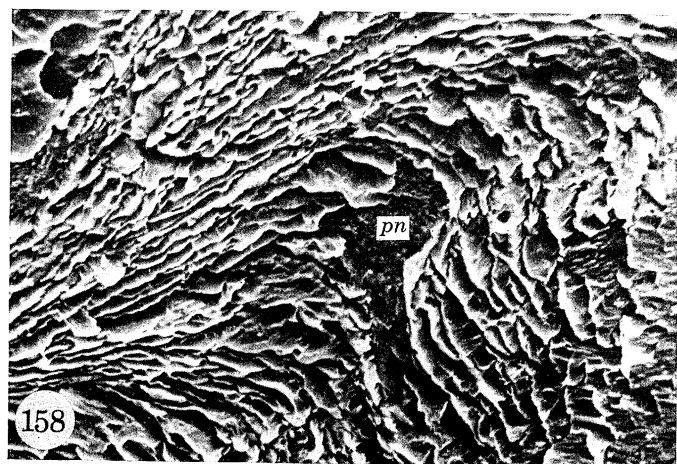
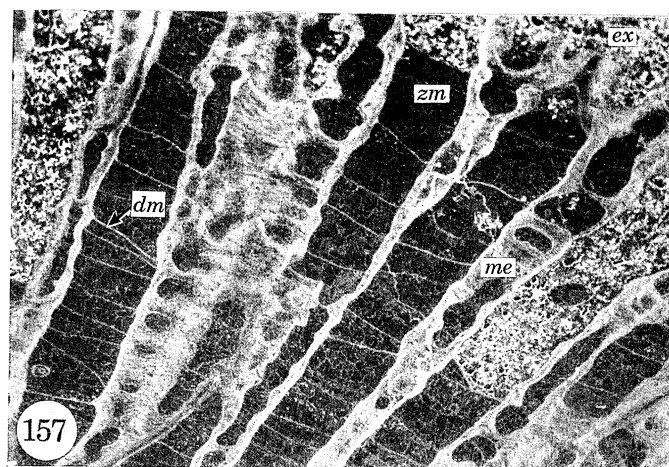
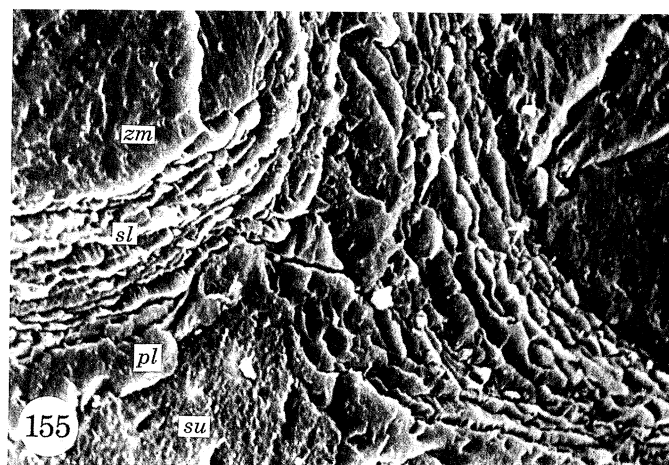
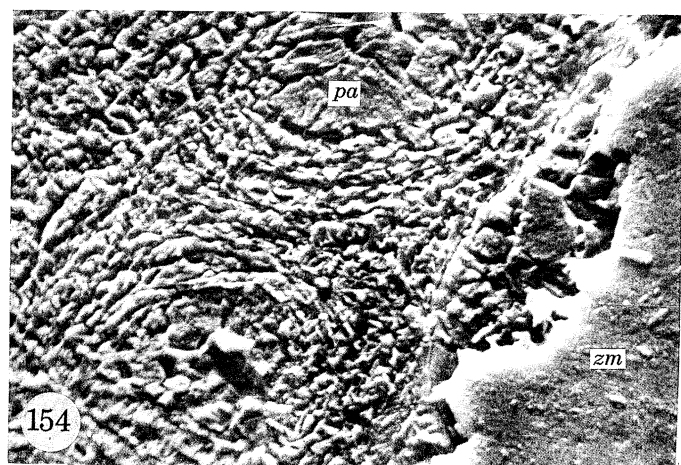
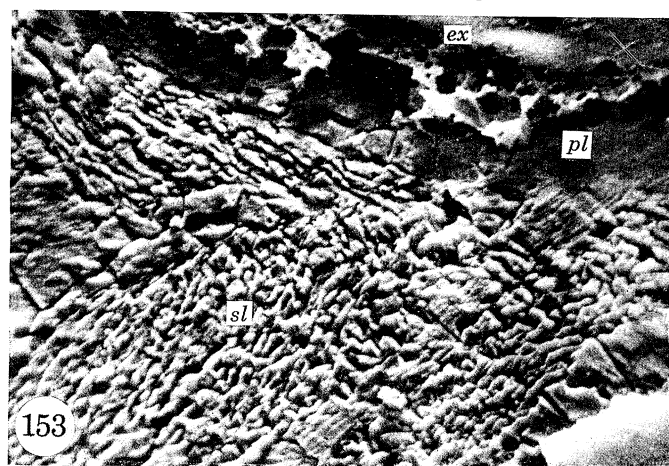
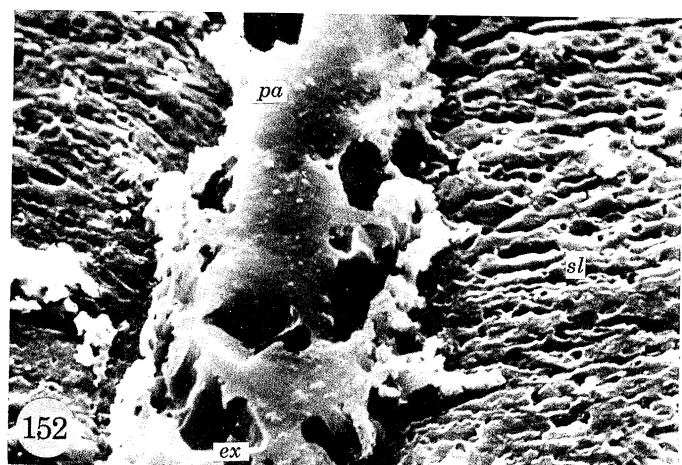
Scanning electron micrographs of fossil cyclostomes:

FIGURE 149. Section of a zooecial wall of *Heteropora* sp. from the Cretaceous (Upper Chalk), Chatham, England, showing mural pores ( $\times 2600$ ).

FIGURE 150. Section of a zooecial wall of *Hederella* sp. from the Devonian (Norway Point Formation), Michigan, showing silicified laminae ( $\times 650$ ).



FIGURES 143 TO 150. For legends see facing page.



FIGURES 152 TO 159. For legends see facing page.



The carbonate remains of the cytidids, *Bicavea urnula* (d'Orbigny), *Desmepora semicylindrica* (Roemer) and *Homoeosolen ramulosus* (Lonsdale), all from the Cretaceous (Upper Chalk) of England, were secreted in the same way as *Hornera*. In all three, a well-developed primary layer consisting of granules or prisms of calcite, occurs medially in interzoecial walls. The secondary layer is laminar, although the laminae are mainly tabular with a mean thickness of 400 nm in *Bicavea* (figure 141, plate 23), and fibrous and occasionally keeled in *Desmepora* and *Homoeosolen* (figure 143, plate 24) with average thicknesses of 800 and 840 nm respectively. The external surfaces of all colonies are usually recrystallized, but traces of laminae survive sporadically indicating secretion by an external epithelial sheet. Confirmation of this relationship is found in the way mural tubes (nematopores), permeating the colony, affect the arrangement of laminae. Towards the external surface, the laminar edges defining these tubes are directed inwardly, and laminae between them are gently convex outwards in section. Such a disposition could only have been brought about by secretory epithelium migrating outwardly.

Among the Cerioporoida, only an undescribed living species of *Heteropora* from the Antarctic has yielded trustworthy data on the carbonate succession of the colonial skeleton. Two fossil heteroporids, *Ceriopora spongites* Goldfuss and *Reptomulticava mammillata* (d'Orbigny) from the Cretaceous (Upper Chalk) of Chatham, England, were also studied. Sections of both species showed only a fabric of coarsely granular calcite which had probably been recrystallized. However, equally delicate skeletons of other cyclostomes from the same horizon and locality are sufficiently well preserved to reveal details of both primary and secondary shell which suggests that a primary succession of relatively coarse calcite crystallites was the sole mineral constituent of these heteroporids.

The primary shell is well developed throughout the colony of *Heteropora*, forming a medial layer, up to 14  $\mu\text{m}$  thick, in all zoecial walls (figure 144, plate 24) and emerging at the surface as low ridges delineating autozooid and heterozooid openings. It is composed of granules, up to 1  $\mu\text{m}$  in size, forming micritic mosaics on the ridges, and acicular crystallites, up to 3  $\mu\text{m}$  or more long, disposed at high angles to the primary-secondary boundaries.

The secondary shell lining zoecial walls (figure 145, plate 24), is typically laminar as first

#### DESCRIPTION OF PLATE 25

FIGURE 152. Scanning electron micrograph of a section of the secondary layer of *Clausa heteropora* (d'Orbigny) from the Cretaceous (Upper Turonian), Songe, France, showing a punctum ( $\times 2700$ ).

Scanning electron micrographs of the zooecia of *Meliceritites dollfussi* (Pergens) from the Cretaceous (Upper Chalk), Chatham, England:

FIGURE 153. Transverse section of the 'frontal' wall showing the skeletal succession ( $\times 1300$ ).

FIGURE 154. Transverse section of a zoecial wall showing puncta ( $\times 1300$ ).

Scanning electron micrographs of the zooecia of *Leioclema asperum* (Hall) from the Silurian (Wenlock Limestone), Dudley, England:

FIGURE 155. Section of the basal and lateral walls showing the skeletal succession ( $\times 2400$ ).

FIGURE 156. Section showing the junction between a diaphragm and a zoecial wall; distal to the left ( $\times 2600$ ).

FIGURE 157. Section showing the relationship between zooecia and mesopores ( $\times 65$ ).

FIGURE 158. Section of a zoecial wall showing a pseudopunctum ( $\times 2600$ ).

FIGURE 159. Scanning electron micrograph of a section of *Peronopora compressa* (Ulrich) from the Ordovician (Maysville Group), Cincinnati, Ohio, showing the structure of a zoecial wall and diaphragms; distal to the top right ( $\times 1200$ ).



noted by Boardman & Towe (1966, p. 20). The succession begins with a thin layer of relatively coarse, horizontal fibres about  $1\text{ }\mu\text{m}$  thick. These pass inwardly into regular fibre units, on average  $460\text{ nm}$  thick and  $3.2\text{ }\mu\text{m}$  wide, and commonly with an externally facing keel (figure 146, plate 24). The fibres are spirally disposed in overlapping rows (figure 147, plate 24) about  $3\text{ }\mu\text{m}$  apart and their exposed faces are terminated by dihexagonal corner angles. At intervals between  $15$  and  $75\text{ }\mu\text{m}$ , hook-like or rounded outgrowths, about  $13\text{ }\mu\text{m}$  in size, protrude into the zooidal interiors (figure 148, plate 24). They are composed of laminae and are an integral part of the secondary shell (see also Corneliussen & Perry 1970). Mural pores occur (figure 149, plate 24) and were well developed in the only fossil species of *Heteropora* studied, from the Cretaceous (Upper Chalk) of Chatham, England.

The carbonate succession of *Heteropora*, therefore, is consistent with the findings of Borg (1933, p. 260) that the colonial skeleton was secreted within epithelial folds, growing upwards and outwards from the base and secreting primary shell in continuity with the basal layer ahead of the secondary lining of laminae.

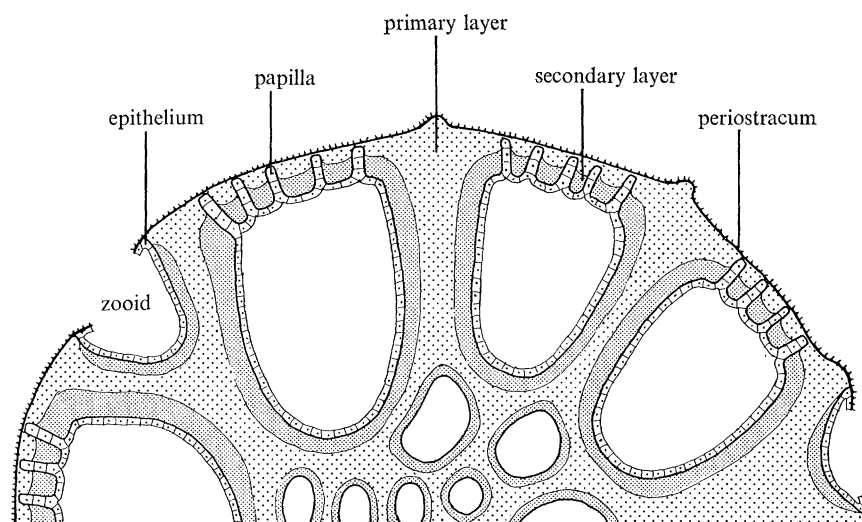


FIGURE 151. Diagram showing the arrangement of secretory epithelium in relation to the skeleton of *Meliceritites* as seen in transverse section.

### (3) *Hederelloid, dactylethroid and salpingoid zooecia*

The three remaining superfamilies assigned to the Cyclostomata are composed exclusively of extinct species so that the relationship between skeleton and secreting epithelium has to be inferred from carbonate successions. In all three, the skeletal fabric shows that zooecia were secreted in the same way as in *Crisidia* and not as coelocysts within epithelial folds as in *Lichenopora*.

The only representative available for study of the small problematic Palaeozoic group known as the Hederelloidea, was a partly silicified colony of *Hederella* sp. from the Devonian (Norway Point Formation) of Michigan. It was, however, possible to identify an external undifferentiated layer, presumably of primary granular calcite and traces of an inner layer of laminae, each between  $1.5$  and  $2.0\text{ }\mu\text{m}$  thick, which could represent replaced secondary shell (figure 150, plate 24). The succession, therefore, could have been deposited between an external periostracum and an eustegal epithelial lining.

Both the dactylethroid *Clausa heteropora* (d'Orbigny) and the salpingoid *Meliceritites dollfussi* (Pergens) from the Cretaceous (Upper Chalk) of Chatham, England, have well differentiated punctate skeletons. In *Clausa*, the autozooea are segregated from one another by clusters of smaller heterozooea (dactylethrae) each closed externally by a punctate wall. *Meliceritites* (figure 151) resembles cheilostomes in certain features including heterozooea which could have accommodated avicularia. In both species, however, the mode of secretion of the skeletal succession is determinable from sections.

In *Clausa*, the succession begins with primary granular calcite with constituents up to 8  $\mu\text{m}$  across. It forms an outer layer about 15  $\mu\text{m}$  thick well seen in the external punctate walls of the heterozooids, and a medial zone about 6  $\mu\text{m}$  thick in zooecial walls. The succeeding laminar secondary layer is composed of fibres, about 850 nm thick, commonly with crests directed externally. In the external walls of heterozooids, the fibres are deflected outwards around puncta which are about 7  $\mu\text{m}$  in diameter (figure 152, plate 25). The puncta must therefore have been occupied by papillose extensions of secretory epithelium lining the internal surface of the wall. Presumably, papillae made contact with periostracum covering the external surface as in *Crisidia* or *Berenicea*.

The shell structure of *Meliceritites* is similar. The granular primary layer, usually about 6  $\mu\text{m}$  thick, is conspicuous externally in gymnocyst-like walls (figure 153, plate 25) and within zooecial walls. The laminar secondary shell is composed of fibres (figure 154, plate 25), on average about 600 nm thick which are deflected outwardly in the walls of puncta piercing the gymnocysts. As in *Clausa*, the puncta (figure 154), typically about 7.5  $\mu\text{m}$  wide, must have accommodated papillose outgrowths of secretory epithelium, lining only the inner surfaces of the gymnocysts.

#### (c) *Structure of trepostome zooecium*

The Trepostomata are extinct Palaeozoic bryozoans characterized by the presence of pseudo-puncta (acanthopores), and by their long tubular zooecia divided into segments by transverse partitions (diaphragms). Both features were attended by modifications of the skeletal fabric, the former as in the cyclostomes *Lichenopora* and *Hornera*, the latter by deceleration in the rate of distal migration of maturing zooids. This deceleration occurred relatively suddenly at about the same stage in zooecial development, so that the entire colony can be divided into two zones: an endozone comprising the proximal immature parts with thin zooecial walls and widely spaced diaphragms secreted by rapidly migrating zooids, and an exozone composed of the distal mature parts with greatly thickened zooecial walls and crowded diaphragms deposited when distal shifts of zooids were comparatively small. There are differences between the skeletal fabric of the exozone and endozone, and neglect of the structure of the latter has been responsible for some past misunderstandings of trepostome skeletal successions.

The astogeny of trepostomes (Cumings 1912) was like that of cyclostomes. In particular, the attitude of the first-formed buds promoted the formation of a basal plate (basal lamina of Ryland 1970, p. 118) by which the colony was attached to the substrate. In life, the plate must have included an adhesive mucopolysaccharide film and periostracum underlying the mineral layers which alone survive as morphological components in fossils. In contrast to the complete skeletal succession of the basal plate, the zooecial walls lack medial breaks in the carbonate succession indicative of periostracal extensions and exhibit structures diagnostic of deposition within epithelial folds. Such folds could only have arisen as invaginations of basal epithelium growing independently of an outer covering of periostracum and eustegal epithelium which

arose at the edge of the basal plate. The model is homologous with that of cyclostomes like *Lichenopora*, and proof of it depends on being able to identify the basal plate within sections of trepostome colonies and determine the exact relationship between the plate and the zooecial walls. This is not usually possible, because most trepostome fossils consist of distal fragments of colonies, and the best chance of finding a basal plate is in encrusting species. Consequently the stenoporid *Leioclema asperum* (Hall) from the Silurian (Wenlock Limestone) of England has been used as the standard trepostome, although the zooecial tubes are shorter than in most other members of the Order.

Although secretion of zooecial tubes within folds of basal epithelium is most easily visualized in encrusting species, there is evidence to confirm that carbonate skeletons of all trepostomes were deposited in this way. Variation in colonial growth is even greater among trepostomes than cyclostomes because it includes bifoliate species in which the basal plate is extended distally as a doubled medial frame supporting zooecia on either side, as well as ramose forms with a comparatively small basal plate acting as a disk of attachment for the main stem of the colony as in the cyclostome *Hornera*. These changes in proportion and orientation of the basal plate did have structural repercussions especially among bifoliate species which are represented in this study by the monticuloporida *Peronopora compressa* (Ulrich) from the Upper Ordovician of Ohio.

A third species requiring special consideration is *Constellaria constellata* (Van Cleve), also from the Upper Ordovician of Ohio, because the endozonal structure of this stock is sufficiently different from that of other Trepostomata to warrant reconsideration of the proposal by some bryozoologists that the genus be transferred to the Cystoporata.

Apart from the three genera mentioned above, eight others have been investigated. They belong to eight of the ten families recognized within the Order, and the close concordance of their skeletal ultrastructure suggests that, in respect of zooecial secretion, they may be regarded as typical of all trepostomes.

#### (1) *Leioclema zooecium*

The growth habit of *Leioclema* is variable, but *L. asperum* (Hall) is an encrusting form and the basal plate is well developed as a foundation for the entire colony. The plate is, on average, 10  $\mu\text{m}$  thick and consists of nodular or irregular bodies of calcite (figure 155, plate 25). The plate has probably undergone recrystallization and the absence of any original textures suggests that, in life, it lacked an organic framework and was composed of crystallites secreted as epitaxial aggregates.

The primary shell of the plate is succeeded by a laminar secondary layer composed of fibres with an average thickness of 750 nm. In the plate, the fibres are arranged horizontally, parallel to the internal surface of secretion (figure 155). In zooecial walls, however, the medial continuation of primary shell wedges out distally, usually within 25  $\mu\text{m}$  of the basal layer. Thereafter the medial zone of the walls is composed of curved secondary fibres which are interleaved with one another to form a succession of outwardly convex arches subtended between two lateral layers of fibres disposed parallel to the internal surfaces of the interzooecial walls (figure 156, plate 25). No cores of non-fibrous calcite yet have been found in these distal parts of the zooecial walls.

The diaphragms connecting zooecial walls are more closely spaced in the exozone where they may be only 50  $\mu\text{m}$  apart (figure 157, plate 25). They are 1.5  $\mu\text{m}$  thick on average and usually consist of two or three layers of horizontally disposed fibres (figure 156, plate 25). In all

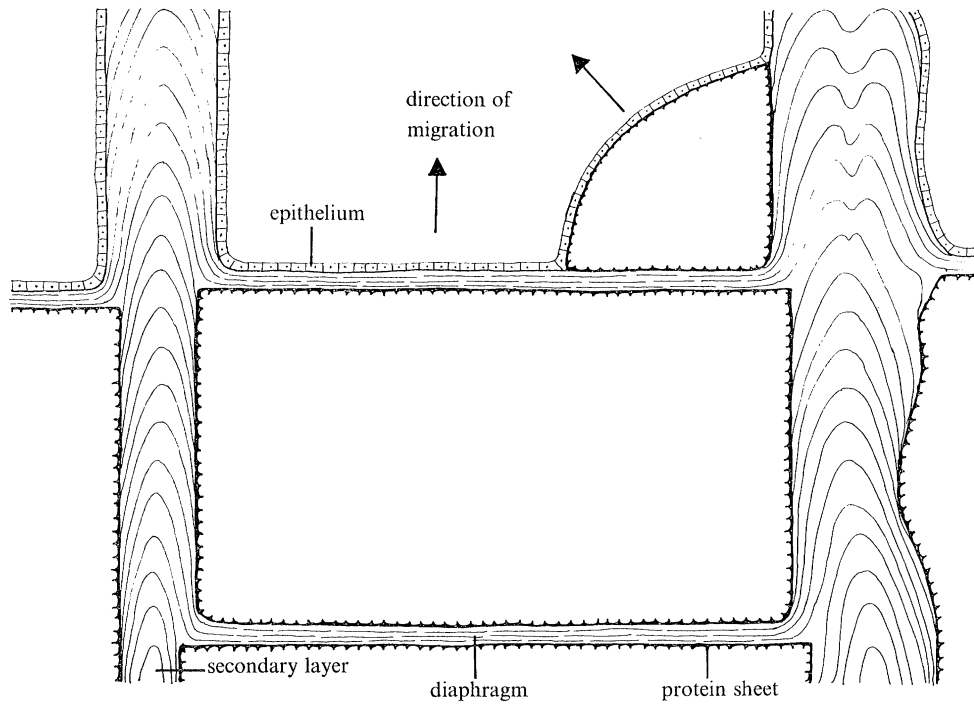


FIGURE 160. Diagram showing the origin of a cystiphragm and diaphragm in the trepostome zooecium.

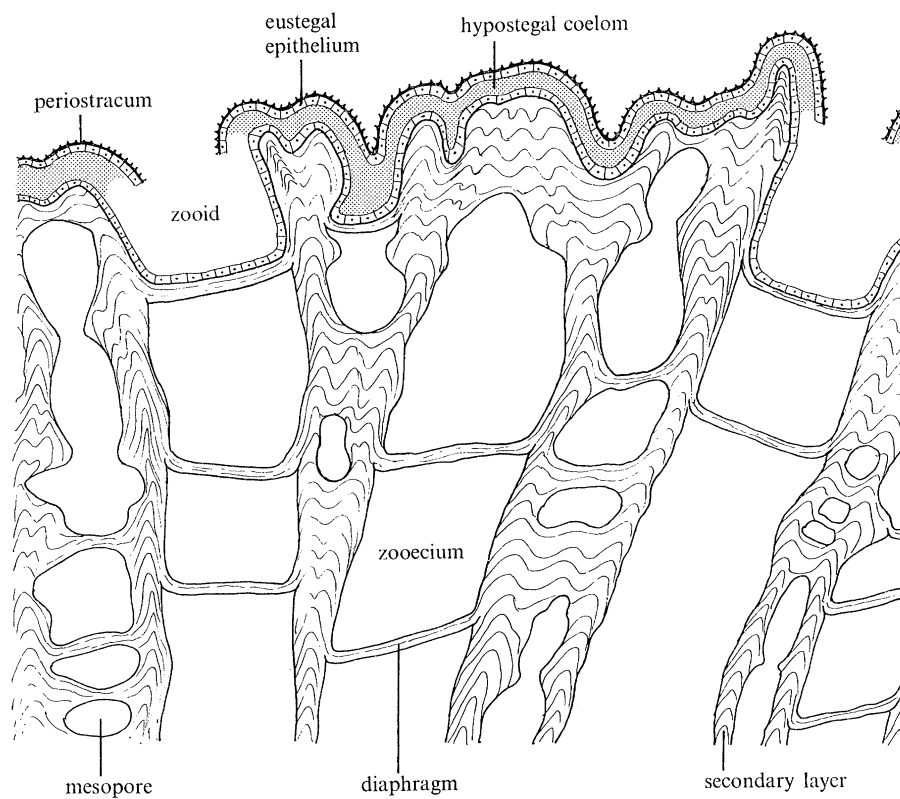


FIGURE 161. Diagram showing the arrangement of secretory epithelium in relation to the skeletal exozone of *Leioclema* as seen in longitudinal section.



trepostomes examined, the relationship between a diaphragm and its bounding zooecial walls is the same in two respects (figure 160). First, the proximal surface of the diaphragm joins the zooecial wall at sharp, high angles, whereas the distal one grades tangentially into the internal surface of the wall. Secondly, the wall distal of the diaphragm is thicker than its proximal counterpart by an amount equivalent to the thickness of the diaphragm.

Two other features merit mention. Zooecia are commonly separated by small heterozooecial tubes (mesopores) bearing rare diaphragms and, more frequently, shelf-like constrictions at intervals of about 7  $\mu\text{m}$ , which give the tubes a beaded appearance in section (figure 157, plate 25). Equally conspicuous are acanthopores (figure 158, plate 25) distinguishable within the zooecial walls as slightly flexured cylindroid bodies about 10  $\mu\text{m}$  in diameter. They are composed of irregular granules of calcite which pass peripherally into outwardly pointing laminae arranged around the acanthopore in cone-in-cone successions.

These morphological features are consistent with the secretion of the *Leioclema* skeleton within folds of basal epithelium (figure 161). The outwardly convex fibres of the zooecial walls and those around acanthopores could only have been deposited by epithelium lining distal surfaces of the colony and simultaneously secreting protein and calcite of spirally disposed fibres. The acanthopores are reasonably homologized with the pseudopuncta of certain brachiopods like the Strophomenida and, as has been inferred for them, may have acted as supports for muscle ties.

Deposition of diaphragms is best considered in the light of researches into the movement of mantle relative to the brachiopod shell. In living brachiopods movement of the mantle is preceded by deposition of a continuous protein sheet which acts both as a 'slide' for the translation of the mantle, and as a seeding sheet when the mantle resumes carbonate secretion. Consequently, it is likely that immediately before a zooid shifted distally within its zooecial tube, a protein film was exuded between the secretory epithelium and the zooecial walls (figure 160). The zooid then migrated forward in one movement and, before carbonate deposition was resumed, the basal part of the epithelial cover must have secreted a transverse organic membrane, which sealed off that segment of the zooecial tube just vacated by the proximal part of the zooid, and also acted as a seeding sheet for the secretion of the mineral constituents of a diaphragm. Curved plates grouped like calcareous blisters around zooecial walls (cystiphragms), which are found in many trepostomes including *Peronopora* and *Prasopora* (figures 166 and 167, plate 26), developed in the same way. The partial segmentation of the mesopores, however, originated quite differently because each constriction was formed by the centripetal growth of a circular ridge secreted within a continuous fold of the epithelium lining the internal walls of the mesopore.

## (2) *Peronopora zooecium*

Colonies of *Peronopora compressa* (Ulrich) grew upright as a bifoliate convoluted frond. Basal attachments are rarely collected and were not available for study, but their structure can be inferred from fragments of the frond. In this part of the colony, two sets of oppositely facing zooecia and mesopores are separated from each other by a medial wall (mesotheca). The zooecial walls, diaphragms and related cystiphragms are exclusively composed of a secondary fibrous shell except for granular calcite forming the cores of acanthopores, which may be only 7  $\mu\text{m}$  in diameter. The fibres are lenticular or crested in transverse section and are, on average, 2.7  $\mu\text{m}$  wide and 1  $\mu\text{m}$  thick. In the diaphragms, cystiphragms and zooecial walls, the fibres

are disposed in the same way as in *Leioclema* (figure 159, plate 25). The mesotheca, however, which is usually about 15  $\mu\text{m}$  thick, consists of two constituents because, among flat-lying secondary fibres, occur lenses of calcite up to 6  $\mu\text{m}$  thick also arranged parallel with the mesotheca (figure 162, plate 26). These lenses constitute a discontinuous layer within the mesotheca. They are probably traces of the primary layer of the basal attachment area, although there are no breaks in the mesothecal fabric indicating the presence of periostracum. Consequently, the mesotheca is not bilamellar in the sense that it represents a tight fold of the basal plate. Presumably it was deposited within a medial fold of basal epithelium growing distally and periodically reverting to the secretion of primary shell in the same way as the epithelial fold containing the transverse wall of *Umbonula* (Tavener-Smith & Williams 1970, p. 249).

### (3) *Constellaria zooecium*

Although the ultrastructure of the base of *Constellaria constellata* is unknown, sections of distal fronds indicate that the genus differs from typical trepostomes in its skeletal fabric. Acanthopores were not seen, although they are known in other species (Ross 1963, p. 52), and the mesopores which are thin-walled and partitioned by diaphragms, are clustered together to form a vesicular tissue segregating groups of zooecia from one another. More importantly the zooecial walls consist of two contrasting fabrics especially in the exozone. Here, identifiable secondary shell, consisting of flat-lying fibres averaging 800 nm in thickness forms two lateral layers separated by a medial shell of massive or granular calcite about 3  $\mu\text{m}$  wide (figure 163, plate 26). In the endozone, smaller deposits of granular calcite may be conspicuous only in the junctions of zooecial walls where they swell out into rods about 9  $\mu\text{m}$  across, although even in walls 4  $\mu\text{m}$  thick a medial layer of granular calcite can usually be identified.

The presence of a layer of granular calcite as the framework for the fronds of *Constellaria* is reminiscent of the way primary shell permeates the colony of the cyclostome *Heteropora* and is, therefore, considered to form a network of primary shell extending from the basal plate.

The other significant difference is the sporadic occurrence of breaks in the zooecial walls of *Constellaria*. These breaks may be up to 7  $\mu\text{m}$  across and, although they bear evidence of having been affected by the crystallization of the matrix (figure 164, plate 26), they are likely to have been pores connecting zooecial chambers before diagenesis began. If this is so, the breaks are identical with the mural pores of the Cystoporata, and may be diagnostic of a close relationship between that Order and *Constellaria*.

### (4) *Other trepostome zooecia*

Study of the skeletal fabric of five other trepostome species (*Batostoma implicatum* (Nicholson), *Hallopora ramosa* (d'Orbigny) and *Heterotrypa frondosa* (d'Orbigny) from the Upper Ordovician of Ohio; *Prasopora grandis* (Ulrich) from the Upper Ordovician of Minnesota; and *Trematopora tuberculosa* (Hall) from the Middle Silurian of New York) confirms the representative nature of the structures just described.

In all species a secondary shell of fibres, varying in thickness from 600 nm in *Trematopora* to 1  $\mu\text{m}$  in *Prasopora* (figure 168, plate 26) is the dominant or exclusive fabric of zooecial walls and diaphragms. The only layer occurring in the distal parts of colonies, which is comparable with the primary shell of *Constellaria*, is a more or less continuous partition of granular calcite, between 2 and 4  $\mu\text{m}$  thick, developed medially in the zooecial walls of *Trematopora* (figure 165, plate 26). The medial zone of zooecial walls of *Batostoma* (figure 169, plate 26) is also superficially

like the primary layer of *Constellaria* (Ross 1964, p. 944); but its constituents are mostly finely granular grading into fibres indistinguishable from those of the secondary layer. This structural gradation is similar to that found in *Hallopora* and affirms the rejection by most bryozoologists (Boardman 1960, p. 26) of a segregation of the Trepostomata into two subordinal groups; one (Amalgamata) with undifferentiated zooecial walls; and another (Integrata) with zooecial walls divided into two discrete parts by a medial dark line 'representing probably remains of animal matter' (Bassler 1953, p. G. 92). The zooecial walls of *Hallopora* (figure 170, plate 27) which, together with *Batostoma* and *Trematopora*, has been classified as an 'integrate' trepostome, consist exclusively of laminar secondary shell with laterally placed constituents averaging 850 nm in thickness. Medially there is no trace of either primary shell or periostracal residue, although the laminae there, unlike their gently curving counterparts in the 'amalgamate' *Heterotrypa* (figure 172, plate 27) and *Prasopora* (figure 168, plate 26) are sharply arched distally and up to three times as thick as the lateral units. Changes in the disposition and dimensions of laminae are, therefore, as much responsible for the optical impression of a distinct medial sheet separating two normal laminated layers as the development of a primary layer. Such features are unrelated structurally and, being neither exclusive to the so-called 'Integrata' nor constantly developed within the same colony, are of no taxonomic importance.

In the structure of other features, like mesopores, diaphragms and cystiphragms which are especially characteristic of *Prasopora* (figures 166 and 167, plate 26), all species are closely comparable. Acanthopores are more variable in distribution, being well developed in *Heterotrypa* and *Prasopora* with non-fibrous cores up to 20 µm in diameter but rare in the specimens of *Batostoma* and *Hallopora* (figure 171, plate 27).

(d) *Structure of cystoporate zooecium*

The Order Cystoporata was established by Astrova (1964) to accommodate Palaeozoic species, allegedly alike in a unique combination of features that distinguishes them from contemporaneous bryozoans. The species belong to two groups of families, the Ceramoporidae and Fistuliporidae, and the Constellariidae and Dianulitidae, which had previously been assigned to the Cyclostomata and Trepostomata respectively. In expatiating on the distinctiveness of

#### DESCRIPTION OF PLATE 26

FIGURE 162. Scanning electron micrograph of a section of the mesotheca of *Peronopora compressa* ( $\times 2500$ ).

Scanning electron micrographs of the zooecia of *Constellaria constellata* (Van Cleve) from the Ordovician (Maysville Group), Cincinnati, Ohio:

FIGURE 163. Section showing the skeletal succession in a zooecial wall ( $\times 2400$ ).

FIGURE 164. Section of a zooecial wall with a break believed to represent a mural pore ( $\times 2400$ ).

FIGURE 165. Section of the junction of zooecial walls of *Trematopora tuberculosa* (Hall) from the Silurian (Lower Rochester Shale), Lockport, New York showing the presence of primary shell ( $\times 2600$ ).

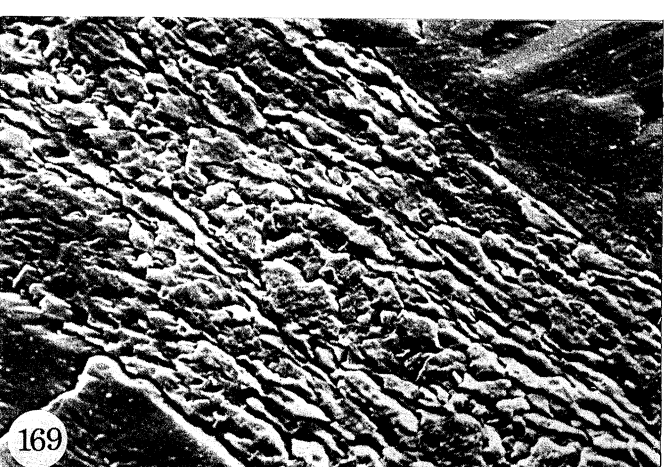
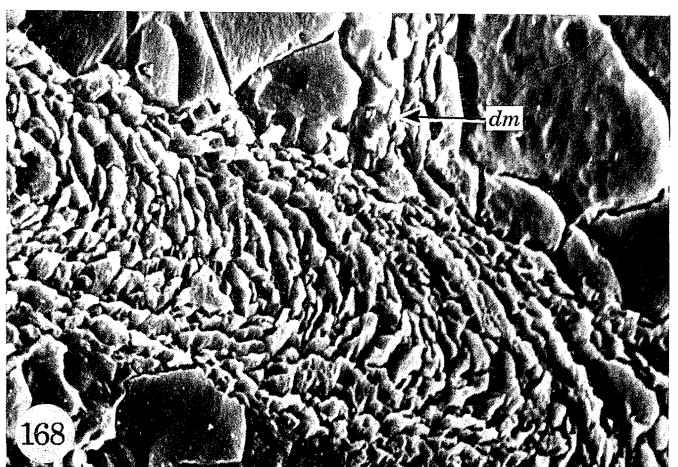
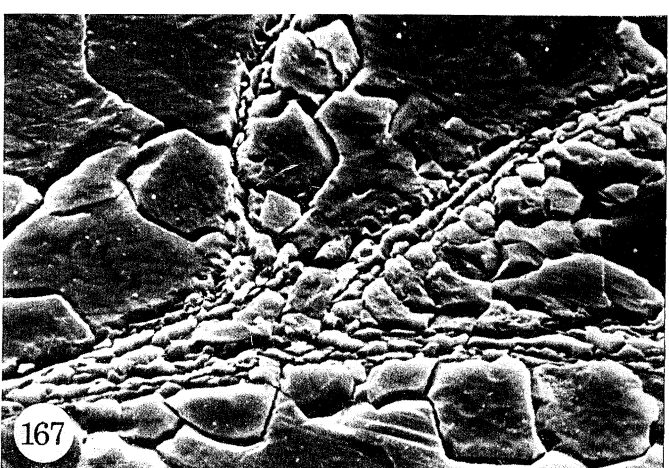
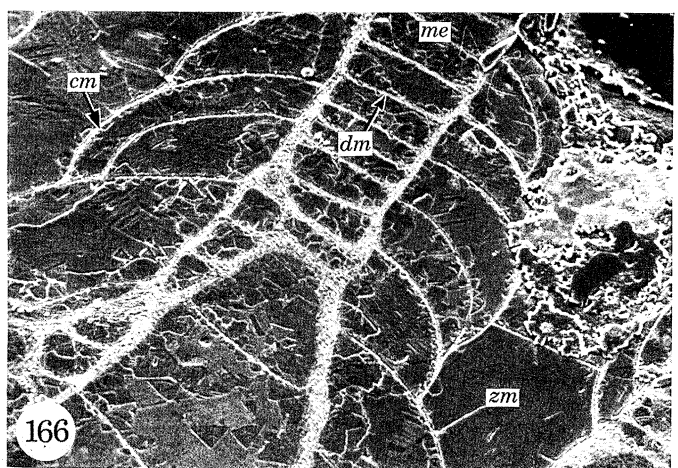
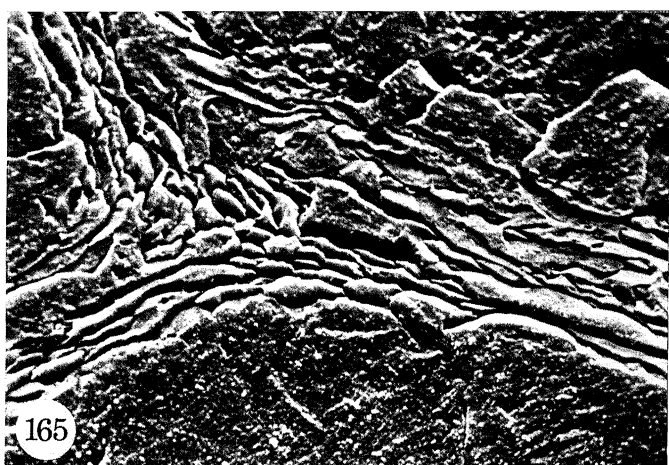
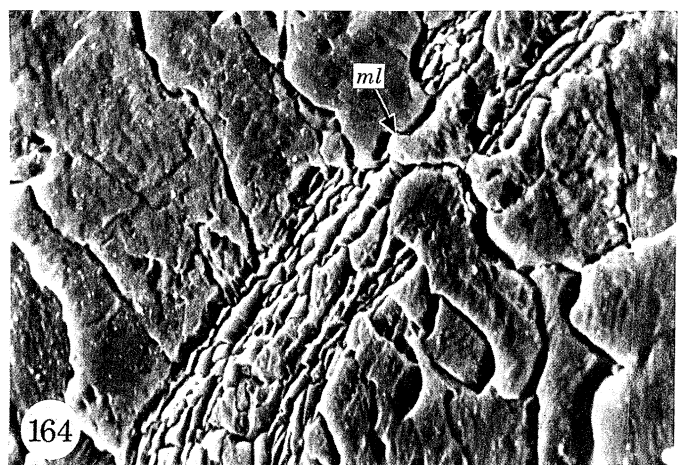
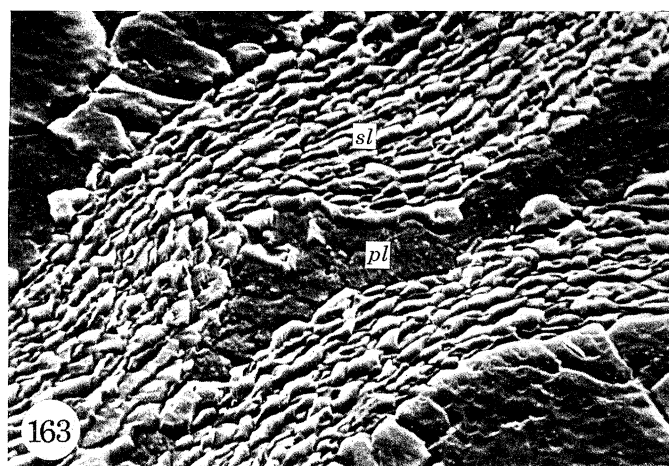
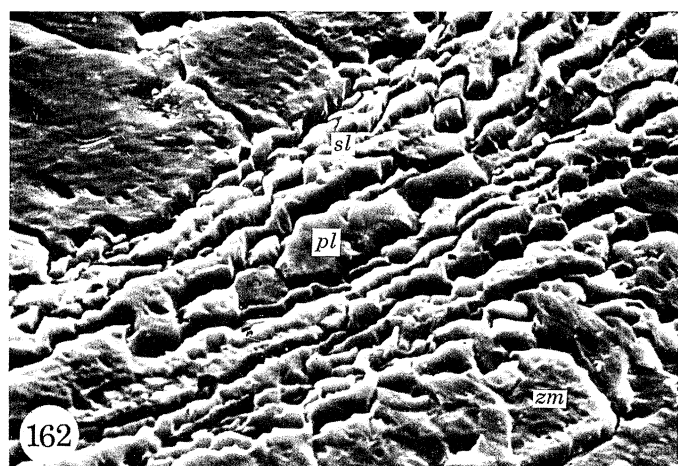
Scanning electron micrographs of the zooecia of *Prasopora grandis* (Ulrich) from the Ordovician (Trentonian), Cannon Falls, Minnesota:

FIGURE 166. Section of part of a colony to show the relationship between zooecia and mesopores ( $\times 225$ ).

FIGURE 167. Section showing the junctions of three cystiphragms ( $\times 2300$ ).

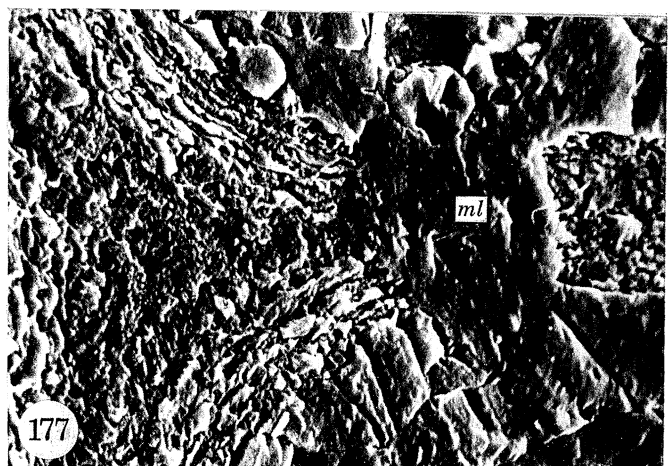
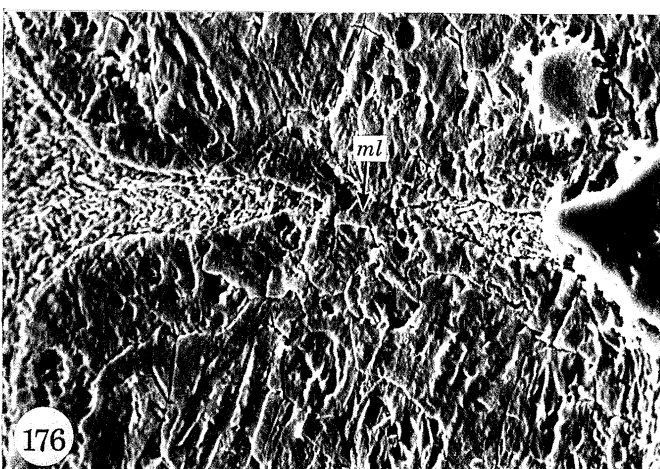
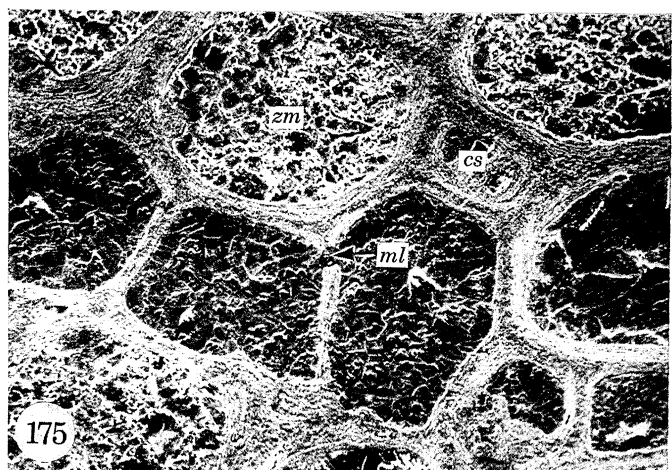
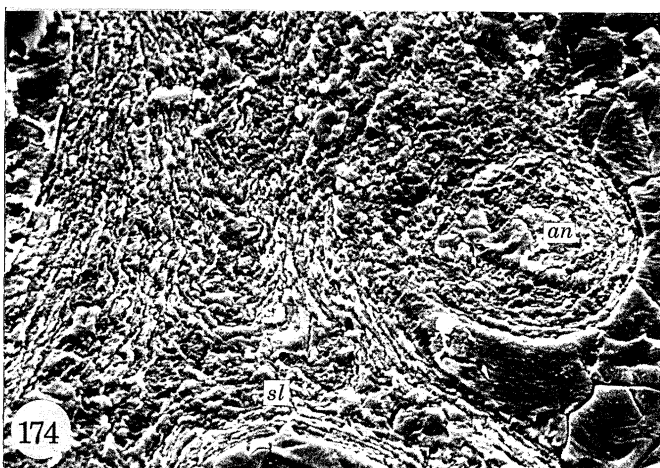
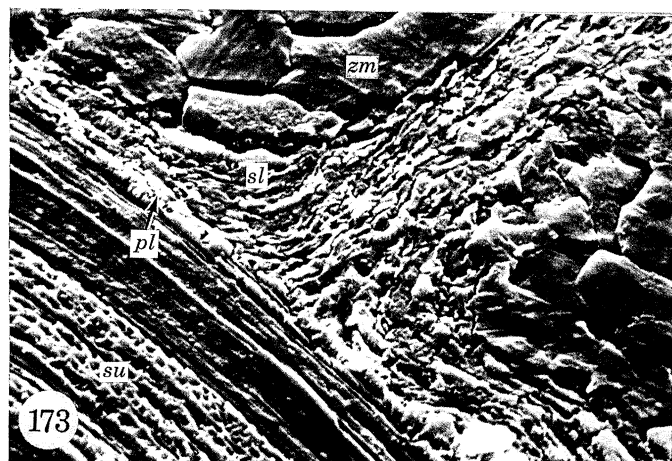
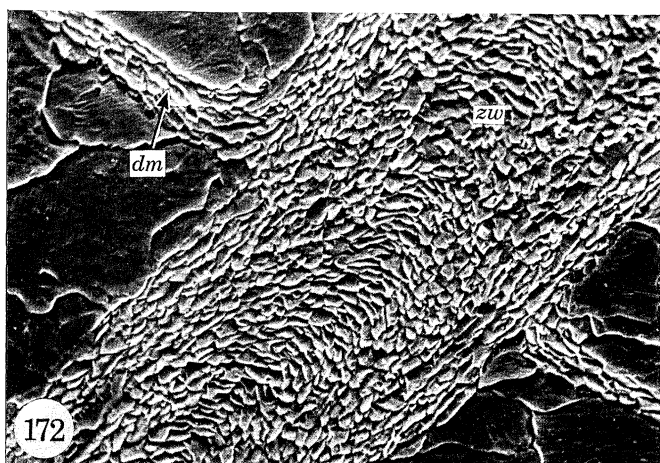
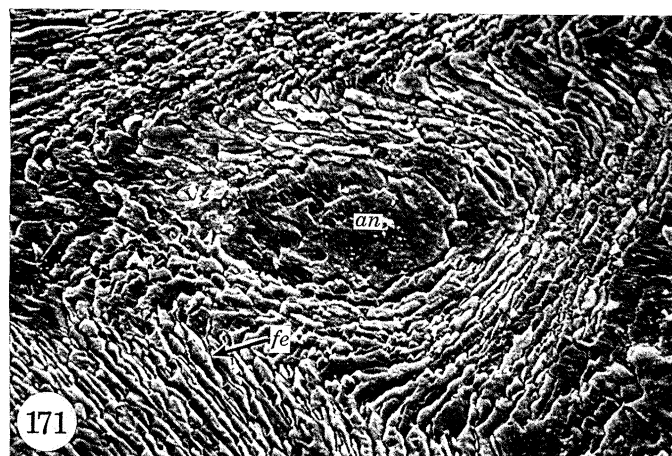
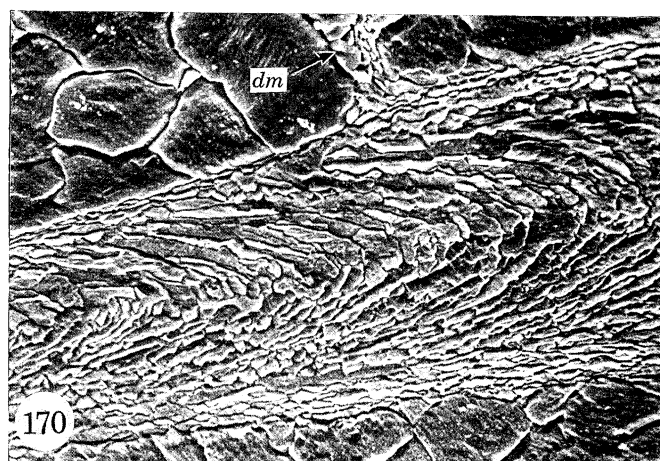
FIGURE 168. Section of a zooecial wall showing the disposition of fibres; distal to lower right ( $\times 2300$ ).

FIGURE 169. Section of a zooecial wall of *Batostoma implicatum* (Nicholson) from the Ordovician (Upper Cincinnati), Cincinnati, Ohio ( $\times 2400$ ).



FIGURES 162 TO 169. For legends see facing page.





FIGURES 170 TO 177. For legends see facing page.

these species, Astrova drew attention to the shape of the zooecial aperture, the segregation of zooecia by tubular partitioned cavities (cystopores), mural pores penetrating homogeneous fibrous-granular walls, and small needle-like cavities within the zooecial walls (minutopores). It is not the purpose of this paper to explore the taxonomic merits of characters like apertural shape, but the growth of cystopores and minutopores affect the skeletal structure and can, therefore, be considered in that context. Only four ceramoporoid species have been studied: *Ceramopora lindströmi* Hennig from the Upper Llandovery of Gotland, Sweden, *Ceramoporella distincta* (Ulrich) from the Upper Ordovician (Maysville Group) of Indiana, *Fistulipora incrustans* (Phillips) from the Lower Carboniferous (Benbulbin Shale) of Ireland and *Coeloclema alternata* (James) from the Upper Ordovician (Maysville Group) of Ohio. *Constellaria* has already been described in association with trepostomes following the lead given by Ross (1966, p. 218) and Utgaard (1968, p. 1035) who do not believe that the Constellariidae and Dianulitidae are closely related to *Fistulipora* and its allies. It seems to us, however, that a case may yet be made for accepting the grouping originally proposed by Astrova although, with regard to this study, the validity of the Order rests on the distinctiveness of the Ceramoporoidea.

In *Fistulipora*, a primary layer of granular calcite is found only in the proximal part of the colony where it forms a basal layer (figure 173, plate 27) up to 2  $\mu$ m thick, and a series of medial wedges extending distally from the base for about 20  $\mu$ m within zooecial walls. The basal layer and both sides of the wedges are succeeded by a secondary laminar layer of fibres, each about 500 nm thick and disposed parallel to the internal zooecial surfaces. Distally, however, the zooecial walls are composed exclusively of fibres with the medial ones arranged as outwardly convex arches in contrast to two flanking sets disposed parallel to the surfaces of deposition (figure 174, plate 27). Diaphragms within the zooecia and the cystopores are also composed of flat-lying fibres. Indeed the only significant changes in attitude occur where calcite rods, representing sporadically distributed acanthopores (figure 174, plate 27), have caused the inward deflexion of adjacent fibres; or around gaps in the walls purporting to represent mural pores (figure 175, plate 27). In section, these gaps are up to 18  $\mu$ m long and may occur, in any part of the zooecial walls. The walls defining some gaps taper towards the centre (figure 176,

#### DESCRIPTION OF PLATE 27

Scanning electron micrographs of the zooecia of *Hallopora ramosa* (d'Orbigny) from the Ordovician (Corryville Formation), Cincinnati, Ohio:

FIGURE 170. Section of a zooecial wall showing the sharply arched laminae of the secondary shell ( $\times 1300$ ).

FIGURE 171. Transverse section of a zooecial wall showing a pseudopunctum with a calcitic core (acanthopore) ( $\times 1300$ ).

FIGURE 172. Section of a zooecial wall and diaphragms of *Heterotrypa frondosa* (d'Orbigny) from the Ordovician (Corryville Formation), Cincinnati, Ohio ( $\times 1300$ ).

Scanning electron micrographs of the zooecia of *Fistulipora incrustans* (Phillips) from the Carboniferous (Glencar Limestone), Gleniff, Co. Sligo, Ireland:

FIGURE 173. Section of the basal and lateral walls showing the skeletal succession ( $\times 2400$ ).

FIGURE 174. Transverse section of zooecial walls showing the arched disposition of secondary fibres and an acanthopore ( $\times 1300$ ).

FIGURE 175. Transverse section showing a mural pore in a cystopore wall ( $\times 250$ ).

FIGURE 176. Transverse section of a zooecial wall showing a mural pore with its original outline ( $\times 1300$ ).

FIGURE 177. Transverse section of a zooecial wall showing a mural pore with its original outline destroyed by recrystallization ( $\times 2500$ ).

plate 27) and the arrangement of constituent fibres, more or less parallel with this attenuation, is consistent with their having been formed by centripetal growth and resorption of zooecial walls around epithelial-bounded tissue as in living cyclostomes. In the majority, however, the boundaries are truncated by calcite crystallites (figure 177, plate 27). These cut across growth surfaces like the medial arches of fibres, and may bear traces of an incomplete replacement of fibres that originally filled at least part of the gap. Yet the absence even of breaks like these in the walls of trepostomes from the same localities and horizons as other cystoporates examined suggests that all gaps in cystoporate walls represent mural pores, although many of them have been altered by diagenetic processes.

The skeletal structure of *Ceramopora*, *Ceramoporella* and *Coeloclema* confirms the prevalence among cystoporates of features seen in *Fistulipora*. Only distal fragments of colonies were available for study but, as in *Fistulipora*, they were composed exclusively of secondary fibres varying in thickness from 700 nm in *Coeloclema* (figure 178, plate 28) to 1 µm in *Ceramoporella* (figure 179, plate 28) and disposed as outwardly convex arches in the medial zone of zooecial walls. Acanthopores with non-laminar cores up to 15 µm in diameter occur in all three genera (figures 178 and 180, plate 28), as do traces of mural pores up to 35 µm across in zooecial walls, and variably spaced diaphragms in the cystopores and zooecia.

Ultramicroscopic study of representative cystoporate skeletons, therefore, shows that many features believed to be diagnostic of the Order occur on other bryozoans. The shell structure of the interzooecial walls is not 'fibrous-granular' as reported by Astrova but exclusively secondary fibrous and, as in trepostomes, must have been secreted within distally expanding folds of basal epithelium. Indeed comparison with trepostomes is apt because, apart from an identical mode of colonial secretion, cystiphragms and diaphragms were also well developed within cystoporate zooecia and cystopores. Whether cystopores accommodated heterozoids or papillose extensions of hypostegal epithelium like those permeating the skeleton of the cheilostome *Cupuladria*, is unknown. In view of their simplicity, we believe they were occupied by papillae, like the trepostome mesopores with which they should be homologized. No trace has been found of any canals comparable with those described as minutopores. Presumably those identified by Astrova

---

#### DESCRIPTION OF PLATE 28

FIGURE 178. Scanning electron micrograph of a zooecial wall of *Coeloclema alternata* (James) from the Ordovician (Maysville Group), Madison, Indiana, showing an acanthopore ( $\times 630$ ).

Scanning electron micrographs of the zooecia of *Ceramoporella distincta* Ulrich from the Ordovician (Maysville Group), Madison, Indiana:

FIGURE 179. Section of a zooecial wall showing the arched fibres of the secondary shell ( $\times 1200$ ).

FIGURE 180. Transverse section of a zooecial wall showing an acanthopore ( $\times 1200$ ).

Scanning electron micrographs of the zooecia of *Escharapora subrecta* (Ulrich) from the Ordovician (Decorah Shale), St Paul, Minnesota:

FIGURE 181. Longitudinal section showing the disposition of the zooecial walls relative to the mesotheca ( $\times 630$ ).

FIGURE 182. Section of the mesotheca showing the skeletal succession ( $\times 1300$ ).

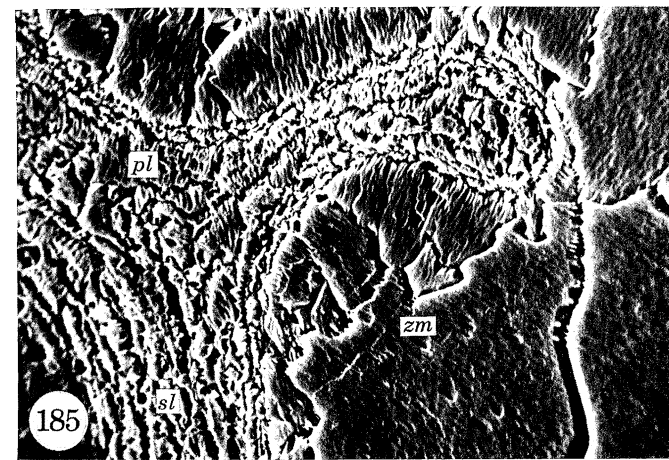
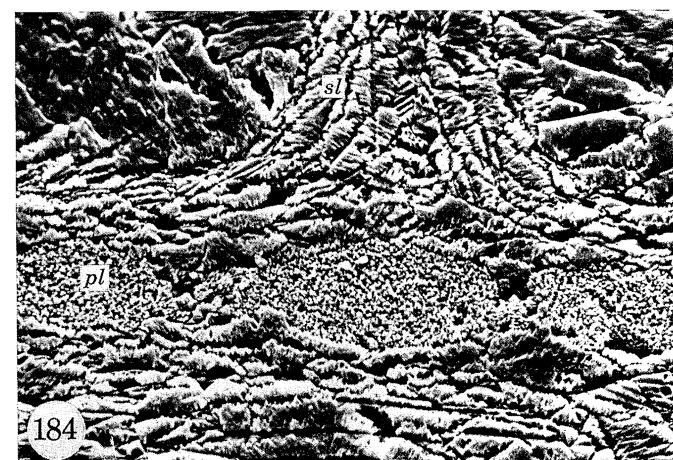
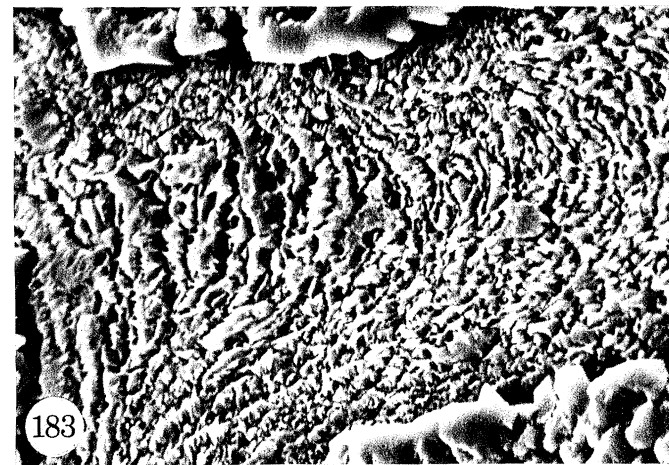
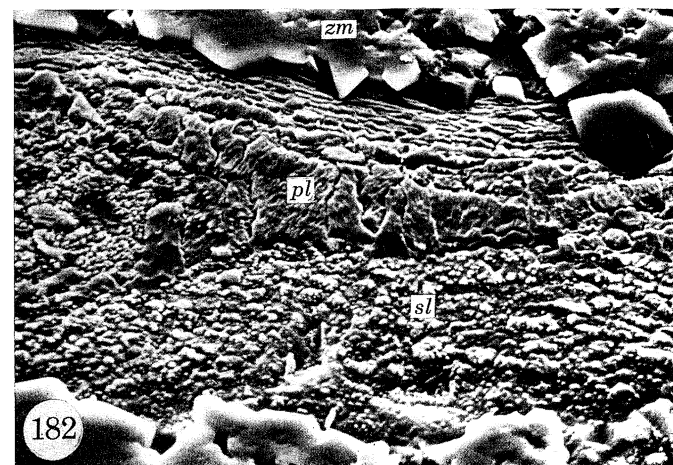
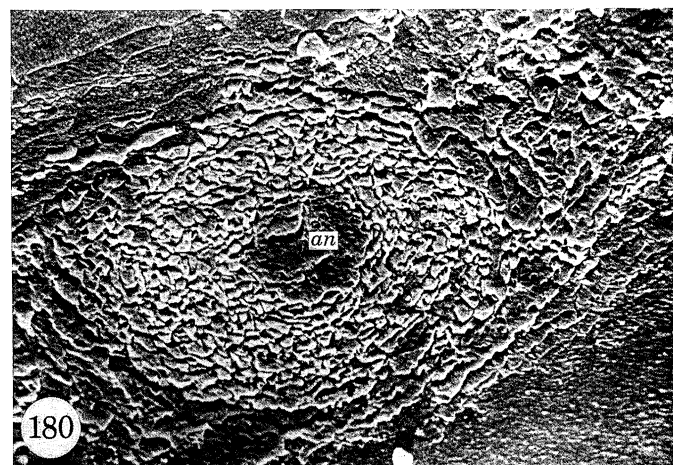
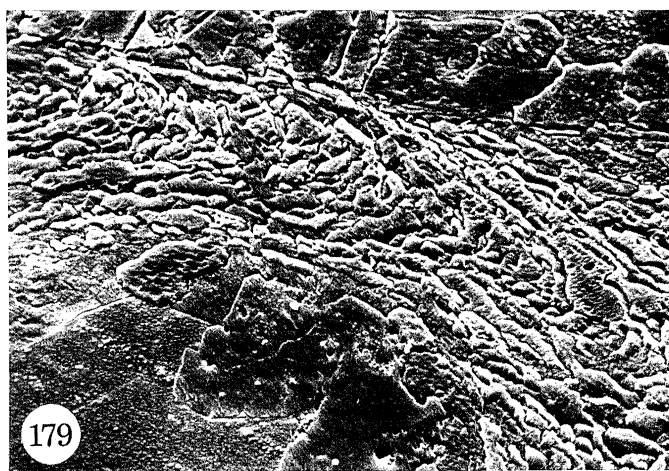
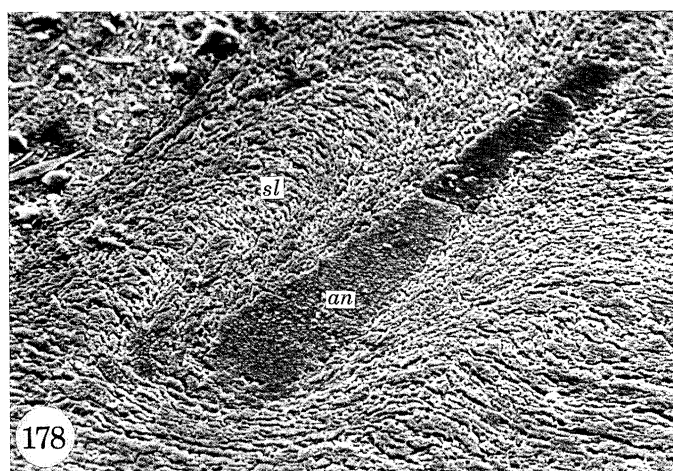
FIGURE 183. Section of a zooecial wall showing the arched arrangement of secondary fibres ( $\times 1300$ ).

Scanning electron micrographs of the zooecia of *Stictopora mutabilis* Ulrich from the Ordovician (Decorah Shale), St Paul, Minnesota:

FIGURE 184. Section of the mesotheca showing the skeletal succession ( $\times 1200$ ).

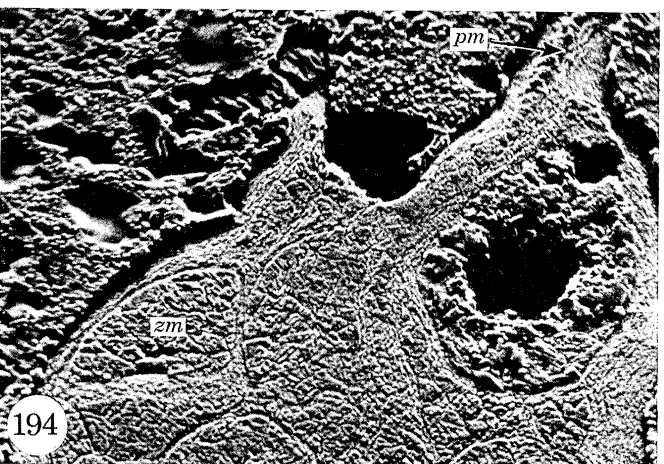
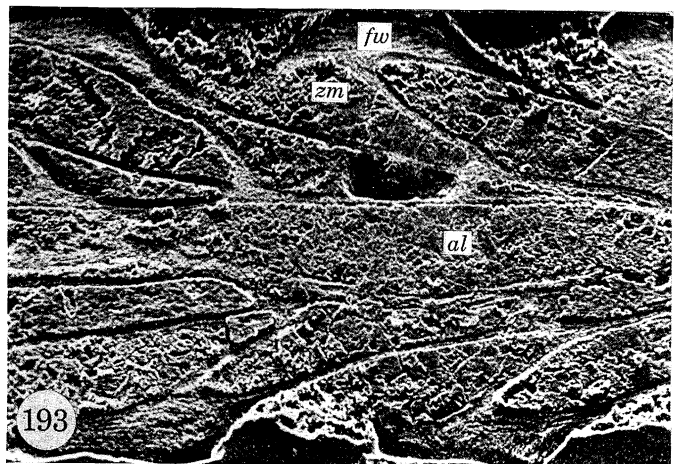
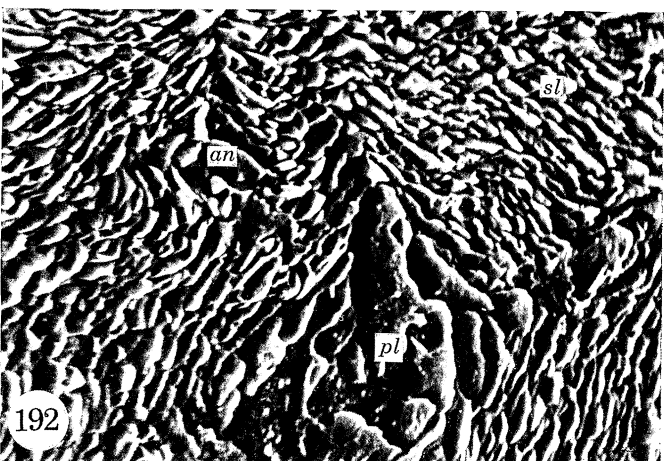
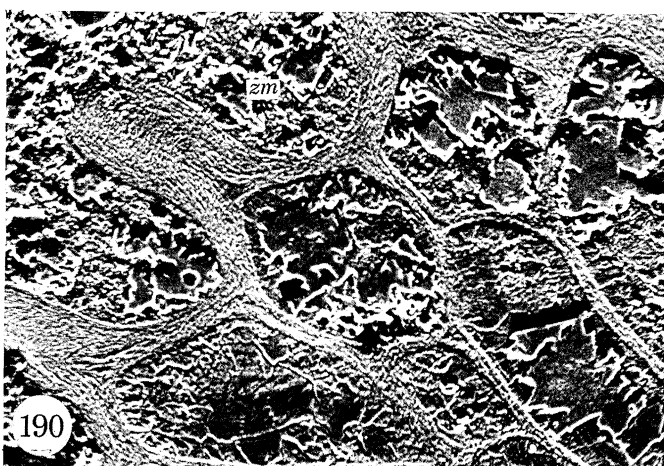
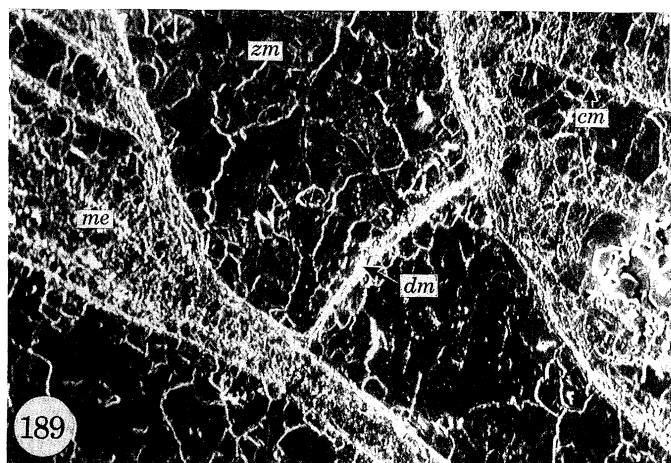
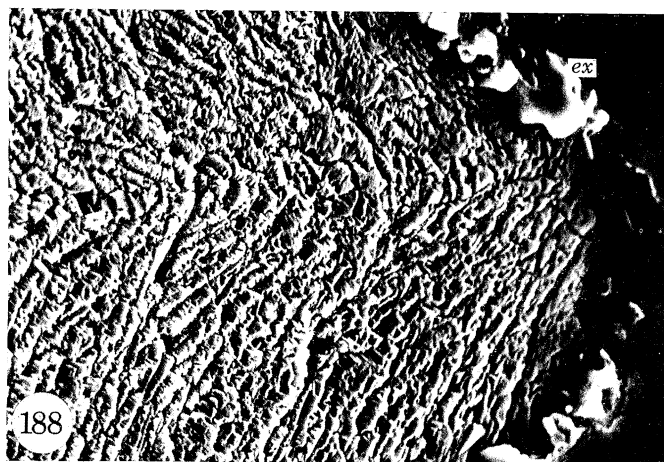
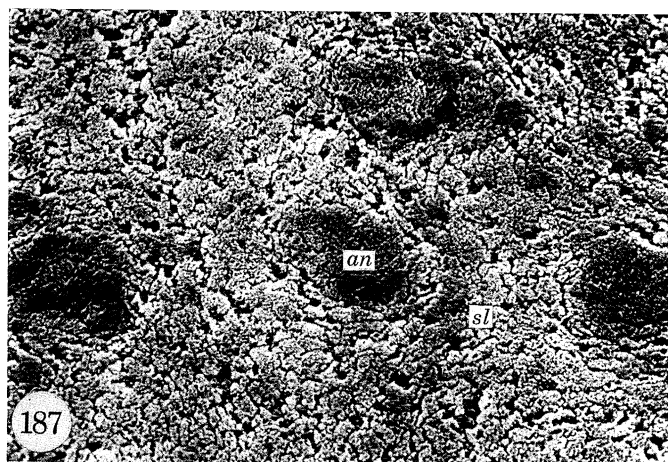
FIGURE 185. Section of a hemiseptum within a zooecial chamber showing the skeletal succession ( $\times 1300$ ).





FIGURES 178 TO 185. For legends see facing page.





FIGURES 187 TO 194. For legends see facing page.

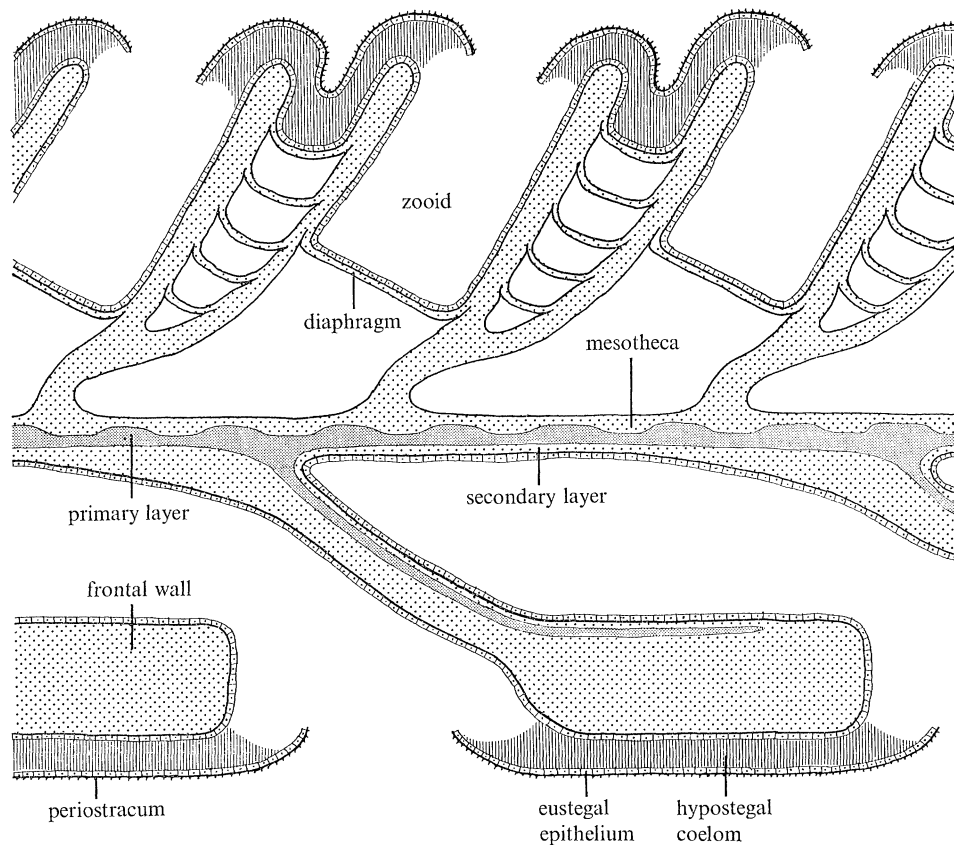


FIGURE 186. Composite diagram showing the arrangement of secretory epithelium in relation to the ptilodictyoid zooecium, based on *Arthrophragma* above and *Escharopora* below.

#### DESCRIPTION OF PLATE 29

Scanning electron micrographs of the zooecia of *Stictopora mutabilis*:

FIGURE 187. Transverse section of a zooecial wall showing skeletal rods ( $\times 1200$ ).

FIGURE 188. Longitudinal section of a zooecial wall showing folds in the fibres representing the zooecial boundary ( $\times 1300$ ).

FIGURE 189. Longitudinal section of the zooecia of *Arthrophragma foliata* (Ulrich) from the Ordovician (Decorah Shale), St Paul, Minnesota, showing diaphragms and cystiphragms ( $\times 250$ ).

Scanning electron micrographs of the zooecia of *Rhombopora exigua* Ulrich from the Carboniferous (Tournaisian), Hook Head, Ireland:

FIGURE 190. Transverse section showing walls in the endozone and exozone of zooecia ( $\times 230$ ).

FIGURE 191. Transverse section showing the primary shell in the junction of zooecial walls ( $\times 2400$ ).

FIGURE 192. Section of a zooecial wall showing a skeletal rod arising from a core of primary shell ( $\times 2500$ ).

FIGURE 193. Scanning electron micrograph of a longitudinal section of *Rhabdomeson gracile* (Phillips) from the Carboniferous (Lower Limestone Series), East Kilbride, Scotland, showing the axial tube in relation to the zooecia ( $\times 120$ ).

FIGURE 194. Scanning electron micrograph of a transverse section of *Carinophylloporina typica* Bassler from the Ordovician (Trentonian), Cannon Falls, Minnesota; the carina is near the top right hand corner ( $\times 230$ ).

were acanthopores or, if originally hollow and opening into zooecial tubes, mural pores. In view of all these striking comparisons with the trepostomes, there seems little doubt that the two groups were closely related and that the only fundamental distinction was the presence of mural pores in the Cystoporata.

(e) *Structure of cryptostome zooecium*

Although the Cryptostomata merit ordinal rank no single feature distinguishes them from other, contemporaneous Orders especially the Trepostomata. Both groups are fundamentally alike in lacking the mural pores found in the Cystoporata and Cyclostomata, and in the secretion of a calcareous skeleton within folds of basal epithelium which were separated from a colonial cover of periostracum and eustegal epithelium by a hypostegal coelom. Indeed differences between the two Orders mainly reflect the variable development of certain features. Thus, the cryptostomes were predominantly ramose, bifoliate or fenestrate in growth forming delicately constructed colonies in contrast to the typically massive encrusting trepostomes, although no habit was exclusive to either Order. Characteristically trepostomatous features like mesopores did not generally develop in cryptostomes, but they occur in species belonging to all three cryptostome Suborders. Moreover, diaphragms and cystiphragms, deposited in the same way as those in trepostomes but more sporadically, occur in the zooecia and mesopores of some cryptostomes. These differences are related to changes in the attitude of zooecia (figure 186). In most cryptostome colonies, the proximal parts of zooecia are only narrowly divergent from a medial plane (or axis) and form short pouch-like chambers (endozone) which may contain a few diaphragms or cystiphragms. Their openings, however, are long passages (vestibules) defined by the differential secretion of a thick frontal wall (exozone) and disposed at high angles to the long axis of the chamber. Consequently the cryptostome zooecium not only lost the tubular appearance characteristic of contemporaneous bryozoans but was served by a frontal rather than a terminal opening in the manner of cheilostomes.

Since changes in emphasis are responsible for the morphological distinctiveness of the cryptostomes, it is not surprising to find that the cryptostome shell structure differs from the trepostome only in the comparatively high incidence of pseudopuncta (acanthopores) and the greater development of the primary layer. This assessment holds for all ten genera examined which illustrate the main structural variation in the cryptostome skeleton.

The Cryptostomata have been divided into three Suborders by Astrova & Morozova (1956, p. 662) on the basis of colonial shape, with the Ptilodictyoidea accommodating all bifoliate forms, and the Rhabdomesioidea and Fenestelloidea all ramose and fenestrate species respectively. This grouping is morphologically acceptable and phylogenetically defensible, because most species assignable to each Suborder are related to one another and so form three independent complexes of descent from the Ordovician to Permian inclusive. No group is so much older than the others as unequivocally to constitute the ancestral stock. The ptilodictyoid *Stictoporellina gracilis* (Eichwald) is recorded from the Arenig of Estonia (Mannil 1959), but fenestelloids and rhabdomesoids occur in the Llanvirn and are well enough differentiated to require antecedents of at least Arenigian age.

(1) *Ptilodictyoid zooecium*

Of the five ptilodictyoid species studied the ptilodictyid *Escharopora subrecta* (Ulrich) from the Upper Ordovician (Decorah Shales) of Minnesota may be regarded (figure 186) as representative of the Suborder. The encrusting base, to which the colonial frond was articulated,

has not been examined, but its composition can be inferred from sections of the frond (figure 181, plate 28). The medial plate or mesotheca, from which arise the two oppositely facing layers of zooecia, is about 4 to 5  $\mu\text{m}$  thick (figure 182, plate 28). It consists of medial lenses of granular calcite, up to 3  $\mu\text{m}$  thick, which represent the primary layer, bounded by two thin secondary layers. The secondary shell of the mesotheca and zooecia is irregularly laminar (figure 183, plate 28) because the chief constituents are rather crudely fashioned fibres between 750 and 1500 nm thick. The fibres compose all parts of the massive frontal zooecial walls except for a thin sheet of granular calcite, about 4  $\mu\text{m}$  thick, embedded in the roof of the proximal part of the zooecial chamber, which is an extension of the primary part of the mesotheca. Their occurrence at the external surfaces of the frontal walls confirms that these surfaces were lined with epithelium responsible for the secretion of all secondary shell lying externally to the primary layer in the roof of the zooecial chamber. A hypostegal coelom must have separated this carbonate-secreting epithelium from an outer coat of periostracum and eustegal epithelium. The carbonate-secreting epithelium must, therefore, have enveloped the entire mineral skeleton, and deposited granular calcite as a primary framework of the immature proximal parts of zooecia, the mesotheca and much of the encrusting base.

The skeletal structure of the rhinoporidid *Stictopora mutabilis* Ulrich from the Upper Ordovician (Decorah Shale) of Minnesota is identical with that of *Escharopora* with a primary layer of granular calcite occurring medially as discrete lenticles within the mesotheca (figure 184, plate 28), and extending into the frontal wall of zooecia where it forms the core of constrictions (hemisepta) at the bases of vestibules (figure 185, plate 28). The secondary shell is composed of fibres about 750 nm thick bent in a frontal direction around rods of calcite (skeletal rods), about 12  $\mu\text{m}$  in diameter, to impart a conspicuous pseudopunctate condition (figure 187, plate 29). Karklins (1969, p. 12) has drawn attention to two sets of boundaries seen, in optical sections of *Stictopora* and other cryptostomes, as dark lines breaking laminar continuity between longitudinally and laterally adjacent zooecia (zooecial and range boundaries respectively). Both boundaries are actually tight, outwardly convex folds of fibres with wavelengths of about 10  $\mu\text{m}$  (figure 188, plate 29) passing into granular calcite here and there. Each zooecial fold was built on a ridge on the outer surface of the primary frontal cover of the zooecial chamber; each range fold on the distal edge of primary calcite occupying the medial zone of lateral walls.

A diaphragm about 6  $\mu\text{m}$  thick normally occurs about 40 to 50  $\mu\text{m}$  above the zooecial base. Its curved distal and sharply angular proximal junctions with the zooecial walls show that its growth was identical with the diaphragms of Trepostomata.

The twofold succession of primary granules and secondary fibres is characteristic of three other ptilodictyoids from the Upper Ordovician (Decorah Shale) of Minnesota; *Arthroporhagma foliata* (Ulrich), *Astreptodictya acuta* (Hall) and *Stictoporella angularis* Ulrich. In the first two species the zooecia are disposed more or less normal to the mesotheca and the resultant inter-zooecial spaces have been given complex covers by distally migrating epithelium. Immediately distal of the mesotheca, an interzooecial space is differentiated into a vesicular zone by a number of cystiphragms (figure 186; and figure 189, plate 29). Towards the outer surface of the colony the vesicular zone is succeeded by a solid layer of secondary fibres. Thus the inter-zooecial spaces are homologous with the trepostome mesopores on the one hand and the massive frontal walls of *Escharopora* and *Stictopora* on the other.

(2) *Rhabdomesoid zooecium*

The rhabdomesid, *Rhombopora exigua* Ulrich from the Lower Carboniferous (Hook Head) of Ireland, illustrates the principal structural features of the branching rhabdomesoid colony. Sections of a branch show that zooecia arose axially and curved outwards in mature stages of growth to form part of the external surface (figure 190, plate 29). In the axial zone the zooecia are defined by walls, about 8  $\mu\text{m}$  thick, with a medial primary layer of granular calcite about 3  $\mu\text{m}$  thick (figure 191, plate 29). This primary framework is flanked by two secondary laminar layers of fibres with an average thickness of 750 nm, each constituting the lining of adjacent zooecial chambers. In the peripheral zone, increasing divergence between adjacent chambers allowed the growth of massive walls up to 80  $\mu\text{m}$  thick. The core of each wall is occupied by primary granular calcite from which radiate large pseudopuncta (figure 192, plate 29), regularly distributed at intervals of about 25  $\mu\text{m}$ , and usually with an axis of granular calcite about 5  $\mu\text{m}$  in diameter. The pseudopuncta permeate the secondary shell which makes up most of the walls, to emerge at the external surface, and their trails are defined by sharp, outward deflexions of surrounding secondary fibres. Their development was controlled at the external surfaces of the walls by hypostegal epithelium.

Sections of *Rhabdomeson gracile* (Phillips) from the Lower Carboniferous of Scotland show the same structural arrangements and skeletal successions found in *Rhombopora*. The axial tube (figure 193, plate 29) which distinguishes *Rhabdomeson* from other genera, is lined by a wall of primary granular calcite about 5  $\mu\text{m}$  thick. The succession confirms that the tube is a cylindroid extension of the base of the colony.

(3) *Fenestelloid zooecium*

Fenestelloid morphology is sufficiently diverse to warrant consideration of the structural variation in two species, the phylloporinid *Carinophylloporina typica* Bassler from the Upper Ordovician (Platteville Group) of Minnesota, and the fenestellid *Polypora corticosa* Ulrich from the Upper Mississippian (Chester Series) of Indiana. The two groups represented by these species are alike in a number of structural aspects, notably the limitation of zooecia to one side (frontal) of the fenestrate skeleton and their segregation into two sets of row(s) by a median ridge (carina). But there are also differences indicating strong affinity between the phylloporinids and trepostomes, including the absence of the dissepiments and the presence of diaphragms within zooecia. However, irrespective of the actual lines of descent, both skeletal structure and succession favour a close relationship between the trepostomes and cryptostomes.

The framework of the *Carinophylloporina* skeleton (figure 194, plate 29, figure 195) is a more or less continuous layer of coarsely granular calcite constituting the primary shell. The layer occurs medially in all common zooecial walls, although it is usually not more than 3  $\mu\text{m}$  thick. It also forms the core of the carina, from which it extends towards the base of a branch as a plate-like feature up to 10  $\mu\text{m}$  thick (figure 197, plate 30). This primary plate is normally identifiable to the base of the frond and is continuous with the primary shell of the zooecia on either side.

The rest of the *Carinophylloporina* skeleton consists of laminar secondary shell composed of fairly regular fibres up to 1  $\mu\text{m}$  thick. The secondary shell lines all zooecial tubes and is the exclusive constituent of sporadically distributed diaphragms which are identical with those found in trepostomes. The external zone of a mature branch is also composed entirely of



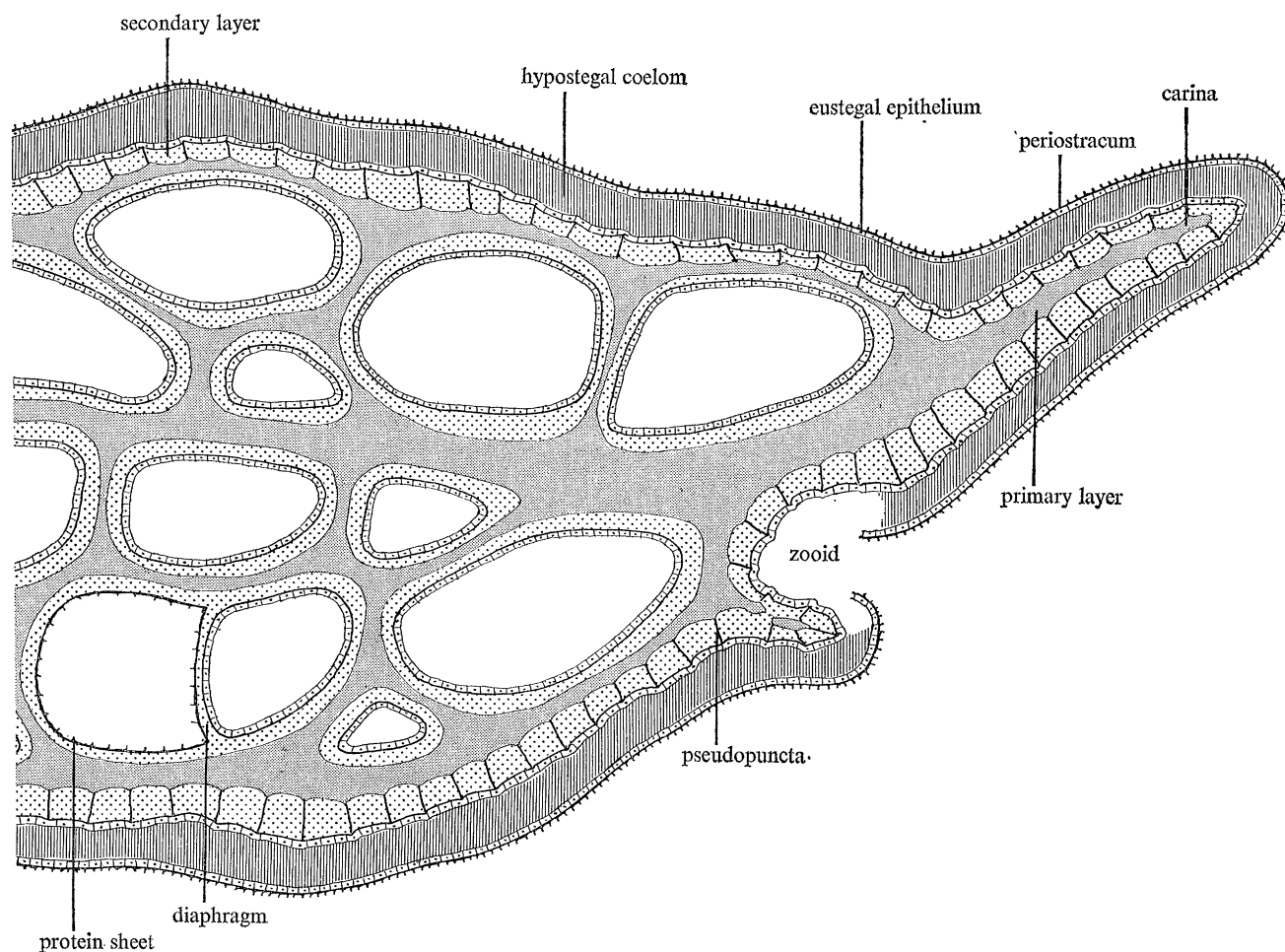


FIGURE 195. Diagrammatic transverse section of *Carinophylloporina* showing the arrangement of secretory epithelium in relation to the skeleton; the primary medial plate extends from the left side of the drawing to the carina; obverse of the branch is to the right.

secondary shell (figure 196, plate 30) because even the carina has an external coat of fibres. Only impermanent rods of granular calcite, about  $4\ \mu\text{m}$  in diameter, in the cores of outwardly deflected pseudopuncta break through this laminar blanket at intervals of about  $20\ \mu\text{m}$  (figure 196). Indeed primary shell could only have emerged at the external surface of the mineral part of the colony near the growing tips. Here granular calcite must have been secreted in advance of secondary fibres by newly generated portions of hypostegal epithelium which enveloped and secreted the entire carbonate skeleton as in *Hornera* (Tavener-Smith 1969a, p. 291).

The skeletal succession of *Polypora corticosa* (figure 198, plate 30) is like that of *Carinophylloporina*, but the primary shell of coarsely granular calcite is relatively more important. Sections show that groups of zooecial chambers are surrounded by a cylindroid layer of primary calcite, which varies from 10 to  $30\ \mu\text{m}$  in thickness because the outer surface is crenulated by rounded ridges with a wavelength of about  $15\ \mu\text{m}$  running parallel to the long axis of the branch (figure 199, plate 30). The ridges support rows of skeletal rods, also of primary granular calcite, with diameters up to  $5\ \mu\text{m}$  (figures 198 and 199, plate 30). They are somewhat irregularly distributed at intervals of 6 to  $14\ \mu\text{m}$  and may branch outwards but all are surrounded by outwardly

deflected laminae of the secondary shell and most if not all of them emerge at the external surface. Thus the entire fabric indicates secretion within an enveloping hypostegal epithelium. The lamination of the secondary shell is attributable to rather irregular fibres between 450 and 900 nm thick. Secondary fibres are also deposited as a layer about 4  $\mu$ m thick on the inner surfaces of the primary shell surrounding zooecia and on the medial layer of the common zooecial walls by zooidal epithelium.

Dissepiments consist of the same succession, namely an axis and radiating skeletal rods of primary granular calcite embedded in secondary shell. A continuous carina, like that found in most fenestelloids, is not developed in *Polypora*. It is represented by scattered nodes each consisting of a core of primary granular calcite about 30  $\mu$ m across. They are embedded in secondary shell and bear skeletal rods splaying out frontally like the branches of a Christmas tree. The structure is identical with the large pseudopunctate cores of *Rhombopora*.

Two other fenestellid species require comment because each is characterized by a feature that is so novel as to provide a rigorous test of the model of secretion proposed in this paper for the cryptostome skeleton.

The main part of the mineral skeleton of *Semicoscinum rhombicum* Ulrich from the Devonian of Spain is orthodox enough, with its fenestrate branches bearing paired zooecia on a carinate frontal surface. This solid part of the colony, however, is encased, both frontally and basally, in vesicular shell (figure 200, plate 30). The vesicles are defined by outwardly convex cystiphragms, never more than 2  $\mu$ m thick but up to 25  $\mu$ m deep and 150  $\mu$ m across. These external cystiphragms, including a pair of flanges developed on either side of the carina, arise from one another as well as from the external surface of the solid skeleton (figure 201, plate 30). They are composed exclusively of secondary fibres between 650 and 850 nm thick which also make up the outer layer of the solid skeleton. The relationship of cystiphragms to one another and to the main part of the colony, shows that the sequence of secretion was from within outwards. In effect the vesicular shell was deposited by an outwardly retreating hypostegal epithelium in the same way as the vesicle walls of the cyclostome *Lichenopora*.

The screw-like fenestellid colony *Archimedes terebriformis* Ulrich from the Upper Mississippian

#### DESCRIPTION OF PLATE 30

Scanning electron micrographs of the zooecia of *Carinophylloporina typica*:

FIGURE 196. Section of the external wall showing the pseudopunctate condition of the secondary shell ( $\times 2900$ ).

FIGURE 197. Section showing the skeletal succession of the primary medial plate ( $\times 1400$ ).

Scanning electron micrographs of the zooecia of *Polypora corticosa* Ulrich from the Mississippian (Glen Dean Limestone), Eckerty, Indiana:

FIGURE 198. Section of the frontal wall showing the skeletal rods in relation to the general succession; obverse surface to the left ( $\times 700$ ).

FIGURE 199. Section of the frontal wall showing the skeletal succession ( $\times 1400$ ).

Scanning electron micrographs of the zooecia of *Semicoscinum rhombicum* Ulrich from the Devonian, Asturias, Spain:

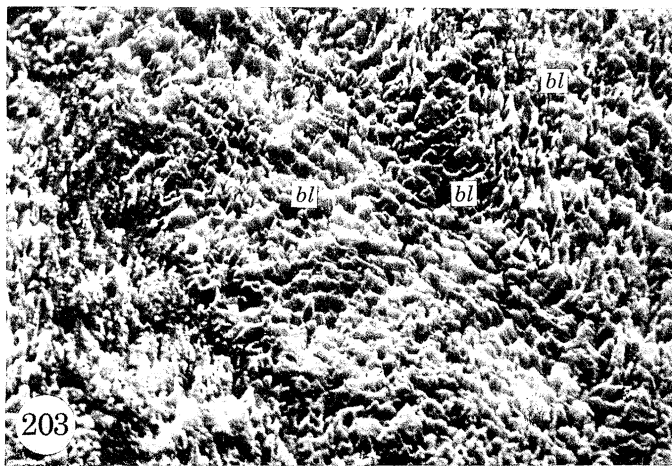
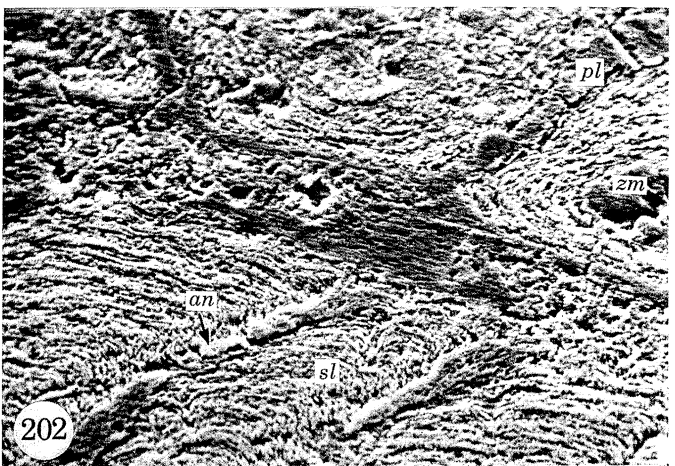
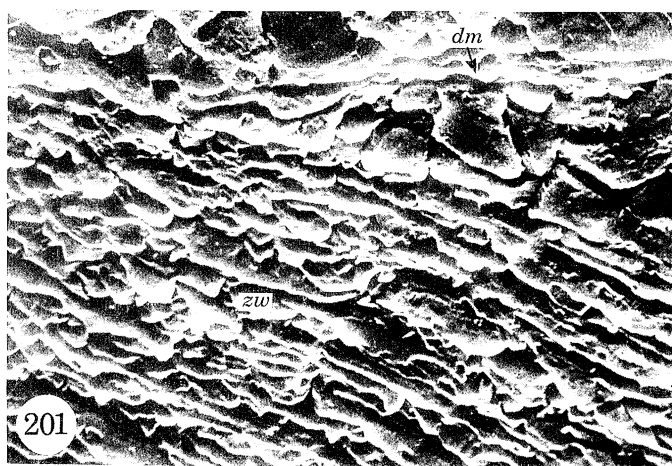
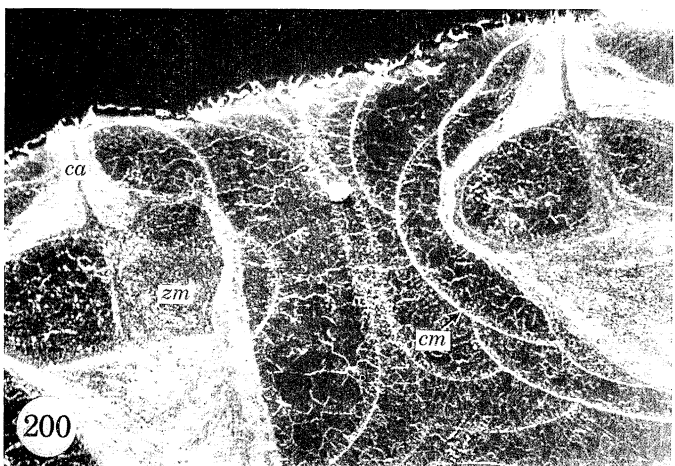
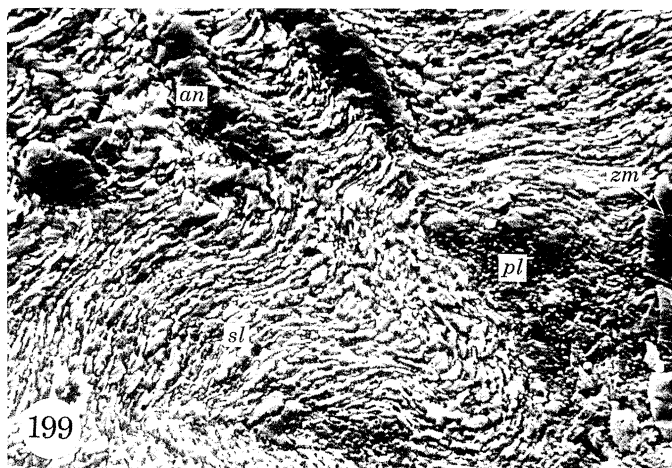
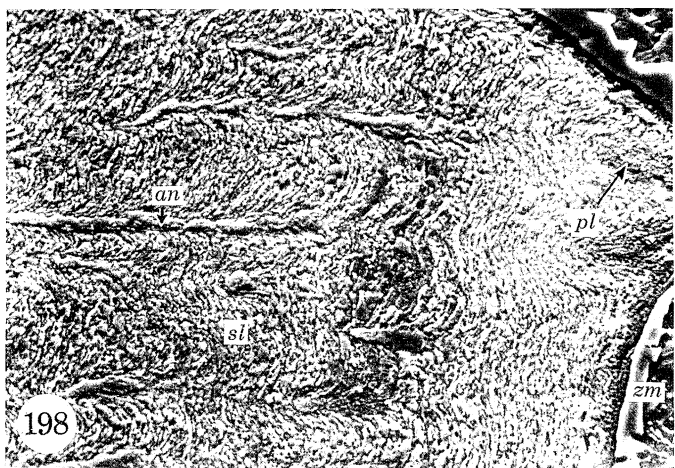
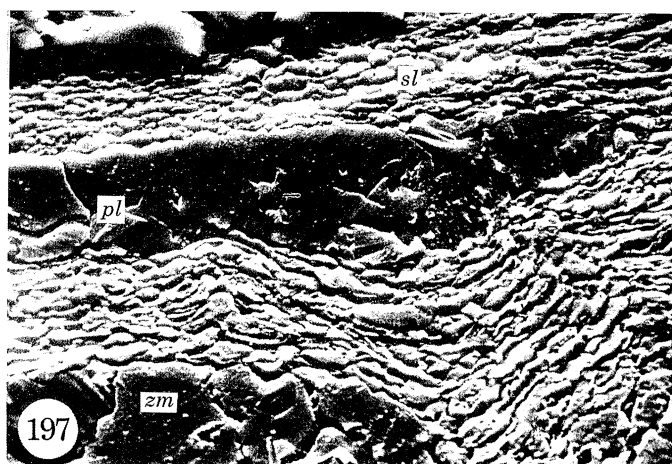
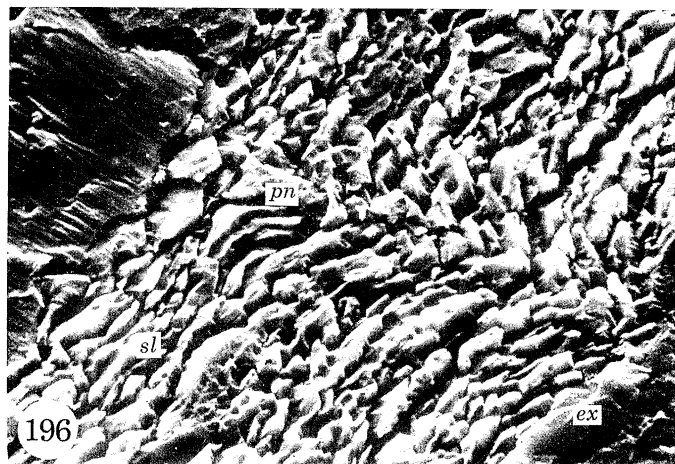
FIGURE 200. Transverse section showing external cystiphragms in relation to the zooecia ( $\times 110$ ).

FIGURE 201. Section of the junction between a cystiphragm (dm) and a zooecial wall ( $\times 2400$ ).

Scanning electron micrographs of the zooecia of *Archimedes terebriformis* Ulrich from the Mississippian (Glen Dean Limestone), Eckerty, Indiana:

FIGURE 202. Section of the basal part of zooecia showing the shell succession in relation to axial rods ( $\times 1300$ ).

FIGURE 203. Section showing alternating bands of laminae in the main skeletal part of the colony ( $\times 2400$ ).



FIGURES 196 TO 203. For legends see facing page.

(Chester Series) of Indiana is a classic example of spiral growth. Functional zooecia were arranged along an outwardly growing edge tracing a helicoid spire about a solid axis. Each zooecium is enclosed, as in *Polypora*, in a frame of primary granular calcite about 3  $\mu\text{m}$  thick and supporting long radiating granular skeletal rods at intervals of about 35  $\mu\text{m}$  (figure 202, plate 30). Large nodes of primary shell, like those of *Polypora*, also occur. Because the spiral edge of the colony expanded outwards and proximally from the axis as successive zooecia were added, their framework of primary calcite extends back to the axial core. This primary fabric except for the edge of newly formed zooecia is buried in a secondary laminar shell composed of regular fibres and plates about 400 nm thick. Laminae line the zooecial chambers and constitute all but the core of the axis as well as the parts sloping down from the axis to the spiral edge. These slopes are ornamented by fine ridges about 25  $\mu\text{m}$  wide which radiate from the axis and consist of alternating bands of laminae disposed parallel with or at an angle to the ridges (figure 203, plate 30).

The structural relationships outlined above, especially the outward deflexion of laminae around skeletal rods and the occurrence of secondary shell at the surfaces of the slopes, suggest that the colony was sheathed in hypostegal epithelium which secreted all the carbonate skeleton except for the lining of zooecial chambers. Secretion of secondary laminae was continuous so that as the edge of the spirally twisted frond expanded outwards, secondary shell encroached on to recently formed parts of the frond and was added to massive deposits already laid down around the axis.

#### CONCLUSIONS

Examination of processes responsible for the secretion of the bryozoan skeleton, and the determination of shell successions for a wide range of species, have provided a reasonably complete picture of the diversity of shell structure attained during the evolution of the phylum, and of the nature of skeletal secretion in extinct groups. Two aspects of shell secretion may be profitably compared among various Orders. They are the skeletal succession, and the punctuation and pseudopunctuation of the mineral layer(s) in relation to variously named cavities in the skeleton. Such comparisons lead to the identification of some interesting homologies, and reveal that the relationship between the skeleton and secreting epithelium was generally more complicated in extinct bryozoans than in living species.

In all living bryozoans, the first-formed part of the skeleton is the periostracum, with or without the external mucopolysaccharide film binding the colony to its substrate. The periostracum, which acts as a seeding sheet for the succeeding mineral layer as well as serving as a protective coat, does not survive fossilization as a morphologically identifiable unit, but may be inferred to have always been present as an external cover. No organized carbonate layer is developed among living ctenostomes so that only trace fossils of this Order are to be expected and current accounts of their geological history are necessarily speculative. With regard to other bryozoans, it is not even possible to deduce the structure of the prototypic periostracum because at least two different types are known to exist. One, found in cheilostomes and certain cyclostomes like *Berenicea* and *Lichenopora*, is bounded externally by a fibrillar triple-unit membrane; the other, occurring in the cyclostome *Crisidia* as well as the ctenostome *Bowerbankia*, by a homogeneous, granular external membrane. The differences between these two membranes may indicate that the former is predominantly proteinous, the latter chitinous, but there is no evidence yet to show which is likely to be the more primitive structure.

The skeletal succession also falls into two categories but involving different groupings of taxa. The carbonate successions of the youngest Order, the cheilostomes, are the most diverse of all calcareous bryozoans. Rucker & Carver (1969) have shown that 14 out of 31 cheilostome families include species with carbonate skeletons composed partly or exclusively of aragonite. In contrast, the preservation of structural detail in all fossil stenolaemates so far examined suggests that the mineral skeletons of extinct cystoporates, trepostomes and cryptostomes like those of living (and fossil) cyclostomes, were always calcitic. From one to three distinctive carbonate layers have been recognized among cheilostomes, whereas a double-layered shell is the only kind of succession so far found in fossil and living stenolaemates. Moreover, even individual layers of the cheilostome skeleton are much more variable in texture. The primary shell, the only carbonate layer present in some genera like *Membranipora*, *Electra* and *Iodictyum*, most commonly consists of acicular crystallites about 300 nm thick and disposed vertically to the inner periostracal surface. But nodular, lenticular and granular bodies of calcite, up to a few micrometres in size, also occur, and tablets about 200 nm thick dominate the primary fabric of *Celleporella*. The secondary and tertiary layers, when developed, are equally variable. The secondary layer is predominantly banded, usually with discrete laminae or lenticles composed of vertically disposed crystallites and interleaved with protein sheets. In *Celleporella*, lamination is more strongly defined because it consists of spirally growing calcite plates sheathed in proteinous membranes. The tertiary layer may be banded, granular or composed of acicular crystallites and, like the primary layer, lacks organized organic constituents.

The fabric of the double-layered carbonate succession of the stenolaemates is much more uniform. The primary layer of living cyclostomes is mainly composed of acicular crystallites, but the constituents are, on average, about twice as thick as those in the cheilostome primary shell, and there is a greater tendency in every species for the calcite to be secreted as granules or, more rarely, tablets. The predominance of a granular texture in all fossil stenolaemates, however, may not reflect original fabric but recrystallization of a crystallite layer like that of living cyclostomes.

The secondary layer in all stenolaemates is laminar and composed of spirally growing plates and/or overlapping fibres, with or without keels. In living cyclostomes, each unit is surrounded by proteinous sheets which interconnect with one another and are secreted by epithelium simultaneously with the carbonate constituents of the shell. The laminae are stable features of the secondary shell being, on average, 400 nm thick in fossil and living cyclostomes. In the remaining stenolaemates, however, the laminae are mainly coarser fibres, varying in mean thickness from 750 nm for the cystoporates to 800 nm for the trepostomes and cryptostomes and tending to be lenticular in transverse section. The clarity of fibre boundaries throughout sections of well-preserved specimens even from Ordovician rocks, suggests that although recrystallization is likely to have taken place, the process occurred within the physical constraints afforded by an anastomosing network of protein sheets pervading the secondary shell, and did not greatly alter the original fabric. In some respects they recall the pattern seen in sections of the brachiopod secondary shell (Williams 1968, plates 11 and 12), and it may be that the faces of fibres exposed on the internal surface were also more or less rhombohedral in outline.

The contrast between the gymnolaemate and stenolaemate calcareous skeleton has an evolutionary significance. All Palaeozoic bryozoans examined possessed a primary layer, now granular but probably composed mainly of acicular crystallites in the unaltered state, and an organic-calcitic laminar secondary shell which was secreted in the form of overlapping fibres or



spirally disposed tablets. Notwithstanding the geological record of the ctenostomes which allegedly first appeared in the Arenig, the cheilostomes must have arisen from the stenolaemates either by way of the ctenostomes or independently of that Order. With their emergence, secretion of the primary shell continued and gave rise to a layer with a similar fabric to that found in cyclostomes. The secondary layer was mainly a later development because, although it is found in a majority of living species, it was identified in only two of the 15 fossil genera examined by us. The layer is also novel involving the aggregation of vertical crystallites into laminae or lenticles separated from one another by proteinous sheets. Only with the evolution of *Celleporella* and other cheilostomes with the same kind of secondary shell was the stenolaemate type of lamination repeated. This was a more important trend than the appearance of a tertiary layer which mainly reflected a reversion to conditions governing deposition of the primary shell.

The order of carbonate secretion is the key to the relationship between secreting epithelium and the bryozoan skeleton. The enclosure within secondary shell of all but the base of the primary framework of a colony is evidence that the skeleton was a coelocyst deposited within an envelope of hypostegal epithelium. This relatively complex arrangement controlled the skeletal growth of cystoporates, trepostomes and cryptostomes including all the earliest known bryozoans of Arenig age (Larwood *et al.* in Harland *et al.* 1967, p. 380). Indeed, the first recorded bryozoans with subperiostracal carbonate skeletons secreted by eustegal epithelium are the Caradocian diastoporids *Mitoclema cinctosum* Ulrich from the Porterfield rocks of Tennessee and an undescribed species of *Corynotrypa* from the Bromide Formation of Oklahoma. Subsequently, unless the cyclostomes were polyphyletically replenished from the cystoporates, a coelocystic skeleton evolved for the second time in bryozoan history during the early Mesozoic with the appearance of the cerioporoids and cancelloids. Yet a third occasion for the independent development of the coelocyst attended cheilostome evolution. The Order is first represented in the Cretaceous by Albian electrids and calloporids (Larwood *et al.* in Harland *et al.* 1967, p. 391) with their subperiostracal carbonate skeletons. Yet coelocystic features like the cryptocyst had already developed in cellariids by late Cretaceous times; and with the appearance of the coelostegoid *Cupuladria* in the Miocene and the ascophorans *Iodictyum* and *Sertella* in Recent seas, an extensive coelocystic skeleton became a feature of gymnolaemate as well as stenolaemate evolution.

Comparison of ancillary skeletal features like punctation, interzoecial cavities and pseudo-punctation shows them to be simple structures obscured by a confused terminology.

Puncta, as distinct from interzoecial connexions like mural pores and rosette plates, are canals opening onto the external shell surface. Two principal types are known. In the cyclostomes *Berenicea* and *Crisidia*, and presumably in other punctate species of the same Order with a subperiostracal skeleton, the external opening of a punctum is plugged by a thickening of periostracum. The papilla within the canal is an extension of eustegal epithelium and acts as a storage centre. These so-called 'pseudopores' are homologous with the 'tremopores' of the cheilostome *Schizoporella*, although the latter are extensions of hypostegal epithelium penetrating the frontal wall and having no connection with zooids. On the other hand, the basal canals of the cheilostomes *Cupuladria* and *Sertella*, which were described by Harmer as 'basal kenozooids' are different. Like tremopores, they contain extensions of the hypostegal epithelium which include storage cells in *Cupuladria* at least; but, unlike tremopores, they connect zooids with the basal hypostegal coelom. Clearly any simplification of terminology will have to take these differences into account. Consequently, it seems advisable to retain 'basal kenozooid' for the tissue occupying the 'basal canals' of *Cupuladria*, and to use 'punctum' in place of 'pseudopore'

and 'tremopore'. If there is any need to distinguish puncta according to the nature of the epithelial extensions accommodated by them, they can be referred to as 'eustegal' or 'hypostegal'.

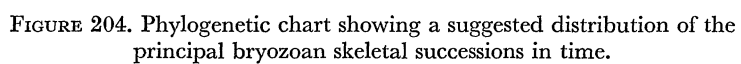
This clarification of terminology makes correlation of canal-like structures in other Orders easier. Puncta are unknown in extinct stenolaemates except for the 'accessory apertures' in certain fenestelloid cryptostomes like *Fenestrapora biperforata* Hall and a species of *Septopora* reported by Shishova (1952, p. 159). The 'mesopores' of the trepostomes are not puncta, but spaces created in a coelocyst by divergent growth of adjacent zooecia. Each space was occupied by a fold of hypostegal epithelium which periodically secreted vesicular tissue of diaphragms and cystiphragms as it retreated distally. Such spaces are identical with the 'alveolar' (i.e. 'vesicular') tissue of convex partitions (i.e. diaphragms and cystiphragms), in *Lichenopora*. They are also identical with the interzooecial 'vesicular zones' of the cryptostomes and the 'cystopores' of the cystoporates, and it would reduce ambiguity to use the terms 'mesopores', 'vesicles', 'diaphragms' and 'cystiphragms' for appropriate structures in all three groups.

The mesopores have also been compared with the 'dactylethra' of cyclostomes like *Clausa*; but such spaces were briefly occupied by autozooids and sealed off during subsequent growth of the subperiostracal skeleton. They need not be considered further.

Inwardly pointing cones of secondary shell known as pseudopuncta, with or without axial rods of granular calcite, have a significant distribution among bryozoans. They are unknown in cheilostomes, present in certain living cyclostomes like *Hornera* and *Lichenopora*, and strongly developed in almost all trepostomes, cystoporates and cryptostomes, among which they are known as acanthopores, minutopores and skeletal rods respectively. It seems, therefore, that pseudopuncta are restricted to skeletons of coelocystic origin. This distribution supports the assumption that pseudopuncta have always acted as muscle bases because such a function would have improved the attachment of highly folded hypostegal epithelium to the skeletal surface.

Our interpretation of the structural evolution of the bryozoan skeleton is illustrated in figure 204. The skeletal succession of the prototypic bryozoan which must have appeared sometime during the Cambrian may be visualized as an outer periostracal coat of chitin or protein underlain by a layer of vertical crystallites and an additional layer of protein-bound calcitic laminae in at least the immediate antecedents of the earliest recorded bryozoans. The skeleton was probably secreted as a pseudopunctate coelocyst within folds of hypostegal epithelium, and consisted of loosely aggregated zooecia which promoted the formation of mesopores.

Four main lines of descent evolved from the prototypic bryozoans including the cystoporates which, through the presence of mural pores alone, are as taxonomically viable as the trepostomes or cryptostomes. These three groups became extinct by the end of the Palaeozoic but the fourth, the cyclostomes, survived to the present day and was differentiated from the others by a radical change in shell secretion. The change involved a simplification in the arrangement of secretory epithelia so that the entire mineral skeleton not just its base, was deposited between the periostracum and eustegal epithelium. The skeletal succession remained the same except for the loss of pseudopuncta. Mesopores also disappeared because the gaps developing between diverging zooecia were no longer internal cavities enclosed by hypostegal epithelium but external depressions of a periostracum-covered surface. Punctuation developed in some of the younger stocks, but a more important change led to the appearance of coelocystic cyclostomes. *Lichenopora*, for example, down to the pseudopunctate condition of the shell and the vesicular tissue between zooecial rows, is a remarkable homeomorph of early Palaeozoic stenolaemates.



No new information is available about the early history of the cheilostomes. The great difference between the cheilostome and stenolaemate skeletal succession favours a neotenus derivation of the Order involving the loss of that part of the stenolaemate secretory regime controlling carbonate secretion. A ctenostomate ancestry is consistent with this conclusion because it would not have militated against the evolution of a new kind of mineral succession so characteristic of the cheilostomes in which even the secondary and tertiary layers are normally composed of vertically disposed crystallites. In any event, although the cheilostomes could not have evolved into an independent complex much before the Cretaceous, punctate and coelocystic species have already appeared.

We have received invaluable help and advice from many people in the course of this study. In particular, we wish to thank: Miss P. L. Cook of the British Museum of Natural History, and Dr D. E. Owen of the Manchester Museum, who kindly arranged for the loan of specimens in their care; Professor E. Voigt of the Geologisch-Paläontologisches Institut, Hamburg, Dr S. Reguant of the University of Barcelona, and Dr O. L. Karklins of the United States Geological Survey who were most generous in the provision of fossil material for sectioning; and Mr W. Pople of the University of Ghana and Dr J. S. Ryland of the University College, Swansea, for the supply of living material.

We also wish to express our indebtedness to Professor G. Owen and members of his staff in the Department of Zoology, the Queen's University of Belfast for affording facilities to maintain living bryozoans under laboratory conditions, and for advice in locating and preparing some of the specimens used; and Dr Jean Graham and Dr Katharine McClure, research assistants in the Department of Geology, The Queen's University, Belfast, for help in the preparation of sections and illustrations.

#### REFERENCES

- Armstrong, J. 1970 Zoarial microstructures of two Permian species of the bryozoan genus *Stenopora*. *Palaeontology* **13**, 581–587.
- Astrova, G. G. 1964 O novom stroyade Palaeozoyskikh Mshanok (A new order of palaeozoic bryozoa). *Paleont. Zh.* **2**, 22–31.
- Astrova, G. G. & Morozova, I. P. 1956 Taxonomy of Bryozoa of the Order Cryptostomata (in Russian). *Dokl. Akad. Nauk SSSR* **110**, 661–664.
- Banta, W. C. 1968 The body wall of cheilostome Bryozoa, pt. 1, the ectocyst of *Watersipora nigra* (Canu & Bassler). *J. Morph.* **125**, 497–508.
- Bassler, R. S. 1953 *Treatise on invertebrate paleontology* (ed. R. C. Moore), Part G: *Bryozoa*. Geol. Soc. Am. and University Kansas Press.
- Boardman, R. S. 1960 Trepostomatous bryozoa of the Hamilton Group of New York State. *Prof. Pap. U.S. geol. Surv.* **340**, 1–87.
- Boardman, R. S. & Cheetham, A. H. 1969 Skeletal growth, intracolony variation, and evolution in bryozoa: a review. *J. Paleont.* **43**, 205–233.
- Boardman, R. S. & Towe, K. M. 1966 Crystal growth and lamellar development in some Recent cyclostome bryozoa. *Spec. Pap. Geol. Soc. Am.* **101**, 20.
- Bobin, G. 1958 Structure et genèse des diaphragmes autozoeciaux chez *Bowerbankia imbricata* (Adams), (Bryozaire Ctenostome, Vesicularine). *Arch. Zool.* **96**, 50–100.
- Bobin, G. & Prenant, M. 1968 Sur le calcaire des parois autozoeciales d'*Electra verticillata* (Ell. et Sol.), Bryozaire cheilostome, anasca. *Archs Zool. exp. gén.* **109**, 157–191.
- Borg, F. 1926 Studies on Recent cyclostomatous Bryozoa. *Zool. Bidr. Upps.* **10**, 181–507.
- Borg, F. 1933 A revision of the Recent Heteroporidae (Bryozoa). *Zool. Bidr. Upps.* **14**, 253–394.
- Borg, F. 1965 A comparative and phyletic study on fossil and Recent bryozoa of the suborders Cyclostomata and Trepostomata. *Ark. Zool.* (Ser. 2), **17**, 1–91.
- Brood, K. 1970 Structure of *Pseudohornera bifida* (Eichwald). *Geol. För. Stock. Förh.* **92**, 188–199.
- Campbell, F. L. 1929 The detection and estimation of insect chitin, and the correlation of 'chitinisation' to hardness and pigmentation of the cuticle of the American cockroach, *Periplaneta americana*. *Ann. ent. Soc. Am.* **22**, 401–426.

- Cook, P. L. 1965 Notes on the Cupuladriidae (Polyzoa, Anasca). *Bull. Br. Mus. (Nat. Hist.) Zool.* **13**, 153–187.
- Corneliusson, E. F. & Perry, T. G. 1970 The ectoproct *Batostoma? cornula* (Cumings & Galloway) and its enigmatic intrazooecial spines. Fort Atkinson Limestone (Cincinnatian), Wilmington, Illinois. *J. Paleont.* **44**, 997–1008.
- Culling, C. E. A. 1963 *Handbook of histopathological techniques* London: Butterworths.
- Cummings, E. R. 1912 Development and systematic position of the monticuliporoids. *Bull. Geol. Soc. Am.* **23**, 357–370.
- Harland, W. B. *et al.* (eds.) 1967 *The fossil record: a symposium with documentation*. Geol. Soc. Lond.
- Harmer, Sir S. F. 1934 Polyzoa of the Siboga Expedition, Pt. III. Cheilostomata, Ascophora, 1. Reteporidae. *Rep. Siboga Exped.* **28c**, 503–635.
- Harmer, Sir S. F. 1957 Polyzoa of the Siboga Expedition, Pt. IV. Cheilostomata, Ascophora 2. Ascophora, except Reteporidae. *Rep. Siboga Exped.* **28d**, 641–1147.
- Hyman, L. H. 1959 *The invertebrates* 5. *Smaller coelomate groups*. New York: McGraw-Hill.
- Illies, G. 1968 Multiseriale Bryozoa Cyclostomata mit gewölbtem zweigquerschnitt aus dem Dogger des Oberrheingebietes. *Oberrhein. geol. Abh.* **17**, 217–249.
- Karklins, O. L. 1969 The cryptostome Bryozoa from the Middle Ordovician Decorah Shale, Minnesota. *Geol. Surv. Minnesota Spec. Pap.* **6**, 1–78.
- Levinson, G. M. R. 1909 *Morphological and systematic studies on the cheilostomatous Bryozoa*. Copenhagen: Nat. Forfatt. Forlag.
- Lutaud, G. 1961 Contributions à l'étude du bourgeonnement et de la croissance des colonies chez *Membranipora membranaeca* (Linneé). Bryozoaire chilostome. *Annls. Soc. r. zool. Belg.* **91**, 157–300.
- Mannil, R. M. 1959 Problems in the stratigraphy and Bryozoa of the Ordovician of Estonia. *Dokl. Akad. Nauk Estonian SSSR*. pp. 1–40.
- Ross, J. R. P. 1963 *Constellaria* from the Chazyan (Ordovician), Isle La Motte, Vermont. *J. Paleont.* **37**, 51–56.
- Ross, J. R. P. 1964 Morphology and phylogeny of early Ectoprocta (Bryozoa). *Bull. Geol. Soc. Am.* **75**, 927–948.
- Ross, J. R. P. 1966 An early Ordovician ectoproct from Oklahoma. *Okla. Geol. Notes* **26**, 218–224.
- Rucker, J. B. & Carver, R. E. 1969 A survey of the carbonate mineralogy of cheilostome bryozoa. *J. Paleont.* **43**, 791–799.
- Ryland, J. S. 1970 *Bryozoans*. London: Hutchinson.
- Schneider, D. 1963 Normal and phototropic growth reactions in the marine bryozoan *Bugula avicularia*. In *The lower metazoa* (ed. E. C. Dougherty), pp. 357–371. Los Angeles: University California Press.
- Schopf, T. J. M. & Travis, D. F. 1968 Skeletal wall structure of a calcified bryozoan (Phylum Ectoprocta) *Biol. Bull. mar. biol. Lab., Woods Hole* **135**, 436.
- Shishova, H. A. 1952 Carboniferous bryozoa of the genus *Septopora* from the Moscow and Don areas. *Dokl. Akad. Nauk. SSSR* **40**, 159–176.
- Silén, L. 1944 On the formation of the interzoooidal communications of the Bryozoa. *Zool. Bidr. Upps.* **22**, 433–488.
- Söderqvist, T. 1968 Observations on extracellular body wall structures in *Crisia eburnea*. *Atti Soc. ital. Sci. nat.* **108**, 115–118.
- Tavener-Smith, R. 1969a Shell structure and growth in the Fenestellidae (Bryozoa) *Palaeontology* **12**, 281–309.
- Tavener-Smith, R. 1969b Wall structure and acanthopores in the bryozoan *Leioclema asperum*. *Lethaia* **2**, 89–97.
- Tavener-Smith, R. & Williams, A. 1970 Structure of the compensation sac in two ascophoran bryozoans. *Proc. R. Soc. Lond. B* **175**, 235–254.
- Utgaard, J. 1968 A revision of North American genera of ceramoporoid bryozoans (Ectoprocta): part 1; Anolotichiidae. *J. Paleont.* **42**, 1033–1041.
- Williams, A. 1968 Evolution of the shell structure of articulate brachiopods. *Palaeont. Spec. Pap.* **2**, 1–55.

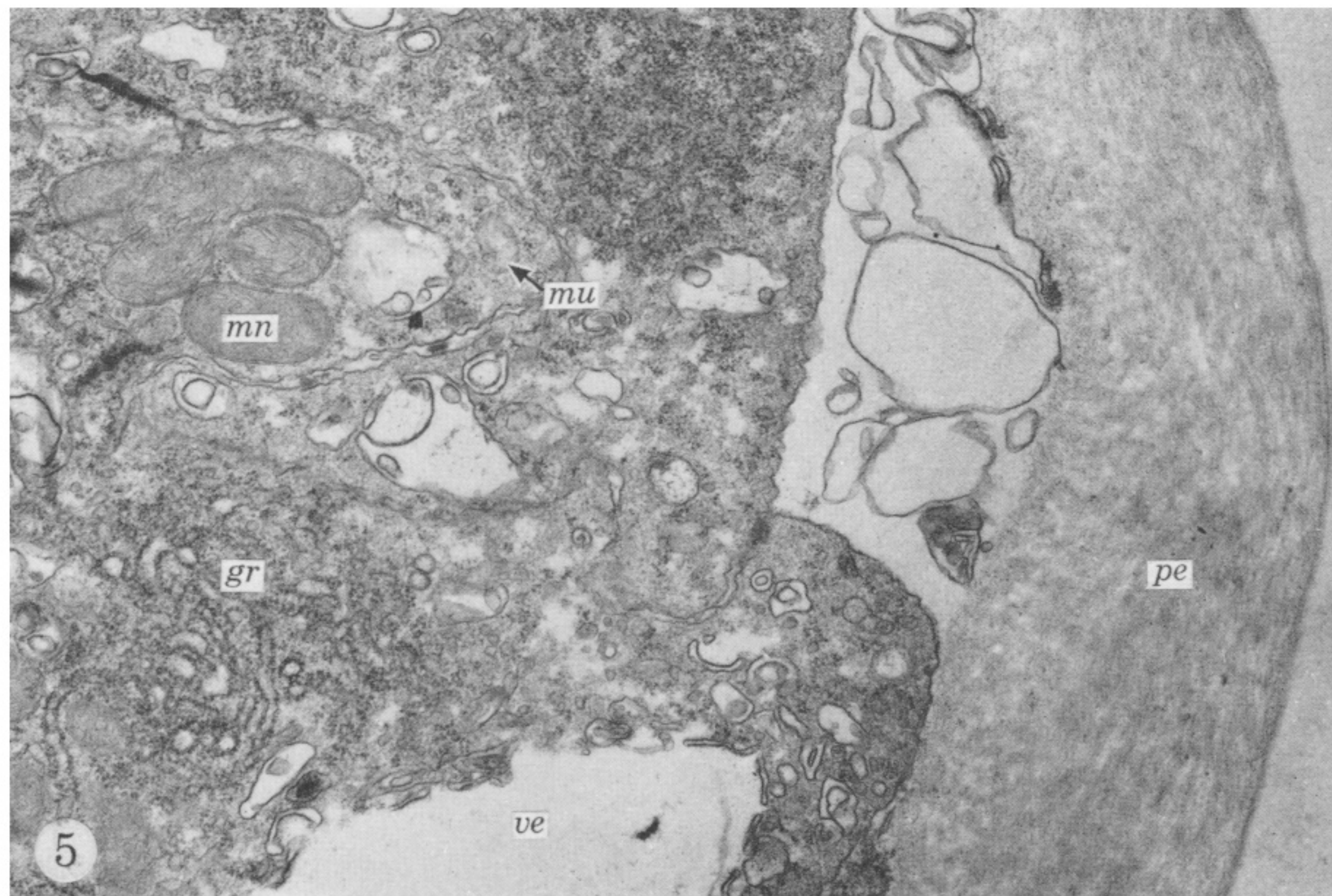
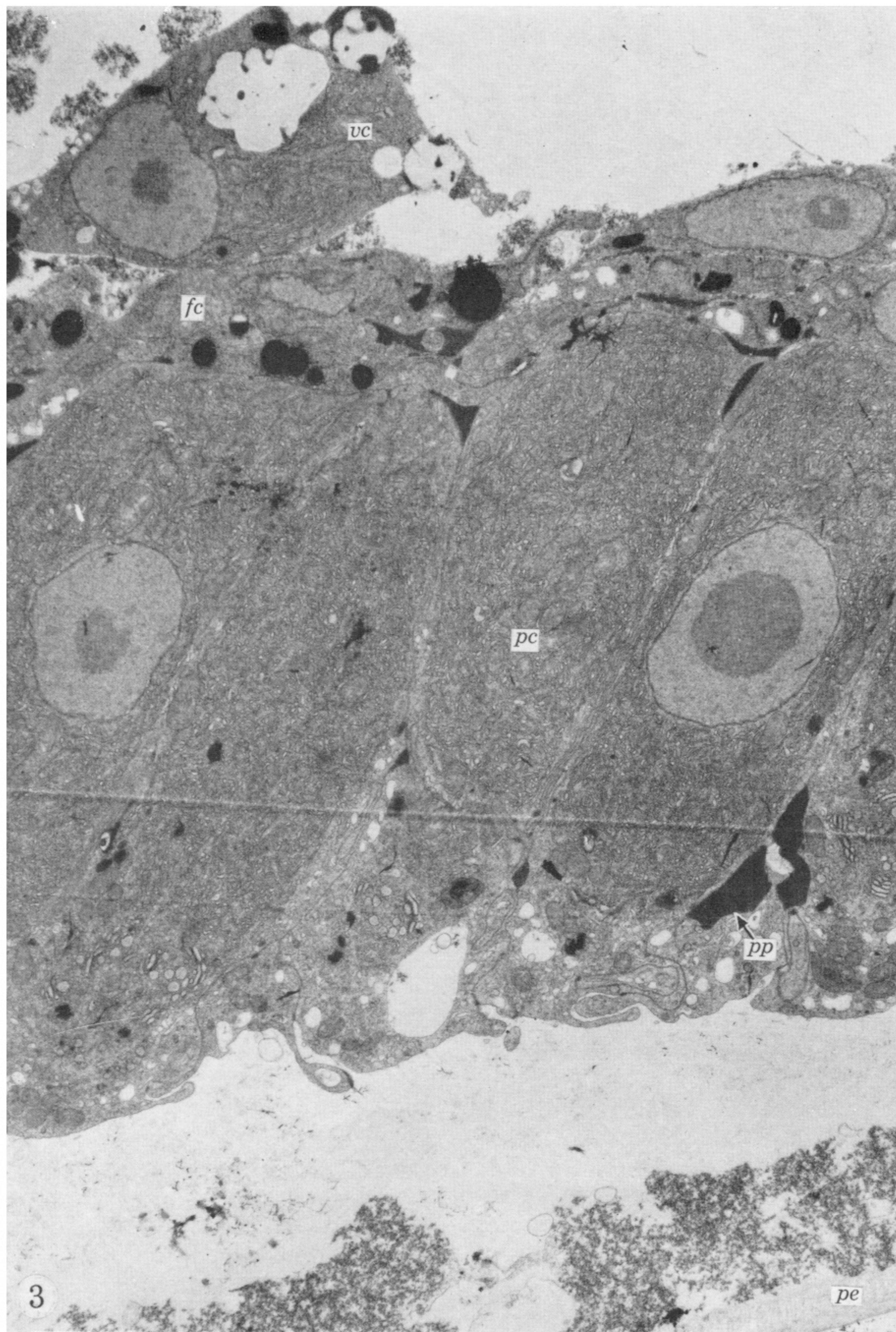


# STUDY OF LIVING AND FOSSIL BRYOZOA

## LIST OF ABBREVIATIONS

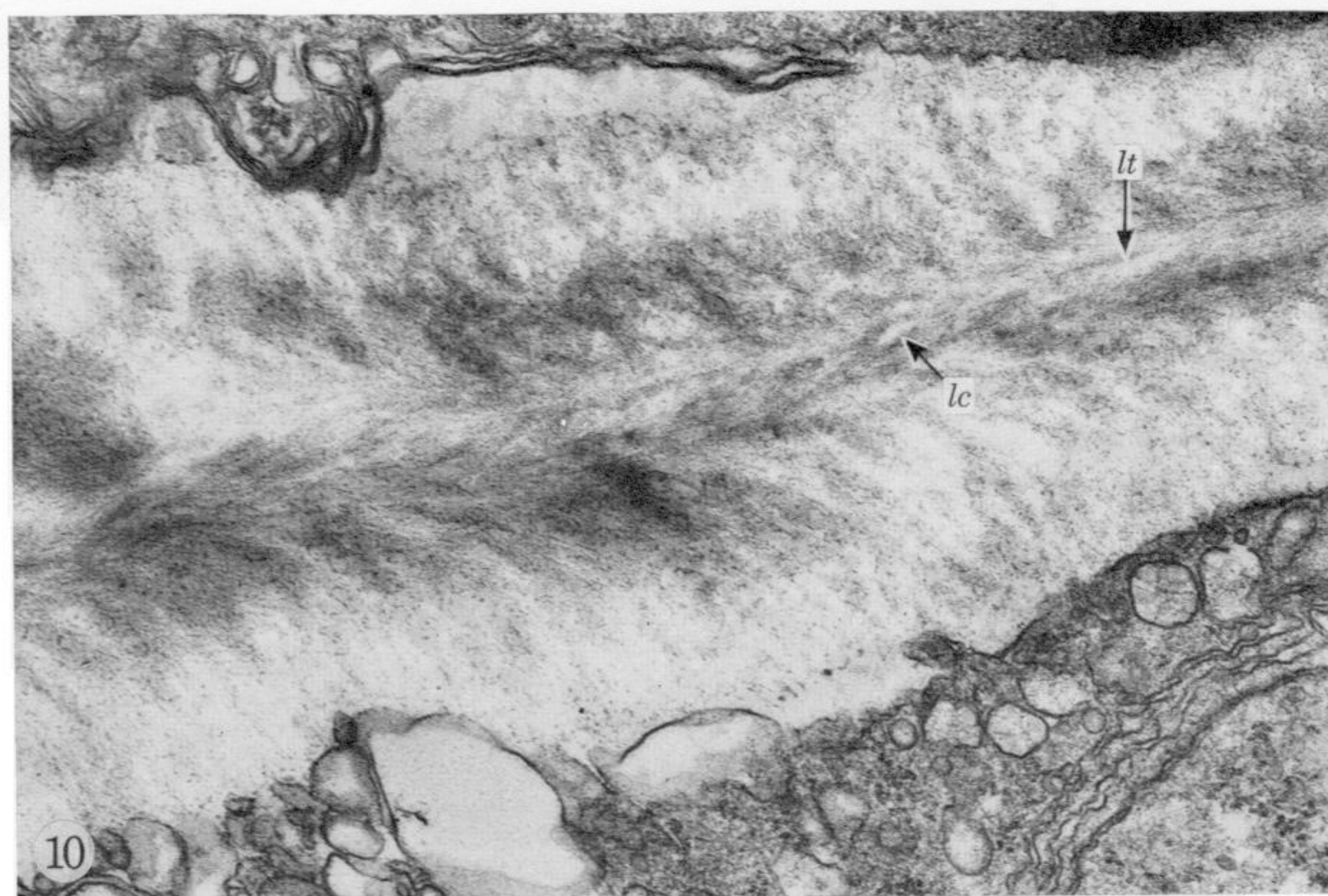
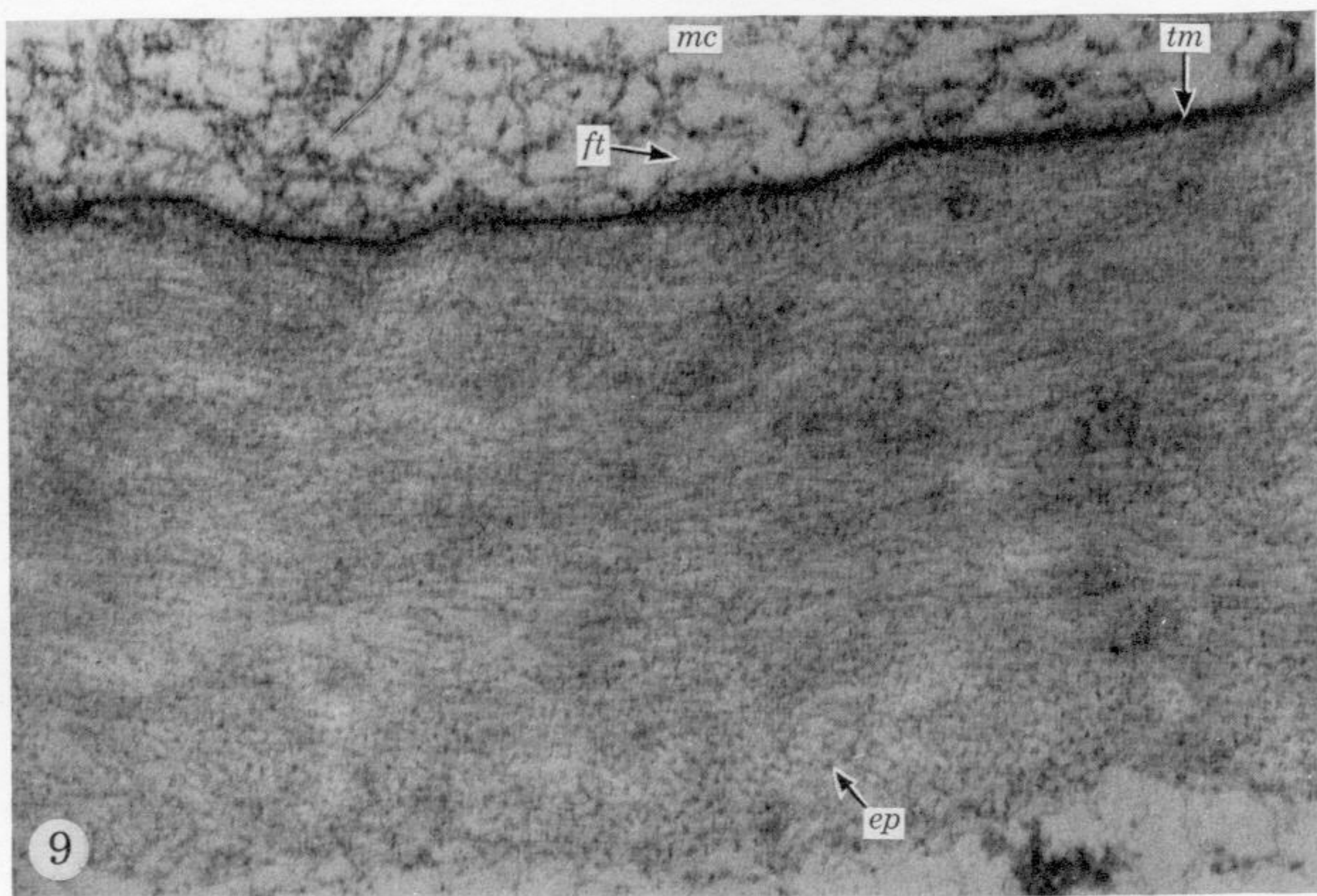
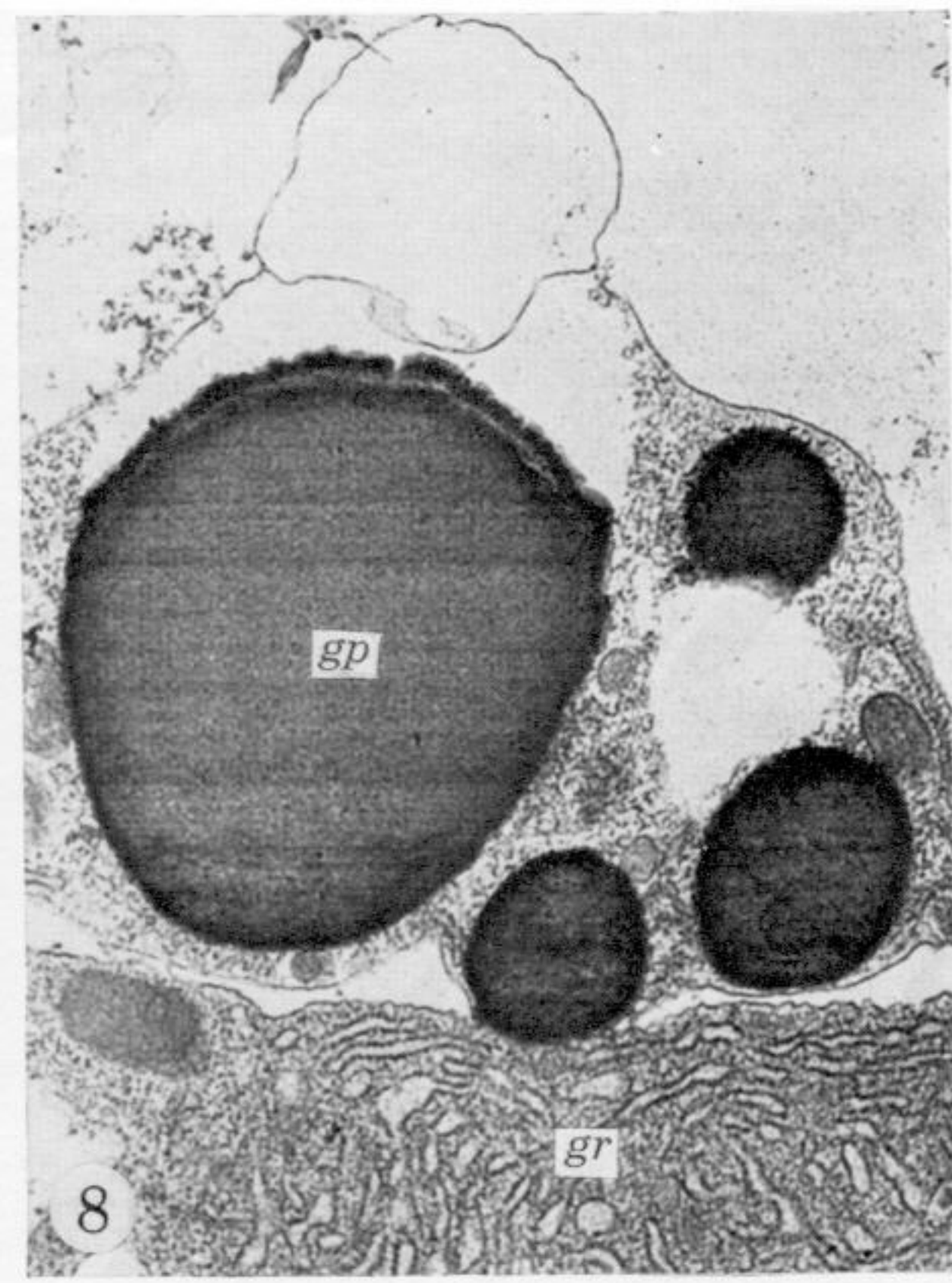
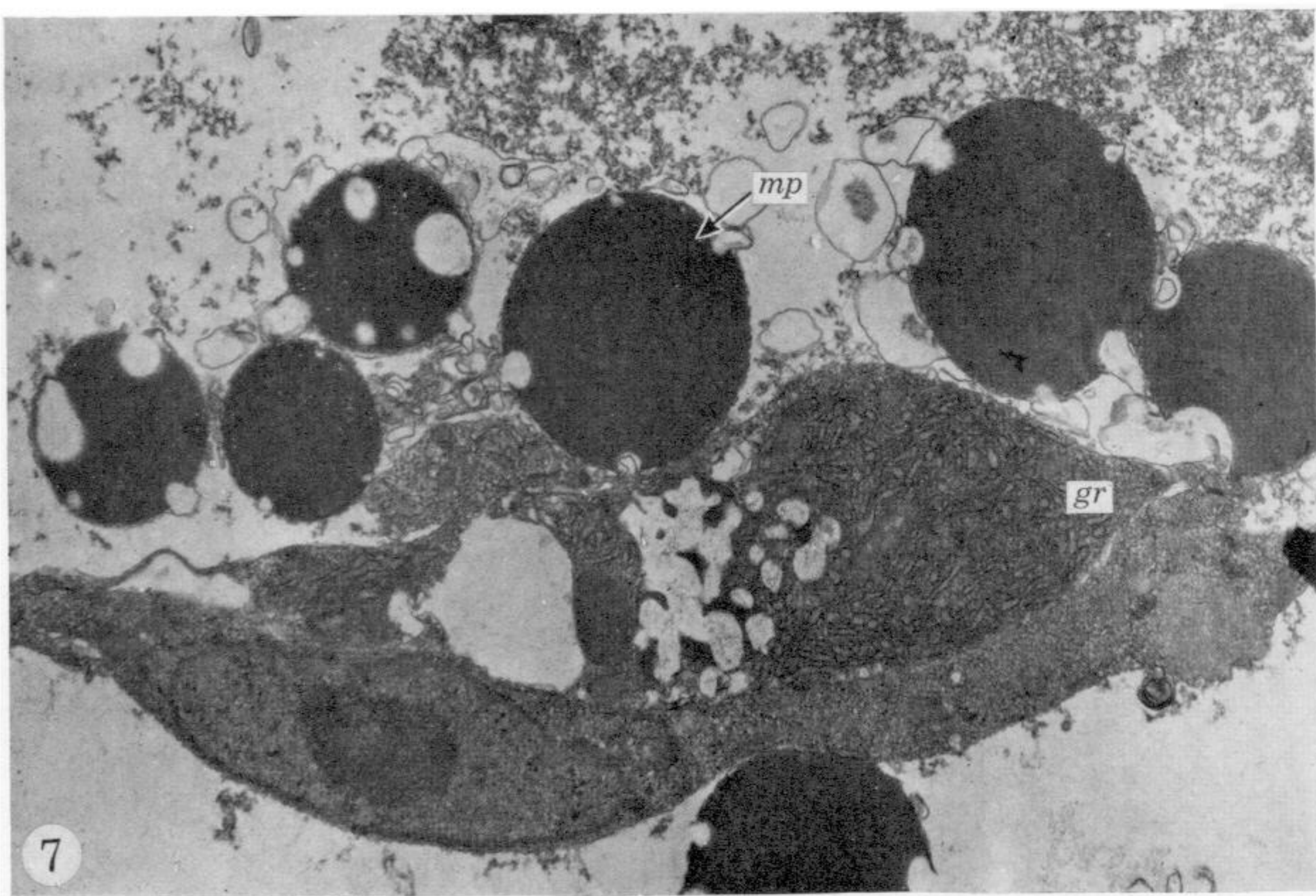
<i>aa</i>	ancestrula	<i>fm</i>	proteinous film	<i>pe</i>	periostracum
<i>ac</i>	acicular crystallite	<i>fs</i>	frontal spine	<i>pf</i>	primary carbonate film
<i>ae</i>	aperture	<i>ft</i>	filament	<i>pg</i>	periostracal plug
<i>al</i>	axial tube	<i>fw</i>	frontal wall	<i>pl</i>	primary layer
<i>am</i>	avicularium	<i>fz</i>	first zooid	<i>pm</i>	primary plate
<i>an</i>	acanthopore (or skeletal rod or minutopore or pseudopunctum)	<i>ge</i>	granule	<i>pn</i>	pseudopunctum
<i>ap</i>	aragonite prism	<i>gl</i>	growth line	<i>pp</i>	polysaccharide protein secretion
<i>as</i>	alveolus	<i>gp</i>	glycoprotein	<i>pr</i>	pore
<i>at</i>	anocyst	<i>gr</i>	granular endoplasmic reticulum	<i>ps</i>	proteinous sheet mainly in secondary layer
<i>bl</i>	laminar band	<i>gs</i>	growth surface	<i>py</i>	primary disk
<i>br</i>	basal layer	<i>gt</i>	gymnocyst	<i>pz</i>	primary zooecium
<i>bw</i>	basal wall	<i>il</i>	intrabasal sheet	<i>rc</i>	rhombic crystallites
<i>ca</i>	carina	<i>ir</i>	internal surface	<i>rg</i>	protein ring
<i>cc</i>	core cell	<i>is</i>	intercellular space	<i>rp</i>	rosette plate
<i>cf</i>	calcite film	<i>kc</i>	kenozooid chamber	<i>sl</i>	secondary layer
<i>cl</i>	canal	<i>la</i>	lamina	<i>sp</i>	scarp of acicular crystallites
<i>cm</i>	cystiphragm	<i>lc</i>	lacuna	<i>sr</i>	smooth endoplasmic reticulum
<i>cp</i>	calcareous partition	<i>le</i>	lenticle (or lens)	<i>ss</i>	inner sealing surface
<i>cr</i>	calcite ridge	<i>li</i>	lipid	<i>su</i>	substrate
<i>cs</i>	cystopore	<i>lt</i>	linear trail	<i>tc</i>	tabular crystallite
<i>ct</i>	cryptocyst	<i>lw</i>	lateral wall	<i>te</i>	tubercle
<i>de</i>	desmosome	<i>ma</i>	mesotheca	<i>tl</i>	tertiary layer
<i>dm</i>	diaphragm	<i>mc</i>	mucin	<i>tm</i>	triple unit membrane
<i>ec</i>	external coat	<i>me</i>	mesopore	<i>tw</i>	transverse wall
<i>el</i>	extraneous layer	<i>mi</i>	microvillus	<i>vc</i>	vesicular cell
<i>em</i>	epithelium	<i>ml</i>	mural pore	<i>ve</i>	vesicle
<i>ep</i>	electron-dense particle	<i>mn</i>	mitochondrion	<i>zc</i>	zoecial crater
<i>ex</i>	exterior	<i>mp</i>	mucoprotein	<i>zm</i>	zoecial chamber
<i>ez</i>	edge of colony	<i>mu</i>	mucopolysaccharide	<i>zw</i>	zoecial wall
<i>fb</i>	filamentous brush	<i>oc</i>	ovicell chamber		
<i>fc</i>	fusiform cell	<i>op</i>	organic partition		
<i>fe</i>	fibre	<i>ot</i>	outgrowth		
<i>fl</i>	folds in plasmalemma	<i>pa</i>	punctum		
		<i>pc</i>	palisade cell		
		<i>pd</i>	pad		





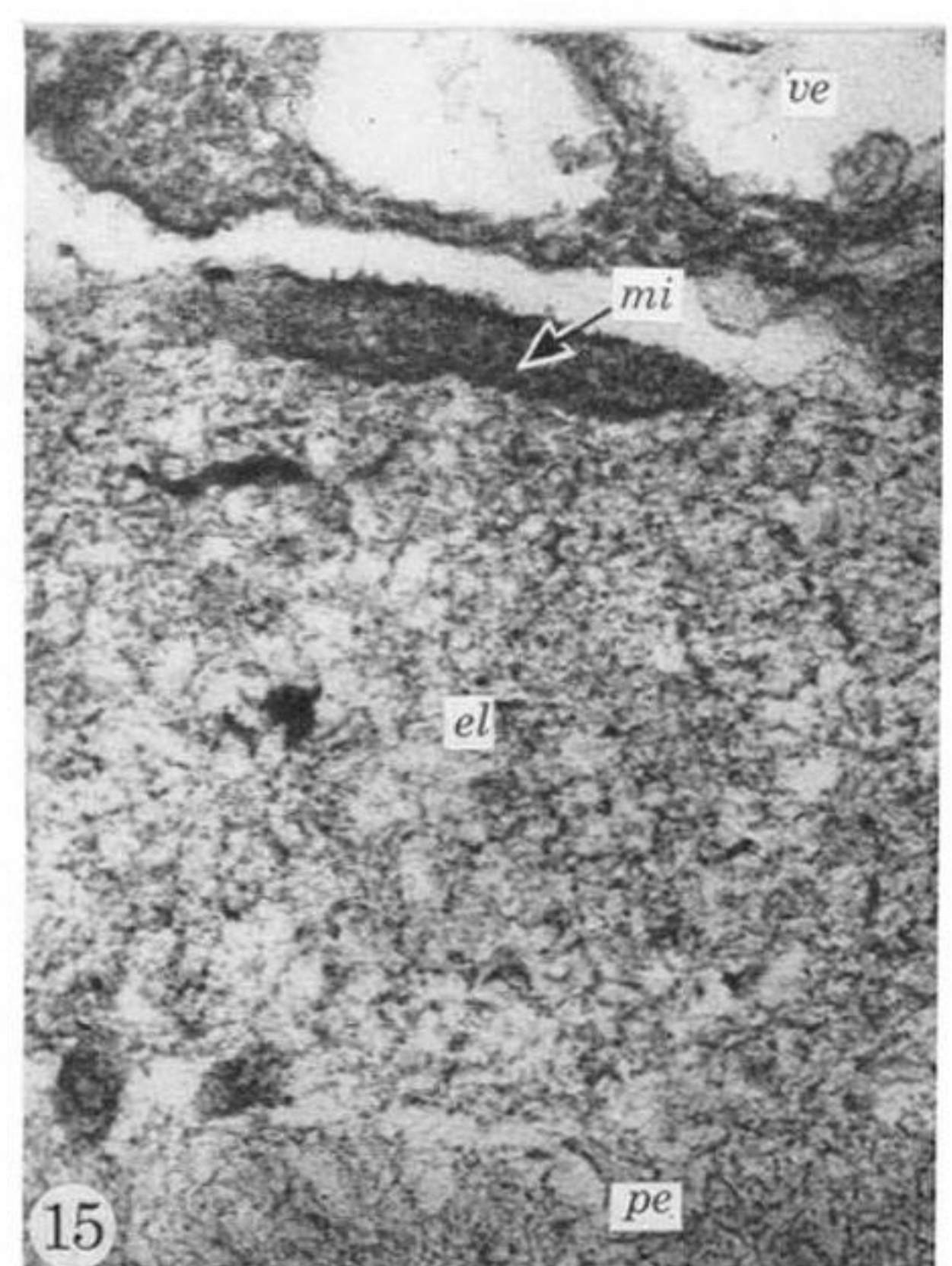
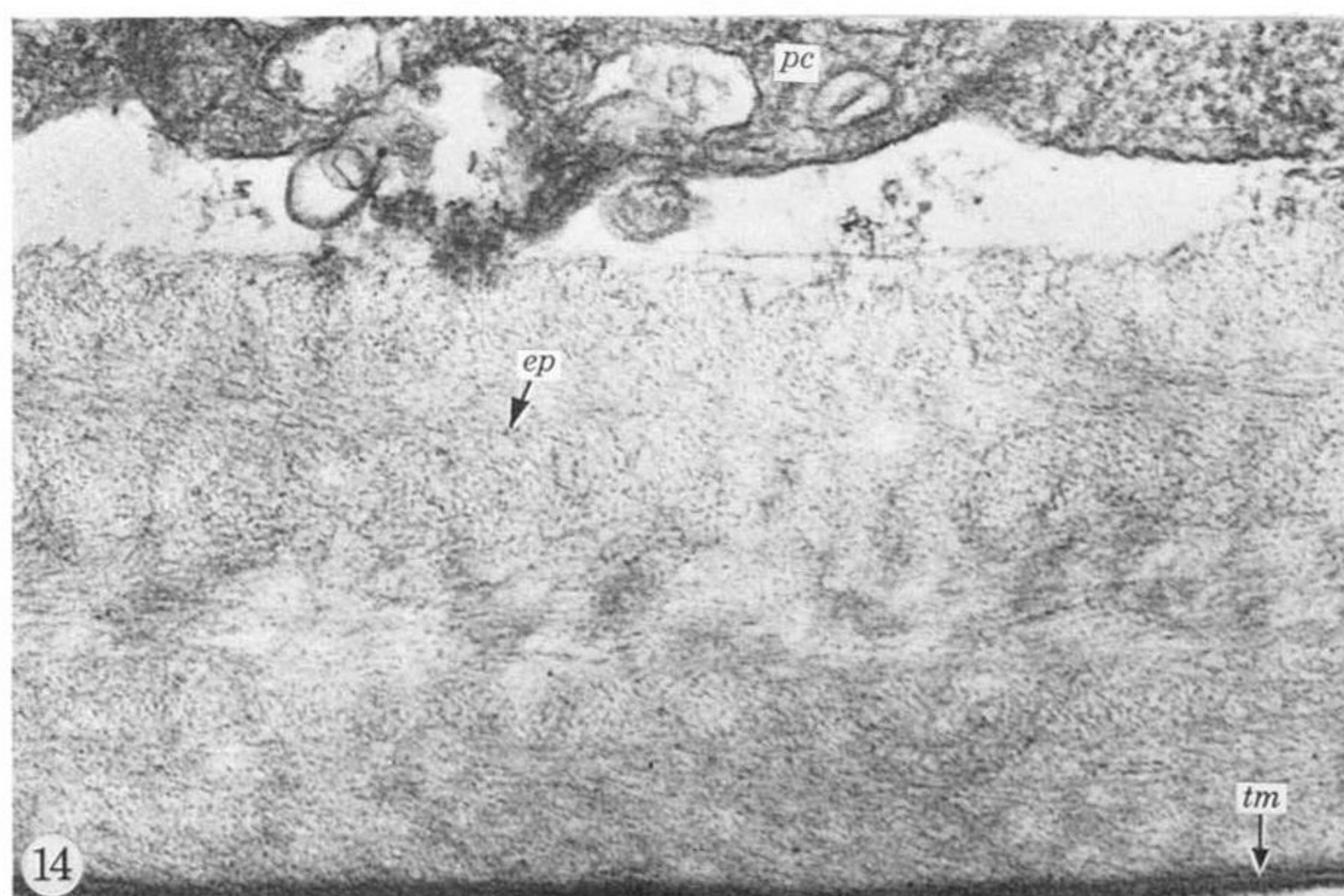
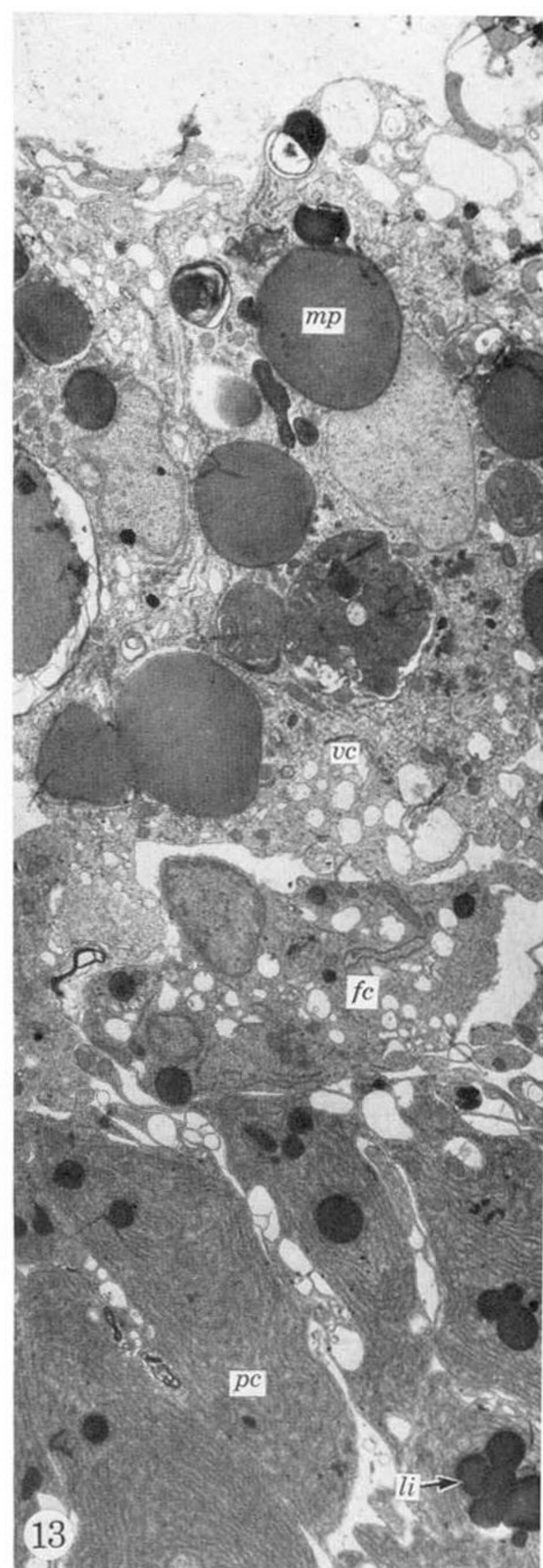
FIGURES 3 TO 6. For legends see facing page.





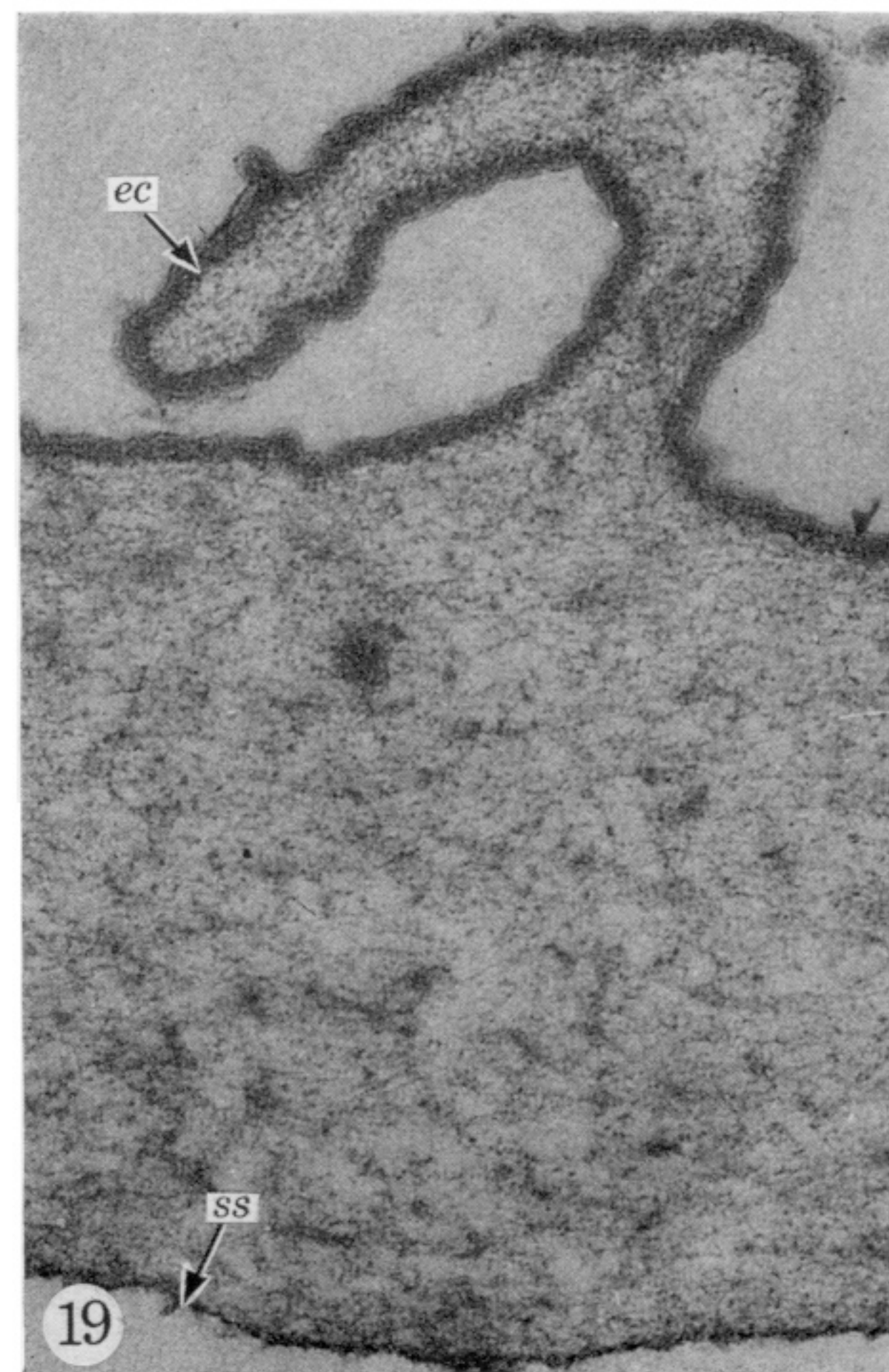
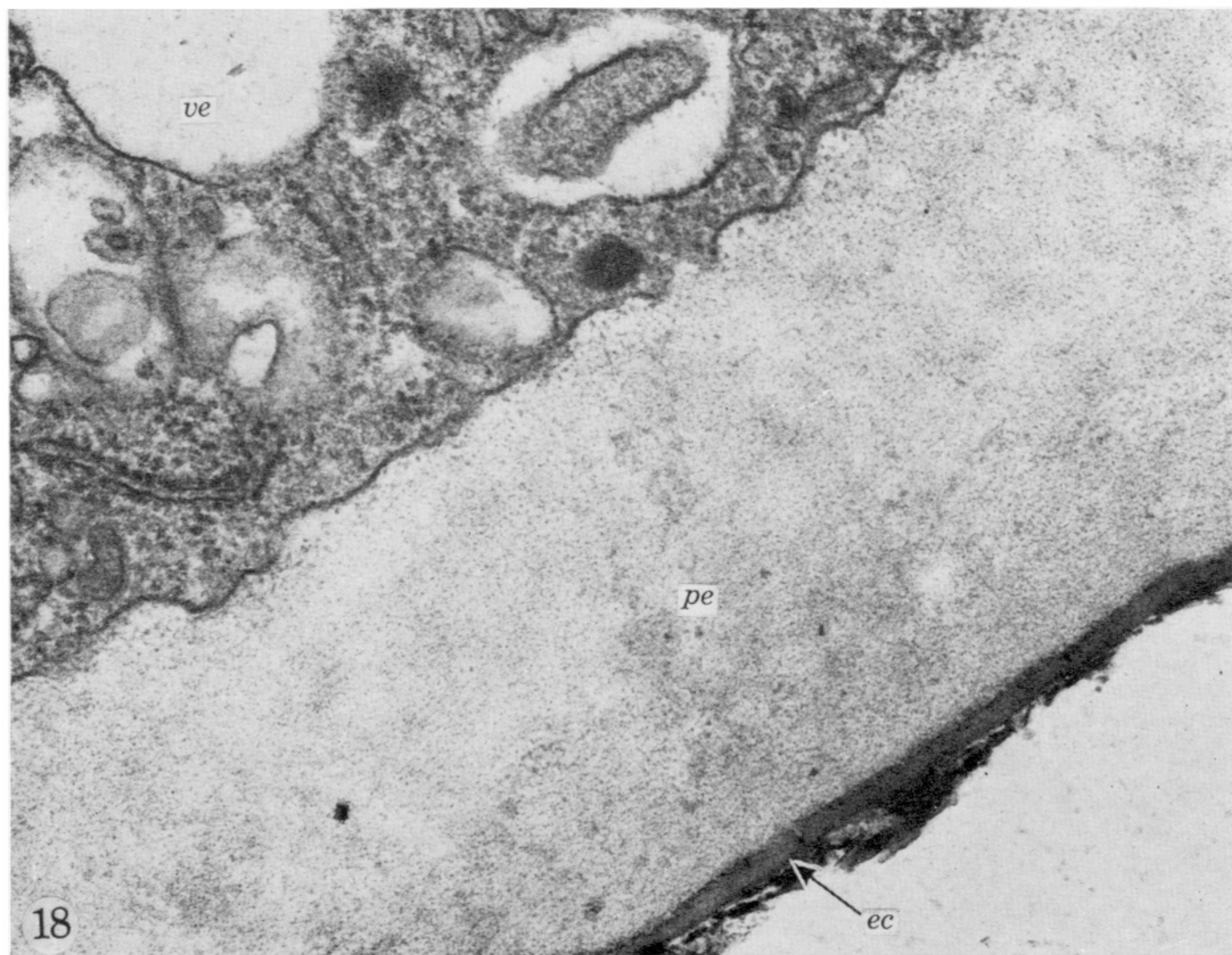
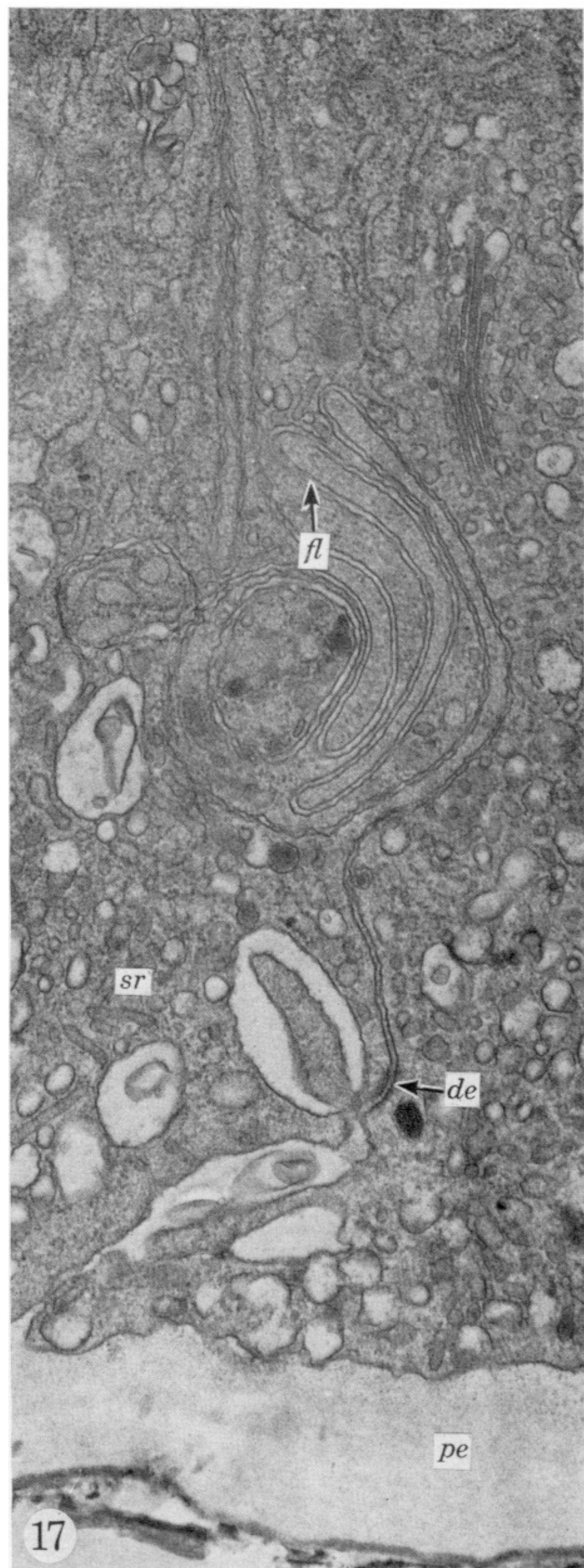
FIGURES 7 TO 11. For legends see facing page.





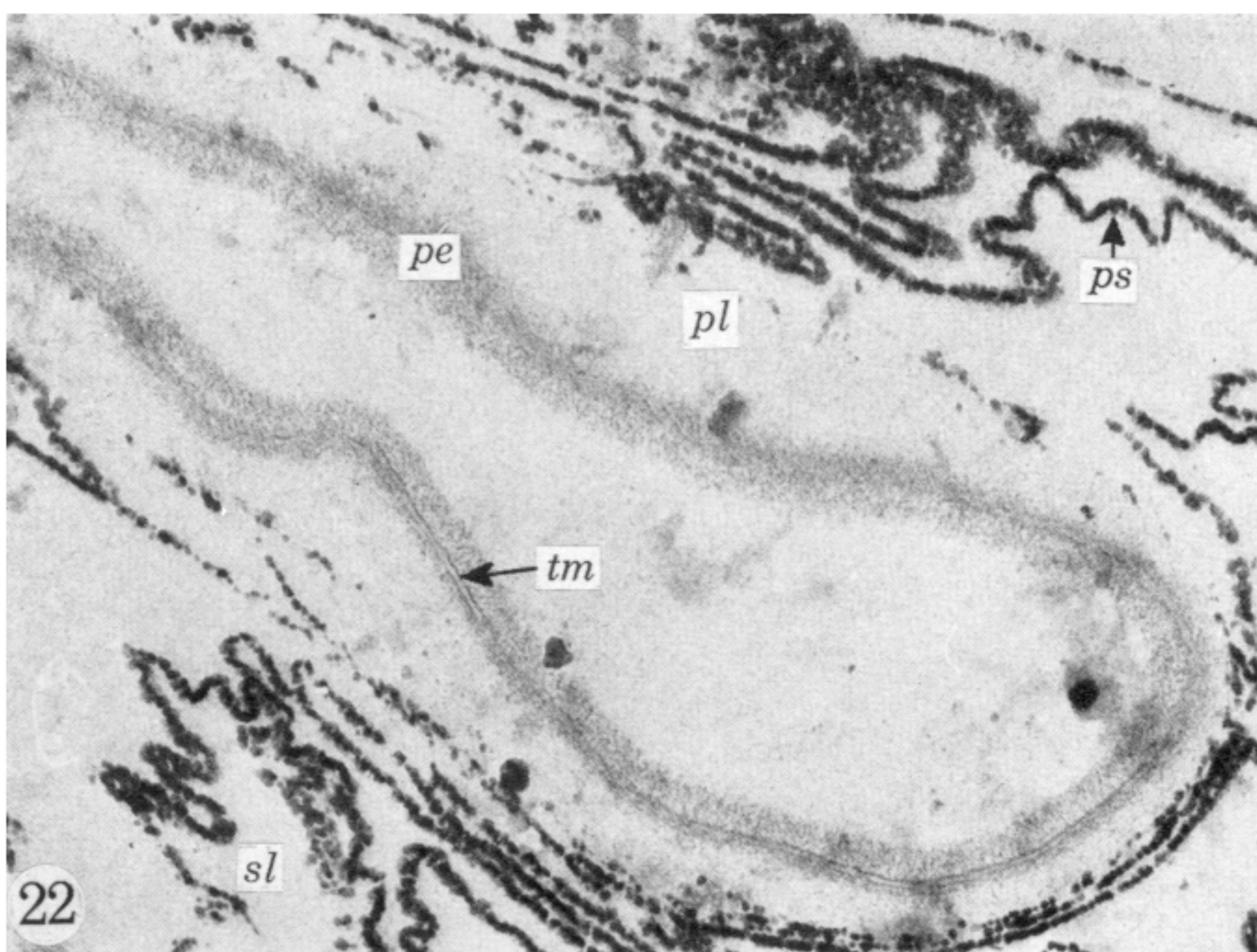
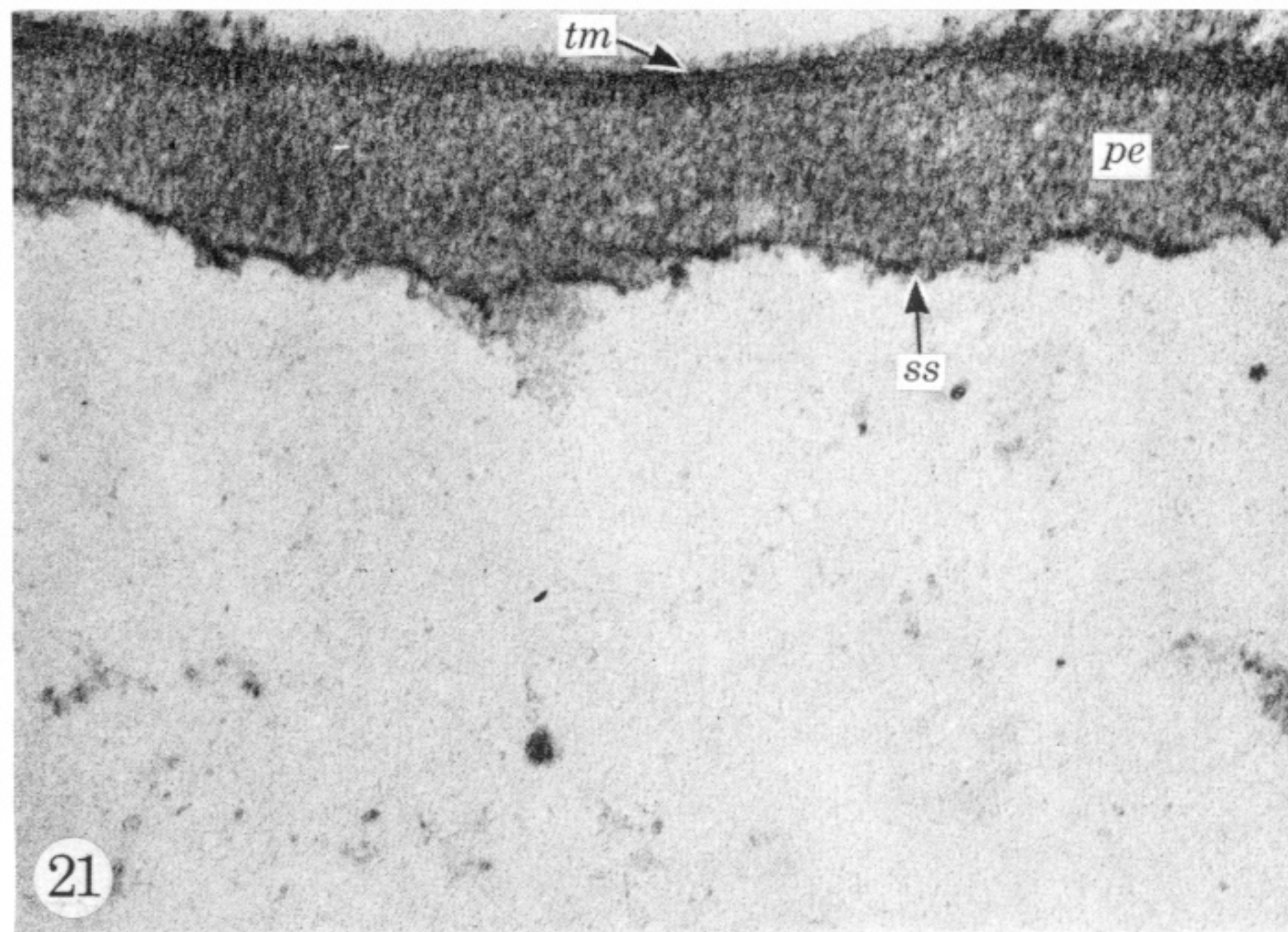
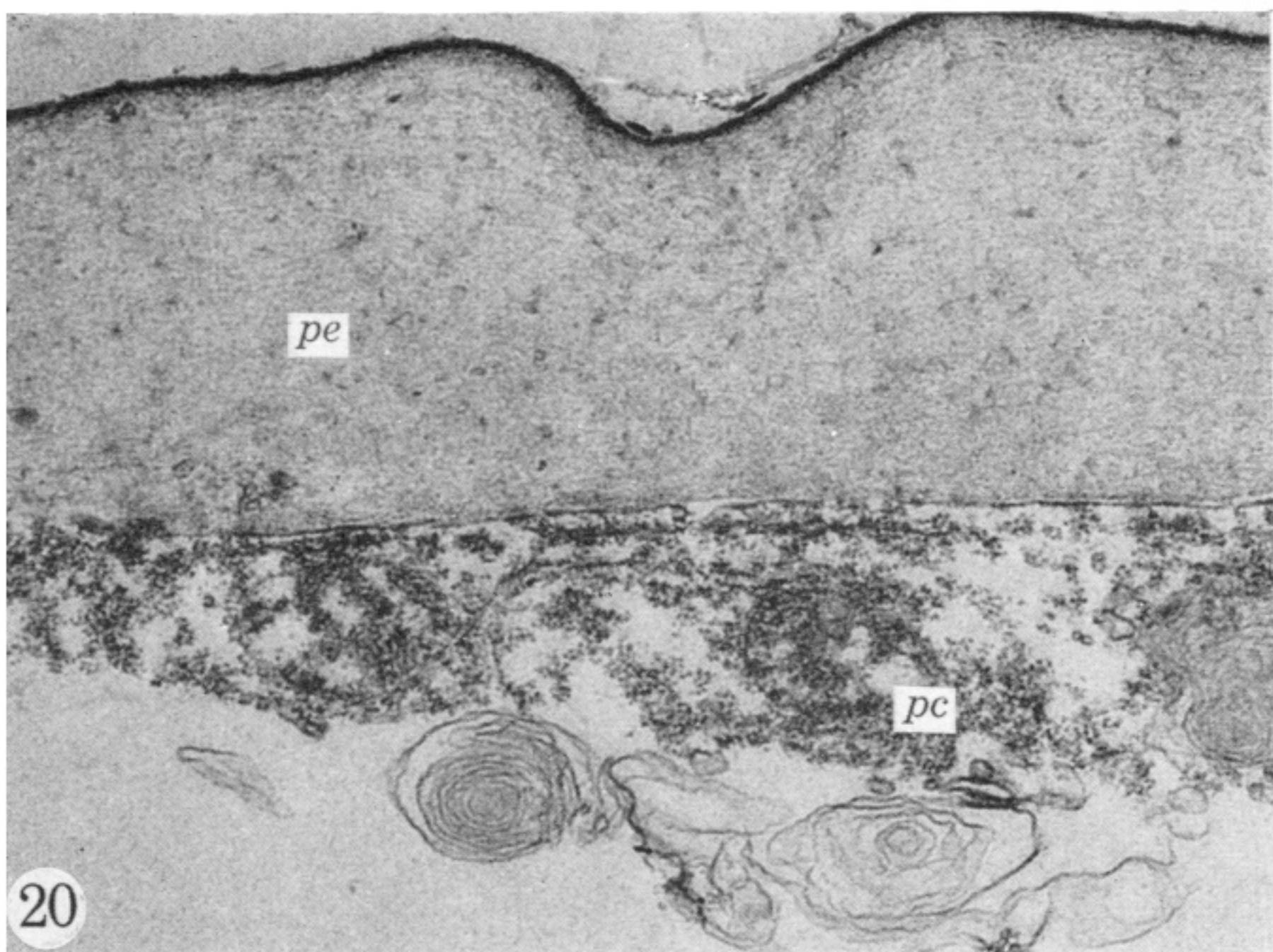
FIGURES 12 TO 15. For legends see facing page.





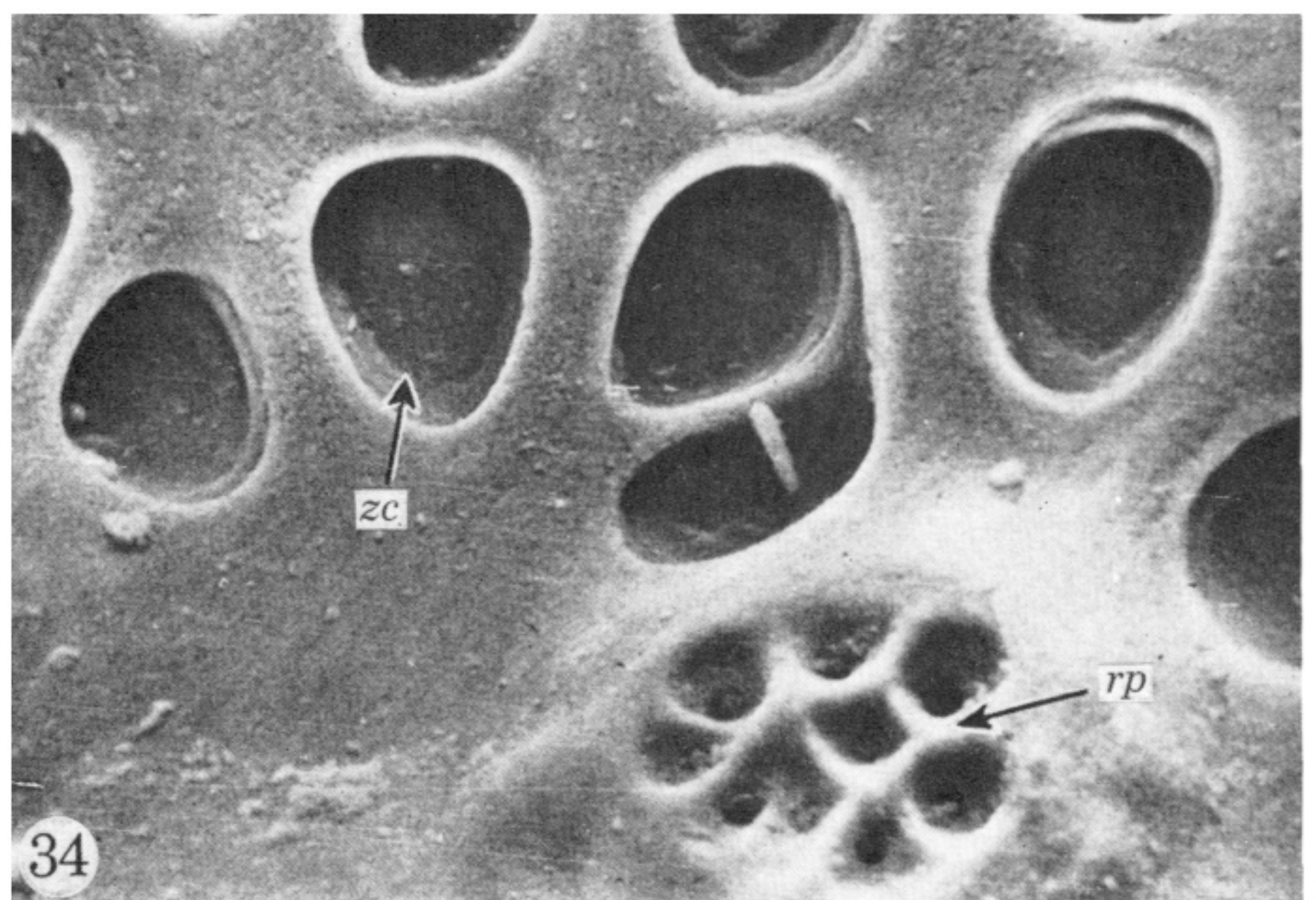
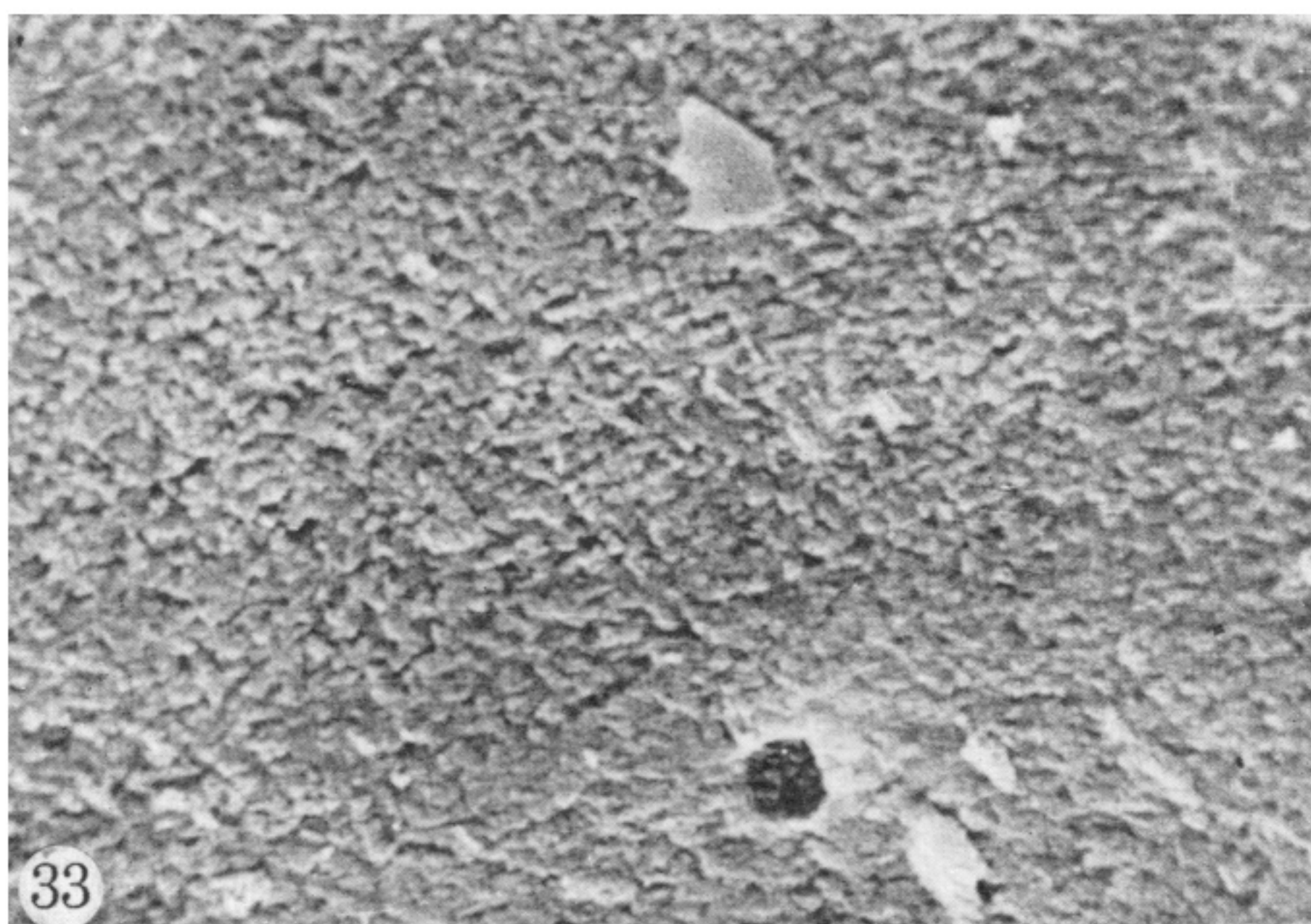
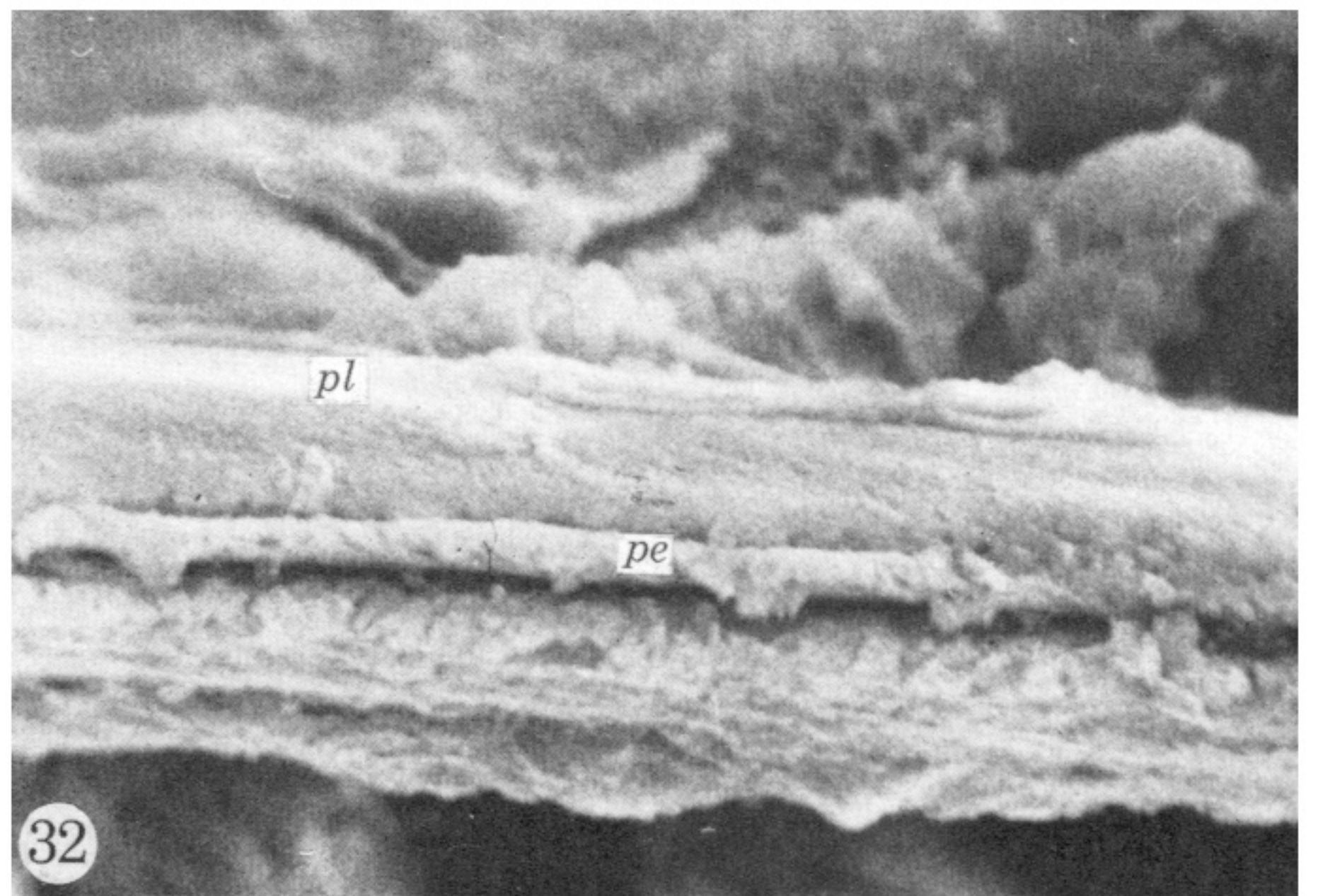
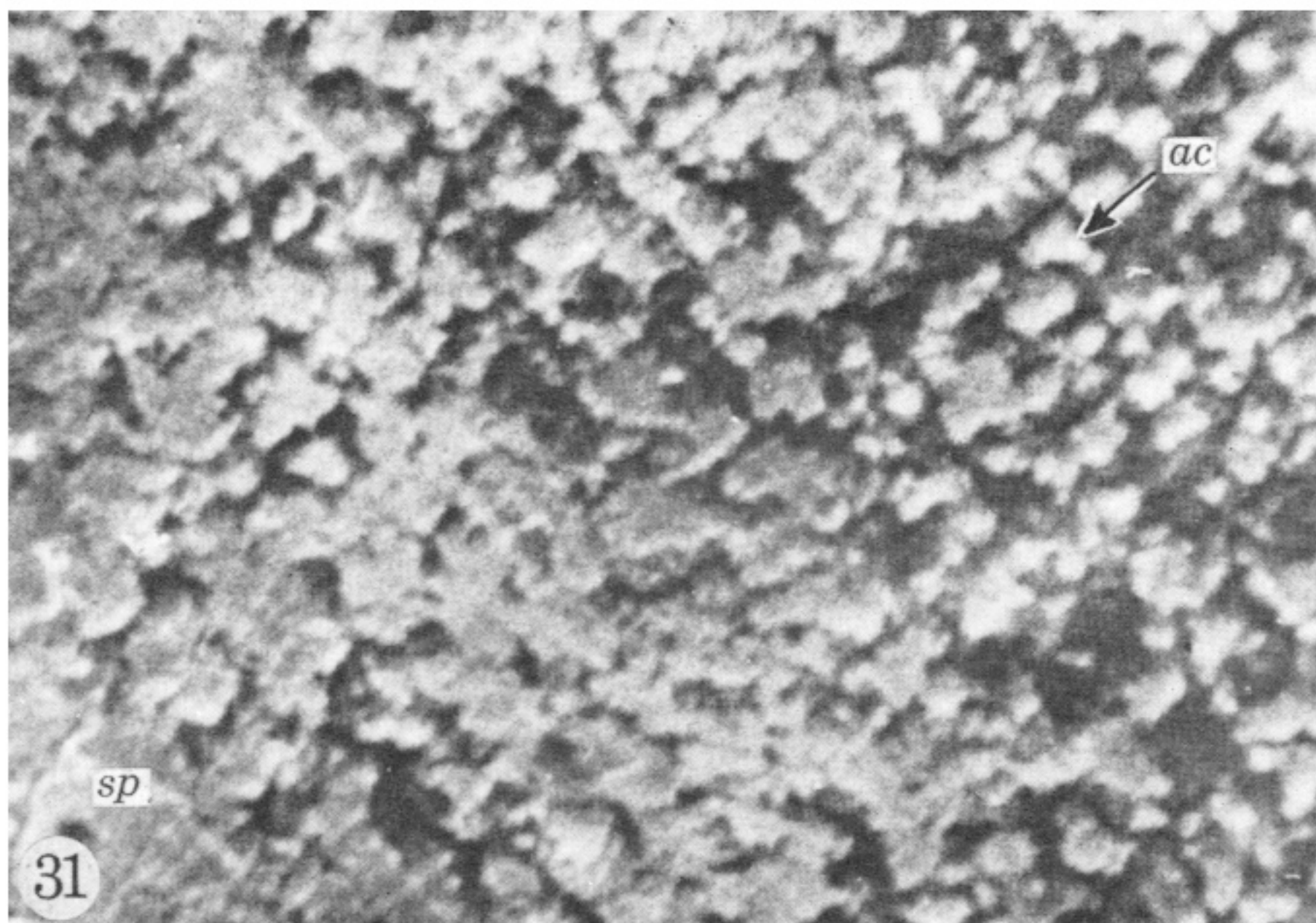
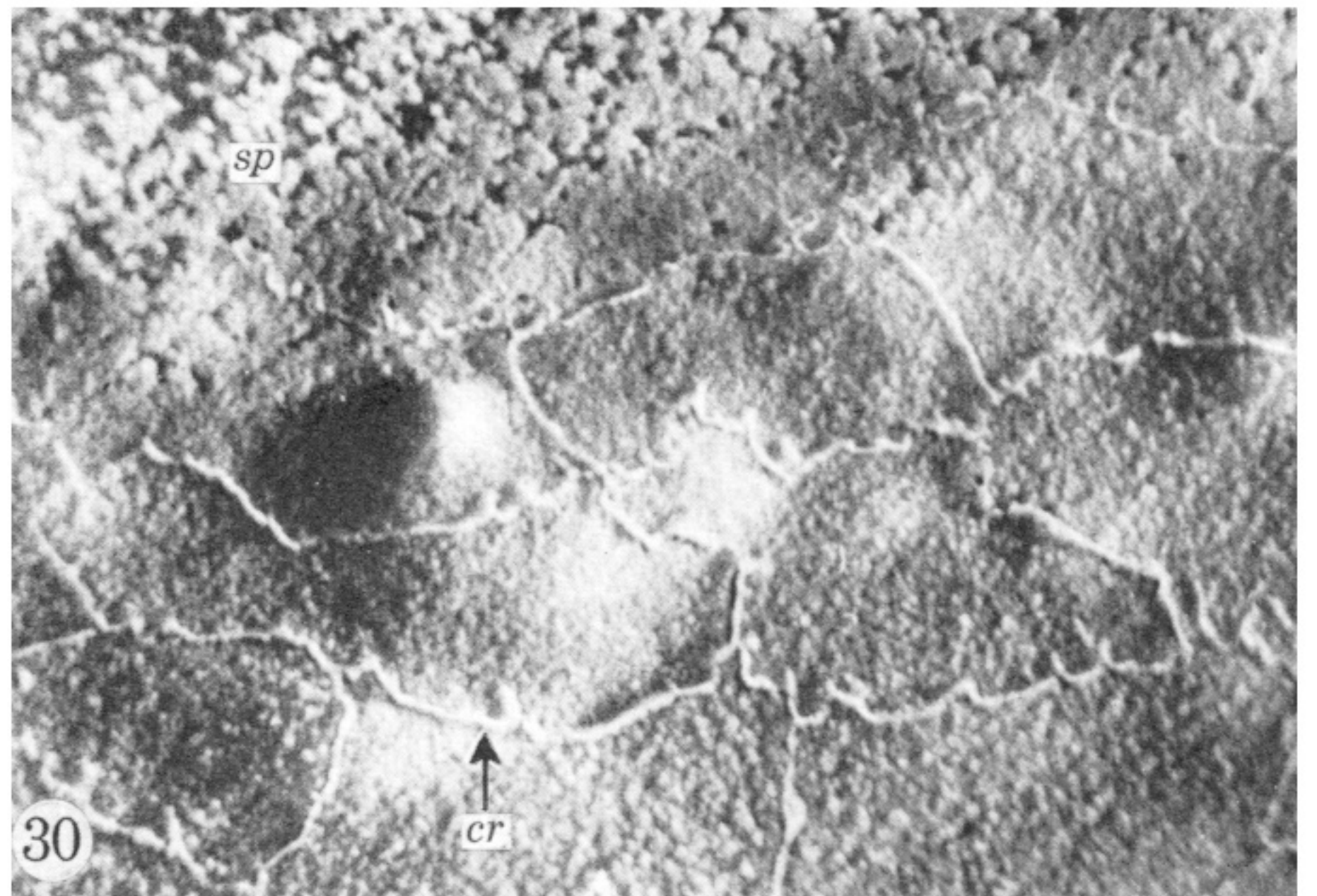
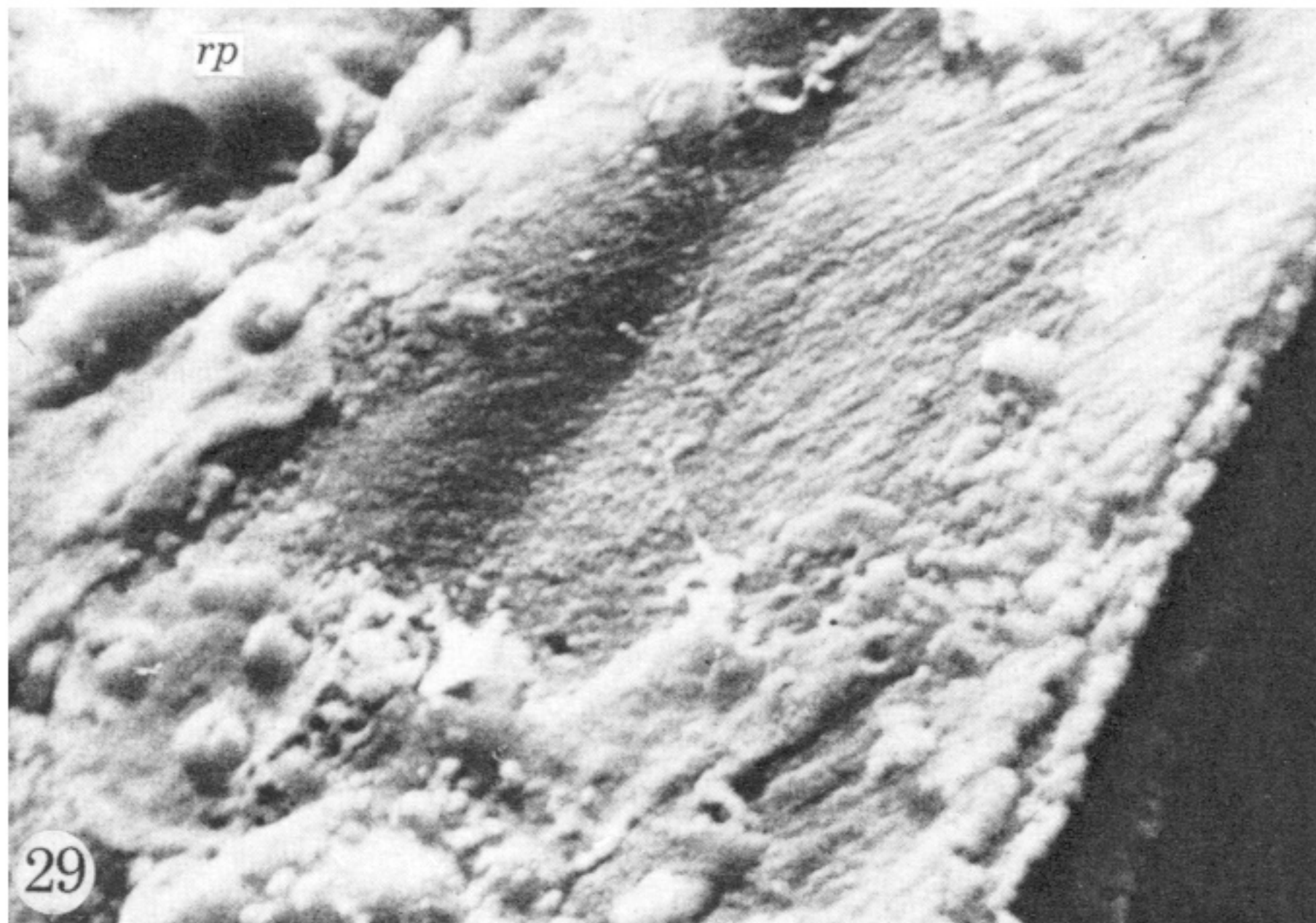
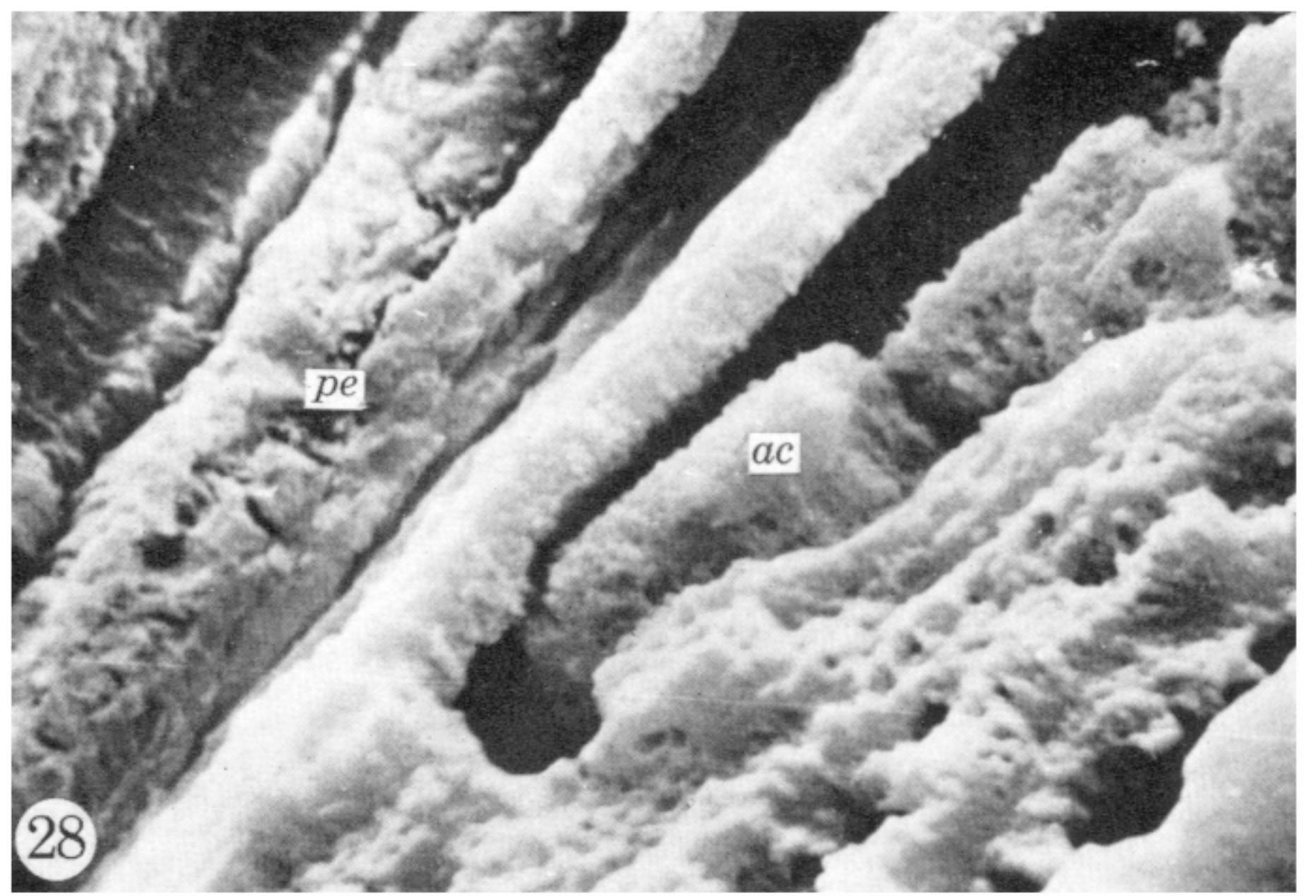
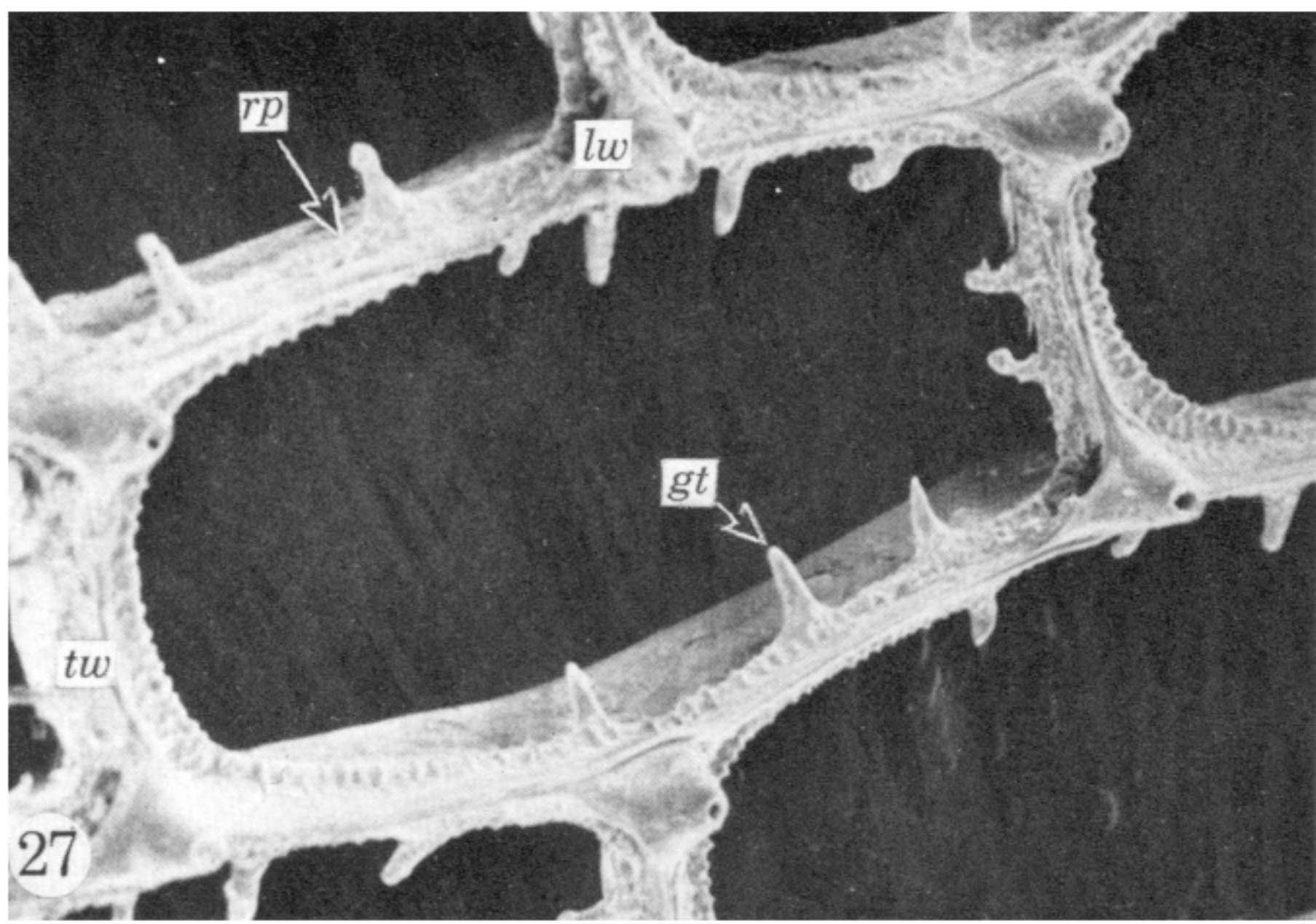
FIGURES 16 TO 19. For legends see facing page.





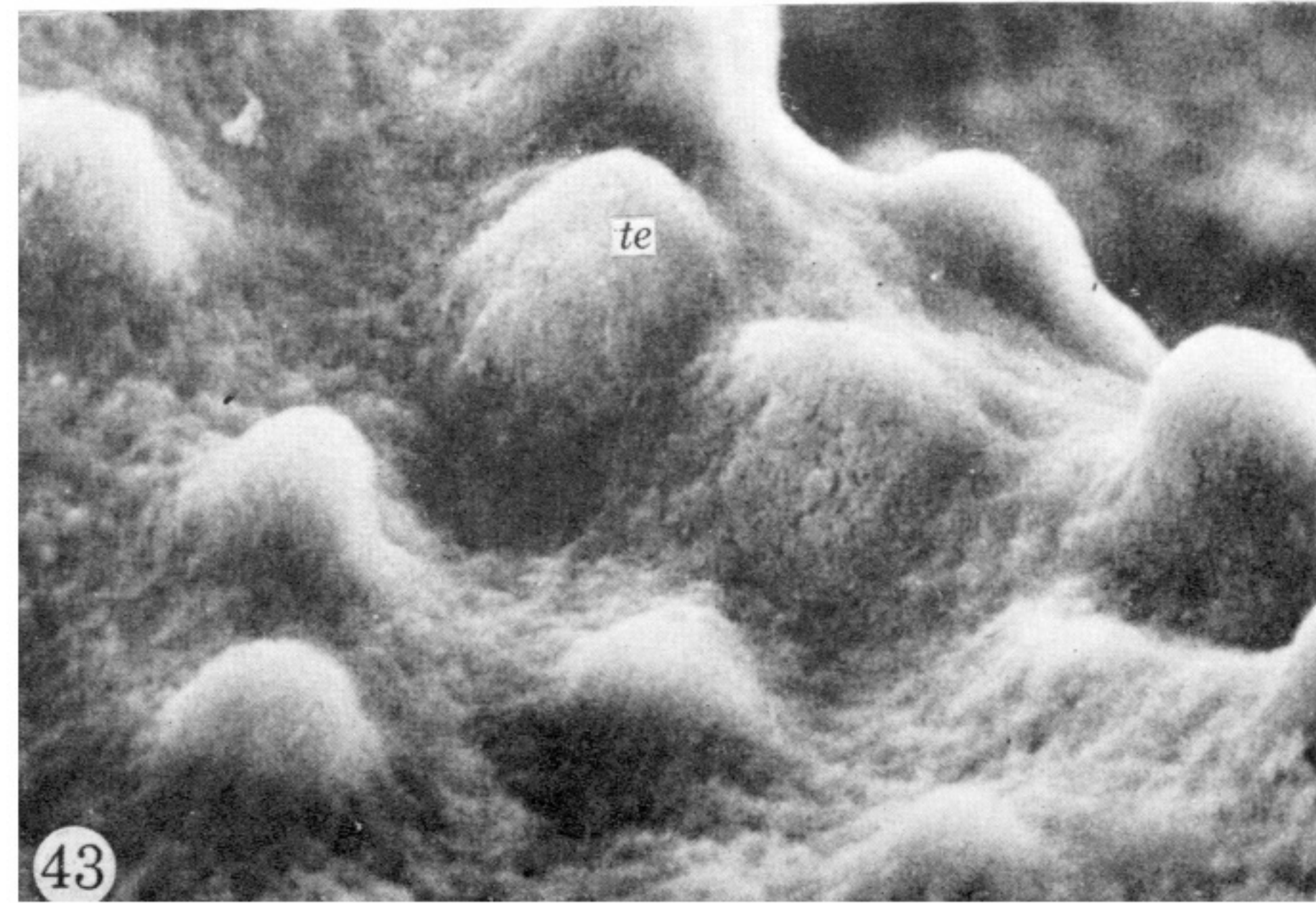
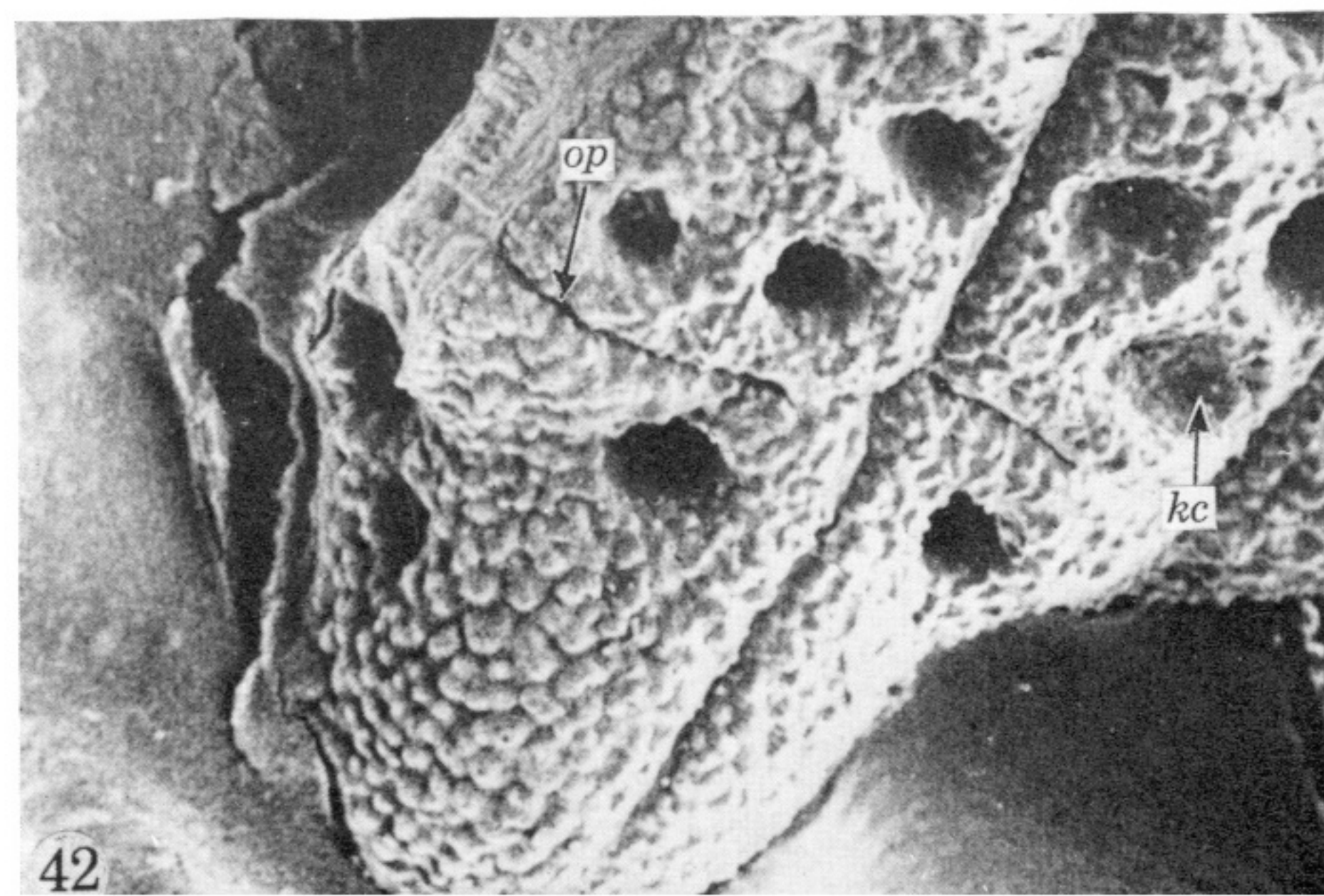
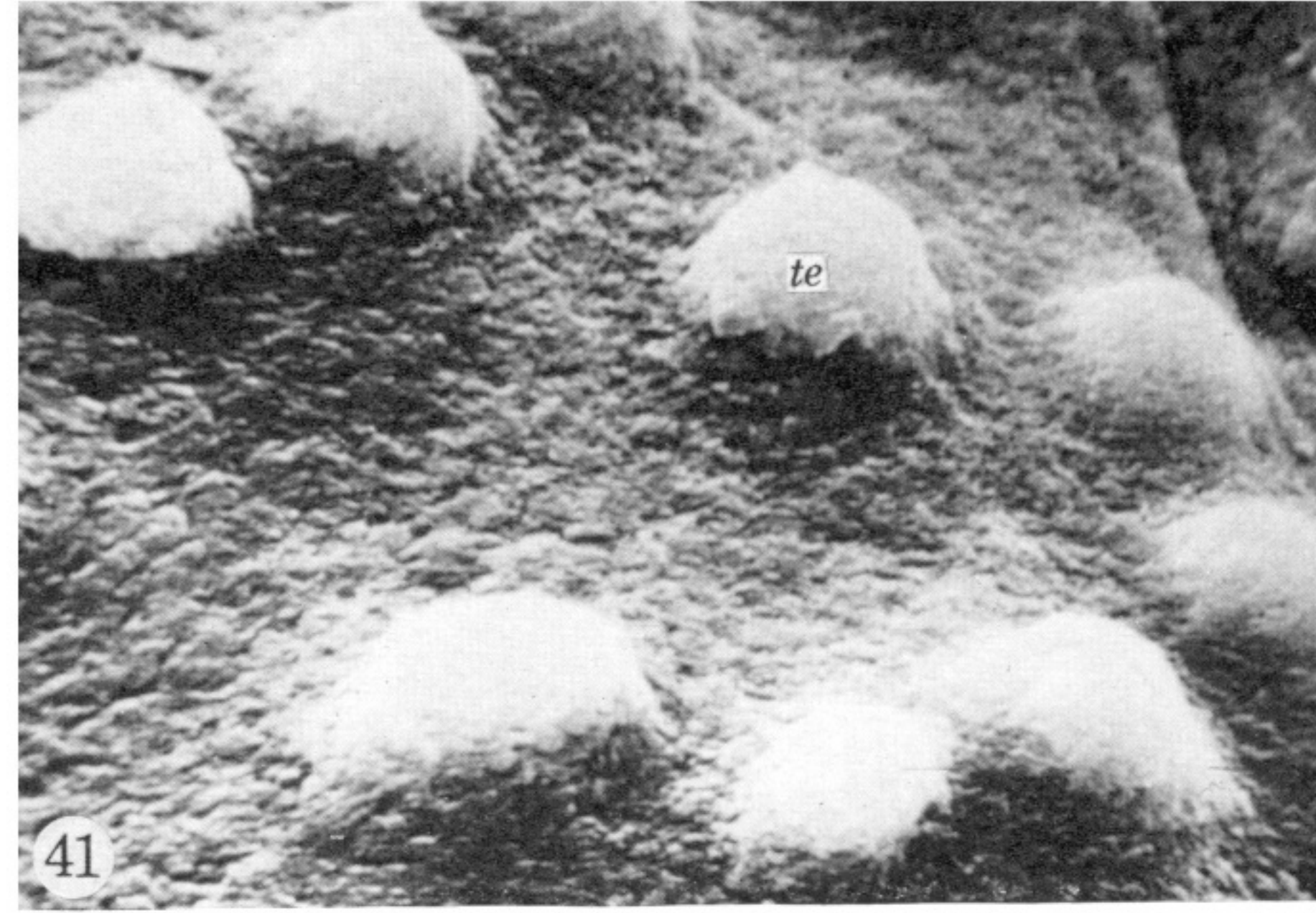
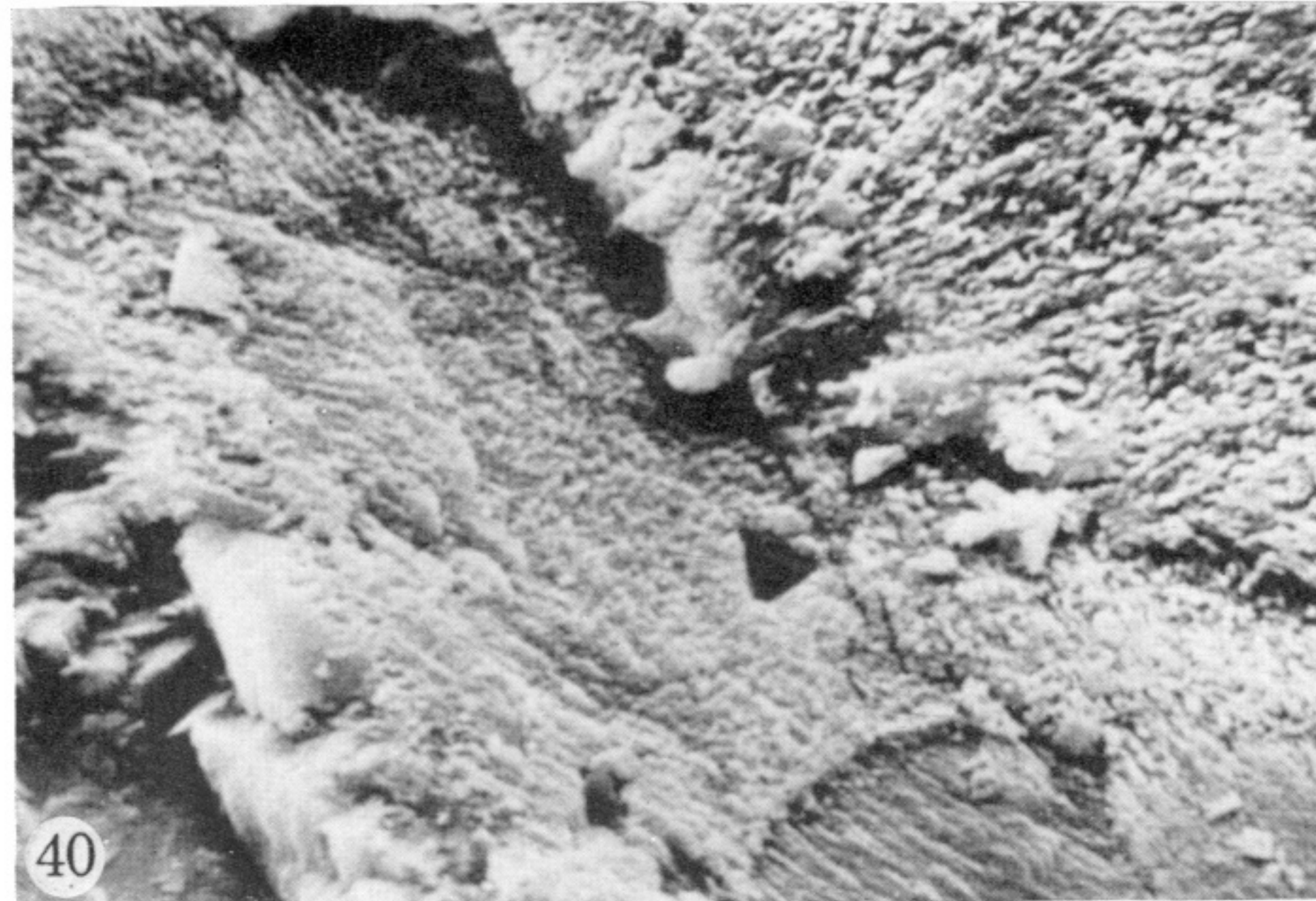
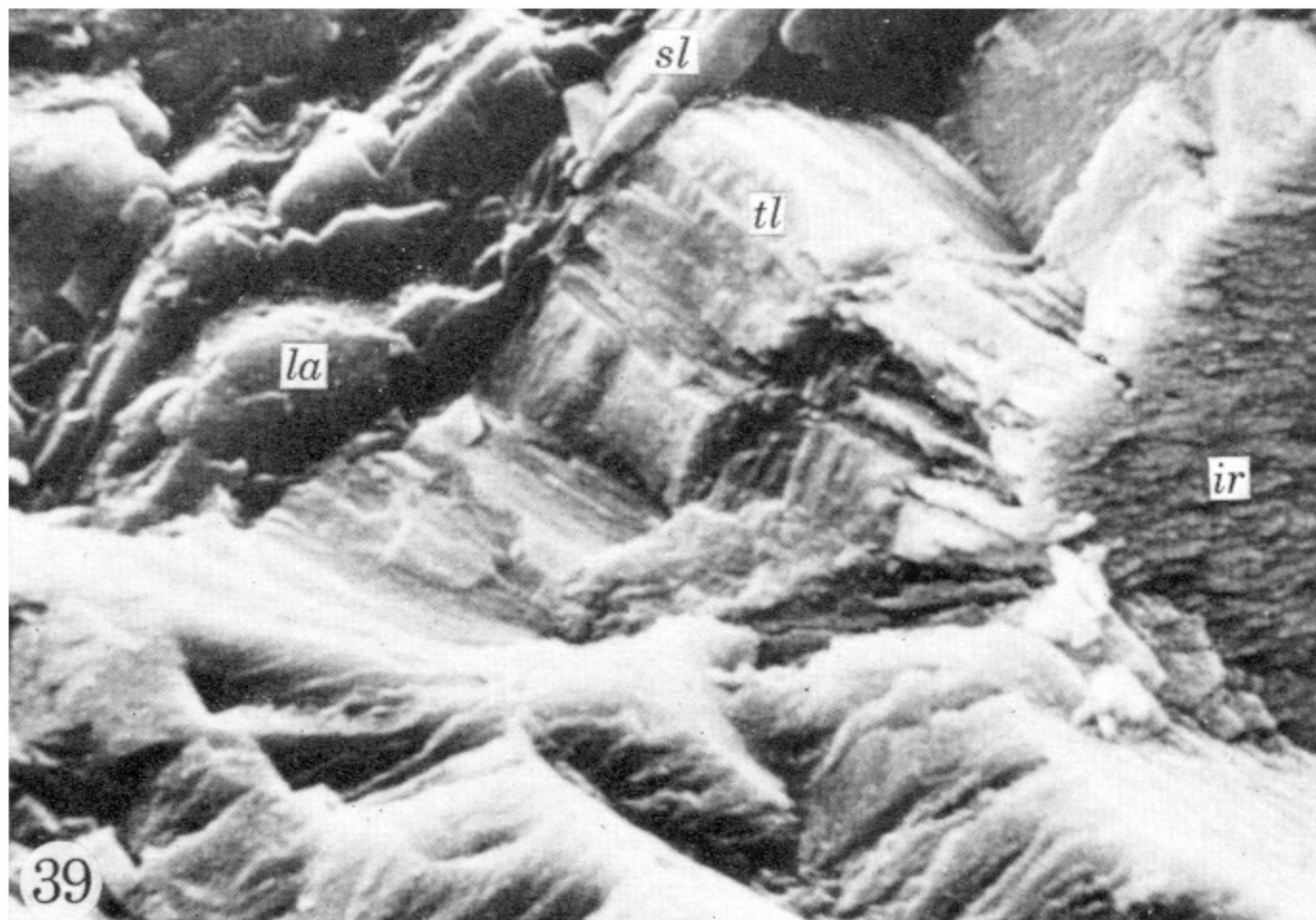
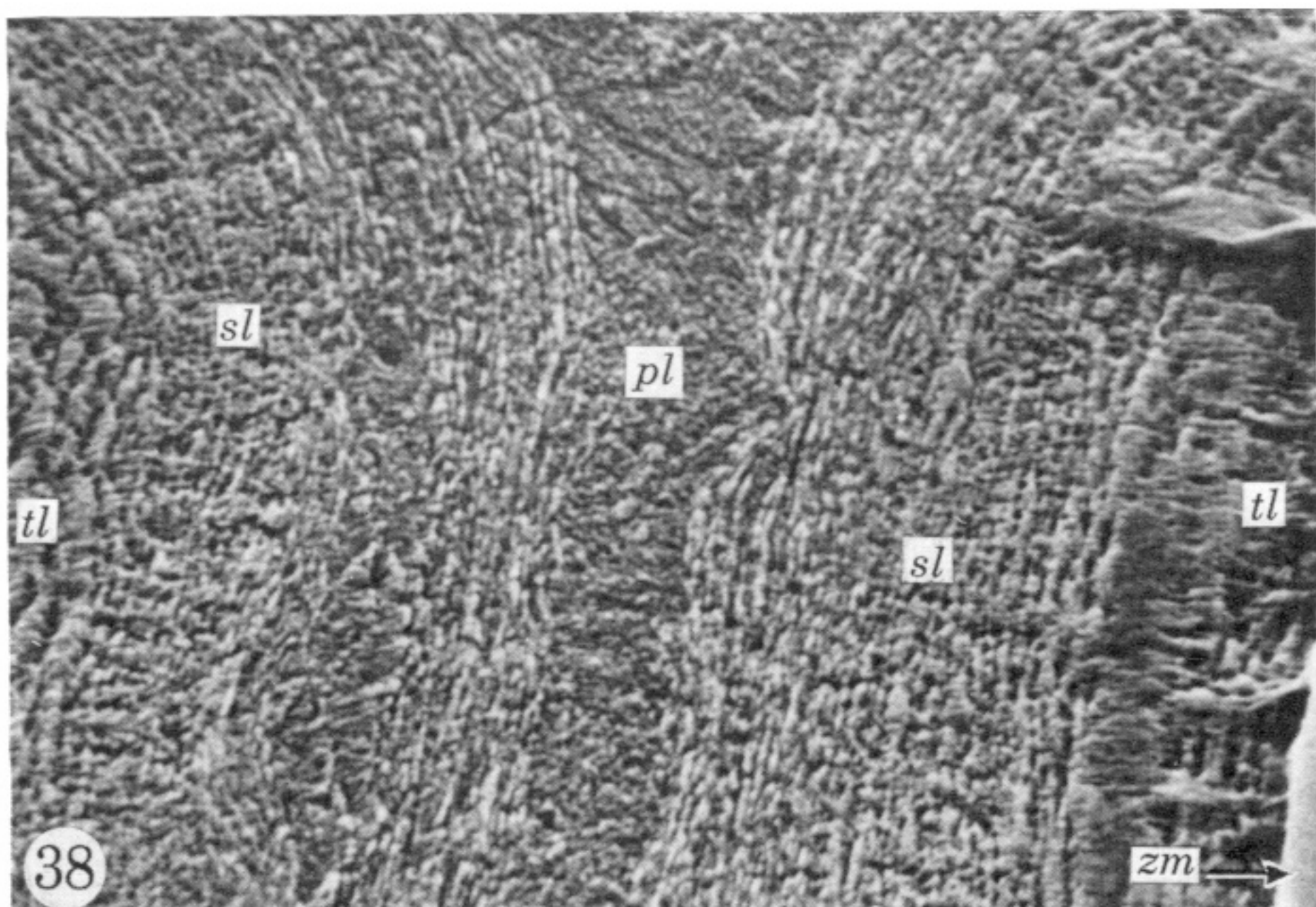
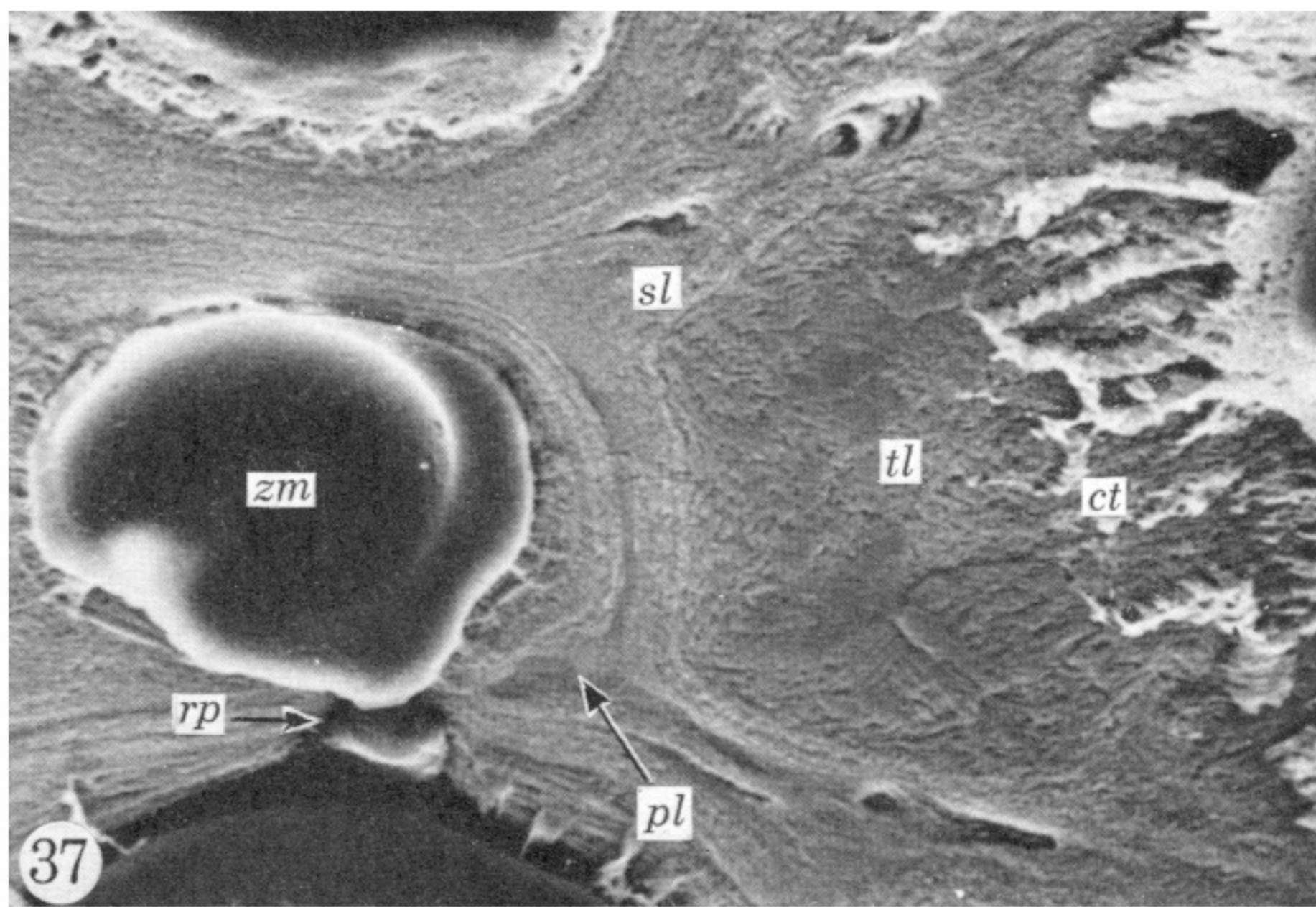
FIGURES 20 TO 24. For legends see facing page.





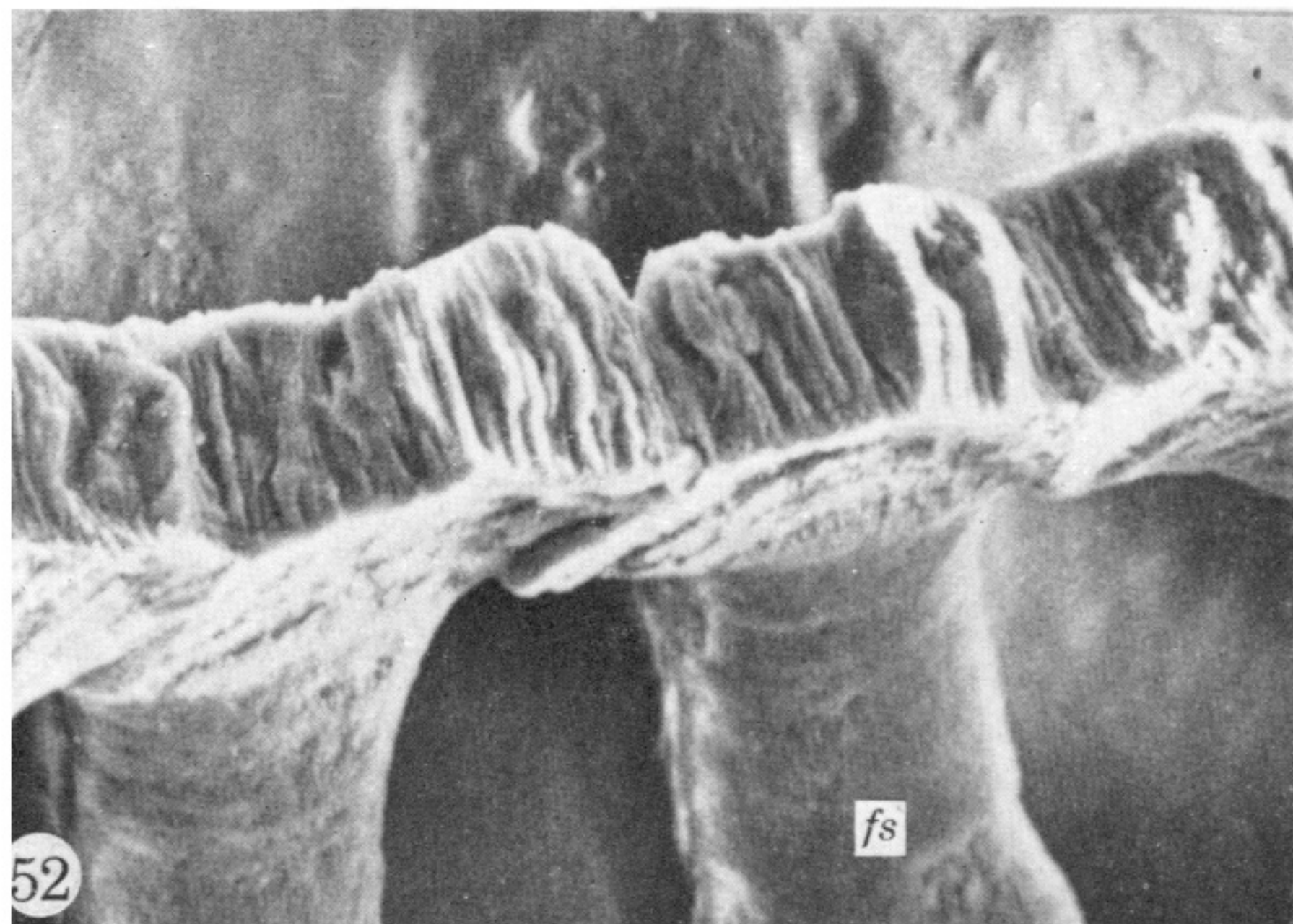
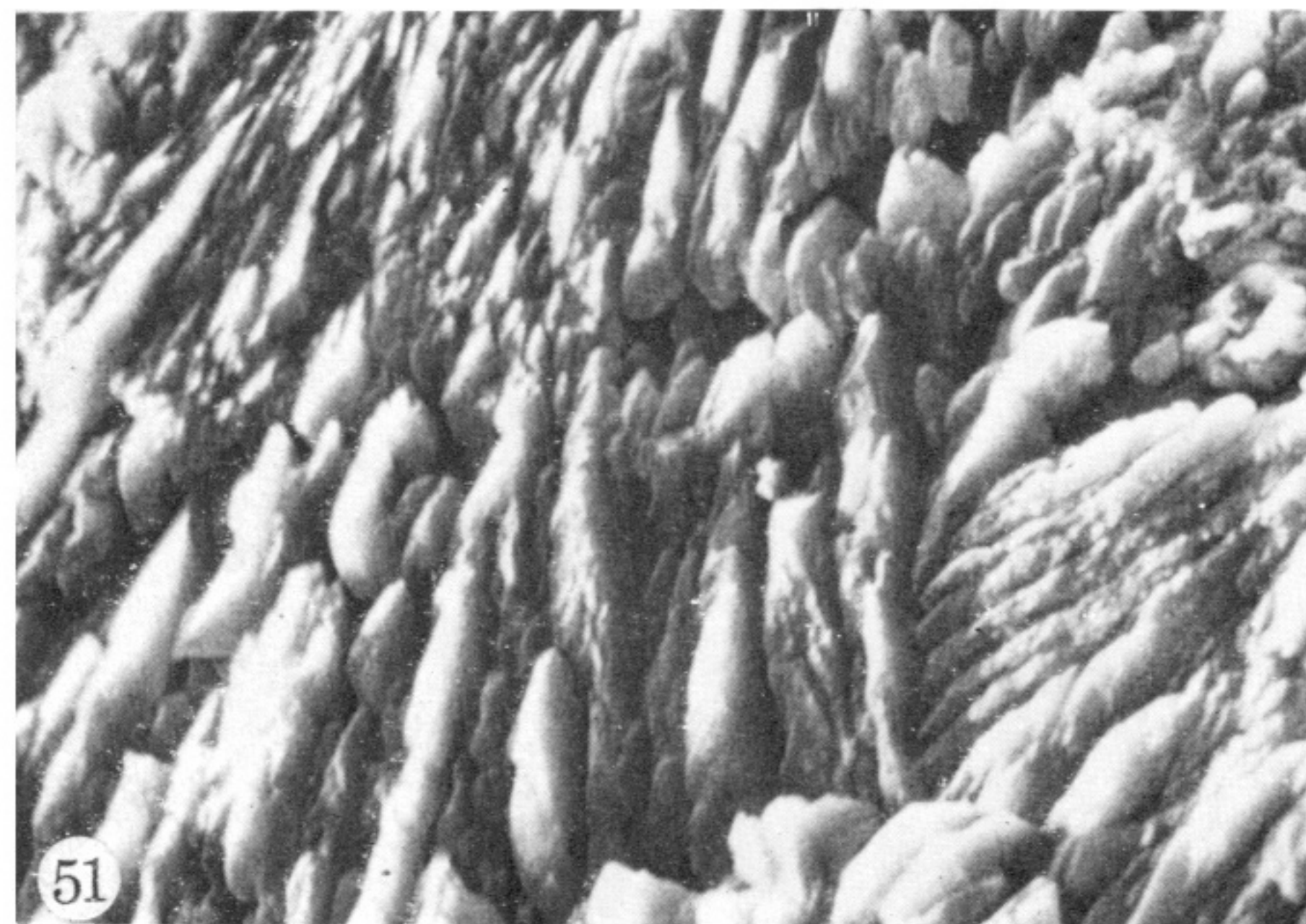
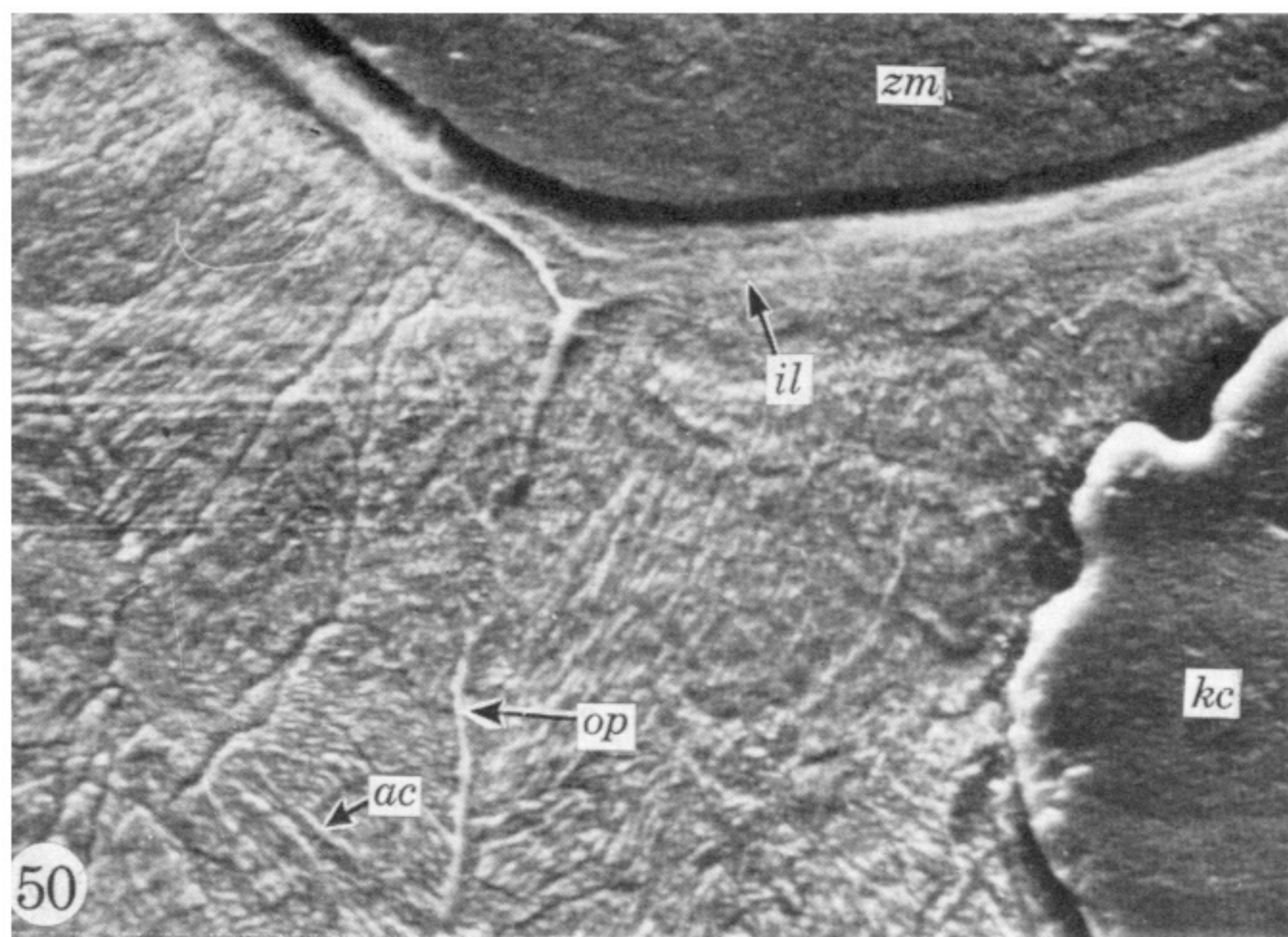
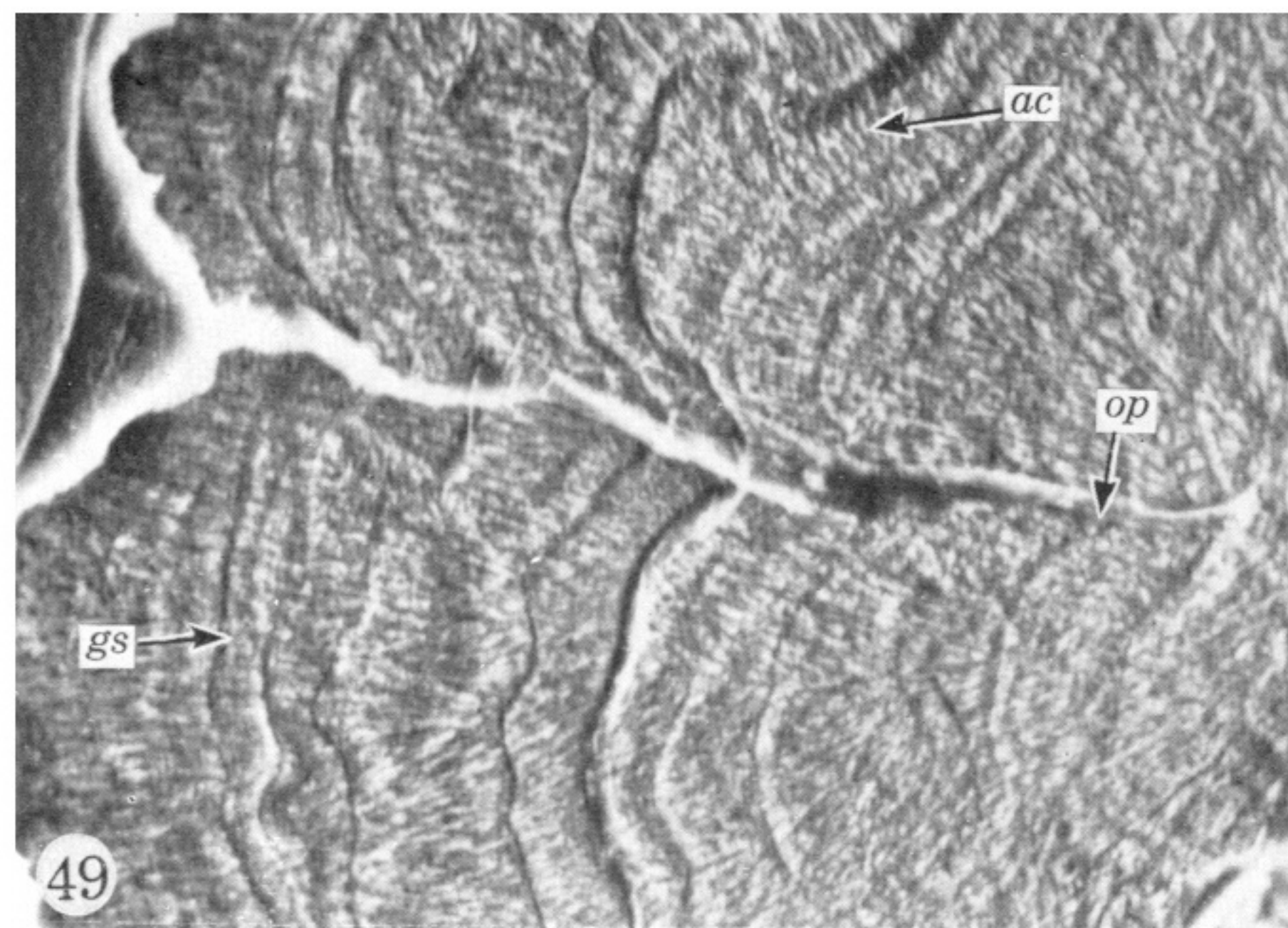
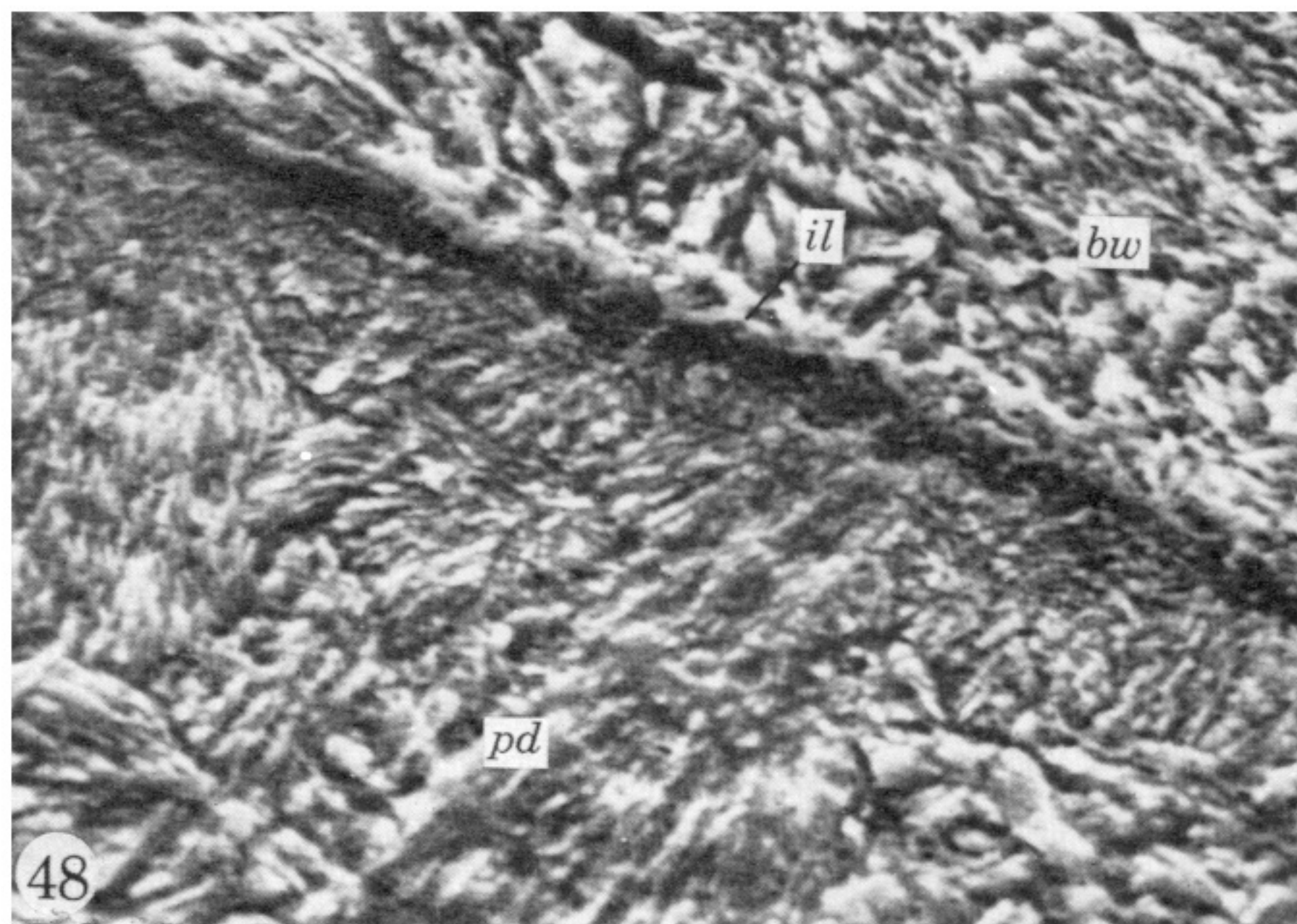
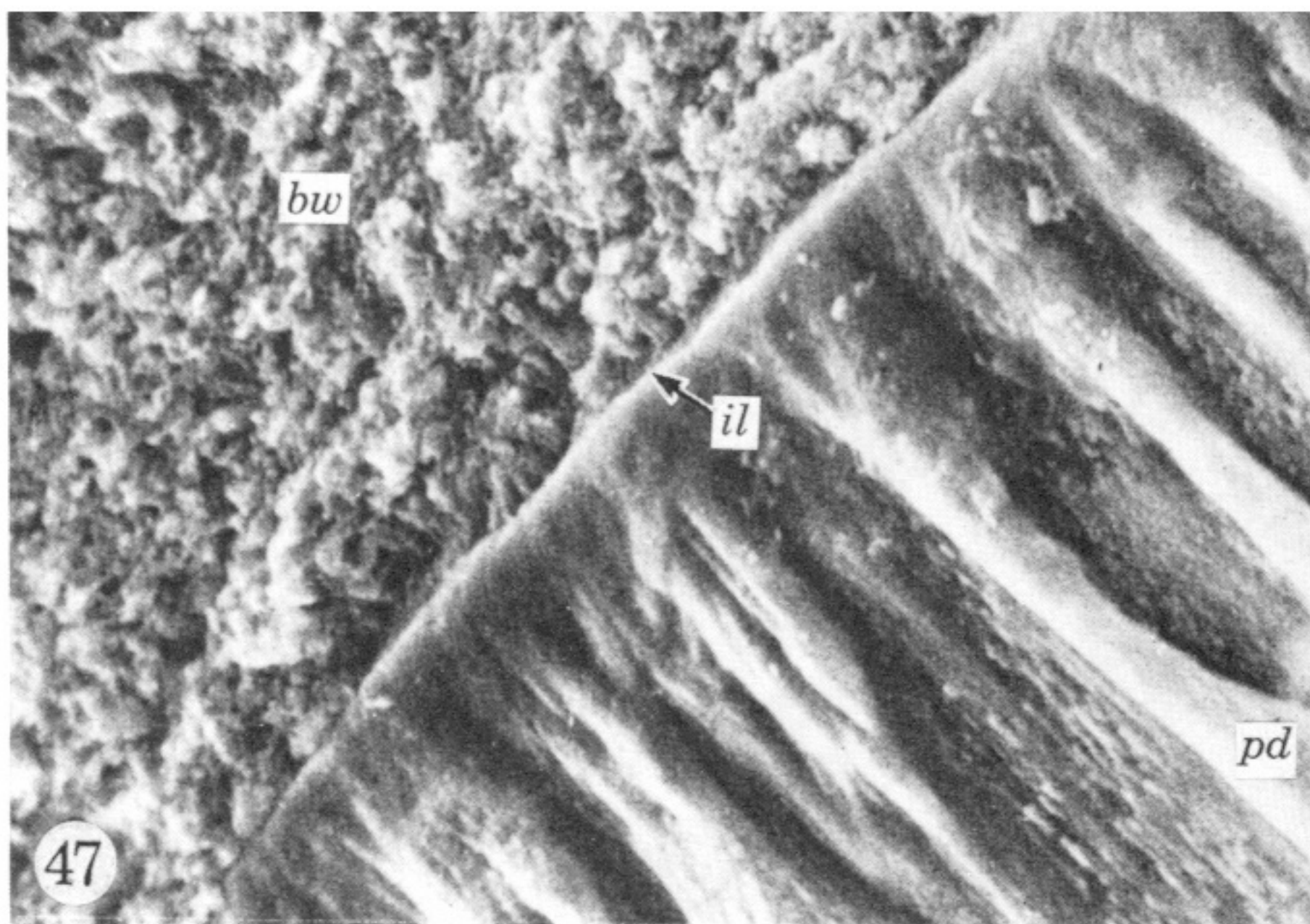
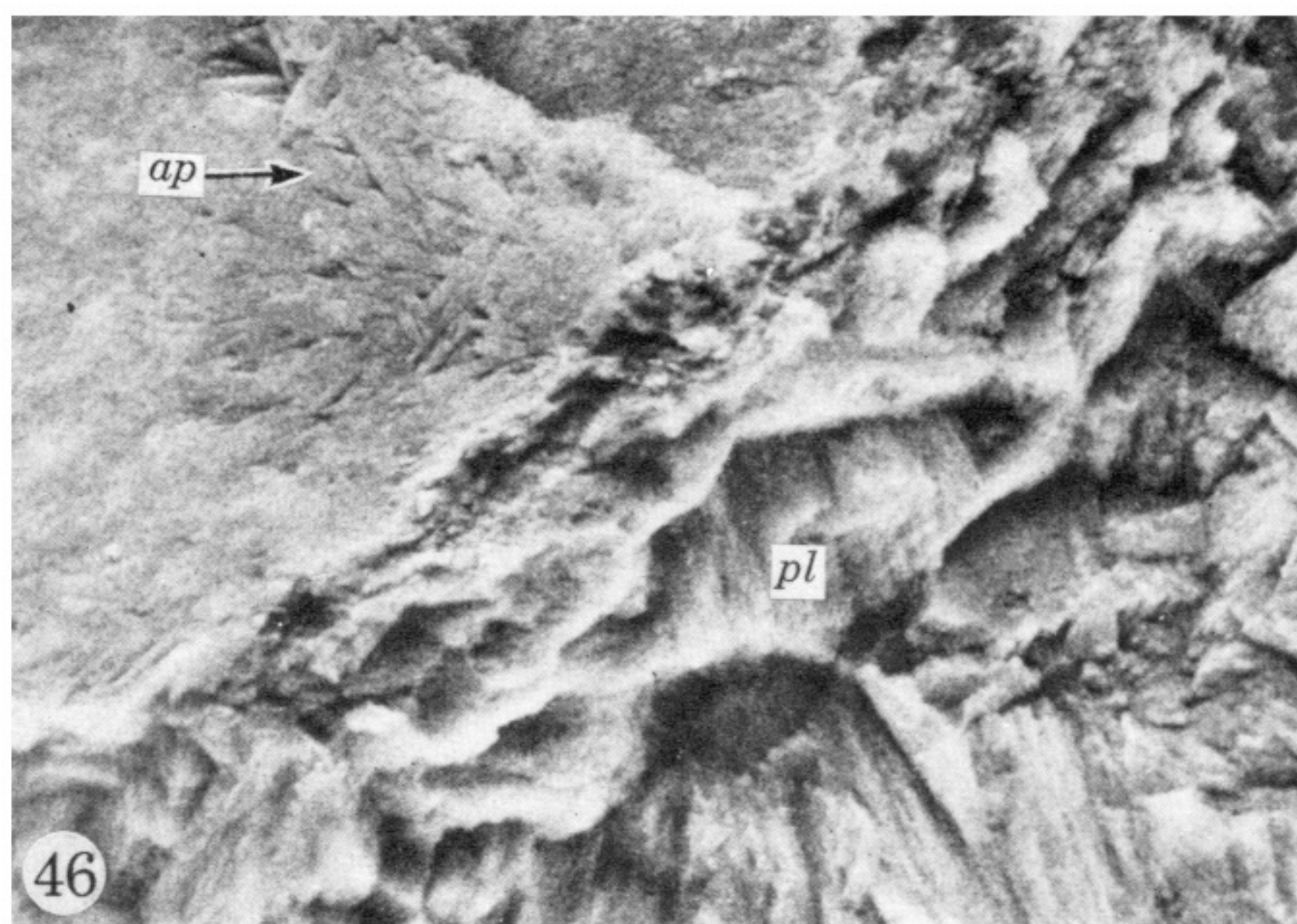
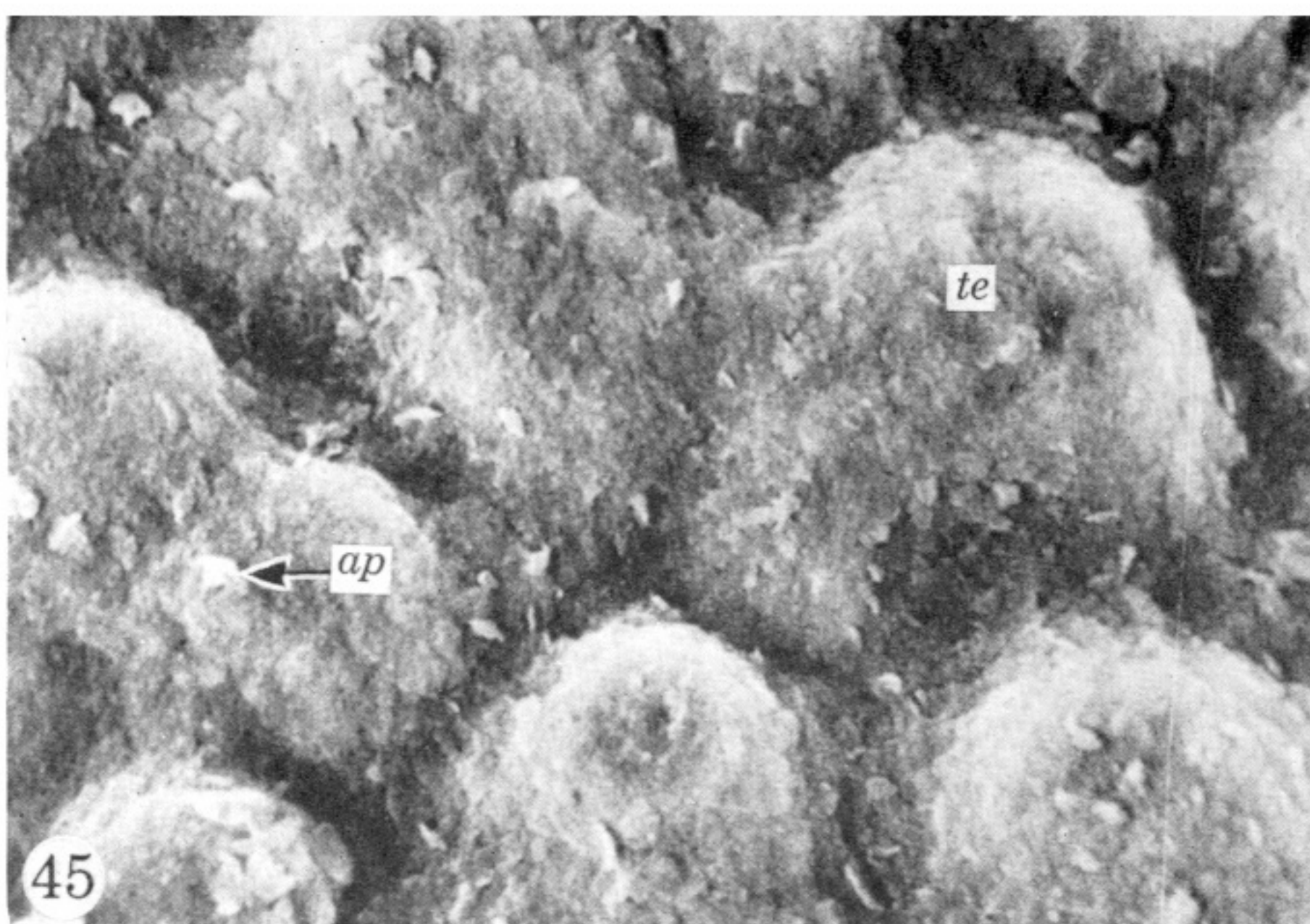
FIGURES 27 TO 34. For legends see facing page.





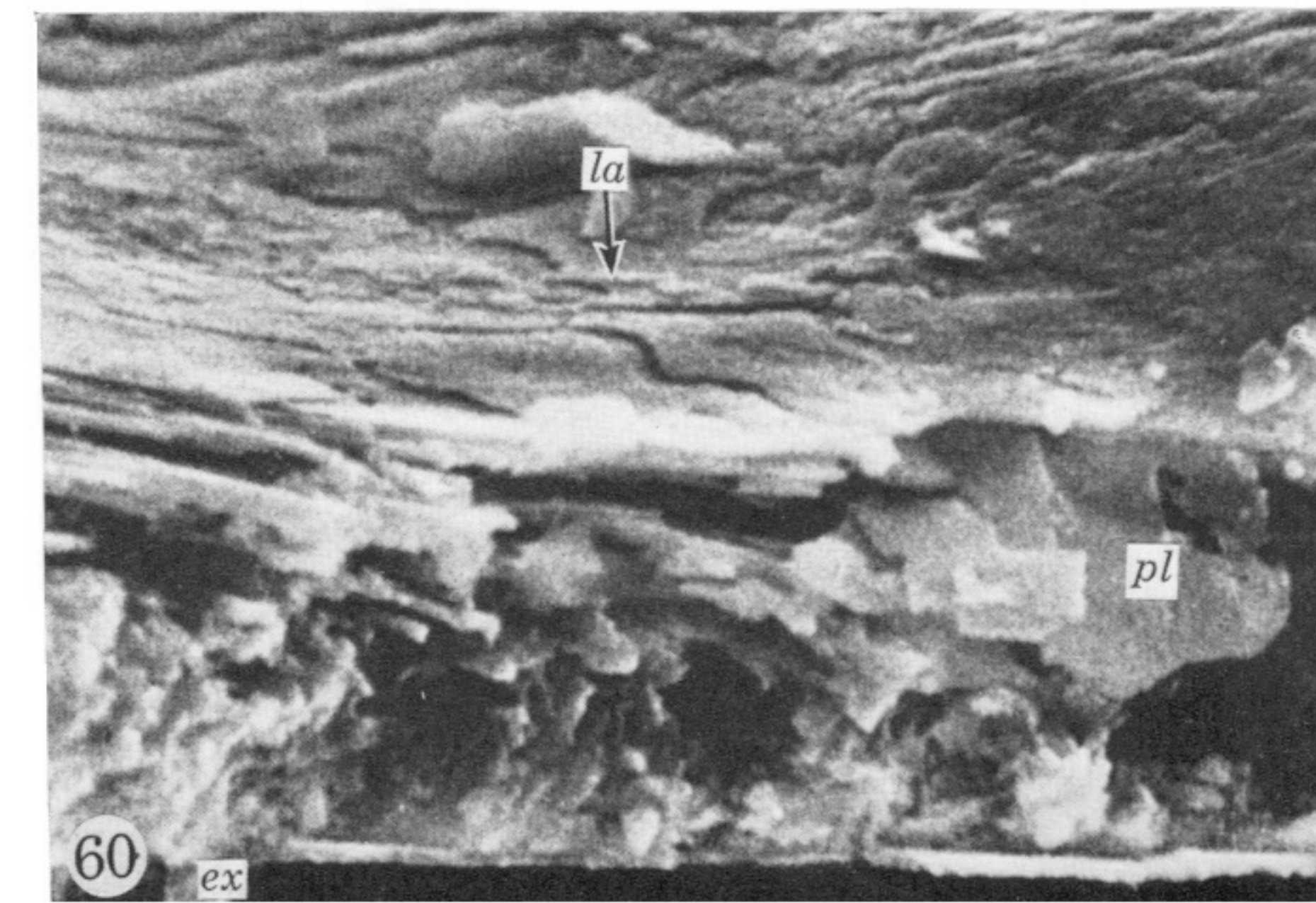
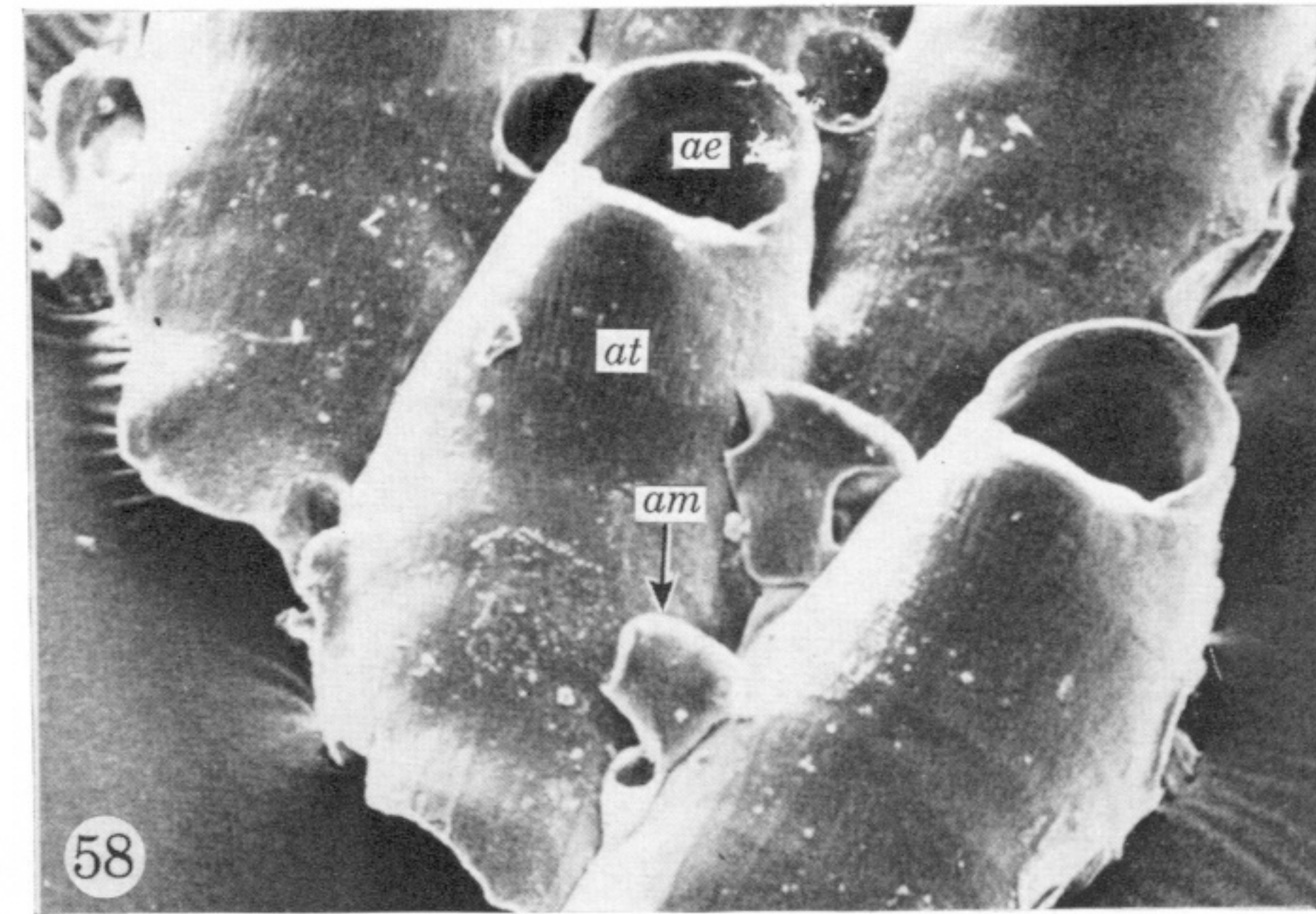
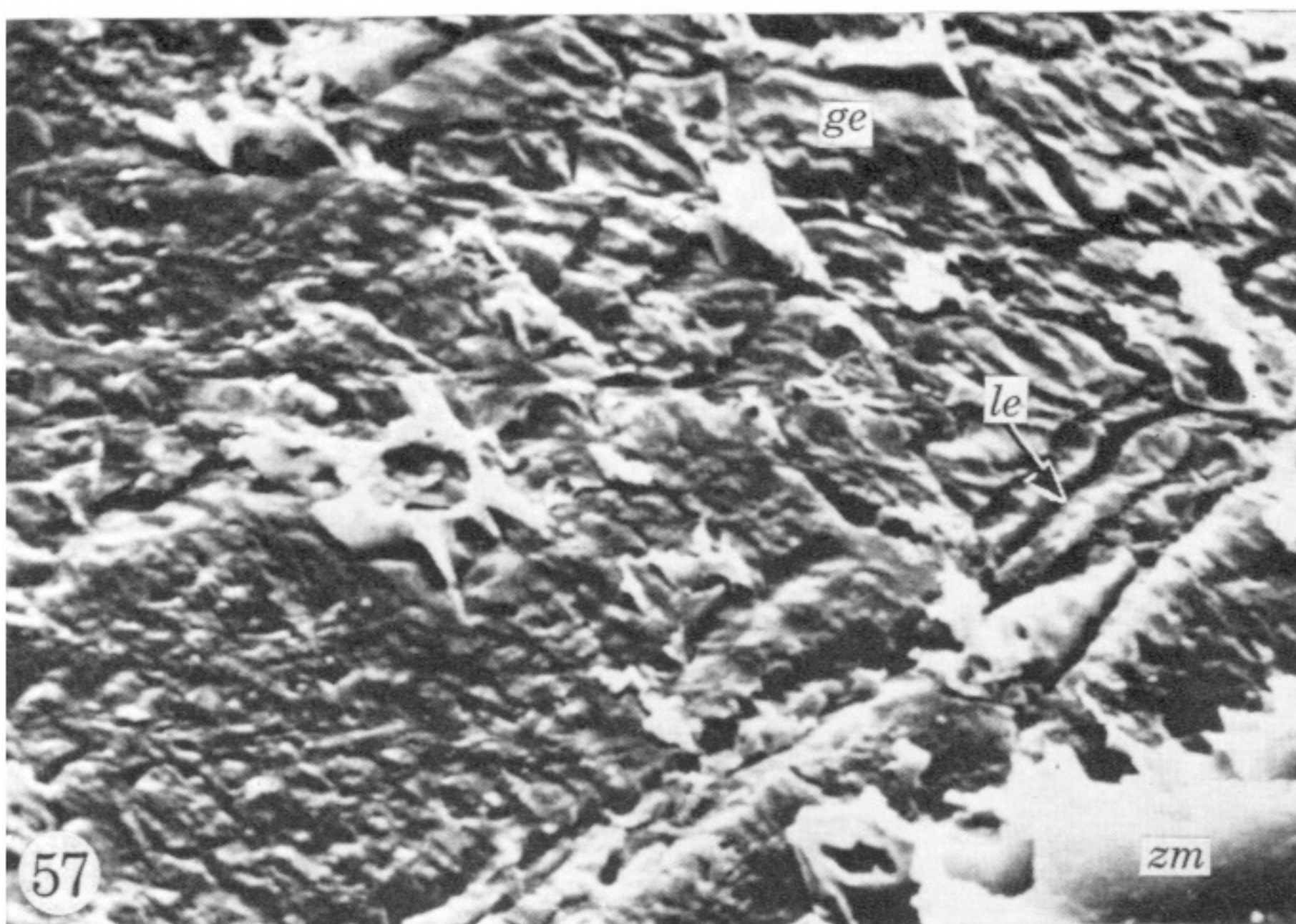
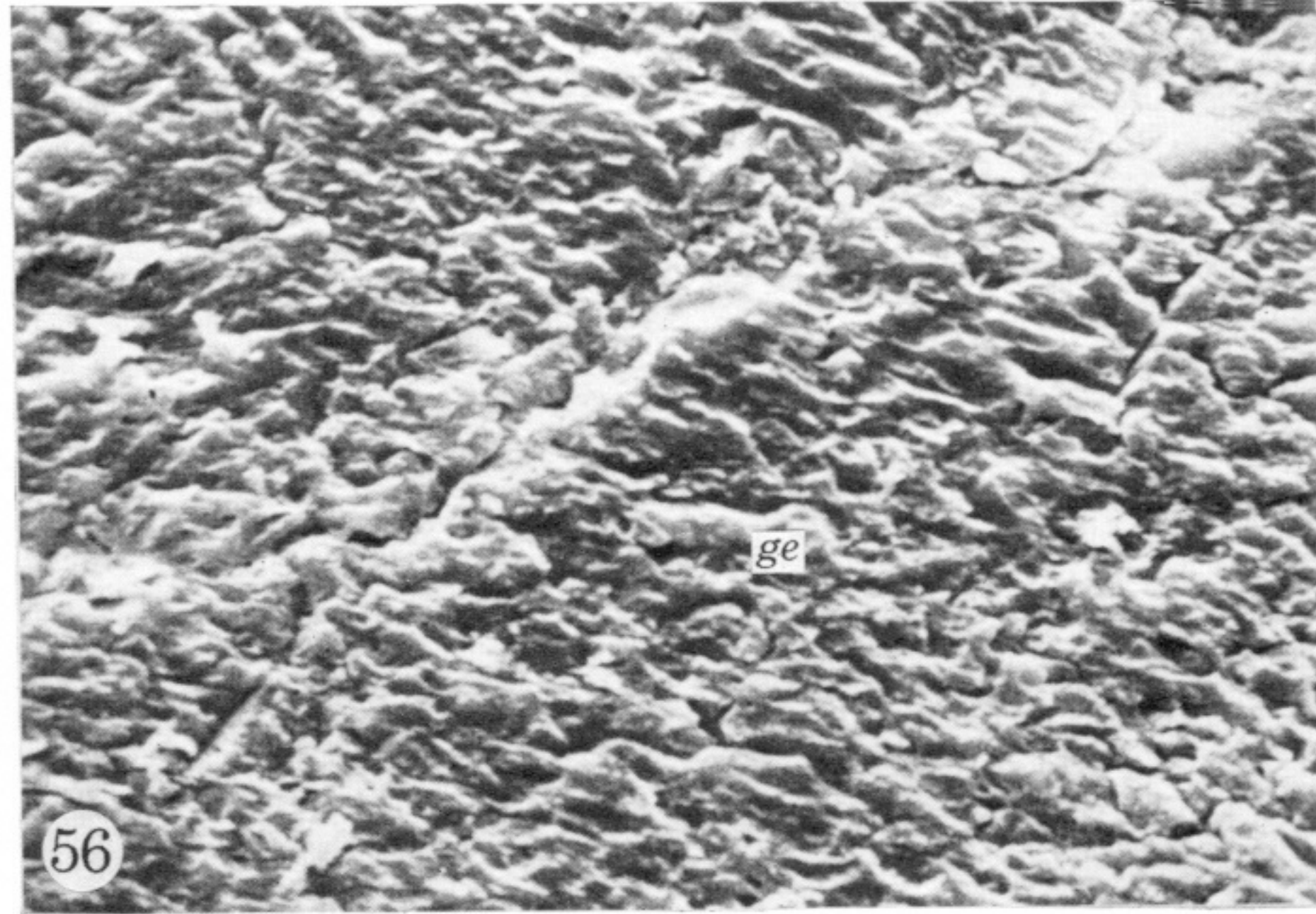
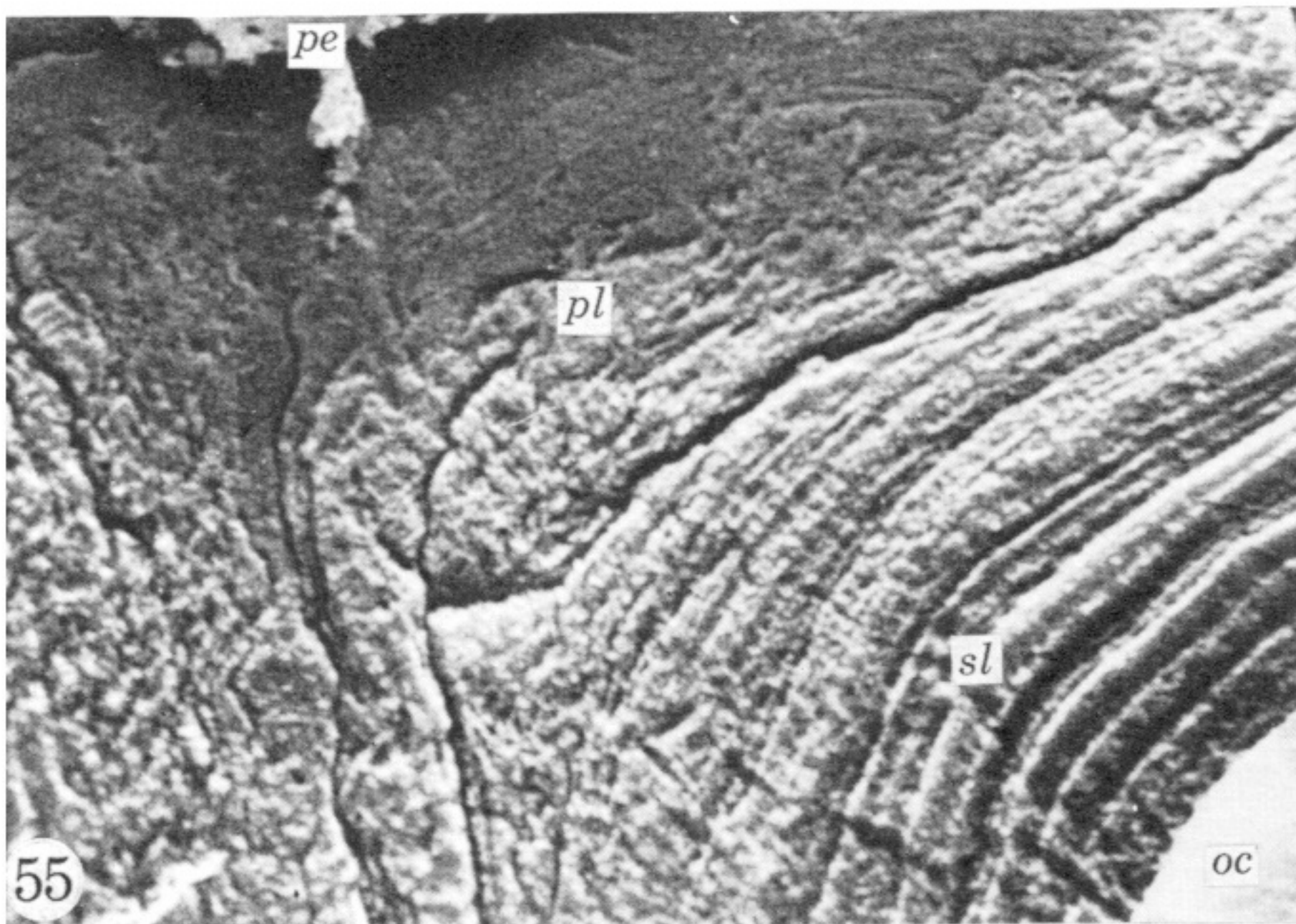
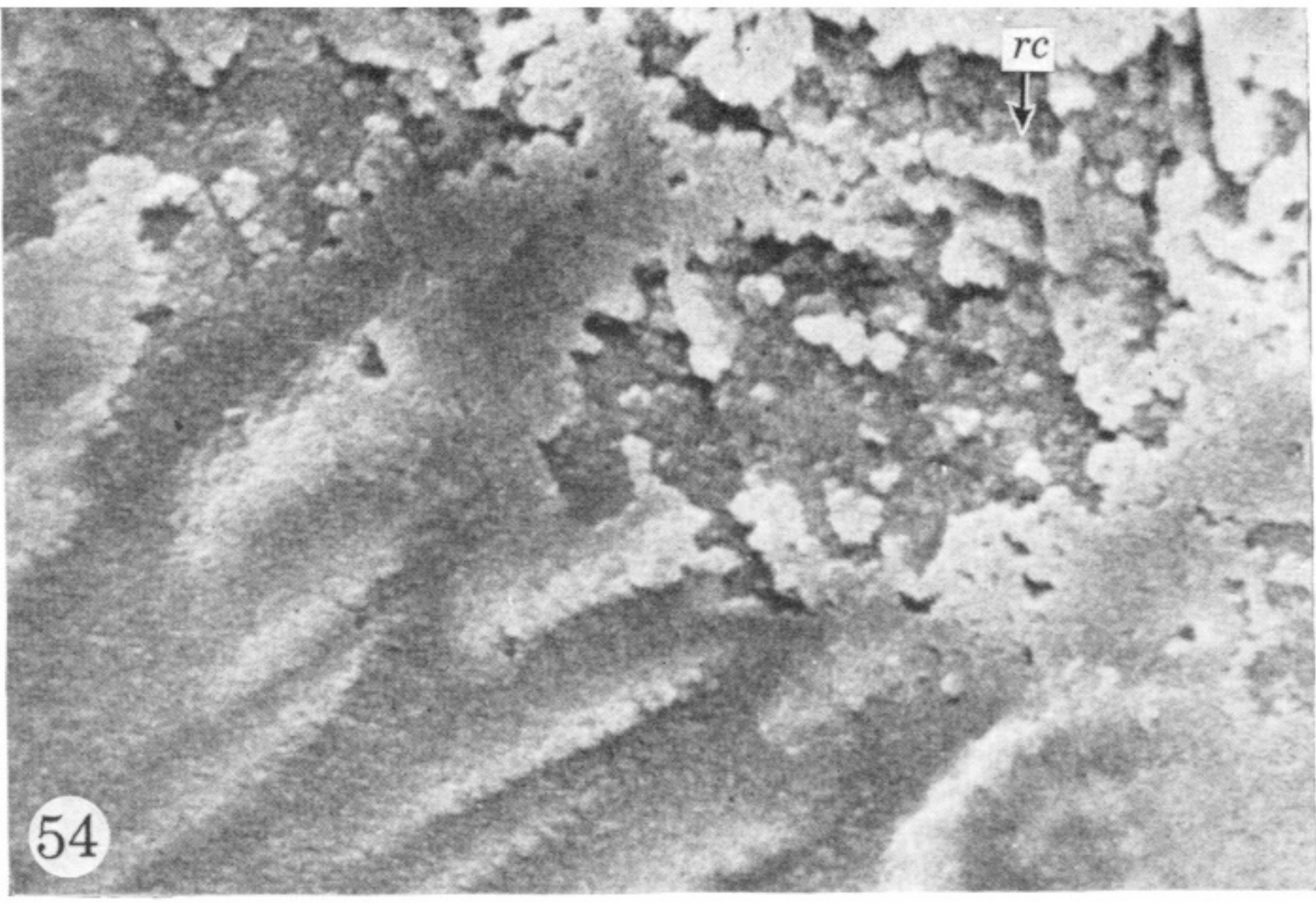
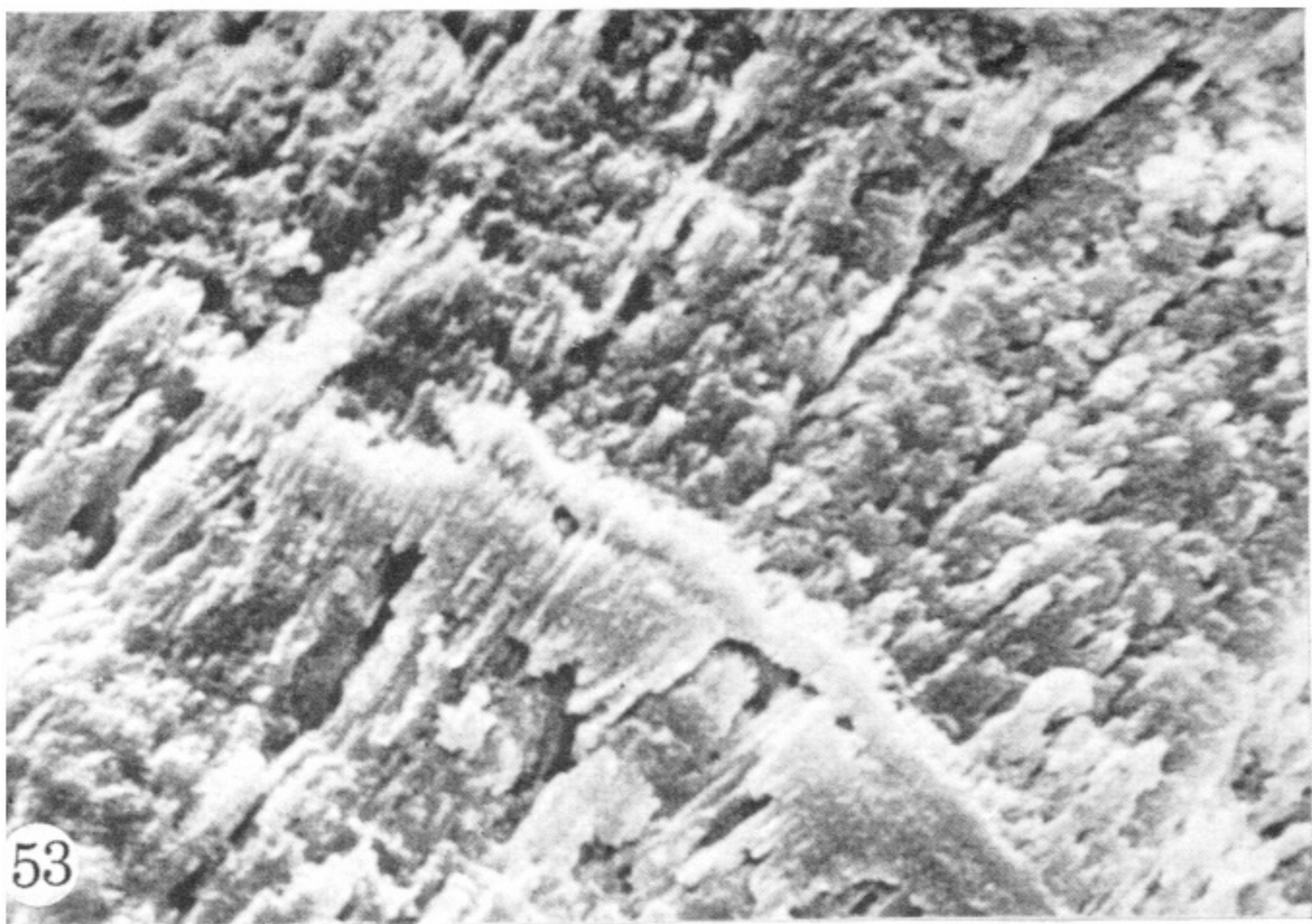
FIGURES 36 TO 43. For legends see facing page.





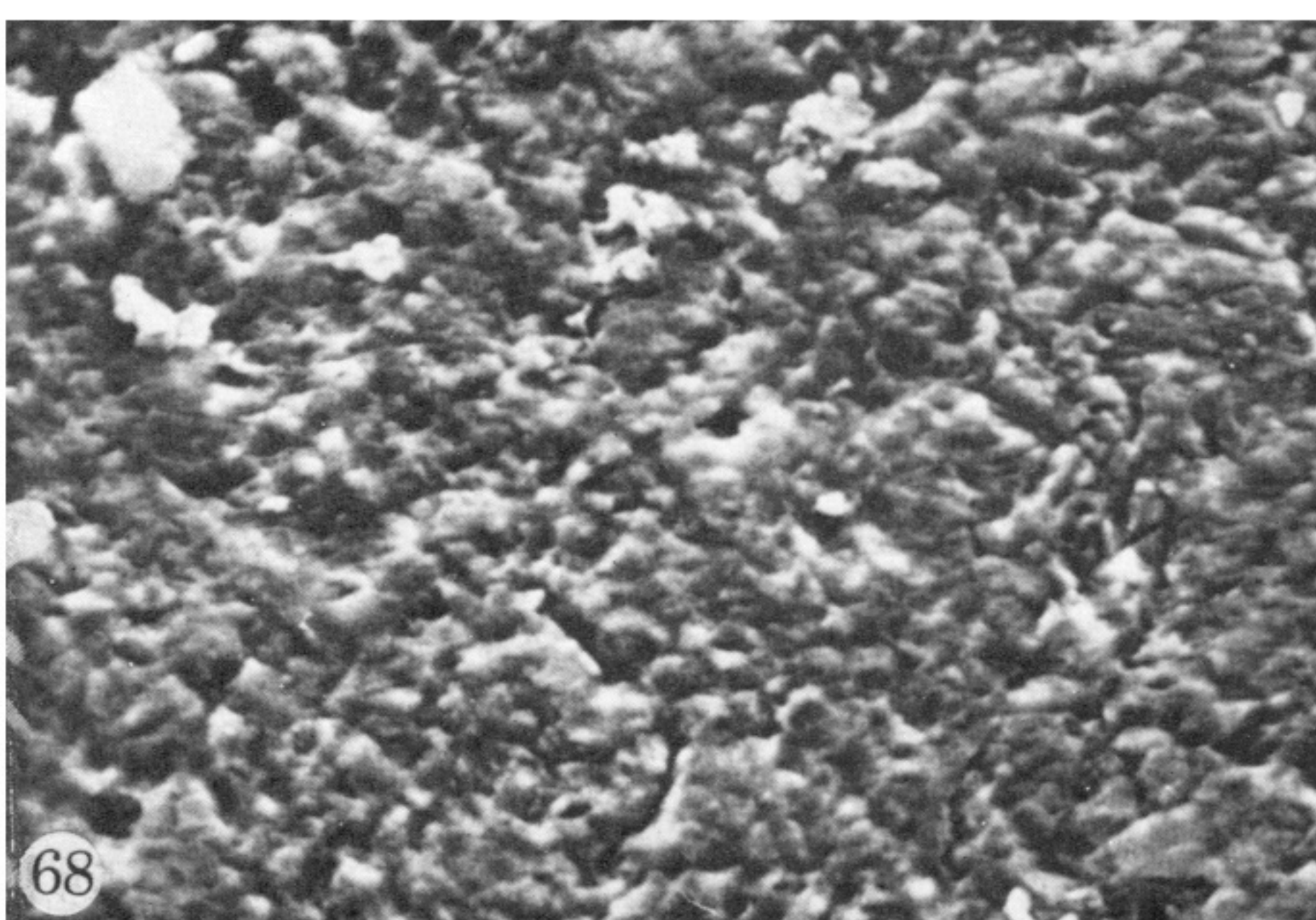
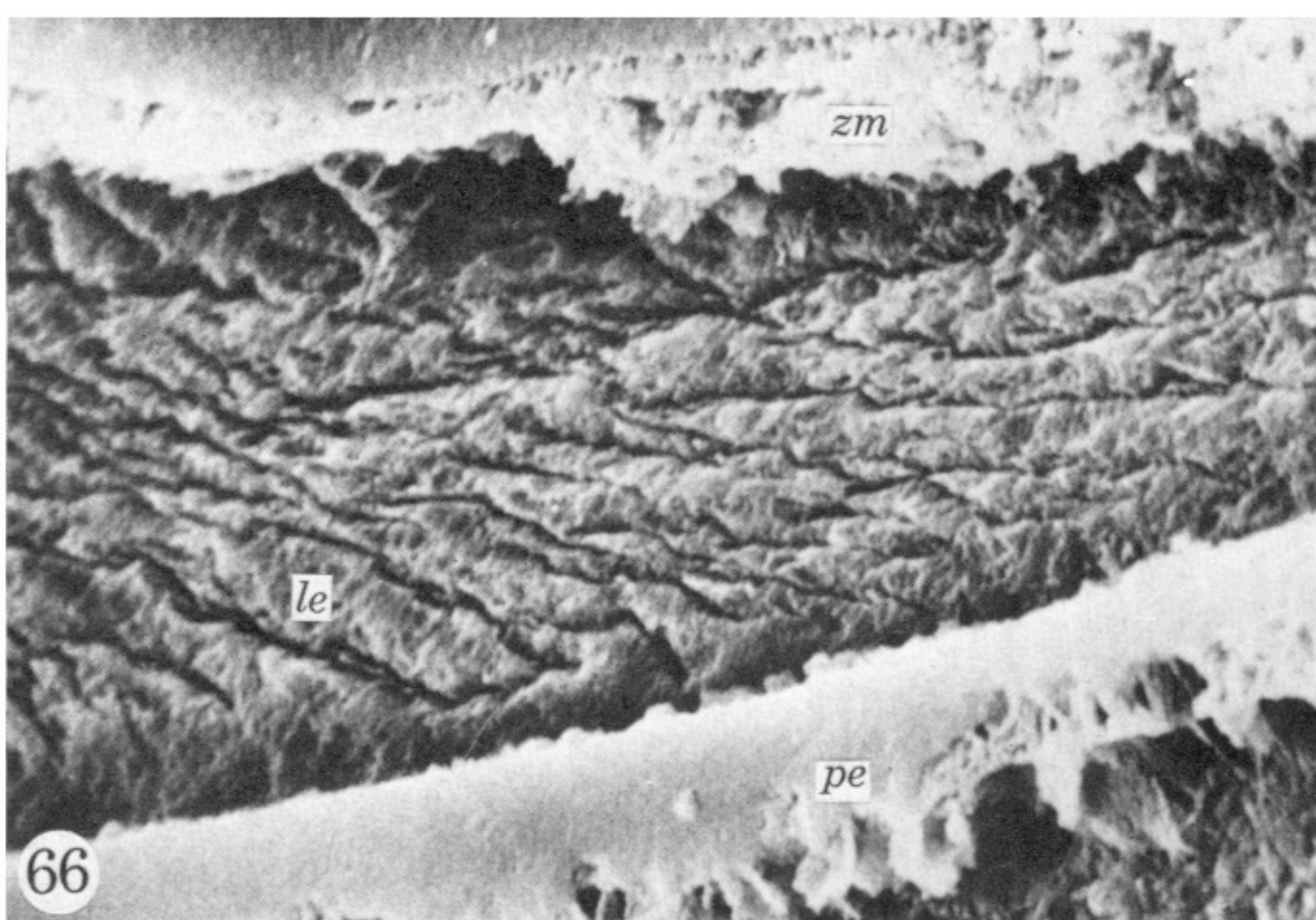
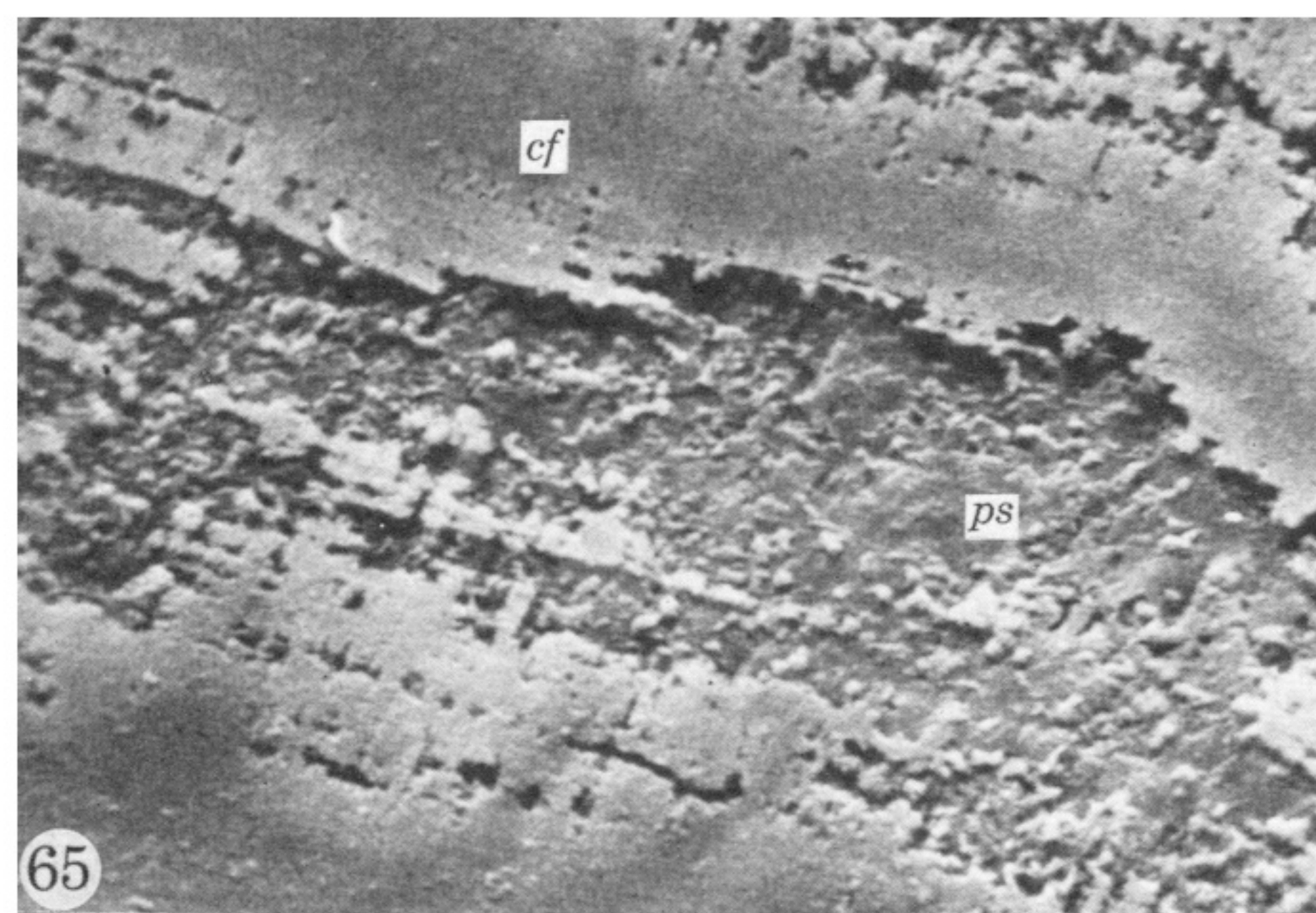
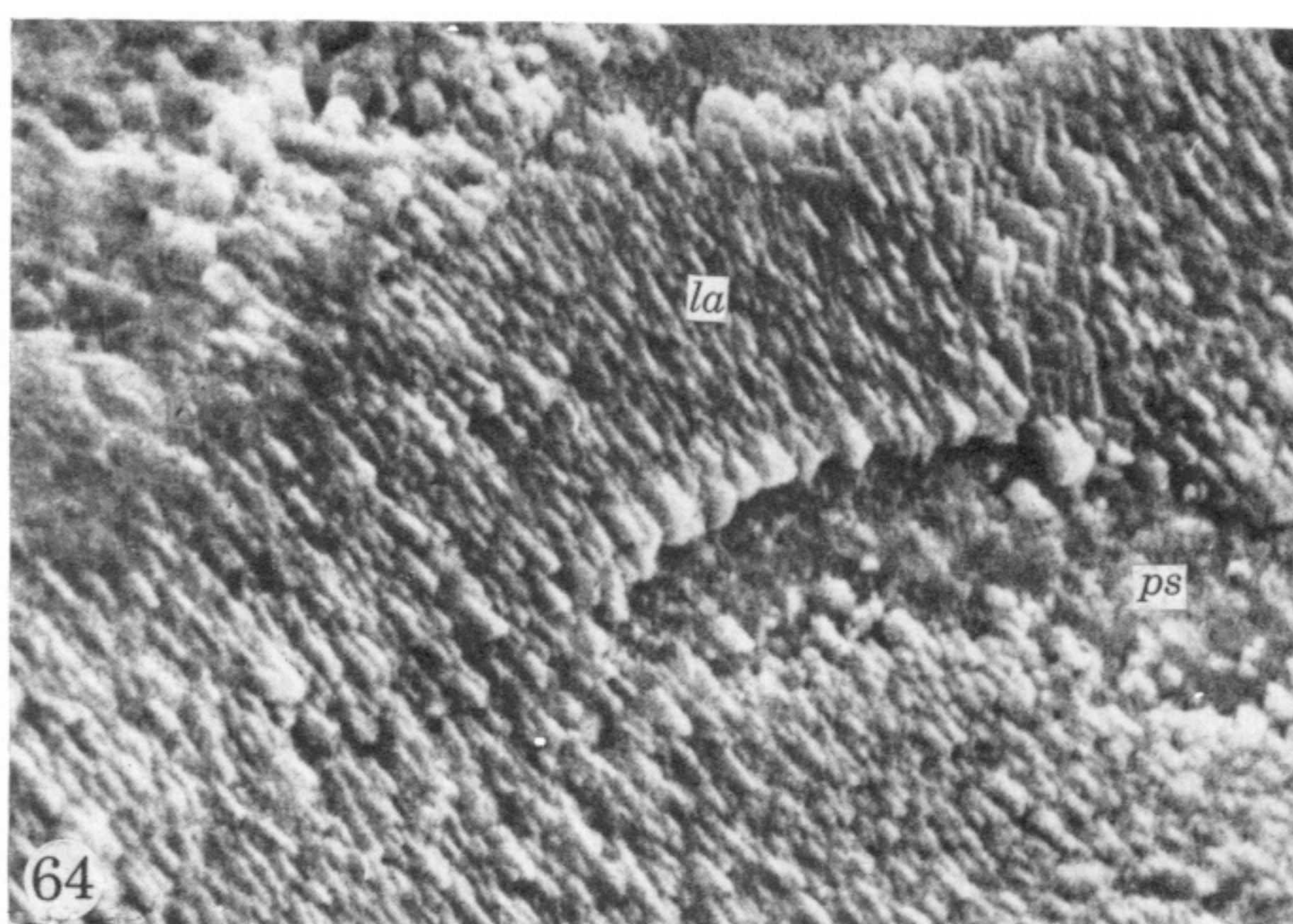
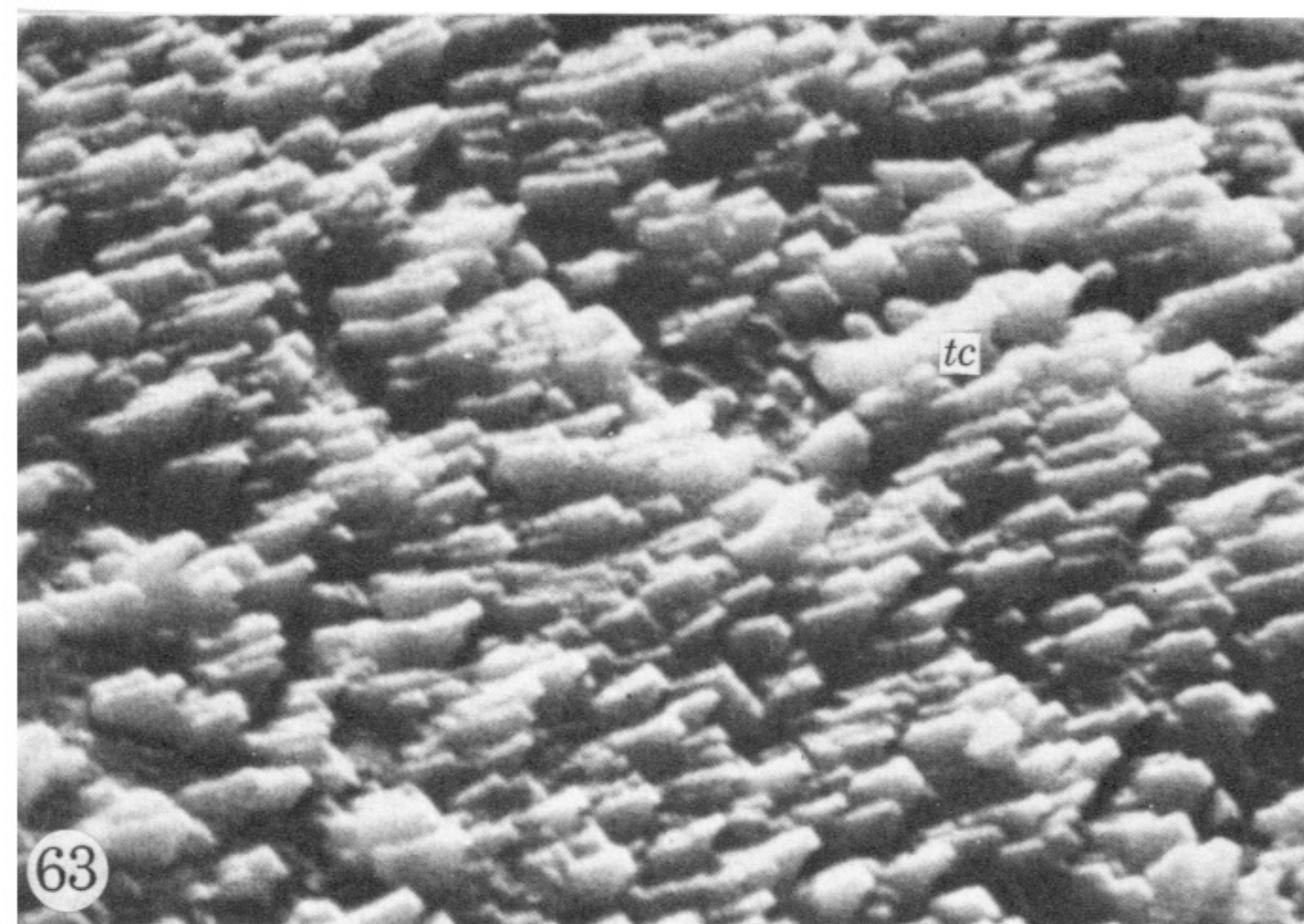
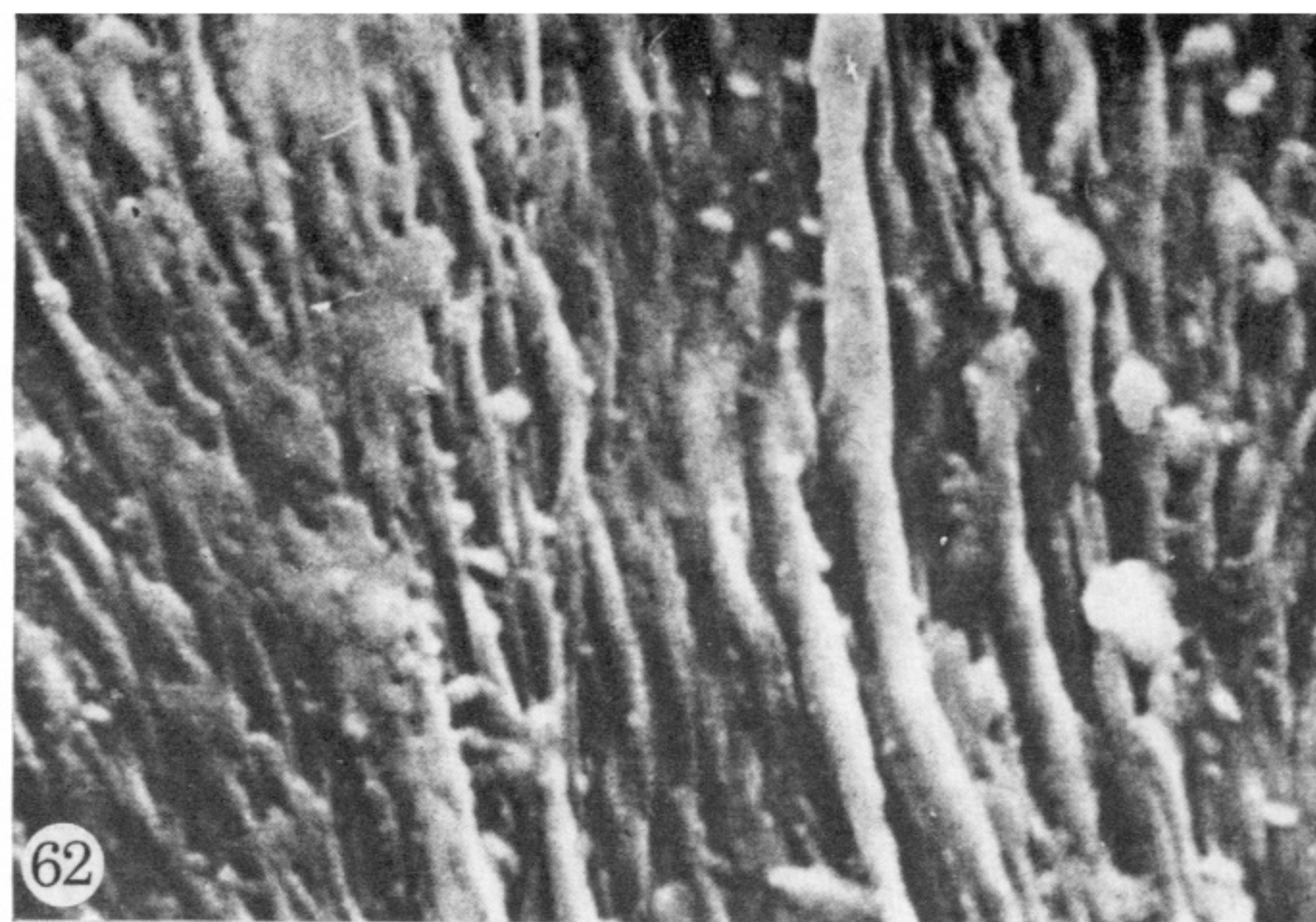
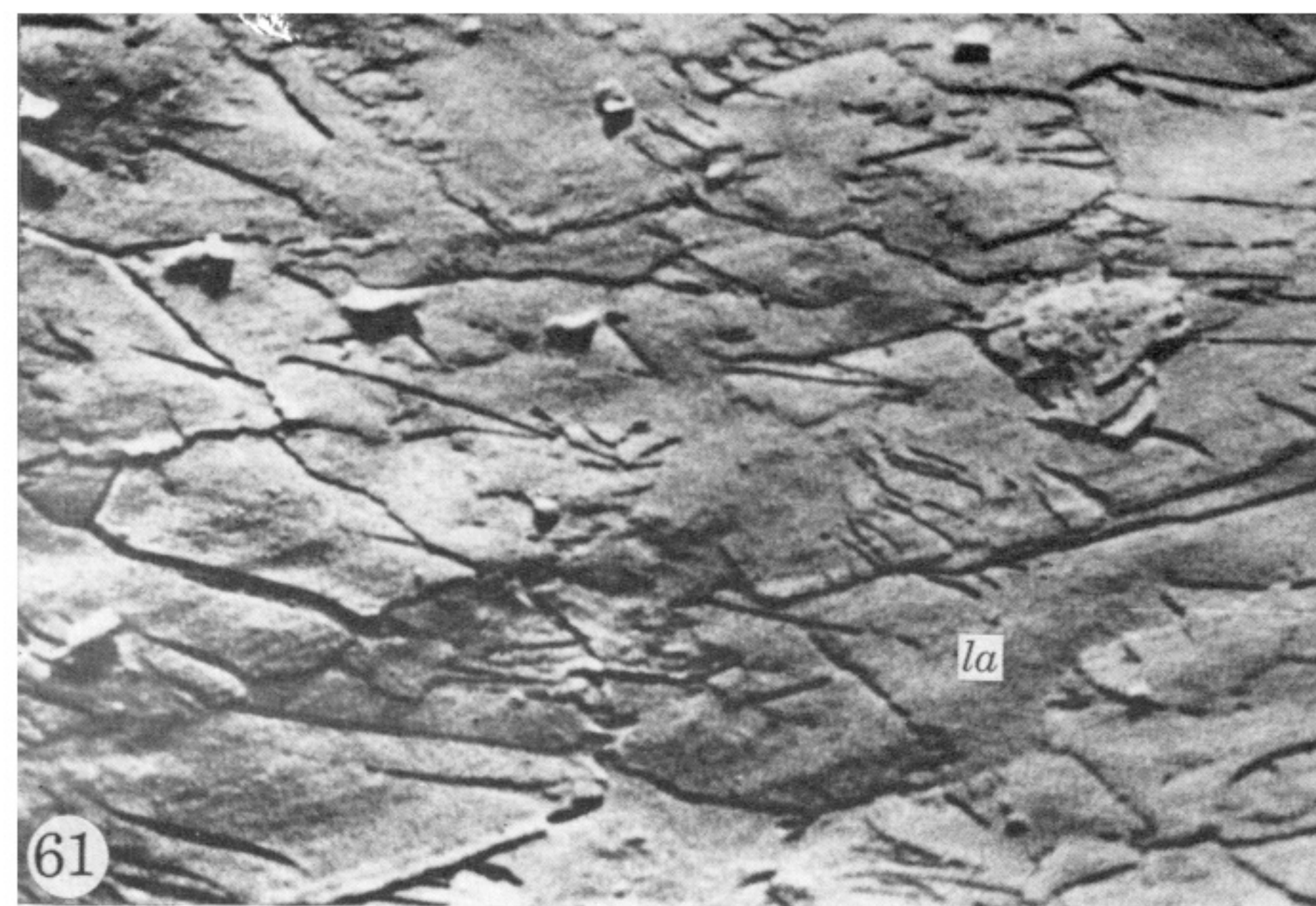
FIGURES 45 TO 52. For legends see facing page.





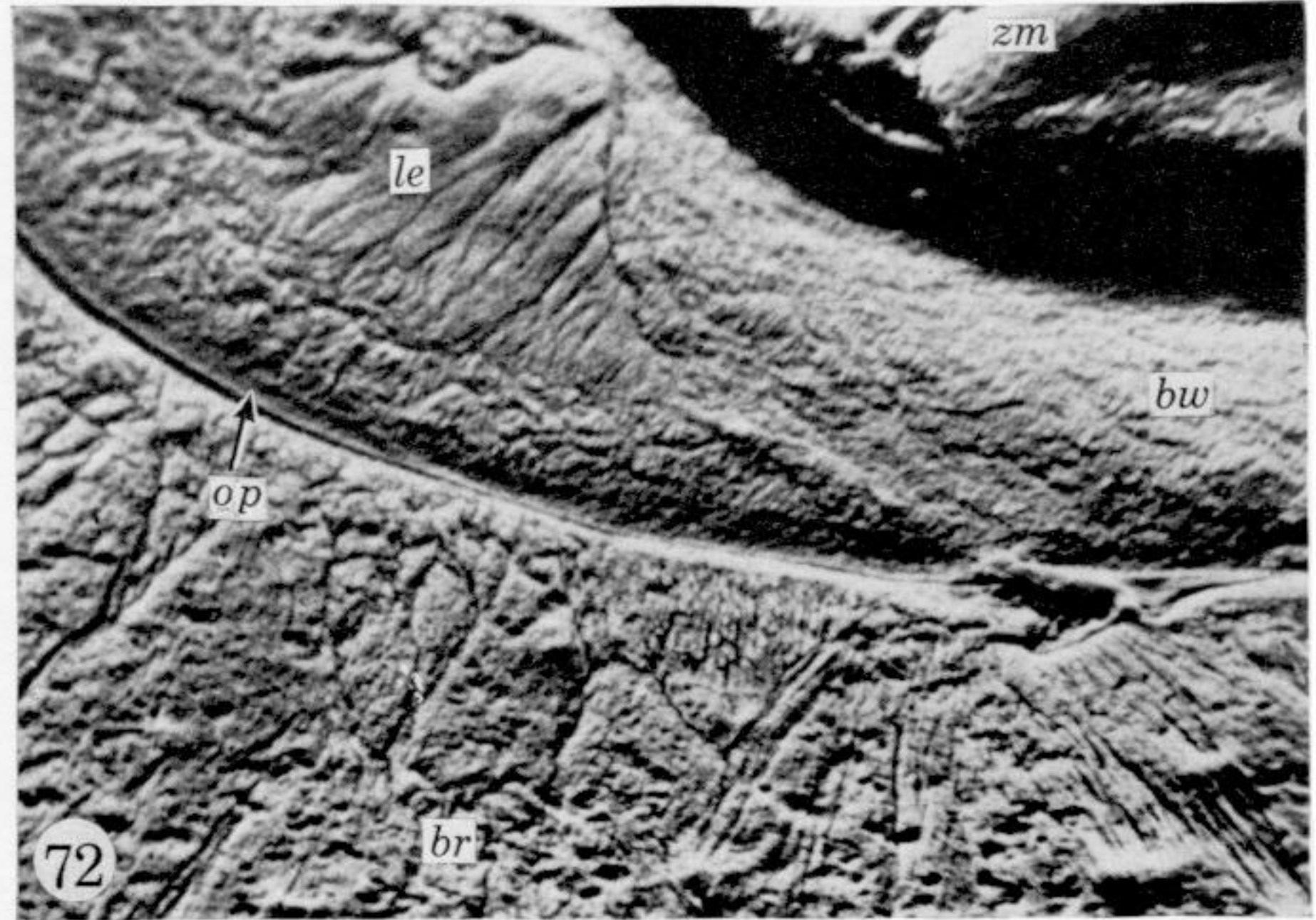
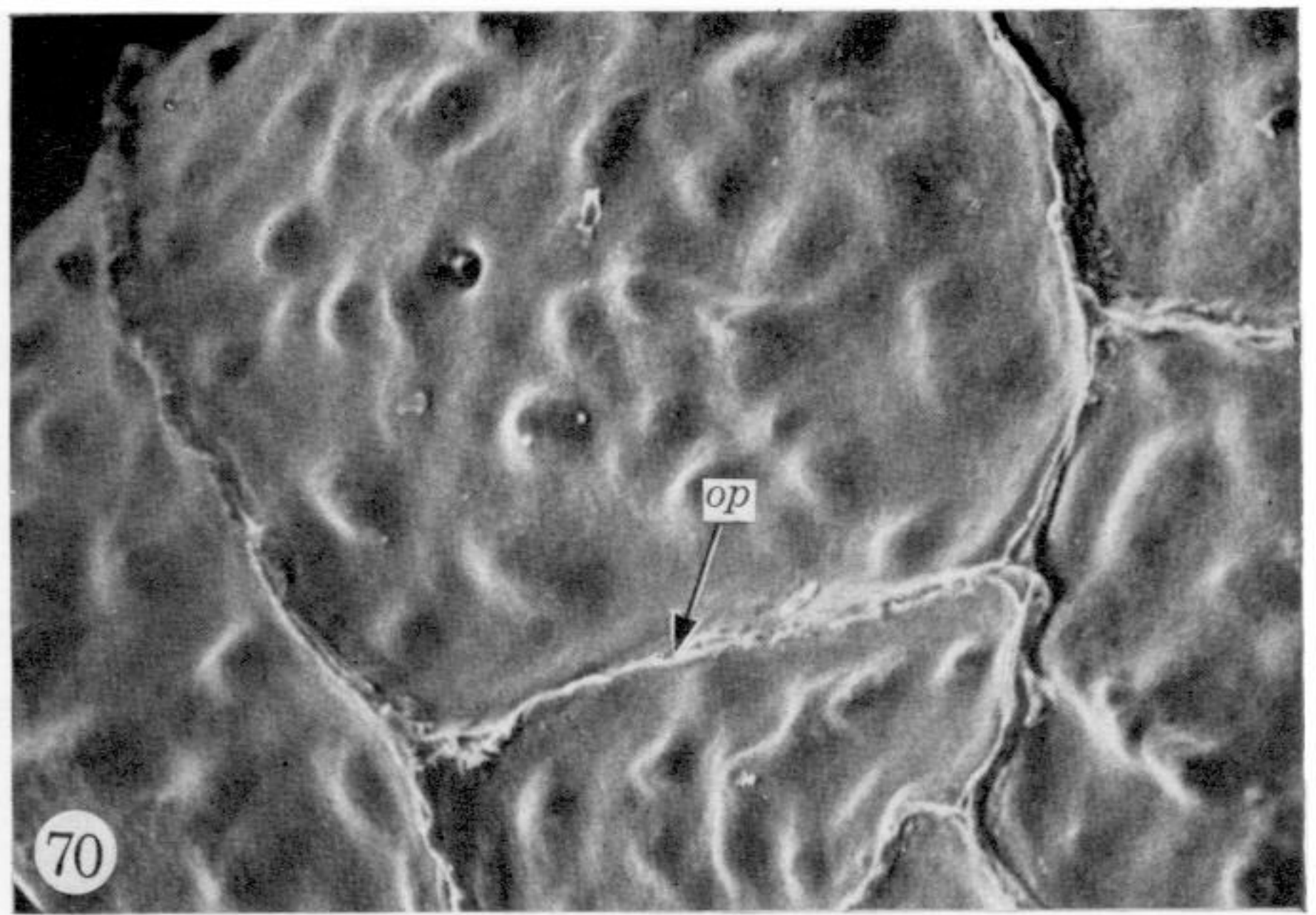
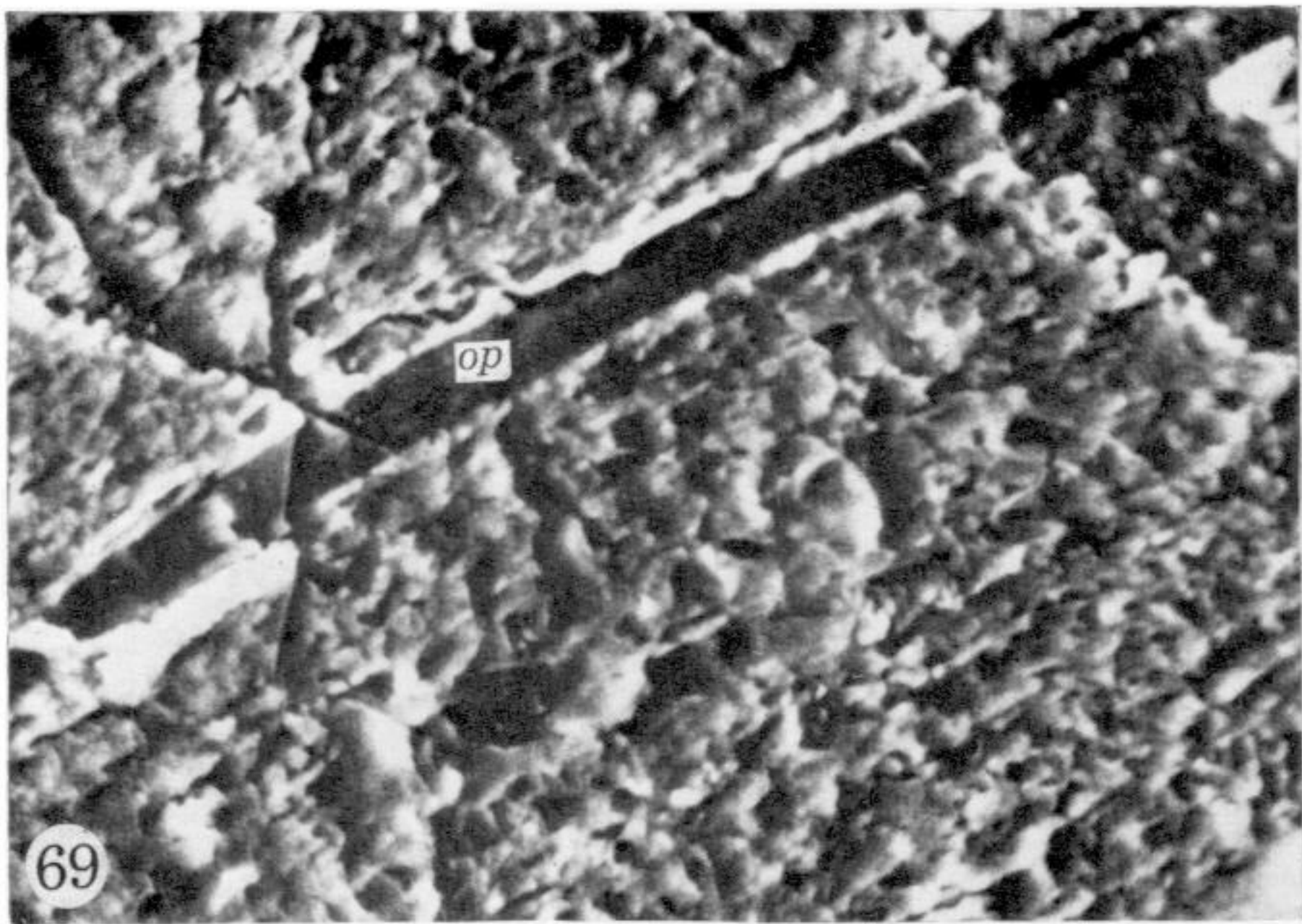
FIGURES 53 TO 60. For legends see facing page.





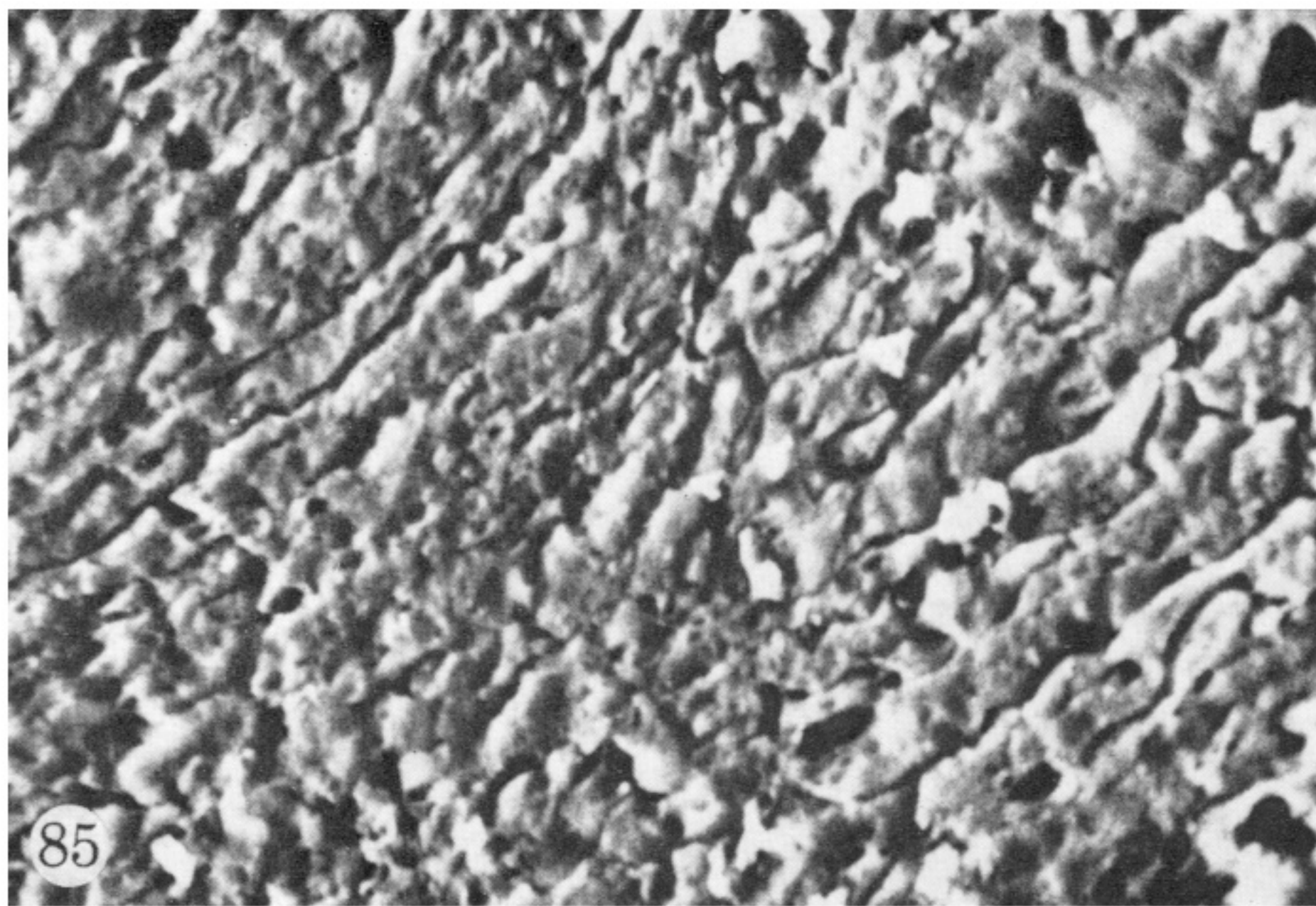
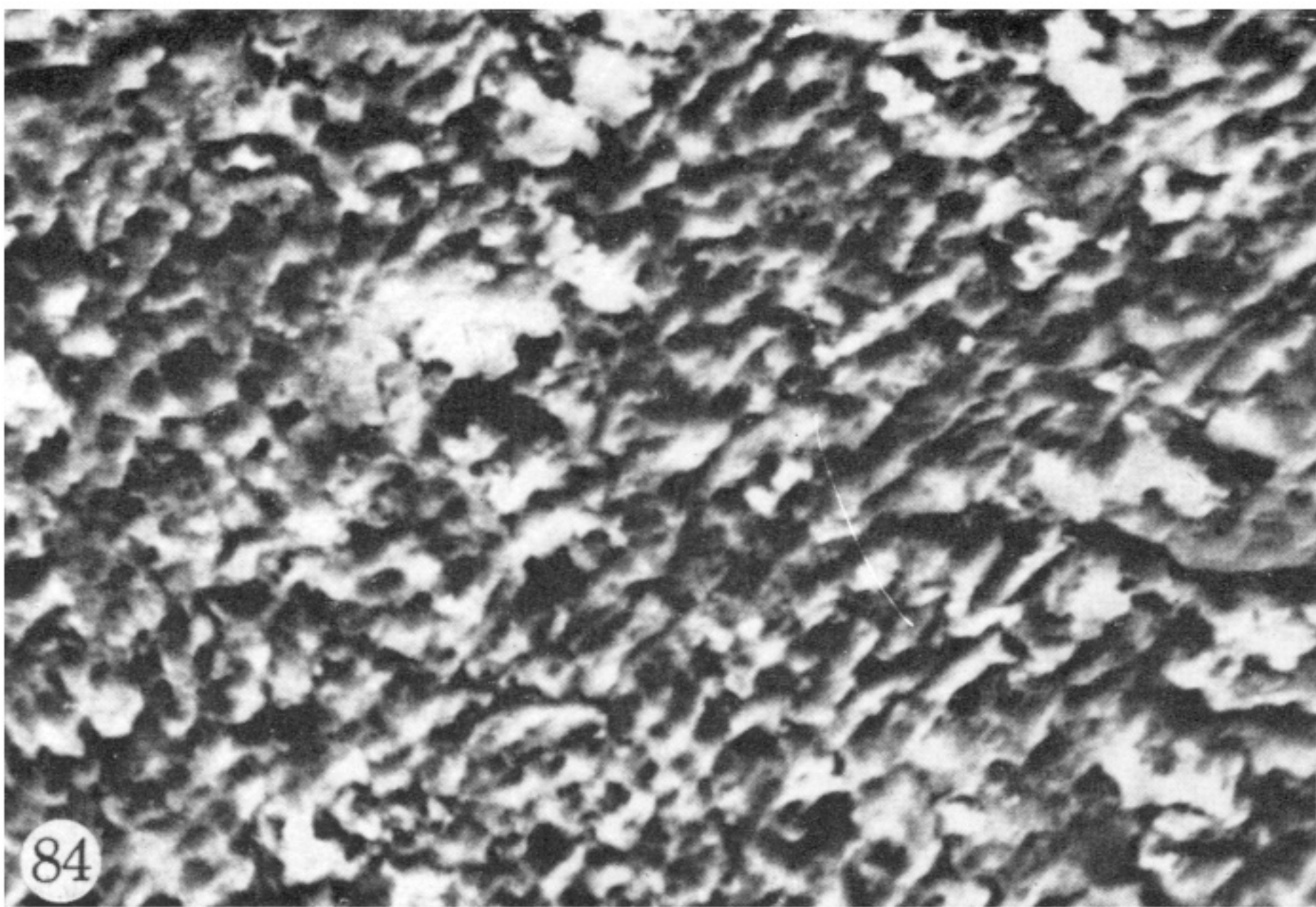
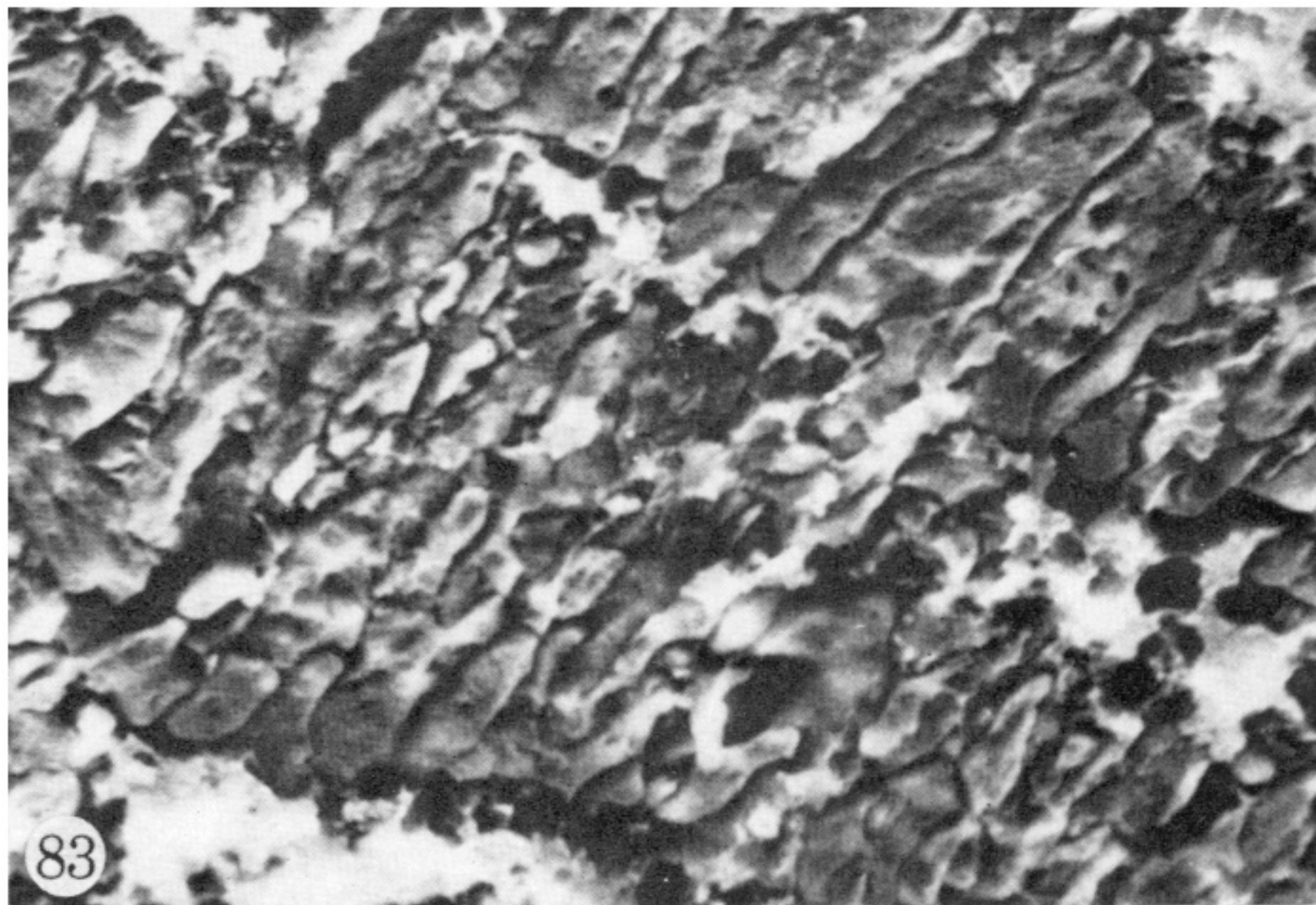
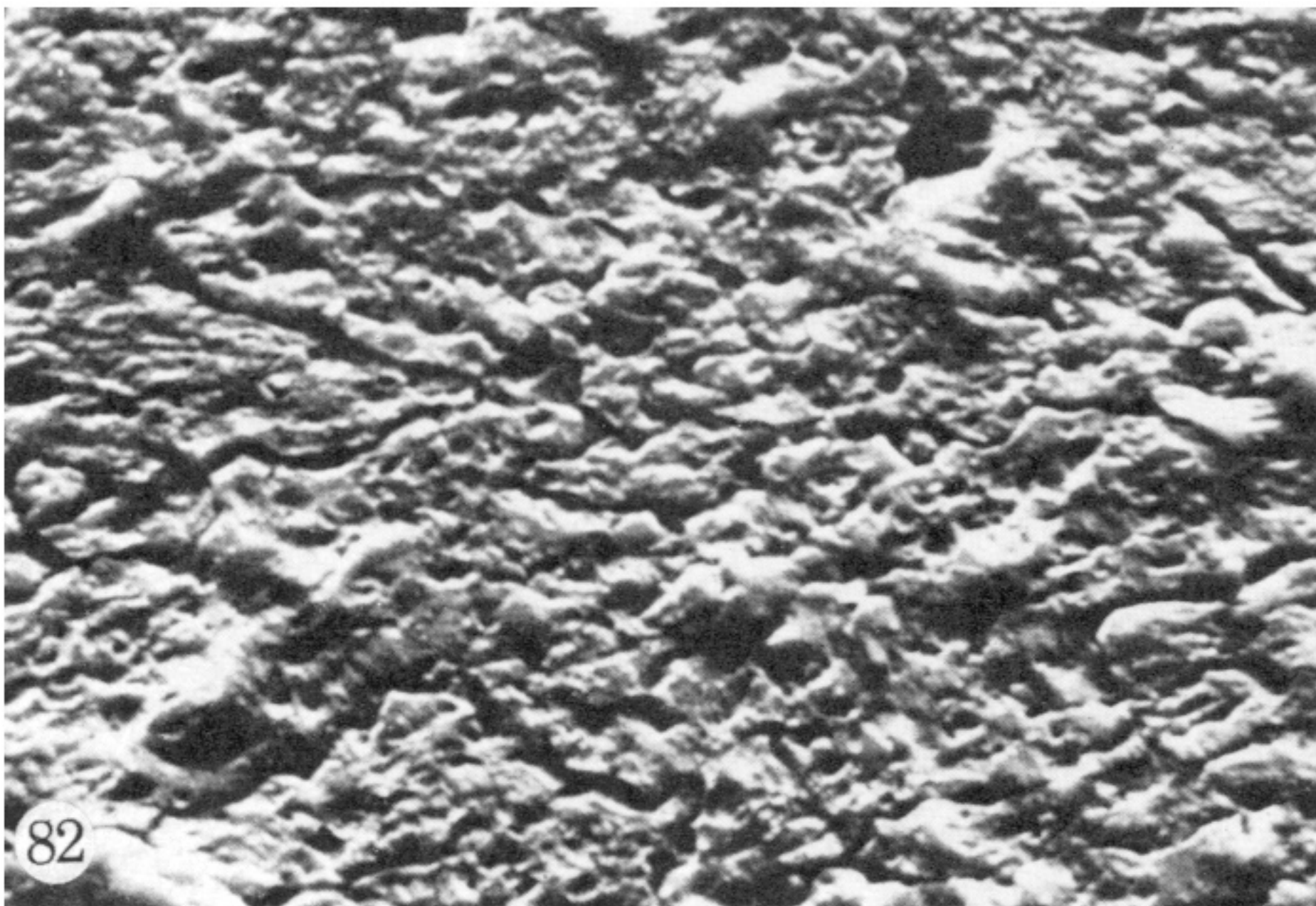
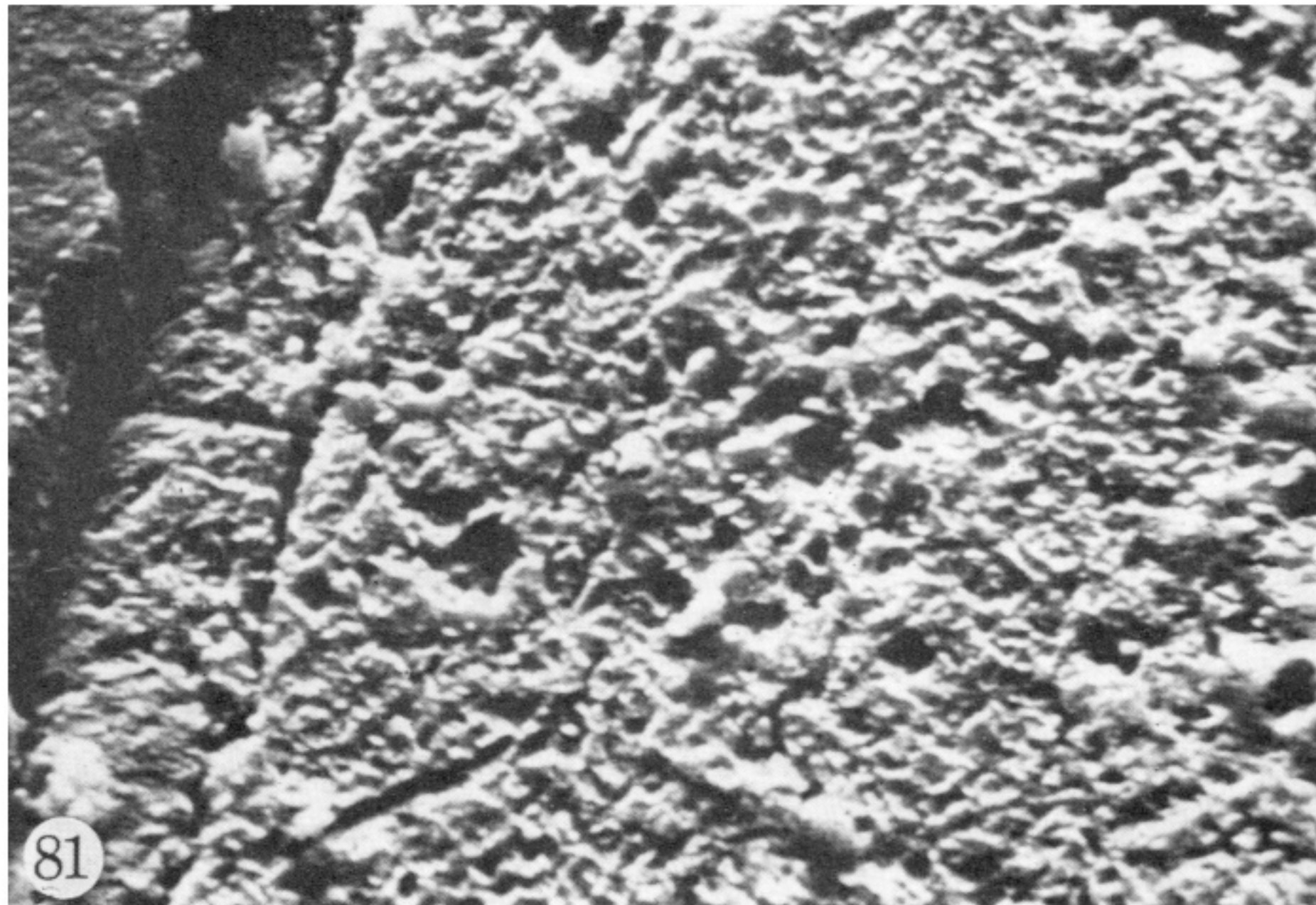
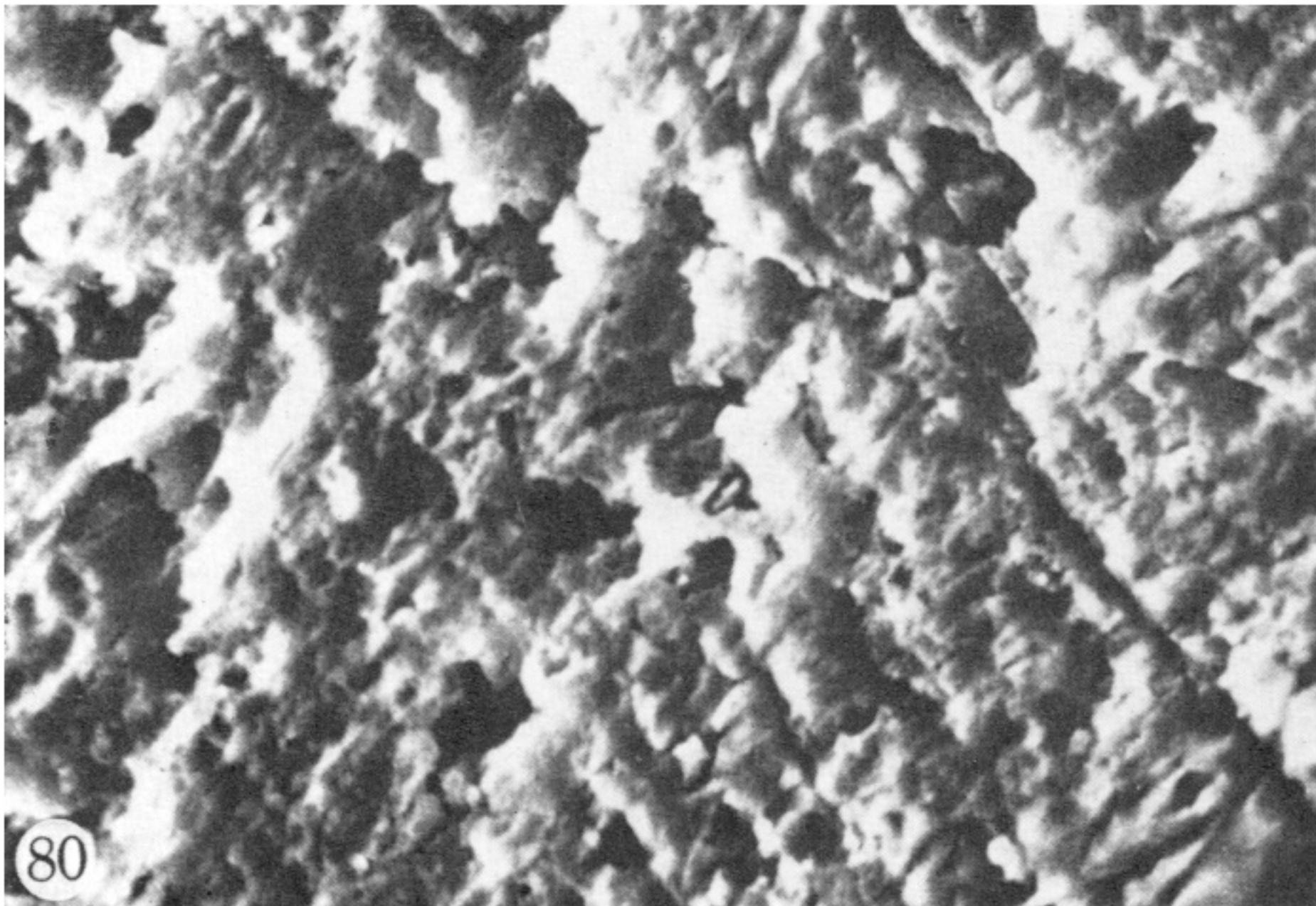
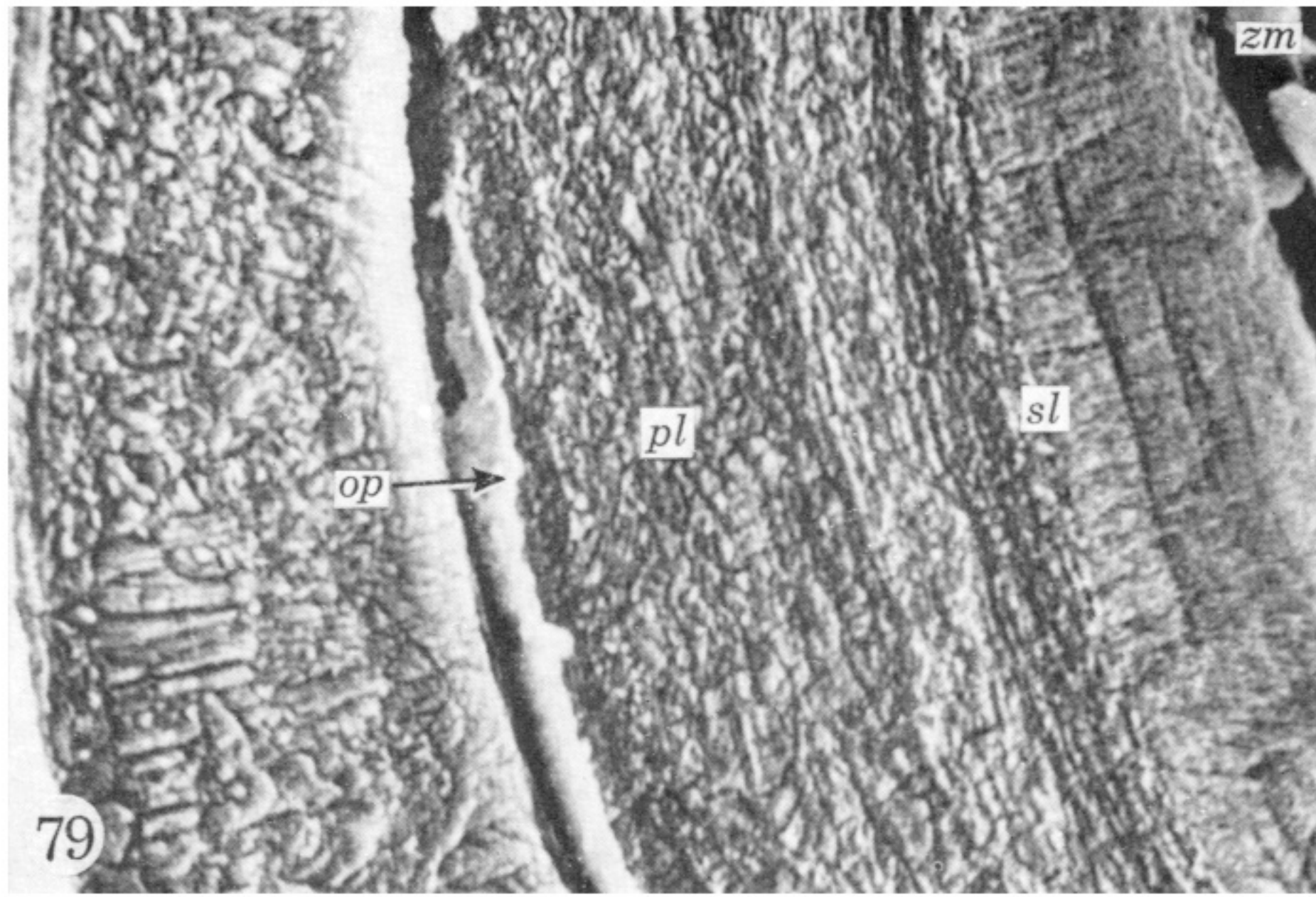
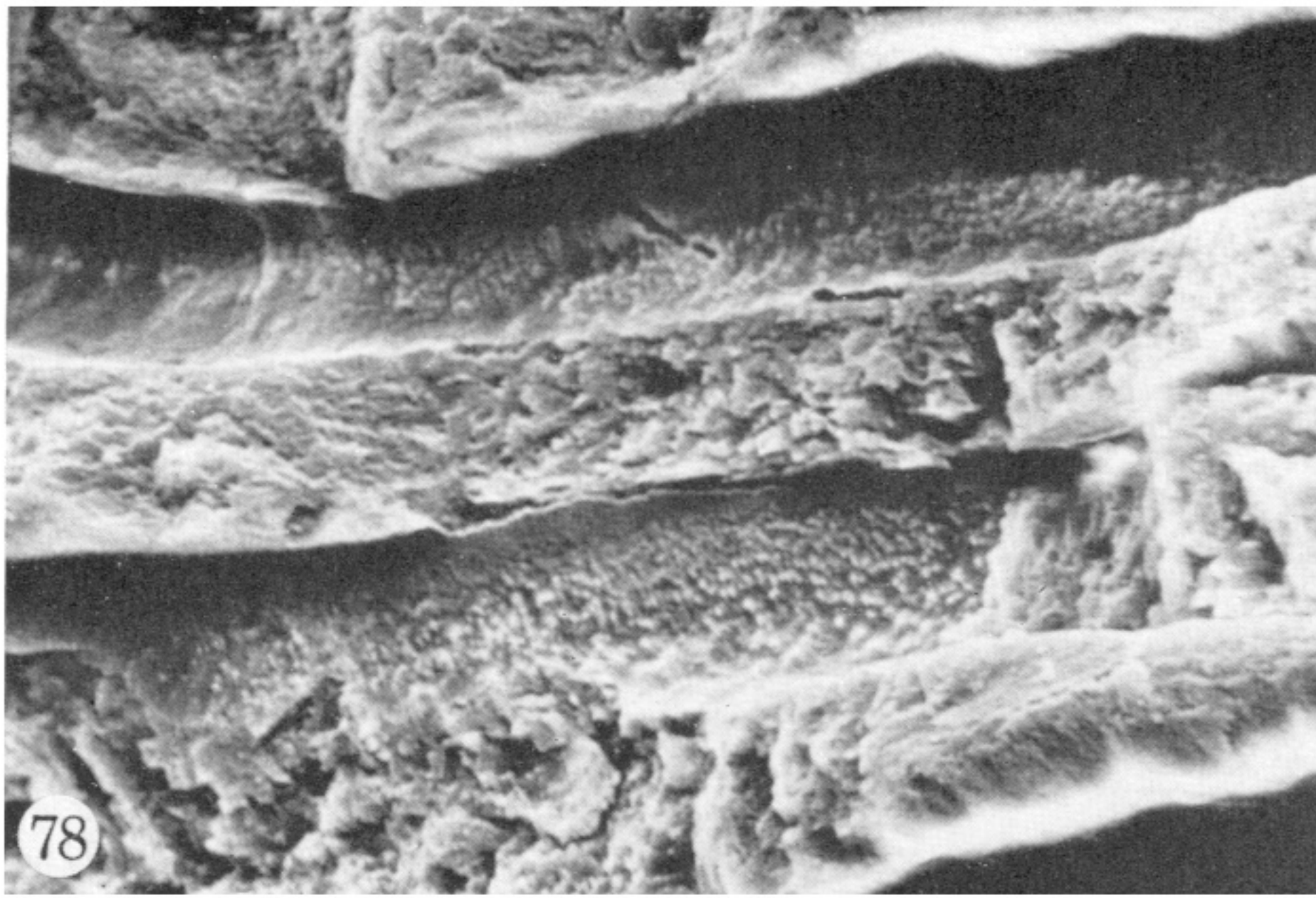
FIGURES 61 TO 68. For legends see facing page.





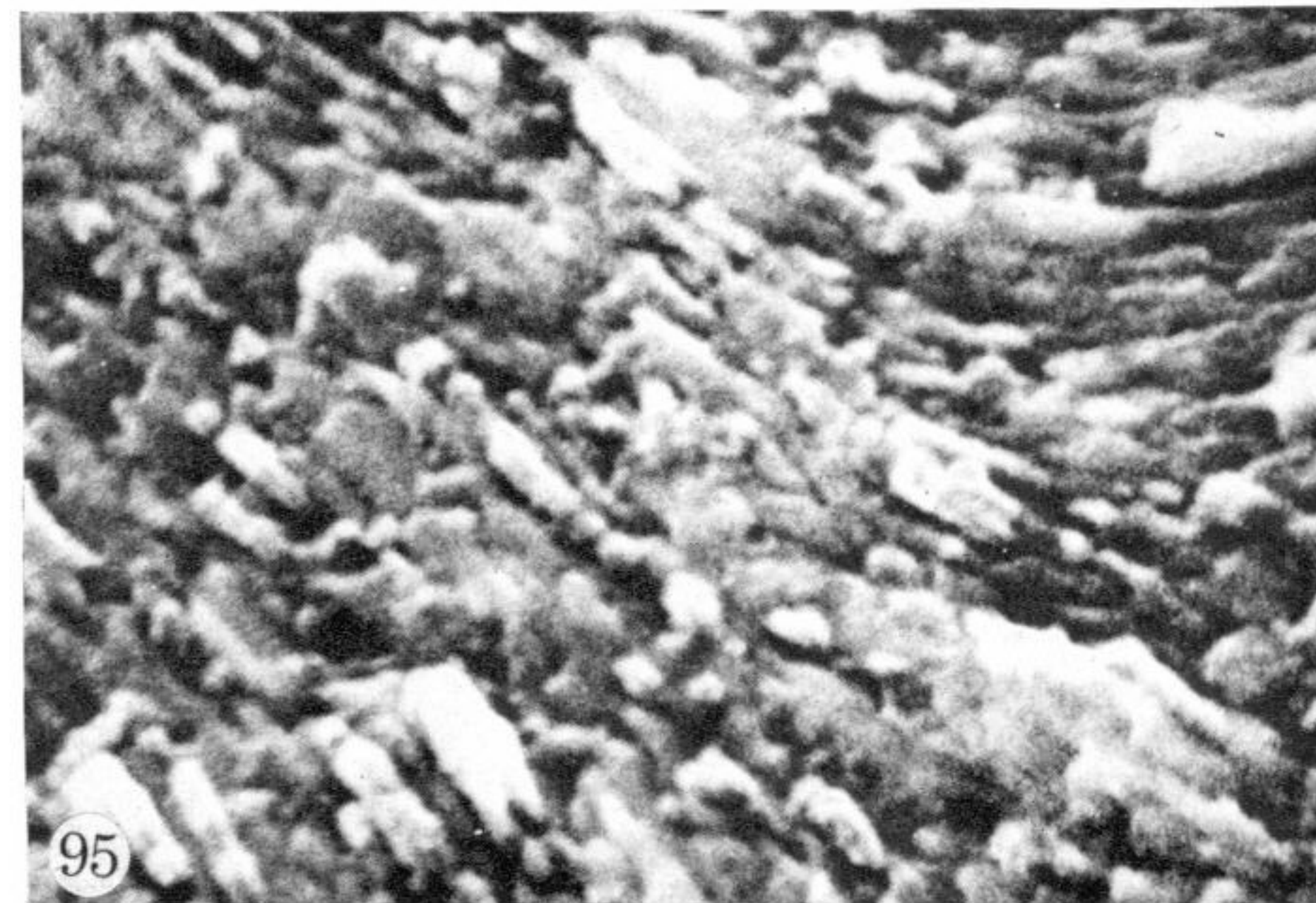
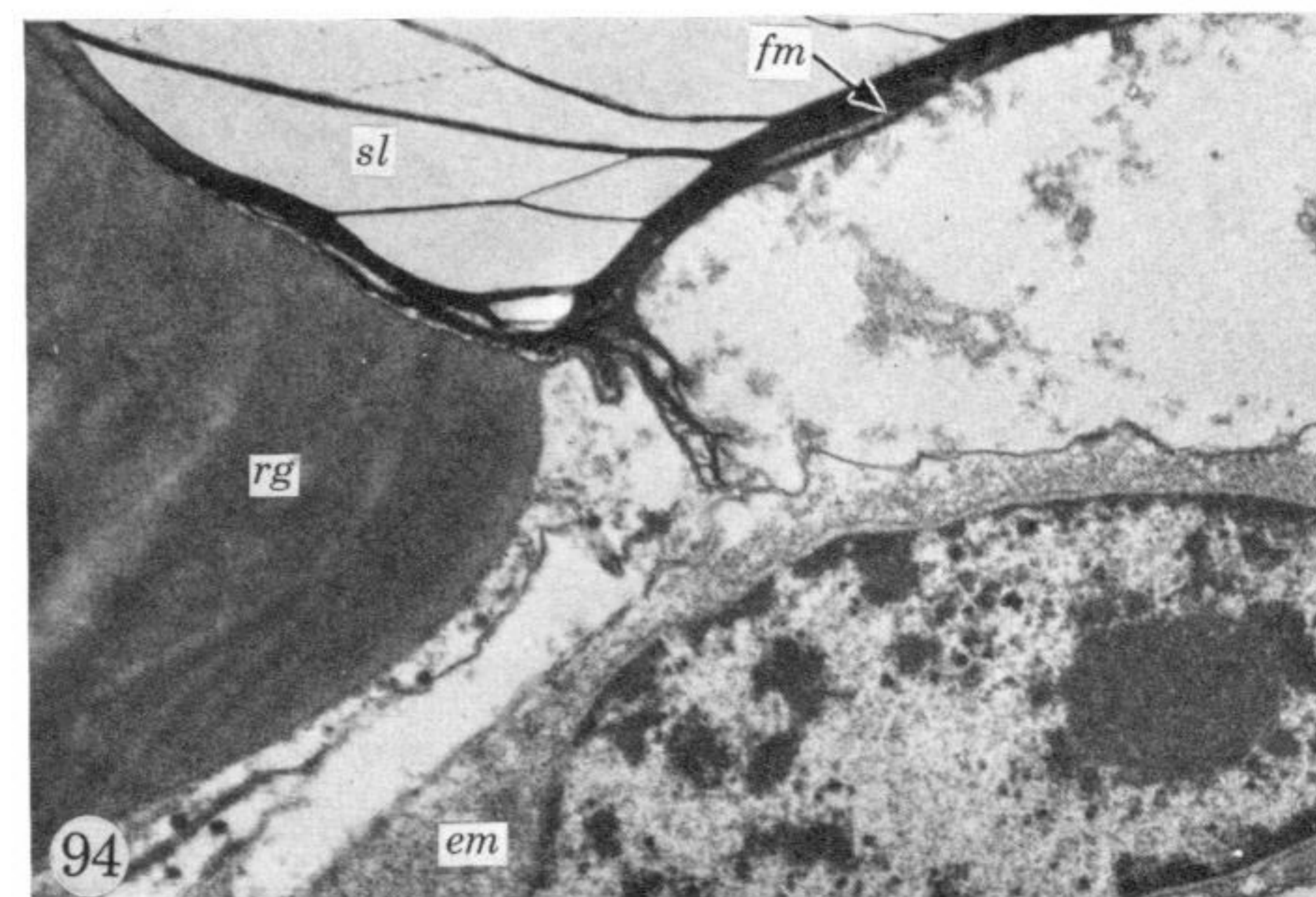
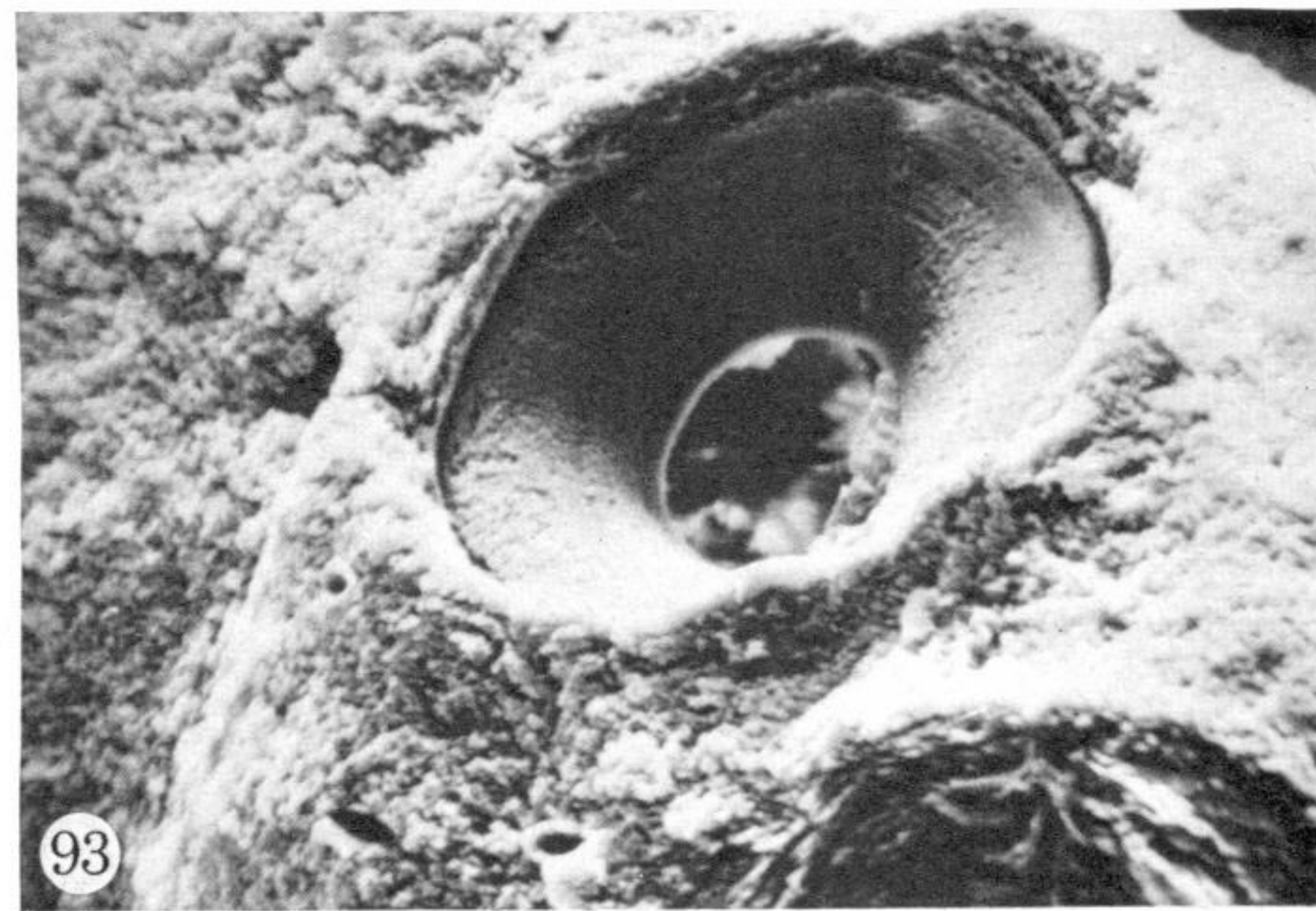
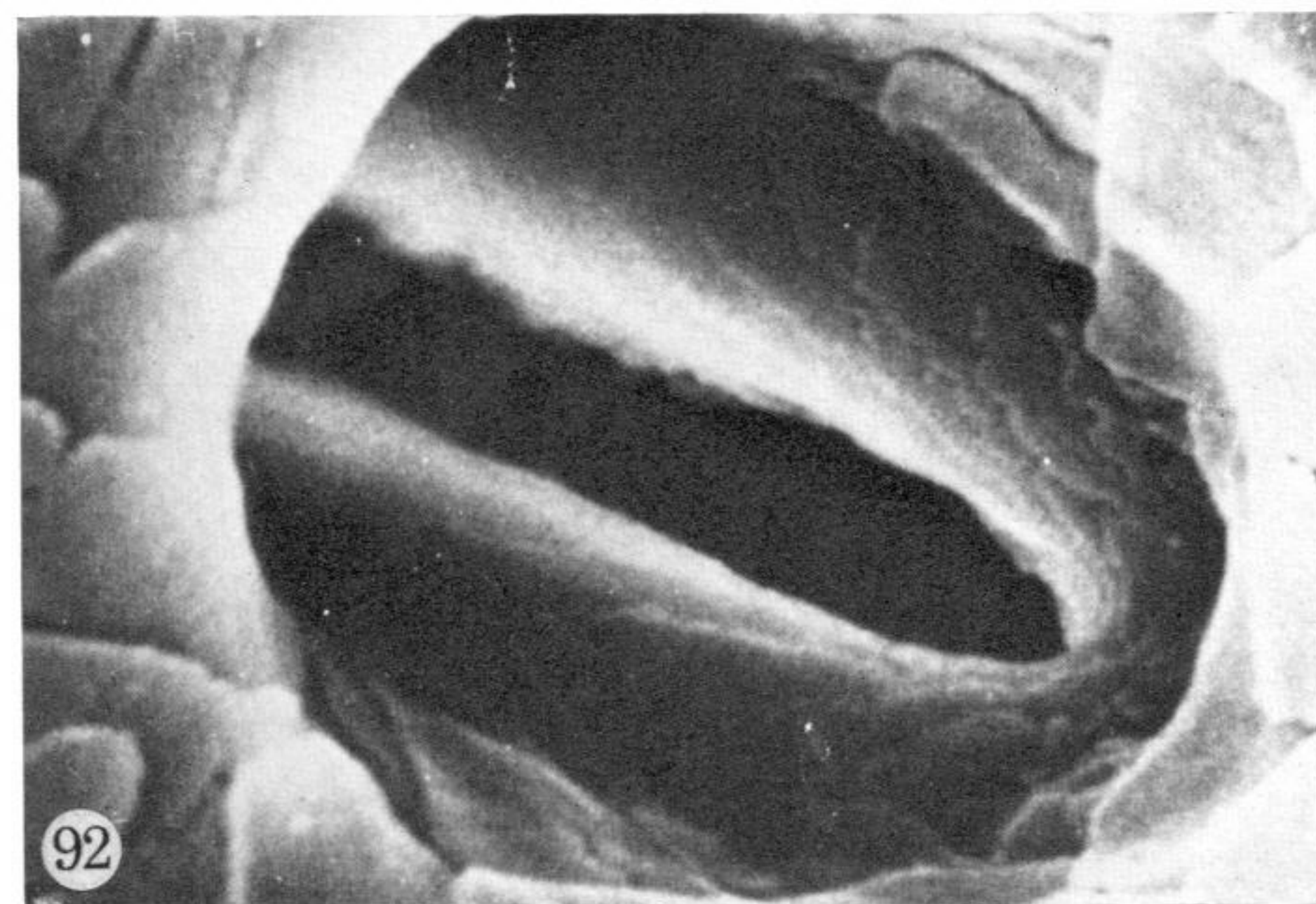
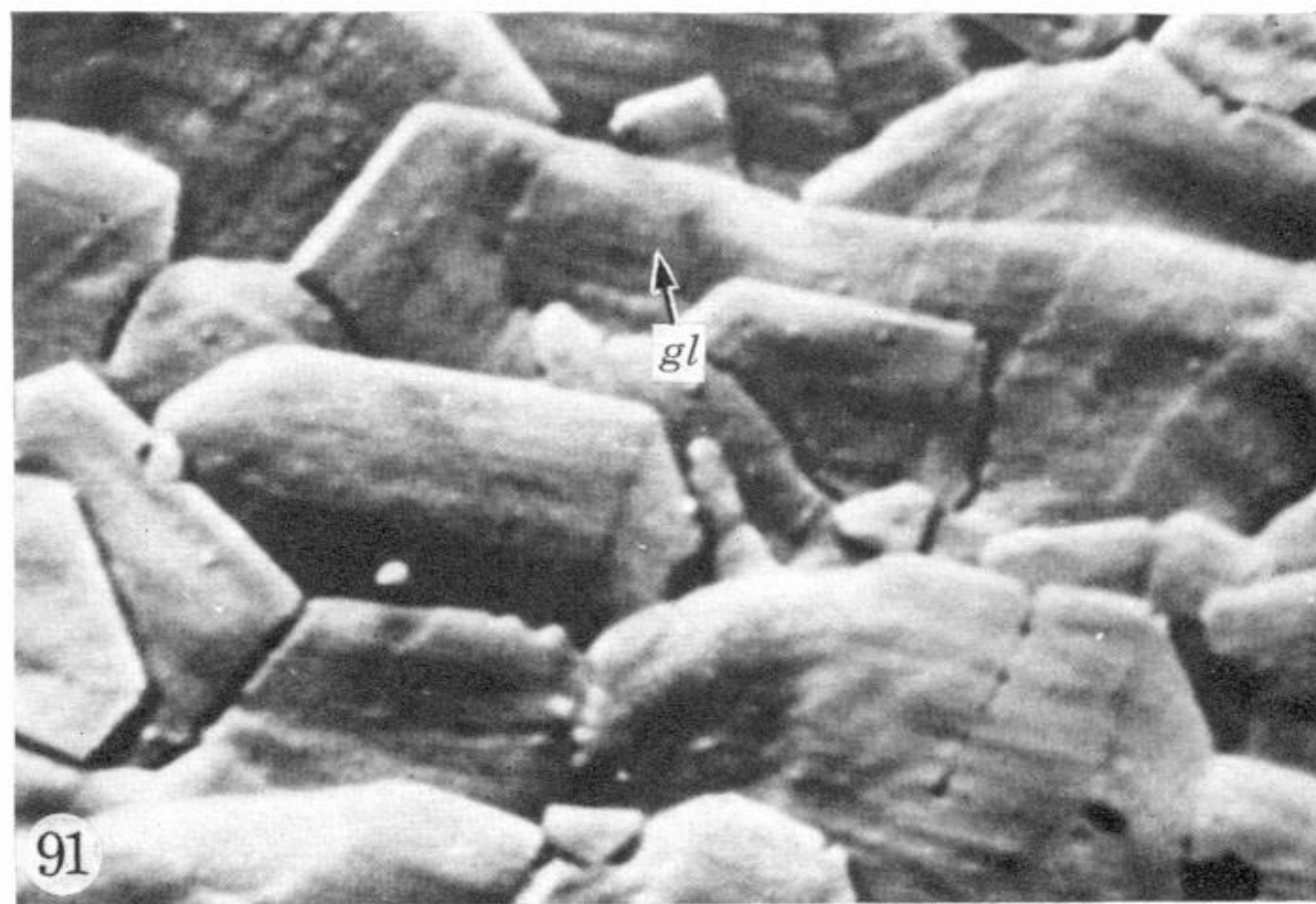
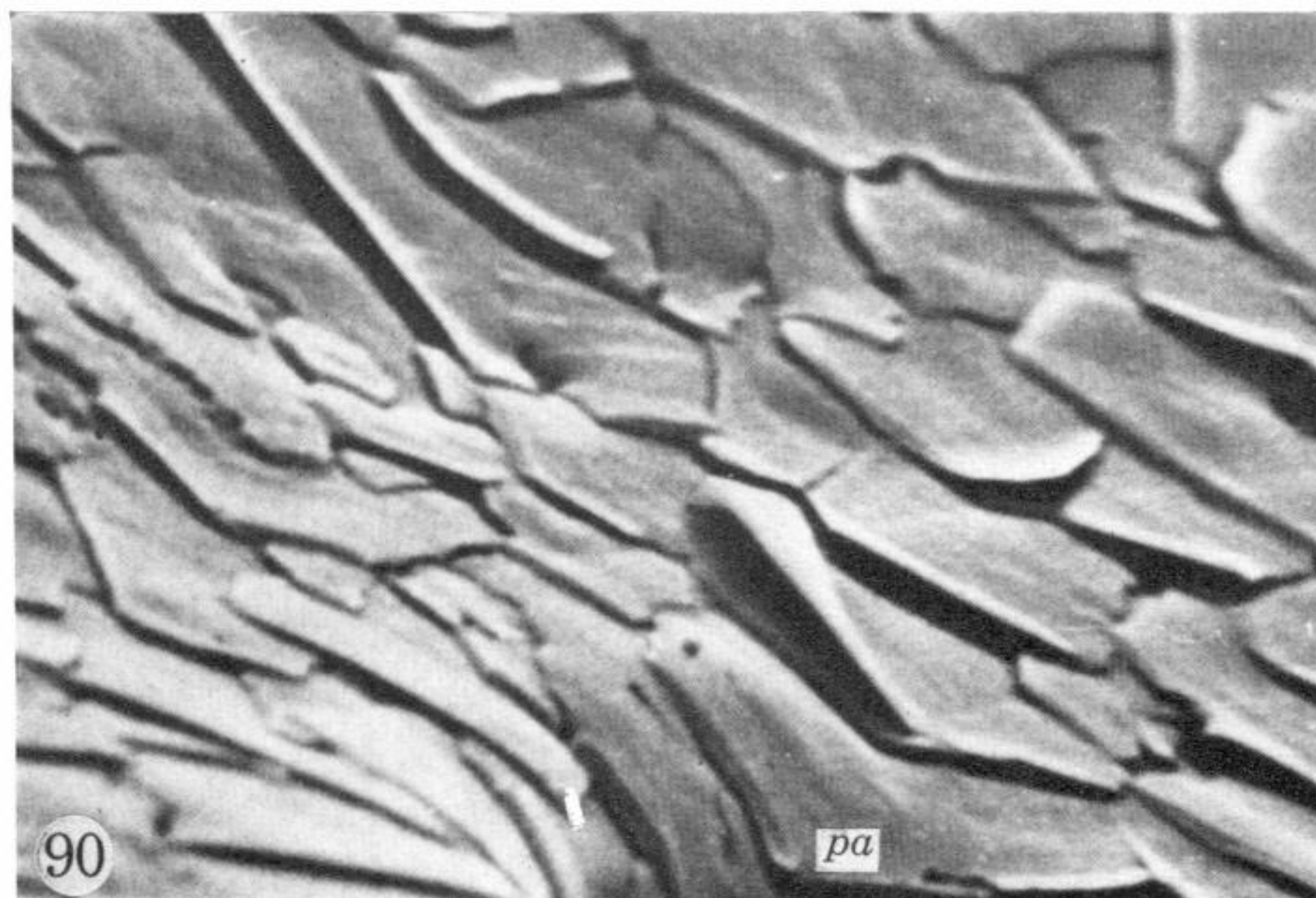
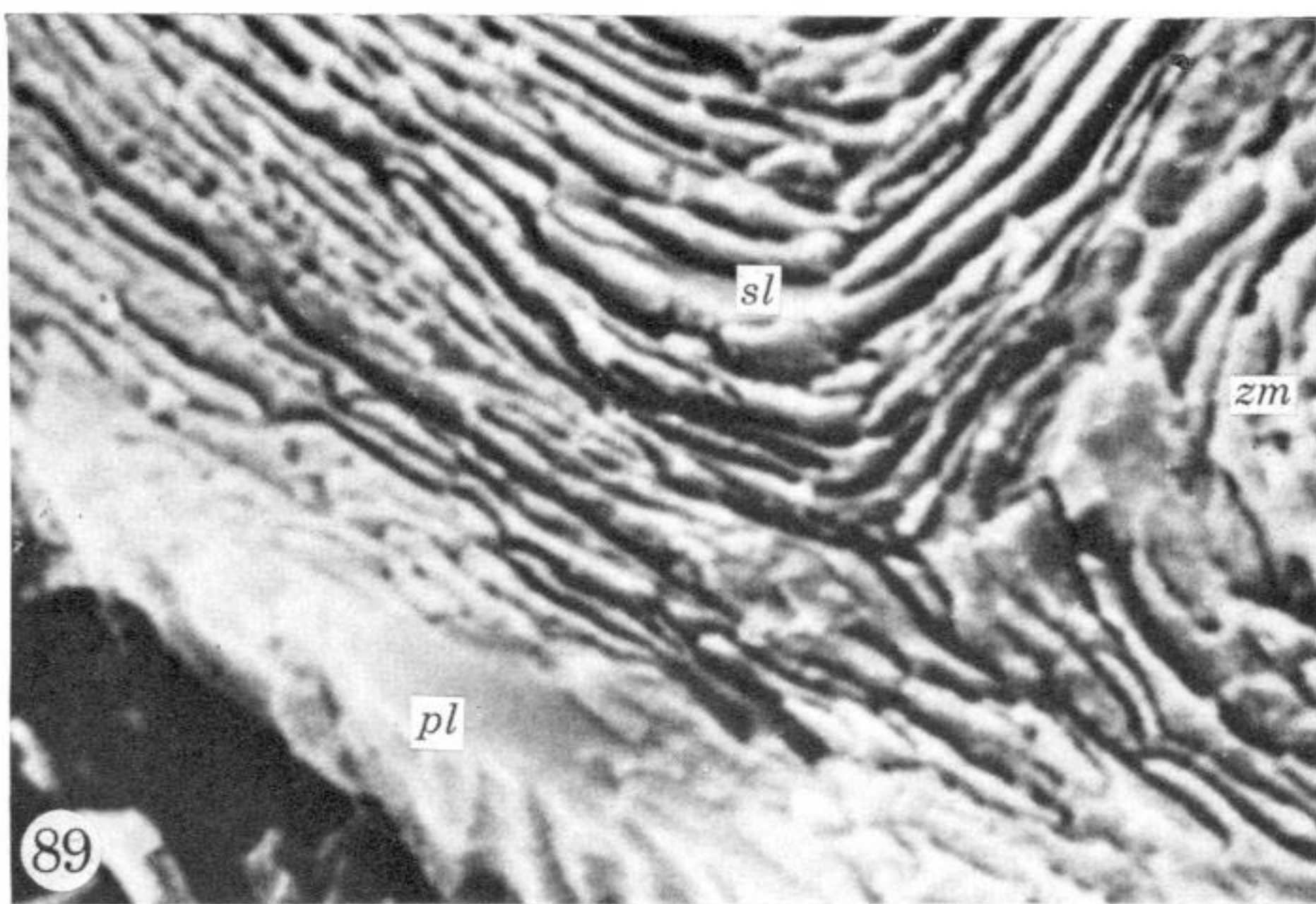
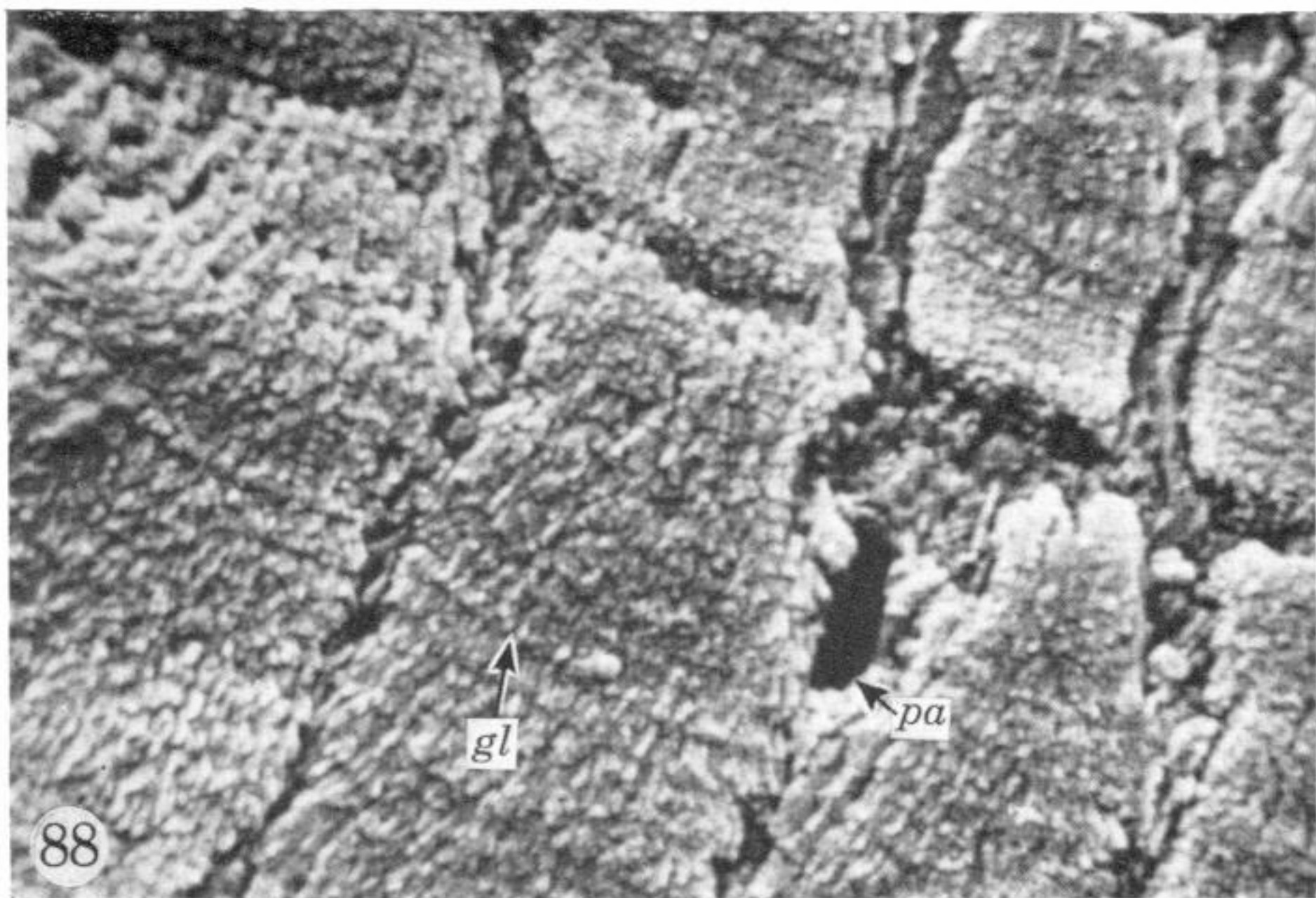
FIGURES 69 TO 76. For legends see facing page.





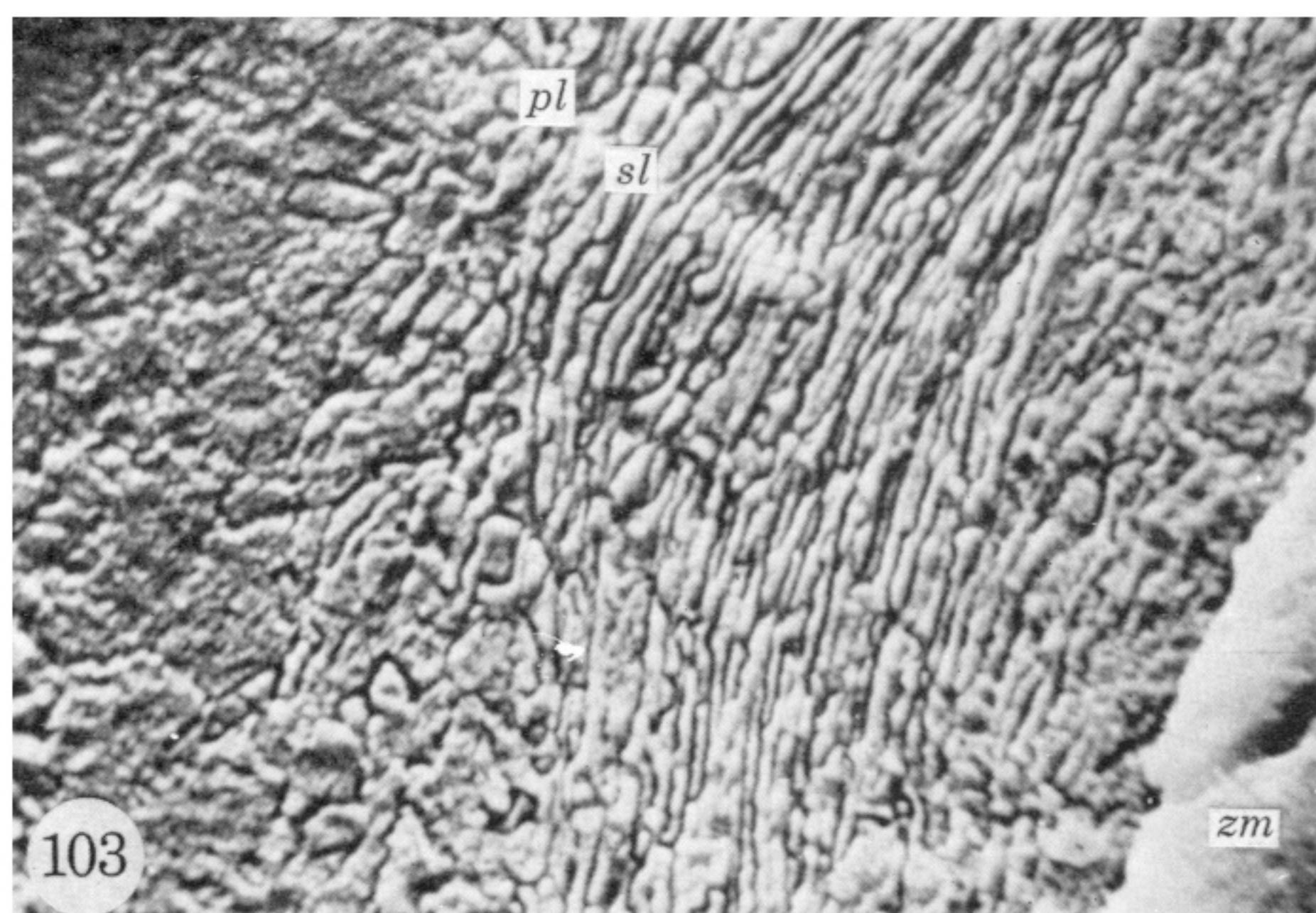
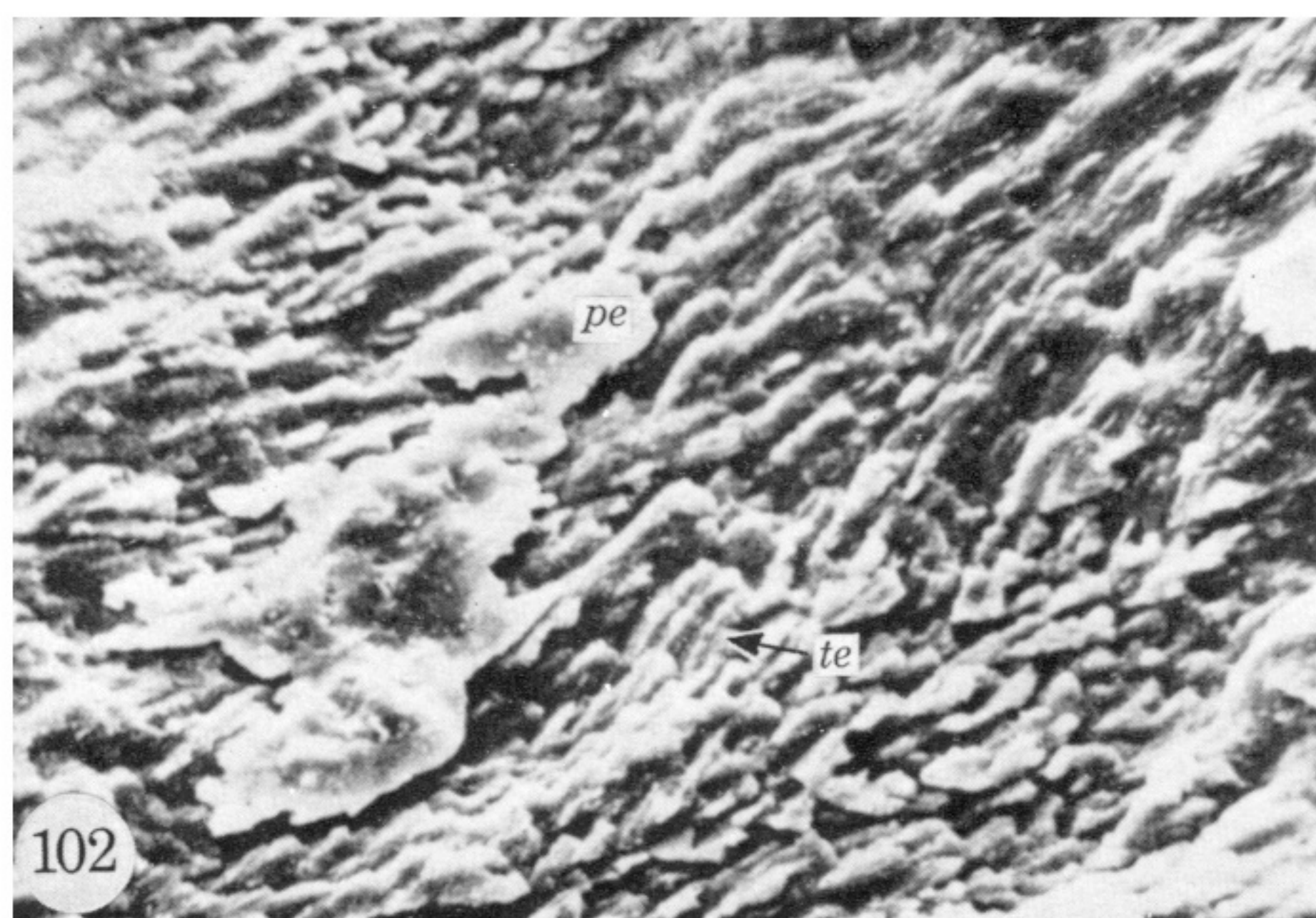
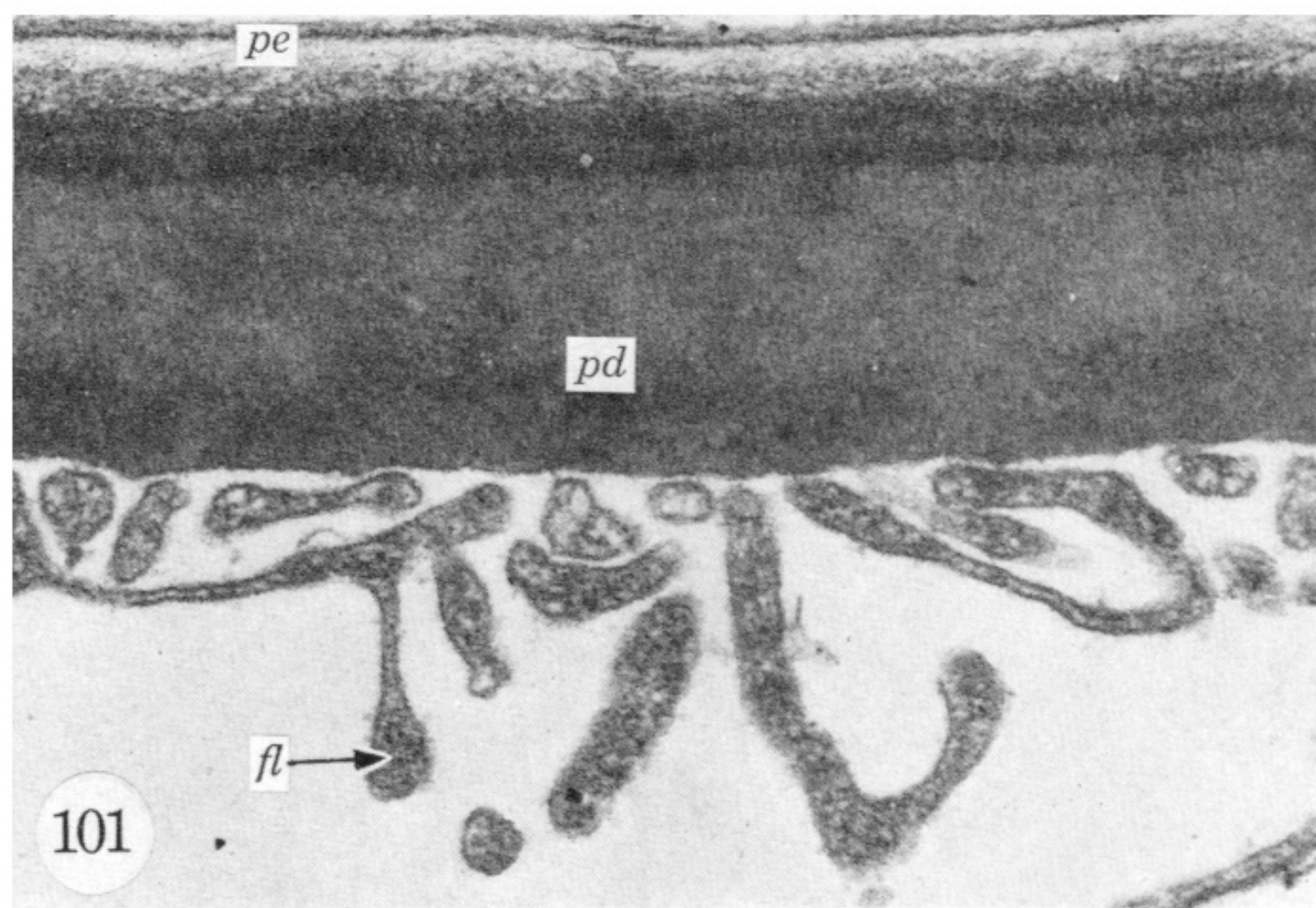
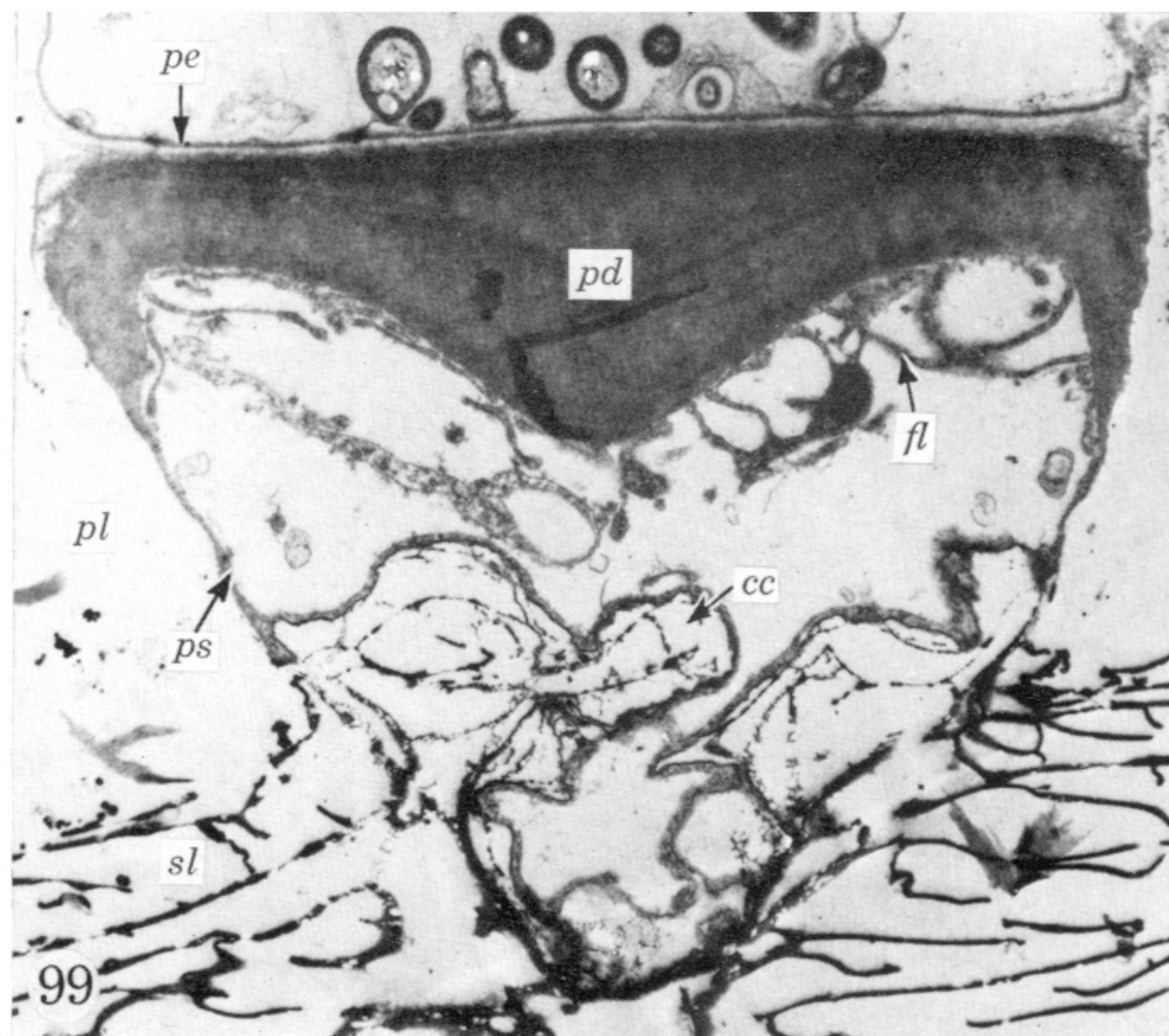
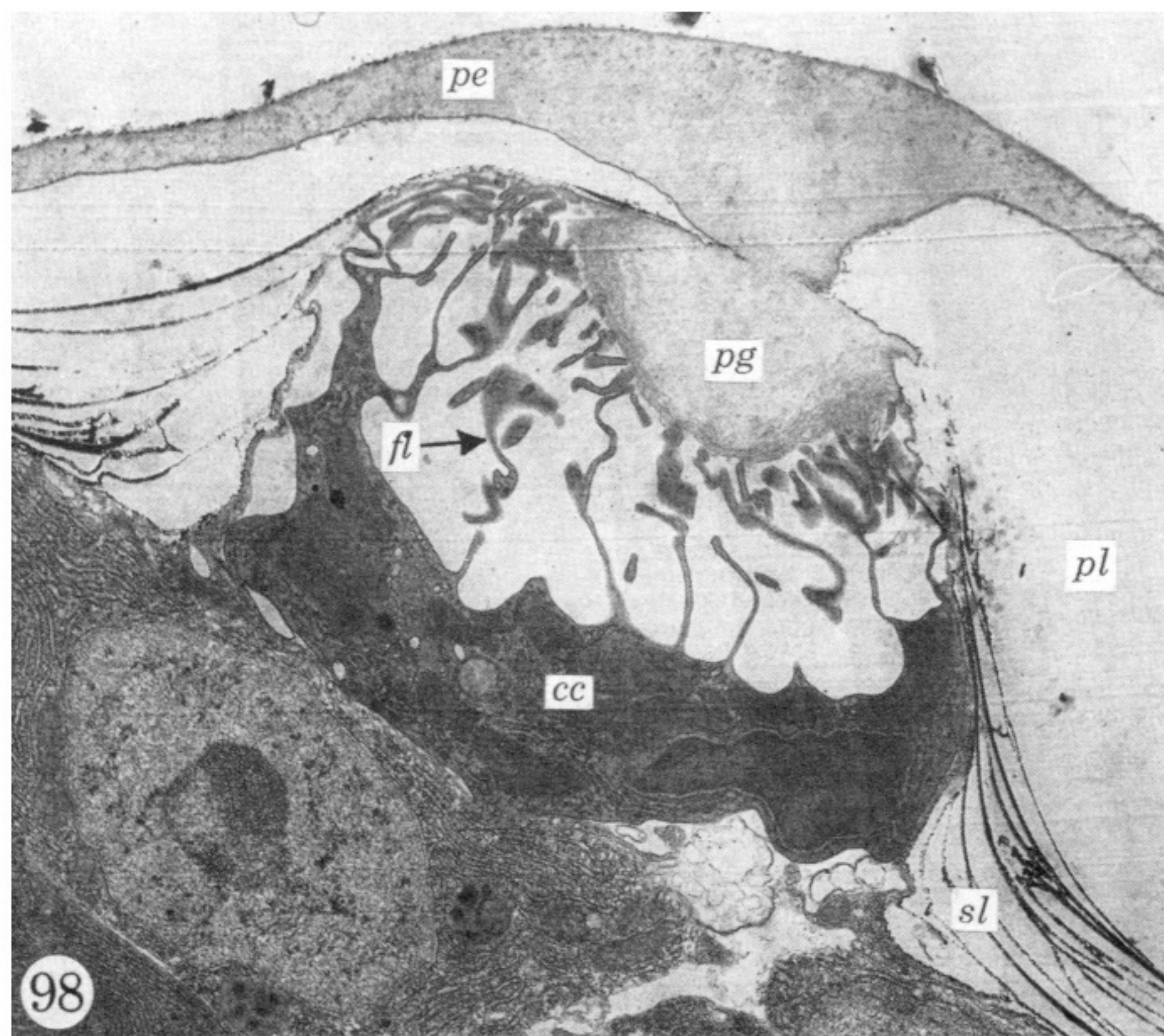
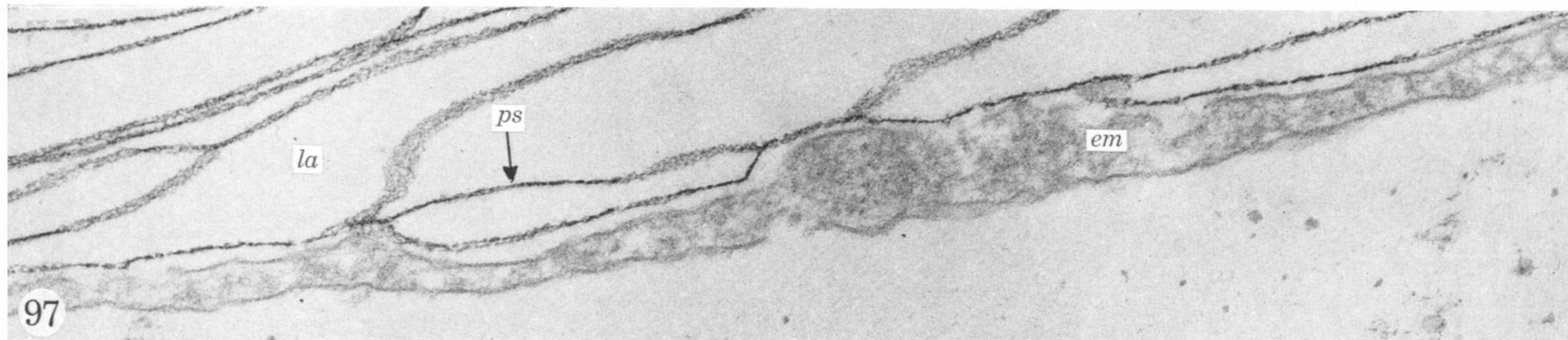
FIGURES 78 TO 85. For legends see facing page.





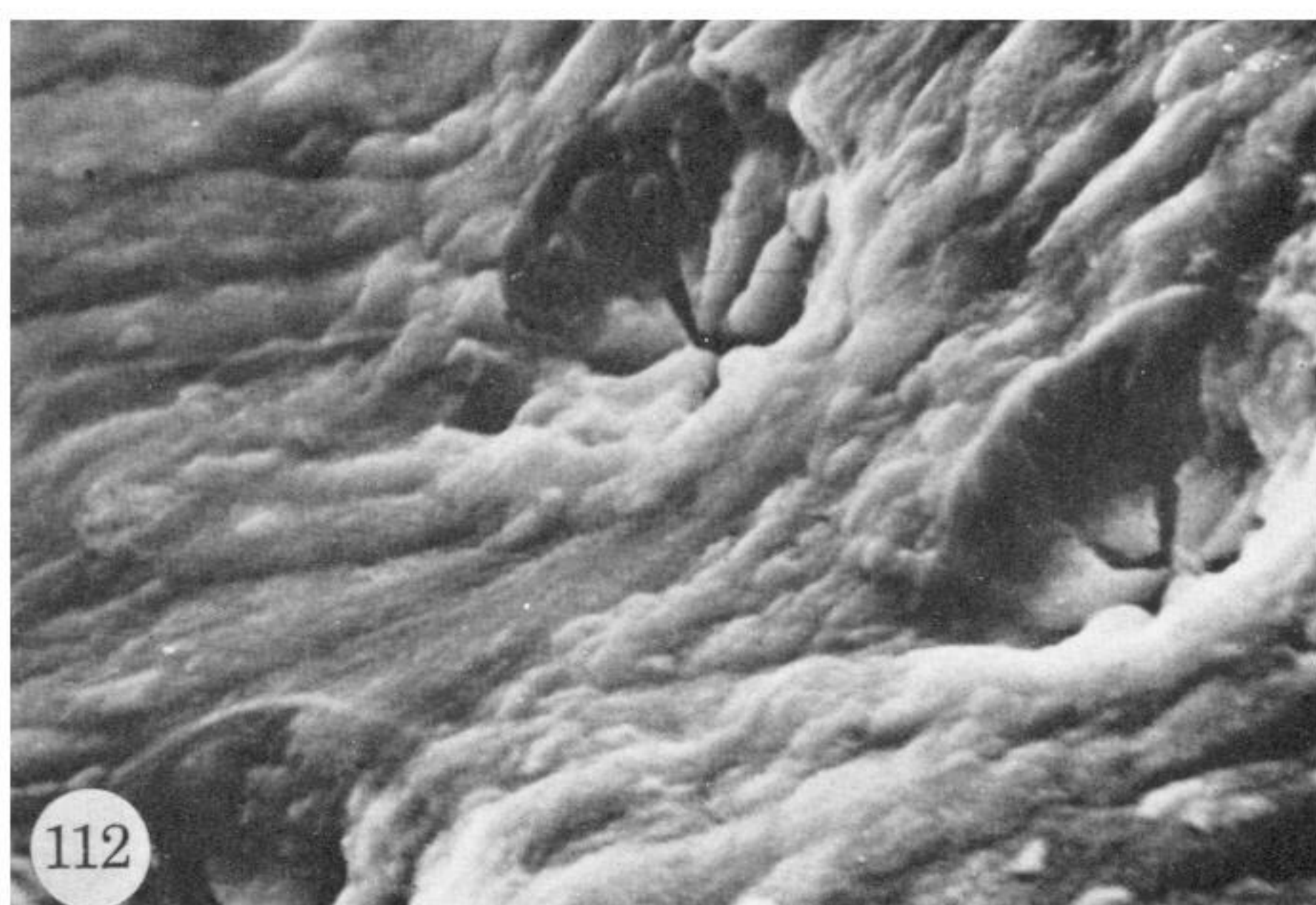
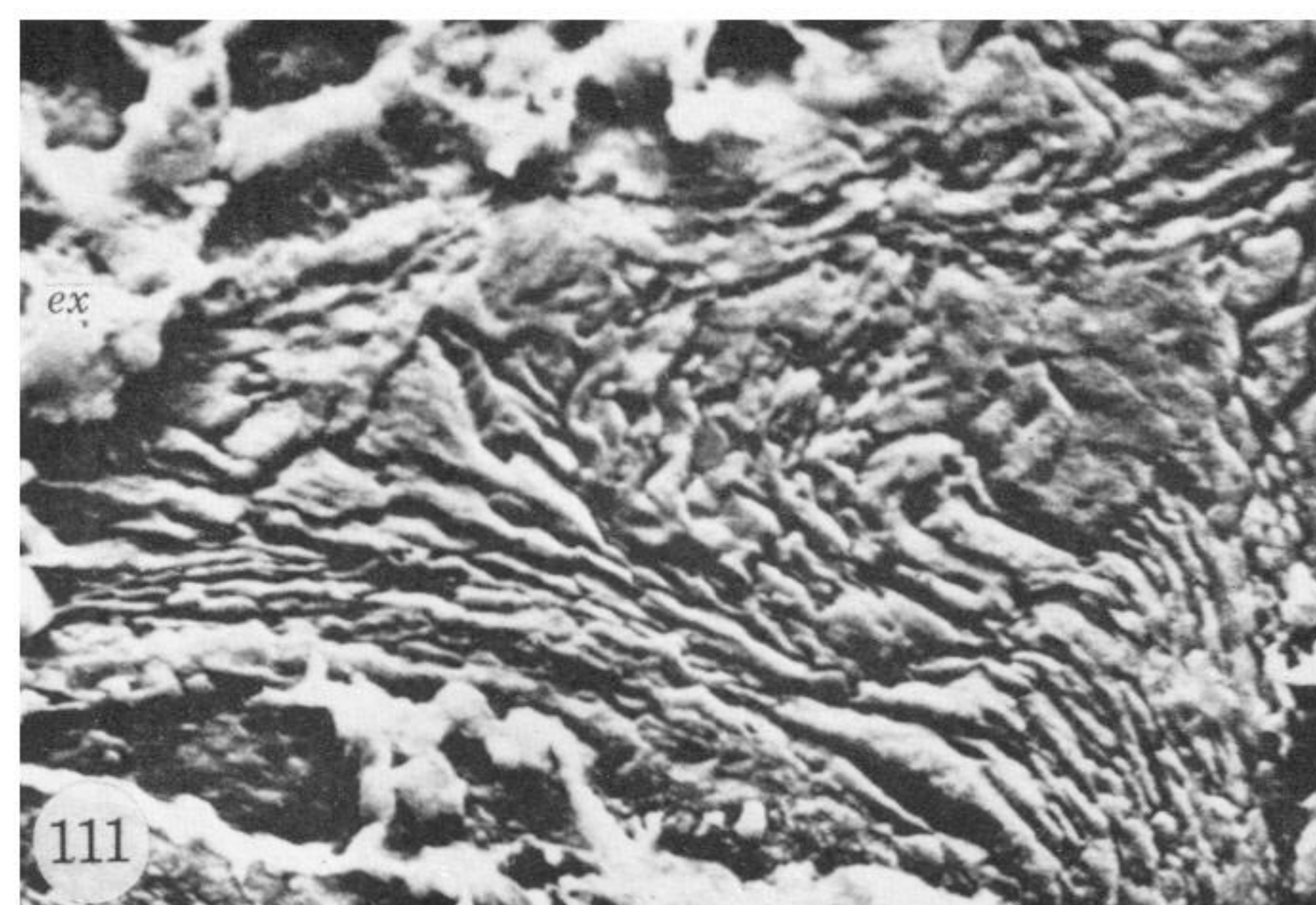
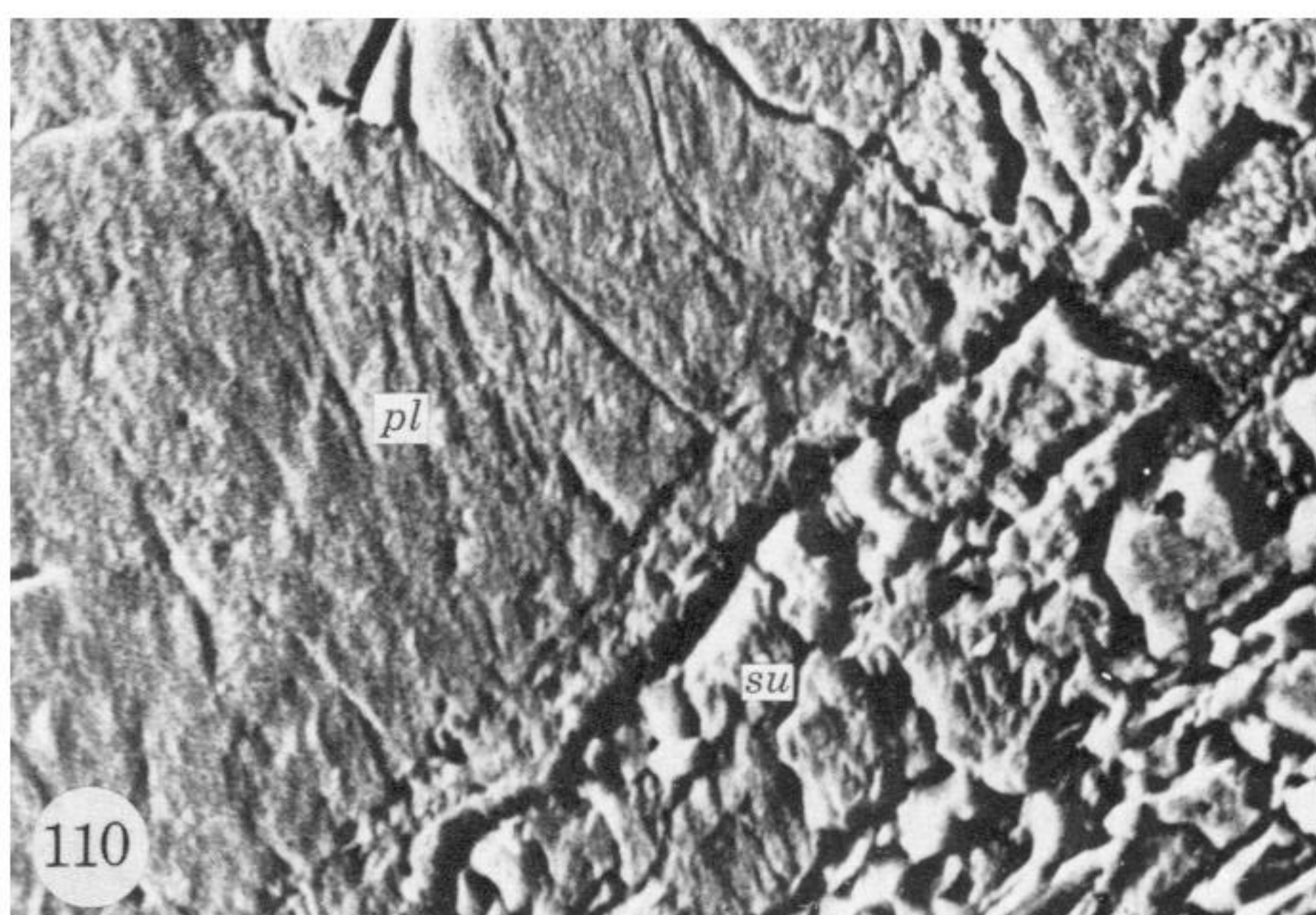
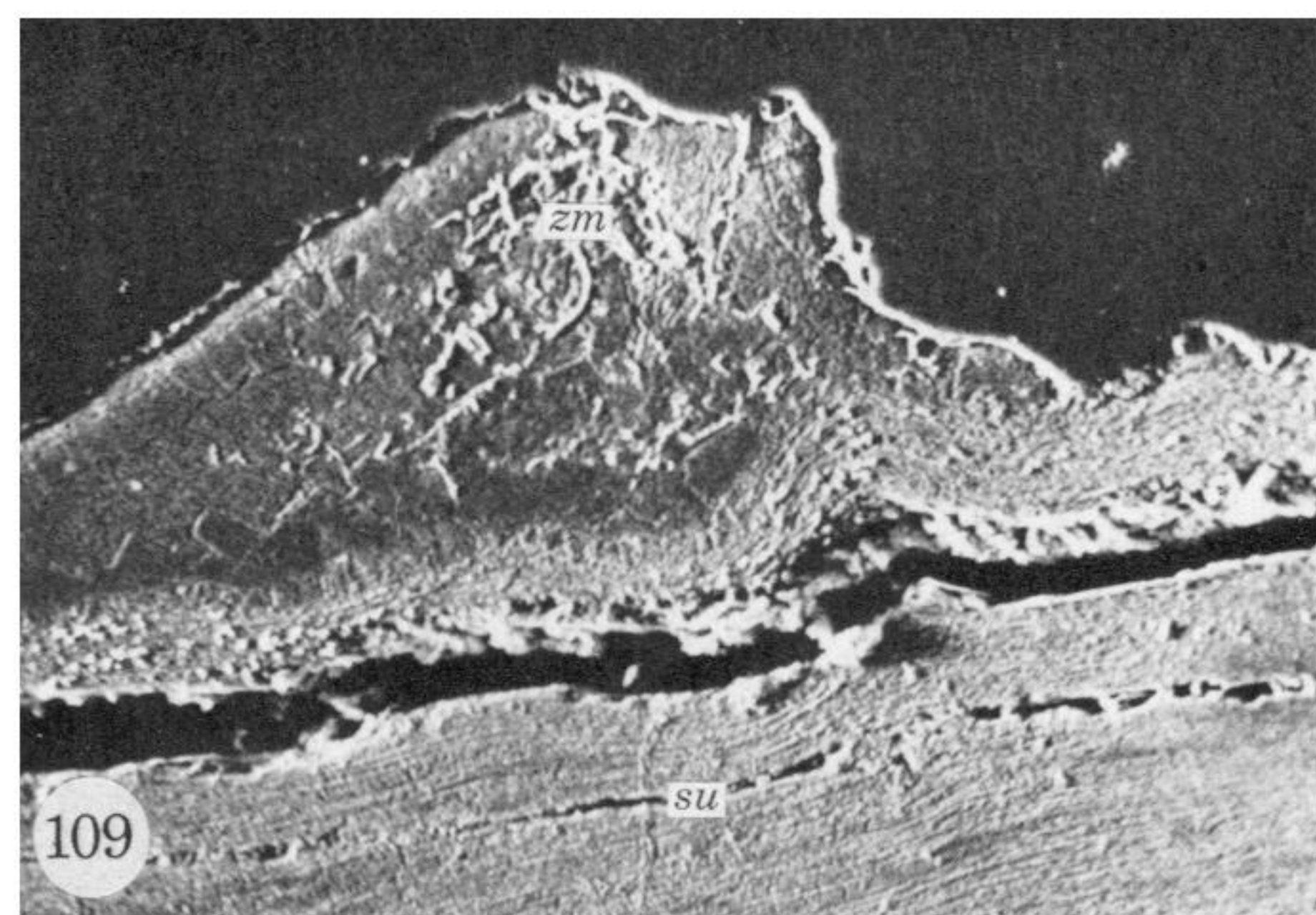
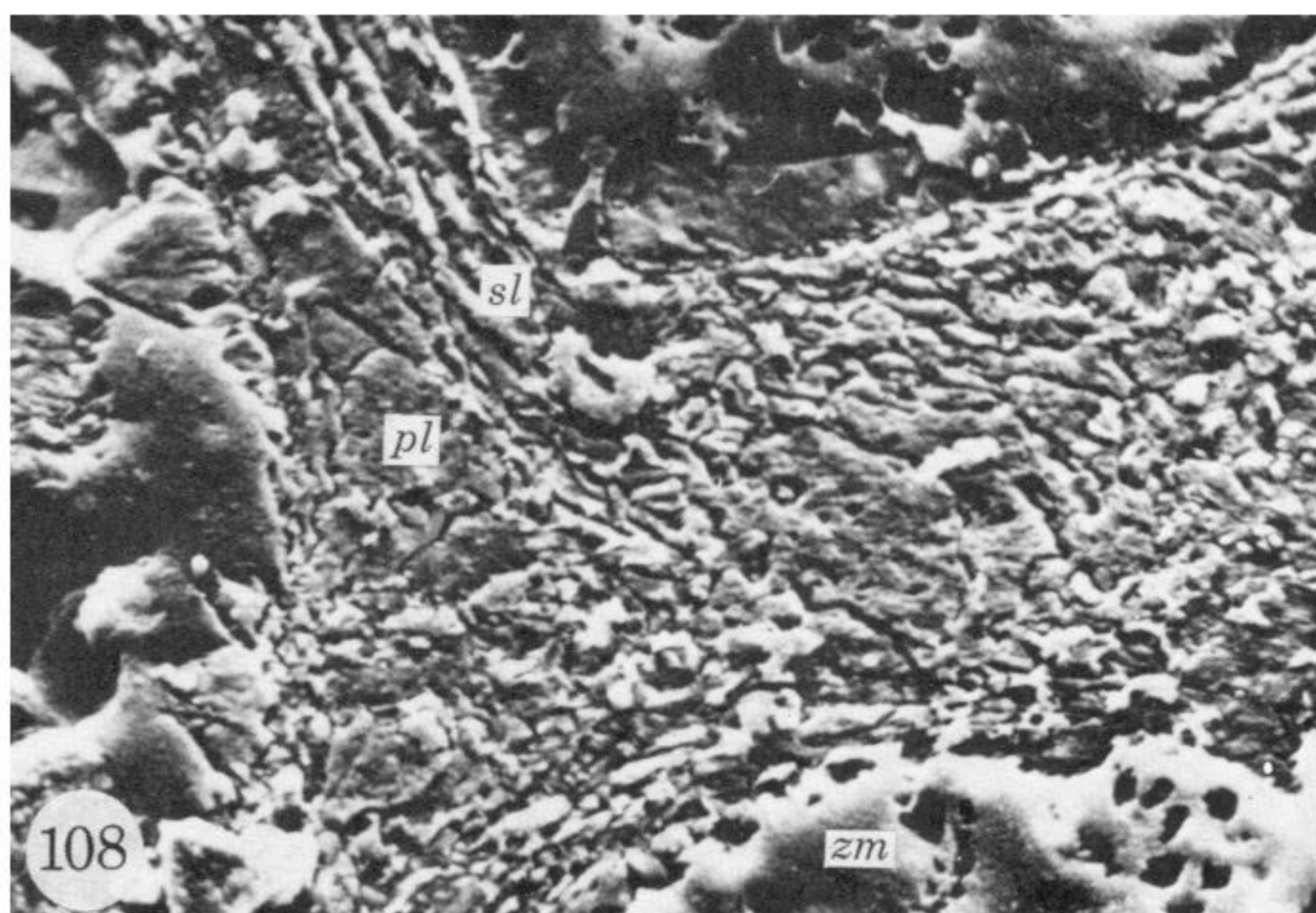
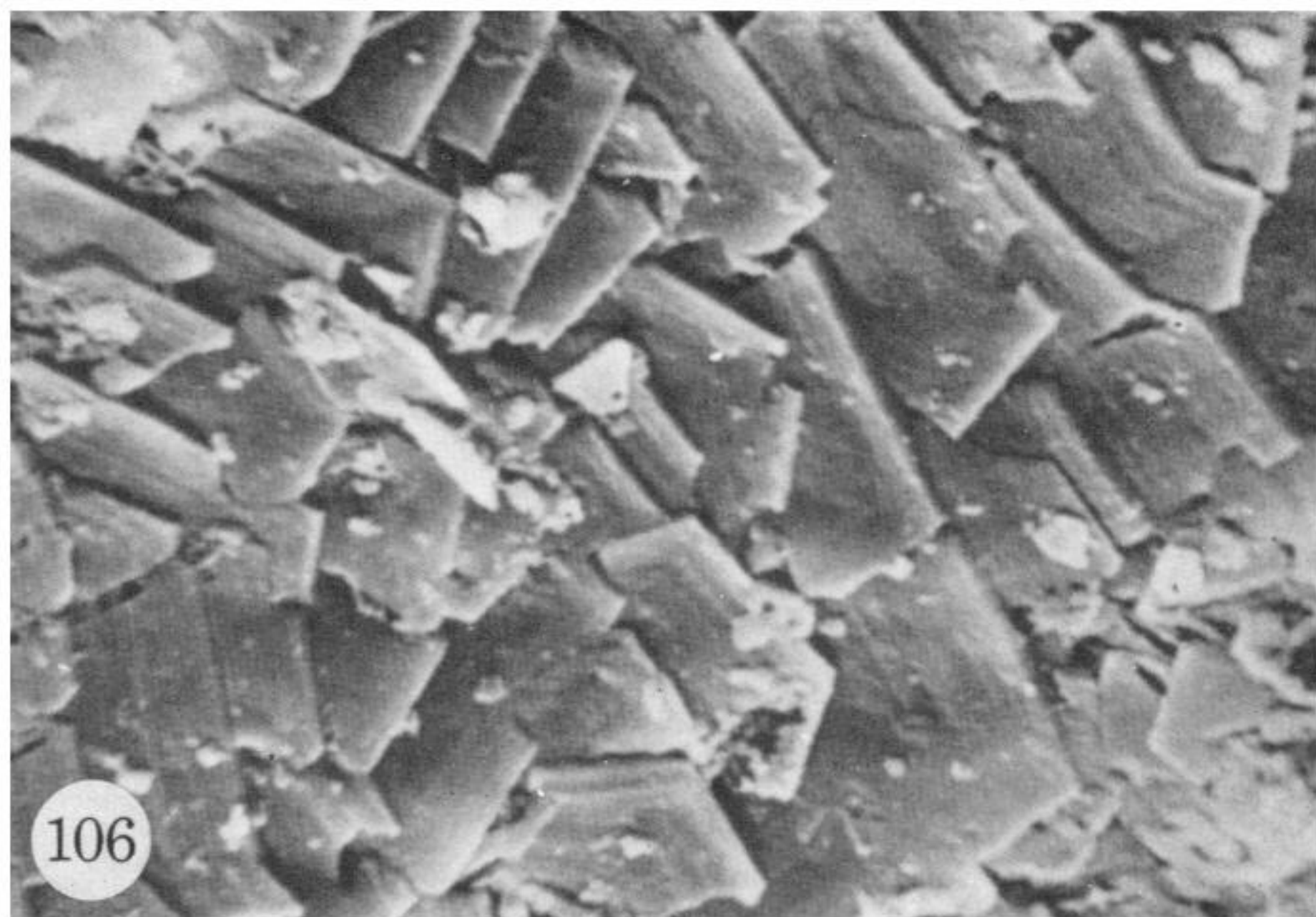
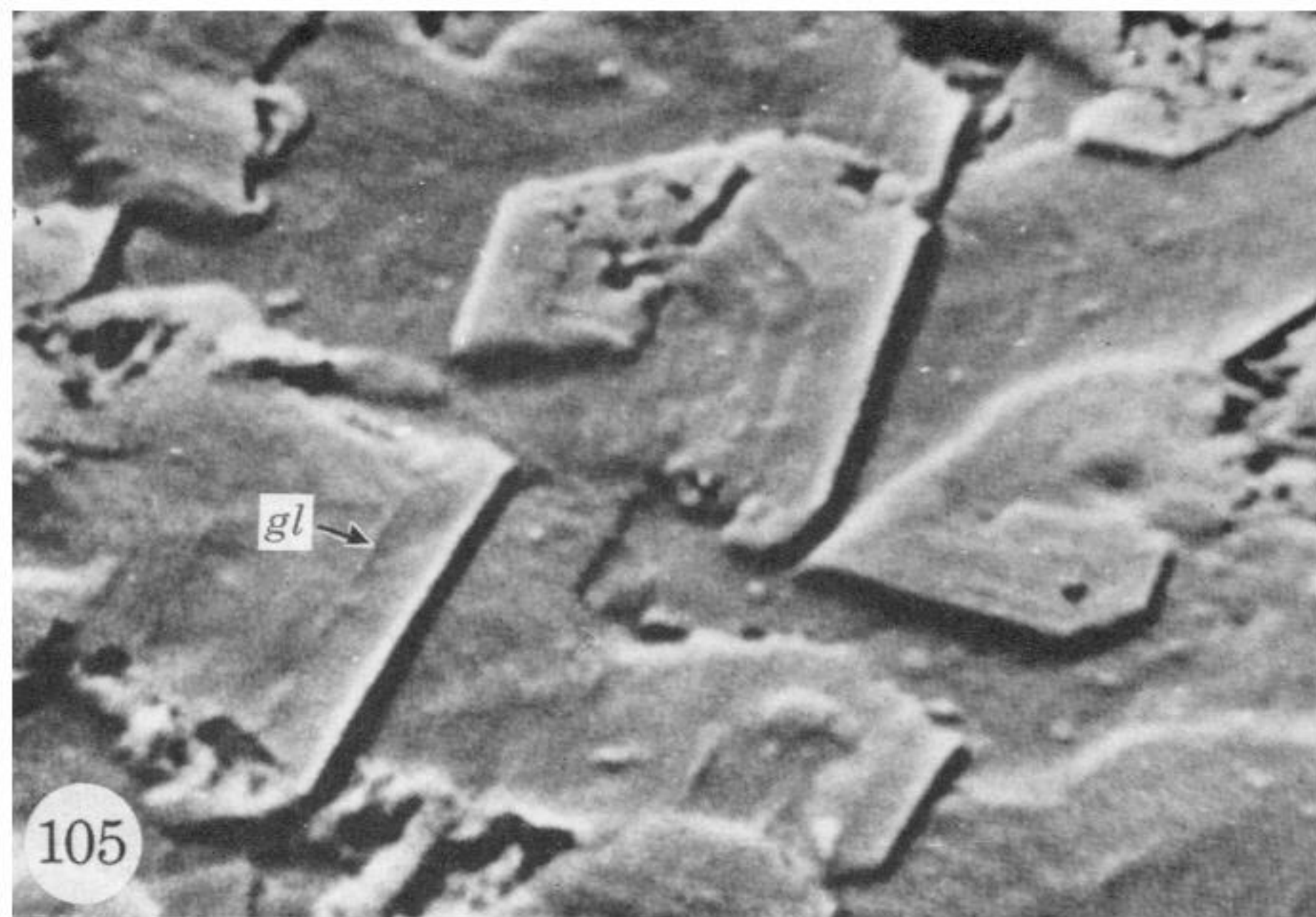
FIGURES 88 TO 95. For legends see facing page.





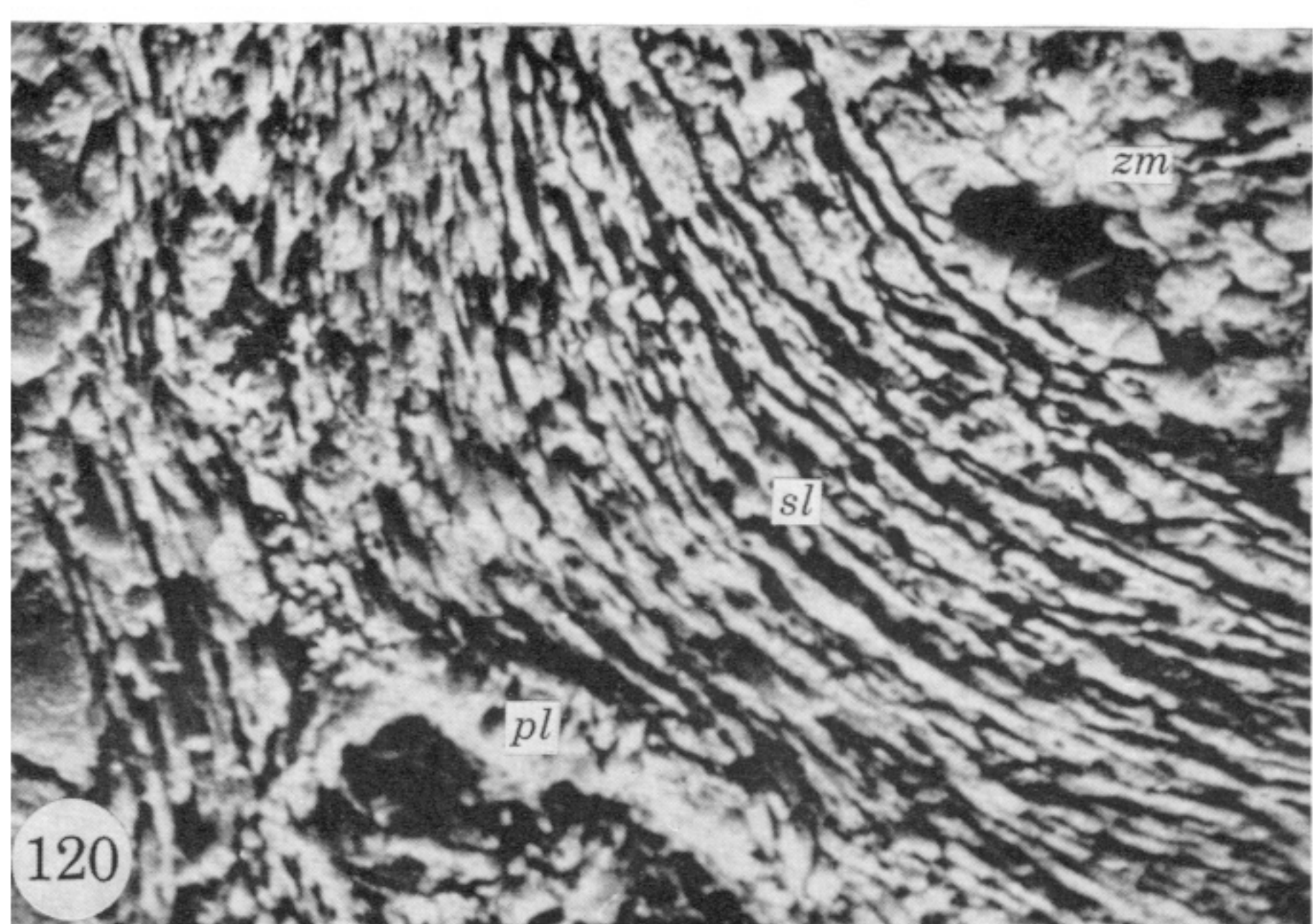
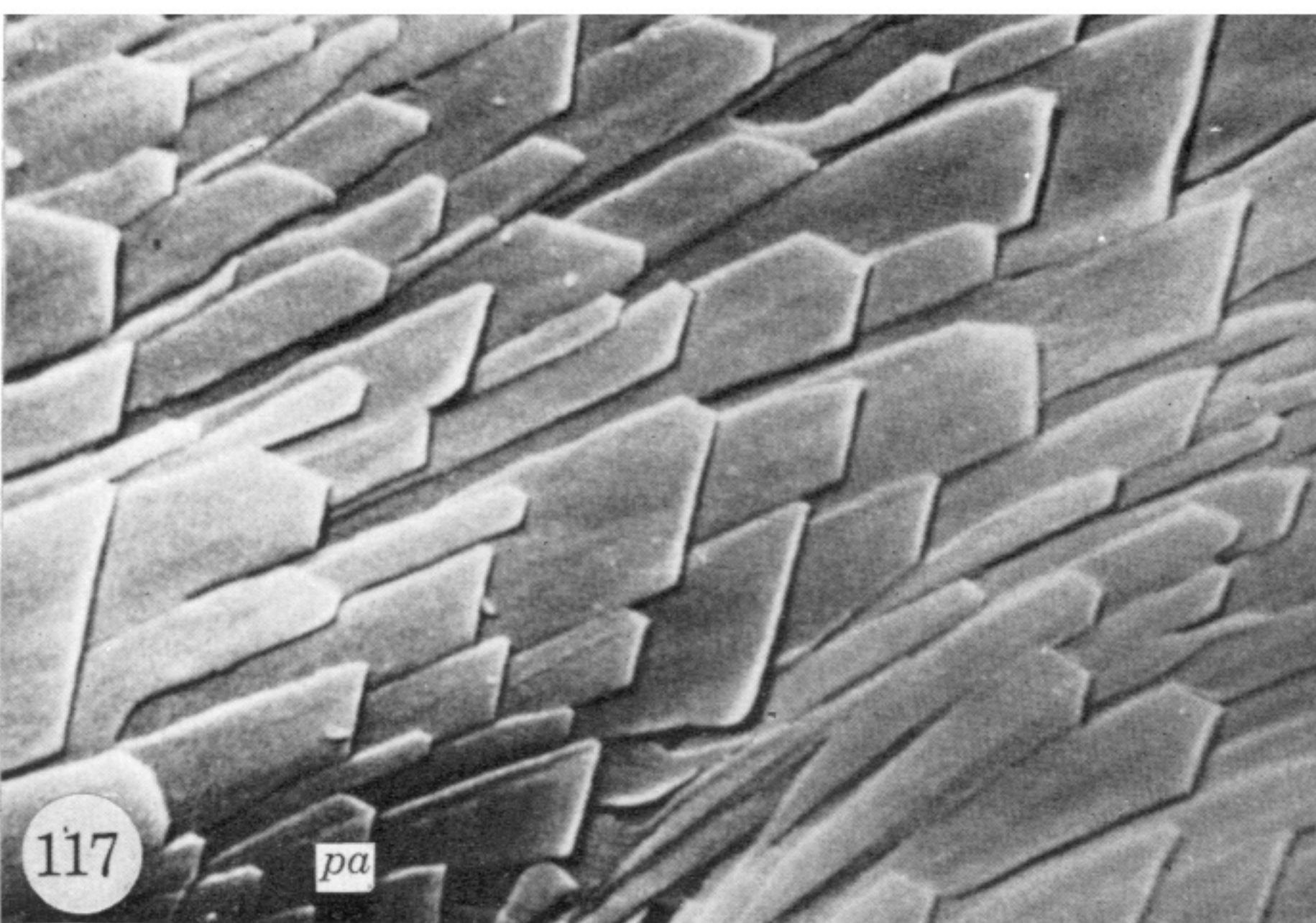
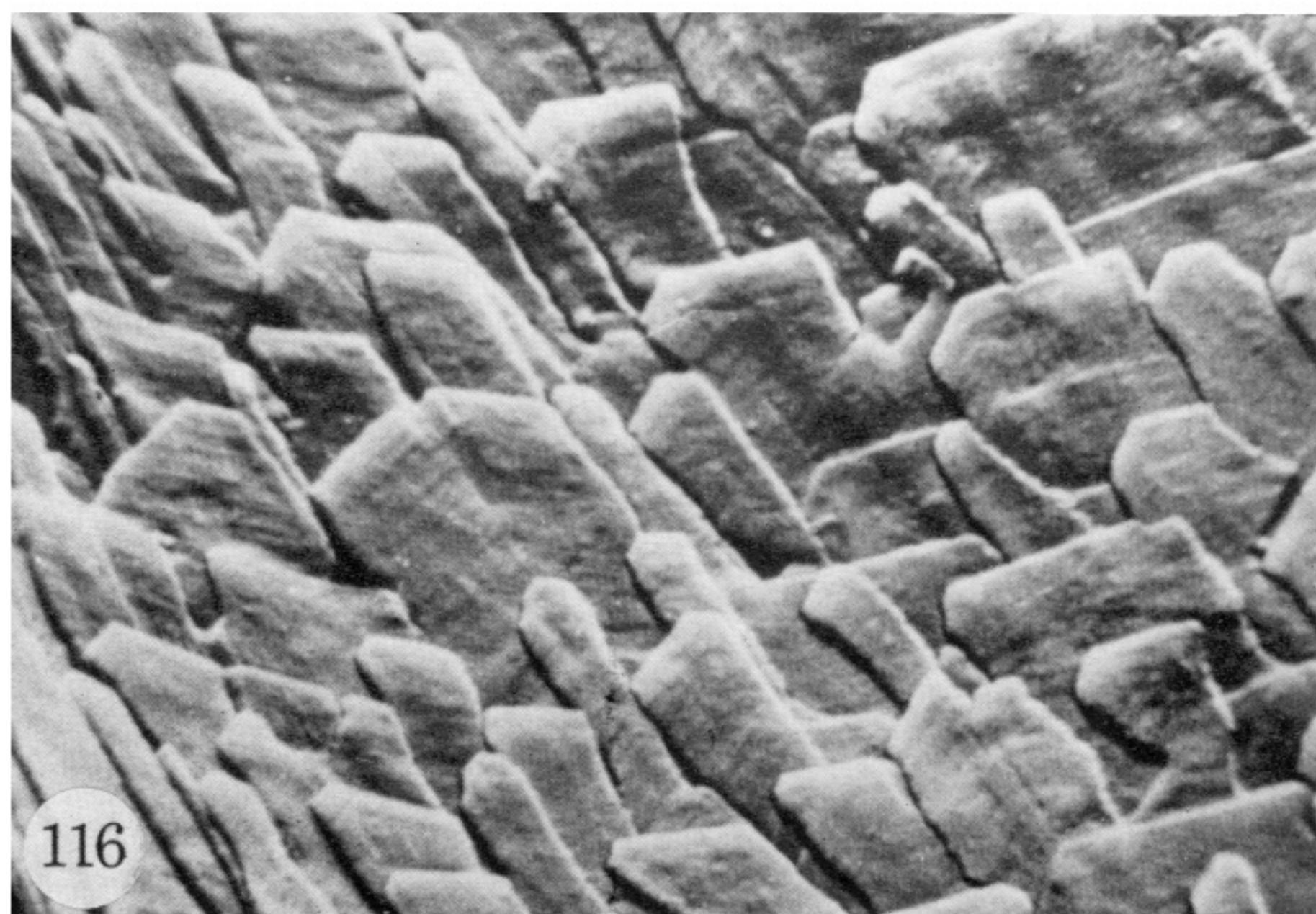
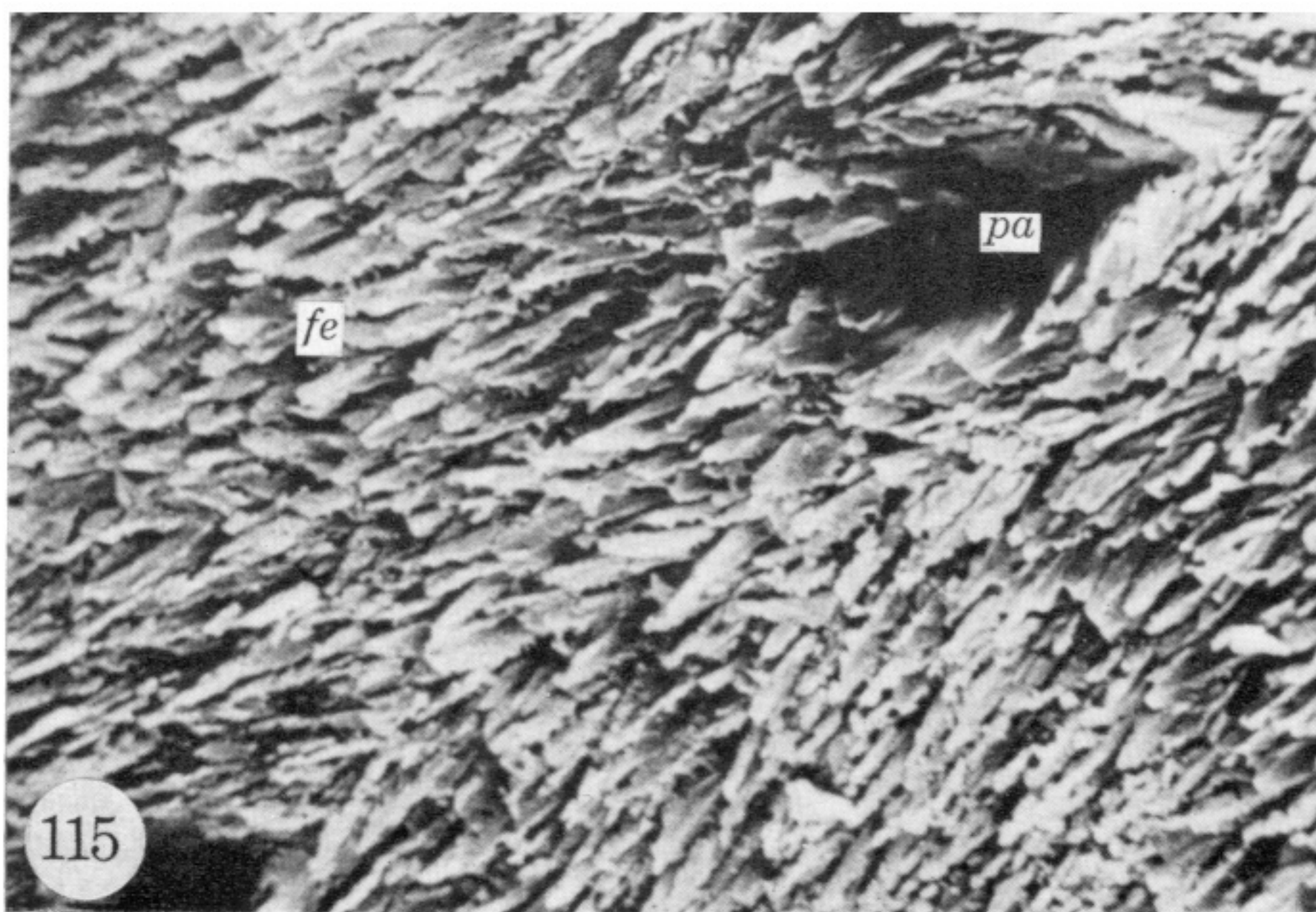
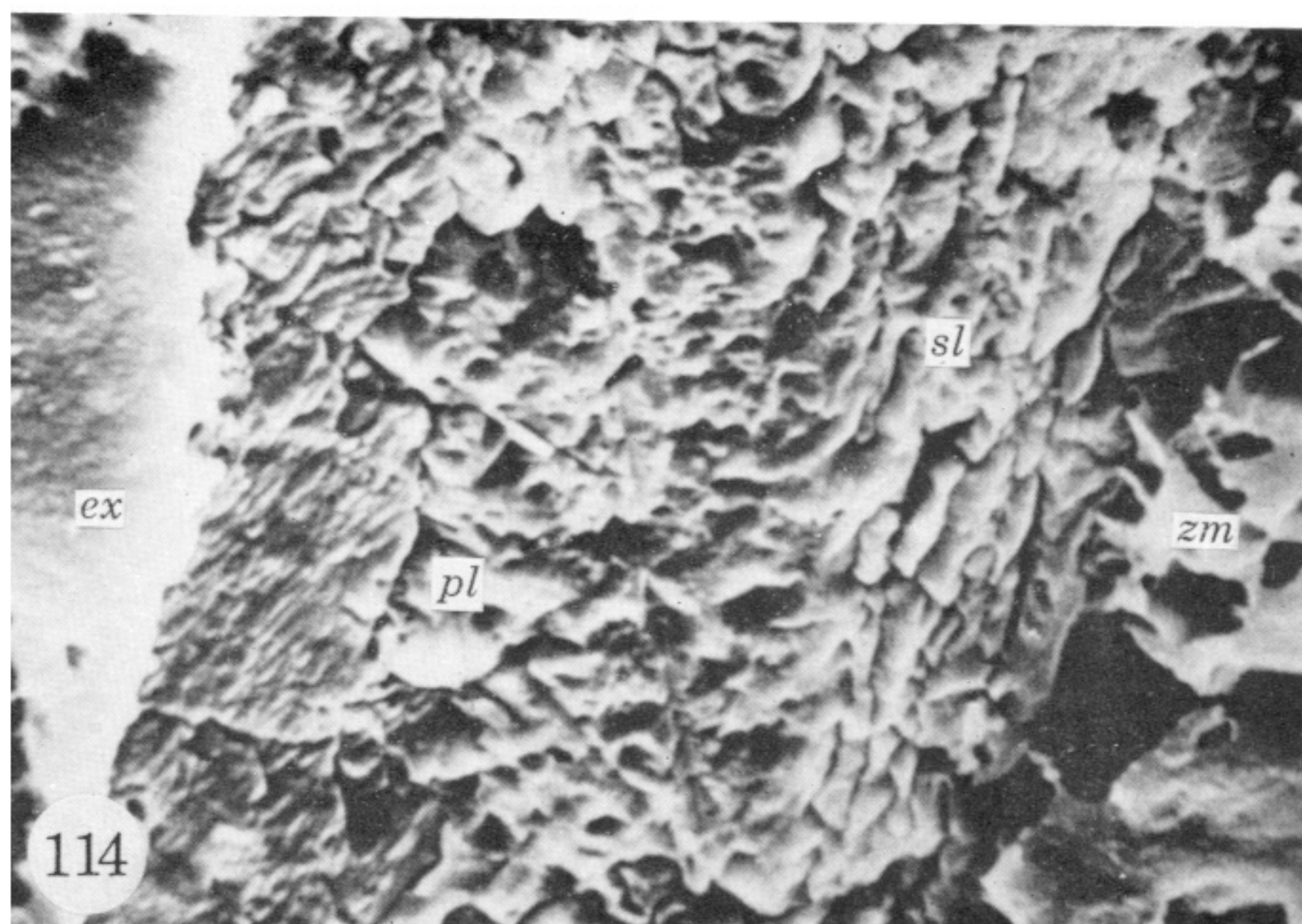
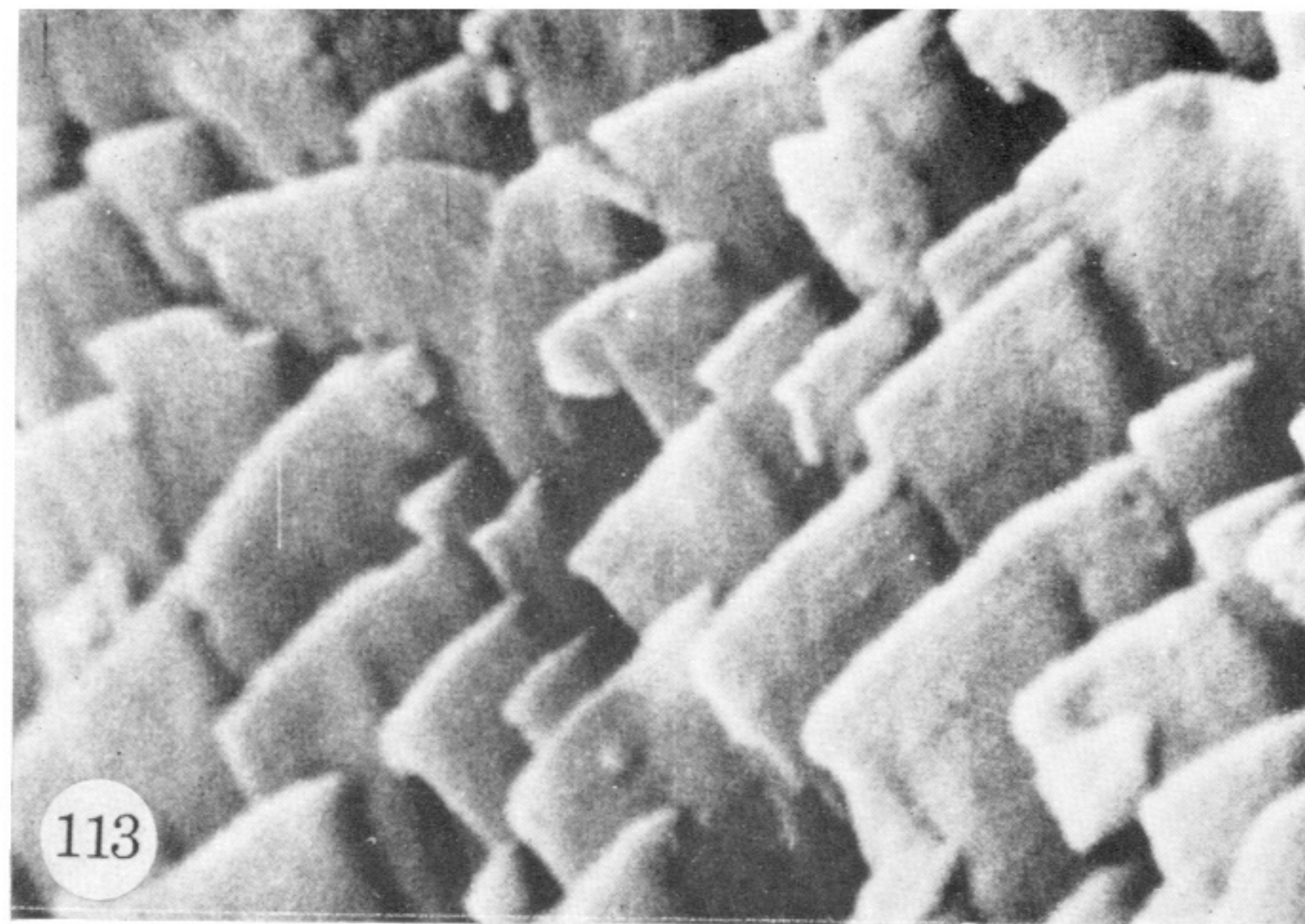
FIGURES 97 TO 103. For legends see facing page.





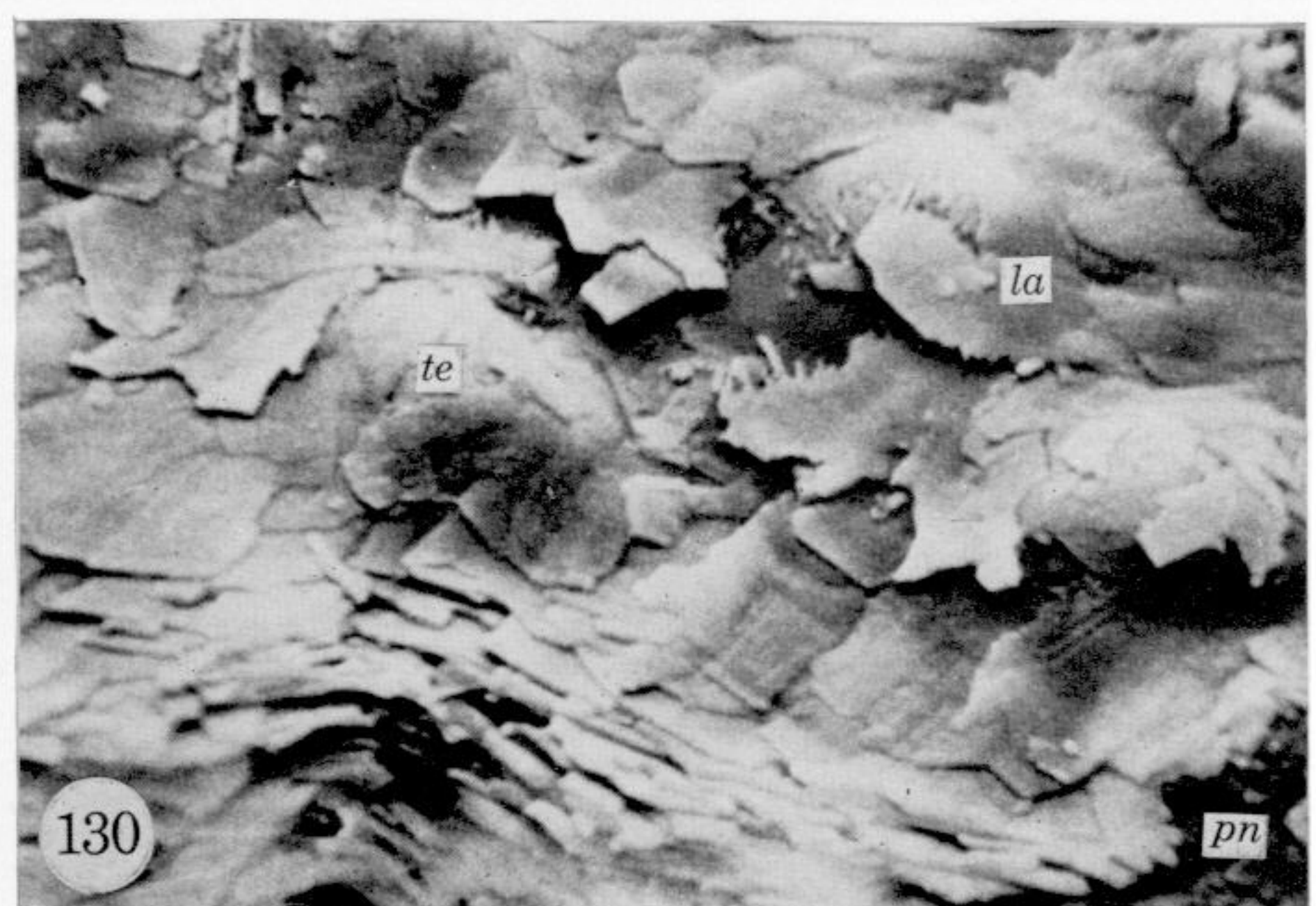
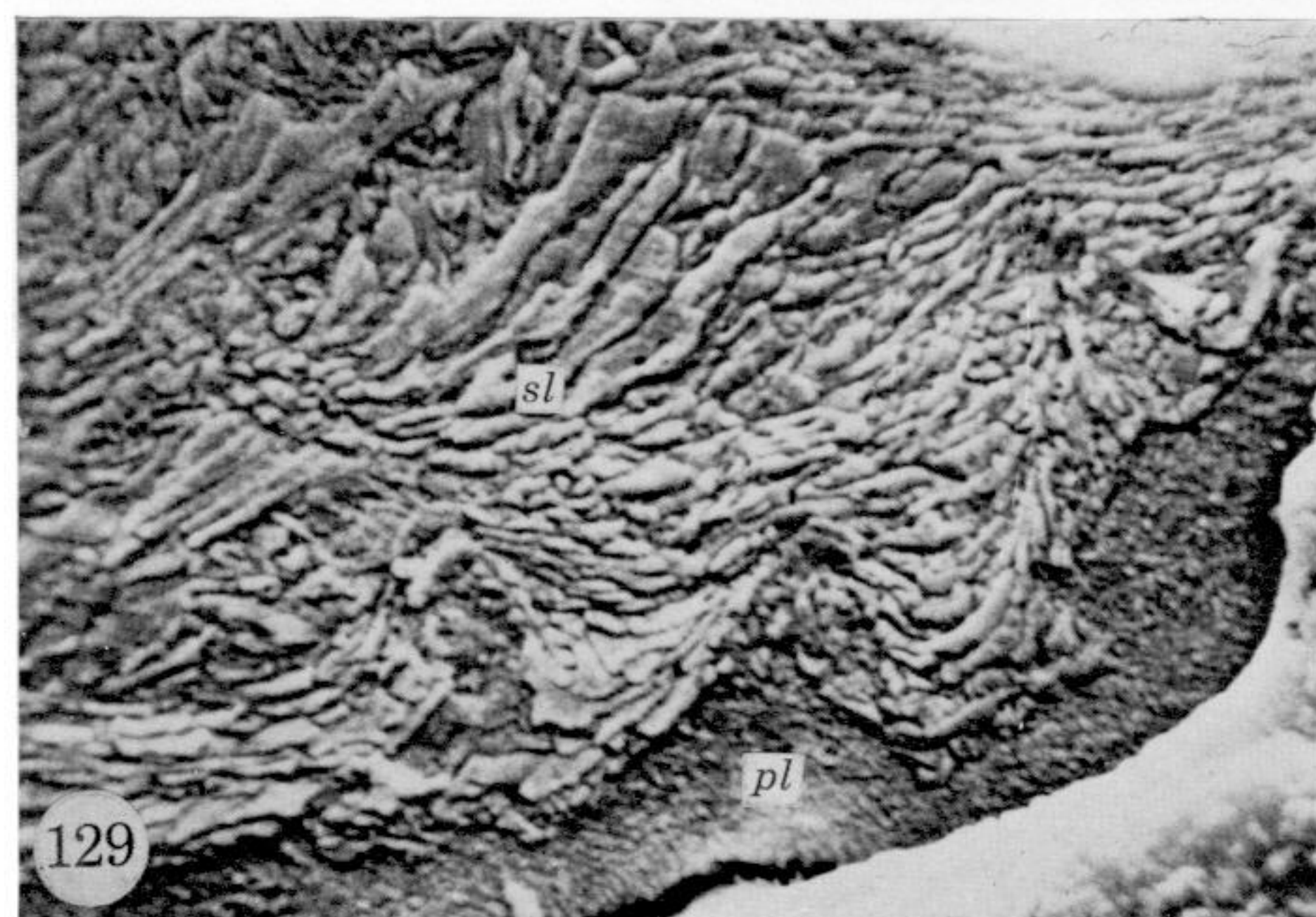
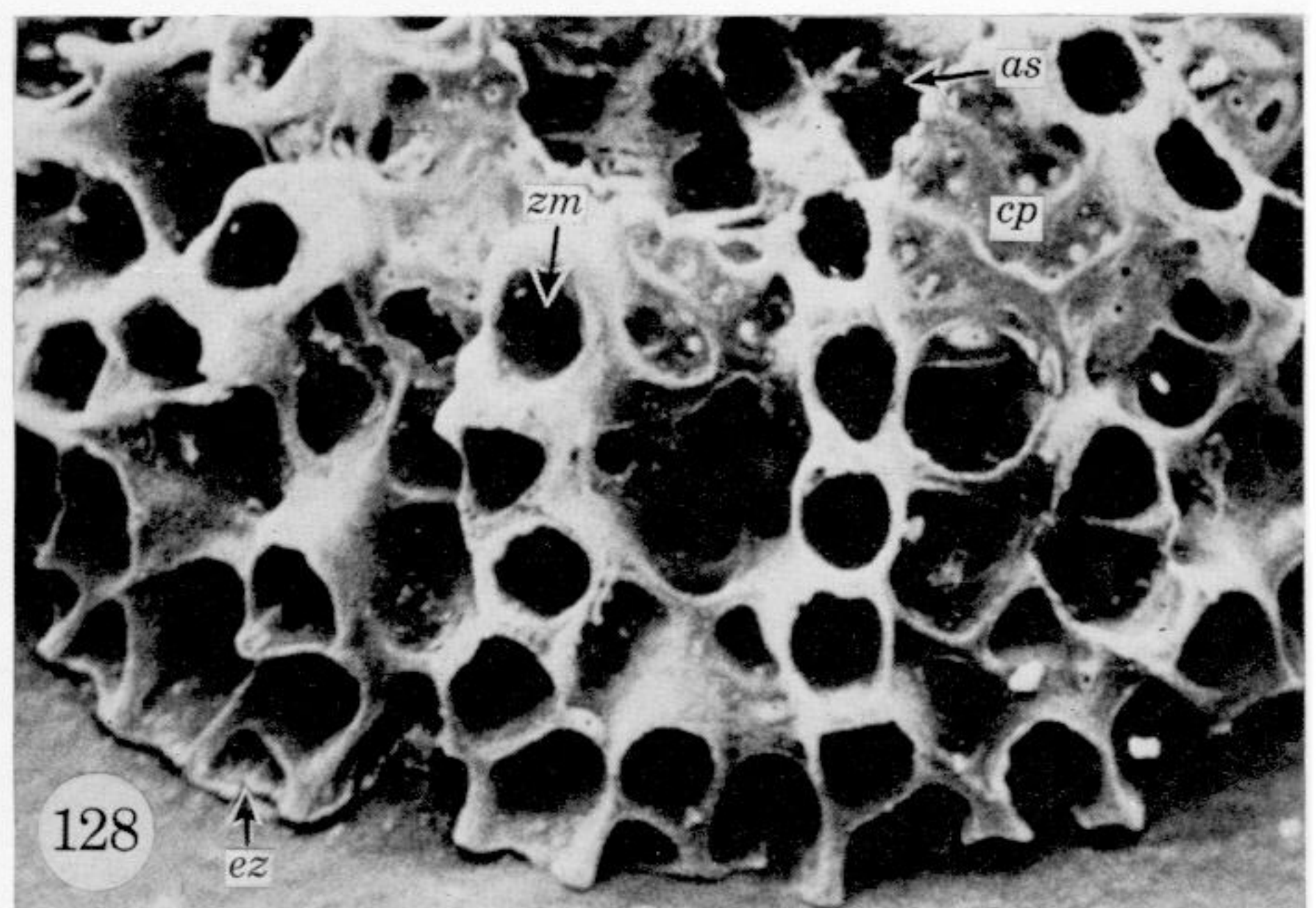
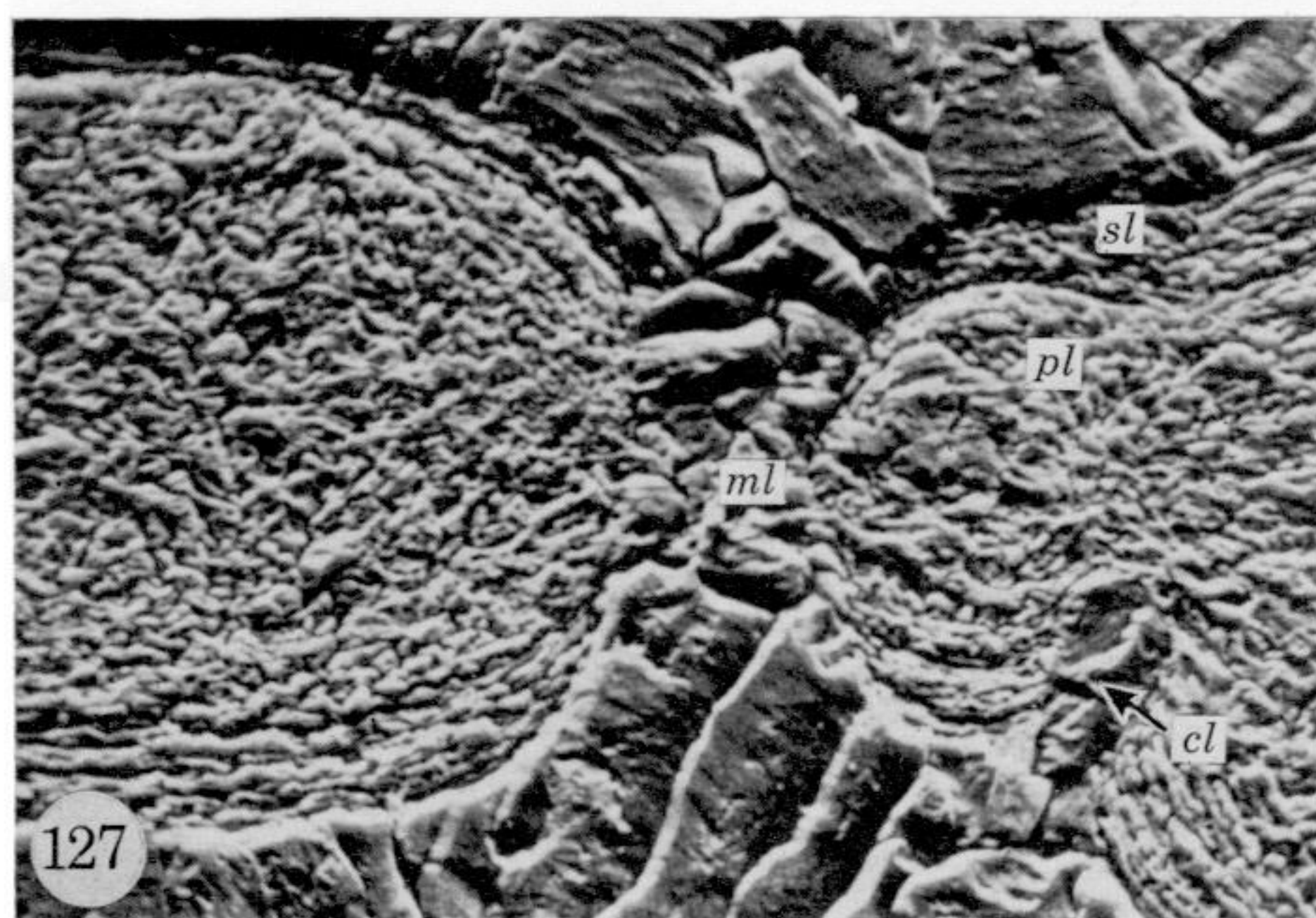
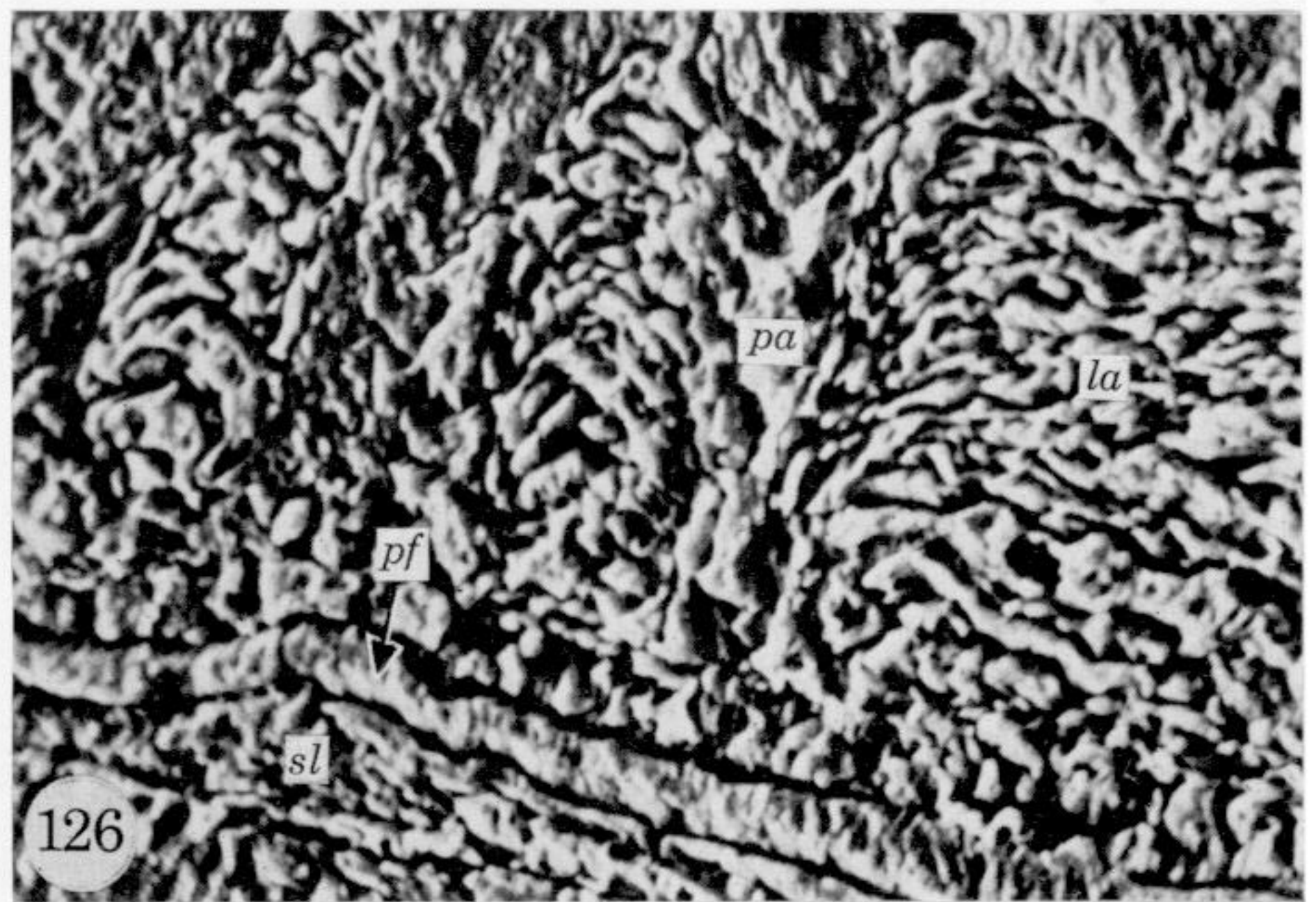
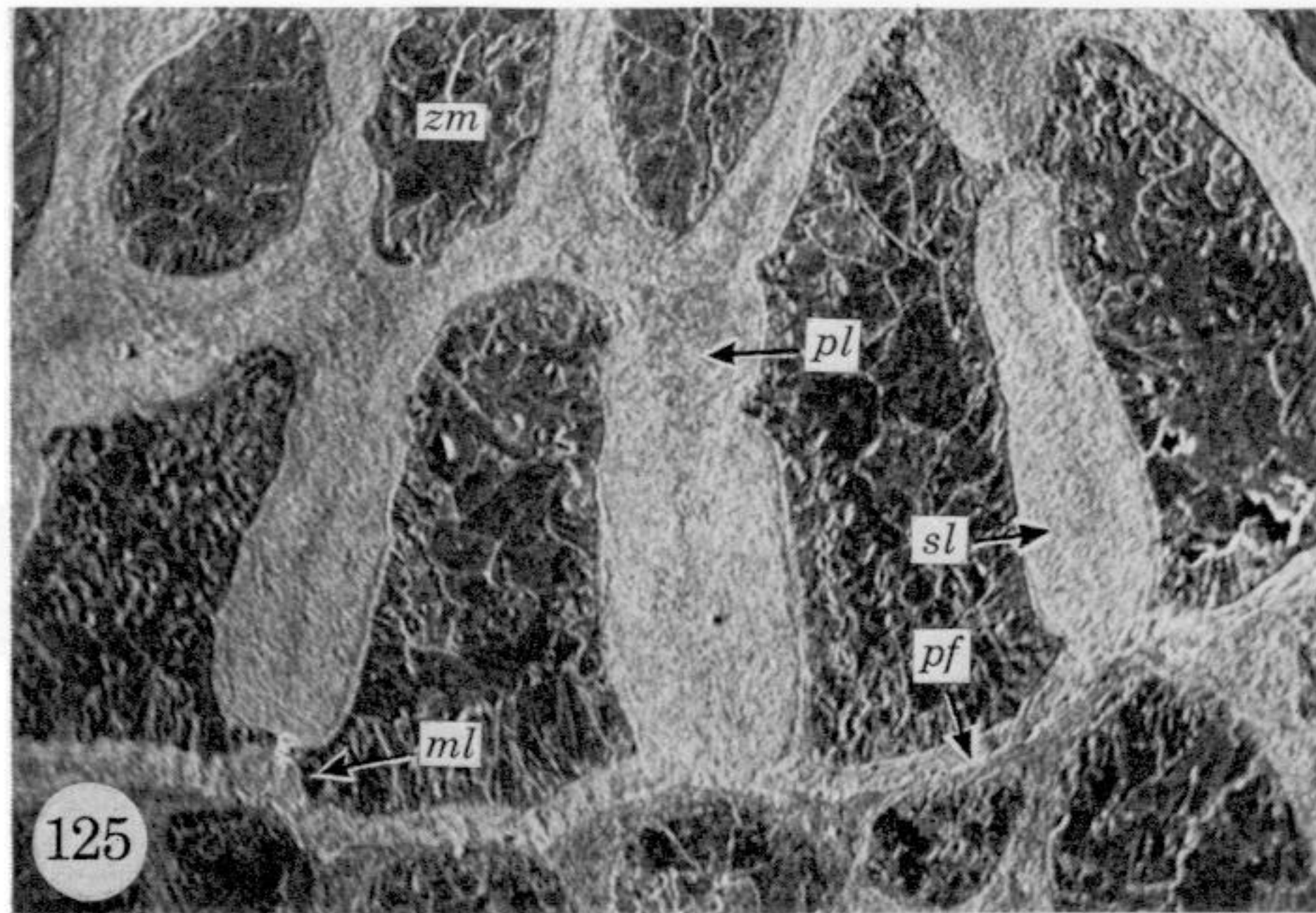
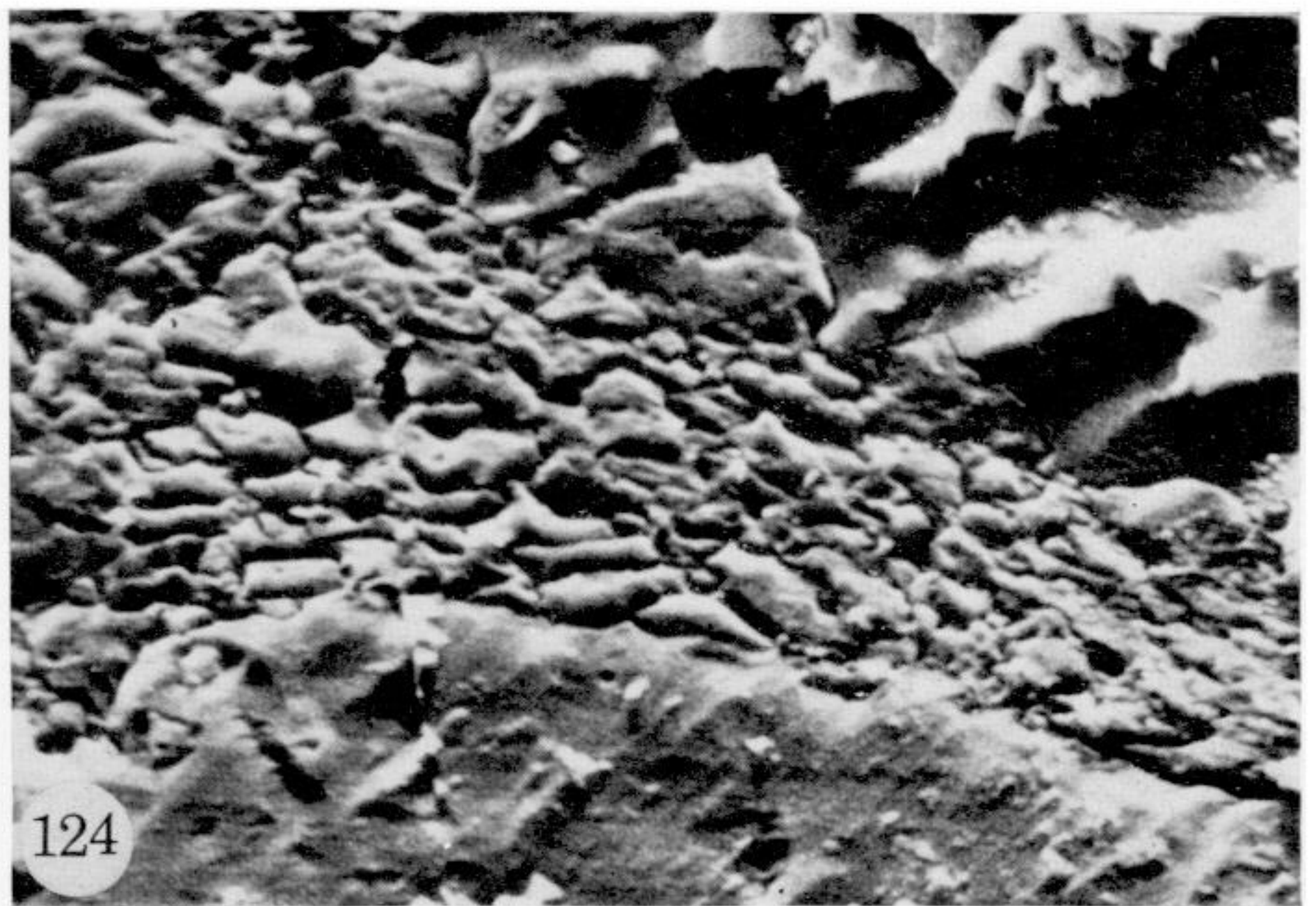
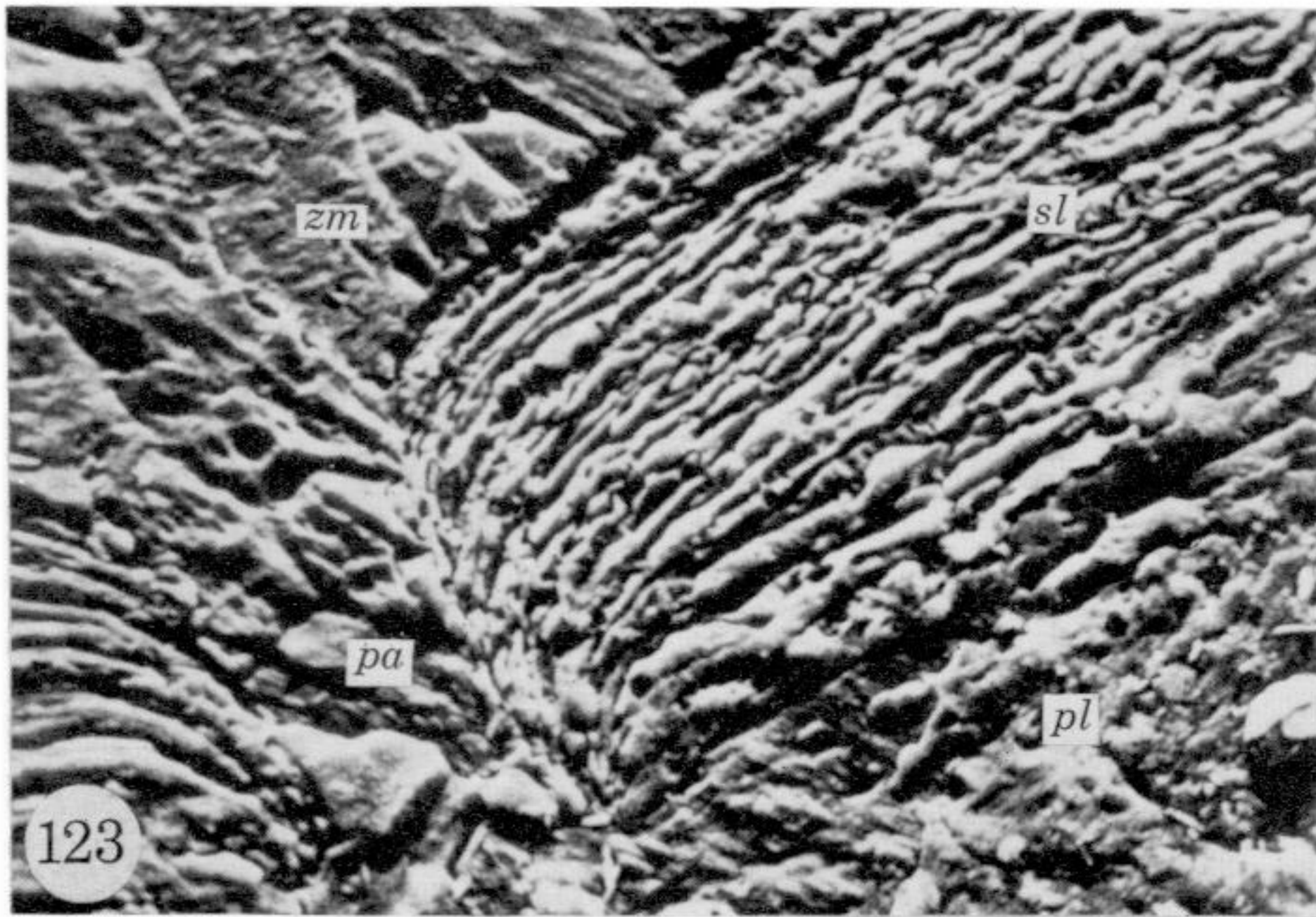
FIGURES 105 TO 112. For legends see facing page.





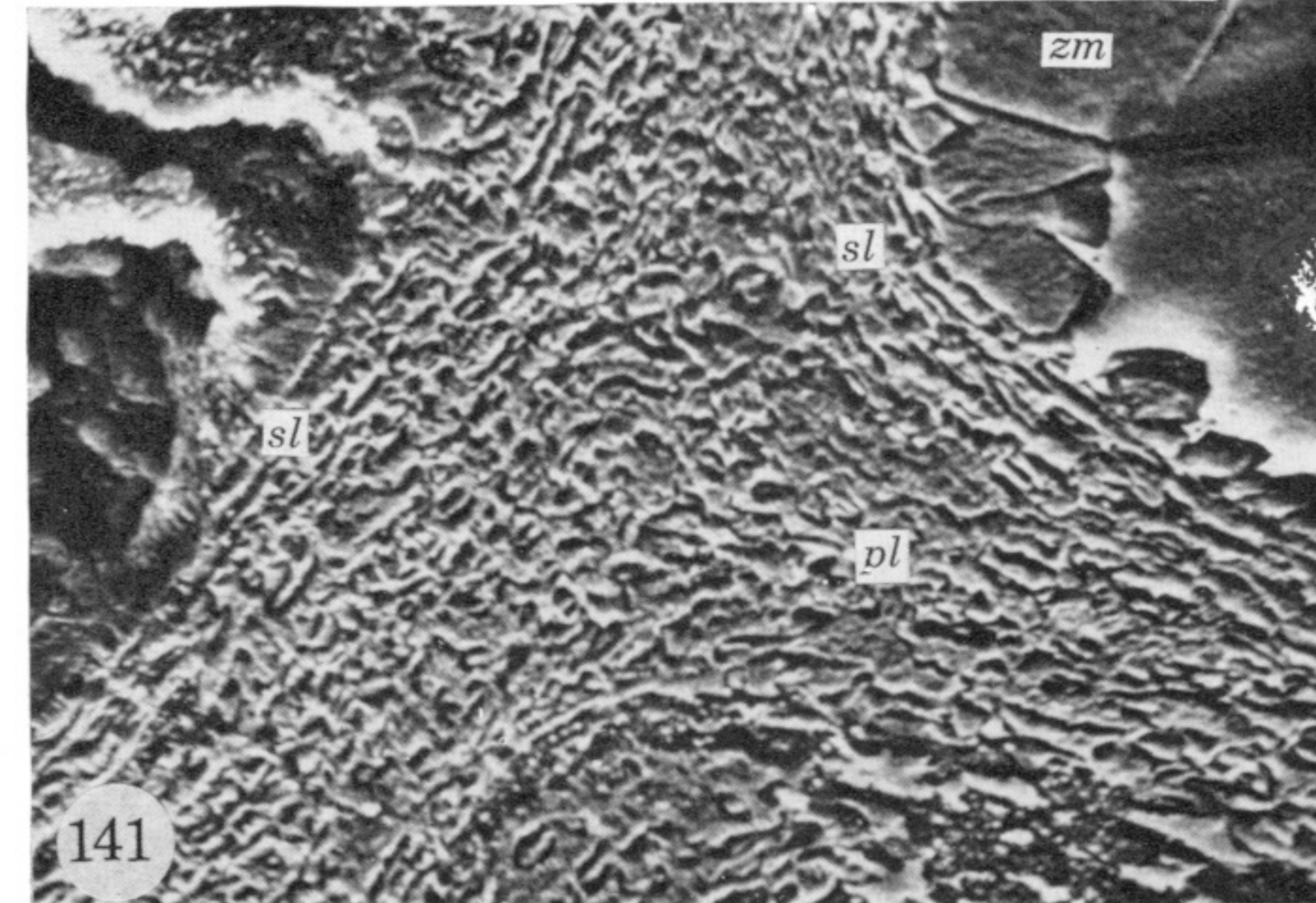
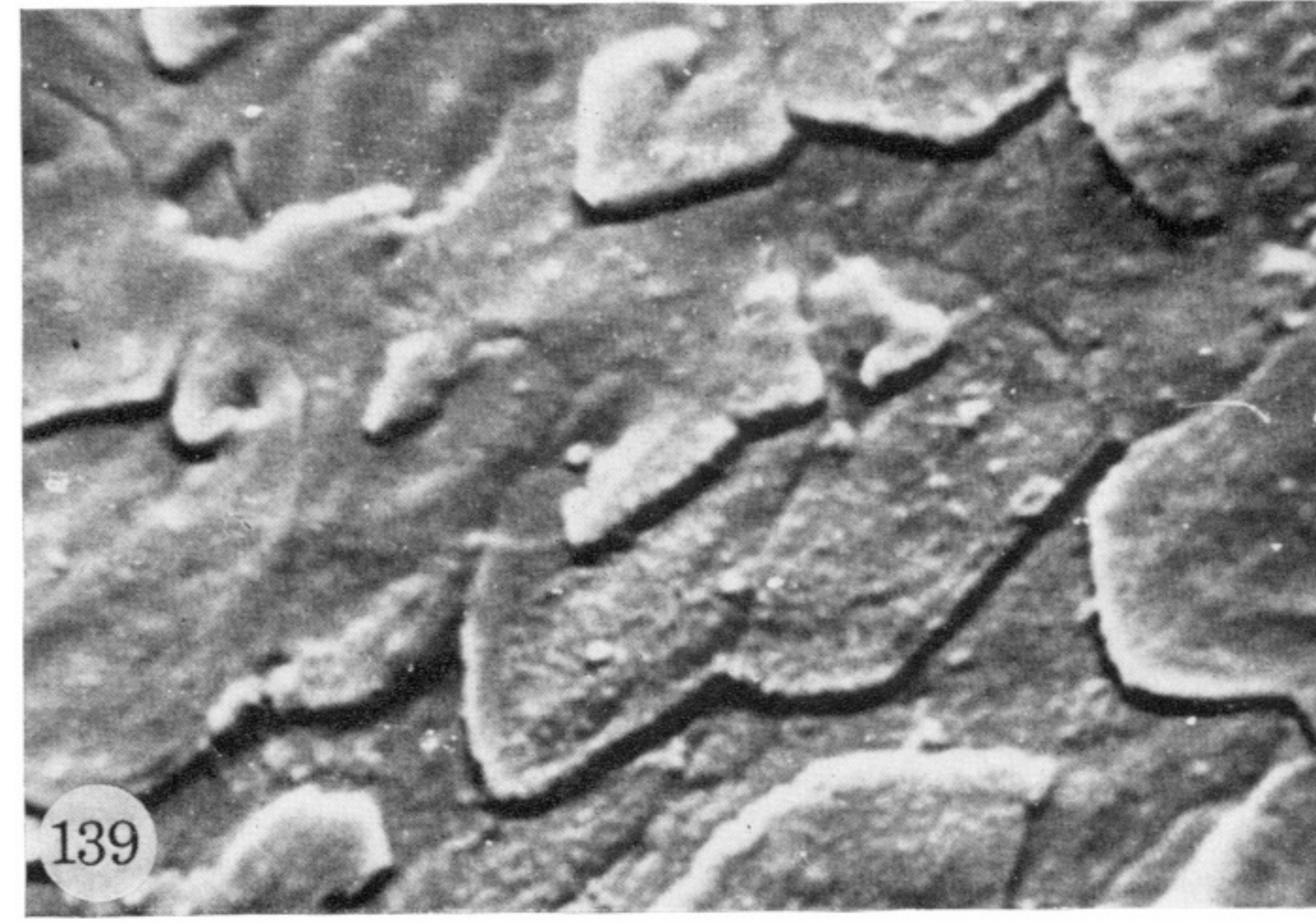
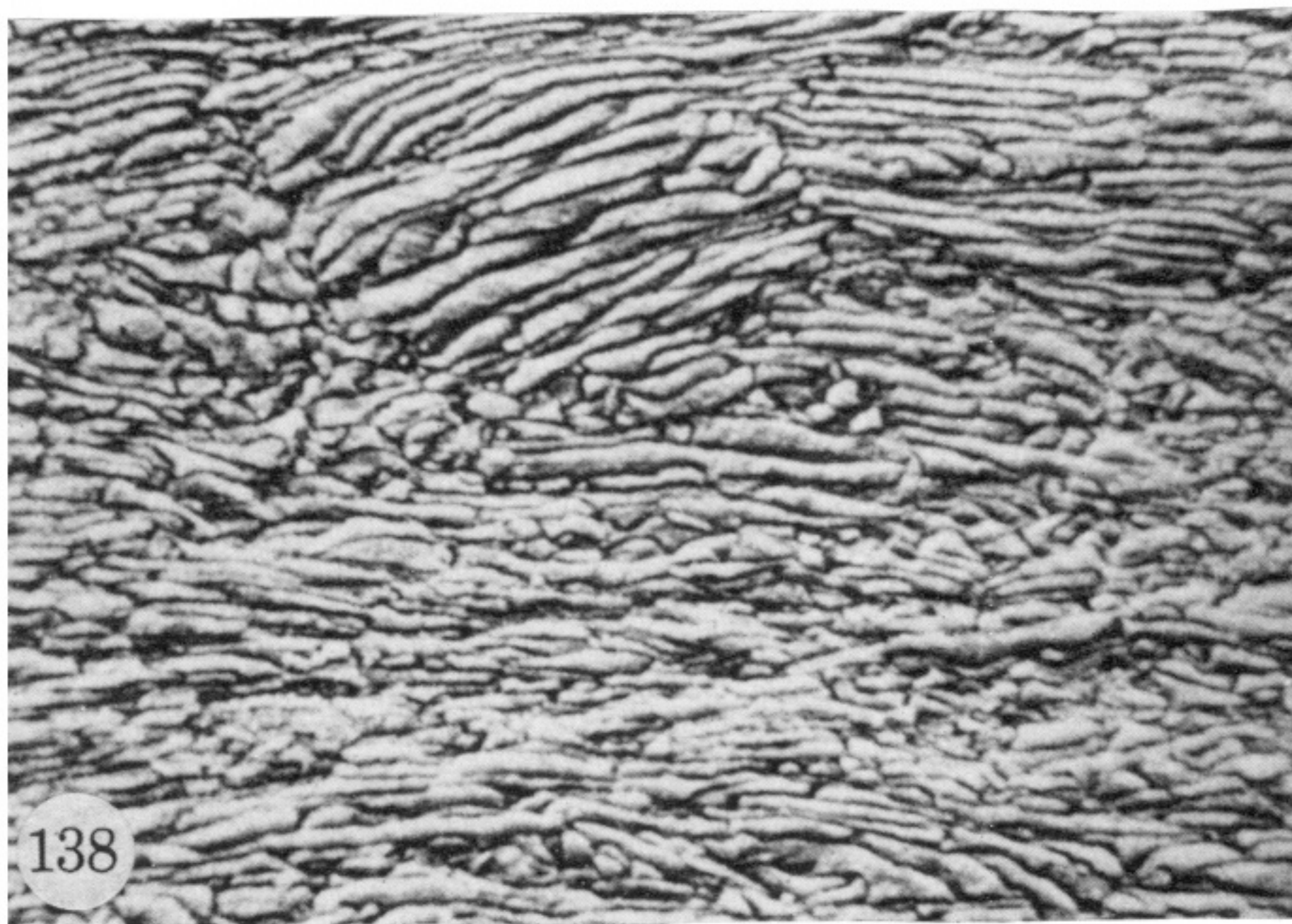
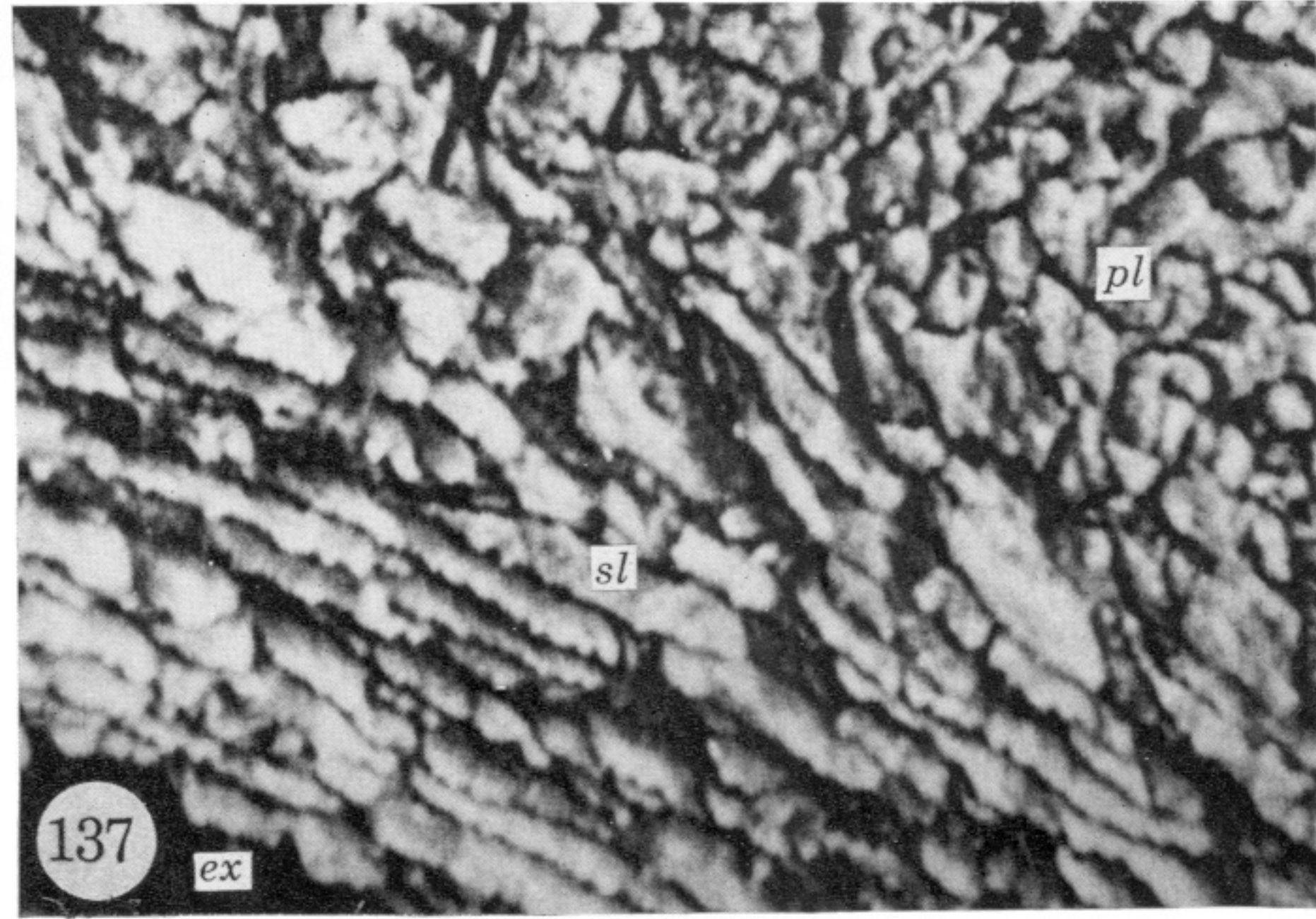
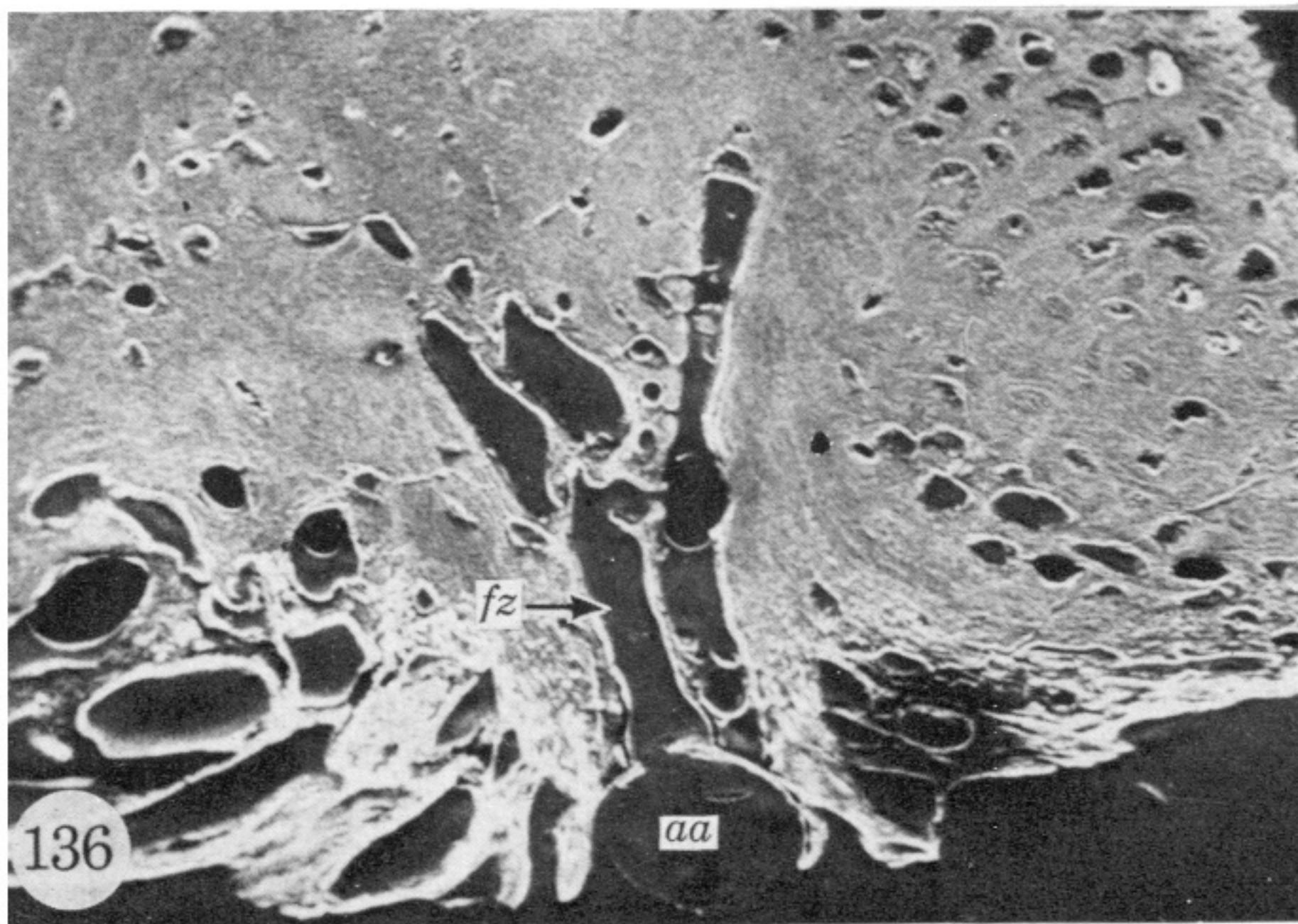
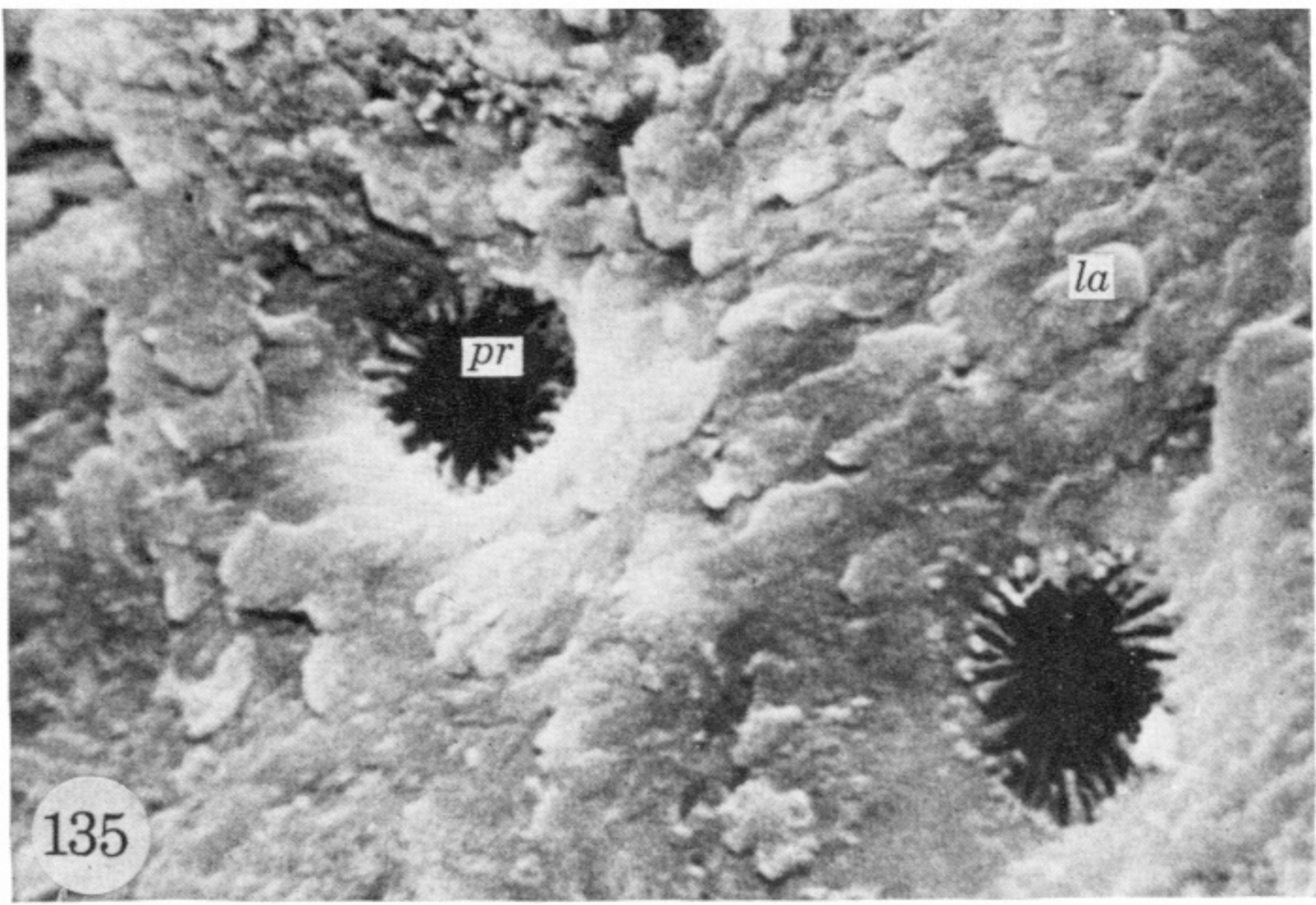
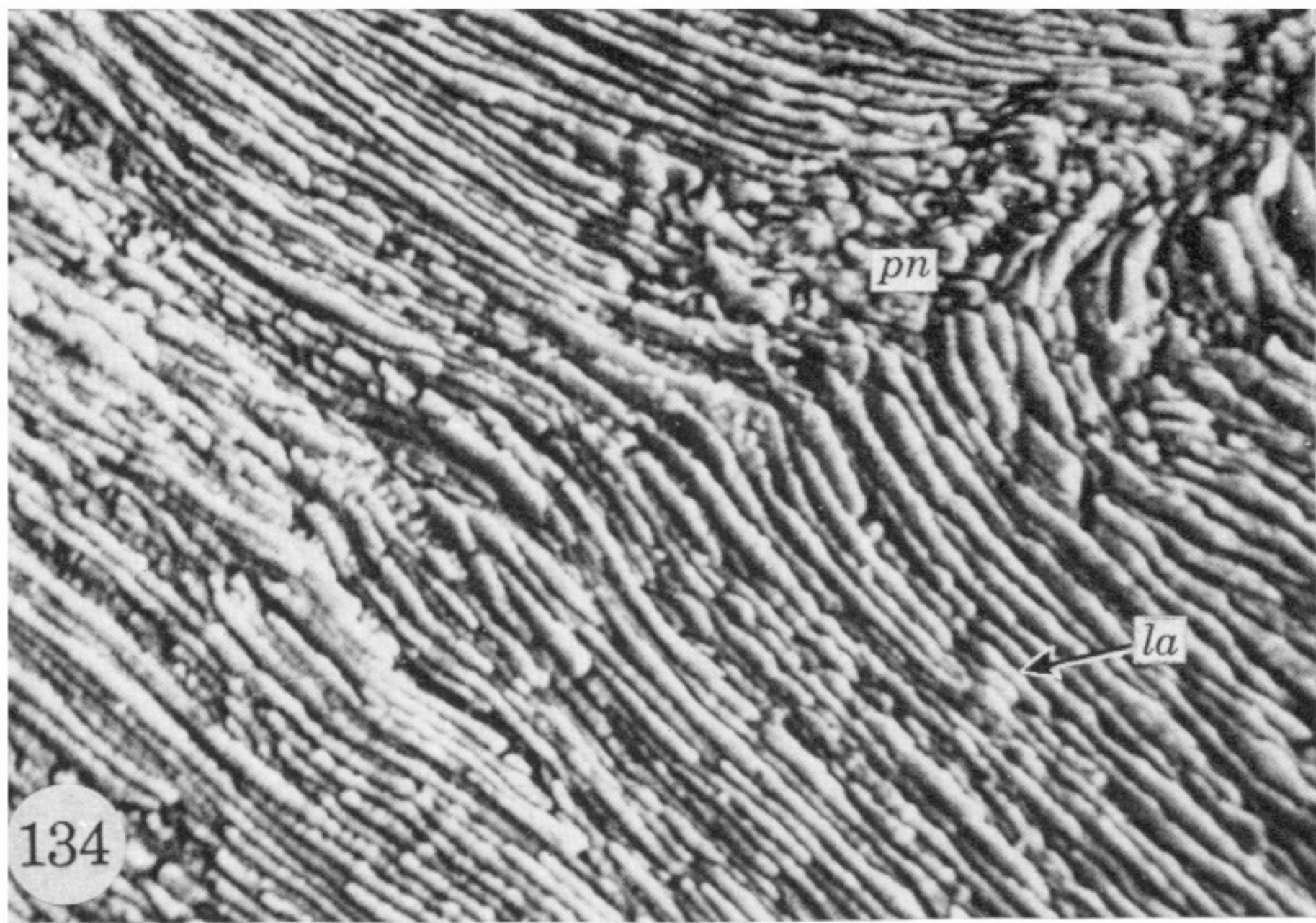
FIGURES 113 TO 120. For legends see facing page.





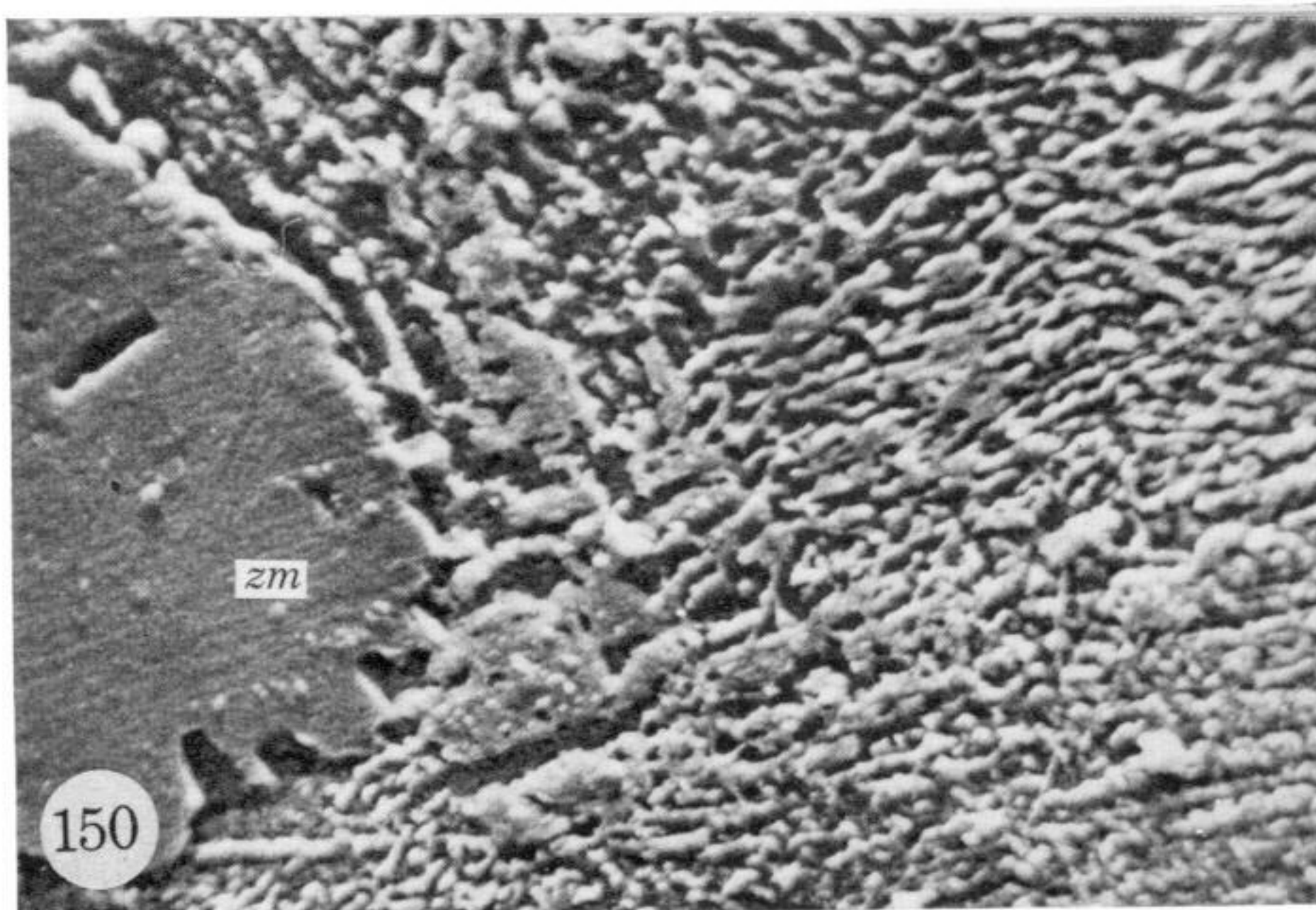
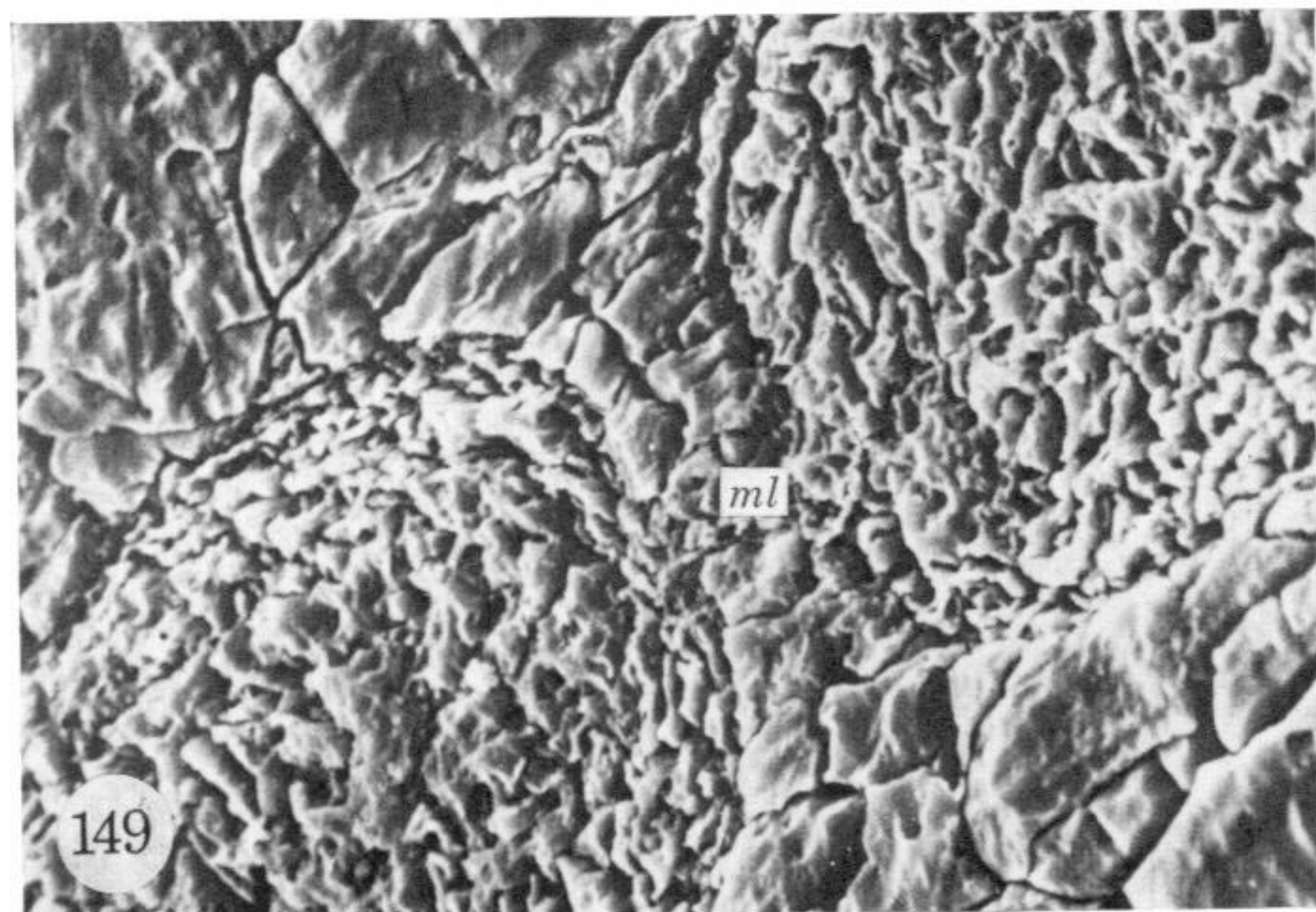
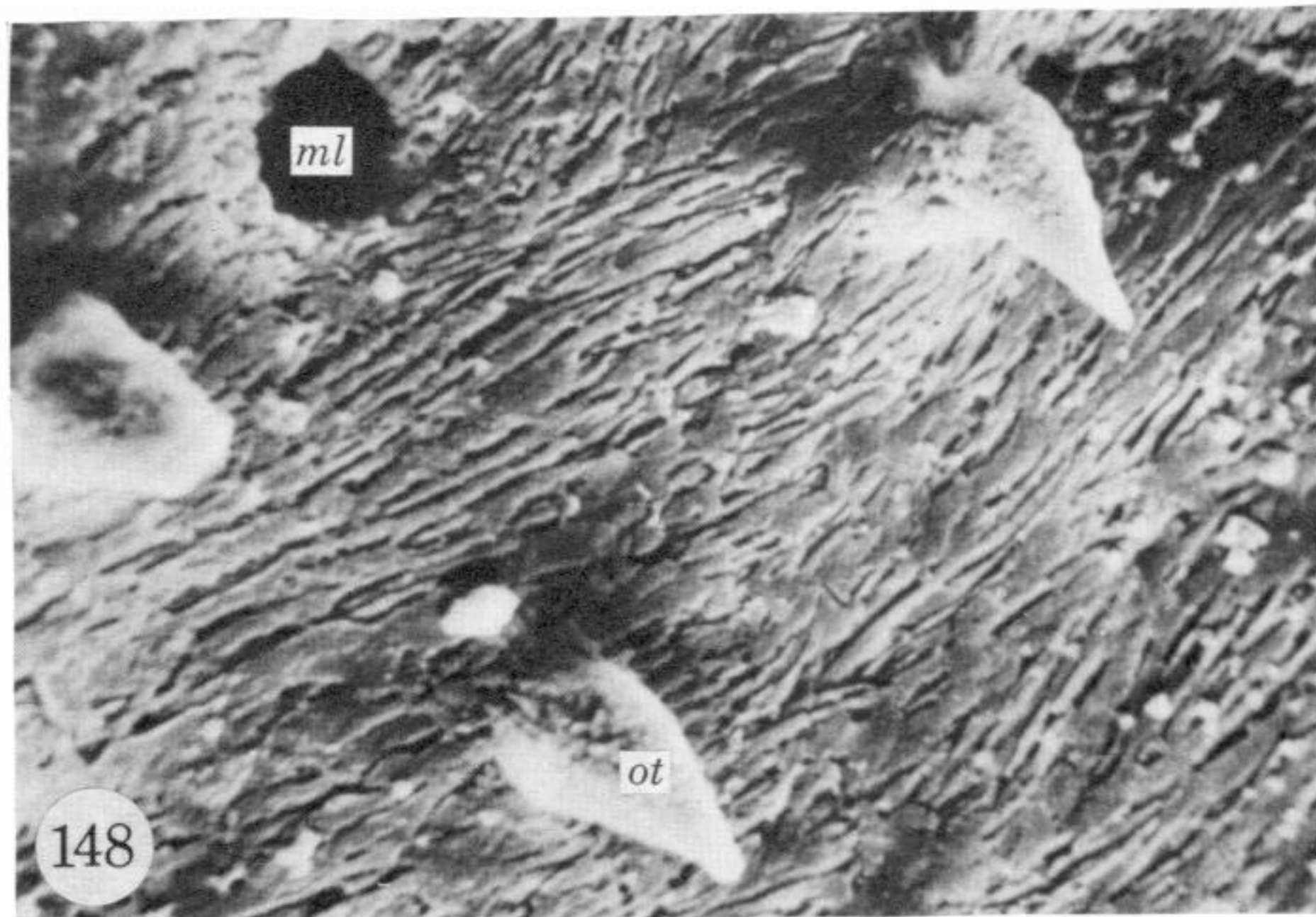
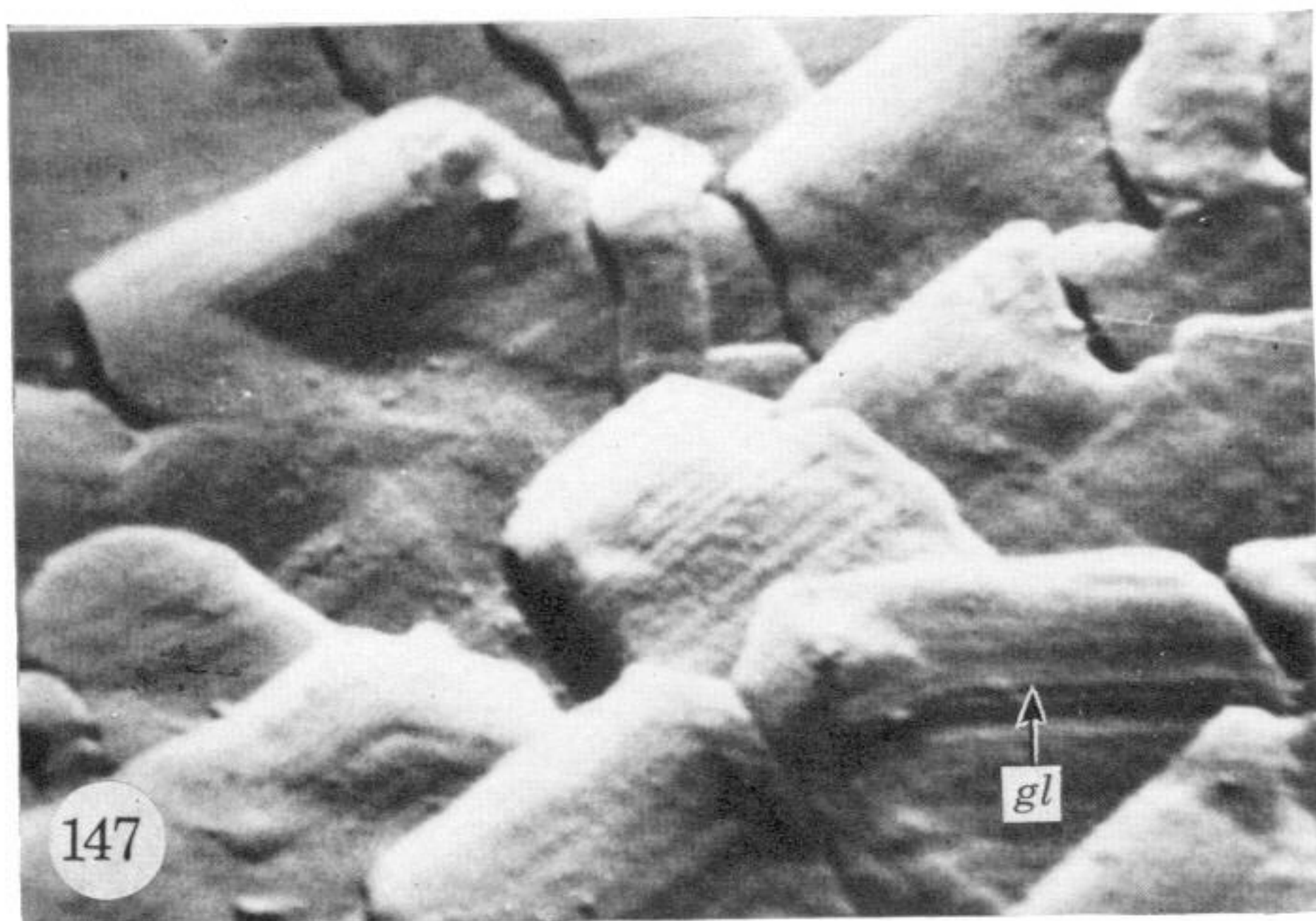
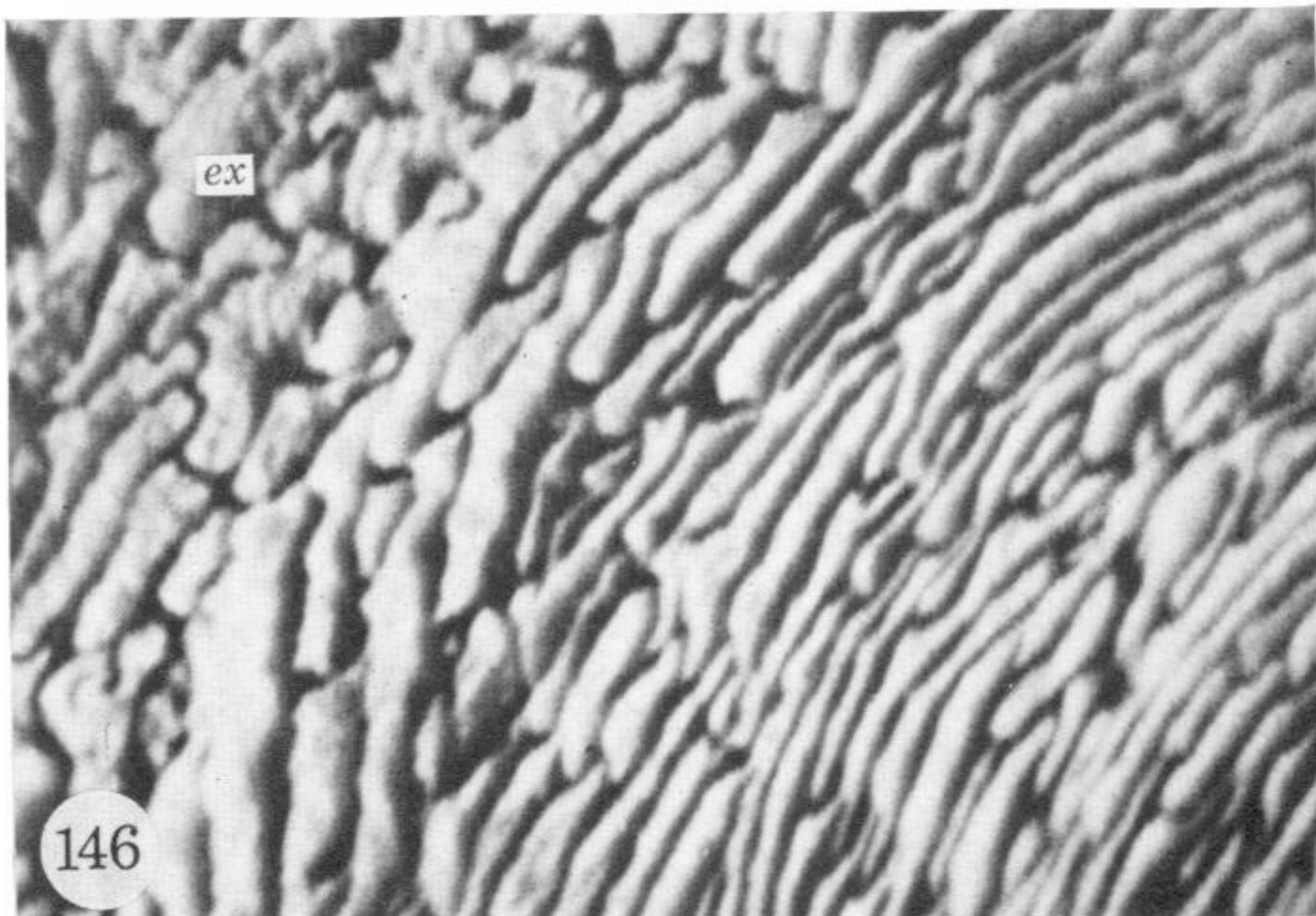
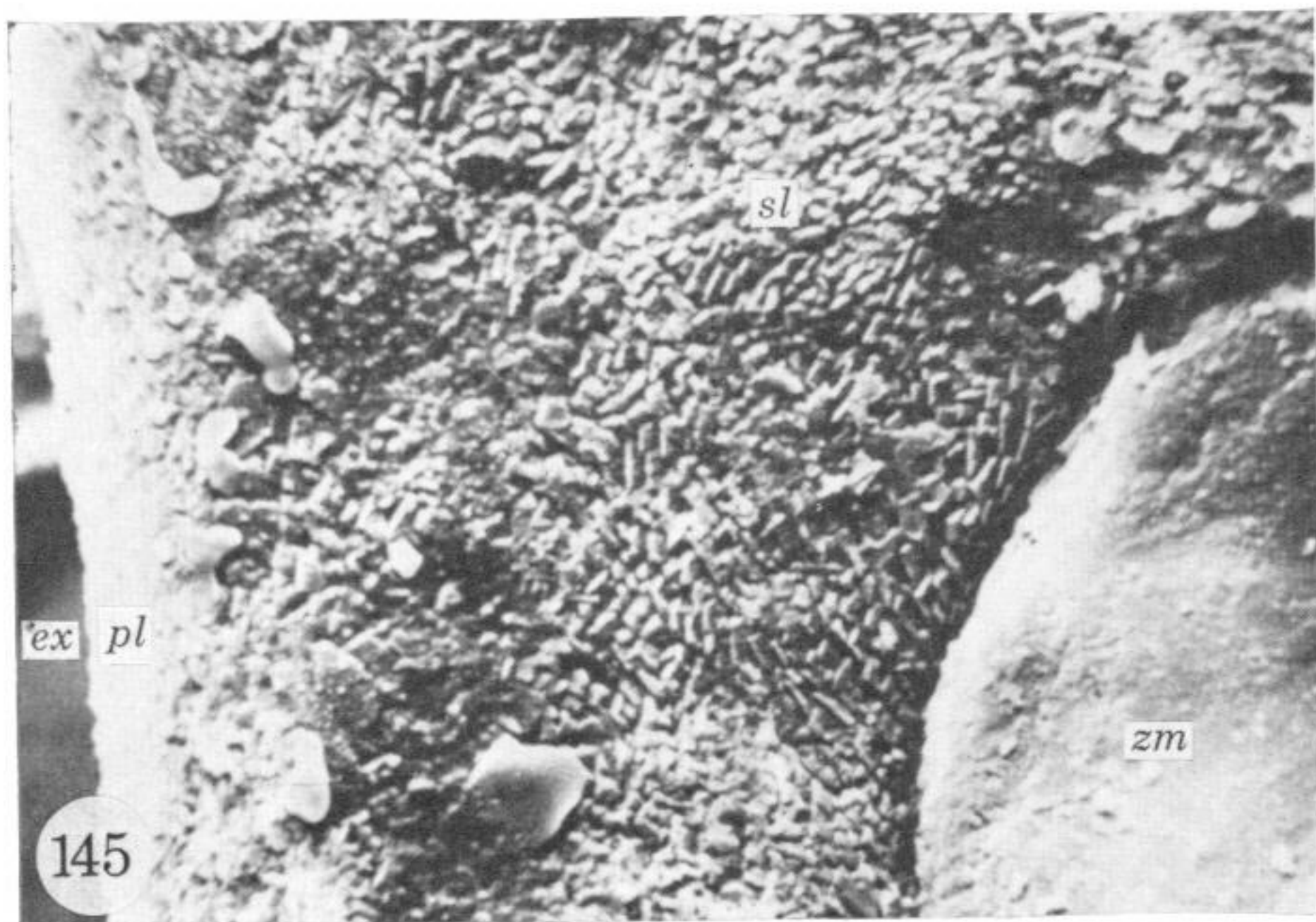
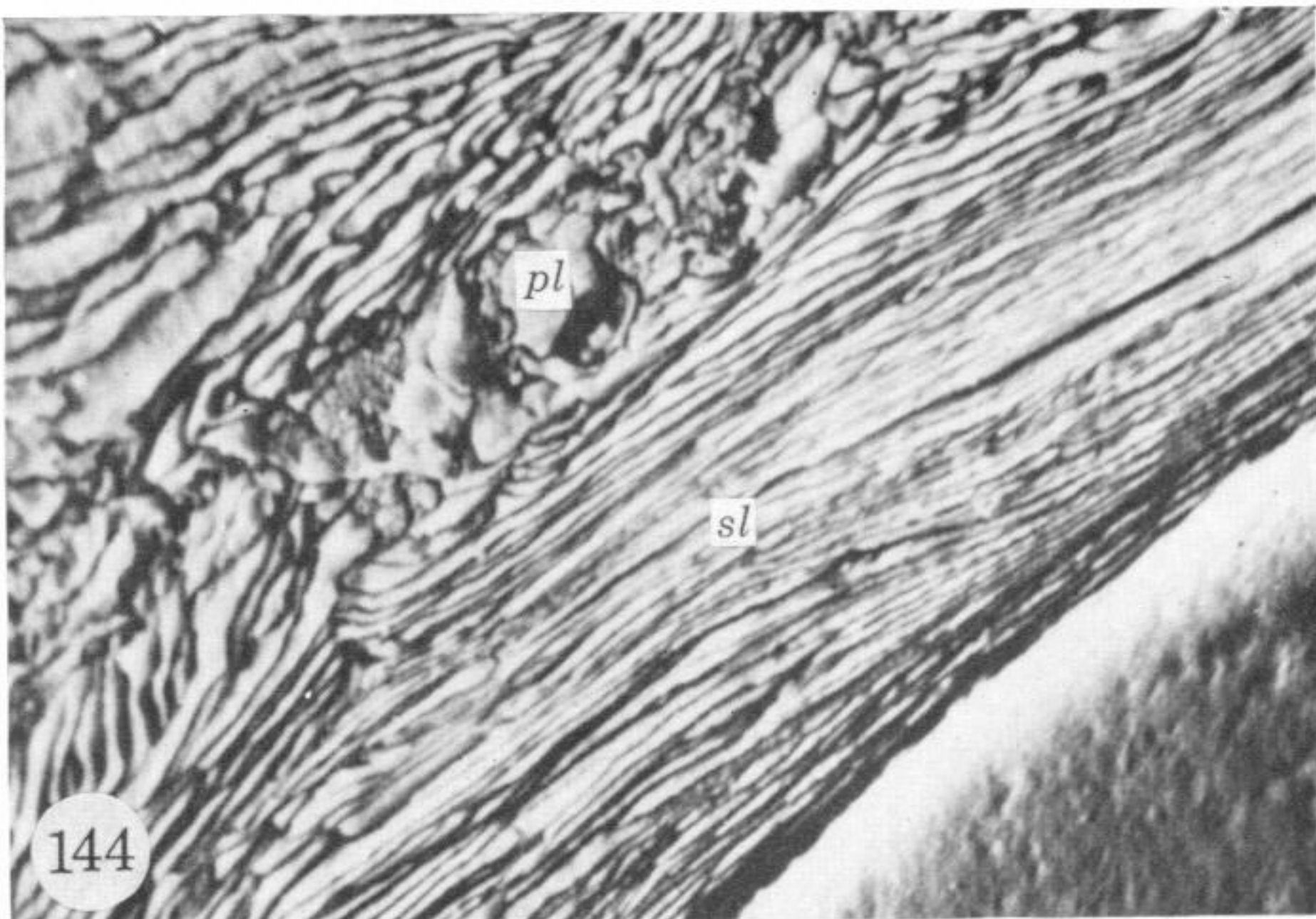
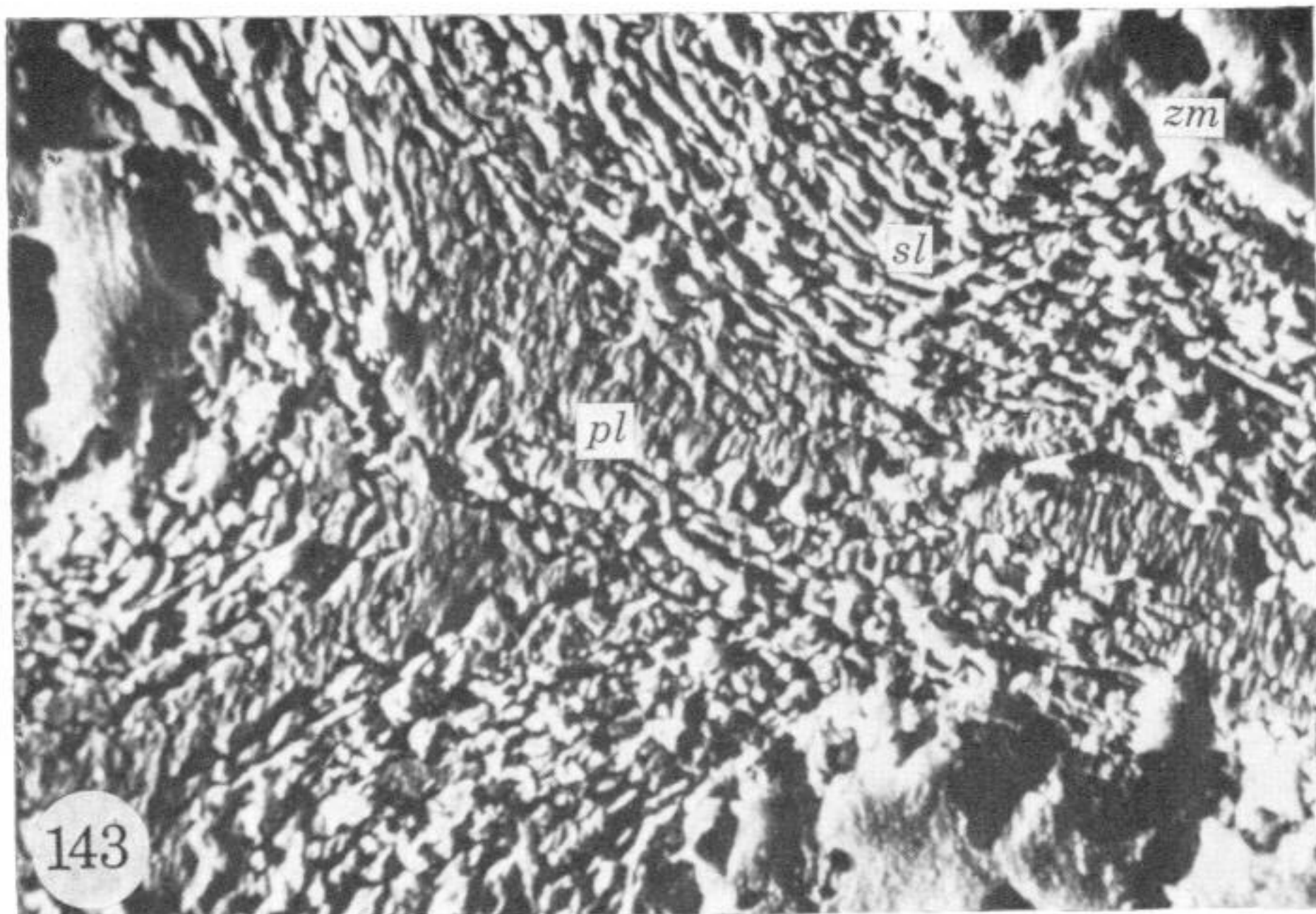
FIGURES 123 TO 130. For legends see facing page.





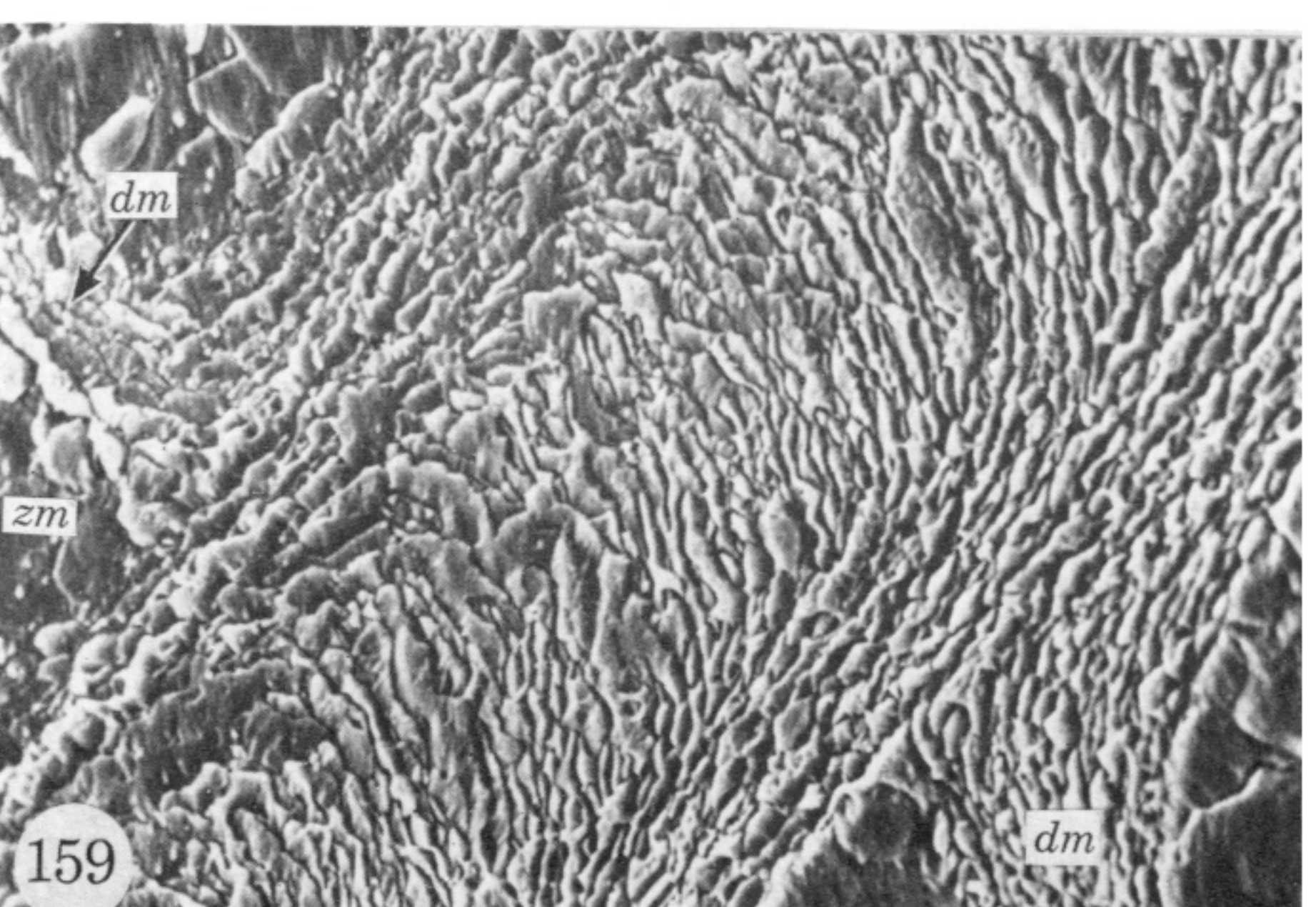
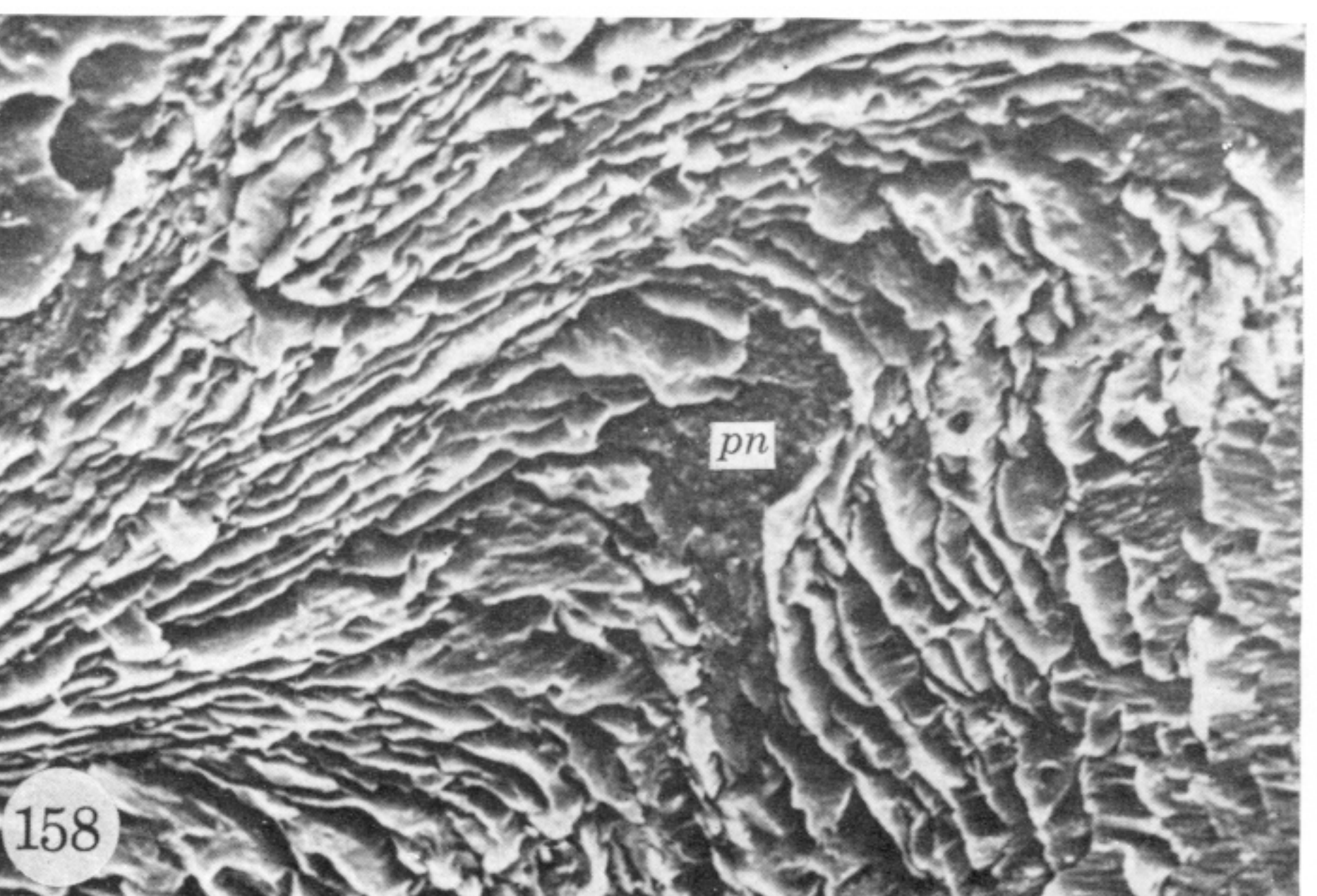
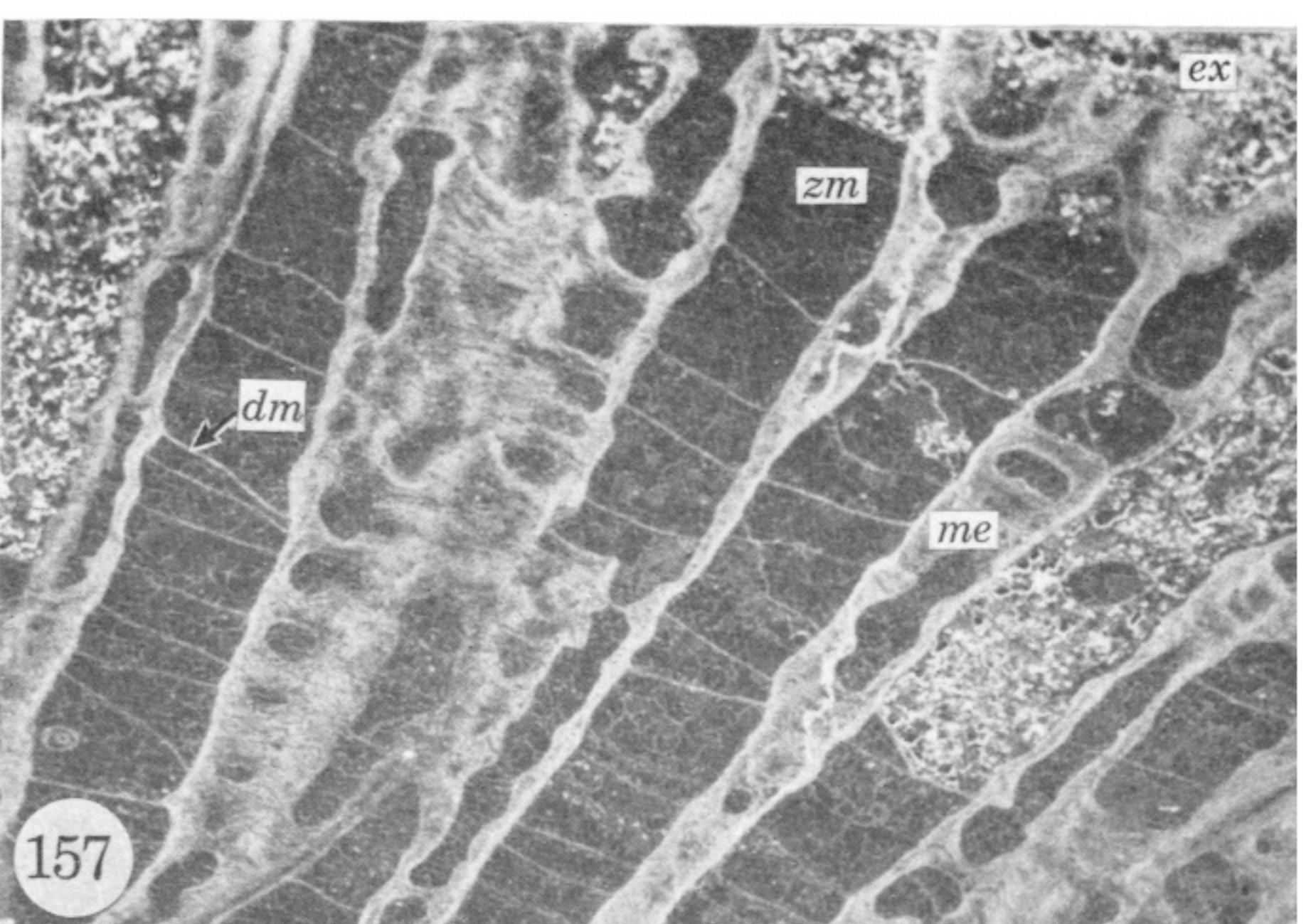
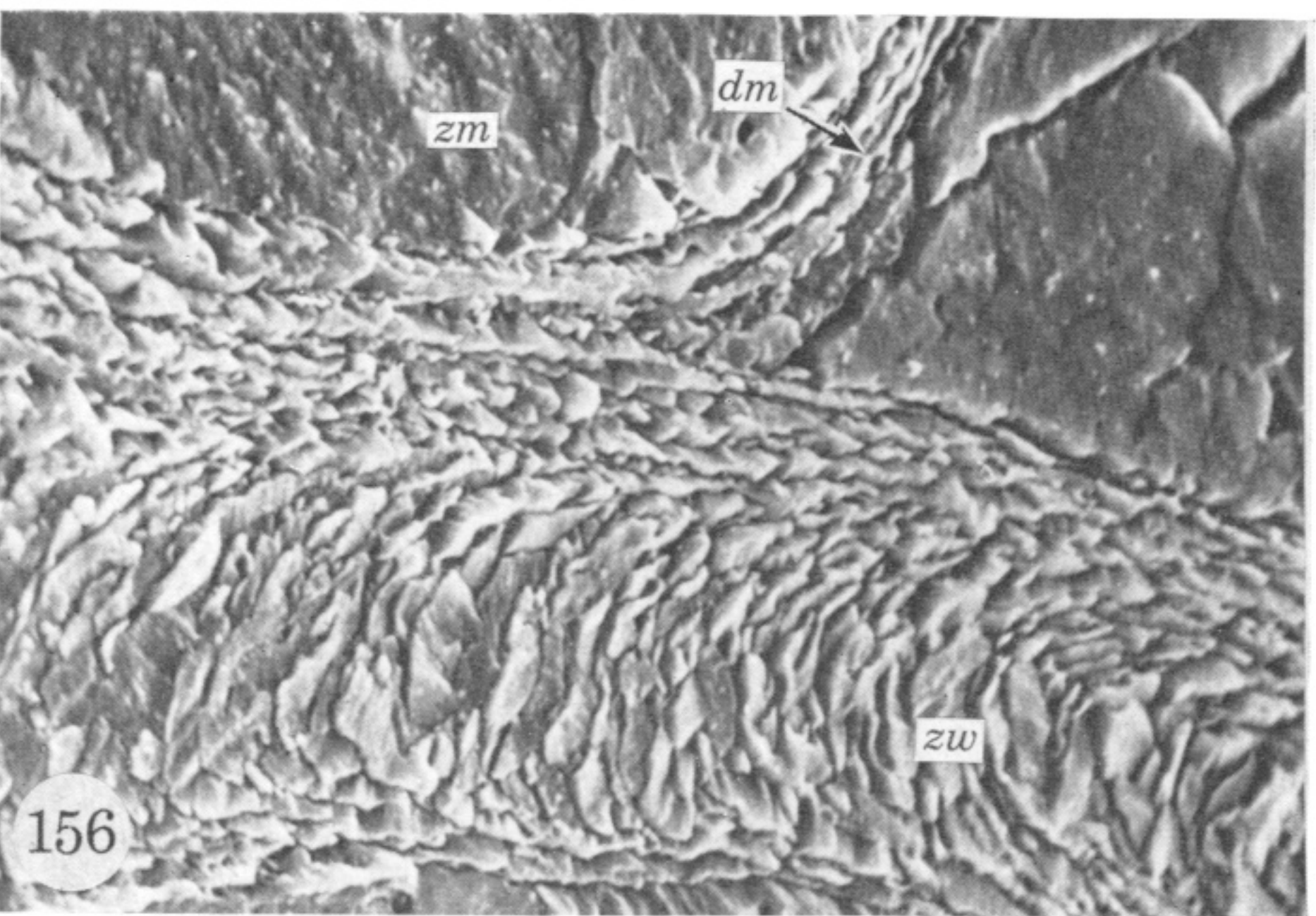
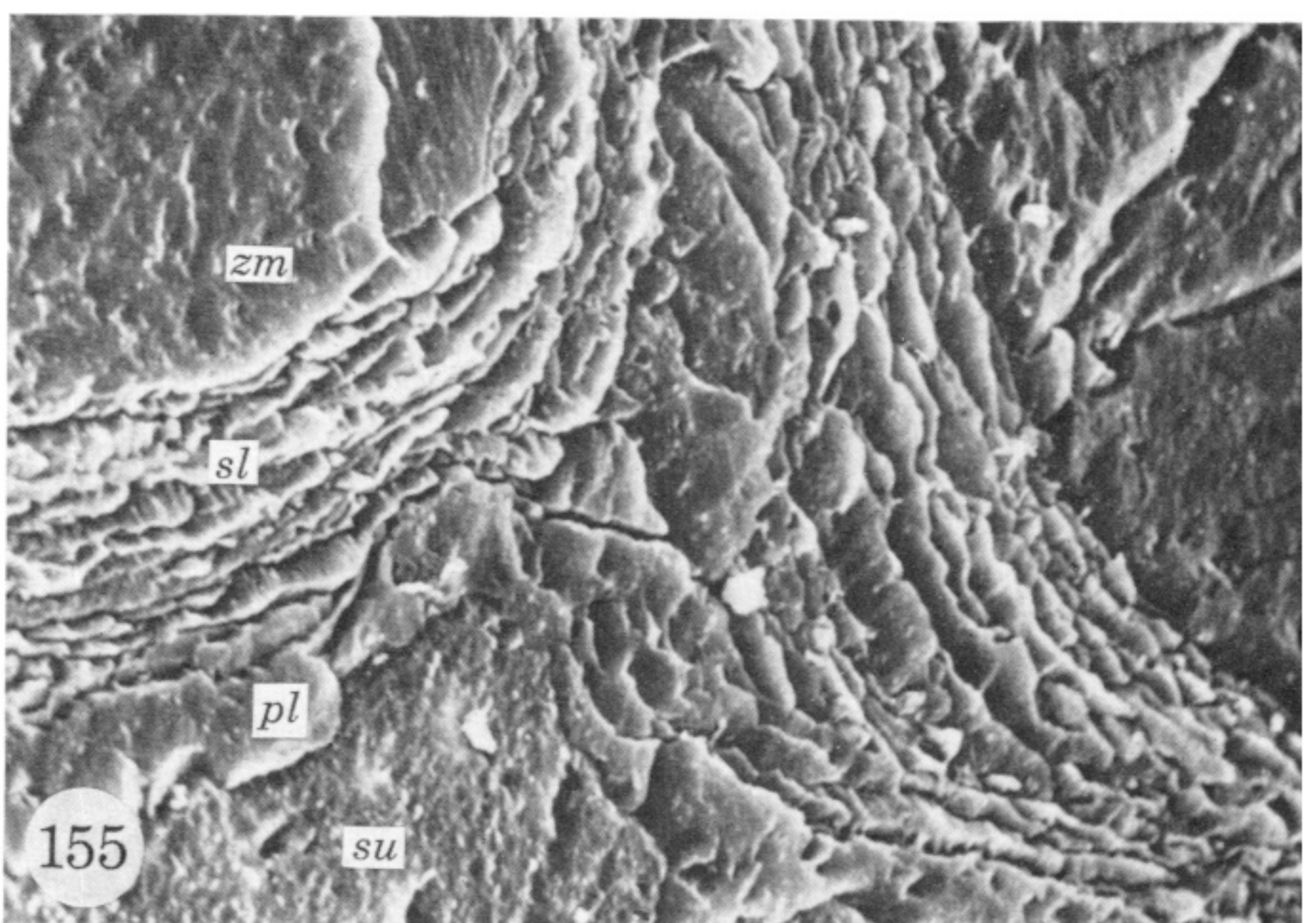
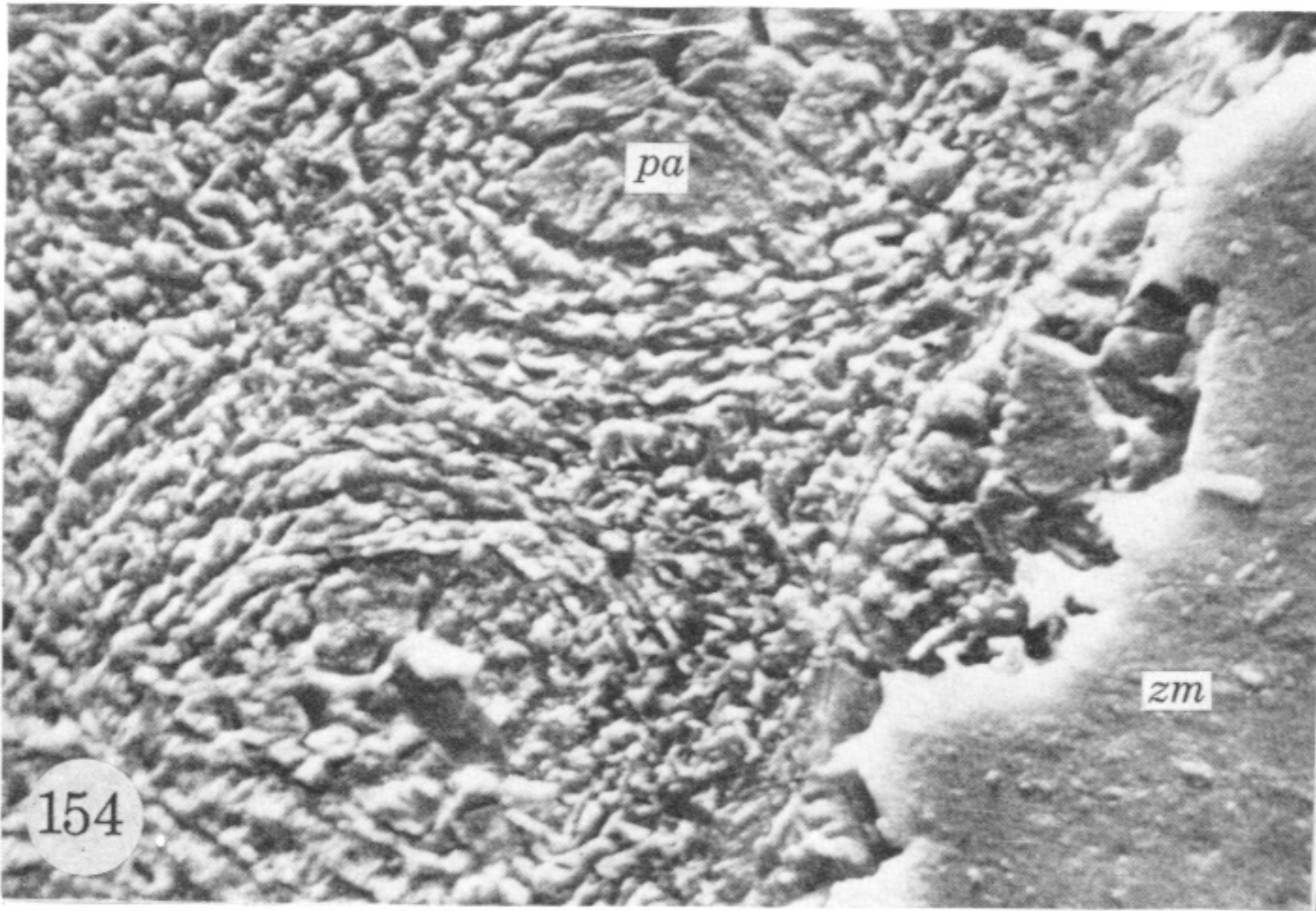
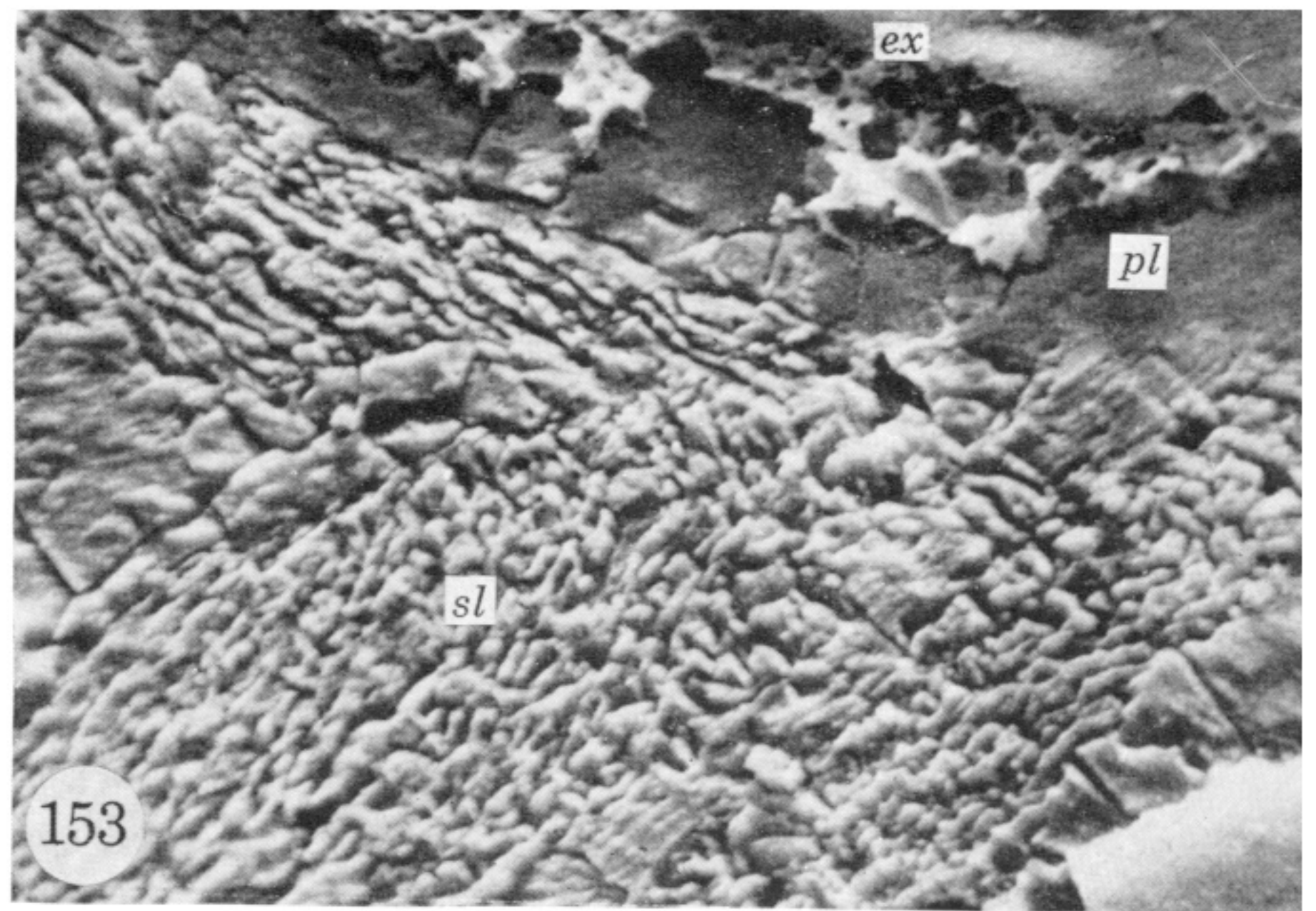
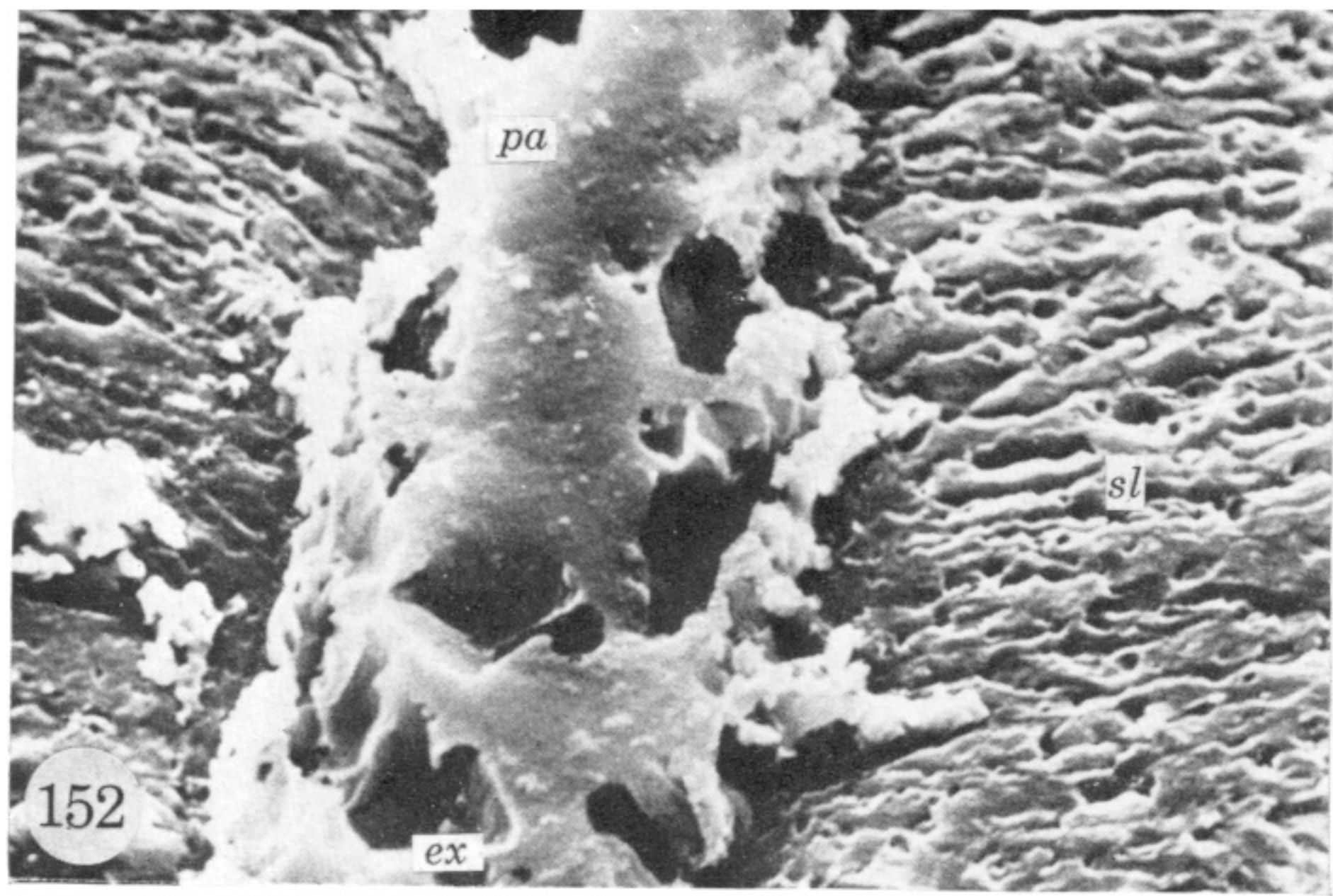
FIGURES 134 TO 141. For legends see facing page.





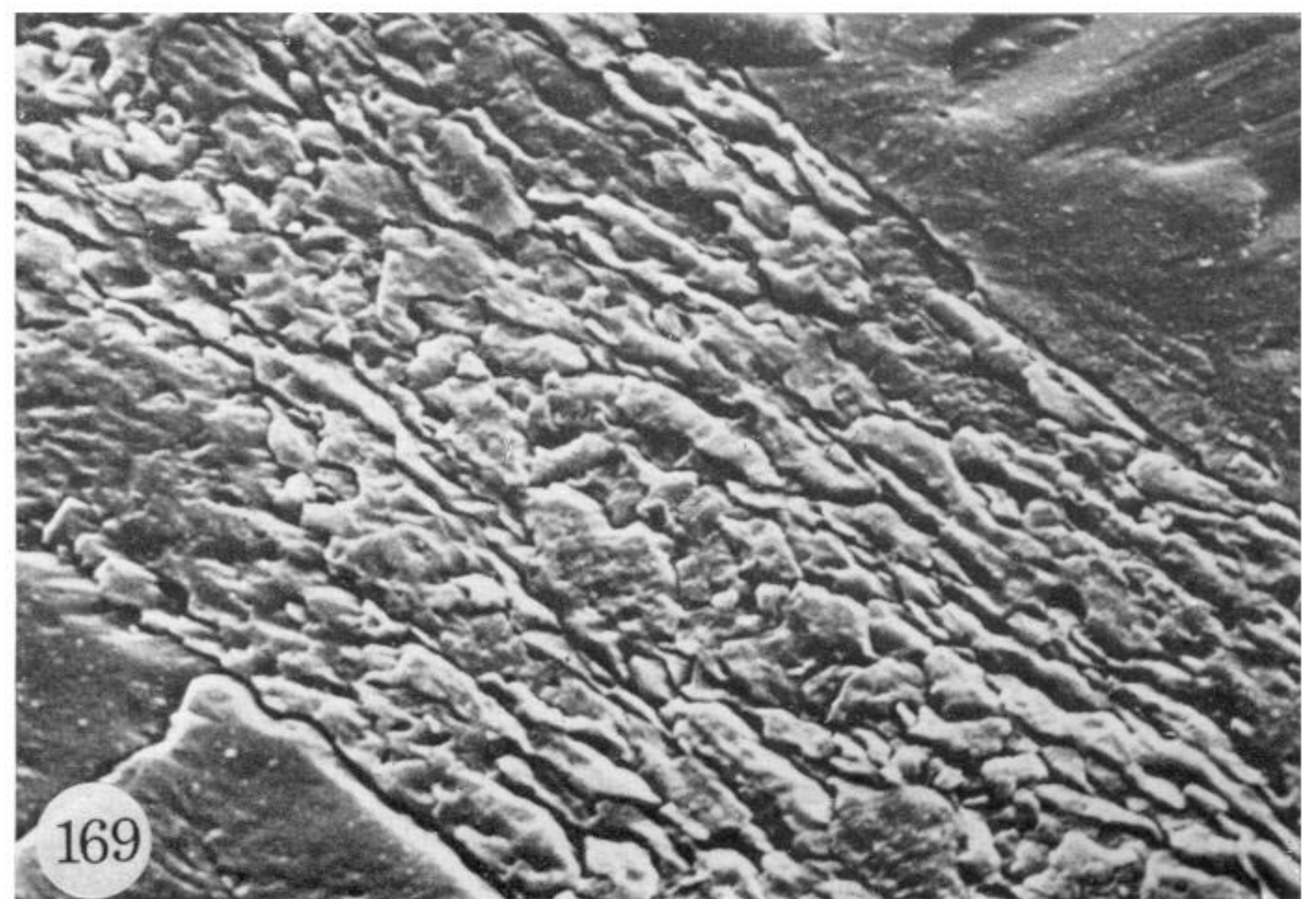
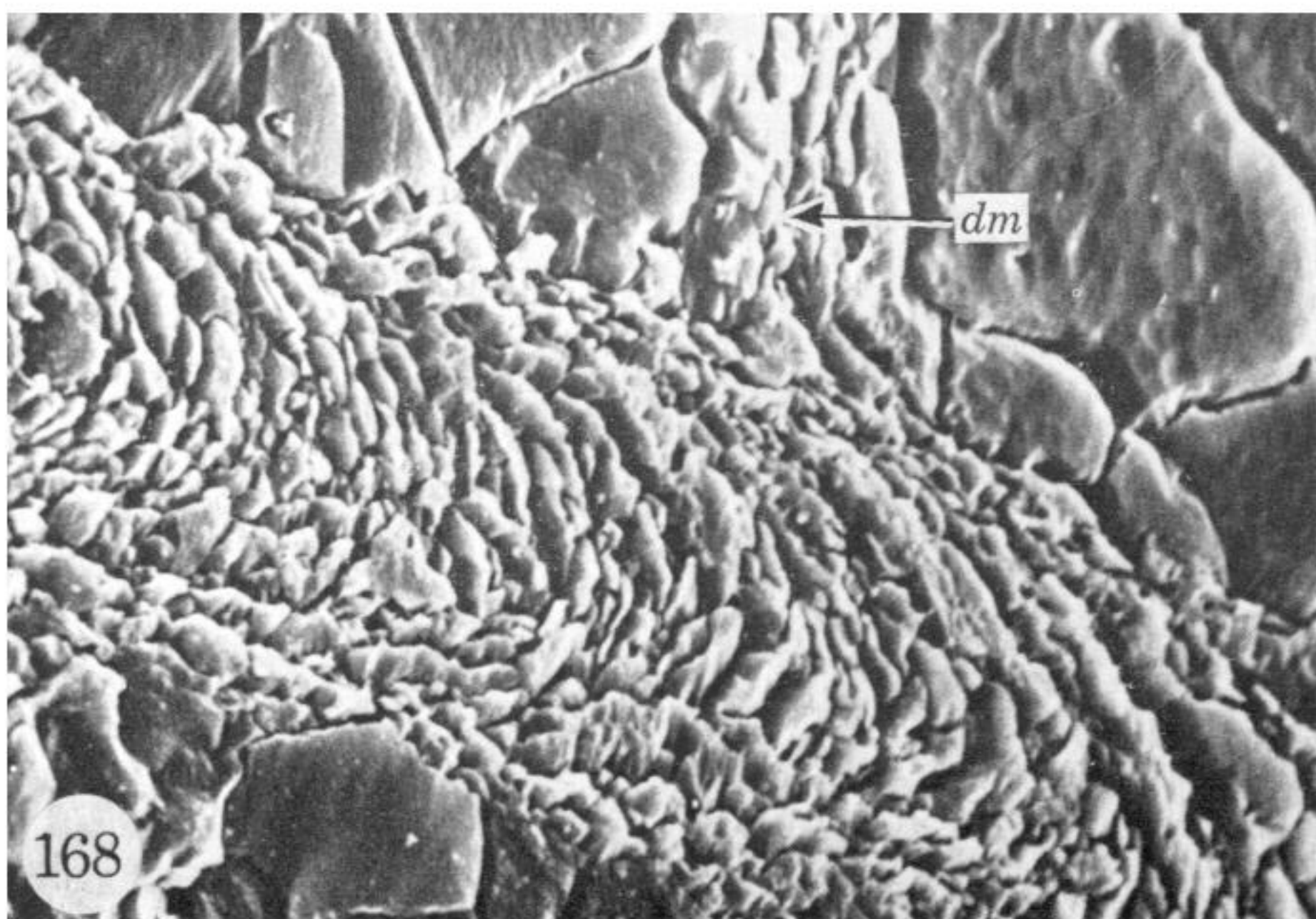
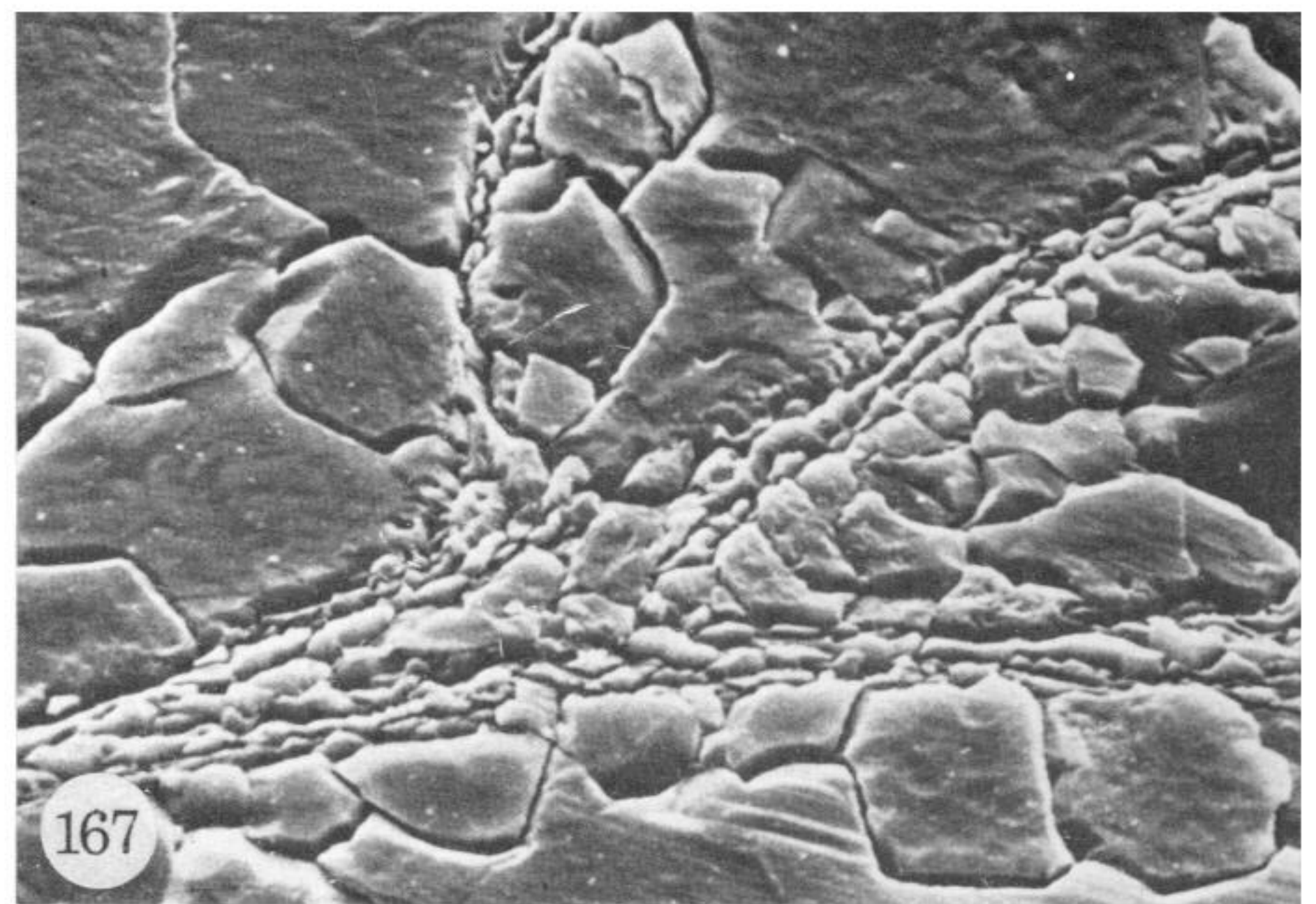
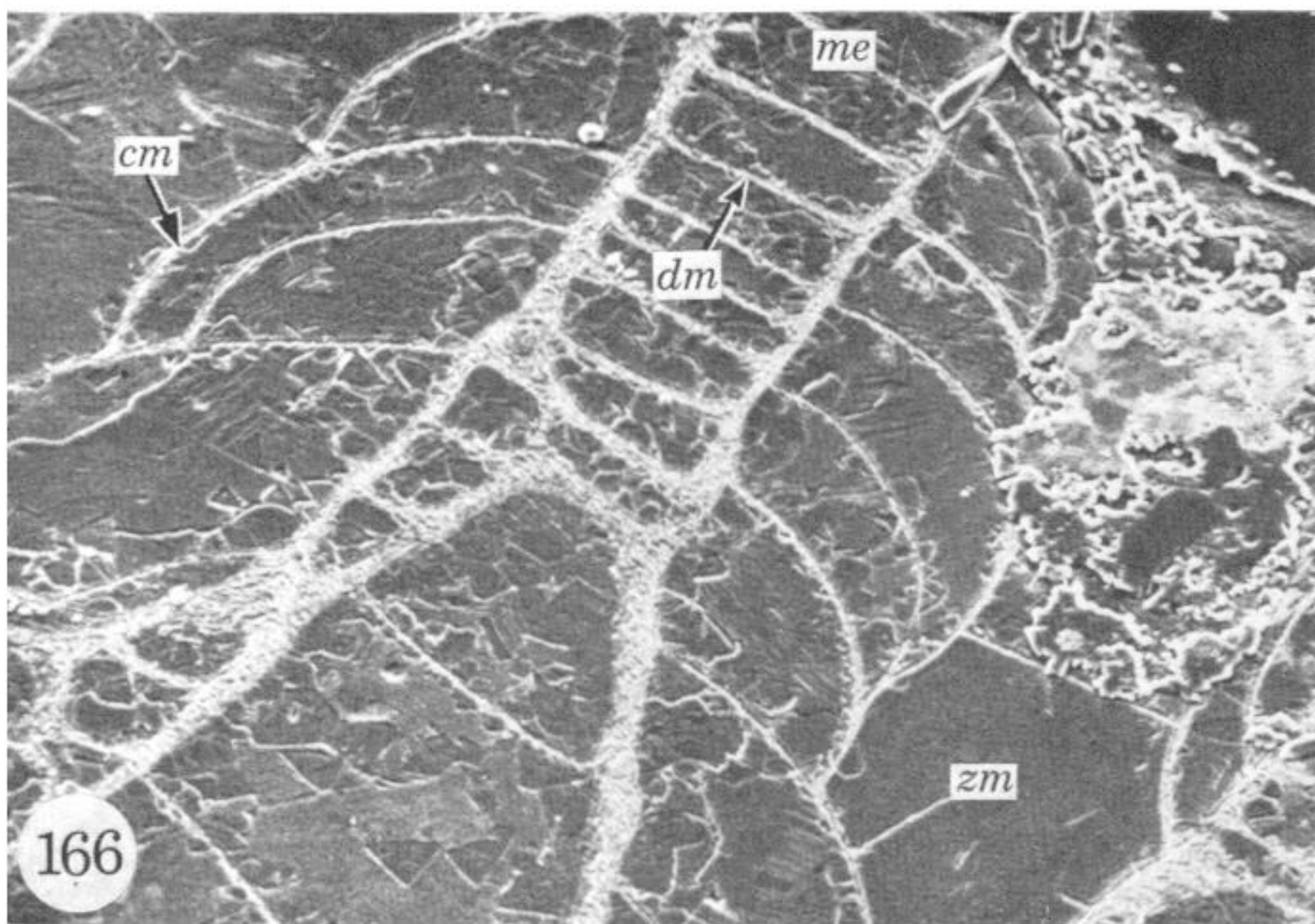
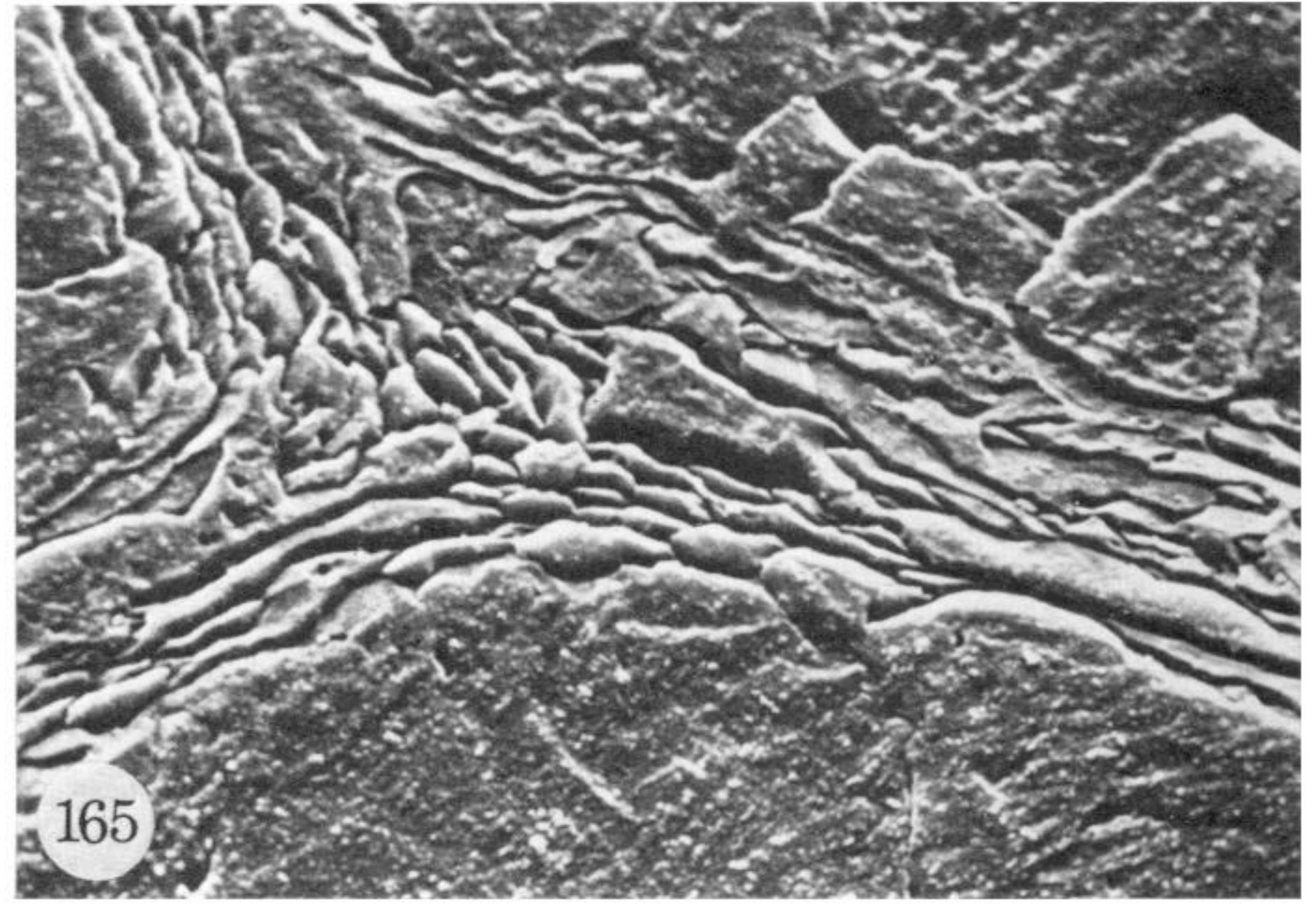
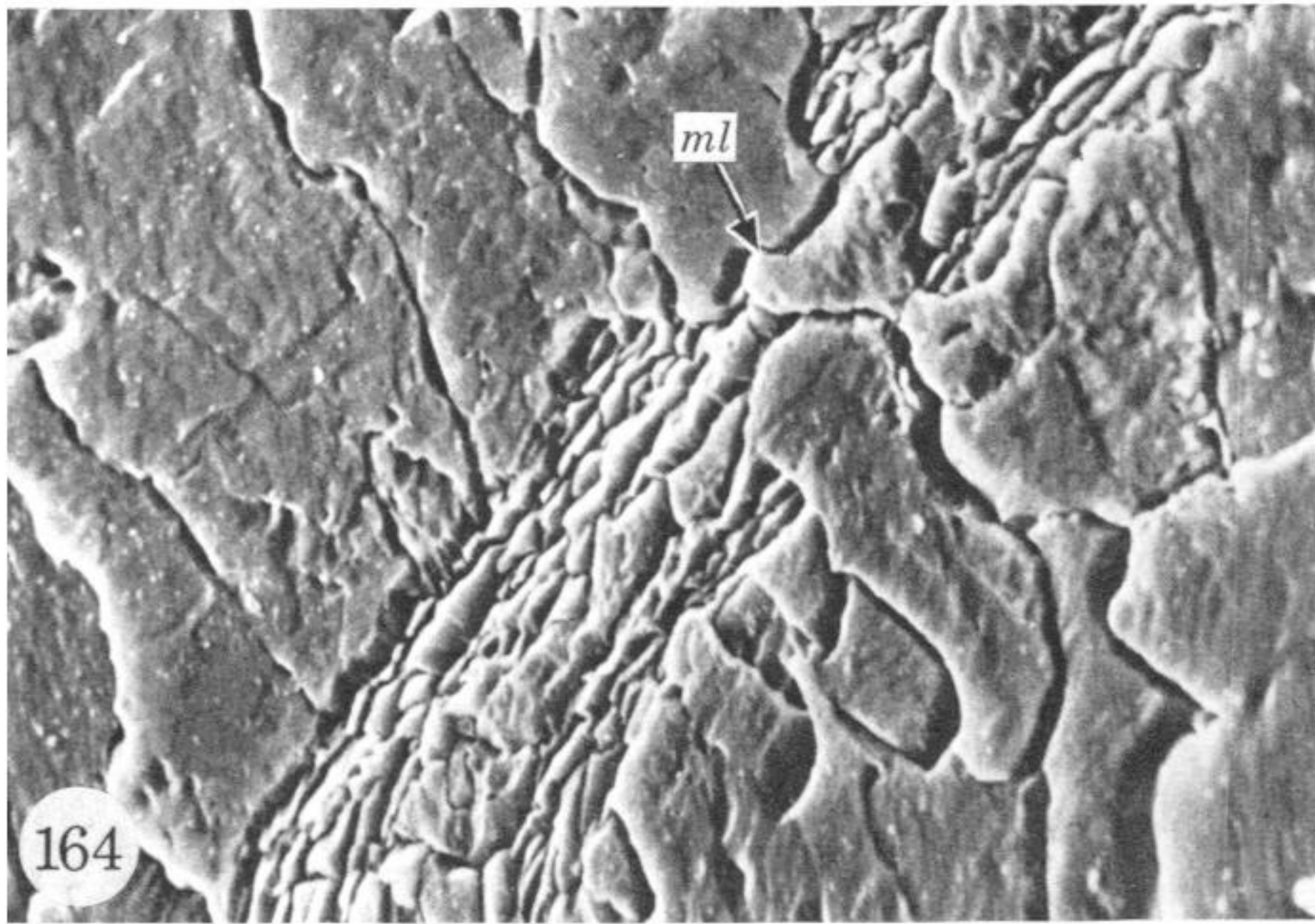
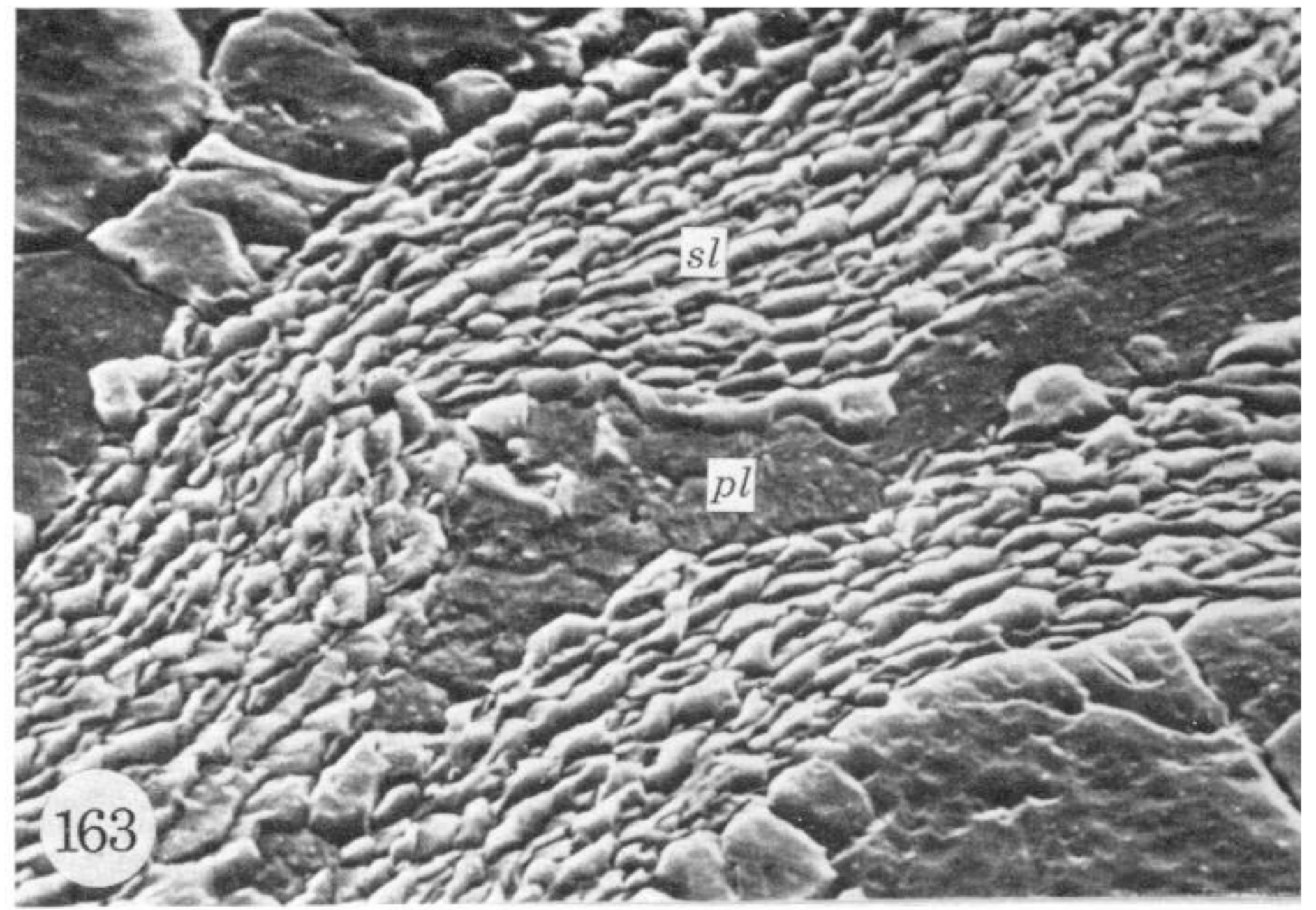
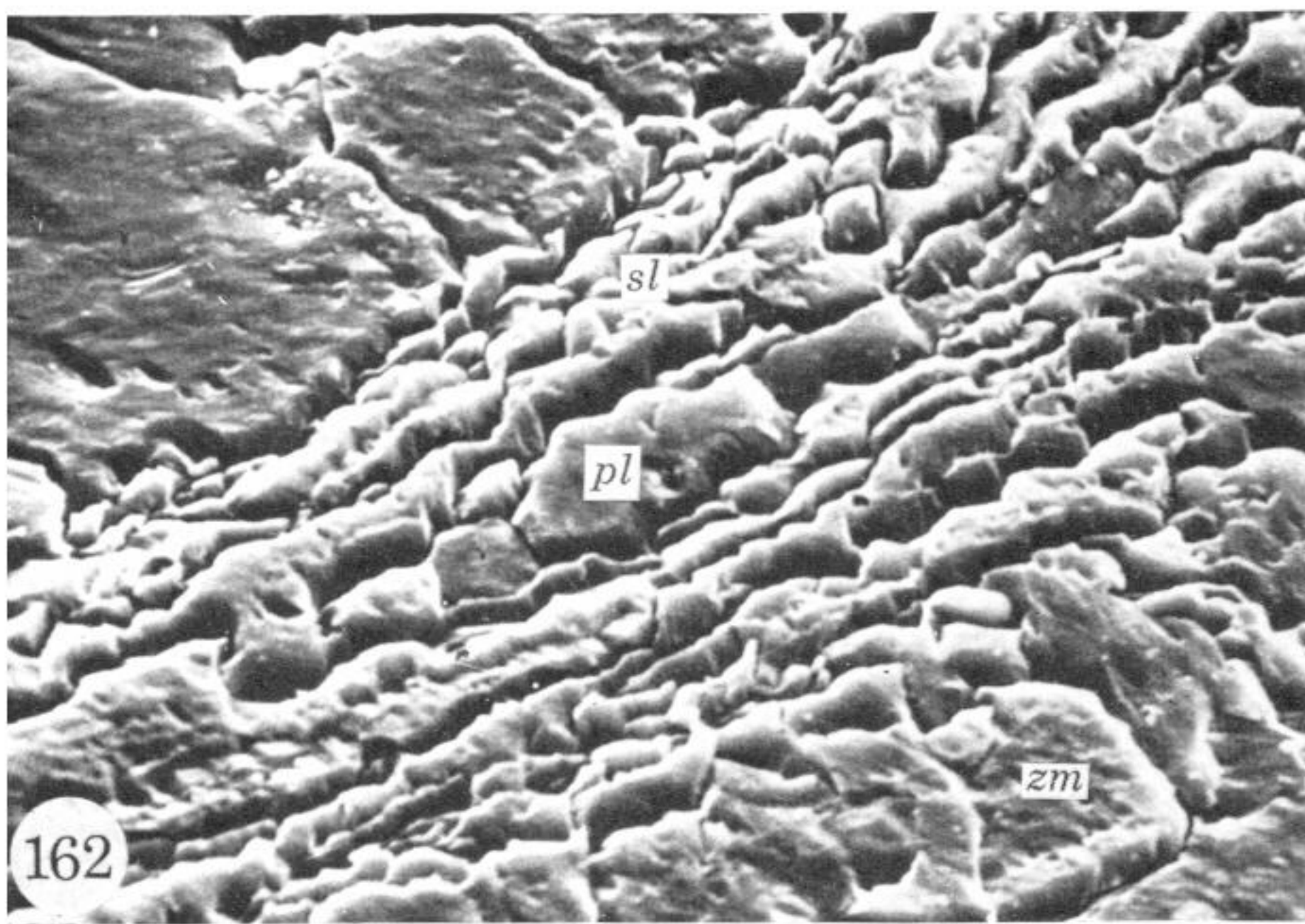
FIGURES 143 TO 150. For legends see facing page.





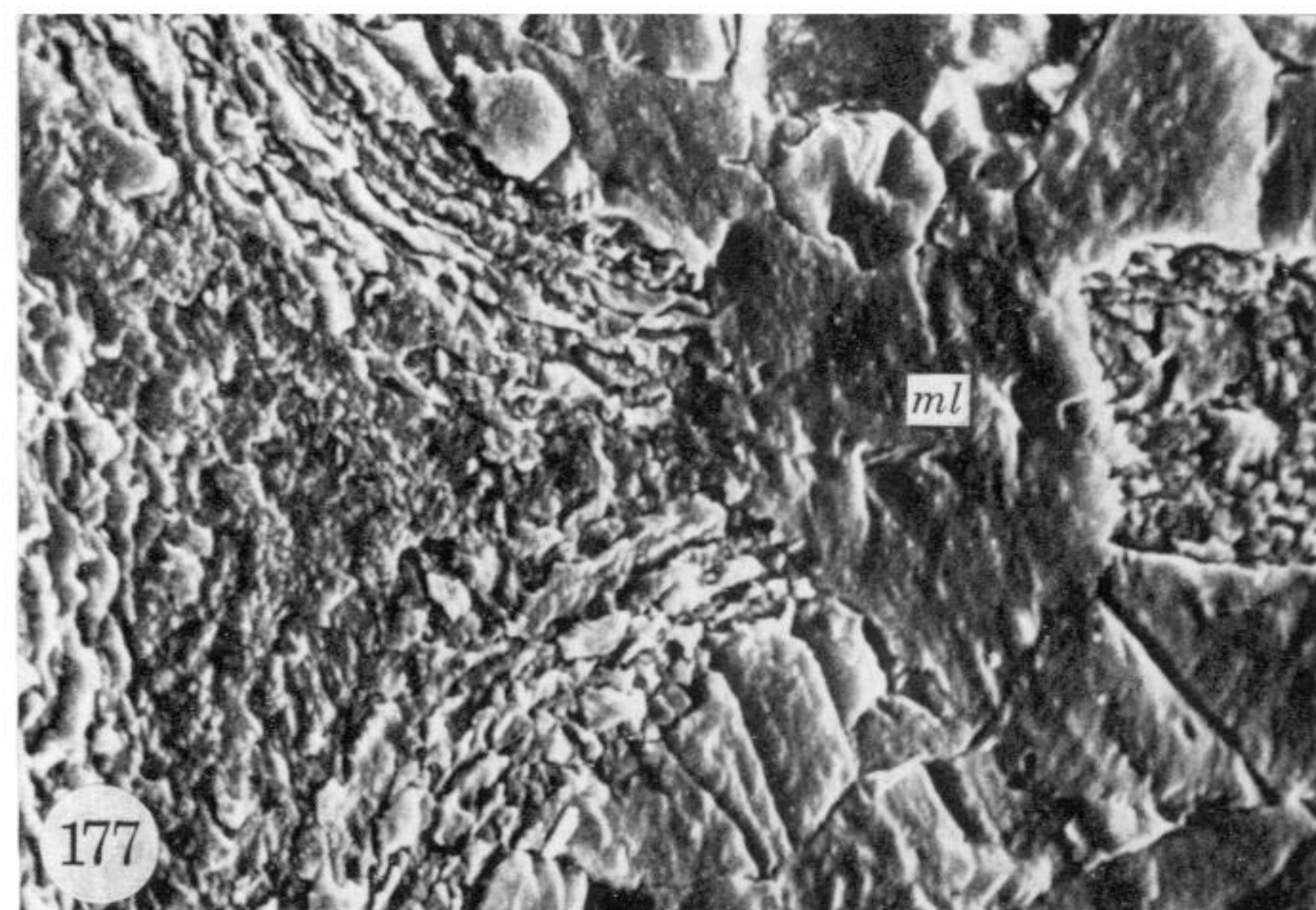
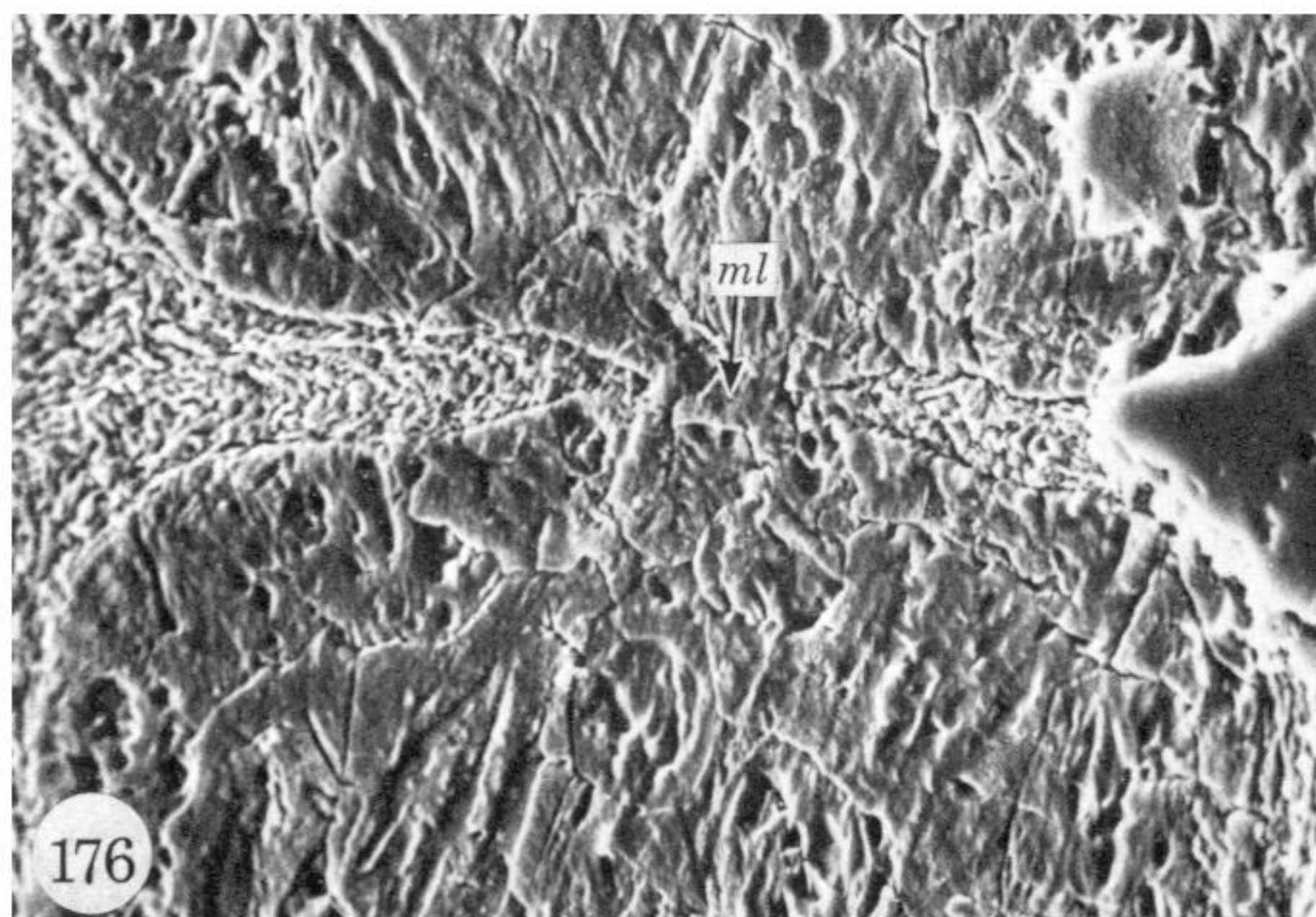
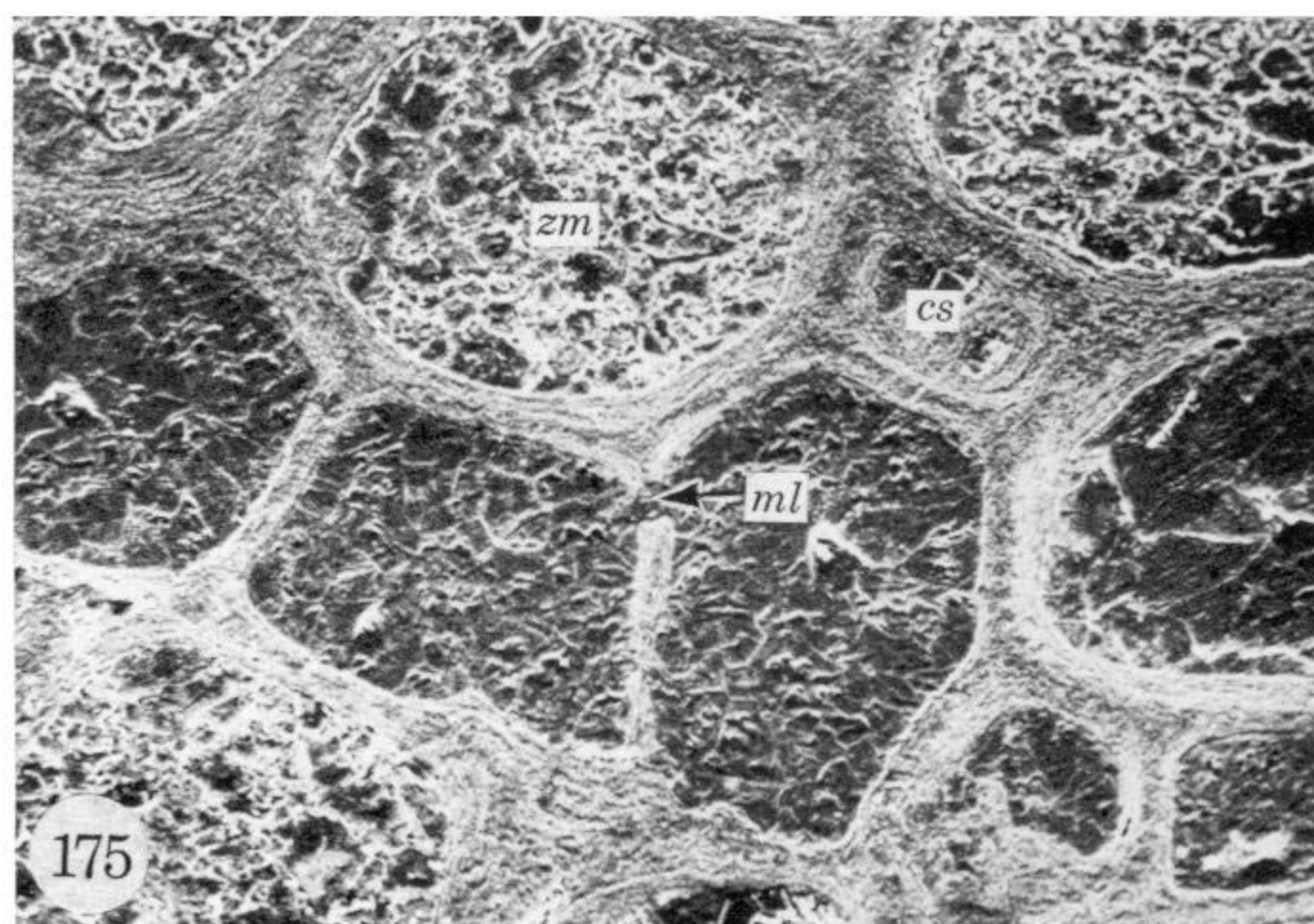
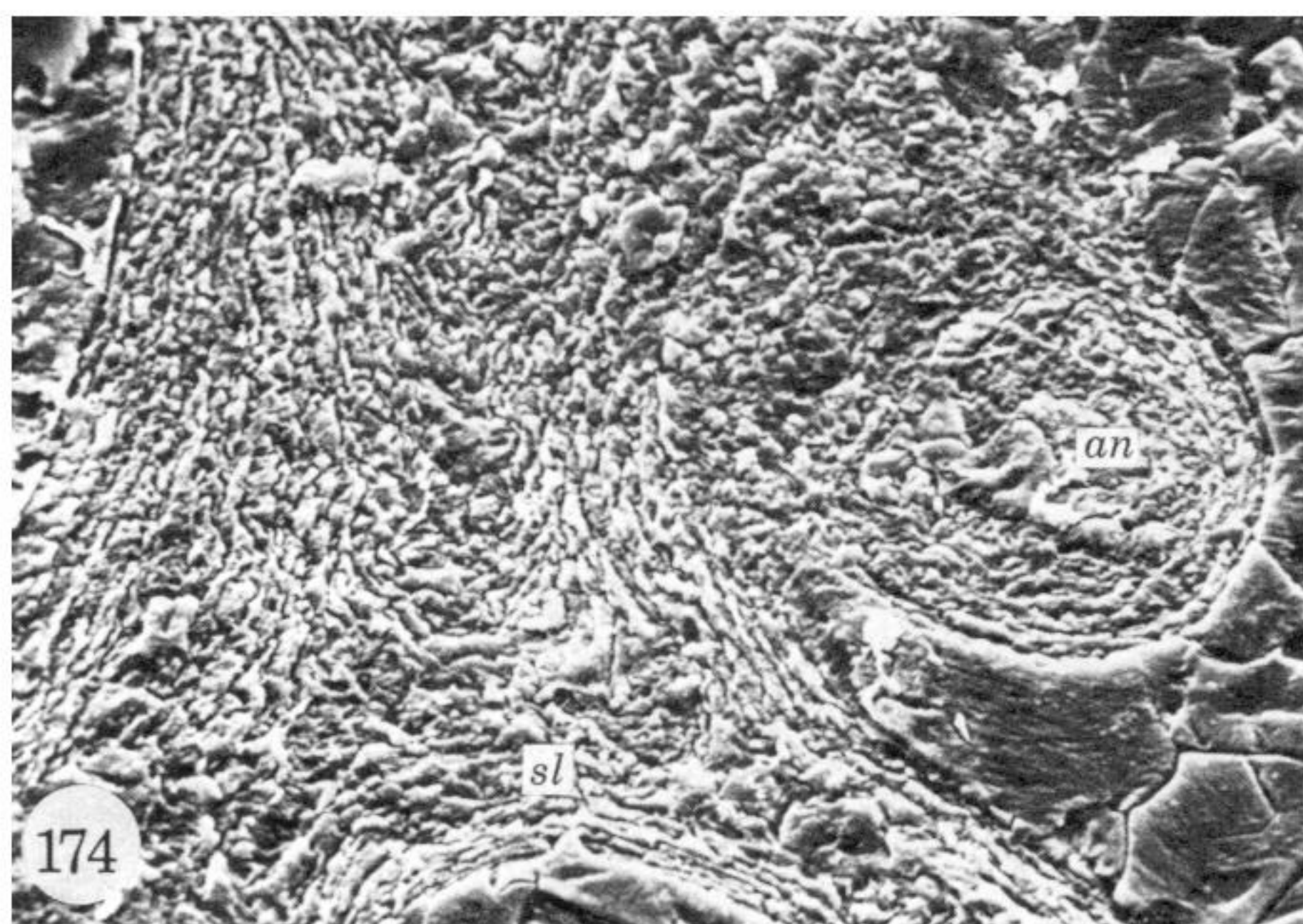
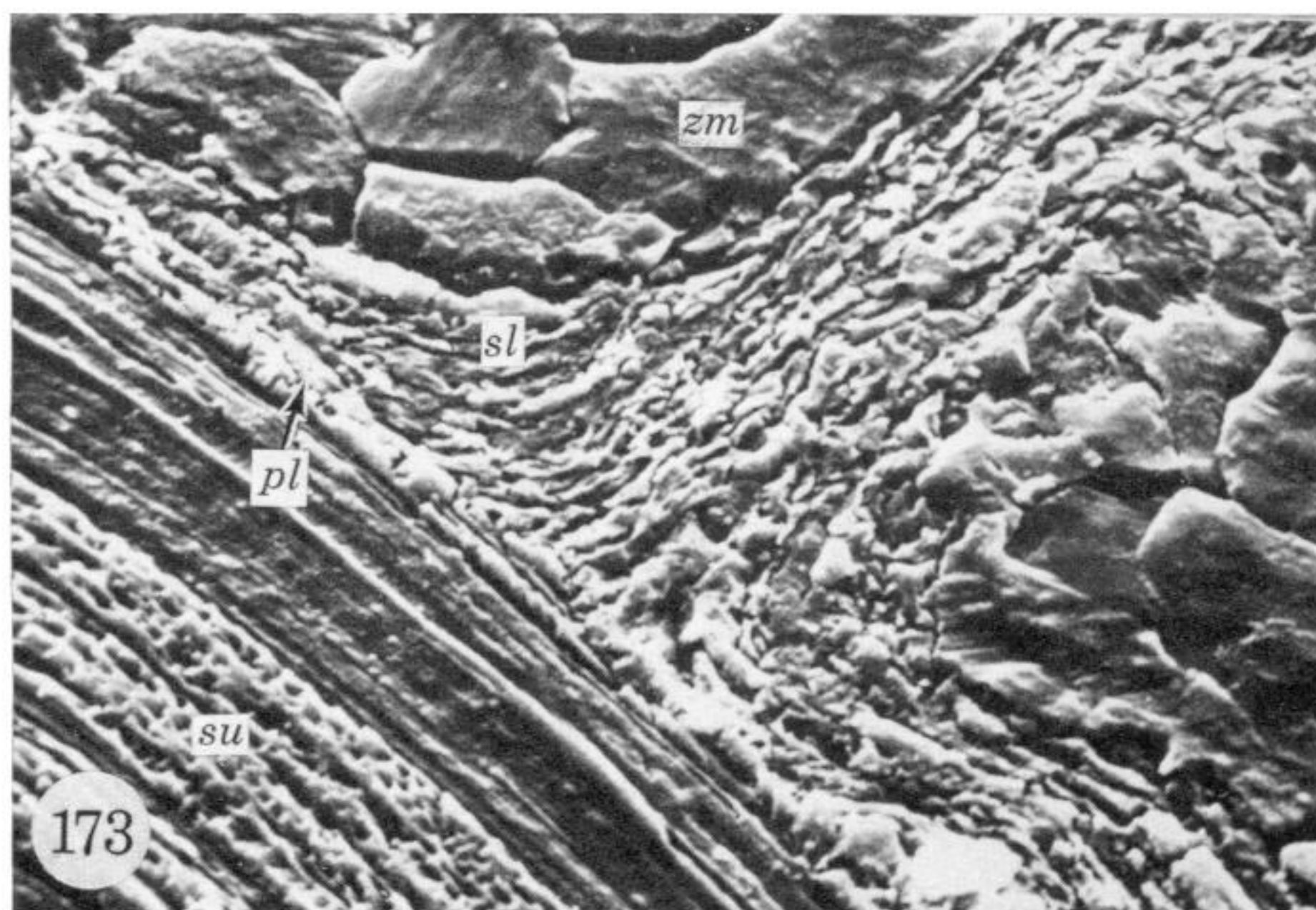
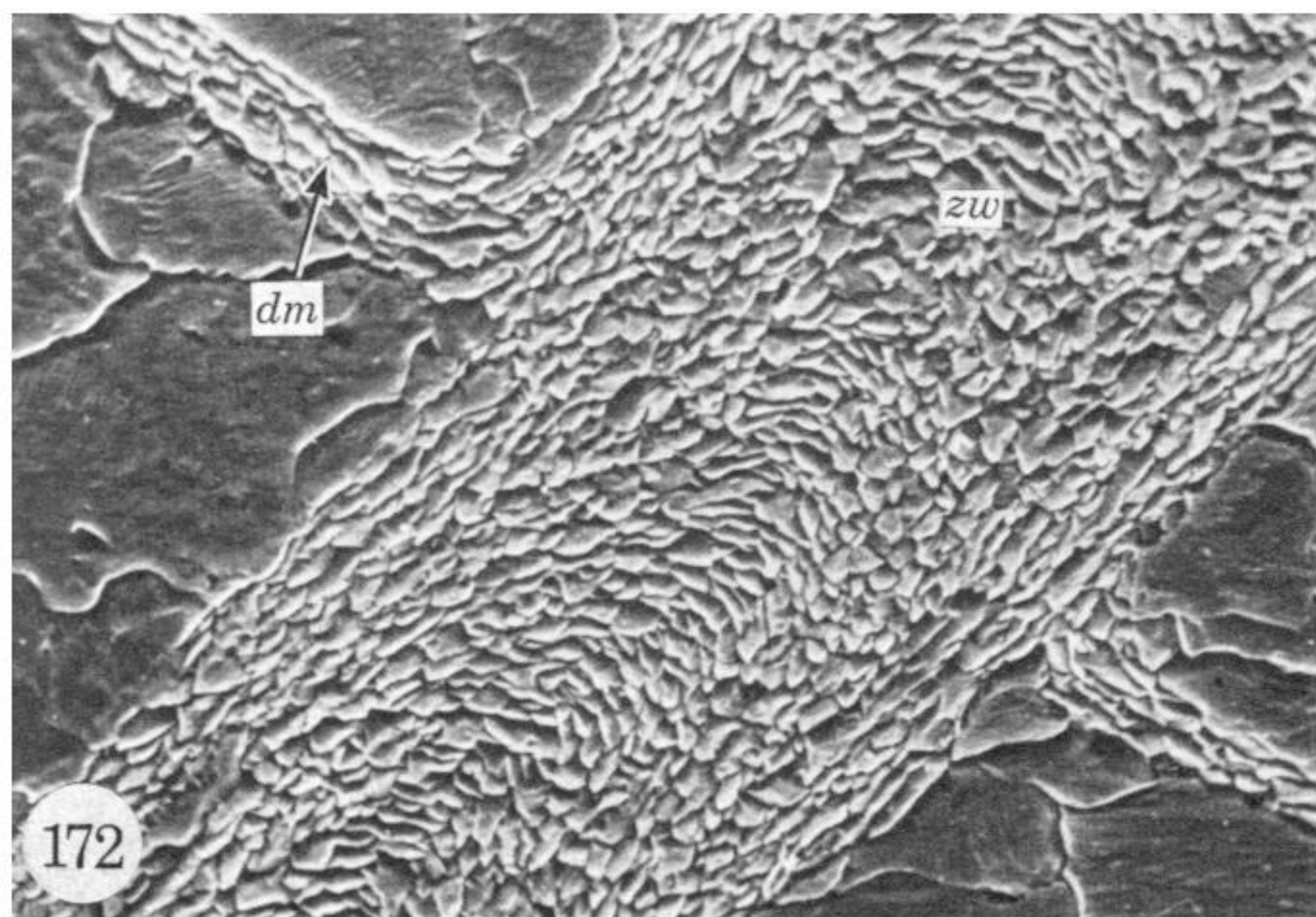
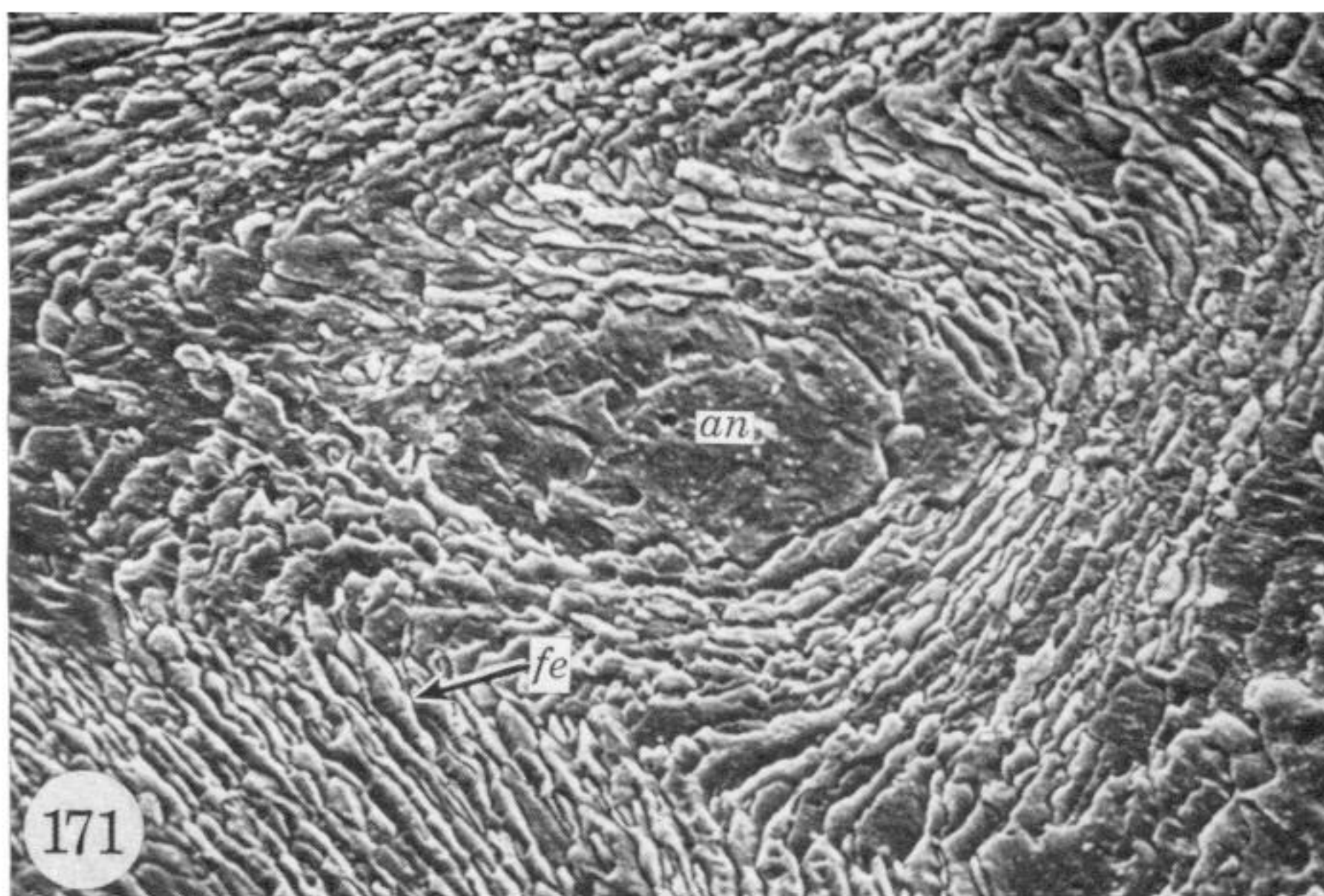
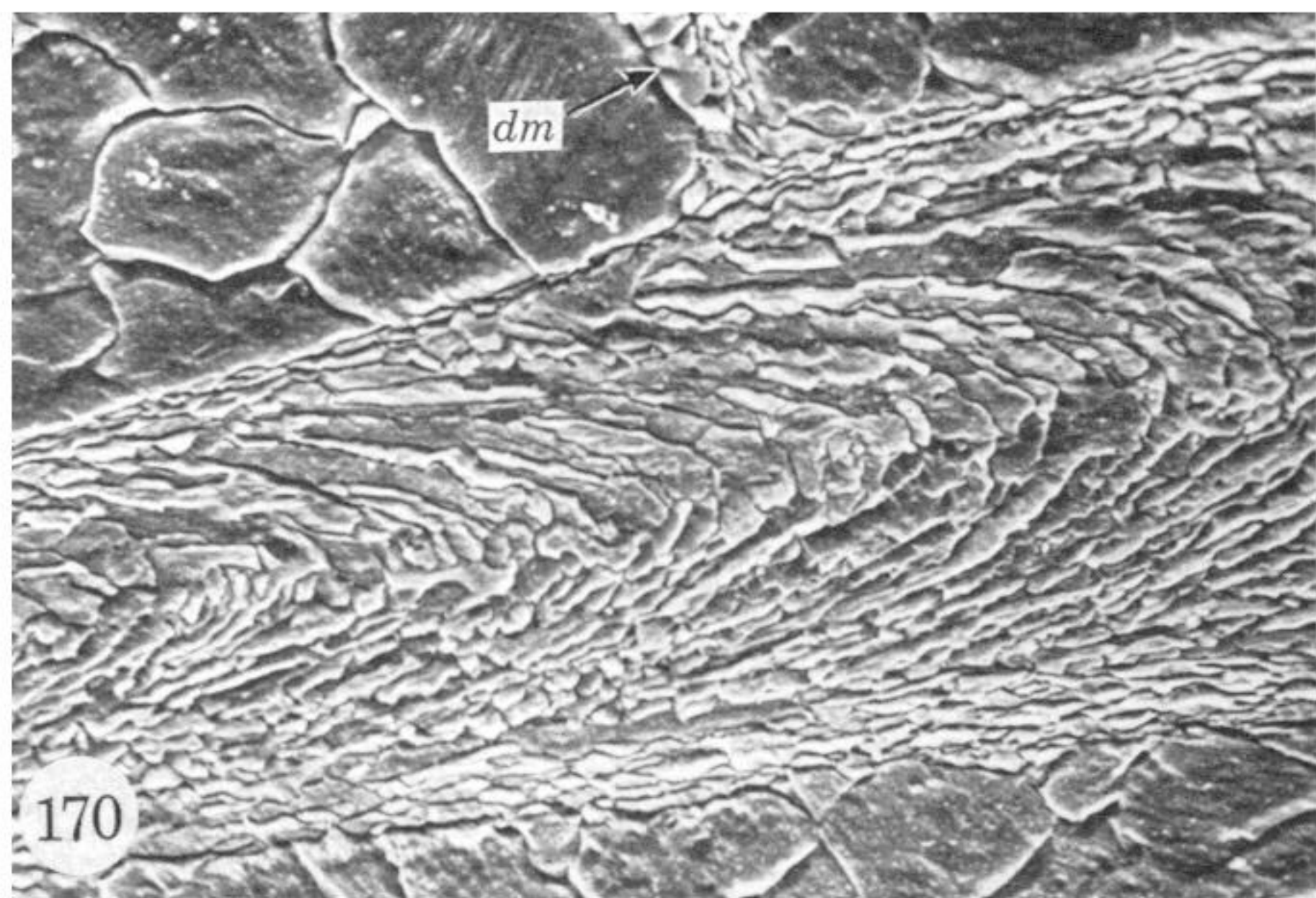
FIGURES 152 TO 159. For legends see facing page.





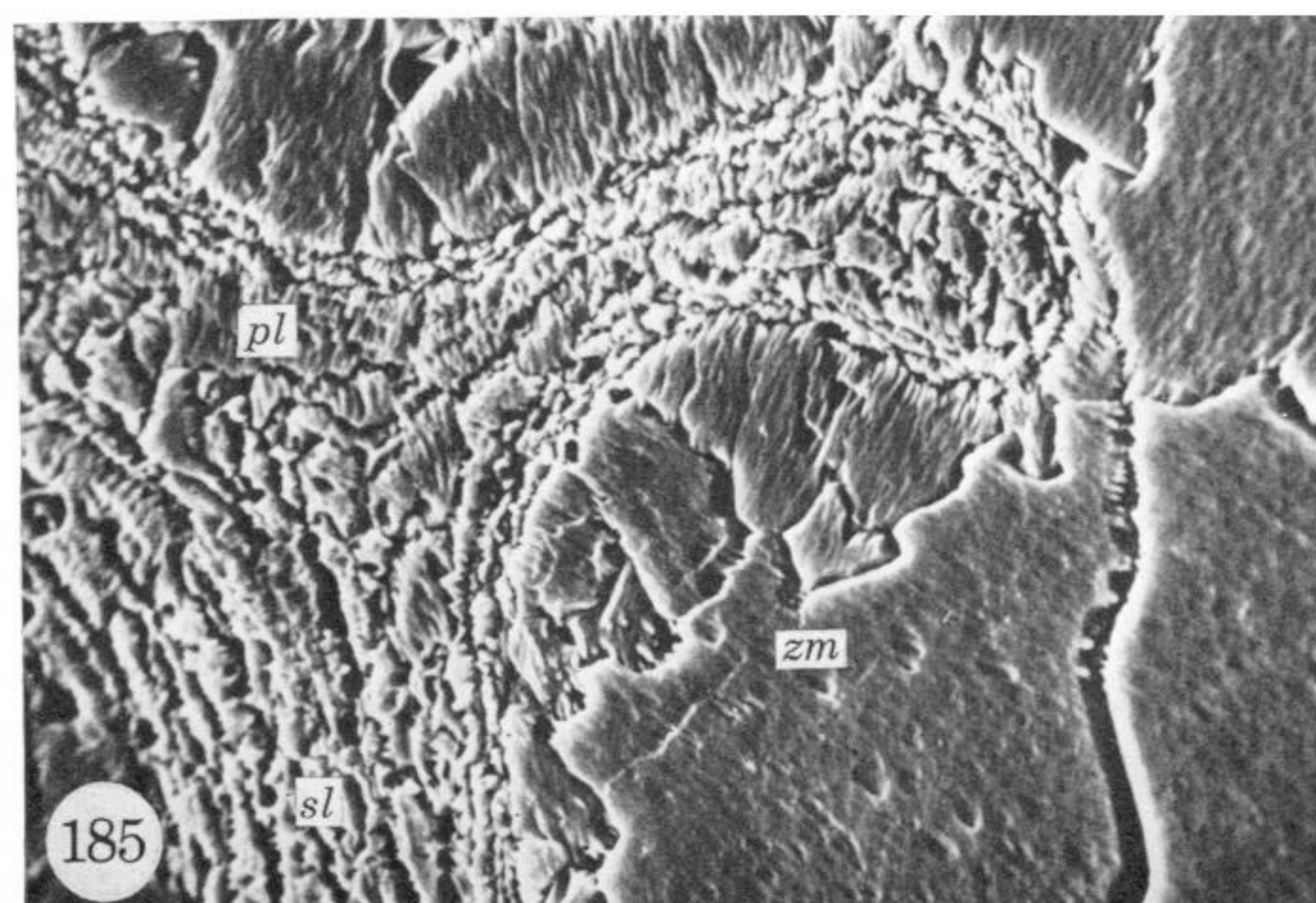
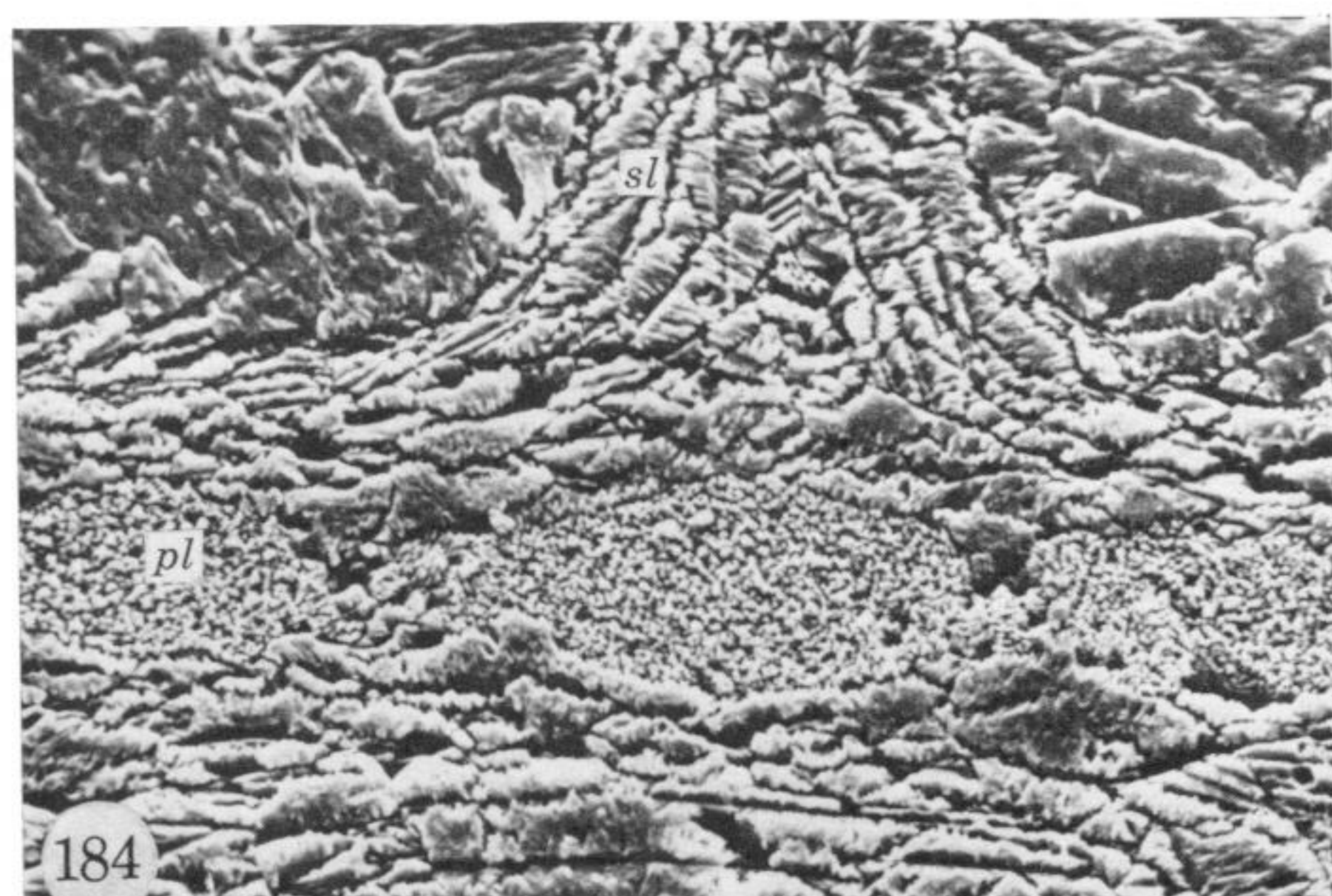
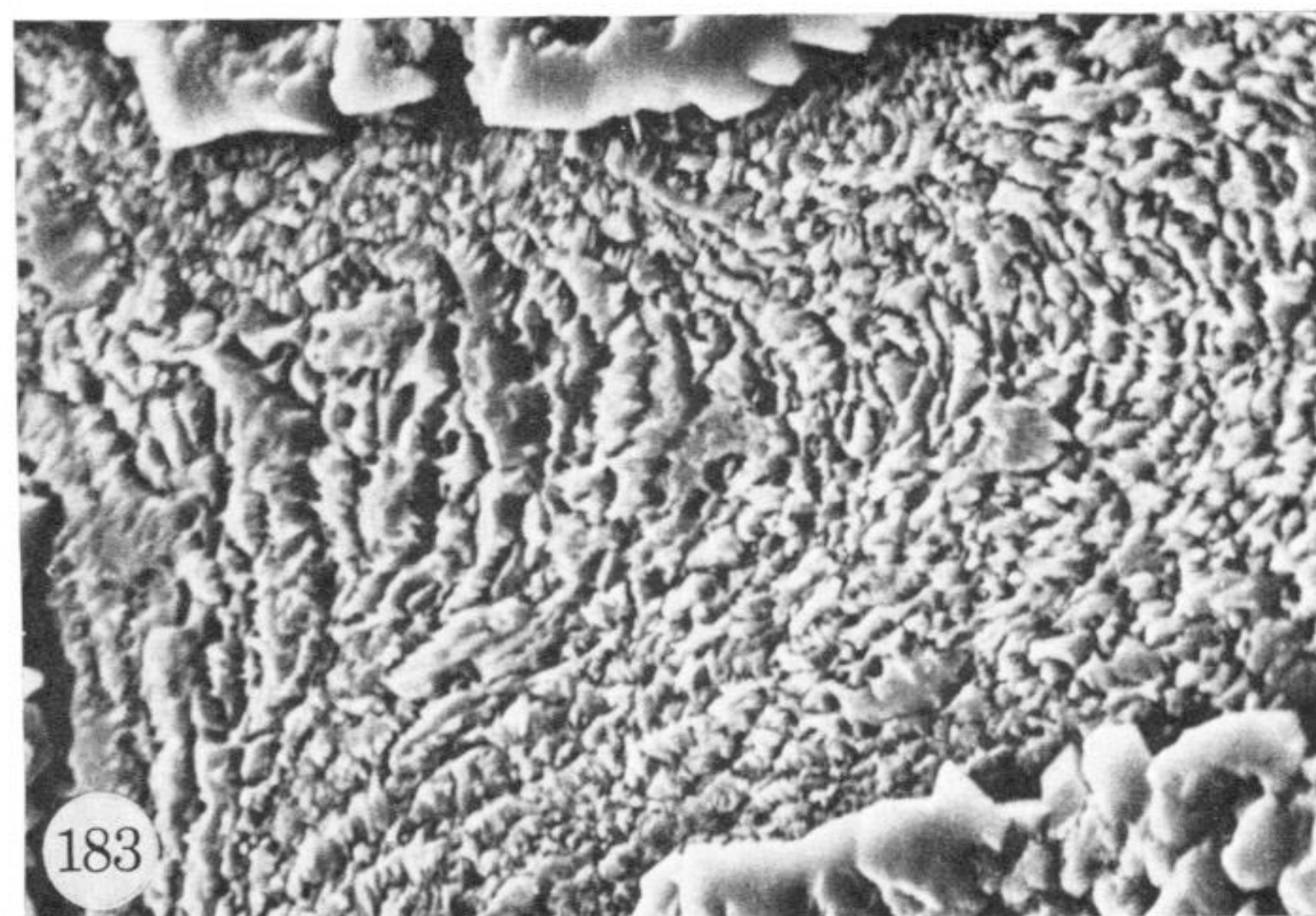
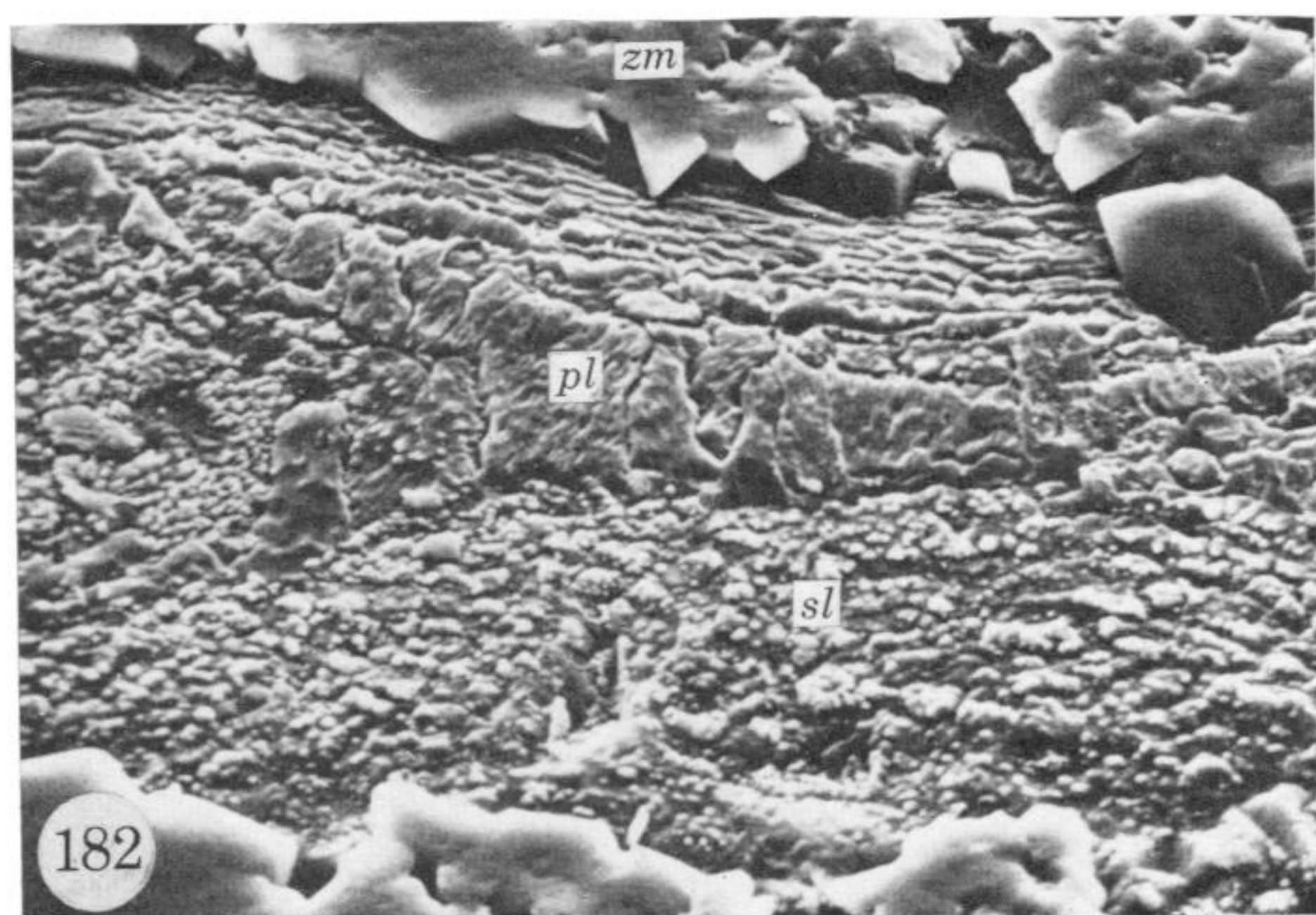
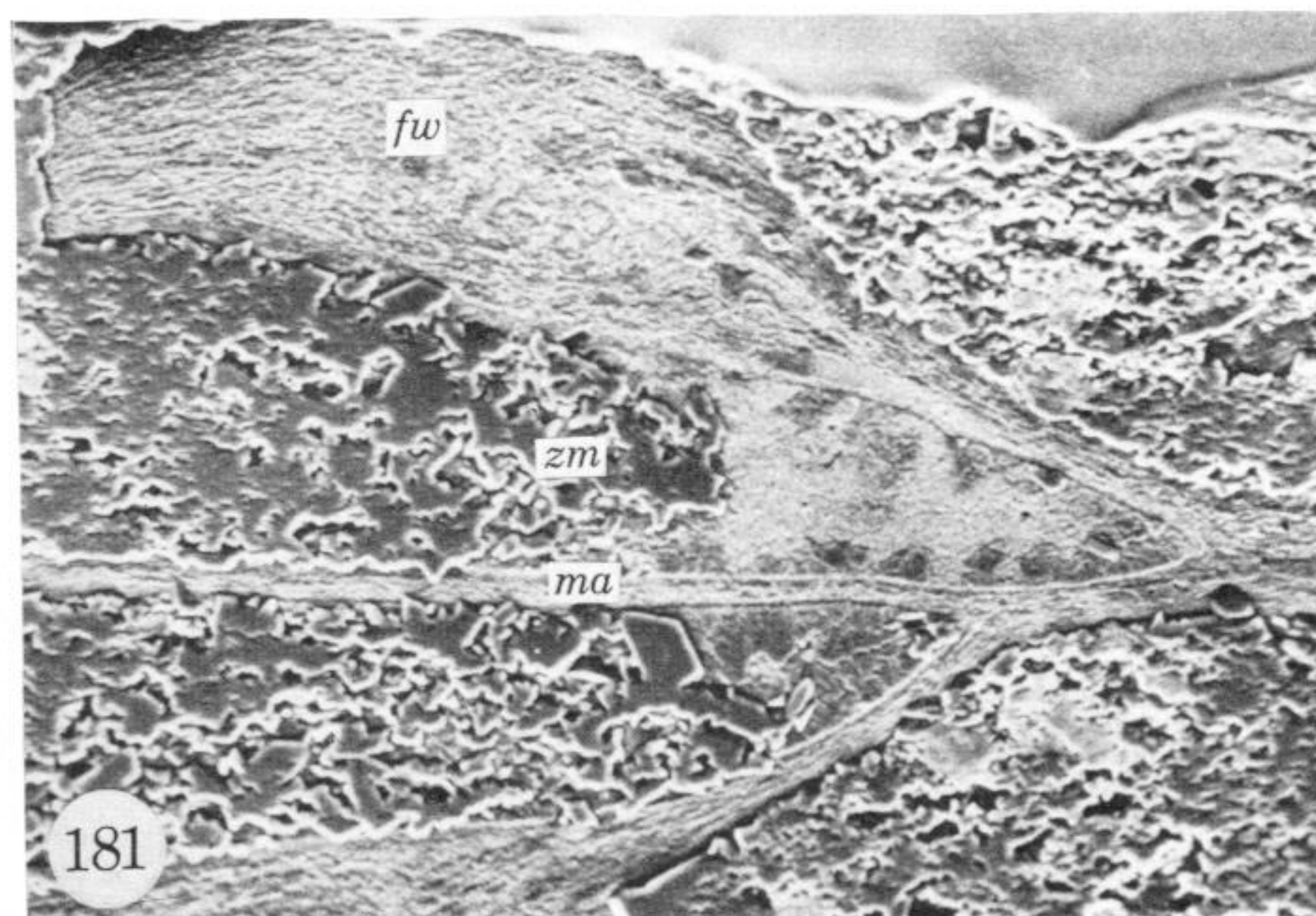
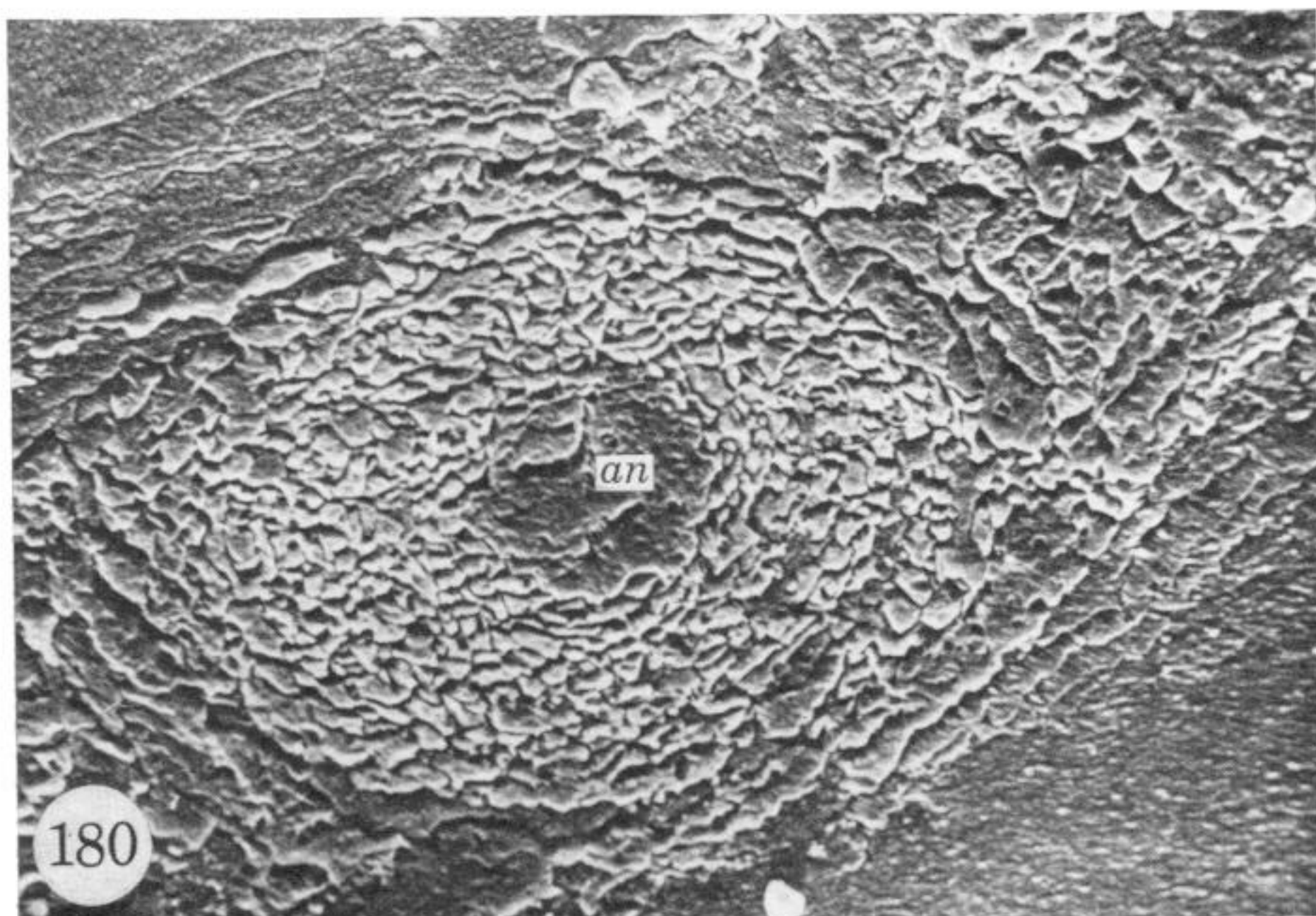
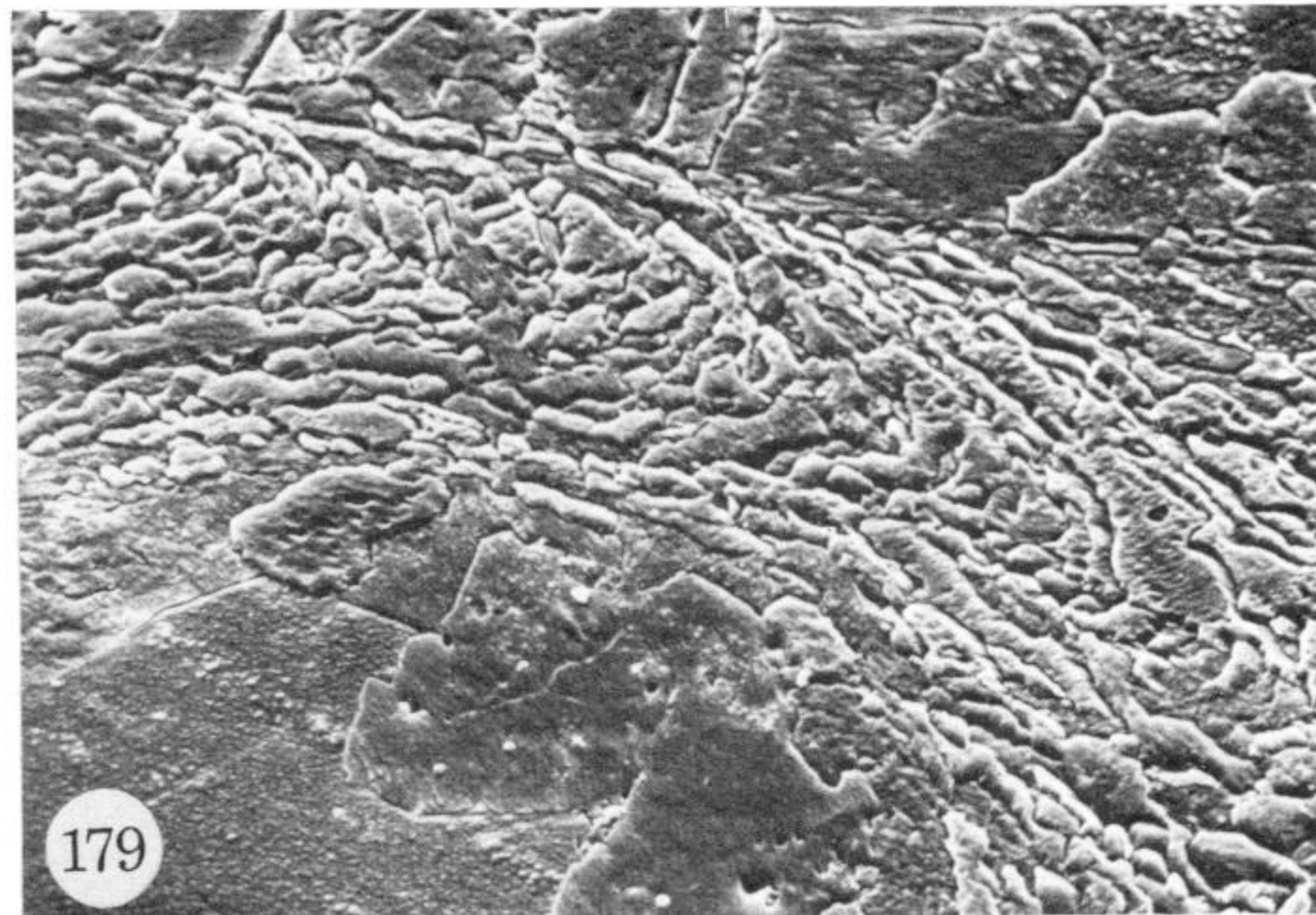
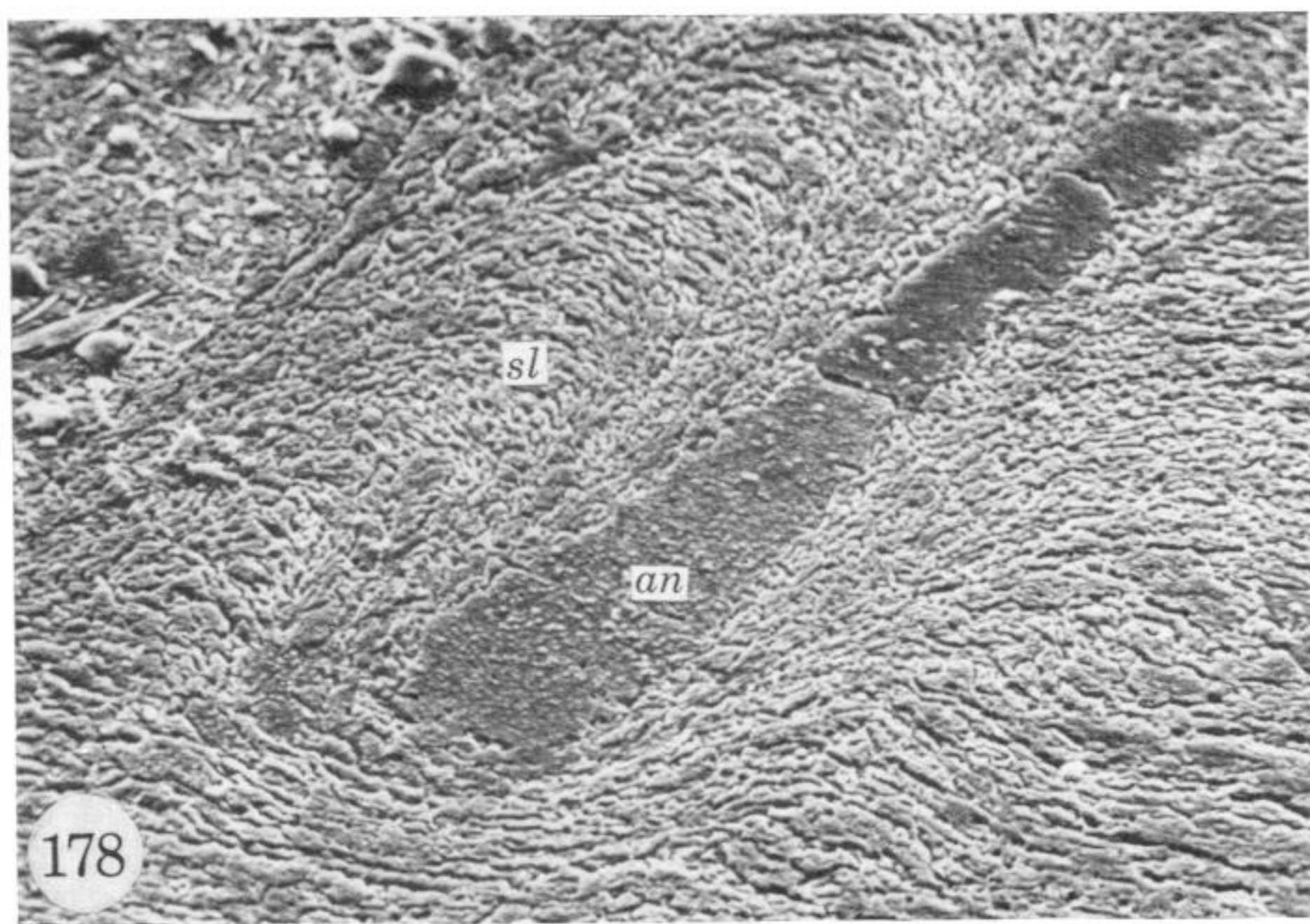
FIGURES 162 TO 169. For legends see facing page.





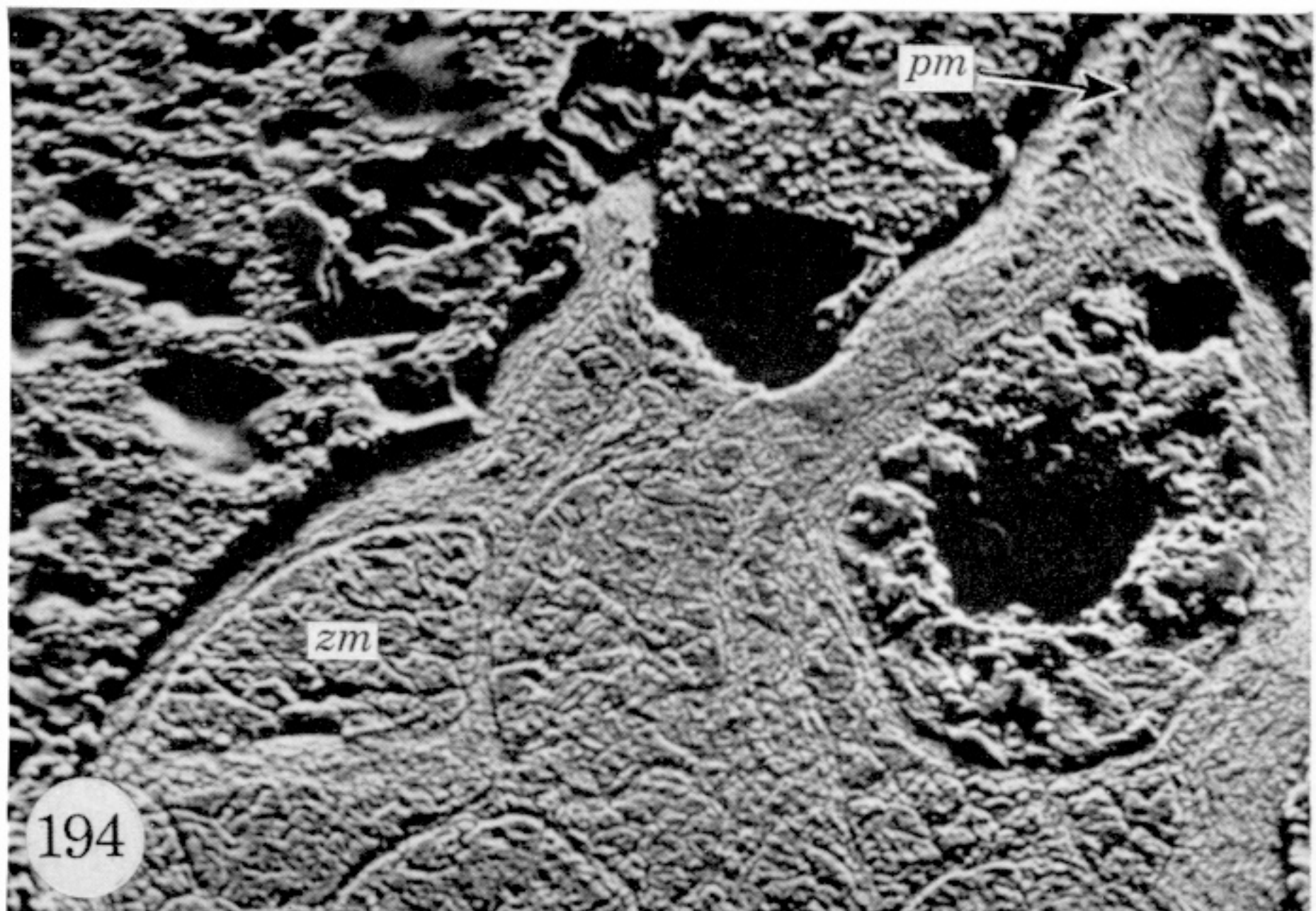
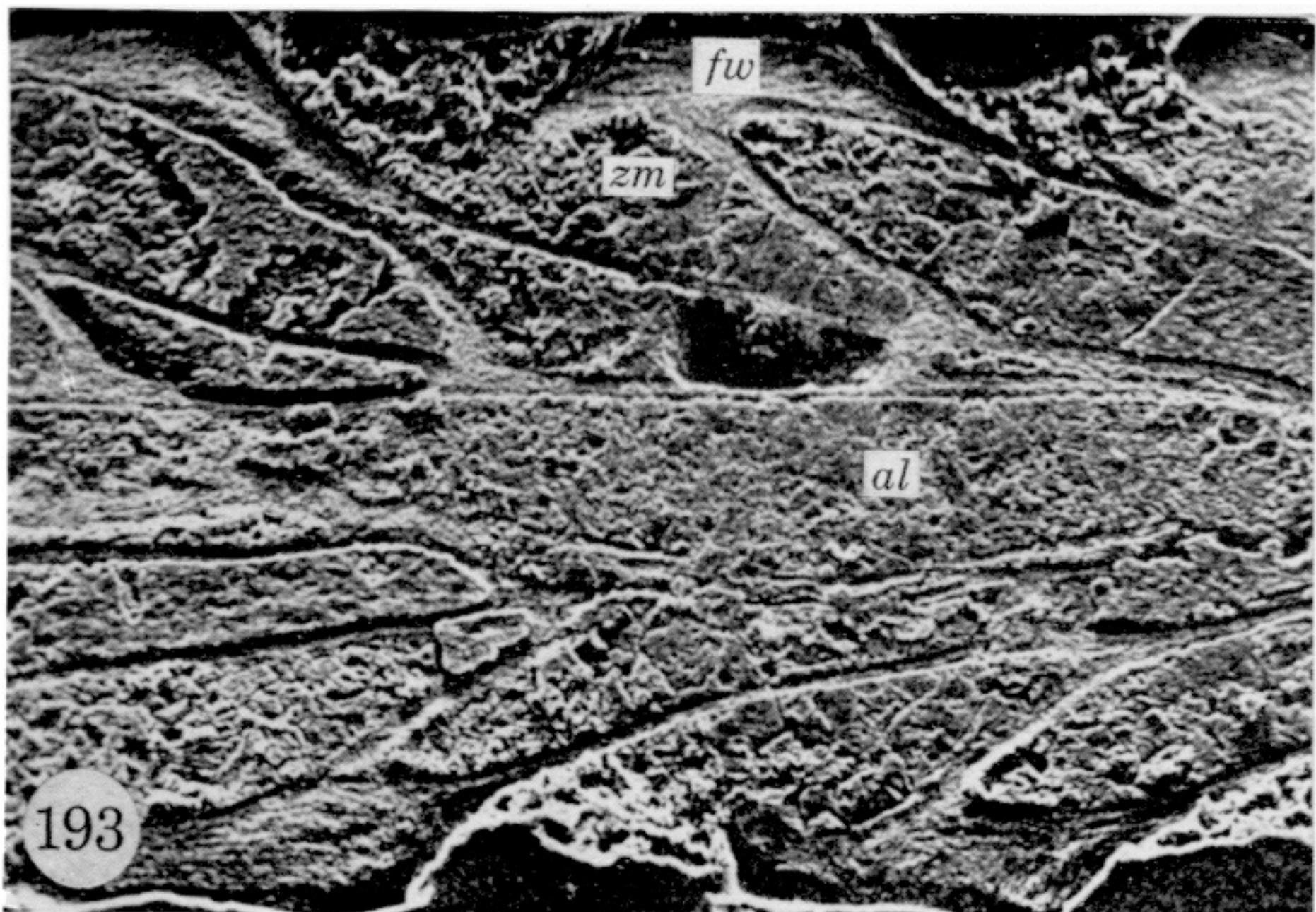
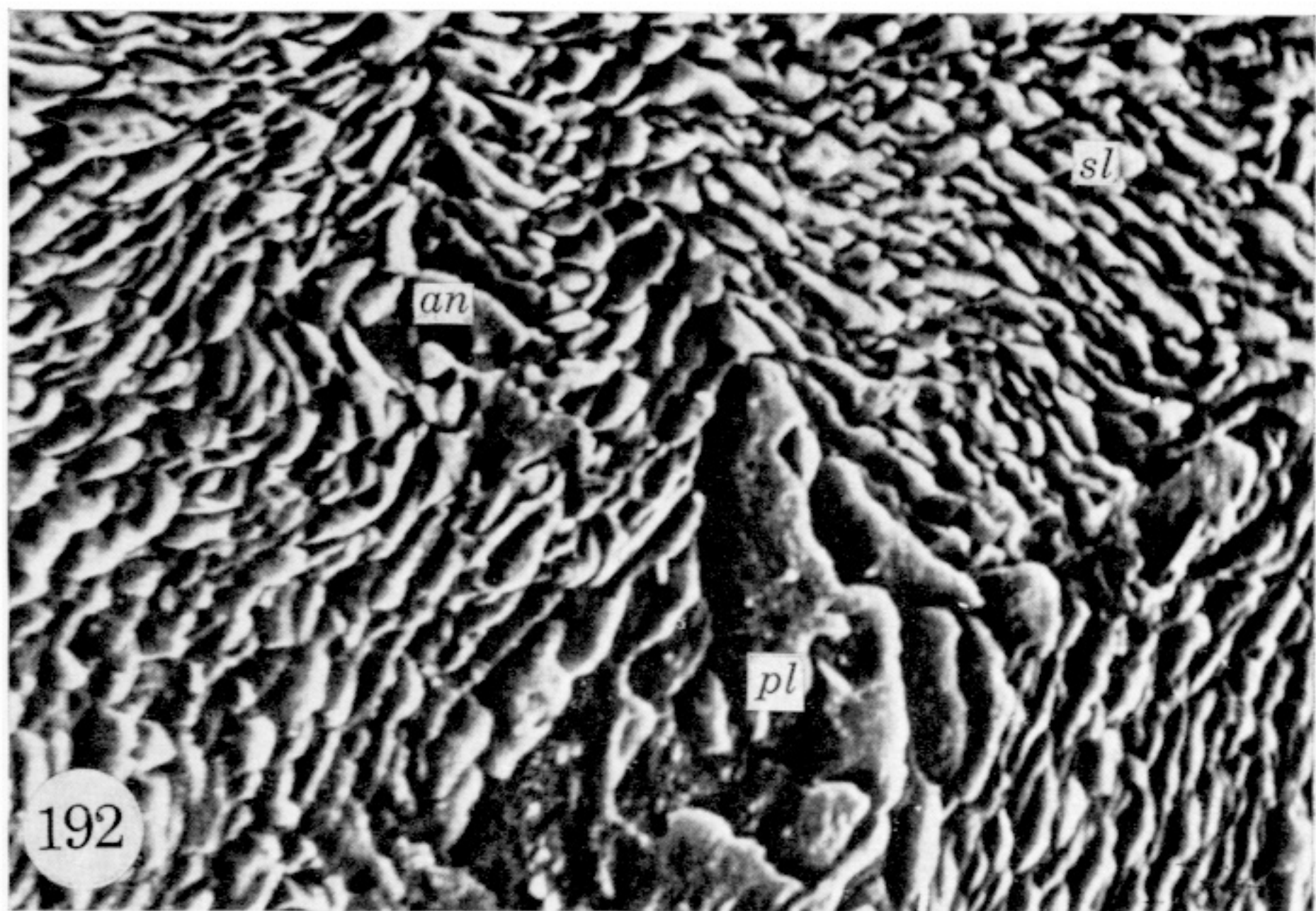
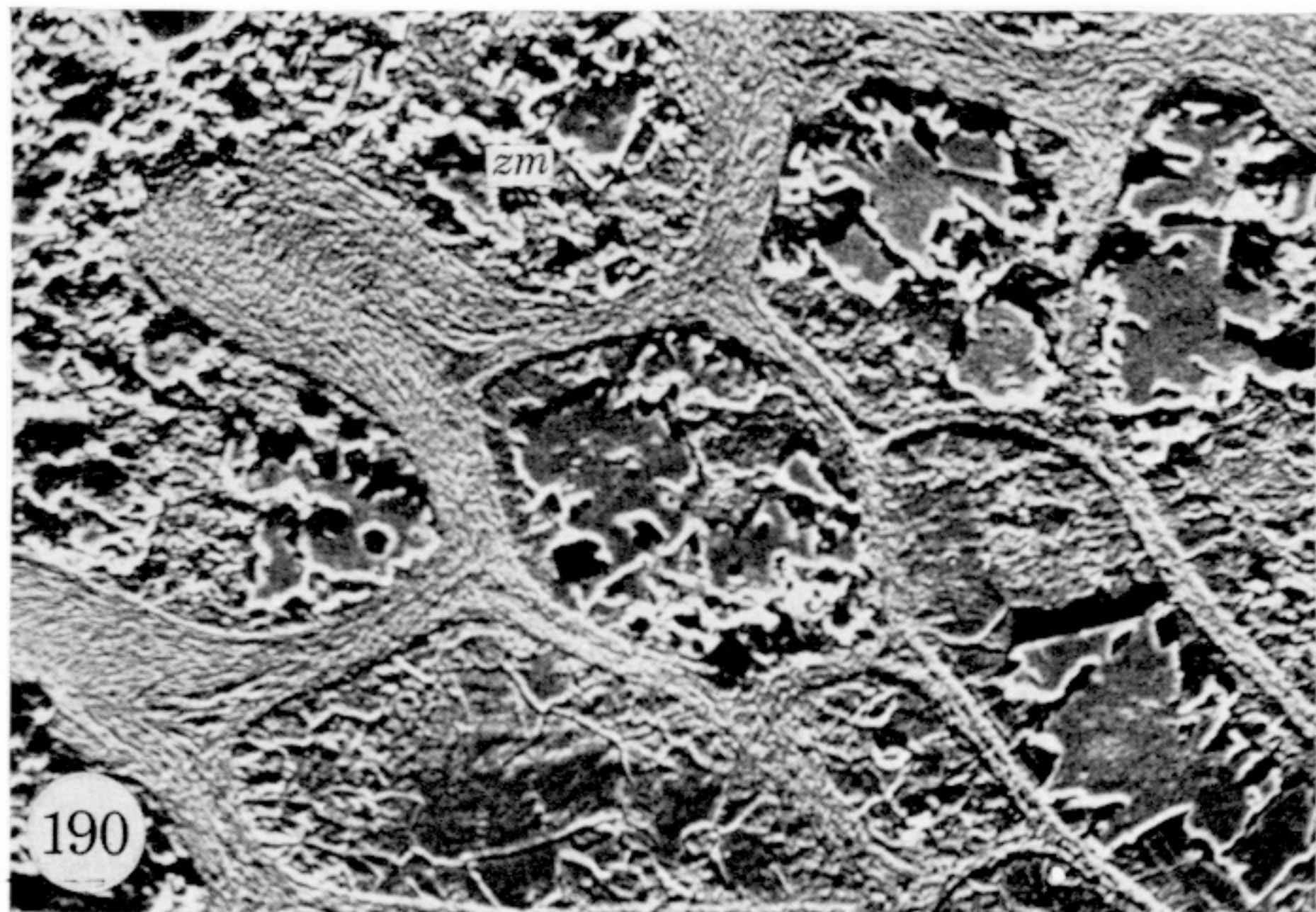
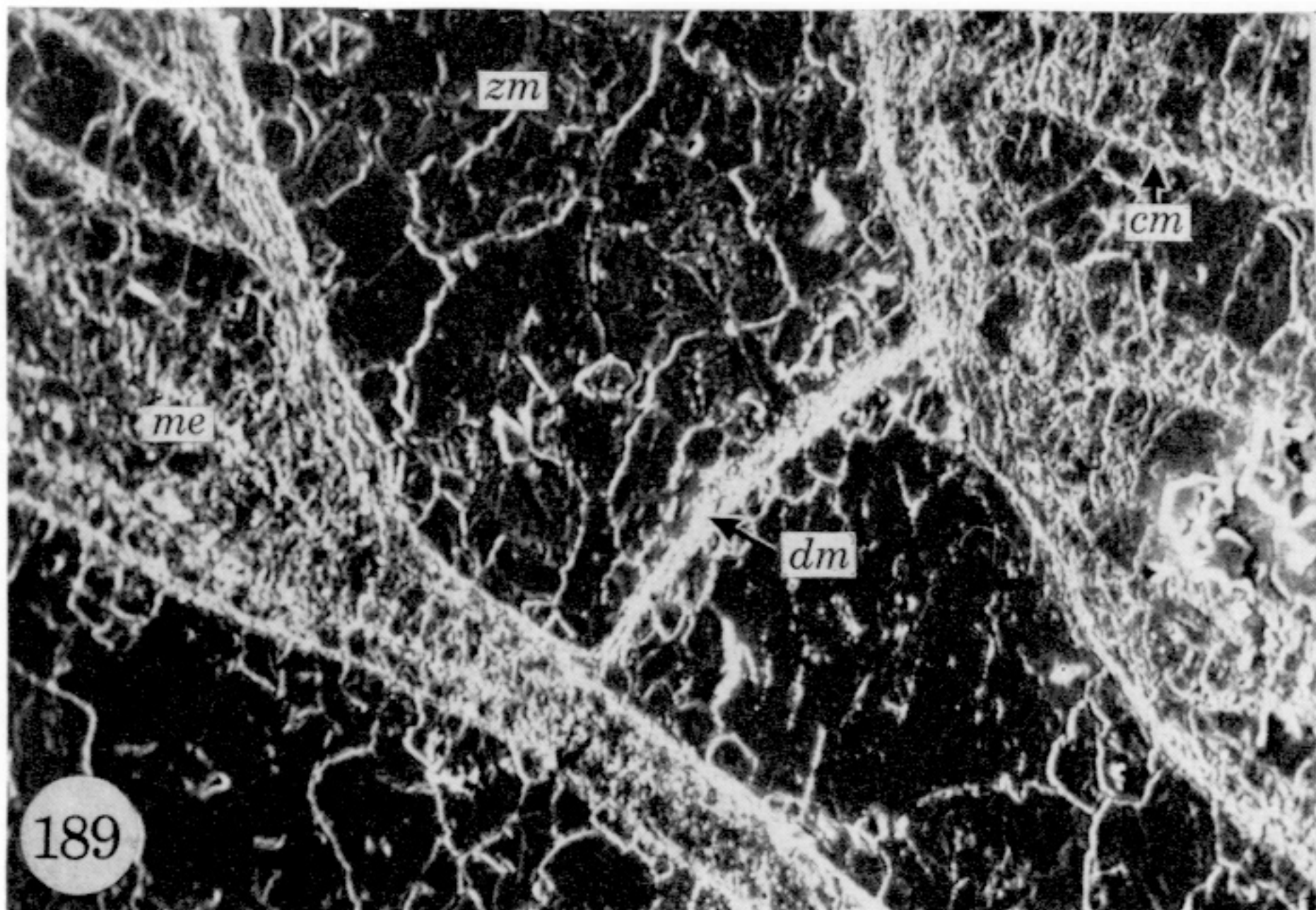
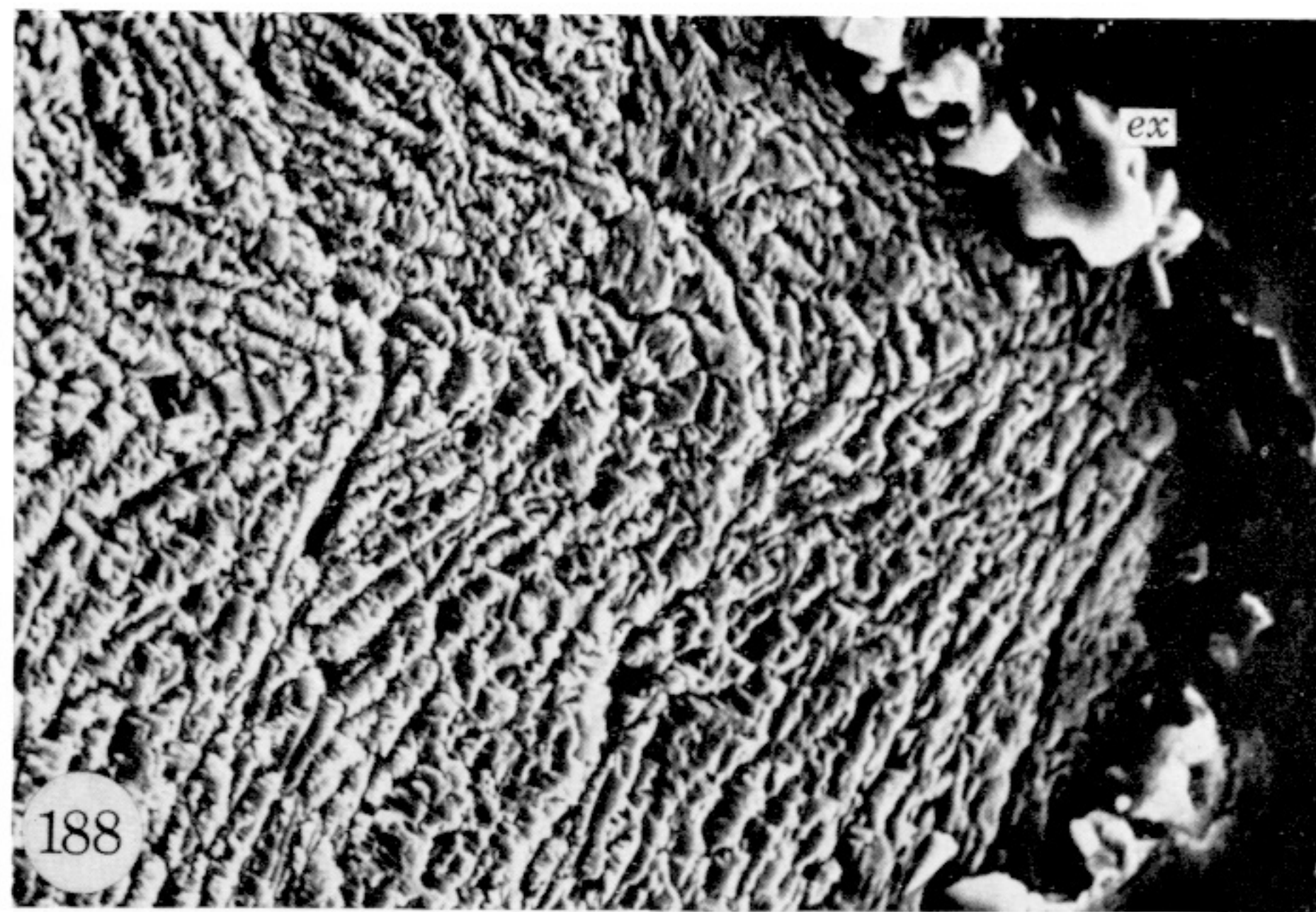
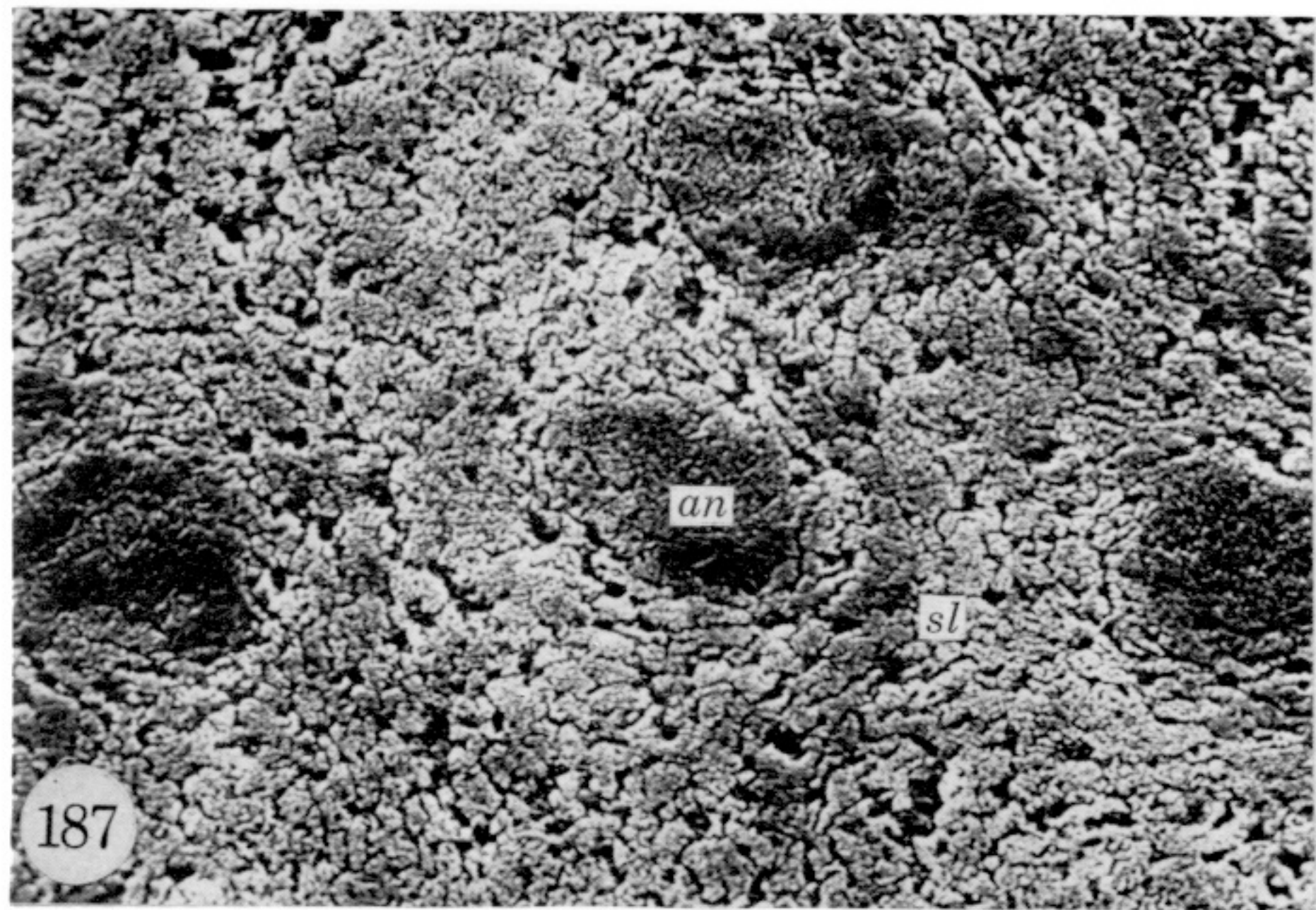
FIGURES 170 TO 177. For legends see facing page.





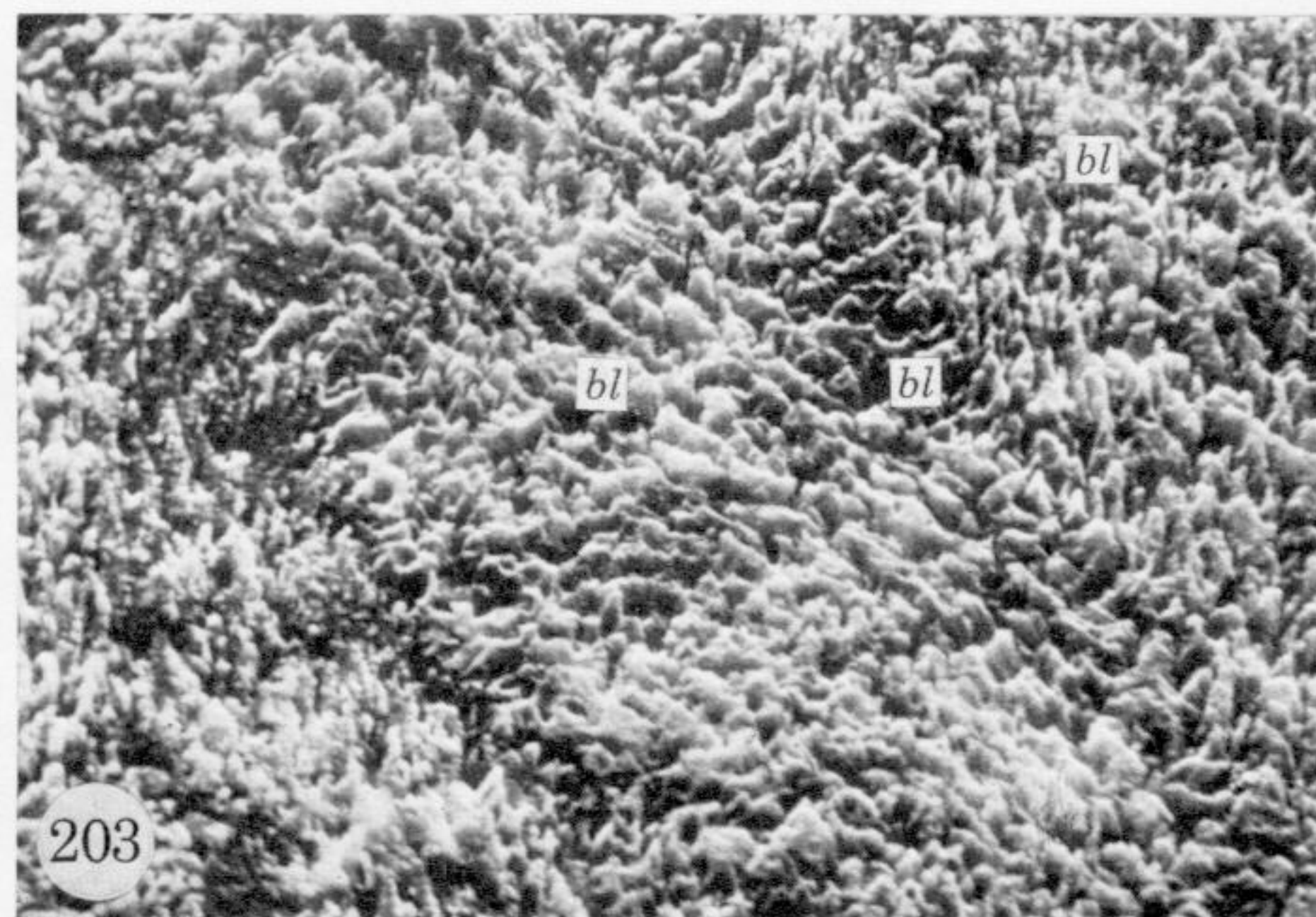
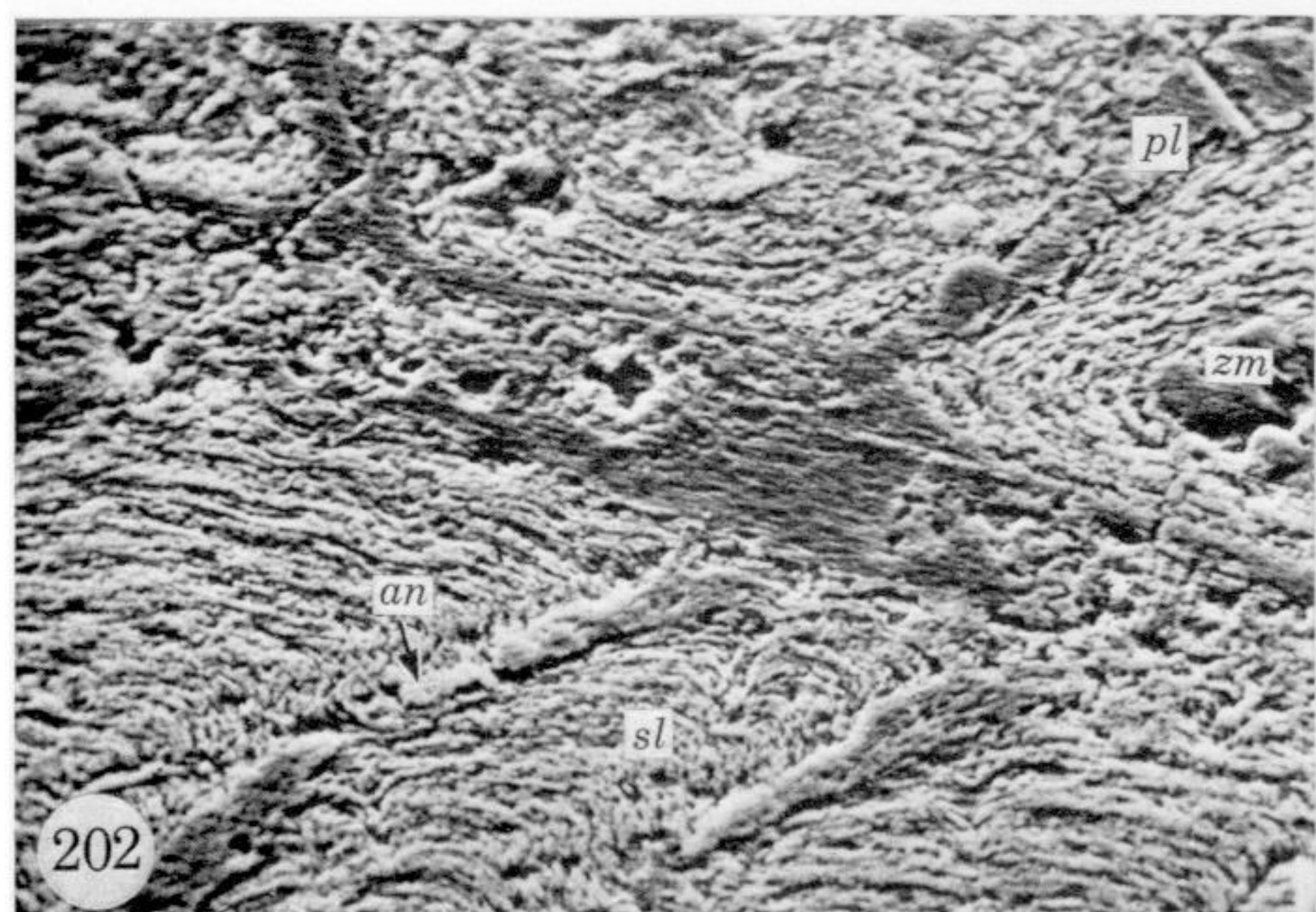
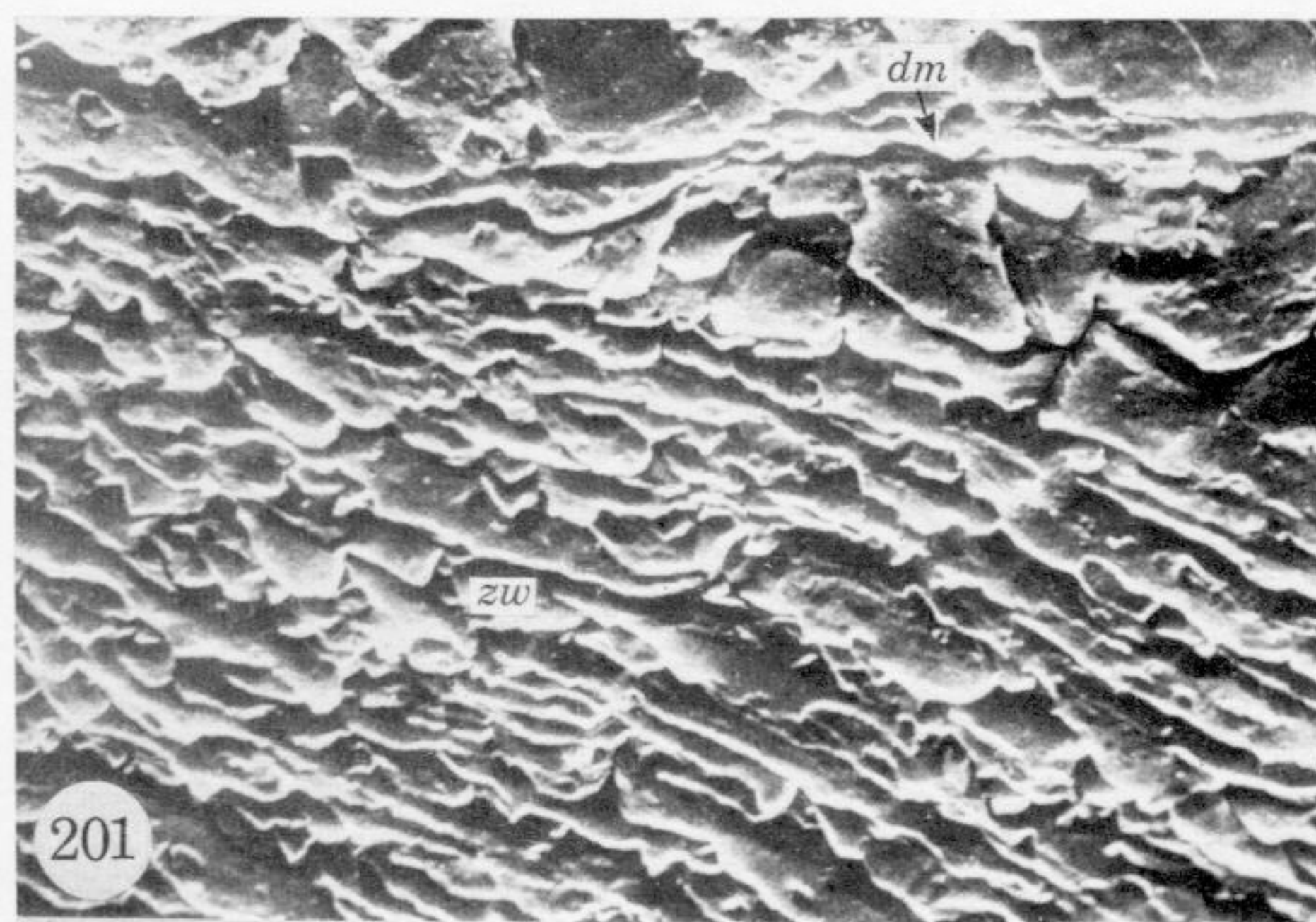
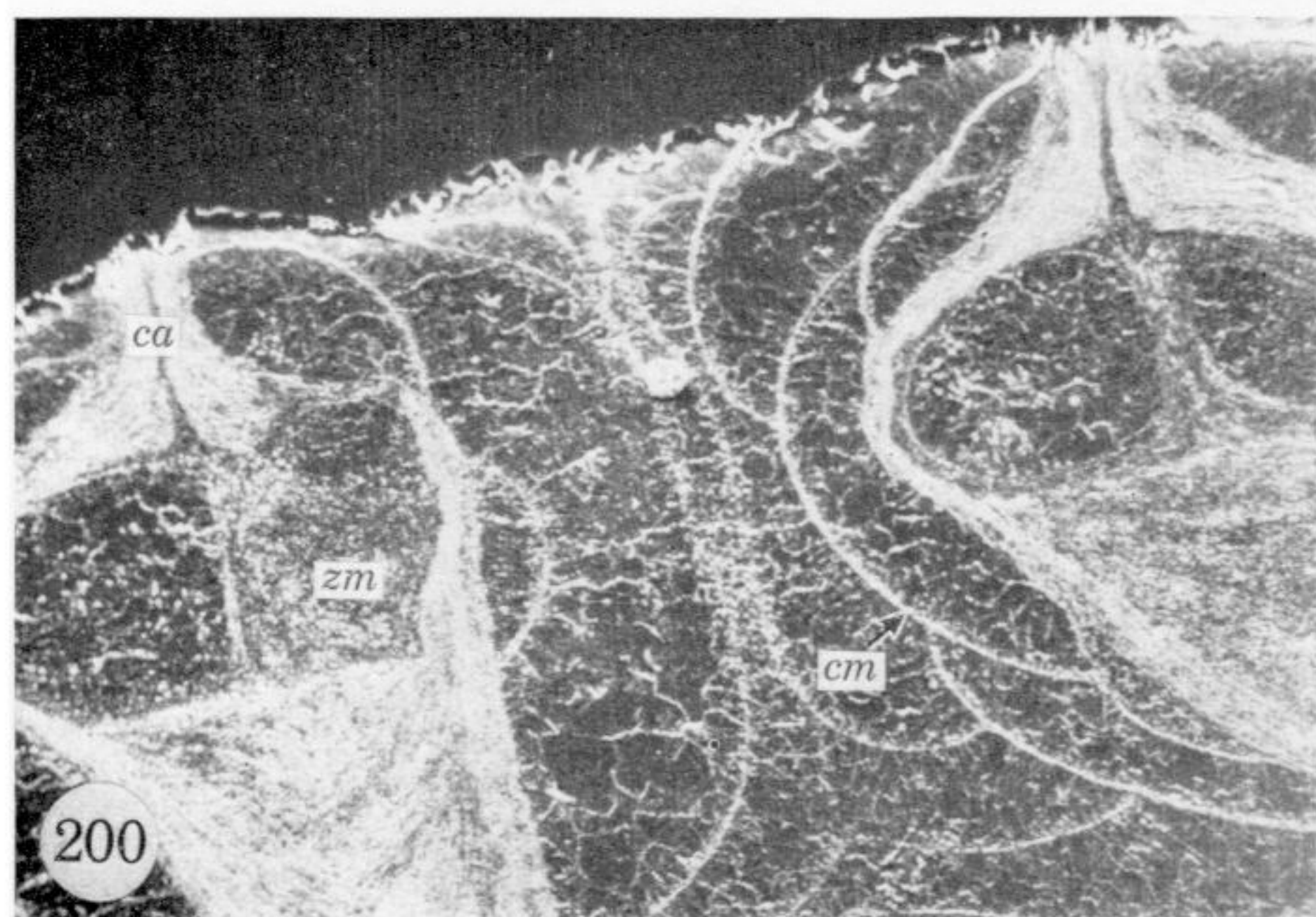
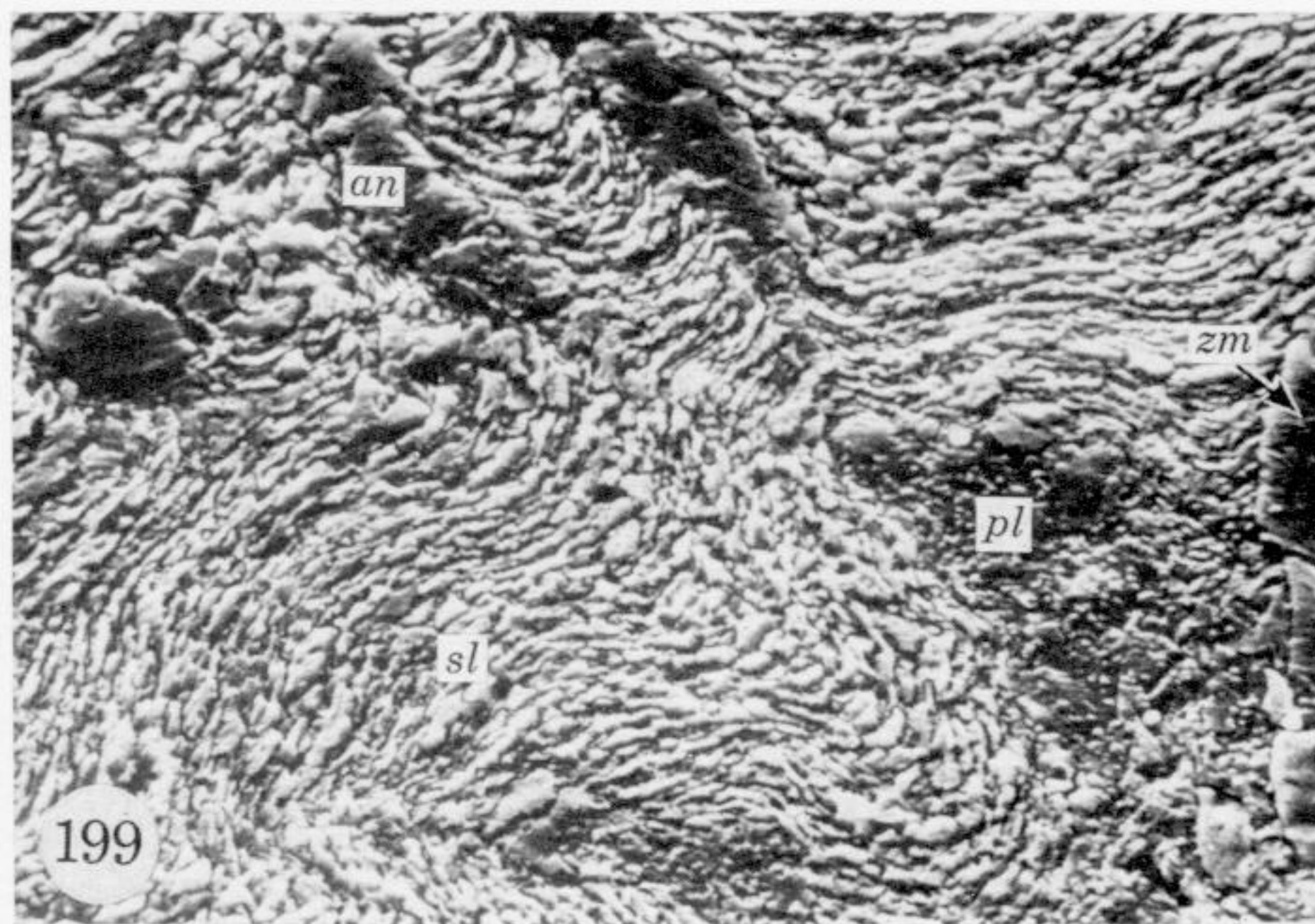
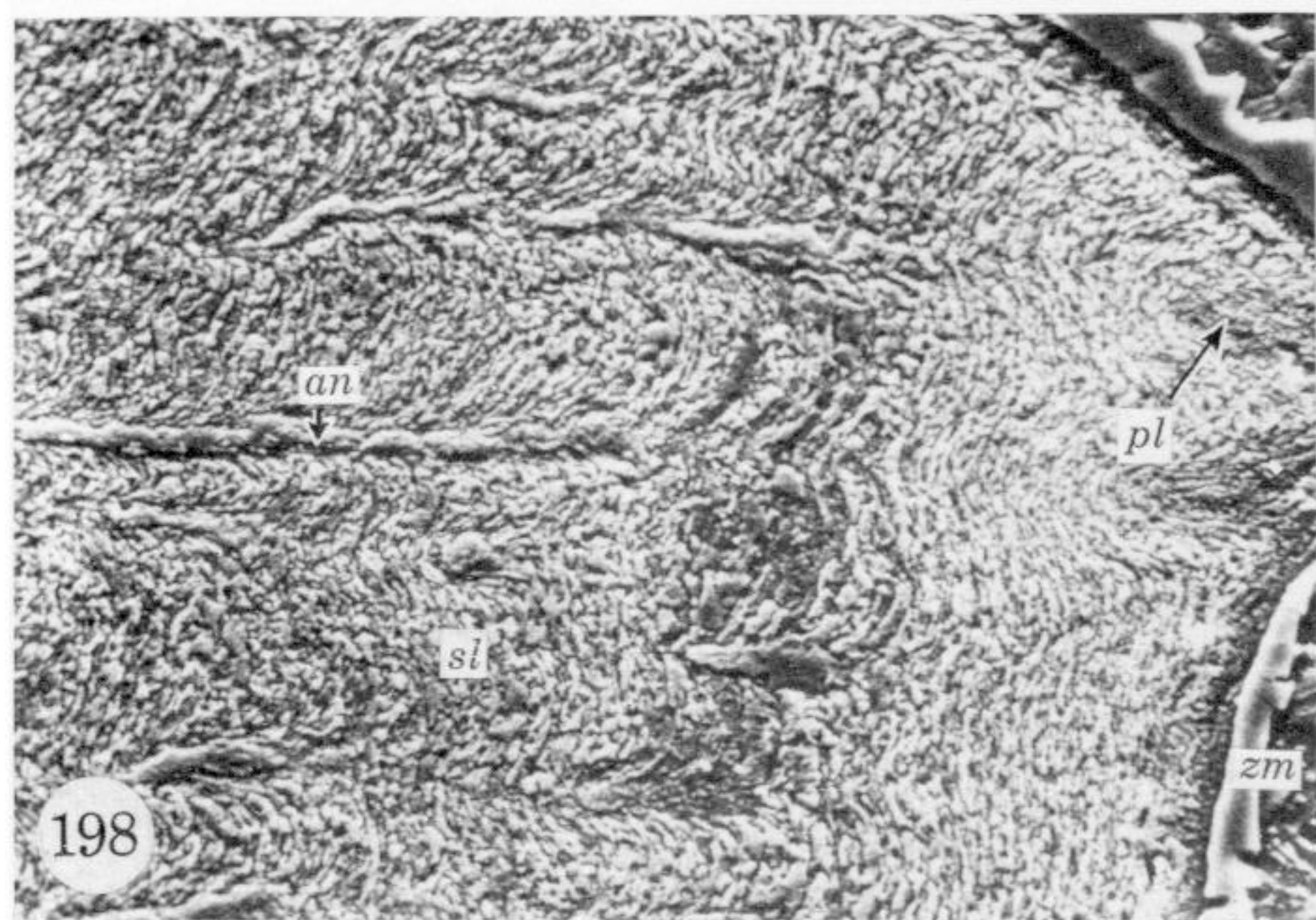
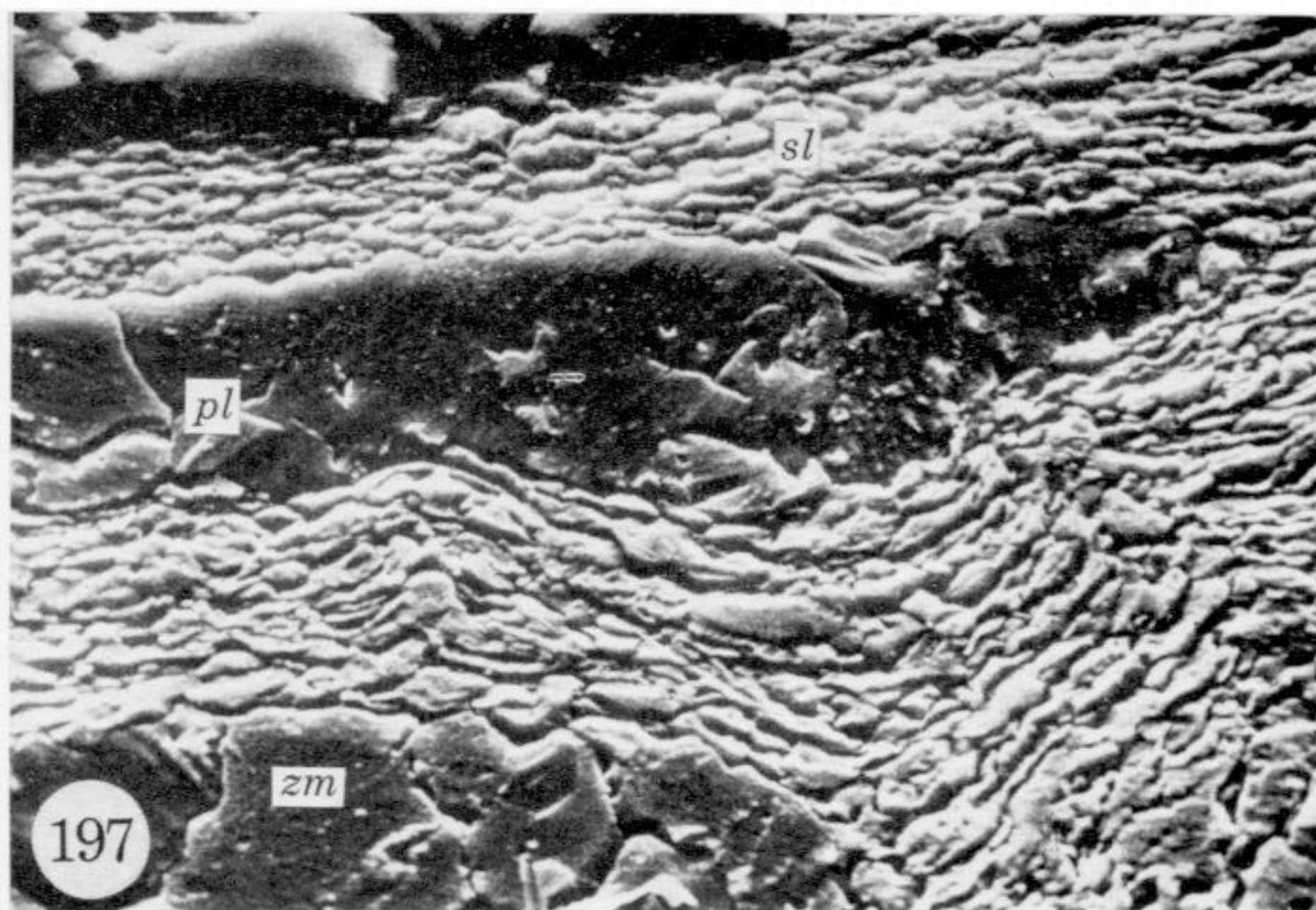
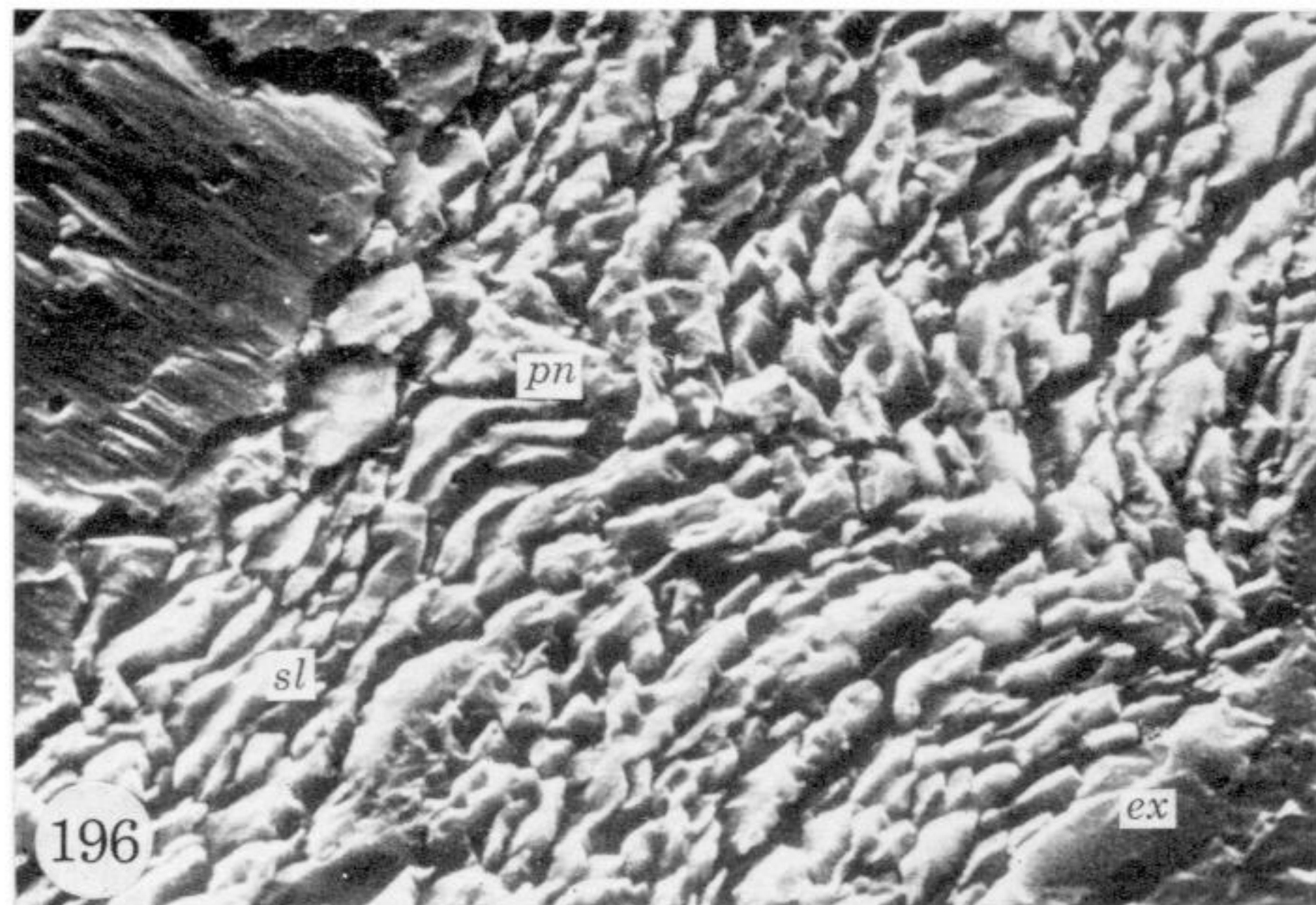
FIGURES 178 TO 185. For legends see facing page.





FIGURES 187 TO 194. For legends see facing page.





FIGURES 196 TO 203. For legends see facing page.